Herausgeber: Prof. Dr.-Ing. Viktor Mechtcherine

Institut für Baustoffe
Fakultät Bauingenieurwesen
Technische Universität Dresden
01062 Dresden

Telefon: +49 351 463 36311
Telefax: +49 351 463 37268
Email: i.baustoffe@tu-dresden.de

Druck: addprint AG, Am Spitzberg 8a, 01728 Bannewitz

ISBN 978-3-86780-519-3

Mitigating autogenous shrinkage of Ultra-High Performance Concrete by means of internal curing using superabsorbent polymers

Verringerung des autogenen Schwindens von Ultrahochfestem Beton durch innere Nachbehandlung mit superabsorbierenden Polymeren

An der Fakultät Bauingenieurwesen der Technischen Universität Dresden
zur Erlangung der Würde eines Doktor-Ingenieurs (Dr.-Ing.)
eingereichte

DISSERTATION

vorgelegt von
Dipl.-Ing. Łukasz Dudziak
aus Gdynia (Polen)

eingereicht am 22. Februar 2016

Tag der mündlichen Prüfung: 13. Mai 2016

Gutachter:
Prof. Dr.-Ing. V. Mechtcherine
Prof. Dr. K. Kovler
Prof. Dr. D. A. Stephan

Abstract

Application of smart curing concept called internal curing (IC) is the most promising strategy for mitigating autogenous shrinkage and related early-age cracking in cement-based materials with low water-to-cement ratio. There are still many theoretical and practical questions that need to be answered before IC could become a standard method. Many of these questions concern the most appealing of water-regulating additives for IC called Superabsorbent Polymers (SAP). The clear linkage between SAP material properties, the moment of water release and the effect on autogenous shrinkage is still missing, which blocks formulating recommendations for use of particular potential IC agents in concrete construction.

In this treatise various aspects that are decisive for effectiveness of IC in mitigating autogenous shrinkage were examined. The choice of materials was purposefully limited to two compositions of Ultra-High Performance Concrete (UHPC), one fine-grained and one coarse-grained mixture, and one particular, in-depth characterized SAP. The objectives of examination which shaped the final experimental programme were: assessment of IC agent absorption capacity, specification of periods of water migration from fresh concrete mixture into SAP and from SAP back into hardening concrete, determination of effect of SAP addition on cement hydration, evaluation of IC influence on and determination of start of effective autogenous shrinkage and, finally, assessment of autogenous shrinkage with selfsame IC agent but for different matrices. Ideally, description of the mechanisms behind the action of IC at different stages of concrete life and reasoning of differences observed for the UHPCs under investigation had to be provided.

First, the main components of the system – UHPC and SAP material – were characterized as to their suitability for IC application. Special attention was paid to the material properties which affect water transport. Usage of different testing methods was necessary here and included: testing with ESEM, FT-IR, tea-bag test, sol fraction content examination and X-ray computed tomography (for SAP) as well as air content measurement and various methods for characterization of the porosity and other features of the microstructure. The observed delay in the start of pozzolanic reactions in case of fine-grained UHPC was rather surprising, but, under consideration of porosity, shed new light on permeability of young UHPC.

The work at hand revealed numerous methods that can be used for studying the absorption capacity of polymers, but hardly representative for the behaviour of those polymers within concrete matrix. Because of its general availability and the relatively robust testing procedure, it was decided to focus on possibilities and limitations of using tea-bag test for evaluation of absorption capacity of SAP. New interpretation of tea-bag test results was deduced which enabled assessment of maximum absorption capacity of SAP from measurement of consistency of concrete before and after modification with IC.

Influence of IC on hydration process was revealed by using two non-destructive methods, in particular ultrasonic measurement and concrete temperature record. It could be shown that the ionic polymer exhibits complex effects including retardation and acceleration of individual chemical processes. Additionally, X-ray computed tomography (CT) and instrumented ring tests were performed in order to understand scientific significance of the characteristic event appearing during shrinkage measurements, taken as time-zero (= starting point for evaluation of autogenous shrinkage data). Linkage of time-zero with certain phenomenon, e.g., changes of the SAP particles volume or specific value of yield stress, but not with final set, was suggested for the future investigations.

By using two setups based on corrugated tube protocol it was possible to register and compare autogenous shrinkage of both UHPCs without and with modification by IC. The effectiveness of IC was shown to be dependent on the matrix in which IC was implemented. This was related to the observed changes in pore percolation that resulted from different absorption behaviour of SAP in the two UHPCs under investigation. Furthermore, the effect of fibres on effectiveness of IC was discussed.

Description and discussion of mechanisms behind IC was supported by measurement of capillary pressure, total shrinkage tests with simultaneous mass loss measurement, free autogenous shrinkage tests and the CT measurement. Valuable source of information was furthermore the in-depth literature review. The most appealing finding of the work and the biggest paradox revealed was high efficiency of IC in mitigating autogenous shrinkage and simultaneously appearance of stage where very clear reverse in mode of polymer volume change was observed. This suggests partial reabsorption of water initially released. This puts interpretation of operative shrinkage mechanisms and ones standing behind IC effect in a new perspective.

Kurzfassung

Die innere Nachbehandlung (Internal Curing – IC) ist die derzeit aussichtsreichste Strategie, um das in zementgebundenen Baustoffen mit niedrigen Wasser/Zement-Werten ausgeprägt auftretende autogene Schwinden wirksam zu verringern und die damit einhergehende Rissbildung in jungem Beton zu vermeiden. Vor einer breiten baupraktischen Anwendung des IC sind noch viele offene Fragen zu beantworten. Die meisten dieser Fragen betreffen die derzeit interessanteste Klasse von wasserregulierenden Stoffen für das IC – die superabsorbierenden Polymere (SAP). Von entscheidender Bedeutung ist hier der noch weitgehend unerforschte Zusammenhang zwischen den Materialeigenschaften der SAP, dem Zeitpunkt der Wasserabgabe und der Auswirkung auf das autogene Schwinden.

In der vorliegenden Arbeit werden verschiedene Einflussfaktoren auf die Wirksamkeit von SAP zur Verringerung des autogenen Schwindens untersucht. Für die Experimente wurde ein feinkörniger und ein grobkörniger ultra-hochfester Beton (UHPC) sowie ein schon detailliert charakterisiertes SAP genutzt. Das experimentelle Programm wurde auf folgende Untersuchungsziele ausgerichtet: Absorptionsvermögen der SAP, Zeitfenster der Wassermigration aus dem Frischbeton in das SAP sowie vom SAP in den erhärtenden Beton, autogenes Schwindmaß sowie effektiver Beginn des autogenen Schwindens. Ziel der Arbeiten ist die Beschreibung der Mechanismen, die IC zugrundliegen – und dies zu verschiedenen Betonaltern und unter Berücksichtigung der an den untersuchten UHPC beobachteten Unterschiede.

Bei der Charakterisierung der Hauptkomponenten des betrachteten Systems – UHPC und SAP – wurde auf die Materialeigenschaften fokussiert, die den Wassertransport beeinflussen. Dazu wurden u. a. folgende Untersuchungsmethoden angewendet: ESEM, FT-IR, Teebeuteltest, Sol-Fraction Test, Röntgentomographie (für SAP) sowie verschiedene Verfahren zur Charakterisierung der Poren im Beton. Im feinkörnigen UHPC wurde überraschenderweise ein verzögerter Beginn der puzzolanischen Reaktion festgestellt, der bei Berücksichtigung der vorliegenden Porosität zu einer Neubewertung der Permeabilität von UHPC in jungem Alter führte.

In der vorliegenden Arbeit werden verschiedene Methoden zur Beschreibung des Wasserabsorptionsvermögens von SAP benannt, deren Aussagekraft bei Anwendung dieser

Polymere im Beton aber sehr eingeschränkt ist. Aufgrund seiner einfachen Verfügbarkeit und Robustheit wurde daher der Teebeutetest zur Bestimmung der Wasserabsorption des SAP genutzt. Die Wasserabsorption der SAP im Beton wurde durch Gegenüberstellung von Konsistenzmessungen am Beton vor und nach Zugabe von SAP und Ergebnissen der Teebeuteltest abgeschätzt.

Der Einfluss des IC auf die Hydratation wurde zerstörungsfrei mit Ultraschall- und Betontemperaturmessungen erfasst. Auf dieser Grundlage konnten Hypothesen zu den komplexen Wechselwirkungen zwischen ionischem Polymer und der Beschleunigung oder Verzögerung einzelner chemischer Prozesse formuliert werden. Mit Hilfe von instrumentierten Ringversuchen und X-ray Computertomographie wurden die Auswirkungen des IC mit SAP auf das autogene Schwinden, den Aufbau von Zwangsspannungen bei behindertem Schwinden und Time-Zero diskutiert. Dabei konnte ein Zusammenhang zwischen Time-Zero und verschiedenen Phänomenen, wie z. B. Volumenänderung des SAP oder der Fließgrenze des erhärtenden Betons, nicht aber zum Ende des Erstarrens aufgezeigt werden.

Das autogene Schwinden beider untersuchter UHPC (jeweils mit und ohne IC) wurde mit Hilfe von Corrugated Tube-Versuchen gemessen. Es konnte gezeigt werden, dass wie Wirksamkeit des IC von der Betonzusammensetzung sowie der in den UHPC infolge Wechselwirkungen mit den SAP verschieden ausgebildeten Porenstruktur der Matrix abhängt. Weiterhin konnte ein Einfluss von Faserzugaben auf die Wirksamkeit des IC gezeigt werden.

Die Beschreibung und Diskussion der Mechanismen des IC wurde durch Messungen des Kapillardrucks, des Gesamtschwindens, des freien autogenen Schwindens, des Masseverlustes und Computertomographie unterstützt. Eine wichtige Erkenntnisquelle war zudem die umfangreich gesichtete und diskutierte Literatur.

Das interessanteste und zugleich paradoxe Ergebnis der Untersuchungen ist die Tatsache, dass die bei Einsatz von SAP beobachtete Verringerung des autogenen Schwindens eindeutig mit einer zeitgleichen Umkehr der Volumenänderung der SAP einhergeht: die bis dahin dominierende Wasserabgabe geht in eine erneute Wasseraufnahme über. Dies stellt die Interpretation der Triebkräfte des Schwindens und die dem IC zugrundliegenden Mechanismen in einen neuen Zusammenhang.

Vorwort des Herausgebers (Preface by the Editor)

Die Entwicklung von Hochleistungsbetonen stellt heute eine wichtige Grundlage für Innovationen im Bauwesen dar. Neben offensichtlichen Vorteilen, wie günstige mechanische Eigenschaften und hohe Dauerhaftigkeit, zeichnen sich solche Betone gegenüber herkömmlichem Beton i. d. R. durch große autogene Schwindverformungen aus, was vor allem auf niedrige W/Z-Werte zurückzuführen ist. Das behinderte autogene Schwinden kann u. U. zu Rissen in Beton führen, die die Vorteile von Hoch- und Ultrahochleistungsbetonen mindern. Diese „Achilles-Ferse“ von Hochleistungsbetonen ist eines der Haupthindernisse für deren breitere Nutzung in der Baupraxis. Eine neue und sehr effektive Maßnahme zur Verringerung des Rissbildungspotentials von Hochleistungsbetonen durch autogenes Schwinden besteht in einer inneren Nachbehandlung durch das Einbringen von hochabsorbierenden Polymeren (SAP = superabsorbent polymers) als Speichermedium. Bisher gibt es jedoch nur sehr diffuse Vorstellungen über die Wirkungsmechanismen von diesem neuen Zusatzmittel in Beton. Mit seiner Arbeit ist es Herrn Dudziak gelungen, viele wichtige Erkenntnisse zu gewinnen, die auf bestimmte Mechanismen hinweisen bzw. diese klar belegen. Besonders hervorzuheben sind die vorgeschlagene Methodik zur Ermittlung der Time Zero und die sehr aufschlussreiche Analyse der CT-Messungen. Die vorliegende Arbeit trägt maßgebend zur Klärung zahlreicher offener Fragen bei, so dass die Methode der inneren Nachbehandlung künftig zielsicherer und effizienter angewendet werden kann. Dies ist eine der Voraussetzung für die Verbreitung dieser Methode in der Baupraxis.

Viktor Mechtcherine

Acknowledgements

When beginning work on my dissertation, I did not expect this was going to be such an exciting journey. I would like to take this occasion to acknowledge all those who have, in one way or another, been helpful in accomplishing my goal and contributed to making an important step in my professional career.

First of all, I would like to express my deepest gratitude to Prof. Dr.-Ing. Viktor Mechtcherine, my main supervisor and the Director of the Institute of Construction Materials at Technische Universität Dresden. Thank you for initiating this thesis and providing interesting topic thereof. I am deeply indebted for the given opportunity as well as the support, both personal and professional, and the confidence you showed me. Our productive cooperation since 2006 would not bring such fruitful results including this treatise if it wasn't for his encouragement and constructive criticism, combined with full understanding of specificity of my work. For these and the academic maturity I gained throughout the years I am, and will always be, very grateful.

My special thanks go as well to Prof. K. Kovler and Prof. Dr. D. A. Stephan for the interest in my work and the willingness to acts as co-advisors. The expert advice and the hints you gave me had important imprints in the work presented. At the same time I would also like to acknowledge my appreciation for the very friendly treatment and the numerous interesting scientific and non-scientific discussions held with the former on different occasions. You made my introduction to the world of internal curing much easier. Thank you for that!

Furthermore, my sincere thanks are given to all colleagues at the Institute of Construction Materials at the Technische Universität Dresden I had pleasure to work and exchange the daily problems with. Their either tireless assistance in the experimental laboratory testing (Dr. Marko Butler, Renate Franke, Isabell Schur, Christian Stahn, trainess Markus, Toni, Nadine, Oliver), help in manufacturing the necessary aids (Tilo Günzel, Arnd-Eike Brüdern) and performing some of the tests (Simone Hempel, Annett Willomitzer, Martina Götze, Mirella Kratz, Kai-Uwe Mehlisch, Annegret Lindner, Prof. Dr. rer. nat. habil. Michael Schiekel, Kati Wenske, Egor Secrieru) or even in dealing with administrative stuff (Martina Awassi, Birgit Busch, Verena Damme), in addition to always warm treatment, made my work and adaptation to life in new country much easier. Michaela Gorges, Claudia Bellmann, Steffen Müller, Eric

Mündecke and Philipp Kunz are thanked not only for tireless support and exchange of experience but also the necessary distraction, especially the ‚kicker times'. This list of supporters wouldn't be however full without mentioning associates I had pleasure of meeting at the former working place- TU Kaiserslautern (Cornelia Ziegler, Joachim Schulze, Robert Adams, Karl Leidner). To all – vielen Dank!

My special deepest thankfulness and honest appreciation are due Dr. Anastasia Sobolkina, Klaudiusz Holeczek, Helena Stańczyk-Mielewczyk, Dr. Petr Jun, Dr. Frank Altmann, Venkatesh Naidu Nerella, Dr. Wilson Ricardo Leal da Silva, Prof. Dr. Billy Boshoff, Prof. R. D. Toledo Filho. Your work, attitude to it like that to life itself always inspired me and distributed the necessary power when I needed it. And the friendship borne either when sharing office, during enlightening discussions we had or in any other way is gift I will worship forever.

Finally, and most importantly, I would like to thank my Family: My parents Ewa and Walenty Dudziak, my late grandmother Małgorzata, my brother Andrzej and my wife Janina without whom none this would have been possible. Your love and unconditional support throughout good but sometimes hard times was my fuel and helped to make my dreams come true. Dziękuję Wam za to kochani!

God. You are truly almighty and your presence and the support is also acknowledged. Bądź pochwalony na wieki!

Last but not least, I would like to thank you, the reader, for showing interest in this work and taking the time to read it.

Dresden, June 2016

Łukasz Dudziak

Table of Contents

1 Introduction

1.1 Motivation

Production of crack-free, durable cement-based materials is a prerequisite to erecting sustainable concrete structures, from material perspective at least. Existence of so-called autogenous shrinkage phenomenon in group of high and ultra-high strength/performance cement-based materials can put that ultimate goal for concrete practitioners at risk. This volume change results from bringing water-to-cement ratio (w/c) to very low values, even as low as 0.2, that is a step necessary to obtain high strength concrete. The parameter fixation while having positive output however also exposes materials such as Ultra-High Performance Concrete to internal dry-out, a phenomenon called self-desiccation. No moisture loss to the ambient is needed to provoke this process. When the resultant shrinkage deformation is restrained, stresses are generated and if they exceed tensile strength of material, cracking takes place. Since allowing ingress of hazardous substances, cracking due to regarded cause can render concrete structures unserviceable and lead to high rehabilitation costs.

To fully take advantage of attributes that UHPC delivers e.g. enhanced mechanical behaviour and superior durability, a reliable preventative measure against autogenous shrinkage is obviously needed. Presently, no standardized solution for very dense thus little permeable materials exists. Smart curing method called internal curing has however the potential requested: By providing water from the evenly distributed internal water reservoirs, IC acts directly at the origin of autogenous volume change and not only compensates for the dimensional changes, at least according to theories known to date.

1.2 Problem and goal definition

The main obstacle hindering acceptance of internal curing as standard mitigation method is still insufficient understanding of mechanisms that trigger the effect behind it. One reason for particular situation is the difficulty in indication which shrinkage mechanisms are truly operative, also when the cement-based material is maintained in sealed conditions. Currently, only certain recognized mechanisms can be described quantitatively and be used in modelling, e.g. capillary pressure. The experimental data of this variable for concrete ages when autogenous shrinkage development rates are highest is nearly missing and is often charged with methodological errors, this being especially the case of relative humidity measurements. This, in comparison to modelling, rules out prediction approaches.

Another complexity relates to the modified material. Concrete is a very complex composite. Therefore, in majority of studies reporting on IC effect, the cement pastes are mainly under research. While being hardly representative material for final use of IC, cement paste is also much more likely to crack compared to mortar [Pir 06], for instance. This cracking will obviously influence the way and the speed curing fluid is transported to self-desiccating zone. It must be also taken into account that concrete like UHPC relative to the paste is much denser and much less permeable even if basic w/c is set equal; it furthermore is expected to be virtually deposed of capillaries, where curing fluid supposed to be distributed to from the IC agent. This list of differences between materials is regrettably not all: Role of creep in shrinkage and cracking phenomena [Gra 06a] as well as varied presence of other source of moisture e.g. stored at the interfacial transition zones [Ben 00][Est 09] are another parameters hardly taken into account when discussing shrinkage (mitigation) mechanisms. Eventually – unless mixing with vacuum is applied – high air contents are sometimes the attribute of concrete of increased viscosity and density, like the finely grained UHPC [Sch 04]. The role of air pores is vague and may become important for curing effectiveness for very different reasons related to shrinkage [Mor 01][Est 09], concrete permeability [Won 11][Tam 12] and cracking [Kus 05][Gra 10][Tam 12].

Another apparent challenge is that there are no recommendations regarding choice of materials useful for IC purposes, yet. Superabsorbent Polymers, although being closest to be used as ‘standard’ IC agent owing to freedom of material design, are often obtained from different producers. Not surprisingly, they characterize with incomparable properties, starting with shape/size and sorption properties. This complicates judgement whether water is distributed to all water-lacing zones of desiccating material, being as difficult to estimate experimentally as the absorption capacity of IC agent itself. The obvious idea behind IC is to use materials of fast absorption but which do not allow curing water to be released before self-desiccation is initiated, as to maintain effectiveness on the highest potential level.

The complexity also regards tools allowing evaluation of the IC effectiveness. Today, the standardized corrugated tube method is widely accepted but concrete age for autogenous shrinkage data evaluation is still live topic of debate and is relevant source of differences in effectiveness estimates. Reliable criterion for choosing so-called time-zero from which ‘true’ autogenous shrinkage starts and simultaneously fit for assessing true effect of IC is obviously required.

In short, the current knowledge about internal curing mechanisms as well as the precision of determining its effectiveness cannot be considered as satisfying, especially from perspective of IC usage in more complex cement-based materials than cement paste or some mortars. It is intention of this thesis to contribute to improvement of this knowledge by investigating internal curing of UHPC. The experimental focus is on evaluation of free and restrained autogenous shrinkage in different curing conditions, using corrugated tube protocol and instrumented ring tests as the main testing methods. Time-zero is determined with help of non-destructive methods mainly. Another non-destructive method that is alternative to relative humidity measurement is used to trace capillary pressure. These observations are confronted with behaviour of SAP itself, both as tested in concrete and on pure material, with special focus on the properties of the IC agent and their role in water-control processes.

1.3 Structure of the thesis

The treatise is divided into six chapters plus references and appendices, beginning with an introduction of the topic and aims of this thesis in **Chapter 1**. The following **Chapter 2** gives a survey of the literature where state-of-the-art in the fields relevant to this work of is presented. General introduction to topic of volume changes and cracking, selection of volume change that is most important for cracking in case of UHPC and time-zero aspect are reviewed firstly. Subsequently, the origins of depicted autogenous shrinkage and associated cracking are treated in more detail. This gives basis to discussion on potential mitigation strategies, critical discussion on which then follows. Finally, the solution chosen, particularly internal curing methodology by means of Superabsorbent Polymers, is screened in terms of known working mechanisms and microstructural changes exerted. Preceding these, literature research on properties of SAP material itself is performed. The materials as well as test methods used in own investigations are subject of description in **Chapter 3**. **Chapter 4** presents the main experimental results and their discussion. Whenever found necessary, supplementary literature review related to topic of concern is performed first, and additional interpretation and analysis are carried out after presentation of results, with a summary part complimenting each section. This is followed by **Chapter 5** where it is tried to provide answer whether IC truly acts at the origin of autogenous shrinkage with help of supplementary tests and discussions. The most pertinent findings of this work are summarized in **Chapter 6** where some suggestions as to possible investigations for improving the knowledge in the subject of concern are given as well.

2 Literature review

2.1 Introduction

The review of literature consists of four main parts. Section 2.2 gives, firstly, general introduction to the topic of volume changes and associated cracking. Subsequently in selfsame section, the attention is paid to the most critical volume change and main reason for cracking in case of UHPC, viz. autogenous shrinkage. Important metrological issues related with its measurement are finally discussed here as well. In the following Section 2.3, all potential mechanisms and driving forces that contribute to the net result of volume change in focus are pointed out and, if possible, their applicability to UHPC is critically discussed. This helps in defining all potential mitigation strategies for material under investigation and choosing the best one, being subject of review in Section 2.4. Because the selected solution requires introduction of new concrete component, i.e. SAP, in Section 2.5, complex nature and various characteristics of product to be added are brought to attention. Then current knowledge about the use of SAP in the mitigation strategy against autogenous shrinkage and origin of effect on other concrete properties are analysed, this finally allowing argumentation of goals of current study.

2.2 Volume changes and cracking of concrete

2.2.1 General

When cement contacts and then subsequently reacts with water, so-called hydration initiates, becoming the most fundamental process to take place in life of concrete. By involving several phenomena of chemical and physical nature that undergo further modifications in presence of certain additives/admixtures (e.g. superplasticizer), hydration products glue the aggregates together, while hydration reactions convert the initially fluid-like matter/viscous suspension initially formed into porous elastic solid of changing microstructure and saturation with water. This transformation is inherently accompanied by emission of hydration heat and by volume changes.

Unlike this transition being limited mainly to first 24 hours, volume changes of concrete can occur at any concrete age and will be either induced autogenously or they will be invoked under present curing conditions. The principal underlying stimuli are moisture/hygral changes (as related to both chemical and physical causes), temperature fluctuations and application of loading [Min 81]. Shall any of these conditions and especially their combination be

evidenced, more than one phenomenon from the group: shrinkage, swelling and creep are likely to occur.

At stake of competition and frequently superposition of volume changes is premature deterioration of concrete as caused by concrete cracking. Cracks are disadvantageous in several aspects, reduction of load carrying capacity of the structure and loss of durability and serviceability due to ingress of hazardous substances being the most critical instances.

2.2.2 Classification of volume changes

Important from engineering viewpoint, categorisation of volume changes due to shrinkage to be followed in this treatise is one put forward by Aïtcin et al. [Aït 97]. In line with the proposal, five fundamental shrinkage types can be distinguished: thermal dilation, plastic shrinkage, drying shrinkage, autogenous shrinkage and carbonation shrinkage. This list may be still complimented by another (sixth) volume change. The respective total shrinkage is commonly associated with structural concrete and is considered to be mainly sum of autogenous shrinkage and drying shrinkage, with some simplification made on particular occasion [Ish 99][Yan 05][Sol 11].

Table 2.1: Types of volume changes and their particularities.

Type	Name	Age or state of concrete at activation	Nature (hygral, other)	Acquisition	Typical record/ occurrence conditions	Main trigger
Due to shrinkage	(Effective) Thermal dilation	After hardening	Other	Calculated from temperature change and α_T	On decreasing T of concrete	Hydration heat, ambient temperature change
	Plastic shrinkage	Before hardening	Hygral	Direct	Exposure of concrete surface to ambient	Rapid loss of water by evaporation
	Drying shrinkage	When plastic shrinkage finishes = after hardening	Hygral	Extracted from superposition principle	Exposure to ambient	Moisture diffusion
	(Effective) Autogenous shrinkage	**After hardening**	**Hygral**	**Direct**	**Constant temperature, sealing**	**Lack of water for continued hydration**
	Carbonation shrinkage	Months or years	Other	Direct, but after termination of other shrinkage types	Exposure to environment of sufficient CO_2 concentration	Ingress of carbon dioxide
Due to creep	**Basic creep**	**After hardening**	**Hygral**	Excess volume change with respect to un-loaded specimen	**Load, sealing**	**Microsliding between adjacent C-S-H**
	Drying creep	After hardening	Hygral		Load, exposure to ambient	Microcracking and stress-induced shrinkage

The net result of each shrinkage type under the conditions specified in Table 2.1 is volume decrease of the concrete member[1]. However, differentiation between absolute and apparent volume variations leads to observation that shrinkage and swelling can take place simultaneously, e.g. [Bar 01][Bar 05]. Whether the swelling occurs only microscopically or, after becoming more important part of volume change than shrinkage, on the macro-level, this is decided by concrete composition as well as curing conditions. Should the relative humidity be maintained at 94% or higher, the latter is expected [Lorman *Ibid.* ACI 224R-01]. As such, different causes of swelling rather than specific types are being recognized, see Section 2.3.4.

Application of load and the consequent visco-elastic response bringing about increase in concrete strain is reserved from volume change called creep. It might be differentiated between creep components or, using simplified approach, the creep types (Table 2.1). The latter are two, viz. basic creep and drying creep and, similarly to shrinkage types, will pay different contribution to the total volume change in strict dependence on curing conditions, fluid-to-solid transition stage of concrete and its composition.

Since driving forces and underlying mechanisms are different for each volume change, e.g. [Bel 11], recognition of operative volume change and its origin for concrete under investigation becomes fundamental step for successful choice of prevention measure.

2.2.3 Autogenous shrinkage: Main volume change of UHPC

Ultra-High Performance Concrete examined in this treatise is relatively new class of concrete and most appealing outcome of quest for stronger and more durable cement-based material. The worldwide research efforts towards the goal intensified when silica fume and new generation of superplasticizers became available as they provided the possibility of realizing the idea of concrete porosity reduction[2] in a new way, viz. without necessity of concrete vibration, heat treatment or even significant advancement of hydration. Numerous important contributions to this subject, especially that of Bache as well as French researchers (e.g. [Bac 81] and [Ric 95][Ver 98], respectively), led finally to development of the so-called Ultra-High Performance Concrete (UHPC). This class of concrete is by definition characterized by compressive strength of at least 150 MPa [Bor 01]. Still, and the definition aside, UHPC will

[1] It should be noted that volume change due to temperature could be subdivided into thermal dilation (when the temperature of concrete is increasing) and thermal contraction (in the opposite case).
[2] Note this is the main prerequisite for material properties improvement, understood since Powers.

present general enhancement in other properties compared to other concrete, though typically smallest for the tensile strength.

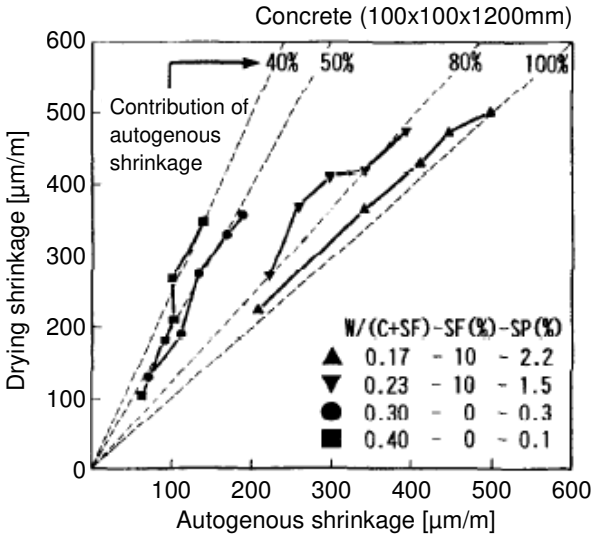

Figure 2.1: Contribution of autogenous shrinkage to total shrinkage (here erroneously named drying shrinkage) in dependence on mix parameter variation [JCI 99].

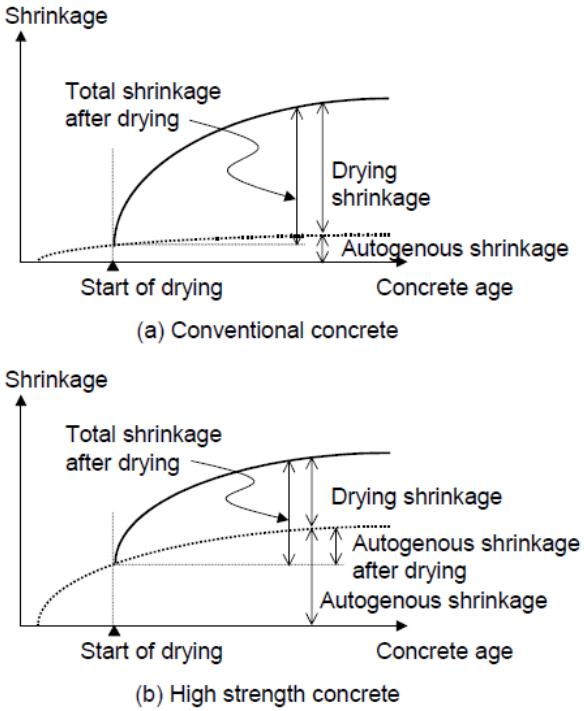

Figure 2.2: Total shrinkage and its components in case of conventional/ordinary concrete (top row) and high strength concrete (bottom row), after [Sak 04].

UHPC can attain its superior properties as it succeeds to overcome some of characteristic shortcomings of conventional concretes by the special mix design. Usage of coarse aggregate is an option but not a 'must' when composing the UHPC recipe, e.g. [Ma 04][Cwi 08]. On the other hand, the necessary optimization steps involve, as a rule of thumb, lowering w/c to about 0.2, introduction of silica fume as well as superplasticizing admixture [Ric 95]. Regrettably, such design approach and main way to obtain maximization of packing density also bring about very high autogenous shrinkage of UHPC. This particular type of volume change has prevailing contribution to total shrinkage of UHPC, while its contribution to total shrinkage of ordinary concrete becomes neglectable with increasing w/c, see Figure 2.1 and 2.2.

2.2.4 Cracking due to autogenous shrinkage

Autogenous shrinkage, even when attaining high values as for UHPC, is of little concern as long as concrete can deform freely. However, a truly free deformation hardly exists in the practice of construction as the contracting matter becomes in different ways restrained. The barriers hindering volume changes to undergo freely are originating directly from the concrete

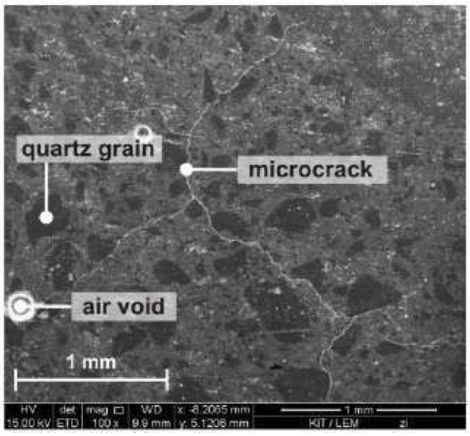

Figure 2.3: Microstructure of 28-day-old water-cured coarse-grained UHPC without fibres exhibiting micro-cracking associated with autogenous shrinkage, after [Sch 12a].

components or the fresh concrete contacting any elements of relatively higher stiffness, see Section 2.3.4 for more details. In most critical case scenario, specific interplay between the volume changes, the mechanical properties of concrete and different types and degrees of restraint leads to stress generation that could finally turn into cracking, see Figure 2.3. Cracks are unwanted given that they impair concrete quality.

Luckily enough, despite the stress generation by the restrained shrinkage deformation, cracking isn't always the case. The UHPC mix design is certainly important. E.g. short steel fibres are useful in avoiding the most concrete quality-detrimental macro-cracking, e.g. [Ros 87]. As the tiny reinforcement stitches/bridges the microcracks and, in doing so, limits their propagation, with adequate type of fibre used and sufficient fibre-matrix bond strength attained, development of macro-cracks can be constrained and certainly delayed.

Interestingly enough, only micro-cracking seems inherent to internally restrained UHPC without fibres due to autogenous shrinkage origin [Lou 99][Fey 01][Sch 12a]. The phenomenon occurrence is noted to have little dependence on maximum aggregate size used in the design, in agreement with past studies [Bis 01][Pir 06][Mou 11]. However, it certainly depends on time, having highest likelihood during first 24 hours, [Sch 02][Epp 10], i.e. when the rates of autogenous shrinkage and the 'stress-carrier'-Young's modulus development are typically highest.

The lack of macro-cracking – despite no fibres present and in spite of high autogenous shrinkage of UHPC – is often related to designed material behaviour. As a rule of thumb, it may be attributed to specific differences in development of Young's modulus and tensile strength [Sch 02][Sch 07a] as well as certain favourable phenomena taking place endogenously, especially stress relaxation [Sch 02][Sch 07a][Epp 10]. Decisive factor for the stress generation as such will be nonetheless the advancement of the so-called fluid-to-solid transition. This transition is crucial in terms of development of elastic properties of concrete

[San 09] and therefore effective autogenous shrinkage, i.e. part of volume change that actually leads to rise of tensile stresses under restraint. The so-called time-zero roughly related to development of solid with non-zero stiffness will be often named in this context.

2.2.5 Relevant aspects of autogenous shrinkage measurement

Despite continuously broaden knowledge about factors controlling autogenous shrinkage and allowing choice of preventative measures, conflicting information regarding rate of development and magnitude of autogenous shrinkage of UHPCs is often found in literature. In particular, same levels of deformation are demonstrated for two theoretically different UHPC compositions (see Figures 2.4 and 2.5 at reference concrete age of 200 days) while the opposite finding is sometimes presented when nearly identical matrix is tested (compare result for M2Q and M1Q matrices in Figure 2.4 and Figure 2.6, respectively). The effect of fibres also becomes somewhat masked, see Figure 2.6.

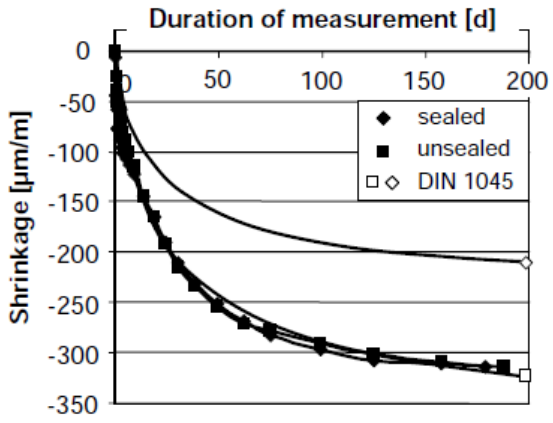

Figure 2.4: Autogenous shrinkage of finely grained UHPC based on M2Q matrix, after [Bur 08].

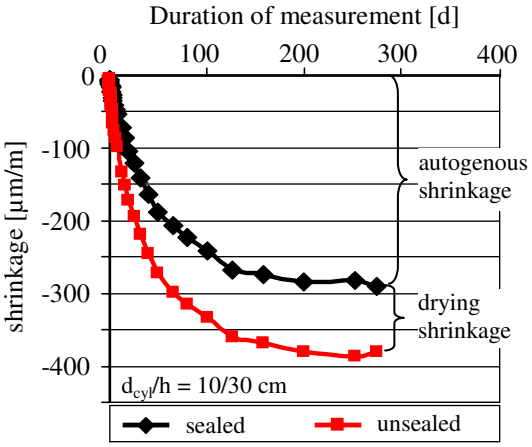

Figure 2.5: Autogenous shrinkage of coarse-grained UHPC based on B5Q matrix, after [Mue 10].

When temperature effect is accounted for, can be neglected (for temperature rise of max. 2K [Ham 06a]) or is directly excluded within measuring principle, it is observed that the major point of disagreement leading to the above-mentioned paradox could be attributed to the differences in the start of shrinkage investigation. The fact is that many of existing design standards followed, e.g. DIN 1045-1 [DIN 1045-1], give the beginning of autogenous deformations as one day after mixing. In other cases, record is delayed to even later ages since assessment of particular volume change solely supplements the main scope of studies, evaluation of visco-elastic behaviour from the age of 1 day or later being one example [Bur 08][Mue 10]. If development of shrinkage-induced stresses is taken into account, however, this means ignoring important part of autogenous shrinkage developed in the first 24 hours.

Consequently, without correct definition of so-called time-zero, i.e. concrete age at which 'relevant' AS starts, effectiveness of mitigation strategy undertaken may be misjudged too.

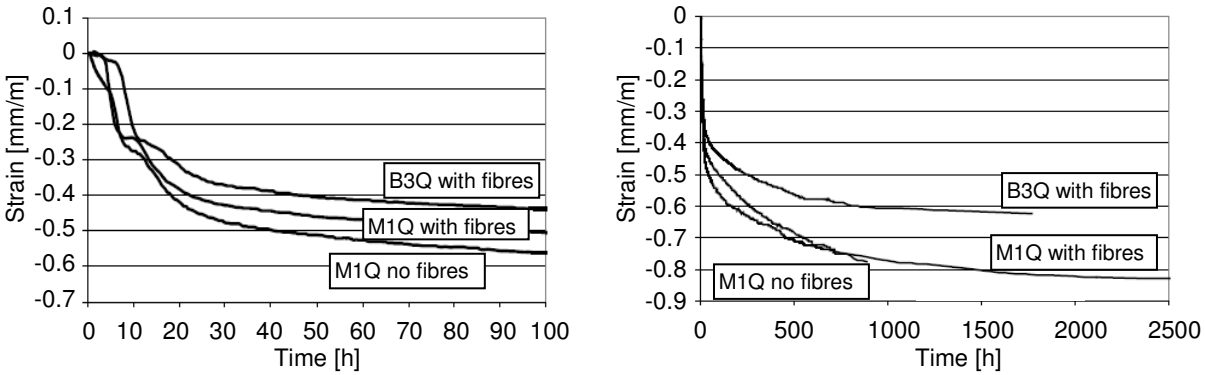

Figure 2.6: Autogenous shrinkage of two chosen UHPC mixtures studied in the framework of SPP1182 programme in respect to the effect of fibres and changes of concrete composition [Feh 05].

From scientific point of view, one essential point is to begin with the measurements as early as possible, best directly after mixing, in order to record the entire history of the early age deformations and any of pronounced secondary effects occurred. However, to delimit the deformation captured to most relevant part from engineering and/or phenomenological perspective, the goal-oriented definition of time-zero is required.

Time-zero can be defined as 'duration between the instant when the water comes in contact with cement and the time at which the concrete develops sufficient structure to enable tensile stress transfer through the concrete' [TC 196-ICC]. In other words, time-zero corresponds to concrete age when internal stresses start to develop within concrete material and the autogenous shrinkage becomes effective i.e. has practical consequences such as residual stress development. It is a general consensus that particular time instant is closely associated with the fluid-to-solid transition (e.g. [Med 11b]) and, simultaneously, likely coincides with final setting time (e.g. [Dar 11]), even if various approaches used for purpose of determining the characteristic transformation may lead to different results [San 09]. However, even to date, none of the methods prove to be optimum. E.g. the onset of tensile stress development in the restrained ring test and end of setting period are commonly taken as time-zero but suffer from serious shortcomings: while former gives result dependent on degree of restraint provided by set-up and certainly decided by steel ring thickness [Hos 04][Yoo 14], the value of latter starts to vary as soon as different measurement standard for penetration method is used [Gra 06c]. Scientific approach in which shape of shrinkage-time curve is taken into account and some important phenomena are recognized might thus become an important alternative in determining time-zero.

2.3 Driving forces and mechanisms behind autogenous shrinkage and related cracking

2.3.1 Hydration and microstructural development

Conceptually, autogenous shrinkage may be regarded as common effect of two events, viz. chemical shrinkage (also called Le Chatelier's contraction after the founder) and the self-desiccation, to be further discussed in Section 2.3.2. The nucleus of both phenomena is hydration.

Due to high complexity, the hydration is still a live scientific topic and the object of much controversy and debate. According to the newest in-depth studies though, it closest to be described as a dissolution-precipitation process [Smi 02][Bul 11]. In course of hydration, free water is gradually bound in both chemical and physical way and the microstructure (i.e. matter heterogeneous over extended length scales) is developed. The most relevant processes and events bringing about these outcomes include [Tay 97][Bul 11][Scr 11][Zha 12b]:

- gradual dissolution of anhydrous cement grains with simultaneous release of different ions into pore water (Figure 2.7), i.e. pore solution formation,
- precipitation of hydration products corresponding to reacted clinker compound at the respective ionic supersaturation state,
- filling of the water-filled spaces (so-called capillary pores) with hydration products and their spatial arrangement bringing about of own, much smaller pore system (so-called gel pores and small gel pores, see Figure 2.8),
- coalescence of hydrations shells from adjacent cement grains and the resulting solid phase percolation, followed by 3D-percolation and setting,
- continuous gain in strength of the load-bearing skeleton of the hardened cement paste,
- capillary depercolation and, in subsequence, potential repercolation [Ben 06a].

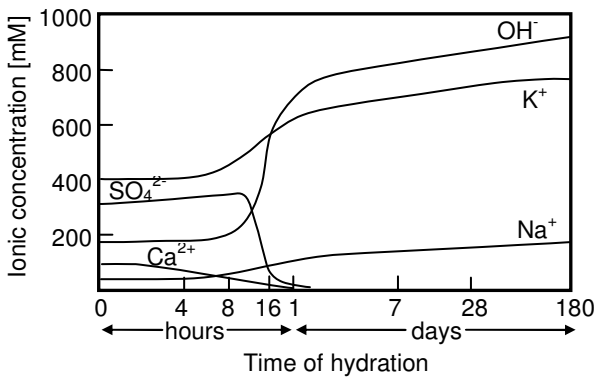

Figure 2.7: Typical changes in pore solution in hydrating cement paste. Courtesy of Sidney Diamond, Purdue University.

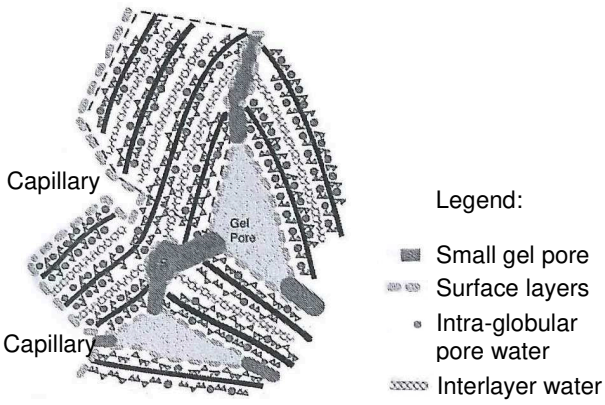

Figure 2.8: Schematic of most abundant component of hardened cement paste, so-called C-S-H phase [Jen 13].

All abovementioned events fall in-between five stages of hydration commonly depicted based on evolution of hydration heat and named pre-induction period, dormant/induction period, acceleration period (note: the most important stage in the fluid-to-solid transition and microstructural development!), deceleration period and final period of hydration. The process halts when the relatively humidity (RH)[3] drops to approx. 80 % [Pow 47] rather than due to lack of space for hydration products deposition[4]. Autogenous shrinkage as closely related to hydration understandably will be therefore also limited by the same RH level, being easily and rapidly attained in UHPC even when sealed conditions are maintained, e.g. [Lou 99].

The changes in volume fractions of paste constituents and the hydration advancement could be assessed using Powers' model [Pow 47][Han 86][Jen 01b] or its modified version for cement-silica systems [Jen 93]. Having it applied for low w/c or w/b systems like UHPC, it is immediately noticed that while the conversion of cement into hydration products is less than for conventional concretes, a remarkable volume of cement paste will be occupied by internal voids produced due to chemical shrinkage, see Section 4.5.4 and Appendix D.

2.3.2 Chemical shrinkage and self-desiccation

Chemical shrinkage could be understood as the entire volume reduction of cement due to hydration. It reflects the fact that the absolute volume of hydration products is smaller than that of reacting constituents (i.e. cement and water), even if solid phase volume in fact increases. Thus, in view of cavitation phenomenon occurred, chemical shrinkage from principle ends up with formation of empty (gas) pores[5] often classified as capillaries [Nev 96].

Unlike chemical shrinkage, self-desiccation is only inherent to systems with w/c lower than 0.42 [Pow 47/48]-0.44 [Pow 47], with very few exceptions. The phenomenon yields the fact that water consumption and formation of internal voids proceeds at faster rate than pore volume reduction due to filling capillary pores with hydrates. Thus while (capillary) pores progressively de-saturate and dry out beginning from largest water-filled void, the relative humidity drops and the hydration slows down, this happening under isolated/sealed conditions

[3] Note that relative humidity may be considered as partial vapour pressure in the pores and not a direct measure of moisture content or degree of saturation of concrete [Gra 06b]. For more detailed information on relative humidity phenomenon, please see [Gra 06b].
[4] Note here that capillary water is generally used up at faster rate than these pores are filled with gel acc. to Hansen [Han 86].
[5] It should be noted that, as discussed by Acker [Ack 04a], air is the only phase of cement paste with ability to expand by the same amount as volume change of cement. That is to say, at least some new empty pore space may also result from expansion of existing air voids.

without mass loss. Which phenomenon contribution to autogenous shrinkage is most important at which stage of hydration, this finally depends on the form of structure of hydration products (= microstructure), where the time-zero, i.e. the point at which the hydrating system is able to support its own weight and can be regarded as solid (note: the phenomenological definition), provides the decisive threshold mark.

Before time-zero or the time-vicinity of setting, autogenous shrinkage can be regarded as equal to chemical shrinkage, i.e., the internally occurring and the externally measurable volume changes are alike. It is attributed to the fact that cementitious material in liquid-like state is not able to sustain the internal voids created by chemical shrinkage. Thus, these pores are relieved either by (plastic) shrinking, because of which one speaks of system collapsing onto itself. After the formation of a solid skeleton of hydration products, however, the bulk, macroscopically observed deformations of the entire concrete system are clearly smaller than the changes in the internal volume of the material. Under microscopic observation the formation of a large number of fine pores in the cement stone can be noted as the manifestation of significant volume changes due to the hydration processes. Macroscopically measured reduction in concrete specimen volume (= autogenous shrinkage) can be therefore only a fraction of the real material shrinkage (= chemical shrinkage).

To what extent chemical shrinkage is transformed into autogenous shrinkage depends obviously on the water content in the system. Due to limited permeability, systems like UHPC are more difficult to cure compared to ordinary concrete; they possess amount of water that is insufficient to complete the hydration process due to the low water-to-cement ratios. Thus, pores forming due to chemical shrinkage are filled with air of relative humidity lower than 100 %. With ongoing hydration a significant internal drying occurs and the thermodynamic equilibrium of the system becomes disturbed, initiating the RH drop-associated autogenous deformation.

2.3.3 Mechanisms associated with water transport and surface tension

Hydration in system of low w/c is not only responsible for chemical shrinkage and self-desiccation but also the pore structure that develops. The changes occurring within particular microstructural element can be finally used to explain the triggers of autogenous shrinkage.

Notably, as cement reacts with water, both chemical shrinkage-associated voids and the hydration products fill the space initially occupied by mixing water, and named capillary water after type of pore it reveals. It will be observed that this water is being used up at a faster rate than filling with the hydrates can proceed. Pore walls showing high affinity for water molecules become thus deprived of the adsorbed water film. This film of water molecules controlling e.g. surface tension of the solid is otherwise bound: As estimated, about three layers of water molecules are adsorbed strongly, while further water layers may still attach and are bound by weak forces [Lur 03]. Should any disturbance in particular complex occur, a volume change may be triggered.

The consequences are not immediate. All cement-based materials show important ability to self-cure, therefore to transfer free water from zones rich in particular ingredient to ones lacking. It could be, for instance, transport of fluid from so-called Interfacial Transition Zone of locally higher w/c [Ben 00a][Est 09]. The migration is granted through the pore system, thus, follows easiest of routes and involves different transport mechanisms depending, among others, on pore size. Typically capillary forces will be involved. Should the water-rich zones be missing and/or the pore connectivity change to extent disabling rapid water rearrangement, thus hindering the self-curing effect, the following mechanisms come in play:

- *surface tension change (= surface free energy variation = Gibbs-Bangham shrinkage)*

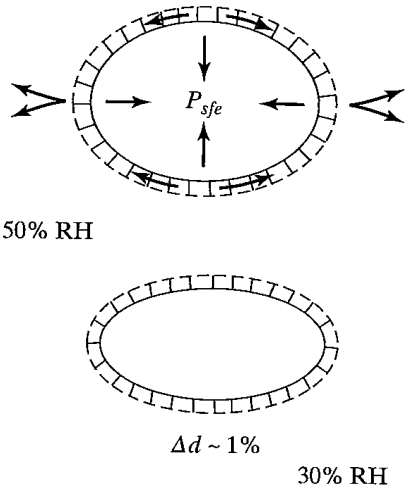

Figure 2.9: Schematic illustration of the surface tension mechanism and its stages at the somewhat arbitrary RH levels [Min 81].

Surface tension is the basic phenomenon named in relation to volume changes occurring in cement-based materials due to removal of water that is not free. Its existence proves that not only water but also the adhesive, cohesive, colloidal solid, that is the hardened paste, yields the same consequence of lacking symmetry in cohesive forces acting at surface molecules, viz. development of perpendicular tensile force trying to minimize the surface area. If not counteracted, which for cement-based materials means maintaining liquid water film cover of adequate thickness on solids (or, more precisely, inner pore walls), the hydrostatic pressure generated puts the solids under compressive stress. The paste thus deforms elastically and macroscopically. As believed, interpretation of mechanism made on isolated particle (Figure 2.9) can be applied to whole porous body [Pow 68b].

The modelling approaches, some of which have been successful in validating the mechanism in case of autogenous shrinkage of cement-based materials [Koe 97] including UHPC [Far 07] (somewhat similar to modelling a part of total shrinkage [Han 87]), give clearly contrasting impression about surface tension theory applicability compared to some experimental and theoretical works, e.g. [Wit 09][Bel 11]. Therefore, it might be more appropriate to address the two important derivatives of the surface tension phenomenon, viz. capillary pressure and disjoining pressure, which are discussed in the following.

- capillary pressure (also named capillary depression and capillary tension)

Capillary pressure is the most widespread of the shrinkage mechanisms, having validation in both autogenous shrinkage modelling (e.g. [Hua 95][Lur 03][Ish 99][Wyr 11][Zha 12a][Li 14]) and theoretical deliberations [Ack 04b] but, at the same taken, still the most questioned one for a hygral volume change [Bel 05][Wit 09][Bel 11]. As suggested by name, it takes place in capillaries and originates from emergence of three immiscible phases viz. solid, liquid, gas, i.e., air plus water vapour in the hydrating medium (Figure 2.10). Because of the pressure difference occurring in such situation and particularly motivated by chemical shrinkage, there will be molecular interaction taking place at the interface with solid phase in the partly emptied pores.

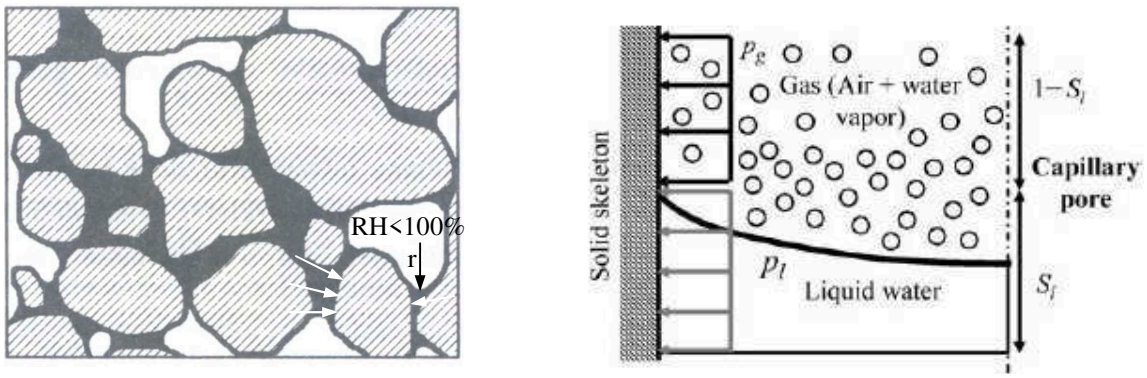

Figure 2.10: Schematic representation of conditions for the formation of meniscus at different scales of observation, picture to the right after [Ben 07].

In gist, as water is removed due to hydration, a special kind of liquid bridge or interface being referred to as water-air or liquid-vapour meniscus is formed between solid walls of the initially water-filled pore (Figure 2.10, right) when physically allowed, i.e., for capillaries in size range of 5 to 50 nm [Hua 95]. To bring the body to its minimum energy, liquid tends to spread from the interior across exposed solid surface thus developing negative pressure within pore fluid (inside the meniscus) that is determined by changing meniscus curvature.

Accordingly, the meniscus and water phase as such is found to be in hydrostatic tension which pulls the pore walls inward (Figure 2.11); meanwhile the equilibrium is restored by subjecting the solid skeleton of hydration products to hydrostatic compression. In response to resultant mechanical load and elastic deformation generated, the colloidal system yields macroscopically observed volume change (shrinkage). Some pores are observed to collapse on smaller scale of observation.

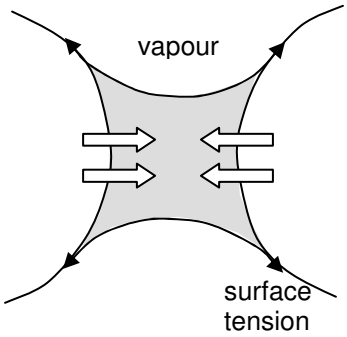

Figure 2.11: Schematic illustration of the capillary tension mechanism, inspired by [Gra 06a][Gra 06b].

The essence/merit of the mechanism is often explained by the referring to Kelvin-Young/Laplace equation (Eq. 2.1) that has been derived from respective laws originally for circular cylindrical pores. When corrected by important contribution from changing composition of the pore fluid (Rault's law) [Lur 03][Lur 08b], it reads as following:

$$p_c = p_l - p_g = -\frac{2\gamma \cdot \cos\theta}{r} = -\frac{RT}{V_l}\ln\left(\frac{RH}{RH_s}\right) \tag{2.1}$$

where p_c is the capillary pore pressure/stress, p_l is the pressure of the liquid water phase, p_g is the pressure of the gaseous phase, γ is the surface tension of water, θ is the contact angle on the liquid-solid interface, r is the radius of the meniscus, R is the ideal gas constant, T is the absolute temperature, V_l is the molar volume of the fluid, RH is total relative humidity and RH_s is the relative humidity due to dissolved salts in the pore fluid.

According to Equation 2.1, the highest capillary stresses are produced on emptying the smallest of pores from the 5-50 nm range and/or on increasing concentration of dissolved salts in the pore fluid, especially alkali hydroxides [Lur 03]. On the other hand, only very small pores are acknowledged to exist in UHPC, hence the noted immediate drop of RH [Lou 99] and consequent build-up of the capillary pressure. From early ages, when the strain-stress ratios will be the highest [Zhu 08], capillary pressure may thus contribute to rise of the very high autogenous shrinkage of UHPC.

- disjoining pressure

Disjoining pressure is the second of the mechanisms yielding existence the surface forces in cement-based materials. It originates from the fact that diffusion or mass transport occurring in mono- and multilayers of water molecules is restricted by adsorbent walls [Baž 72], being solid adsorbent walls (= pore in hardened cement paste), see Figure 2.12.

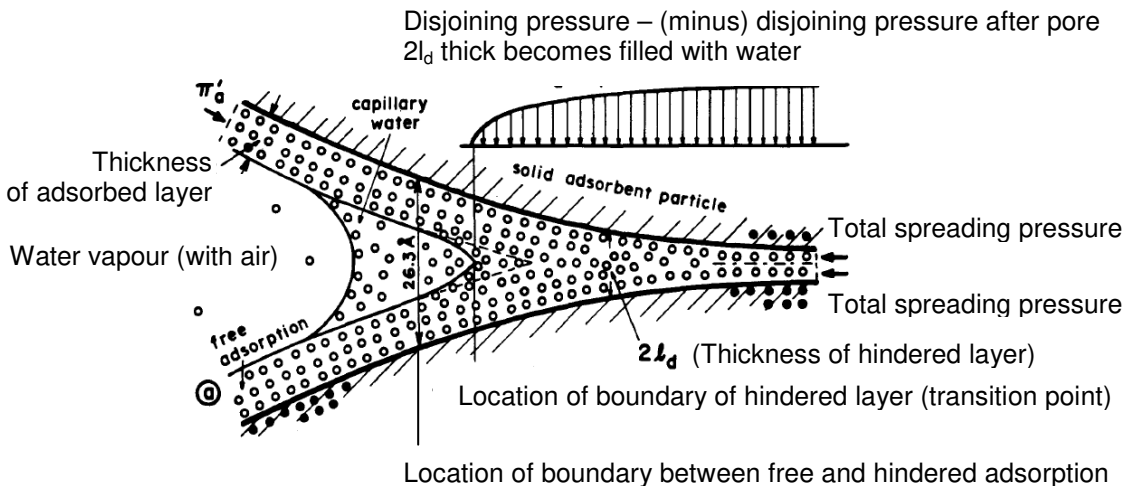

Figure 2.12: Schematic illustration of the space where disjoining pressure operates [Baž 72].

Whether disjoining pressure is activated separately or operates in some difficult combination with capillary pressure, this is still under debate [Der 87][Ack 04b][Bel 05][Wit 09][Duc 09]. The fact is however that in cement-based materials mechanism reflects the net result of multi-component phenomenon, involving both attracting and repelling forces [Der 87][Fer 87][Bel 08][Wit 09]. Disjoining pressure furthermore operates in smaller pores compared to capillary stress-based mechanism, called hindered absorbed layers or micro-pores. These are best described as narrow pore spaces not wide enough to accommodate the water that otherwise would be freely adsorbed by isolated solid particle [Pow 68b] and, simultaneously, approached so close that their mutual (surface) force interaction becomes appreciable [Baž 72], i.e. distanced by 1 or 2 to max. 10 water molecules, which translates into pores having diameter smaller than 2.63 nm and located in the main hydrate phase (C-S-H).

In gist, the change in surface free energy occurring due to disjoining pressure is compensated and the counterforce is derived from elastic strain [Pow 68b]. In particular, as self-desiccation takes place and RH drops due to hydration, structured water diffuses along the layers of hindered adsorption [Baž 72] to maintain hygrometric balance. Thinning of adsorbed film is then observed. As consequence, disjoining pressure diminishes (along with increase in solid

surface free energy) and solid layers (= C-S-H surfaces) come closer due to attractive forces, mainly Van der Waals forces [Bel 05]. Particular action is counteracted by cohesive bonds [Pow 68b] and stresses develop in the solid microstructure to balance the reduction in disjoining pressure. In turn, macro-scale shrinkage deformation is evidenced [Bel 05] whereas the porosity reduces.

Notably, in cement-based systems with low w/c one-halph to three quarters of surface area can be located in micro-pores [Odl 72a]. Confronting it with possibility of moisture transport through such pores [Mar 97][Asa 06][Che 15], this makes disjoining pressure important candidate as far as the autogenous shrinkage mechanisms are concerned.

- Interlayer water movement (= changes in the basal spacing of layered hydrates, hydration pressure)

For the statement of another relevant mechanism related to water migration, findings of the studies conducted by Beltzung [Bel 11] and Wittmann et al. [Wittmann 2006 *Ibid*. Wit 09] must be taken into account. In half of the specimens investigated, capillary pores (and thus associated capillary pressure mechanisms) were eliminated purposefully, particularly by material impregnation. Despite no change to original recipe as such, a noticeable decrease in the mass loss was observed, as excepted. The hygral volume change course, however, was affected to much lower, if not negligible, extent. In this way, disjoining pressure was originally concluded to be main operative shrinkage mechanism.

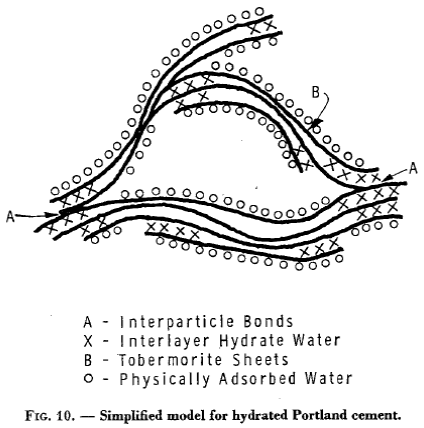

FIG. 10. — Simplified model for hydrated Portland cement.

Figure 2.13: Simplified model for hydrated Portland cement [Fel 70].

Another mechanism that could be imagined as paying a dominant role or at least one of primary contributions in this situation is movement of water from smallest of pores present in hardened cement paste. Such water could be located in-between the C-S-H sheets (Figure 2.13), and is often referred to as interlayer (hydrate) water [Fel 70]. Migration of particular water type, if occurred, could be at origin of large macroscopic strains [Fel 70].

Most researchers ascribe activation of each of potential shrinkage mechanism to certain RH range, despite no consensus on the limiting RH values as such, see e.g. [Kov 06]. As for currently treated mechanism, low RH is typically predicted; this needn't be very surprising given that below RH of approx. 30 % or higher decomposition of hydrates [Fel 70] and thus the accompanying dehydration shrinkage [Wittman 1982 *Ibid.* Kov 06] starts. On the other hand, this knowledge is derived for a much simpler system, containing no chemical and mineral admixtures as such. Especially superplasticizer could be the origin of changing the characteristics of hydrates, e.g. [Gey 04][Fla 09]. This could be finally among reasons why the knowledge may appear outdated and simultaneously why the treated mechanisms require new look in terms of application in the hydration/self-desiccation RH range.

2.3.4 Other mechanisms

- *swelling/expansion*

As signalized earlier (see introduction to Section 2.3.3), there is important and positive contribution to mitigation of autogenous shrinkage emerged from self-induced and water transport-related phenomena. On another occasion, this aspect was explicitly and in an experimental manner treated by Barcelo et al. [Bar 05]. The so-called autogenous swelling being in focus, i.e. the second component of net volume change measured macroscopically, was showed to be cement characteristics-dependent.

As literature review showed, other reasons may exist for particular shrinkage-counterforce generation, having direct or secondary relation to water movement and which origin is other than thermal effects. The several important theories call for crystal growth-triggered crystallization pressure [Coh 83][Bar 01], absorption [Nev 96] or transportation [Bar 01] of water through C-S-H layers, water adsorption on [Coh 83] or imbibition by [Min 95] other hydrated phases, osmotic pressure [Powers 1961 *Ibid*. Rah 82][Bar 01], bleeding water absorption [Bar 01][Tia 08][Moh 10], and/or capillary distension [Kov 96]. A complex nature of swelling mechanisms, involving many concurrent driving forces at once [Ros 82] as well as controlling factors (e.g. level of restraint [Mat 70][Min 95], w/c and free water content [Mat 70], presence of silica fume [Lob 93], composition of pore solution and especially free lime content [Min 95], and many other [Mat 70]), should be expected too.

The reason for potential and instantaneous swelling observed on macroscopic level immediately after casting and before setting also in case of UHPC [Hab 06a][Kam 08]

appears less clear. In less advanced systems, however, such an early volume change was related with dissociation of cement in pore solution, addition of chemical admixtures and silica fume [Pau 94], whereas increasing solvation process by repulsive forces [Pau 94] or ettringite formation [Odl 99] in view of little restraint existent was noted as potential origin. Important to acknowledge though, the swelling, while being to much lower extent dependent on material composition or curing conditions [Aït 99a][Odl 99] in contrast to autogenous shrinkage, induces some changes in porosity [Odl 72a] similarly to latter.

- restraint

Although concrete as whole composite may shrink or swell, not all its elements are notably involved in the processes behind the net result observed macroscopically. Should the solid component shrink slower, if at all, and further characterize with stiffness higher than that of surrounding paste, it will act as restraint, thus limiting the volume change of composite.

Table 2.2: Types of restraint and their particularities [Mat 70][ACI 207.2R-95].

Type of restraint	Restraint attribute	Examples	Typical crack type ascribed
External	Continuous restraint along contact surface of concrete and adjacent one	Adjacent subgrade/structure, formwork, reinforcement, concrete joints, or testing set-up	Macro
Internal	Discontinuous restraint purely relating to material	Aggregates, fibre reinforcement and/or self-restraint	Micro

The two important examples of restraint often reported are replacing part of volume fraction of paste by aggregates and casting new concrete on old concrete subgrade. General distinction will be also made between external and internal restraint. The list of their examples given in Table 2.2 needn't be though considered final. Indeed, since Carlson [Car 39] arguments have been continuously delivered enabling qualifying clinker residues as well as the new stable solid phases emerged due to hydration as the restraint somewhat similar to aggregate, e.g. [Hea 99][Ben 04][Pic 13]. The like ability of load-bearing solid skeleton or even its constituents to restrain isotropic shrinkage that is autogenous deformation could be thus giving new meaning to the so-called self-restraint, i.e. the internal restraint otherwise originating from non-uniform (= differential) shrinkage caused by moisture [Bis 01] or temperature gradient [ACI 207.2R-95][6]. On the other hand, as proved in case of usage coarser

[6] Stresses generated due to local gradients of moisture or temperature will be often classified as eigenstresses, see e.g. [Epp 10] and further discussion.

cements, it seems important that also other chemical and physical effect and not the self-restraint as such are taken into account [Ben 99a][Ben 01c].

Whatever the source of restraint is, due to restraining autogenous shrinkage or swelling a complex stress-state incorporating eigenstresses[7] and/or stresses due to external restraint may be generated and cracking, micro- or macro-, can be triggered. As such, no cracking is expected from sealed system before the stiffness develops [San 09]. Once the sine qua non occurs, however, and given concrete is relatively weak and brittle in tension, cracking will develop as soon as tensile stresses (generated due to restrained shrinkage) exceed the tensile strength. Cracking will relax the tangential stresses around aggregates that may coincide with shrinkage reduction of the composite [Gra 06a], as signalized earlier.

Concrete that is not cracked despite provision of high degree of restraint shows yields important fact, in particular existence of more factors decisive for the concrete behaviour. It should be considered that, beside influence from thermal effects, cracking phenomenon is a complicated function of free shrinkage (magnitude and rate), stress relaxation, degree of restraint, fracture toughness, structural geometry, and age-dependent material properties development [Wei 99][Ben 01a][Yoo 14], especially tensile creep characteristics, Young's modulus and tensile strain capacity [Sch 02][Med 11b]. Because of existence of phenomena relaxing the tensile stresses (creep, micro-cracking), the so-called residual stresses are measured by stress sensors and in the restrained/instrumented ring test.

- microcracking

Cracking, because of its generally detrimental effect on concrete properties, makes the upsides of phenomenon occurrence less evident. However, the latter seem to exist particularly in terms of volume changes due to shrinkage. Due to increasing the internal porosity of material being associated with dilation effect [Mou 11] or expansion, as well as due to relaxation of tangential stresses created otherwise around aggregates [Pow 59][Gra 06a], the formation of microcracks very likely contributes to reduction of shrinkage deformation. This has been noted for overall (total) shrinkage since Powers [Pow 59][Lan 03], but it is believed

[7] Eigenstresses are stresses produced in the paste autogenously and/or due to drying to ambient when volume change is restrained. They will typically develop around restraining elements like aggregates [Ben 01c] or any other heterogeneity/inhomogenity of different stiffness or inner pressure (air voids [Gra 10], …) and will result from both shrinkage and expansive strains. A special kind of eigenstresses is brought about from self-restraint and structural restraints.

also to occur when a cement-based system is sealed from ambient, i.e. in case of autogenous shrinkage [Mou 11].

Whether the special role of microcracking is truly revealed and balances the contraction remains vague, especially when to consider other experiences noted [Lou 99]. On one hand, lowering w/c, i.e. factor which generally increases risk of cracking [Pai 89][Wei 99][Pea 04], does not reflect this clearly and rather masks the potential contribution since, as rule of thumb, results in increasing free autogenous shrinkage, e.g. [Wei 99][Pea 04][Ack 04a]. This suggests that some tiny cracks initially formed probably close despite increased chemical activity recorded at early stages of hydration, especially for UHPC [Fey 01]. One reason for this could be for instance existence of compressive stresses [Lan 03] that will certainly appear when the specimen undergoes additional drying to the ambient [Bis 01]. Before the closure, microcracking could also 'produce' new surfaces of paste that want to hydrate or at least to be covered with water. On the other hand, by providing new transport pathways and increase of permeability as such [Hea 99], microcracking can motivate movement of water from any of the water inclusions present, including water carried by curing agent [Hua 10]. The consequent rise of RH may be thus leading to healing of microcracks while filling the exposed space with new hydrates, analogously to exposure of UHPC to humid air [Epp 10]. Eventually, it should be considered that microcracking may be another reason for the so-called repercolation phenomenon [Ben 06a] which if occurred and analogously to microcracking theory may have positive influence on autogenous shrinkage.

- creep

When a specific load is exerted, the shrinkage is either being produced (the case of internal load [Gra 06a]) or it notably increases (the case of additional, external, sustained load, e.g. [Fel 70]). Important in selfsame respect, other events, viz. movement of interlayer water (Section 2.3.3) and microcracking discussed above, are likely also to be induced under load, and thus may separately or combined, with or without further input from other mechanisms [Tam 00][Lan 03], lead the cement-based material to creep. While this explains close interrelation between shrinkage and creep and the respective mechanisms couplings [Ulm 00][Ack 04a], it also implies potential contribution of basic creep to autogenous shrinkage.

Separation of basic creep from other driving forces leading to shrinkage of a sealed system as well as microcracking [Lan 03] (note: assuming no contribution to creep origin) is hard to

make, especially experimentally. Not surprisingly, verification of the creep role and information regarding operation age are nearly lacking. E.g. Zhutovsky and Kovler [Zhu 08] largely excluded autogenous shrinkage as being affected by basic creep. Lura et al. [Lur 03] remained more sceptical in this respect, but assumed later involvement of phenomenon in regarded volume change, i.e. after the RH drop slowed down. More recently, and supported by modelling, Grasley [Gra 06a] demonstrated that autogenous shrinkage could be in fact considered as a viscoelastic mechanical response to internally applied stresses. This researcher importantly pointed out that the role of creep will finally depend on type of material considered (cement paste, concrete) and the aging phenomenon involved.

In another important publication particularly on volume changes of UHPC, Acker [Ack 04a] came to conclusion that shrinkage and creep of UHPC, similarly to pastes [Bar 01], involve the same mechanism being viscous strain in C-S-H. The same could be understood when addressing microcracking which could [Ass 14] although needn't necessarily be alone [Tam 00] if at all [Lan 03] the reason behind basic creep of cement-based material. The finding is that the phenomenon initiates soon after time-zero, i.e. within first 24 hours [Pir 06]. This finally confirms what was (also indirectly) showed to be taking place about similar age in case of finely grained UHPC by Feylessoufi et al. [Fey 01]. Cracking tendency might though still be revealed in later ages due to decreasing stress relaxation and induced otherwise by the reducing creep.

2.4 Mitigation strategies

2.4.1 General

From discussions in the foregoing sections it becomes clear that study of and counteracting to cracking caused by restraint of shrinkage deformation belongs to important tasks of the research program regarding mitigation of autogenous shrinkage of UHPC. Assessment of cracking risk can be very challenging owing to number of metrological issues involved, see e.g. [Wei 99][Sch 02][Epp 10]. Important in selfsame respect is one of the most fruitful finding of study by Eppers on UHPC [Epp 10], i.e. the proportionality between the level of free autogenous shrinkage (where the word 'free' means free of external restraint) and the risk of cracking caused by it under exposure to additional restraint, see Figure 2.14.

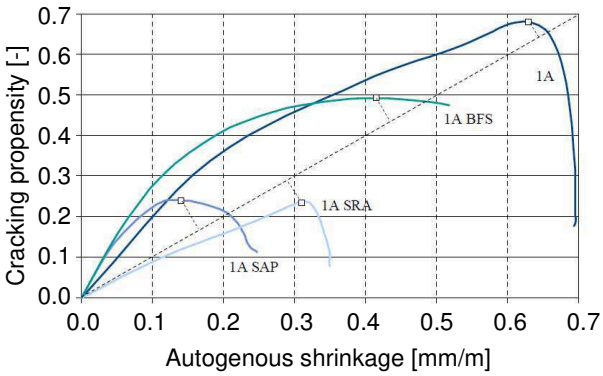

Figure 2.14: Relation between autogenous shrinkage cracking propensity and free shrinkage [Epp 10].

The abovementioned conclusion was made for material very similar to one of two UHPC recipes investigated in this treatise. This allowed limiting the main focus of this work to be evaluation of mechanisms behind mitigation strategy chosen. That is to say, it is assumed that by having mitigation of free autogenous shrinkage reassured, the cracking propensity decreases as well. Nonetheless, the very basic tests on cracking tendency, especially owing to more curing conditions studied (sealed, unsealed) and specific attributes of curing technique used, will be performed as well.

2.4.2 Minimizing free autogenous shrinkage

An excellent review of available mitigation strategies in fight against development of autogenous shrinkage and related cracking, to which novel strategies are basically extension to, is that of Bentz and Jensen [Ben 04]. The two schools of thought regarding the approach to take seem to be supported in this important publication. In particular, in some solutions representing the first group, it is accounted for the true gist and origin of autogenous shrinkage as well as imprints and remedies to potential shrinkage mechanisms. In comparison, the second group consists of these approaches that allow strengthening the role of components contributing to the net result of particular volume change but in other way than shrinkage. The short summary with examples for both groups with update is presented in Table 2.3.

Table 2.3: Approaches to mitigate free autogenous shrinkage.

Group 1	Group 2
• Replacing cement or silica fume by inert materials [Ben 04][Che 10][Cou 13] or water repellent-treated powder [JCI 99] • Using a specific, shrinkage-'friendly' cement type [JCI 99][Sch 02][Ben 04][Bar 05]	• Utilization of expansive cements or additives [Ben 04][Pié 06]
• Coarsening pore structure, e.g. by usage of coarser cement [Ben 04] • Increasing entrapped [Tam 12] or entrained air [Est 09] for increasing permeability or other reason	• Higher fraction of aggregates with a high Poisson's ratio and high Young's modulus [Ben 04][Gra 06a]
• Usage of Shrinkage-Reducing Admixture (SRA) [Wei 99][Ben 04][Med 11a] • Usage of other chemicals: surface treatments and liquid chemicals [Xu 00], latex [Wei 99] or special, multi-functional superplasticizer	• Increasing particular hydrate content (CH, …) [Ben 04] or related usage of Partially Hydrated Cementitious Materials [Sol 11]
• Early initiation [Aït 99b] and extension of wet curing durations during construction, especially for small cross-sections of concrete members having capillary continuity still present [Sol 12]	• Usage of adequate fibres [Ben 04] (see also Appendix B)
• Internal curing / water-entrainment [Jen 01][Jen 02b][Ben 04]	

As experience shows, not all solutions and especially composition changes (Appendix B) could be successfully applied for UHPC, if the effect on other concrete properties is taken simultaneously into account. E.g. utilization of Shrinkage-Reducing Admixture (SRA), being a very popular choice due to effective reduction of drying shrinkage, seems problematic to incorporate in the material of interest. The arguments are potential delay in setting, reduced rate of cement hydration and strength development in concrete [Wei 99] as well as interaction with other admixtures [Tam 12]. These negative influences are hardly overcome by combining SRA with other admixture/additive, although particular approach allows reducing autogenous shrinkage to a higher extent and, important enough, maintaining the positive effect exerted longer relative to SRA used alone [Med 11a][ref. 12 Ibid. Med 11a][Sol 11][Sol 12]. In comparison, an extended moist curing in addition to adequate choice of expansive additive is necessary to avoid some of the drawbacks related with application of the latter [Wei 03]. The problem yet may still persist for UHPC as conventional curing (where water is delivered from external source) will generally fail in view of expected and very limited moisture influential depth of this material [Sol 12], with exception for very young UHPC.

In view of arguments presented above and since high-tech materials generally demand smart solutions for the problem prevention, internal curing (IC) appears to be an attractive alternative. In this methodology, a new component of high water storage capacity, referred hereafter to as IC agent, is added to other mix components along with amount of water it can absorb and return back when needed. As water becomes both thermodynamically and kinetically available, IC enables replenishment of water consumed by chemical shrinkage. This turns directly into much higher RH of system otherwise undergoing self-desiccation and thus much lower, if not negligible, autogenous shrinkage or even expansion.

The effectiveness of IC will be decided by many factors, which may include but needn't be solely limited to: (1) amount of water available for the internal curing, (2) mobility of the internal water released from the reservoir and (3) distribution of the reservoirs themselves [TC 196-ICC]. For accomplishing the goals of curing, however, the choice of appropriate IC agent remains still fundamental and many works, with most recent ones by [Est 09][Zhu 11b][Sch 12c][Mec 12][Ass 13], yield this issue very clearly. As such, decision for IC agent could be made between different natural and artificial materials, including Light-Weight Aggregates (LWA), polymeric materials/hydrogels, recycled or other porous materials, wood-derived products [TC 196-ICC] and, promoted most recently, rice husk ash [Tua 10]. Among them, Superabsorbent Polymers (SAP) appear presently to be the most promising water-regulating additive in case of curing of UHPC, having effectiveness verified e.g. by present author [Mec 06][Dud 08b], Soliman [Sol 11][Sol 12] and Hua with Wang [Hua12]. The associated methodology will be discussed in more detail in Section 2.5.

2.4.3 Minimizing restrained autogenous shrinkage

Mitigation of autogenous shrinkage under additional external restraint and stresses it generates until cracking is commonly approached by solutions enabling at least partial elimination of its most important trigger, i.e. free autogenous shrinkage. This typically is (Figure 2.14), but, given other contributions to stress generation, needn't prove always sufficient, see e.g. [Sch 02]. However, to approach it in any other way may require introducing pronounced changes in original material composition, this allowing the increase of tensile strength or decrease of stiffness. The available solutions are few and involve e.g. using cocktail of different steel fibres [Sta 04b][Ros 02 *Ibid.* Appendix C] or replacing cement with metakaolin [Qia 01] for tensile strength increase.

In spirit of maintaining the UHPC performance, including its workability in fresh state, as well as aiming at eliminating the cause and not only avoiding the consequence of restraining the volume change, the approaches involving changes in mechanical properties cannot be accepted. The remaining alternative (to mitigation of free autogenous shrinkage) could be thus limited to increasing the creep/relaxation properties of the matrix, in agreement with [Gra 06a]. This aspect remains seriously under-investigated. Nonetheless, because application of SAP is likely to present advantage also in regarded respect [Ham 07] (somewhat rivalry to effect on tensile creep [Ass 14b]), other potential but still very limited solutions such as usage of wollastonite microfiber [Sol 14] were considered by present author as solely optional ones.

2.5 Internal curing using Super Absorbent Polymers (SAPs)

2.5.1 Super Absorbent Polymers (SAPs)

- general

Superabsorbent Polymers, also known as Super Absorbent Polymers (accordingly shortly abbreviated: SAP, SAPs), are an interesting example of hydrophilic material. It is next generation of product in practical use since 1950s when first water-swollen cross-linked hydrogel was applied for biological use [Lin 06]. Due to significant development especially during last three decades, their unique characteristics of swelling under absorption of aqueous solutions and high water retention towards mechanical pressure have been exploited and found successful in broad applications, from use in agriculture/soil science [Joh 84][Var 97] to production of diapers. Currently, the knowledge gained can be utilized in production of smart curing compound customized to needs of curing.

SAPs are generally speaking hydrogels[8], i.e. loosely cross-linked macromolecular three-dimensional polymeric networks containing ionic/ionisable functional groups attached to polymer backbone (= chains) facilitating absorption of aqueous medium in which they are placed. In SAP, the absorption takes place without polymer dissolving and, owing to existence of non-zero shear modulus of the network [Li 90], change of original shape. The subclass of hydrogel represented by them is however even more special. The exceptional features include the amount of solution this hydrogel can 'process' (i.e. absorb, retain and release, if favourable condition has occurred), this being many times of own weight and by definition exceeding 95 % of total weight (or volume). SAP furthermore can be made non-degradable (if such is request), possess higher (wet) mechanical stability than any other hydrogel[9] as well as may be to high extent insoluble, although never entirely [Shu 11]. They can also form either amorphous gelatinous mass or, being most spectacular advantage, discrete gel particles, depending on their original dehydrated physical form [Joh 84]. Solutions are continuously delivered allowing refine material in terms of toughness, morphological homogeneity and especially swelling properties [Gon 12]. Obviously, such attributes as well as potential of further improvements make particular hydrogel type a perfect

[8] In terms of definition, a certain simplification is often used. As such, hydrogels are two- or multicomponent systems existing as swollen polymeric networks. They are containing two main parts one of which is the solid part (which is constant in quantity) and another one- liquid part (aqueous solution, which could vary), filling the spaces between macromolecules/macromolecular chains (so-called interstitial spaces). These coexist without or with additional presence of air/porosity (the third potential component). In a two component configuration, the network structure is sometimes described as mesh. The mesh is represented by certain shear modulus.

[9] SAP must withstand pressure of minimum 0.67 g/cm² according to JIS- Japanese Industrial Standards [Mas 14].

candidate for applications where operation with water reserves is important, including concrete. Example of most conventional type of SAP is presented schematically in Figure 2.15.

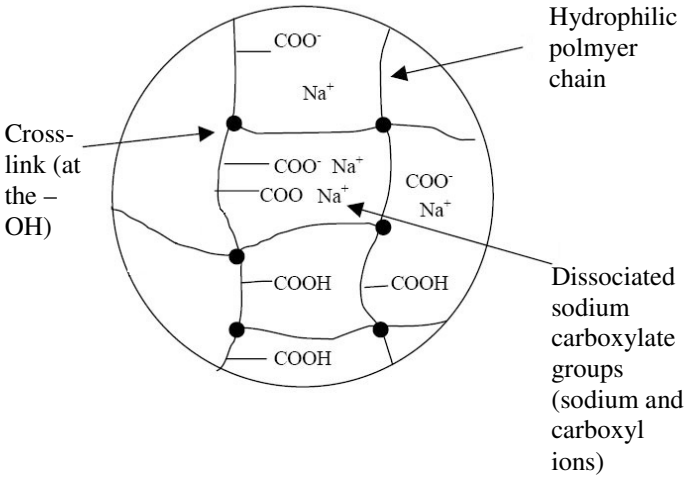

Figure 2.15: Illustration of a typical acrylic-based SAP [Ell].

- production

To attain their unique properties, SAP are typically fabricated as petroleum-based synthetic products rather then being obtained from natural sources. Compared to physical/reversible gels, cross-linking of chains constituting the network of SAP also differs: the degree of linkage is higher and due to chemical nature each chain junction is permanent. That is to say, by saying SAP, it is typically meant chemical or, if referring to strength of bonding between chains, a permanent gel.

The production method is the free-radical polymerization, for which two synthesis techniques are engaged: either solution polymerization or inverse suspension polymerization. It is the choice in-between latter which decides whether resultant products attains irregular (Figure 2.16) or spherical shape (Figure 2.17), respectively.

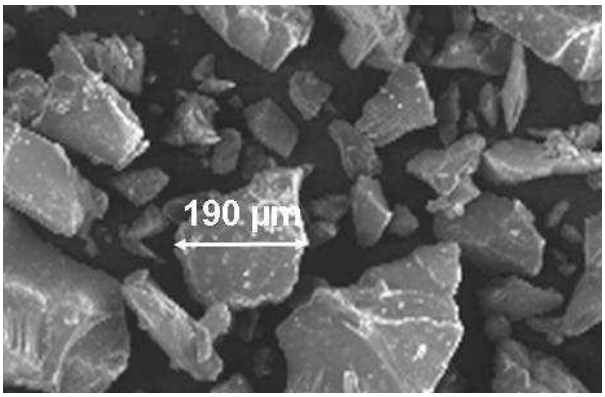

Figure 2.16: ESEM micrograph of dry SAP obtained by solution/gel polymerization technique.

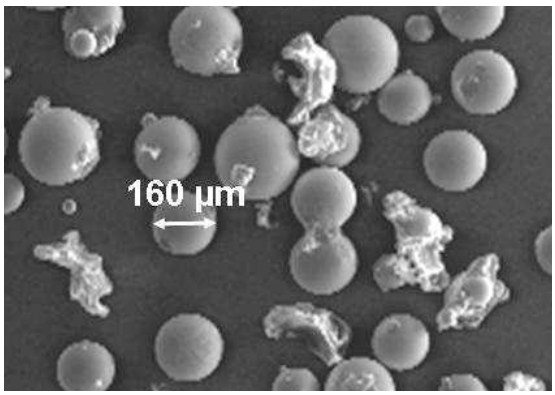

Figure 2.17: ESEM micrograph of SAP obtained by inverse suspension polymerization technique.

- SAP networks and their composition

SAPs are commonly composed of two or more hydrophilic monomers, without or with modification by hydrophobic one for sorption property-tailoring reasons [Phi 96][Shu 11]. This combination of mono- or multifunctional components in any of network type (which

could be [Bou 00] cross-linked gels of copolymers (random gel network), interpenetrating polymer networks, …) often leads to creation of so-called 'smart/intelligent' hydrogel, i.e. one sensitive to change of various external stimuli such as pH, ionic strength, and temperature, and, although rarely mentioned, exposed to load-regulating exchange of (counter-) ions of varied valency [Bow 91][Var 99][Sir 12][10]. Furthermore, for enhancing sorptivity and mechanical properties, partial neutralization of ionic monomers (i.e. pairing with counter ions such as Na^+, K^+, NH^{4+}, NH^+ and/or H^+) and, as additional to that for bulk or core, surface cross-linking [Ell], respectively, is not infrequent too[11]. Overall, the production particularities chosen can lead to formation of complex SAP structures e.g. core/shell structure [Tak 91].

- *volume changes*

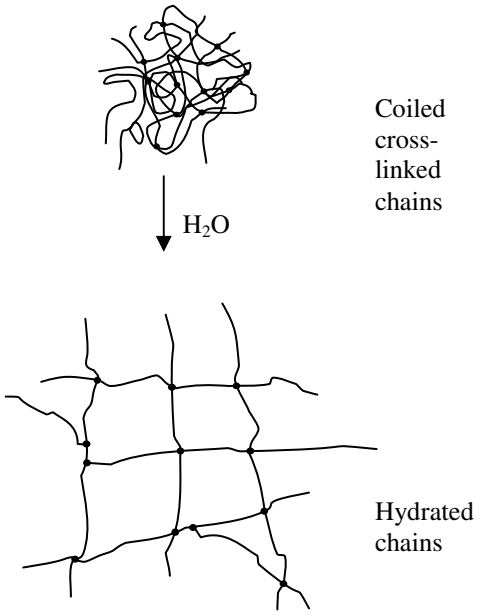

Figure 2.18: Reorganization of chains of SAP during swelling and state transition.

Demonstration of physical changes exerted by the basic/primary stimulus (i.e. presence of aqueous solution) and secondary ones (i.e. the aforementioned chemical and physical stimuli or other[12]) is the partial and, without change in the latter, fully reversible volume-phase transition. Should the molecules of aqueous solution be accommodated or removed, each SAP particle will either swell or shrink, respectively. With regard to the polymer structure, such change provokes shift between two states referring to organization of the chains, i.e. collapsed state (when chains are coiled, which is original solid state) and swollen state (flexible chains are stretched while mesh size attains 'local' maximum), see Figure 2.18.

For hydrogel having sufficient chain stiffness and/or required amount of ionized groups [Hir 84] (with supplementary condition: before all acidic groups dissociate [Sas 97]), volume-

[10] Note that the first three are the same parameters which in concrete can undergo changes within hydration time. The last parameter mentioned must be yet considered as relevant given that time-spread diffusion of ions into IC agent and/or adsorption on its surface was found to be sometimes the case.
[11] Neutralization can be performed as pre- or post-neutralization [Ell][Omi 12]. For maximization of sorptivity, neutralization should only be performed to certain limited extent [Tsu 97].
[12] The amount of fluid under attraction by polymer or one already absorbed could also easily change under exposure to shear [Ver 03], substantial compression [Ver 05] or pressure [Lee 90][Var 97], and/or suction [Wit 14]. All of them notably appear at some stage in life of concrete.

phase transition is discontinuous and is completed when reaching definite point referred to as equilibrium swelling[13] or limiting swelling capacity [Shu 11] in case of swelling and shrinking (to highest possible extent at specified conditions), respectively. As will be showed also in own work, maximum swelling capacity can differ from equilibrium swelling and these terms needn't coincide in time e.g. [Pou 13]. Eventually, depending on many factors (e.g. polymer structure, type of solvent used and/or direction of changes observed), the phase transition may, but needn't be, interfered by formation of skin/gel surface layer [Mat 88], other surface instabilities/morphology modifications [Gon 12][Tan 87] or, in extreme case, appearance of cracks/fractures [Sch 90][Ghi 97][Siv 12]. These are further contributions controlling sorption alike the ones hypothesized for surface film formation [Che 07] and presence of superplasticizer [Tak 91][14]. In consequence, the solvent release may be sometimes limited [Zhu 15] or, in other special case and alike in case of drugs [Bra 94], is burst/rapid [Siv 12].

- *mechanisms behind volume changes*

Upon cross-linkage enhancement, in particular covalent cross-links provided, the typically amorphous (otherwise semi-crystalline) hydrogel is expected to undergo volume changes instead sol-gel transitions. In gist, the phase transition is a result of interplay of few balancing and otherwise opposing forces, including ones acting to expand the polymer (repulsive forces) and another ones forcing the network to shrink or at least maintain the structural integrity (attractive/retractive forces). At equilibrium for fixed pH and salt concentration, these forces are equal while the physical situation in case of swelling can be expressed in terms (minimization) of the (total) Gibbs free energy ΔG:

$$\Delta G = \Delta G_{mix} + \Delta G_{el} + \Delta G_{ion} \tag{2.2}$$

In short, Eq. 2.1 yields that swelling behaviour may result from thermodynamic force of mixing (a result of spontaneous mixing of fluid/solvent molecules with polymer chains, cf.

[13] Alternatively, equilibrium swelling may be sometimes referred to as equilibrium volume degree of swelling, equilibrium swelling capacity, equilibrium degree of swelling, equilibrium volume swelling ratio, equilibrium mass swelling, equilibrium weight swelling ratio or is translated into so-called hydration, and otherwise referred to as hydration ratio or hydration power. To address state of volume changes on way to equilibrium, terms such as mass swelling, degree of swelling, swelling ratio, swell index, absorption/gel capacity, water absorbency, ratio of absorption, absorptivity and water retention value are applied. Equilibrium water content is term close to equilibrium swelling; however, in this case the reference is made to weight in the swollen state giving water content of hydrogel.

[14] It should be mentioned that formation of polymeric complexes or some kind of interaction occurred due to absorption of surfactant agent or polyelectrolyte by hydrogel is possible, e.g. as exhibited in [Phi 96] and [Yoo 97], respectively.

energy term ΔG_{mix}), elastic retractive force of polymer chains (term ΔG_{el}) and force due to ionic contribution (osmotic pressure, term ΔG_{ion})[15].

Whether all three forces are active in swelling mechanism in general, and whether the third force mentioned (which is much stronger than mixing force) is activated in particular, this, similarly to secondary stimuli-dependent behaviour, depends on type of polymer under consideration.

- classification of SAP types and stimuli-responsiveness

Important classification with regard to last aspect involves dividing SAP according to nature of the side/pendant groups attached to the polymeric chains, i.e. potential ionization. In turn, SAP could be recognized as either non-ionic (neutral) or, similarly to superplasticizers (another polymeric material used commonly in concrete technology), ionic polymers (polyelectrolytes), the latter type being further subdivided into anionic and cationic hydrogels[16] [Zoh 08]. As a rule of thumb, volume changes induced by pH and ionic strength change are associated with polyelectrolyte-type of SAP, while uncharged SAP are more likely to respond to changes in temperature or osmotic pressure [Lee 90]. Apparent sine qua non for phase transition due to pH is attaining pH above pK_a or lowering it below pK_b of ionisable species/moieties tethered on polymer chains of anionic and cationic hydrogel, respectively, in subsequence to which two opposite behaviours depending of polyelectrolyte type could be exhibited, see Figure 2.19. Excessive exceeding the respective thresholds is typically unwanted due to/given appearance of adverse change in course of swelling [Vas 90].

[15] The paramount importance of osmotic response (assumption: the mechanism is applicable to the gel), without accounting for other effects, is doubt by Bowman et al. [ref. 1 *Ibid*. Bow 91]

[16] Certain simplification is used as particular classification does not include other, yet very seldom used types of hydrogels. For full classification acc. to nature of pendant groups, reader's attention should be paid to e.g. [Zoh 08].

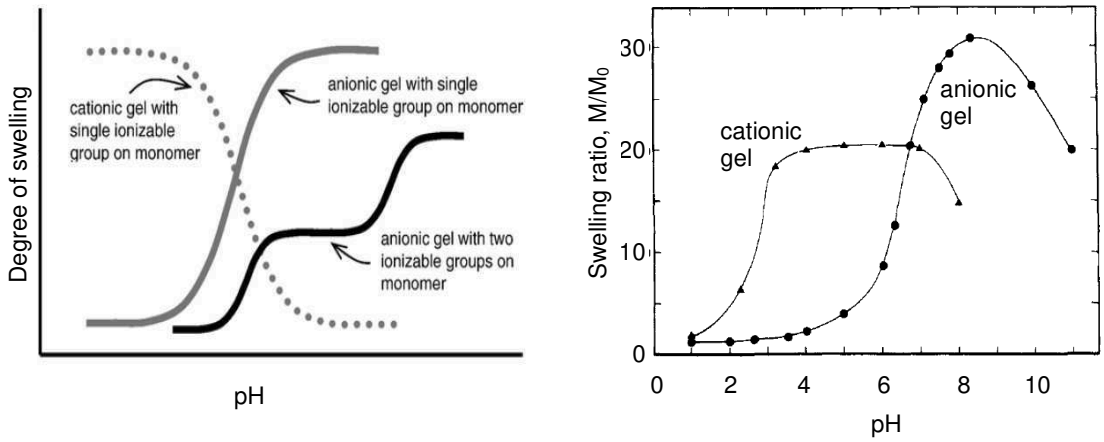

Figure 2.19: Typical change of swelling degree of ionic SAP in dependence on pH value (to the left) and the effect of exceeding critical threshold (to the right), after [Lin 06] and [Vas 90], respectively.

Similarly to pH stimulus, one of two different responses and rarely complex one is expected from the hydrogels undergoing volume changes in response to temperature variation. Important in this respect is acquiring characteristic thresholds: upper critical solution temperature (UCST) or lower critical solution temperature (LCST) for positive and negative temperature-sensitive hydrogel, respectively (Table 2.4). Each behaviour can become modified while, as also known from different studies [Fei 92][Yoo 97], mutual influence of both pH and temperature, in addition to individual one, is not excluded. Temperature-induced transition phenomenon may eventually sometimes disappear [Fei 92][Don 91][Yoo 00]. Given the number of controlling factors and discussed in [Don 91][Fei 92][Yoo 97][Yoo 00][Zho 03], it is generally found that responsiveness to temperature is more complex that that to pH stimulus.

Table 2.4: Type of responses presented by temperature-sensitive hydrogel systems and the response modifications.

Type of temperature responsiveness (corresponding CST)	Representative polymer	Response of hydrogel to exceeding threshold	Control, modification
Positive (UCST)	Poly(acrylic acid-co-acrylamide) with UCST 34-3 °C at pH 2.5-8.0 [Zho 03]	Cooling below UCST: hydrogel is shrinking Heating above UCST: hydrogel is swelling	Ionization effect: shifting of UCST towards lower temperature with increase of pH [Zho 03] Dependant on molecular weight and concentration, as well as co-solvent (if applicable)

(continued on the following page)

Table 2.4: Type of responses presented by temperature-sensitive hydrogel systems and the response modifications *(continued)*.

Type of temperature responsiveness (corresponding CST)	Representative polymer	Response of hydrogel to exceeding threshold	Control, modification
Negative (LCST)	Homopolymers: Cross-linked Poly(N-isopropylacrylamide) with LCST~32-34 °C and Poly(methacrylic acid) with LCST~75 °C or copolymer: poly(N-isopropyl acrylamide-co-acrylic acid)	Below LCST: polymer chains are fully hydrated and polymer behaves as a hydrophilic structure (gel becomes swollen, hydrated and hydrophilic) Heating above LCST: hydrogel looses majority of absorbed bound water and is contracting e.g. due to hydrophobic interactions (gel becomes collapsed, dehydrated and hydrophobic)	Ionization effect (case of increased hydrophilicity): shifting of LCST towards higher temperature on increasing pH, e.g. [Don 91] Copolymerizing with other monomers: The more hydrophobic monomer incorporated, the lower LCST as opposite to incorporating hydrophilic monomers 'Additives': (simple) salts, surfactants, and co-solvent/co-solute added to polymer/water solution (polymer/solvent system) e.g. formation of **polyelectrolyte complex** [Yoo 00]

- types of water held by SAP

In the swollen hydrogel, free water[17] constitutes important if not the major component of the hydrogel's liquid part. Restated, that is to say free water is not the single water type held by these materials. Since water becomes compartmentalized by hydrogel and furthermore undergoes various interactions (water-polymer, water-water), other water types must obviously result, as being schematically showed in Figure 2.20.

As a rule of thumb, the further a water molecule belonging to specific layer is from the polymeric chain, the lower binding strength therefore the higher its mobility, as well as higher likelihood of unperturbed/unchanged structure i.e. closer to that of free water [Omi 10]. In SAP with and owing to extraordinary swelling, the belief is that the unbound or, assuming worst case scenario, weakly bound water prevails, making other water types[18] to exist in

[17] Free water is the water physically entrapped within polymer network and is first to be removed under mild conditions e.g. due to temperature. It is water type of transition temperature, enthalpy and DSC curve similar to these of pure water. In hydrogel, it belongs to the outmost layer and is unable to permeate into region of bound water. In comparison, other water types will have other activity, freezing and melting behaviour as being trapped by stronger binding forces. (Thermodynamic properties different from those in the bulk liquid phase)

[18] Classification of water state/types/classes has been showed to strongly dependent on measuring method used, analysis of data and thermal history of the sample, e.g. [Roo 94]. To avoid dividing water into types being unrealistic for room temperatures (e.g. freezable and non-freezable water), other classifications have been proposed. Alternatively to that presented by Omidian and Park [Omi 10] and similar to [Tsu 97], important one appears to be that presented by Roorda [Roo 94], distinguishing between free water and perturbed (a kind of bound) water.

negligible amounts, in agreement with Koda et al. [Kod 94]. This follows observation of significant amounts of water taken up in superabsorbents at high relative humidity and only little (around 10 %) amount of water that is spent on formation of hydration shell surrounding polymer chains, e.g. in the case of poly(acrylic acid) sodium salt presented by Thijs et al. [Thi 07]. The results of Mönnig [Moe 09] seem in general agreement with this statement, although some difference in desorption behaviour compared to pure water remained for SAP. On the other hand, as more studies show [Don 91][Kim 04], free liquid content seems to be individual attribute of chosen SAP and used solvent type. E.g. in copolymers of hydrophilic monomers, where poly(acrylic acid) constitutes the major solid part, the free water content is sometimes reported relatively low, even as low as 37 % [Kim 04]. Not surprisingly, in cases of some SAP large water part cannot be extracted even if very high suction pressures are applied [Ver 05].

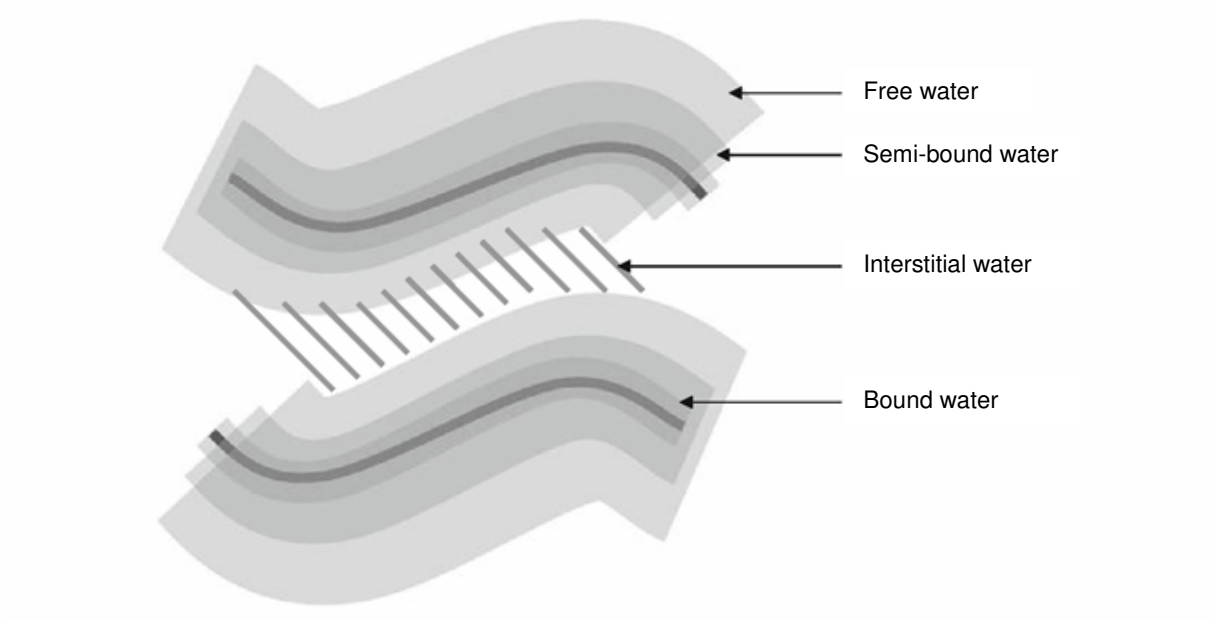

Figure 2.20: Classification of water types according to Omidian and Park [Omi 10].

- factors controlling behaviour of SAP

Obviously, for successful application of SAP, water not only has to be absorbed; it also has to either bound or, as for one of the concrete applications considered, to remain reasonably free, in order to allow its release at appropriate time and in controlled manner/fashion. The rule of thumb is that highly swollen hydrogels contain large amount of unbound water enhancing release transport [Don 91]. Nonetheless, the general observation is that mechanisms of hydrogel's swelling are in principle polymer shape dependant [Li 90] and differ from these associated with the absorbed aqueous solution return. Indeed, whereas swelling can be

diffusion- or relaxation-controlled, the release of load carried in and from polymeric material can be already of the diffusion-controlled, chemical-controlled or solvent-activated type [Lan 83]. The mechanisms leading to both behaviours remain interrelated on some level, e.g. via porosity [Zho 03]. This could be further extended to a number of parameters related to polymer structure and environmental conditions (especially liquid composition in which SAP is placed). As Table 2.5 exhibits, they are in common and taking control over state of water bound, sorption behaviour and mechanical properties.

Table 2.5: Review of different factors related to polymer production details and the solvent with regards to SAP sorption-related properties with particular focus on anionic-type superabsorbents.

Parameter undergoing increase[1]		**Response**				
		Free water	**Swelling capacity**	**Swelling rate**	**Deswelling**	**Mechanical properties (wet strength)**
Hydrogel production details	Porosity/particle porosity	↑ [Gan 10]	↑ but effect doubt by [Zoh 08]	↑ [Zoh 08][Gan 10][Omi 12]; also in case of open and interconnected pores [Omi 12]	Unknown, hypothesis: ↑ (due to less constraint provided)	↓ [Zoh 08][Omi 12], unless new generation of SAP [Gon 12]
	Cross-linking ratio/density (assuming minimum low crosslinking density threshold has been acquired); Flory's theory	↓ (in terms of molecular motion of water); effect questioned by Roorda [Roo 94]	↓ [Zoh 08][Omi 12]	↑ [Omi 12] in contrast to ↓ [Zoh 08]	↓ (screening effect; with occurrence dependent on approaching the mesh size by exiting solute molecules)	↑ [Zoh 08] until optimum [Omi 12]
	Hydrophilicity	↑ but also dependent on type and ratio of hydrophilic monomers used [Kod 94]	↑ [Omi 12], with limitation [Shu 11]	↑ [Omi 12]	Unknown	↓ [Omi 12]

[1] Given little investigation in past (with one of very few exceptions being excellent publication of Philippova et al. [Phi 96] and literature referred to), as well as upon only general view on parameters concerned, important effect of surfactants, i.e. additives decreasing surface tension of water, is not presented.

Table 2.5: Review of different factors related to polymer production details and the solvent with regards to SAP sorption-related properties with particular focus on anionic-type superabsorbents *(continued)*.

Parameter undergoing increase		**Response**				
		Free water	**Swelling capacity**	**Swelling rate**	**Deswelling**	**Mechanical properties (wet strength)**
Hydrogel production details	Neutralization degree (until optimum)	↑ [Tsu 97]	↑ if degree of crosslinking=const. and the swelling medium is salt solution [Ell]; [Lee 01] with limitation	↓ with only small variations [Lee 01]	Unknown	Hypothesis: ↓ given the relation: the higher the water content of the gel, the poorer the mechanical properties gel by [Jen 01]
	Particle size	Effect is vague considering hypothesises established in [Moe 09] and [Jen 02]	Not straightforward: ↑ for single particle [Est 09] but ↓ in terms of absorption per gram SAP [Soh 03]; additional dependence on synthesis technique [Sir 10]; effect doubt by [Zoh 08];	↓ [Zoh 08][Est 09]	Hypothesised as not straightforward e.g. could be affected by different surface phenomena (skin formation, cracking, …)	↑ [Zoh 08] in contrast to [Jen 01] and [Omi 12]
Physical and chemical stimuli-related	pH	↑ [Don 91]; dependent on composition and ionization state of hydrogel	Dependent on type of stimulus responsiveness, if any; if applicable, also dependent on ionization state of weakly acidic (or basic) active sites	Hypothesis: ↑; dependent on stimulus responsiveness and ionization state	Unknown	Hypothesis: if more water absorbed at high pH, then ↓
	Temperature	Dependent on amount of water absorbed and polymer composition [Kod 94]	Dependent on type stimulus responsiveness, if any; no effect [Zoh 08]	↑ [Zoh 08]	Unknown	no effect [Zoh 08]

Table 2.5: Review of different factors related to polymer production details and the solvent with regards to SAP sorption-related properties with particular focus on anionic-type superabsorbents *(continued)*.

Parameter undergoing increase	**Response**				
	Free water	**Swelling capacity**	**Swelling rate**	**Deswelling**	**Mechanical properties (wet strength)**
Ionic strength = f(mobile ion concentration, ion valency) $Q_{eq}^{5/3} = A + Bi^2 / I$ [Lee 01][Lee 97] with Q_{eq} = the water absorbency at equilibrium i = the concentration of the charges bound to the gel I = the ionic strength of the external solution A, B = the empirical parameters	Hypothesis: ↓ (due to perturbation of water structure by some ions e.g. small alkali metal ions such as Na^+ [Tsu 97]); but in general, indirect and direct effects possible, effects depend on size of alkali metal ion present [Tsu 97]	↓ [Zoh 08][Omi 12]; resulting mainly from screening of the ionic charges bound to the network and osmotic pressure difference decrease[2, 3, 4]	↓ [Zoh 08] but also dependent on neutralization degree [Lee 01]	Unknown	Depending on the other various factors [Zoh 08]
Counter ions (ions of charges opposite to side groups) or their valences; for a given ionic strength [Lee 97]	As in case of ionic strength effect	↓ [Omi 12]; resulting mainly from shielding of repulsive counterion on the polymeric chain by the bound ionic charge [Lee 97] and switch from weak bonding to complexation between side groups and multivalent cations [Lee 97][2, 3, 4]	Unknown	Unknown	Hypothesis, case of di- and trivalent cations: ↑ (due to additional cross-linking provided)

[2] Presented trend is only general and does not include possible changes in composition of surrounding medium which could take control over swelling behaviour as well, e.g. [Bow 91][Var 99][Sir 12].

[3] In case of anionic hydrogels and cations 'regulating' the hydration, the valence of accompanying anion was found to have no impact on hydration of polymer acc. to reference 1 in [Bow 91]. At any given ionic strength and regardless of cation valence, similar secondary role is likely played by radius of cation and nature of the anion, with some exceptions in case of former [Lee 97]. However, whether valence of anion has influence on swelling or not, this was showed to be still dependent on polymer composition [Zha 06].

[4] Screening effect was reported as reversible, however, only on condition of chelating monovalent cations and multiple treatment with distilled water, see reference 1 in [Bow 91]. This generally fails in case of divalent or trivalent cations. The bond developed by the some multivalent cations can be nonetheless sometimes unstable [Zhu 15], in view of which replacement of ions of higher valency on exchange sites by the monovalent ones becomes possible, e.g. case of calcium ions [Bow 91] and less plausibly aluminium cations [Zhu 15].

For more in-depth information on different aspects regarding SAP (preparation, structure, characterization, testing of hydrogels, etc.), reader is asked to refer to recent book and article reviews published, for instance, Zohuriaan-Mehr and Kabiri [Zoh 08] as well as Masuda and

Ueda [Mas 14] or older ones by Frank [Fra 02] and Staples with Chatterjee [Sta 02], in addition to the references mentioned and many reviews by Peppas and co-workers.

2.5.2 SAPs as IC agent

- brief historical review

SAP is relatively new material for purposes of IC but it is hardly new admixture in the concrete technology. Potentially the first application could be dated back to year 1989 when a water-absorbent polymer was used in production of high-strength concrete with aim of improving strength and durability [Has 89]. Many other uses have been successively accomplished since that moment [Tak 91][Ito 94] until the admixture was finally suggested for curing [Tsu 99]. In-between 2001-2002 the most efficient curing methodology using SAP, so-called water entrainment, was introduced and theoretically background by Jensen and Hansen [Jen 01b][Jen 02]. Due to their input, the hypothesis and experimental evidences of curing method effectiveness forwarded since 1950s and ascribed to same process, i.e. internal curing [Mat 70], could be scientifically validated for yet another IC agent.

- the advantages of using IC in general and SAP in particular

Proper curing, while being a mitigation strategy against shrinkage, is one of the most important requirements for optimum performance of a cement-based material in any environment or application [Mee 99]. Best mix designs cannot overcome all imperfect properties related to associated material, with cracking sensitivity due to autogenous shrinkage being the Achilles' heel for UHPC, see Section 2.2.3.

The review of advantages resulting from applying internal curing using SAP in various cement-based materials is presented in Table 2.6. It can be summarized that internal curing seems truly acceptable if not optimum curing methodology for UHPC. It indeed provides the solutions for attaining all fundamental goals of curing in least invasive way, therefore in spirit of UHPC design. When SAP is used as IC agent, some disadvantages related to usage of rival materials can be furthermore overcome too. Last but not least, as signalized in Section 2.5.1, the polymeric materials do show best perspectives with regard to IC optimization which can be attained by engineering properties of the polymers. All these elements add up to great potential of SAP in the IC perspective.

Table 2.6: Analysis of curing requirements in terms of fulfilment by IC using SAP.

Curing requirement aimed at or specific benefit resultant	Manner of fulfilment
Adequate water content [Mee 99]	By supplying curing fluid water from the tiny internal reservoirs, the problem of capillary discontinuity that would limit curing water migration distances is prevented. The experimental evidence of maintaining satisfactory moisture content is the higher RH compared to systems without IC under sealed conditions [Jen 02][Ben 02][Wan 09][Pié 06][Est 09], and in theory reflecting free access to water. When material is additionally exposed to drying to ambient, RH distribution seems yet improved too [Zha 06].
Maintenance of adequate temperature and preservation of reasonably uniform temperature throughout the concrete body [Mee 99]	Since the IC agent can be distributed uniformly throughout concrete member (e.g. [Lur 08a][Dud 08b]), no humidity and thus heat of hydration-related temperature gradients are expected to occur. Further benefit especially from using SAP refers to advantageous control over α_T [Wyr 14][Wyrzykowski and Lura 2013 *Ibid*. Wyr 14].
Adequate time for sufficient hydration [Mee 99]	Because the water of curing fluid needed and to be carried by the IC agent can be precisely assessed (Powers' model based estimations [Jen 93][Jen 01b], other [TC 196-ICC]), and it will be released only when needed (i.e. in controlled manner), hydration can continue until maximum attainable degree of hydration is obtained.
Adequate protection from damaging disturbances during the early period of curing [Mee 99]	Although any curing type must protect concrete from mechanical disturbances especially when microstructure is being developed, IC does it internally. Stresses due to restrained autogenous shrinkage and cracking likelihood are indeed reduced when IC is applied. Nonetheless, fast loss of water from IC agent particles and their pronounced volume decrease, without corresponding changes in the surrounding matrix, may sometimes lead to local defects in direct vicinity of the IC agent particles, e.g. [Lam 05].
Improvement of concrete properties [TC 196-ICC]	Hydration is prolonged with IC which provides trigger for improvement in all properties related to degree of hydration. Final effect depends on SAP particularities used e.g. smaller IC agent particles may appear to be more preferable choice in enhancing strength owing to secondary effects exerted, see Section 2.5.3 for more details.
Minimizing shrinkage [TC 196-ICC]	Autogenous shrinkage is reduced or even becomes converted into expansion with IC, e.g. [TC 196-ICC][TC 225-SAP][RILEM pro052][RILEM pro074]. Observations of positive impact of IC are also made for plastic shrinkage [TC 225-SAP][Dud 10b] and total shrinkage [Mec 06], including that of UHPC, see [Geo 10b] and [Sol 11][Sol 12], respectively. However, little changed [Pié 06] or even higher [Mec 09] total shrinkage of concrete with IC has been also noted, showing dependence of final effect on the time-zero choice or other factors (mix composition etc.).
Other benefits related to operation with moisture (flow barrier function, moisture buffer performance)	Beside poor curing practices, concrete can be exposed to various environmental conditions. Important in this respect, SAP as contrary to many absorptive materials characterizes with very favourable moisture buffering capacity and velocity of adjustment to RH changes [Cer 09]. In terms of durability, the potential function of cutting off capillary network ascribed to SAP [Pai 09] might be very useful too.
Other benefits	SAP unlike light-weight aggregates can be added dry to the mix, known since 1989 [Has 89]. This assures homogenous distribution of polymers (e.g. [Lur 08a][Dud 08b]) and prevents them from formation of gel-blocks, being a serious problem related with usage of SAP in the pre-saturated form [Lam 05][Wan 09]. Dry application makes furthermore handling of the IC measure easier. It might be though required to make addition moment adjusted to size and content of SAP [Moe 09].

- mechanisms of IC by means of SAP

The effectiveness of IC by means of SAP is closely linked to ability of distributing the curing fluid from the particle of polymeric material to furthest region undergoing self-desiccation in its vicinity. The associated travel distance referred to as 'paste – IC agent particle proximity' [TC 196-ICC] and constituting so-called sphere of influence [Zhu 11] or protected paste volume [Jen 01b] will be decided by the properties of the matrix developed, on one hand, and properties of SAP, on the other hand (Section 2.5.1). It can be very complex and specific property and for each material must be investigated individually. The general belief is though that water discharge proceeds in stages (Figure 2.21) and, as recent modelling findings reveal, is governed by demand-supply mechanism rather then being triggered by capillary suction [Wyr 11]. However, should this be disturbed and/or microcracking [Hua 10] as well as growth of hydrates in pores occupied by SAP occur [Jen 02][Kle 13][Jus 15], different and more complex scenario might be expected.

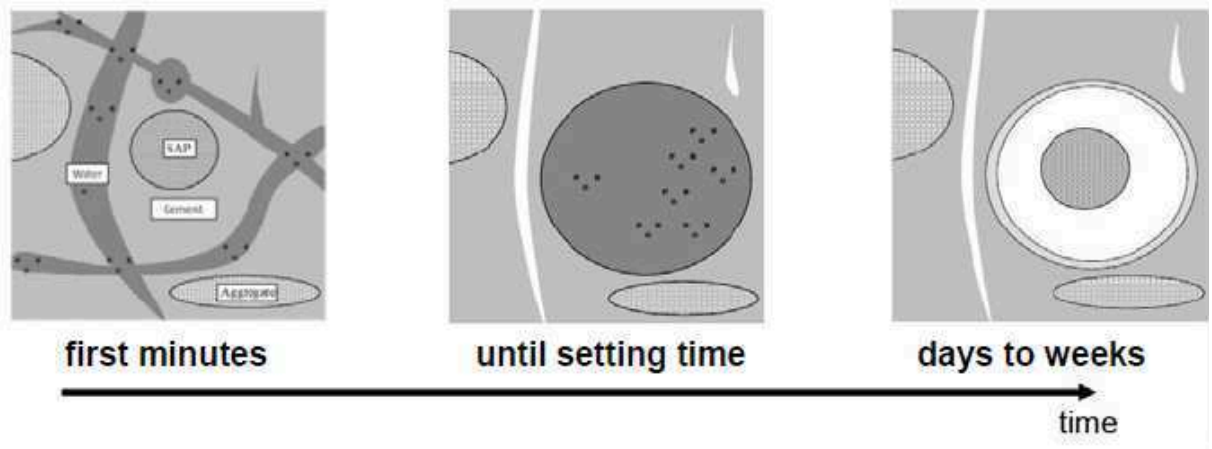

Figure 2.21: Generalized scheme of internal curing obtained using SAP from dispersion stage (left), through finalized solution absorption of IC agent (middle) until cessation of IC activity (right) [TC 225-SAP], adopted from [Moe 09]. Measurements prove in general this view in cement paste, see e.g. [Trt 10].

- other remaining questions and problems related to usage of IC

Since no regulations regarding use of superabsorbent polymers in concrete technology have been proposed to date, although being among goals of running RILEM Technical Committee 260-RSC, there is understandable lack of consensus regarding method of implementing SAP and manner of determining the amount of water to be absorbed by it. With intention of IC purposes, the former is currently conducted with extra water ('water entrainment'), with partial workability adjustment using superplasticizer or with SAP being applied alone ('water sealing'). Although using SAP in option 'water entrainment' seems most meaningful among them when taking into consideration the origin of autogenous shrinkage, two other

combinations mustn't be ruled out. In fact, since phenomena triggering autogenous shrinkage are taking effect in pores, modification of the pore system structure is reported to appear as important factor in reducing AS as the amount of curing water [Jen 01b][Lur 06]. Meanwhile, very little is known about the outcomes of e.g. pure SAP addition (i.e. without extra water) and potential benefits that could be imagined for UHPC.

Implementation also regards the method both IC variables, i.e. SAP and extra water, are introduced in the mix. Common solution is addition of SAP and extra water during dry and wet mixing, respectively, and, on stage of mix design, some replacement of fine aggregates having size similar to that expected from swollen SAP. In case of cement-based materials without aggregate of required diameter, the optional 'on top' method certainly appears important alternative to consider.

It is eventually noted that the most controversy continuously regards estimation of water absorbed by SAP. Many methods has been advanced and used for purpose of estimating absorbed IC fluid so far. The most goal-fit methods are certainly protocols in which fluid absorption of SAP is assessed both under load and excluding factor of changing absorption in dependence on concrete composition, therefore, where the SAP behaviour is examined in the particular cement-based material under modification. These may include, although needn't limit to, tests on fresh concrete [Mec 06][Dud 08b][Moe 09][Ass 14a], refined pore analysis of concrete cross-sections [Jen 02][Ass 13] or, less handy and more costly, X-ray microtomography [Lur 08a], Neutron Tomography [Trt 10] or Nuclear Magnetic Resonance [Nes 09]. However, only little attention has been devoted to the tea-bag test [Zoh 08][WSP 11], which, although not perfect, is easy to perform and can be applied for any liquid, therefore also pore solution, while giving surprisingly good results in comparison to other methods [Ass 14a]. It could be an important alternative in light of changing absorption of SAP in time and being specific for SAP type applied.

2.5.3 Effect of IC/SAP on concrete properties

From previous discussions direct conclusions applicable to this section can be made. In particular, since SAP used in concept of internal curing:

(1) provoke certain changes in original composition of concrete,

(2) absorb water/pore solutions and swell in fresh concrete,

(3) lead to formation of geometrically predesigned macro-inclusions of variable content,

(4) rivalry to hydration regulate the water balance (the action of which takes place irrespectively the concept of internal curing is executed or not), and
(5) act as a flow barrier,
impact of the internal curing methodology is expected to regard majority of concrete properties. It seems reasonable to divide particular field of importance into two, i.e. effect of internal curing (or, intuitively, SAP themselves) on autogenous shrinkage and another one, accounting for influence on all other properties.

Because nearly every addition of SAP with extra water leads to reduction of free autogenous shrinkage, it is most reported effect of IC and currently the best comprehended one in terms of controlling factors. It is seen that effectiveness of IC is governed by the amount and properties of SAP [Jen 02][Lur 06][Sch 12b], especially the particle size [Jen 02][Lur 06] and desorption kinetics [Gor 11][Sch 12c], and generally any factor contributing to distribution of sufficient amount of water at right time (e.g. curing fluid content). These particularities must be adjusted/fit while considering limited travel distance of curing fluid from the stretches of SAP, but precisely how much restricted, is still under debate [Øst 01][Iga 10][Lur 14][Wyrzykowski et al. 2012 *Ibid*. Lur 14][Zhu 11b]. As signalized earlier, it is simultaneously not excluded that certain physical changes in microstructure exerted by IC variables will decide about the extent of curing success too [Jen 01b][Lur 06][Est 09].

Additionally, the characteristics of original cement-based materials, i.e. before modification by internal curing, must be taken into account. In recent RILEM TC 225-SAP Round-robin Test [Mec 14], it has been clearly demonstrated that the same IC agent and amount of curing water will provide only somewhat similar effect when the raw materials properties of mix to be cured (and not the original proportions) are slightly changed. Similar finding was made by the author after comparing introduction of one type of SAP to two different matrices of mortar and finely grained UHPC. This obviously adds up to conclusion that evaluation of internal curing must remain material-orientated, as being established in this thesis.

As far as second group is considered, experience gained by different scientists pioneered by Jensen and Hansen [Jen 01b][Jen 02] through two conferences [RILEM pro52][RILEM pro74] and PhD theses [Moe 09][Est 09][Sol 11][Ass 13] to the state-of-the-art reports [TC 196-ICC][TC 225-SAP] allows to state a considerable list of properties undergoing simultaneous changes. These are widespread over all concrete life states. In particular, of

concern are properties in fresh state (workability, air content, density), ones ascribed to transition from fluid to solid (e.g. setting behaviour) as well as properties in the hardened state (mechanical, elastic, visco-elastic). Upon application of IC agent, especially ones without individual sorptivity taken into account, some changes in permeability and diffusivity, therefore important durability-related properties, may result too.

Unlike the influence of IC on concrete in its fresh state (typically leading to compensable changes of workability, some air content increase and decrease of density, e.g. [Dud 10a][Dud 10b]), one straightforward course of changes on particular property of hardened concrete is from principle hard to find. The fact is that positive impact of one factor can be easily offset by a rival negative one, the best examples being increased degree of hydration at simultaneously increased porosity and much higher moisture content. Furthermore, some parameters may be found of greater importance for one property than the other e.g. tensile strength being more dependent on microcracking and its elimination than compressive strength. In Table 2.7, the most important variables influencing hardened properties from the time of mixing has been collected; more detailed information can be found in current section's references.

Table 2.7: Review of effects of internal curing on concrete properties, based on references from Section 2.5.3.

Potential change due to IC or pure SAP	Microstructural effect	Condition required
Hydration kinetics / course alteration (early ages)	Time-shifted accomplishment of specific thresholds and related events, in accordance to the change	Ability of SAP for invoking particular sorption course, or other, except for level of relative humidity (maintained as a rule of thumb high)
Increased degree of hydration (later ages)	Reduction of capillaries, lower porosity, denser paste phase	Sufficient quantity of water (criterion e.g. level of relative humidity) and hydration product deposition allowed also in the modified material capillaries
Reduction of effective w/c	Strength increase-favourable changes in capillary pore structure	Pure addition of SAP or quantity of extra water not covering the absorption of IC agent used
Increased relative humidity	Existence of pores of high saturation influencing strength	Sealed conditions and/or low diffusion coefficient
Increase in gel porosity	Pore size distribution shifted towards smaller pore diameters	Internal curing takes effect while the SAP pores have been completely eliminated
Increased porosity with simultaneous emptying of SAP pores	Additional voids (especially if large SAP particles applied), lower gel-space ratio, but perhaps increased fracture toughness; elimination of fine, irregular capillary pores	Usage of SAP of specific type and perhaps particle size

(continued on the following page)

Table 2.7: Review of effects of internal curing on concrete properties, based on references from Section 2.5.3 *(continued)*.

Potential change due to IC or pure SAP	Microstructural effect	Condition required or speculated
Creation of porosity of irregular shape	Higher stress concentrations	Usage of robust SAP that show irregular shape in any state (collapsed, swollen)
Diminished autogenous shrinkage	No internal stresses due to shrinkage restraints, no cracks	Efficiency of curing (criterion, e.g. relative humidity or capillary pressure evolution)

Careful analysis of available experimental data and variables just mentioned is important for another reason. In fact, it may serve as valuable source for drawing general conclusions with regards to variations of internal curing effects or their extent. Many of the parameters collected in Table 2.8 will mostly apply to compressive strength, as this mechanical property has been preferably investigated. In general, however, it seems proper to assume that some negative impact may regard many mechanical properties including compressive and tensile strength as well as Young's modulus. While the loss of strength is typically not high (if any), it should not be overestimated since the primarily goal of internal curing especially in materials of much improved mechanical properties compared to ordinary concretes is in fact mitigation of autogenous shrinkage and associated cracking. Important enough, due to complex nature of stress generation, some loss in elasticity, for instance, may be found favourable too.

Table 2.8: Parameters decisive for internal curing effect on strength, based on references from Section 2.5.3.

Parameter and its specification (if applicable)	Influence on strength
Increasing SAP and IC water dosages	Higher loss of compressive strength, especially in early ages
Increasing age of material	Decreasing relative difference in strength (if occurred); possible reasons: (1) hydrates growing inside original boundaries of the SAP particles, (2) carried moisture redistribution
Composition of unmodified material	In case of mortar with normal quartz aggregate, it is decisive about largest defect size, contrary to cement paste and likely finely grained UHPC/RPC
Decreasing effective w/c of material before modificiation	General higher sensitivity to changes due to IC; possible reasons: less capillaries to deposit new hydrates, material also becoming more brittle
Curing conditions	No or some sensitivity to external curing conditions; loss in mechanical resistance, if occurred, resultant from e.g. stress gradients or microcracking caused by moisture gradients

2.6 Summary and conclusions with respect to own work

Autogenous shrinkage can be defined as the bulk deformation of a closed (sealed), isothermal, cementitious material system not subjected to external forces [TC 196-ICC]. It is mainly volume change due to shrinkage for cement-based materials having w/c lower than 0.42, therefore, a fundamental one in case of UHPC with the w/c reduced to about 0.2. The precise magnitude of autogenous shrinkage depends on point selected for the volume change evaluation, so-called time-zero.

The causes of autogenous shrinkage are linked with the special conditions in which hydration takes place. Chemical shrinkage combined with self-desiccation give rise to mechanisms closely related to surface forces, including capillary pressure and/or disjoining pressure. Engagement of other mechanisms and contributing to net result either positively or negatively, i.e. causing less or more shrinkage to develop, respectively, cannot be excluded, yet. The potential candidates are, although needn't be limited to, autogenous swelling, microcracking, and creep.

Internal curing involving implementation of an IC agent and extra water to cure concrete internally appears a mitigation strategy able to overcome permeability-ascribed limitations set to more conventional and externally applied curing measures even in extreme case of UHPC. Meanwhile it is believed to eliminate the source of autogenous shrinkage and not only compensate for the volume change occurred.

Among all natural and artificial products which can be potentially utilized for the purpose of IC, superabsorbent polymers (SAP) appear presently to be the most promising water-regulating additive. These polymers consist of cross-linked chains having dissociated ionic functional groups which facilitate the absorption of large amounts of aqueous solutions, eventually resulting in the formation of a stable hydrogel. Amazingly, the water stored in SAP can survive presence of gentle mechanical stress, making desorption process to be related to other stimuli which are typically ascribed to self-desiccation of the surrounding cement matrix. After all the water is drained out from the tiny inclusions, the only remnants are then small air-filled macropores of uniform distribution in the hardened matrix.

IC has a chance to become a 'standard' curing method in field of low w/b materials. Before practical recommendations for use of SAP in concrete construction can be formulated, a

number of theoretical and practical questions are still to be answered. In fact, the introduction of IC requires making few fundamental choices which affect the effectiveness of IC in mitigating autogenous shrinkage. This especially concerns SAP material appropriate for the purpose which properties, as current literature review importantly revealed, can be very different. Assessment of absorption capacity of IC agent chosen appears as critical too, in both cases yet assuming that material under modification is sufficiently permeable, often doubt for UHPC. Eventually, time-zero, i.e. the beginning of effective autogenous shrinkage, seems to be one of the major parameters when evaluating the effectiveness of internal curing.

It is purpose of this work to contribute to further gain of knowledge on these aspects and especially on the mechanisms of IC. For own investigations, UHPC has been used as it is currently one of most high-tech materials in group of cement-based material and of increasingly widen applications, including construction of bridges and the sky-scrapers.

3 Experimental

3.1 Introduction

Despite exhibiting largely comparable concrete behaviour, compositions of UHPC can vary significantly from one study to another, especially in terms of aggregate graining (Appendix C). It was important aspect covered also in framework of the present study. Meanwhile, even small changes in concrete composition may lead to different values of autogenous shrinkage (Section 2.5.3), thus calling for new look on working mechanisms of internal curing. Being another aspect often ignored, the efficiency of preventive measure chosen will be furthermore decided by particularities related to the IC method, on one hand, and the shrinkage measurement procedure (Section 2.2.5 and [Epp 10]), on the other hand.

Keeping all these in mind, this chapter comprises two main parts that are further split into more subparts. In Section 3.2 which is fully dedicated to concrete materials, the compositions used and the modifications introduced in relation to internal curing implementation are presented in detail. Reasoning or otherwise criteria for the IC implementation approach chosen, IC agent selected as well as use of fibres are given here as well. The section finishes with description of procedures used in mixing, casting and curing. The second main part, Section 3.3, focuses mainly on test procedures. As far as SAP in concerned, all details regarding characterization as well as supplementary phenomenological investigations on material chosen can be found here. With regards to concrete, described are all methods that were found helpful in understanding effect of IC on different properties of UHPC and, beside compressive strength, being strictly related to development of autogenous shrinkage under varied conditions (exposure to external restraint, storage conditions). The order of presentation is according to concrete states, i.e. from fresh to hardened state. For the review of criteria allowing classification of fresh concrete behaviour (note: self-compaction aimed at), please see Appendix F.

3.2 Material under investigation and specimen production

3.2.1 Initial UHPC compositions

All UHPC mixtures examined in this thesis were composed on the basis of two recipes: one of finely grained UHPC and another UHPC containing coarse aggregates, referred to as M2Q and B5Q, respectively [Sch 14]. These compositions were originally developed and optimized by University of Kassel [Bor 01][Feh 05], the work on which was largely continued under the aegis of the Priority Program 1182 of the German Research Foundation (DFG) "Sustainable Building with Ultra High Performance Concrete (UHPC)"[19]. To ensure comparability and synergy of research efforts in the program, some mixtures including M2Q and B5Q, i.e. Ff-R and Cf-R in this thesis, were suggested to be applied by all project partners. When joining the project, both UHPCs but especially M2Q have been suffering from very high autogenous shrinkage, see Section 2.3.3. This fact clearly resulted from specificity of the mixture compositions although they appeared to be no fundamentally different compared to commercial/patented UHPC products or mixtures remained known strictly on laboratory research level. For details, see Appendix C.

3.2.2 Main UHPC ingredients

The basic ingredients used for mix formulation remained identical to those originally proposed for M2Q and B5Q matrices. Yet, for number of reasons (1) since the type of binder used may affect effectiveness of internal curing [Klemm and Sikora 2012, ref. 3 *Ibid*. Kle 13], (2) given that novel superplasticizers are rival polymeric materials in the UHPC mix but also (3) for general clarity, their short description is given in the following.

- binder

In both types of UHPC, Portland cement CEM I 52.5 R-HS/NA produced by Holcim was used as the main binder. In accordance to classification of DIN EN 197-1, this product should be rich in grinded Portland cement clinker and assure high early-age strength, translated into cement strength class of expected 52.5 MPa. It furthermore was expected to exhibit high sulphate resistance owing to low C_3A content, and to be characterized by low alkali fraction. Alike all other concrete components, it was used in number of few batches originating from more production dates.

[19] Priority Program 1182 was a comprehensive research program on UHPC covering a wide range of topics related to this material. Its work finished in 2011 though some work on the mixtures, like the case of this study, continued afterwards as well. Summary of the projects could be found in [Sch 14].

As far as pozzolanic additive is concerned, two sorts of silica fume having appearance of dry powder were used. Microsilica called Elkem 971-U and obtained from BASF company served as the component of finely grained mixtures. In contrast, Silicoll P produced by Sika was utilized when preparing coarse-grained UHPC.

The chemical composition, basic granulometric parameters of the binders are presented in Table 3.1. By theoretical values, it is meant that the data was taken from technical sheet of product or one commonly used in calculations. Measured values, on the other hand, refer to own investigation results or data distributed among project partners.

Table 3.1: Characteristic values for the cement and silica fumes used for production of UHPC.

Particulars	Unit	Cement		Microsilica			
		CEM I 52.5 R-HS/NA *		Elkem 971-U*		Silicoll P*	
		Theor.	Meas.	Theor.	Meas.	Theor.	Meas.
Density	[kg/dm³]	3.10	3.18-3.23	2.20	2.33	2.20	
Specific surface (Blaine)	[cm²/g]	4890	4530-4880	20 x10^4	-	18-22 x10^4	-
C	[%]	-	-	0.5	-	-	-
SiO_2	[%]	-	21.1-21.3	97.5-98.4	-	94.5-97.5	-
Al_2O_3	[%]	-	3.31-3.54	0.2-0.4	-	-	-
Fe_2O_3	[%]	-	5.21-5.23	0.01-0.1	-	-	-
CaO	[%]	-	64.1- 66.4	0.2	-	-	-
SO_3	[%]	-	1.93-2.04	0.1	-	-	-
MgO	[%]	-	0.79- 0.82	0.1	-	-	-
Na_2O	[%]	-	0.19-0.23	0.1-0.15	-	-	-
K_2O	[%]	-	0.38-0.39	0.2-0.3	-	-	-
Na_2O-eq. (=Na_2O+0.658 K_2O)	[%]	-	0.44- 0.51	-	-	-	-
P_2O_5	[%]	-	0.28	0.03-0.1	-	-	-
Chloride	[%]	-	-	0.01-0.1	-	-	-
Water	[%]	-	-	0.4	-	-	-
Max particle size	[µm]	-	50	-	-	>1 = 30 %	1
d_{95}	[µm]	-	37.5	-	-	-	-
d_{50}	[µm]	-	9.5	-	-	0.1-0.3	-
Loss of ignition	[%]	-	1.19	0.5-0.6	-	-	-

* value obtained from technical data sheet or used in calculations (Theor.) or measured or alternatively forwarded by project partners (Meas.)

- aggregates

To create an aggregate cocktail, two combinations of fine aggregates with or without coarse stones were utilized. Quartz aggregate appearing in two forms, i.e. quartz flour named Millisil W12 and granules of rounded fine quartz sand called H33 as obtained from selfsame source (Quarzwerke company), was used for the finely grained mixtures. When producing coarse-grained UHPC, firstly, the part of fine aggregate blend was supplemented with another quartz

powder called Millisil W3. Secondly, the volume fraction of aggregates was completed with basalt split of particle size ranging between 2 and 8 mm, referred to as coarse aggregate.

The chemical and basic granulometric parameters of fine and coarse aggregates used are presented in Table 3.2.

Table 3.2: Characteristic values for the aggregates used for production of UHPC.

Particulars	Unit	Fine aggregate						Coarse aggr.	
		Millisil W3*		Millisil W12*		H33*		Basalt*	
		Theor.	Meas.	Theor.	Meas.	Theor.	Meas.	Theor.	Meas.
Density	[g/cm³]	2.65	2.67	2.65	2.67 - 2.69	2.65	2.66	3.0	3.06
Specific surface (Blaine)	[cm²/g]	1000	-	3800	4423	91	90-100	-	-
SiO_2	[%]	99	99	99	98.7	99.6	99.5	-	-
Al_2O_3	[%]	0.3	-	0.3	0.5	0.2	-	-	-
Fe_2O_3	[%]	0.05	-	0.05	0.05	0.04	-	-	-
SO_3	[%]	-	-	-	0.03	-	-	-	-
CaO+MgO	[%]	0.1	-	0.1	0.21	-	-	-	-
Na_2O+K_2O	[%]	0.2	-	0.2	0	-	-	-	-
Loss on ignition	[%]	0.25	-	0.25	-	0.2	-	-	-
Water	[%]	0.1	-	-	-	-	-	-	-
Maximum particle size	[µm]	-	300	-	60	-	500	8000	8000
Upper grain size (d_{95})	[µm]	220	-	50	55.2	-	412	-	-
Average grain size (d_{50})	[µm]	90	-	16	14.7	260	291	-	-

* value obtained from technical data sheet or used in calculations (Theor.) or measured or alternatively forwarded by project partners (Meas.)

- *superplasticizers*

Two high-range liquid water reducing admixtures, to be referred to as superplasticizers, being based on polycarboxylate ether were used within the studies. For fluidisation of finely grained mixes, product Glenium 51 from BASF company was applied. The workability of coarse-gained UHPC mixes was controlled by means of ViscoCrete 20 Gold, an admixture obtained from Sika company. Both water reducers were characterized with binary composition where the content of aqueous matter was assessed to be approx. 65 %. Their density was nearly identical, in particular approx. 1100 kg/m³.

- *steel fibers*

Whenever foreseen, selfsame type of steel fibre reinforcement 0.15 mm thick and 9 mm long called Weidacon FM 015/9 as produced by Stratec was used.

- mixing water

Usage of distilled and de-aired water is unrealistic in concrete practice and production of large concrete quantities. For this reason, in all investigations, only tap water was used.

3.2.3 SAP material and extra water

- IC agent and its selection

One SAP product was set to be used in all investigations. The material was selected in preliminary studies where SAP of various morphologies, absorption capacities and kinetics thereof were tested for effect on autogenous shrinkage and strength. Since harder to achieve, the decisive criterion for the choice was effect exerted on former (i.e. highest possible autogenous shrinkage reduction) for constant amount of extra water and no significant change of slump flow spread. Only then, the effect on compressive and flexural strength was analysed and SAP promising more favourable result was preferred.

According to selected product supplier, in terms of chemical composition, the SAP material used was inverse suspension-polymerized covalently cross-linked acrylamide/acrylic acid copolymer. On way to fulfil the goals of own study, knowledge on the product, to the highest possible extent, was verified and extended in numerous experiments presented in this thesis.

- dosage of IC agent

The preliminary studies showed that minimum amount of IC agent necessary for pronounced autogenous shrinkage reduction equals approx. 0.3-0.4 % by weight of cement. This well agrees with observations made in different studies, although mainly performed on pastes, e.g. [Jen 02][Lur 06][Est 09][Ass 13]. For better understanding of the IC phenomenon, as well as for evaluation of IC potential (given no full reduction of autogenous shrinkage at contents initially applied), the quantity range was extended: SAP was introduced in cement mass proportions between 0.3 and 1.0 % by weight of cement.

- dosage of extra water

The necessary amount of water to be added and considered as IC water was established by acknowledging amount of water needed for IC using Powers' model (see Appendix D), on one hand, and that needed to compensate workability loss due to the absorption of mixing water by a given amount of SAP, on the other hand. That is also to say, the selfsame spread of control mixture and UHPC containing both IC variables, i.e. SAP and extra water was aimed

at. The approach has an obvious benefit, particularly, the researcher's ability to assess SAP absorption in concrete, details of which will be clarified in Section 4.2.2.

3.2.4 Mix modifications

Two mix modifications were applied to both groups of concretes studied.

- modification 1

The major alteration was **introduction of internal curing** or, as intended for comparison reasons, one of its elements i.e. either pure SAP or extra water. Unlike the widespread manner of formulating the composition of internally cured concrete, where some part of aggregates of one or more kind is removed in order to maintain original paste content constant (e.g. see [Mec 06] for latter), rival and more practical approach was followed. In particular, both SAP and extra (curing) water or, alternatively, one of the two of variables was added as new components to the concrete mix. In other words, they were put 'on top' of original mix composition, hence the name given: 'on top' approach. This meant that volumetric fractions of ingredients in 1 m³ underwent some reduction, however, mutual proportions including relation to cement mass remained unchanged, see Appendix C and Section 3.2.5, respectively.

Even though above-mentioned approach was not perfect, for fair interpretation of IC effects, it appeared to be more appropriate solution to use. The number of arguments gathered in the short review given in Table 3.3 does in fact show this very clearly.

Table 3.3: Short analysis of different aspects related with 'on top' approach.

Action	Impact[1]	Brief description of the gist and problem solution (if necessary)
Addition of new components	-	Volume of the concrete's shrinking part decreases with every increase of IC variables. On the other hand, because 'on top' approach is used, the degree of internal restraint is largely fixed and thus allows easy elimination of effect caused by original mixture modification with IC. To make comparison fair, the corresponding result for the mixture without IC would only need to be rescaled for the amount of cement, and, consequently, other ingredients equivalent to mixture with IC (i.e. assuming neglected part undergoes no shrinkage).
Maintaining basic ingredient of the mix in their original mutual proportions	+	Degree of internal restraint (attributed to aggregates and perhaps unhydrated cement cores as well as some hydrates) is preserved when 'on top' approach is applied.

Continued of the following page

Table 3.3: Short analysis of different aspects related with 'on top' approach *(continued)*.

Action	Impact[1]	Brief description of the gist and problem solution (if necessary)
Maintaining basic ingredients of the mix in their original mutual proportions	+	Because paste/aggregate interfacial zone can occupy significant part of total cement paste volume in typical concrete (other than UHPC though!), there would be an ease of water transfer between the cement paste/aggregate interfacial zone and the bulk phase, e.g. [Hal 95][Sch 07b]. A small variation in aggregate content such as 5 % for aggregate fraction 50-60 % could change percolation of such zones and thus impact the permeability. With 'on top' approach, however, initial permeability very likely remains unchanged.
	+	Assuming all extra water has been absorbed by SAP, in 'on top' approach, each particle remains covered with selfsame paste and water film thickness. This does not hold true for the alternative approach, see Section 4.2.2 for more details.
	+	Additionally to providing internal restraint, aggregates of any specific surface area or absorption can be involved in various processes related to shrinkage as well as basic cause of its origin in autogenous conditions (hydration). In theory, this involves aggregate shrinkage [Hyo 13] and stimulation of hydration [Haa 75][Tas 98][Mou 11][Rah 12]. By applying 'on top' approach this issue is not a concern.
	+	Because no aggregates are removed in 'on top' approach, there is no interference into secondary phenomena which may affect concrete's workability, ball-bearing phenomenon for instance. This would be of paramount importance given absorption of IC agent can be estimated from consistency measurement (cf. Section 4.2.2).

[1] refers to effect on interpretation precision; could be positive (+) or negative (-)

Important decision made in the framework of modification regarded execution of the IC-incorporating mix design in practice. Of the two possible manners of polymeric admixture introduction, dry application and homogenization of SAP with other dry ingredients was preferred. This meant that the extra water had to be introduced separately, the moment for which was shifted towards wet mixing and involved blending with other wet components to be added beforehand (note that the same solution was also applied when no SAP addition was planned). The basis for such decision was the success of uniform distribution of SAP porosity in rival composition of UHPC studied by the author [Dud 06] and only one study [Lam 05] showing otherwise i.e. poor dispersion of quality-equivalent IC agent. It has been assumed that it is the usage of very low w/c and high superplasticizer content as well as fines, and, consequently, high viscosity that secures preferable distribution of the SAP particles in UHPC. As experience shows, pre-saturation of SAP with tap water prior to mixing clearly fails in this respect, see [Wan 09]. If so, neither alternative approach becomes option for UHPC, for which best possible packing of ingredients is at origin of improvement of mechanical properties, nor could the IC effect be fairly quantified.

Important enough, it must be borne in mind that only on addition in 'dry configuration', there was guaranteed control over IC agent's sorption behaviour. All other reasons aside, this would not hold true in case of the alternative approach due to change of pH. As in such case the pH changes abruptly from lower value (that of distilled or tap water absorbed by SAP) to higher one (immersion of swelled polymer in pore solution), there would be considerable partial release of the fluid carried, in analogy to result showed in Figure 3.2 or the similar study result on pure SAP by Pourjavadi et al. [Pou 13]. Meanwhile, only some of the water deposed of could be absorbed back under the new circumstances. This argument finally prevailed on implementation method chosen.

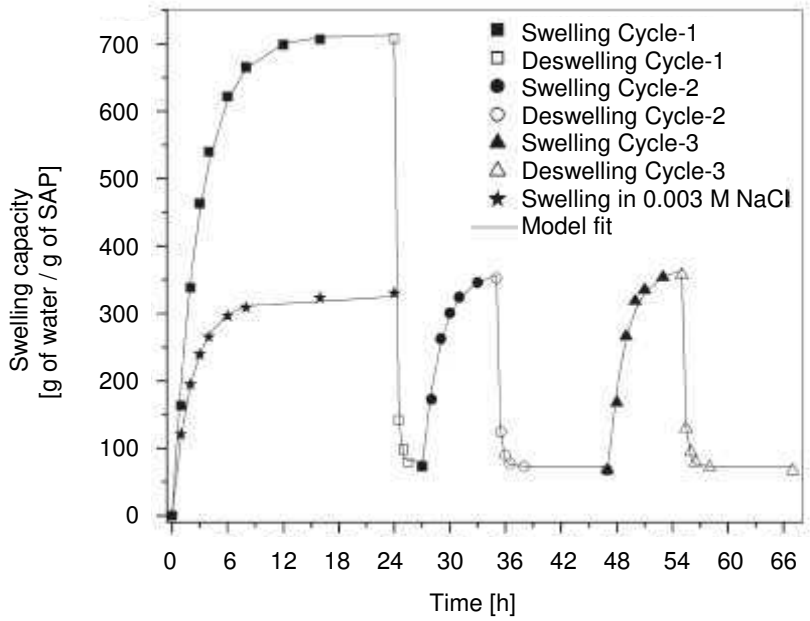

Figure 3.2: Swelling response of an exemplary superabsorbent polymer to cycles of immersion in distilled water and, subsequently, in saline solution in comparison to behaviour after single swelling in the latter, after [Shu 11].

- modification 2

The original M2Q and B5Q were proposed as fibre-incorporating versions of UHPC. In own experiments, however, the **fibre reinforcement was removed for majority of finely grained UHPCs tested** and some of mixtures containing coarse aggregates. This modification was motivated by number of problems related to usage of fibre, largely discussed in [Epp 10].

Usage of steel fibres is challenging for at least two more reasons. Certainly and despite opinion of some researchers [Bon 97], fibres are critical component of UHPC as they play fundamental role mitigation of autogenous shrinkage, see review in Appendix B. The success, however, very much depends on the fibre orientation. Without measures to control reinforcement alignment, being even more difficult for UHPC with coarse aggregate [Cwi

08], it seemed reasonable to exclude fibres from the mix. Only doing so, separation of potential effect of fibres from the one ascribed to IC was possible. Be that as it may, for sake of argument, few mixtures containing steel fibres were tested as well, this including mixtures varied by the presence of coarse aggregates and IC, see UHPCs having additional "f" in their labels in Table 3.4 and 3.5 (to follow).

Whenever the second modification was executed, change in concrete composition analogous to that exerted by inclusion of extra water was attained. Speaking about details, upon elimination of fibres the rest of components increased in content, however, with no change to mutual proportions.

3.2.5 Mixture compositions

Tables 3.4 and 3.5 list the compositions of all finely grained and coarse-grained UHPCs studied. It should be noted that the mixtures have been labelled. In particular, designations address the group of mixtures ("F" for finely grained and "C" for coarse-grained UHPC), reveal the presence of fibres (additional "f"), indicate special production conditions ("vac" for usage of mixer with vacuum unit; "mm" for usage of mortar mixer), signalize change in superplasticizer content ("sp var") and show correspondence to the particular amount of SAP and extra water implemented (comma-separated values after "S" in reference to cement mass; "R" is for reference mix which is either control mix or mix with extra water with content again given after comma).

Thirty mixtures from twenty four compositions were evaluated in total, although not all mixtures were examined in all tests. The major group of mixes studied was finely grained UHPC devoid of steel fibres. It included three control mixtures, i.e. with no SAP and extra water (F-R = F-R-vac = F-R-mm), and fifteen concretes with varied amount of IC variables (F-S.4, F-S.4-sp var, F-S.3.04=F-S.3.04-vac, F-S.3.045, F-S.3.05, F-S.4.06 = F-S.4.06-mm, F-S.4.065, F-S.4.07, F-S.6.08 = F-S.6.08-mm, F-S.6.085, F-S.6.09, F-S.1.0.16). Another five fibre-free mixes contained no polymers but did include extra water in amount equivalent to some SAP-enriched compositions (F-R.04 = F-R.04-vac, F-R.07, F-R.07-sp var, F-R.08) including one with reduced superplasticizer content (F-R.07-sp var). Eventually, three mixtures were studied with fibres present, viz. a new control mix (Ff-R) and two internally cured concretes (Ff-S.3.0.4 and Ff-S.4.07).

Table 3.4: Mass proportions of finely grained UHPC studied in relation to cement in order of increasing w/c.

Mixture	Cement c	Silica fume sf	SAP	w_{IC}	w_{mixing}	w_{total} [1]	$w_{total,eq}$ [1, 2]	Fine aggregate[3]	Coarse aggregate	Steel fibres f	Superplasticizer
F-R / F-R-vac / F-R-mm	1	0.16	-	-	0.20	0.22	0.19	1.42	-	-	0.04
Ff-R	1	0.16	-	-	0.20	0.22	0.19	1.42	-	0.23	0.04
F-S.4	1	0.16	0.004	-	0.20	0.22	0.19	1.42	-	-	0.04
F-S.4-sp var	1	0.16	0.004	-	0.20	0.27	0.23	1.42	-	-	0.10
F-R.04 / F-R.04-vac	1	0.16	-	0.04	0.24	0.26	0.23	1.42	-	-	0.04
F-S.3.04 / F-S.3.04-vac	1	0.16	0.003	0.04	0.20	0.26	0.23	1.42	-	-	0.04
Ff-S.3.04	1	0.16	0.003	0.04	0.20	0.26	0.23	1.42	-	0.23	0.04
F-S.3.045-mm	1	0.16	0.003	0.045	0.20	0.27	0.23	1.42	-	-	0.04
F-S.3.05	1	0.16	0.003	0.05	0.20	0.27	0.23	1.42	-	-	0.04
F-R.07-sp var	1	0.16	-	0.07	0.27	0.28	0.24	1.42	-	-	0.01
F-R.07	1	0.16	-	0.07	0.27	0.29	0.25	1.42	-	-	0.04
F-S.4.06 / F-S.4.06-mm	1	0.16	0.004	0.06	0.20	0.28	0.24	1.42	-	-	0.04
F-S.4.065	1	0.16	0.004	0.065	0.20	0.29	0.25	1.42	-	-	0.04
F-S.4.07	1	0.16	0.004	0.07	0.20	0.29	0.25	1.42	-	-	0.04
Ff-S.4.07	1	016	0.004	0.07	0.20	0.29	0.25	1.42	-	0.23	0.04
F-R.08	1	0.16	-	-	0.28	0.30	0.26	1.42	-	-	0.04
F-S.6.08 / F-S.6.08-mm	1	0.16	0.006	0.08	0.20	0.30	0.26	1.42	-	-	0.04
F-S.6.085-mm	1	0.16	0.006	0.085	0.20	0.31	0.26	1.42	-	-	0.04
F-S.6.09-mm	1	0.16	0.006	0.09	0.20	0.31	0.27	1.42	-	-	0.04
F-S1.0.16	1	0.16	0.010	0.16	0.20	0.38	0.33	1.42	-	-	0.04
vol.-%	Total volume reduced by volume of w_{IC}; individual change in content proportional to mass of c										

[1] includes water from superplasticizer (65 %) and for IC
[2] in reference to mass of binder = c+sf
[3] includes quartz sand (1.17) and quartz flour W12 (0.25) combined

The second group of investigated mixes, coarse-grained UHPCs, included two primary control mixes (fibre-free C-R and fibre-containing Cf-R) and two mixes including selfsame amount of SAP and extra water (fibre-free C-S.3.04 and fibre-containing Cf-S.3.04).

Table 3.5: Mass proportions of coarse-grained UHPC studied in relation to cement.

Mixture	Cement c	Silica fume sf	SAP	w_{IC}	w_{mixing}	w_{total} [1]	$w_{total,eq}$ [1, 2]	Fine aggregate[3]	Coarse aggregate	Steel fibres f	Superplasticizer
C-R	1	0.27	-	-	0.24	0.27	0.21	1.25	0.92	-	0.05
Cf-R	1	0.27	-	-	0.24	0.27	0.21	1.25	0.92	0.30	0.05
C-S.3.04	1	0.27	0.003	0.04	0.24	0.31	0.25	1.25	0.92	-	0.05
Cf-S.3.04	1	0.27	0.003	0.04	0.24	0.31	0.25	1.25	0.92	0.30	0.05
vol.-%	Total volume reduced by volume of w_{IC}; individual change in content proportional to mass of c										

1 includes water from superplasticizer (65 %) and for IC
2 in reference to mass of binder = c+sf
3 includes quartz sand (0.54), quartz flour W12 (0.50) and quartz flour W3 (0.20) combined

3.2.6 Production and preparation of samples (mixing, casting, curing)

i) Mixing procedures

Concrete that has poor workability is hardly considerable as UHPC. Common experience shows that not only the composition of material but also the mixing procedure can have decisive influence on the final product quality. Since SPP 1182 project start, however, no standard manner of manufacturing UHPC existed. Accordingly, much effort has been devoted to development of own mixing procedure.

In the optimization process, different aspects were taken into account. Firstly, concrete compositions as well as attributes of mixing equipment available were analysed. Secondly, own experience in field of UHPC production [Mec 06][Dud 08], knowledge gained by Priority Program 1182 partners as well as in rival laboratory research on UHPC (e.g. [Ma 04]) was made use of. Lastly, power consumption during mixing was monitored on-line.

Regardless whether internal curing was considered or not, it was intended to develop selfsame mixing regime that would also reflect typical order of mixing steps in production of self-compacting high-strength cementitious materials. The decision whether particular mixing regime was used or not was eventually based on slump flow, air content value as well as visual observations made on the fresh mix. Decision finally included compressive strength value obtained after the concrete matured to the age of 28 days.

In result, three mixing regimes including two for one mixer type were utilised to manufacture UHPC. In common to all (Table 3.6-3.8), the fluidisation of mixture was obtained by superplasticizer in two steps, following suggestion of Morin et al. [Mor 01]. The mixing time from the moment of water addition was furthermore maintained less than 10 minutes, which is common and, at the same time, sufficient time for production of high-performance material. The total mixing time of fine and coarse-grained concretes, longer for the former group, was only extended when the inclusion of fibres was foreseen.

Table 3.6: Mixing programme used for production of finely grained UHPC by means of high intensity mixer.

Action	**Duration [s]**	**Speed of mixing [m/s]**	
		Bowl / Drum	**Whirler / Agitator**
Addition of quartz sand and silica fume	Not defined	0.1	0.6
Homogenization	120[1]	0.5	5.0
Addition of remaining dry ingredients incl. SAP (if applicable)	Not defined	0.1	0.6
Homogenization	120	0.5	5.0
Addition of total water and 50 % superplasticizer (mixed together prior to procedure)	Approx. 45	0.5	5.0
Homogenization	120	0.9	5.0
"Pause" (mixing with minimal velocity)	120	0.1	0.6
Addition of rest of superplasticizer	Approx. 45	0.1	0.6
Mixing with moderate speed	10	0.9	1.5
Mixing at higher speed	150	0.9	6.4
('Final') mixing	60	0.9	1.3
Addition of fibres, if applicable	Approx. 120	0.7	1.3
Final mixing with fibres	60	0.9	3.9
Total mixing time from water addition	**550 s (no fibres) or 730 s (with fibres)**		

[1] time which sometimes had to be varied from batch to batch in order to remove silica fume assemblies

Which type of mixer, and in consequence which type of mixing procedure, was used, this depended on volume of concrete produced. For purpose of main investigations and batches of concrete between 25 and 28 litres, a high intensity mixer known as EIRICH R05/T mixer, was used. The main attributes of particular mixer are: an inclined motor-driven mixing drum, specific frequency ranging 4.5 and 90 Hz and power between 1 and 11 kW. The corresponding mixing regime for finely grained and coarse-grained UHPC is given in Table 3.6 and 3.7, respectively.

Table 3.7: Mixing programme used for production of coarse-grained UHPC by means of high intensity mixer.

Action	Duration [s]	Speed of mixing [m/s]	
		Bowl / Drum	Whirler / Agitator
Addition of basalt, quartz sand and silica fume	Not defined	0.1	0.6
Homogenization	60	0.5	5.0
Addition of remaining dry ingredients incl. SAP (if applicable)	Not defined	0.1	0.6
Homogenization	60	0.5	5.0
Addition of total water and 50 % superplasticizer (mixed together prior to procedure)	Approx. 45	0.5	5.0
Homogenization	120	0.9	5.0
"Pause" (mixing with minimal velocity)	120	0.1	0.6
Addition of rest of superplasticizer	Approx. 45	0.1	0.6
Mixing with moderate speed	40	0.9	1.5
Mixing at higher speed	50	0.9	6.4
("Final") mixing	60	0.9	1.3
Addition of fibres, if applicable	Approx. 120	0.7	1.3
Final mixing with fibres	60	0.9	3.9
Total mixing time from water addition	**480 s (660 s with fibres)**		

In case of supplementary investigations on fibre-free finely grained concretes, such as rheological tests (discussed in Section 4.2.3), usage of mortar mixers for production of volume as small as < 5 l became necessary as well. For the purpose, the middle scale paddle mixer called Hobart NCM20 was engaged. This apparatus allows three ranges of paddle rotations and work at the frequency of 50 Hz, with maximal power being established at 0.37 kW.

Because the possibility of establishing a homogenous flowable UHPC from fine materials was technologically limited by mortar mixers, e.g. mixing energies insufficiently counteracted the agglomeration of raw binder material, a premix of dry ingredients was prepared at first. This step forced usage of EIRCH R05/T mixer, the final dry product of which was sealed in plastic bag and kept in closed bucket until the day of utilization. In doing so, technical limitations of equipment could be neglected while a reproducible workability of concrete comparable to that obtained from EIRICH mixer was possible to attain. The corresponding mixing regime is given in Table 3.8. Speaking about details, it reminds the one used for the high intensity mixer with small correction on the velocities of mixing tool and duration of particular steps. Another major difference is shortening of mixing time. Again, the total mixing time matched with objective of study i.e. did not exceed 10 minutes.

Table 3.8: Mixing programme used for production of finely grained UHPC by means of mortar mixer.

Action	Duration [s]	Mixing gear	
		Bowl / Drum	Whirler / Agitator
Secondary homogenization of premix	60	-	I
Addition of total water and 50 % superplasticizer (mixed together prior to procedure)	Approx. 30	-	I
Homogenization	60	-	II
Further mixing at higher speed	120	-	II
"Pause" (stopping the mixer, scrapping off material from walls of the bowl)	120	-	0
Addition of rest of superplasticizer	Approx. 30	-	I
Mixing at highest speed possible	90	-	III
Final mixing	30	-	I
Total mixing time from water addition	**480 s**		

Since none of the mixing equipment possessed ability of mix de-airing, some compositions of finely grained UHPC without fibres had to be produced with usage of mixer belonging to a project partner, TU Munich. When applicable, mixes of 3 litre volume were manufactured by means of high intensity mixer R02 Vac, being another product of EIRICH company but possessing additional attributes. This involved additional and modernized elements viz. vacuum unit attached to mixer, smaller mixing drum and finally different shape of agitator when compared to the model R05/T. Already developed mixing regime adjusted to particular equipment and having verified applicability to UHPC production was used, see Table 3.9.

Table 3.9: Mixing programme for production of finely grained mixtures in collaboration with TU Munich.

Action	Duration [s]	Speed of mixing [m/s]	
		Bowl / Drum	Whirler / Agitator
Addition of all dry ingredients incl. SAP (if applicable)	-	0	0
Homogenization	60	0.5	3.6
Addition of total water and 50 % superplasticizer (mixed together prior to procedure)	30	0.5	3.6
Homogenization	60	0.5	7.3
"Pause" (stopping the mixer)	120	0	0
Addition of rest of superplasticizer	30	0.5	3.6
Homogenization and de-airing by underpressure of 100 mbar	60	0.5	7.3
Release of underpressure and mixer emptying	-	0	0
Total mixing time from water addition	**300 s**		

ii) Casting and placement procedure

As commonly revealed in its properties in hardened state, UHPC is more sensitive to the casting procedure used than ordinary concrete. Indeed, despite significant improvement of concrete workability at low w/c and high binder content, self-compaction is still desired and uncommon property for the finely grained compositions. Rather, this type of UHPC, due to high superplasticizer content, appears as sticky and far from requirement set for "ideally" compacting concrete.

Application of compaction was one crucial issue to consider when casting specimens. As such, this approach neither falls in definition of particular concrete nor is easy to execute. The study of Schachinger et al. [Sch 04] discussed the latter aspect in-depth and pointed out specific type of equipment that is only able to fulfil the demand; as emphasized, these are typically vibrators not usual in concrete construction. Own preliminary studies on fibre-free finely grained UHPC shed new light on the aspect. It was revealed that if the compressive strength level is a criterion for compaction success and standard laboratory vibrating is used, one course of changes is hard to find. Simultaneously, there was no significant effect on porosity of UHPC, especially in the range of smallest pores as measured by MIP. To comprehend this, one has to keep in mind that high viscosity of mixture leads to twofold effect: entrapment of technological air pores (which is inevitable on level of mixing unless mixer is equipped with vacuum unit, but largely avoidable on level of concrete placement) and general restriction to mixture de-airing. In view of these facts, no additional compaction was considered, this being also in agreement with idea behind development of and requirements for UHPC.

Three further arguments speaking against usage of compaction were eventually taken into account. In past, compaction by vibration was acknowledged to affect alignment of fibres or even cause their sedimentation [Sch 04]. This, from perspective of potential effect on autogenous shrinkage and its rival character compared to that of internal curing puts application of particular solution in question. It may be furthermore expected that on vibration, larger SAP particles are possibly separated and may float to the surface [Lur 08a], and so affect effectiveness of internal curing too. Eventually, it is recognized for high performance concrete that vibration may only lead to some reduction of yield stress but not plastic viscosity [Hu 96], meaning that sticky consistency restricting air voids from escape would remain.

Figure 3.3: Flow funnel used during casting of specimen.

Due to the abovementioned reasons, utilization of additional vibration was not considered for the main studies. Instead, as signalized in foregoing section, in all investigations it was aimed to produce mixtures as closest to self-compacting type as possible. Then the freshly mixed concrete was allowed to flow in custom-built and, prior to usage, moisturized C-shaped funnel, see Figure 3.3. With its help, every mould supplemented with wooden collar was filled always from one side and continuously until excess layer of 15 mm was formed. This part of concrete was removed at moment when self-invoked de-airing had finished. This always took place before mix lost its secured flowability (being not longer than 20 minutes from casting). On one hand, the author was aware that such procedure is not typical for UHPC and normally would be difficult to complete on a large scale cast. On the other hand, since the study was performed on laboratory scale and only small samples were set to be produced, it served as sufficient solution to deal with problem of high stickiness of the mix. The proof of appropriateness of this particular approach was eventually compressive strength of concrete at 28 days on cubes with side length of 100 mm. The ultra-high level was obtained irrespectively whether steel fibres were used or not.

One exception from the procedure were mixtures produced with vacuum unit. These mixtures were, in addition to specific mixing regime and after each of two filling layers, heavily vibrated. For the action, a standard vibrator as standardized for production of cement paste or mortar was used. Any pores that appeared on the concrete surface were made to collapse by means of a needle with sharp ending, the action which finished casting procedure.

iii) Curing and storage procedure

Another important element in UHPC specimen production is curing procedure. In major part of the study, it was intended to evaluate the pure internal curing effect, i.e. without impact of the ambient atmosphere. Therefore, unless specified otherwise, all specimens after casting were secured from evaporation as well as water ingress. For this purpose, combination of cover made of thick PCV, moist burlap and at least one layer of plastic foil was applied to

every mould. In subsequence, the standard curing conditions were applied, i.e. temperature of 20 °C and relative humidity of 65 %.

After first 24 hours, the specimens were de-moulded and, if not transported for sample preparation or testing, were wrapped in few layers of plastic foil. Any potential desiccation to ambient was finally prevented from by placing the sealed specimens in PCV box. Meanwhile, the ambient curing conditions remained unchanged.

In case of specimens produced with vacuum, the one alteration processed regarded mould cover which was limited to plastic foil only. No moisture migration was however expected as moulds were subsequently stored under 20 °C and even higher relative humidity of min. 90 %. The selfsame proceeding with specimens at the age of 24 hours as described above then followed.

3.3 Test methods and procedures

3.3.1 SAP material characterization

The choice of SAP suitable/optimal for IC purpose was crucial to current study. Such material was found using the pragmatic approach, see Section 3.2.3. It was the only reasonable solution given that no recommendations or guidelines on choice or testing SAP in terms of IC applicability were proposed to date.

As next step, it was intended to identify these properties which could have led to successful utilization of material selected for curing of UHPC. With regards to the SAP material only, the belief was this should be related especially with these features of material which take control over its sorption behaviour, and which, as reviewed in Section 2.5.1, could be numerous. Luckily, any of these features could be examined using methodology known from field of hydrogel testing, e.g. in form of norms provided by World Strategic Partners [WSP 11] or protocols proposed in literature, including [Pó 94][Buc 98][Sta 02][Zoh 08]. It was decided to make use of most relevant tests meanwhile simplifying the procedures to highest extent with simultaneous adjustment of the available equipment. The final validation of material suitability was eventually provided after application in concrete using non-destructive testing.

In total, three different groups of tests conducted and involving both physical and chemical analysis can be distinguished.

- group 1

Firstly, the SAP selected was investigated for associated physical properties using typical analytical laboratory apparatus. Tested first, **particle size distribution (PSD) of SAP** was examined by means of laser diffraction applying PSD analyzer. Information acquired served as rough estimate of pores to be expected from accommodation of SAP in concrete (assuming particle of average size growth of 2 to 3 times [Dud 08b]) and, more importantly, was used as input data to determine average absorption capacity of SAP based on hardened concrete porosity inspection.

Morphology of dry SAP particles, the second property evaluated, was studied under Environmental Scanning Electron Microscopy (ESEM), see Section 3.3.6 for details. The state of material in examination was ‘as delivered’. Although assuming dry presence, to stay

on the safe side, the **true moisture state of material** was tested as well, which was executed by oven drying at the temperature of 40 °C.

Last property, **density of dry SAP**, was found by means of helium pycnometry and with test apparatus alike in total porosity estimation, see Section 3.3.6.

- group 2

Secondly, the SAP applied was tested for the **quality**. In the test [Dud 08a] referred hereafter as swelling test, the features of main interest were **polymer stability and particle dispersibility after absorption of one of the aqueous solutions considered**. In the procedure, small but constant quantity of polymer (0.5 g) was gradually added while mixing of a fixed amount of liquid on interest (100 ml) in a graduated laboratory vessel. In subsequence of the stirring, the visually observed material behaviour was characterized and presence of unfavourable phenomena (tendency to form clumps, gel-blocking, ...), if any, was reported. This was repeated few times within next 48 hours, during which the vessel remained free of contact with ambient environment to avoid mixing with carbon dioxide.

Two radically different aqueous solutions (so-called swelling media) were used. One was distilled water known of having neutral pH and the other one was pore solution. The latter provided highly ionic environment (pH of approx. 13) and was obtained as filtrate from dissolution of cement used for production of UHPC in overwhelming quantity of tap water (mass proportions c : w= 2.5 : 13) to simulate conditions in fresh concrete.

In **light microscopy tests on swelled material** that followed, the foregoing visual observations were confronted with corresponding evidence under camera. The selfsame batch of material or one produced extra was used.

For more in-depth SAP surface inspection that would allow **detection of porosity, cracks and skin formation**, ESEM was engaged. The samples were prepared in two steps. Absorption of one of the liquids until maximum absorption occurred was executed first. The swelling media contacted with were distilled water and paste filtrates, extension of which included combining cement and silica fume in proportions used in finely grained UHPC mixtures, with or without combination with superplasticizer (note: the selfsame type of material used). Subsequently, desaturation using either freeze-drying or gentle drying at 40 °C

until mass constancy, was applied. Samples delivered in such state were tested in the dry mode and EDX analysis of most interesting newly emerged elements followed.

Swollen gel strength was another important property investigated. In general, execution of rheological measurements or testing absorption under load appear as the most attractive approaches in this respect, see e.g. [Zoh 08]. However, the same property could be followed in indirect manner by observation of physical features of the material before and after it absorbed the liquid of interest. This approach was adapted. Material was assumed to have good gel strength once remained geometrically stable shape with sharp edges and corners, i.e. it was not soft, loose or slimy. In addition to this, the well-accepted 'assessment by observation and feeling' [Pó 94] with modification was applied. In particular, the gel strength was traced by pressing the swelled particles, at best single particle, between the fingers and the global material response to the load was noted. Afterwards, the polymer was analysed under light microscope. It was assumed that material unable to survive this kind of load exerted cannot behave better in case of high shear and load occurring in production of concrete. The same procedure was repeated few times within 48 hours.

The test that finalized qualitative description was **assessment of the spatial homogeneity of SAP**. Two transparent receptacles were placed on top of text pattern, with one containing one layer of dry SAP material on the bottom. Both were sprinkled with distilled water. After SAP attained the maximum absorption, the appearances were compared. Presence or lack of transparency was noted.

- group 3

Thirdly, the IC agents underwent quantitative analysis. Investigated first, **the free absorption capacity and kinetics of absorption of SAP** in environment of one of two main aqueous solution considered were assessed using tea-bag method [Dud 08a][Zoh 08][Gor 11]. As indicated in Appendix E, though not being free of certain drawbacks[20], particular technique was chosen taking into account the standardization documents (e.g. [WSP 11]), its efficiency and suitability aspects for small amount of tested SAP [Zoh 08], as well as good if not excellent swelling kinetics comparability with other methods of testing absorption without load. The method operates somewhat inverse to Darr method. In the particular procedure

[20] Because as for SAP the particles of material tested were relatively large, it was assumed that content of capillary fluid remaining between them limited to some very little value. Accordingly, the drawback that could affect result was largely eliminated.

adopted and improved [Dud 08a][Gor 11], the prewetted gauze-like bag of known weight was filled with fixed (0.2 g) amount of SAP in the original collapsed state. After having the particles distributed evenly at the bottom, the bag was immersed in a beaker full of fluid of interest. In following, the set-up was covered with plastic sheet to avoid carbonation of the liquid. Once the measurement time was attained, this being set at 30 s, 2, 5, 10, 15, 30, 60, 180 min and additionally 24 and 48 hours from the contact made, the tea-bag was withdrawn and any excessive moisture remaining on the its surface was removed. This involved putting the bag on dry cloth and wiping it with another piece of dry material within 30 s. Knowing current mass of tea-bag, the absorption or swelling could be calculated according to Eq. 3.1:

$$S = \frac{\left(m_{tb+SAP,moist} - m_{tb,moist} - m_{SAP,dry}\right)}{m_{SAP,dry}} \tag{3.1}$$

where $m_{tb+SAP,moist}$ is the weight of tea-bag incorporating swollen SAP at testing time t, $m_{tb,moist}$ is the weight of the saturated tea-bag, and $m_{SAP,dry}$ is the weight of SAP in collapsed state, with all masses recorded with precision 0.0001 g.

Three consecutive tea-bag tests per each aqueous solution considered were performed at room temperature. The average is reported.

To determine the **sol (= mobile polymer segments) fraction**, SAP in state 'as delivered' was first dried in oven at the temperature of 40 °C to a constant weight. The dried sample was then sieved into different fractions. The part of material which particles' diameters were larger than the size of filters' perforations to be applied was withdrawn. In next step, suitable pre-dried filter was chosen and its mass with and without sample of known mass (approx. 0.8 g) was measured. Both became soaked into excessive amount of distilled water filling a beaker and the latter was covered immediately afterwards. During next three days, the swelling medium was replaced with fresh one three times. Aiming at the same goal, i.e. removal the any free substances from the gel, the sample was occasionally shaken. Following repeated drying at 40 °C, the final weight was measured and the sol fraction was obtained using Eq. 3.2:

$$Sol\ fraction = \left(1 - \frac{m_{final}}{m_{initial}}\right) \cdot 100\% \tag{3.2}$$

where $m_{initial}$ is the initial mass of SAP after first drying and m_{final} is the mass of SAP after removal of soluble fraction and final drying, with all masses recorded with precision 0.0001 g.

Eventually, the **behaviour of SAP while deswelling** was tested after introduction to concrete by means of non-destructive test. Microfocus X-ray system called FCTS 160-IS located at the Technische Universität Dresden and of configuration showed in Figure 3.4 has been employed in the experiment. Particular apparatus is highly resolving computer tomograph consisting of 160 kV microfocus X-ray tube (its X-ray energy source/source of radiation) and Z250 tension/torsion testing machine from Zwick/Roell. The CT is fit for in-situ measurement in tension, compression and torsion, therefore uses additional to ones set for this study. In the non-traditional arrangement allowed, and being more typical for medical use, the sample is fixed and the tomography rotates, which secures from any movement or vibration of the former during performance of scan. Other important part of CT is the high dynamic flat panel detector used to record images of the analyzed sample to reconstruct the object's internal structure.

Figure 3.4: X-ray computer tomograph used (to the left) and the test sample i.e. hardened sealed UHPC with IC in the mould (to the right). The sample is obtained by pouring fresh concrete into a transparent syringe and, subsequently, sealing it at top and bottom openings.

Scans were taken on small cylindrical sample (diameter of approx. 16 mm, see Figure 3.4 right) which was prepared 10 hours prior to delivery to the testing facility. This time was specifically chosen taking into consideration approximate time of time-zero occurrence, on one hand, and, since the measurement start had to be controlled manually, the first possible working time for performing the CT scan, on the other hand. The size and shape of the

specimen resulted from pouring of fresh concrete into syringe made of PE or similar material, which was chosen based on preliminary studies. After the sample was casted, the main surface exposed to drying was sealed using two types of tape (common isolation tape and self-adhesive aluminium tape) to limit the contact of fresh concrete with glue and therefore to avoid potential reaction between the two as well as to avoid evaporation. Both casting and storage temperature until testing were the same, in particular 20 °C.

Owing of the fixation ability, the same sample was used in all measurements conducted at the concrete age of 10.5, 13.5, 18.5 and 34.5 hours. For each scan, 1350 projections were registered with total exposure time for each projection 1250 ms and with an angle step of 0.2°. This in combination with properties of plat panel detector (viewed image size of 3200 x 2300 pixels with a pixel size of 127 µm) and microfocus X-ray tube (focal spot of 3 µm) enabled one high resolution scan to be obtained in less than 30 minutes. The short exposure times, similarly to using sample of limited cross-section, ensured there was no significant heating of the concrete during acquisition of the samples. This was crucial point of whole investigation given hydration in UHPC is known to take place rapidly within first days of its life, and making information brought from long CT measurements of little value. Fulfilling this condition meant also that desorption of SAP was not attributed to other reasons than those resultant from cement hydration.

Each scan was performed with an accelerating voltage of 80 kV and a tube current of 70 µA. To enable easy comparison of changes occurred in one particular slice or its elements, the same scan parameters and image labelling/numbering were also utilized. The X-ray tube was constant 45 mm away from detector and the distance between X-ray tube and detector was maintained at 840 mm. This led to geometrical magnification of 18.5 and combined with the pixel size guaranteed the voxel size/geometrical resolution of approximately 7 µm, being well above the focal spot size. That is also to say, the features of smaller size were not visible in reconstructed images.

During the whole testing period and intervals between the measurements conditions in the self-contained room were quasi constant, with temperature of 30 °C. This means, there has been difference in heat delivered of about 10 K compared to laboratory environment. As a rule of thumb, this had no effect of scanning performed, unlike some (if any) influence on IC-related phenomena observed.

After obtaining the raw projections (radiographs), data was reconstructed into 14 bit 2D images (so-called slices) using VG Studio Max software. Subsequently, the 2D images obtained were analysed using Photoshop. Stacked up, the slices provided the reconstructed volumetric data of the scanned object.

3.3.2 Properties in fresh state

All tests aiming at evaluation of properties in fresh state were initiated soon after mixing.

In examination of **concrete consistence in terms of flowability**, being the first of workability properties tested, two conceptually similar measuring techniques having relation to yield stress were utilized. The first was a so-called mini-cone test following DIN EN 1015-3, which is a method commonly used for examining fresh mortars. Herein, it was applied to study the properties of finely grained UHPC acknowledging its mortar-like aggregate composition, but also of UHPC mixtures with coarse aggregate[21]. The apparatus is shown in Figure 3.4. In contrast to standardized equipment, a Haegermann cone was used but without flow table which was replaced by a base plate, altogether bringing about exclusion of jolting/beats during testing.

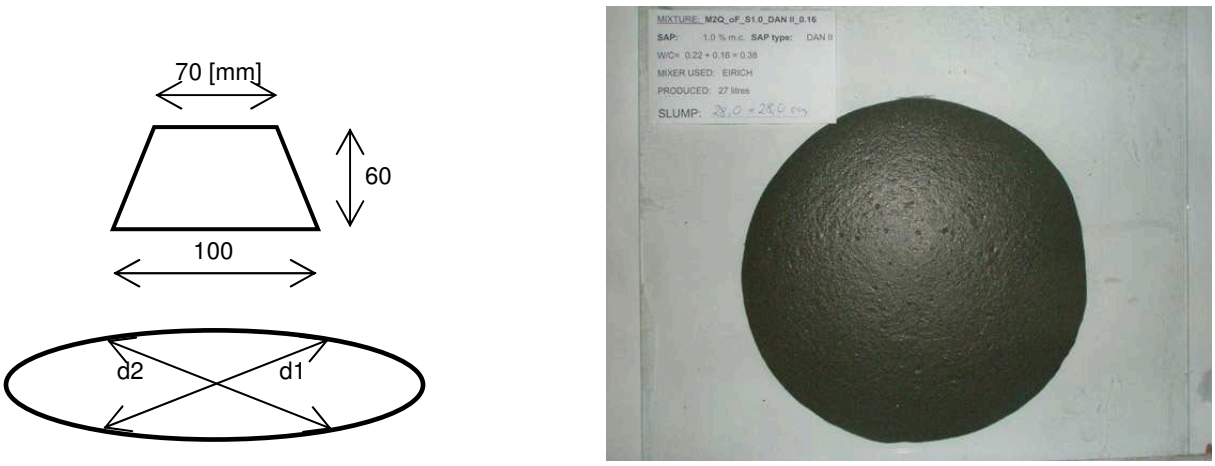

Figure 3.5: Details of testing equipment geometry and information record (to the left) and typical concrete cake obtained from the mini-cone test (to the right).

In parallel to the test or as the test alternative, some batches of both types of UHPC were studied using the larger and fully automatic custom-built set-up, see Figure 3.6. This apparatus was prepared so as to fulfil the requirements of DAfStb code of practice for self-

[21] It was taken into account the low number of coarse-grained UHPC mixtures tested and success of application in previous study on UHPC [Dud 08b].

compacting concrete [DAfStb 03] and method sometimes referred to as inverted slump flow test method. However, the blocking ring (so-called J-ring) was not used.

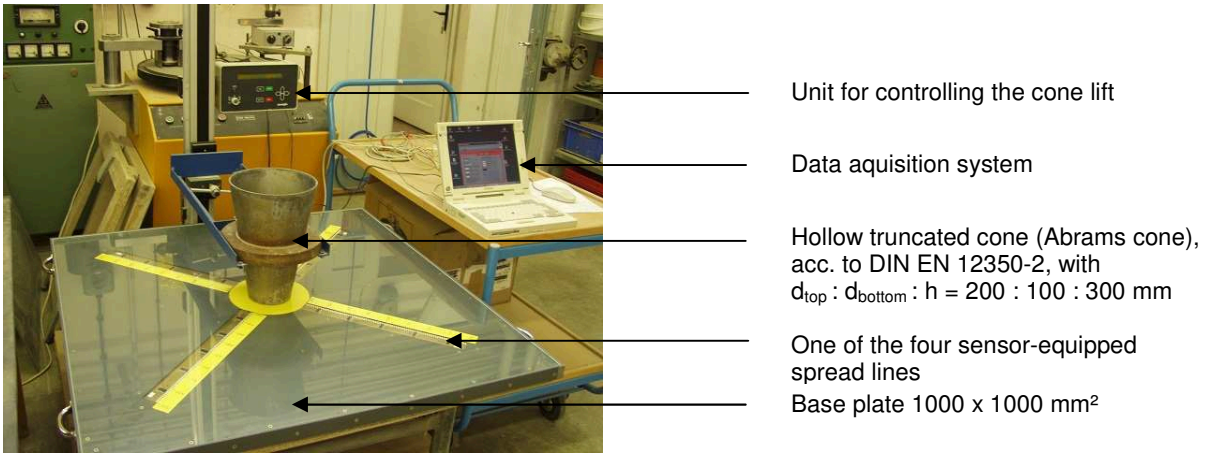

Figure 3.6: Custom-built set-up used in measurement of slump flow with large cone.

During the experiments, two testing conditions were applied. Main condition used for both kinds of tests is referred hereafter as 'moist', according to which the testing equipment was moisturized prior to testing. Such preparation step is intended whenever testing of a self-compacting concrete is considered, see e.g. [DIN EN 12350-8][DAfStb 03][EFNARC 02]. In the procedure, treatment with damp sponge was chosen to avoid the aquaplaning phenomenon. For comparison, the condition addressed as 'dry' was used as foreseen in DIN EN 1015-3 standard, i.e. using dry equipment. According to [Sta 04a], distinction between different states of moisture of the testing equipment might not be necessary for mixtures of high viscosity (therefore UHPC as well) since having little impact on slump flow results. However, this sometimes changes for viscous concretes containing fibres and depends on the type of fibre used. Thus in own study, second slump flow test using dry equipment was performed simultaneously, although mainly for the mini-cone test due to small amount of material needed for the test.

The tests were completed when no particular change of the slump-flow (= the flow spread) was recorded. Subsequently, the final value of spread was read and calculated either manually or automatically from the two perpendicular diameters of the concrete 'cake' obtained.

A visual observation was carried out on occasion of each test performed to determine the **potential for bleeding and segregation**. No other measures were taken in this respect.

The rheological behaviour of selected mixtures, that is which presented target slump-flow after production from one premix (i.e. matching to that of control mix), was studied by employing a concrete rheometer called HAAKE MARS II (Modular Advanced Rheometer System). This Thermo Electron Corporation product is a multicomponent device, the main removable and operational parts of which are measuring cell and a rotor, see. Figure 3.7. The former referred to as unit cell is internally ribbed with demountable longitudinal lamellas. The rheometer itself can operate under one of two main regimes, i.e. defined rotational speed/shear rate (so-called CR mode) or specified torque/shear stress (so-called CS mode); in return, it gives corresponding values of torque force/shear stress or rotational speed/shear rate, respectively. The manual control over apparatus is taken with help of software called RheoWin. With this tool, the test can be performed in one of the two modes, either rotational mode or oscillatory test. The selfsame software can be used for data processing as well.

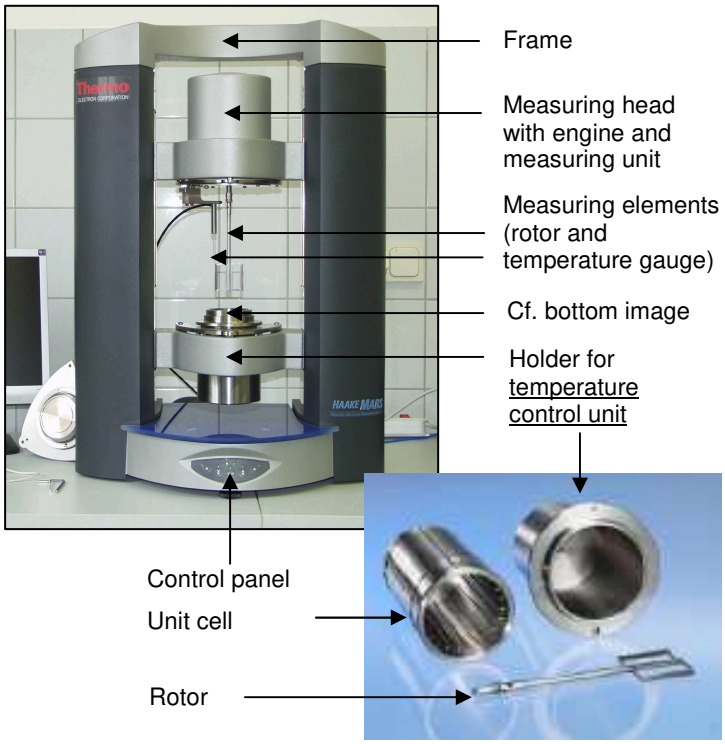

Figure 3.7: Rheometer test set-up.

Because distinction between the two test modes is important for rheological characterization, keeping the goals of study in mind, the experimental programme as given in Table 11 was set.

Table 3.11: Measuring profile for the rheological testing.

Segment	Mode type	Mode type	Duration [s]	Further settings
0	• Lift	•	•	• Setting the rotor in the measurement position
1	• Pre-shear	• CR-Time	• 30	• $\dot{\gamma} = 1.7\ s^{-1}$ (corresponding to $\Omega = 5.2\ [min^{-1}]$), 10 steps
2		• CR-Time	• 60	• $\dot{\gamma} = 0\ s^{-1}$, 10 steps
3	• Rotation (1st)	• CR-RS	• 120	• Controlled shear rate test, $\dot{\gamma} = 0 - 3.2\ s^{-1}$ (corresponding to Ω = 0-10 $[min^{-1}]$), 60 steps
4		• CR-Time	• 30	• Controlled constant shear rate $\dot{\gamma} = 3.2\ s^{-1}$ (corresponding to Ω = 10 $[min^{-1}]$), 10 steps
5		• CR-RS	• 150	• Controlled shear rate test, $\dot{\gamma} = 3.2 - 0\ s^{-1}$ (corresponding to Ω = 10-0 $[min^{-1}]$), 75 steps
6	• Oscillation	• CS-Time	• 45x60	• Oscillation time test, torque M = 0.5 [mNm], f = 1.0 [Hz], 90 steps
7	• Pre-shear	• CR-Time	• 30	• $\dot{\gamma} = 1.7\ s^{-1}$ (corresponding to $\Omega = 5.2\ [min^{-1}]$), 10 steps
8		• CR-Time	• 60	• $\dot{\gamma} = 0\ s^{-1}$, 10 steps
9	• Rotation (2nd)	• CR-RS	• 120	• Controlled shear rate test, $\dot{\gamma} = 0 - 3.2\ s^{-1}$ (corresponding to Ω = 0-10 $[min^{-1}]$), 60 steps
10		• CR-Time	• 30	• Controlled constant shear rate $\dot{\gamma} = 3.2\ s^{-1}$ (corresponding to Ω = 10 $[min^{-1}]$), 10 steps
11		• CR-RS	• 150	• Controlled shear rate test, $\dot{\gamma} = 3.2 - 0\ s^{-1}$ (corresponding to Ω = 10-0 $[min^{-1}]$), 75 steps

Generally speaking, to test effect of IC but also to trace change of rheological parameters, the test profile was composed of two identical rotational modes with separation by a mode of uninterrupted structure reconstruction. During both rotational modes, rather standard measuring sequence known more for cement paste was applied. This means, among other, execution of a so-called pre-shear (i.e. shearing at constant rate) before the main measurement. Such step and in fact stabilization time was necessary to reduce thixotropy effects on one hand and, as for first rotation, remove any traces of the UHPC characteristic elephant skin or agglomerations on the other hand. The main difference to the cement paste was usage of other, lower range of rotational speed (shear rates) leading to higher viscosities obtained. In comparison, the settings of latter test, i.e. second testing mode, were meant to maintain oscillation in the linear elastic range and were fixed based on preliminary studies on this material (amplitude sweep test). With this procedure, all measurements were conducted precisely 12 minutes after addition of water and meaning 5 minutes rest from mix production as it was minimal time for sample casting and transportation to the rheometer. The tests were then processed at a constant temperature of 23 ºC, although the temperature of the material inside the cell varied slightly from the walls to the centre.

The results acquired included torque as a function of rotational speed, or complex viscosity and other parameters of oscillation test in the time scale, presentation of which can be found elsewhere, see Appendix F or otherwise [TC 225-SAP] for the former part. After including calibration of test equipment done by Secrieru [Sec 12], the principal data have become shear stress and shear rate. The ratio of the two at a given shear rate, often addressed as so-called apparent or dynamic viscosity could be then calculated, see corresponding equation in Table 3.10. To determine the parameters yield stress (τ_0) and plastic viscosity (μ), being less direct procedure, Bingham model was assumed. In accordance, the regression analysis was performed for both up-curves (increasing shear rate) and down-curves (decreasing shear rate) from the shear stress-shear rate data obtained; for the purpose, only main data, i.e. without pre-shear underwent processing. The slope of curves was used to calculate the plastic viscosity, while the intercept on the stress axis at zero shear rate was utilized to derive the yield stress. Since so obtained yield stress values were found always positive, application of other fitting models was not considered.

Table 3.10: Calculation basis for finding rheological parameters.

Parameter	Calculation formula
Shear stress (τ), Pa	$\tau = M_d \cdot A_{rheo} \cdot 10^{-6}$ Where: M_d – torque/torsional moment [μNm] A_{rheo}- shear stress (calibration) factor (= 4750 Pa/Nm [Sec 12]) M_{rheo} – geometry (calibration) factor (= 3.0441 (1/s)/(rad/s) [Sec 12])
Shear (strain) rate ($\dot{\gamma}$), 1/s	$\dot{\gamma} = \frac{2\Pi}{60} \cdot \Omega \cdot M_{rheo}$ Where: Ω – rotation/angular velocity [1/min] M_{rheo} – as in foregoing parameter
Apparent/dynamic viscosity η, Pa·s	$\eta = \frac{\tau}{\dot{\gamma}}$
Complex viscosity $\lvert\eta^*\rvert$, Pa·s	$\lvert\eta^*\rvert = \frac{\lvert G^*\rvert}{\omega}$ Where: $\lvert G^*\rvert$ – complex shear modulus [Pa] $\lvert G^*\rvert = [(\tau/(\Phi * M_{rheo}) * \cos\delta)^2 + (\tau/(\Phi * M_{rheo}) * \sin\delta)^2]^{0.5}$ Φ – deformation corresponding arch [-] M_{rheo} – as in foregoing parameters δ – phase difference angle [rad] ω – angular frequency [rad/s]

The **air content** of finely grained and coarse-grained mixes was initially determined by involving pressure method in accordance with the standards DIN EN 1015-7 and DIN EN 12350-7, respectively. The corresponding results obtained were presented in publications [Dud 10b][Dud 10c]. However, this method has met with some criticism and doubts regarding precision of the test, including researchers investigating SAP-enriched mixtures [Has 10]. To stay on the safe side, rival two-step and density-based approach called gravimetric method [Min 81] was therefore chosen. Accordingly, the **bulk density** was determined first, for which DIN EN 1015-6 and DIN EN 12350-6 for concretes without and with coarse aggregates were followed, respectively. For each measurement a minimum of two samples of 1 litre volume was produced whereas, assuming concrete is self-compacting, only in special cases using vibrating table. One such exception was concrete F-S.4 (0.4 % SAP but no extra water), for which intensive vibrating had to be applied to neutralize expected loss of workability. Compaction furthermore was applied for mixes F-R-vac, F-R.04-vac and F-S.3.04-vac as one step in process of air bubble removal (the full procedure involved mixing with vacuum, casting fresh concrete in at least two layers, a heavy compaction following each concrete pouring, excessive material removal and finalization with opening of the surface air pockets). Having done so, the weight of material of known volume was used to assess the bulk density. The air content was then calculated according to Eq. 3.3 [Min 81]:

$$A = \frac{T - W}{T} \cdot 100 \tag{3.3}$$

where A is air content [%], T is theoretical weight of the concrete based on an air-free basis, computed from the proportions and the specific gravities of the mix components and W is unit weight of fresh concrete.

Usage of fresh concrete density instead of that presented in hardened state yielded an obvious advantage given that effect of shrinkage on concrete volume was eliminated. The error made on this occasion owed to changeable specific gravities of some ingredients, especially cement, was insignificant (< 0.5 %). The average from all test performed on particular composition is reported.

Eventually, having the knowledge about all important properties in fresh state, the self-compacting ability of concretes investigated was decided. For acceptance criteria being referred to, please see Table F.1 in Appendix F.

3.3.3 Setting and early-age hydration

The non-destructive monitoring of concrete behaviour during setting and part of hardening stage was conducted using ultrasonic equipment called CELplus®, a product of Geotron-Elektronik. As schematically shown in Figure 3.8, the apparatus consists of main unit and the supplementary components, among which the most important are waveform generator board, pair of piezoelectric broadband ultrasonic transducers and mould meeting high damping specification.

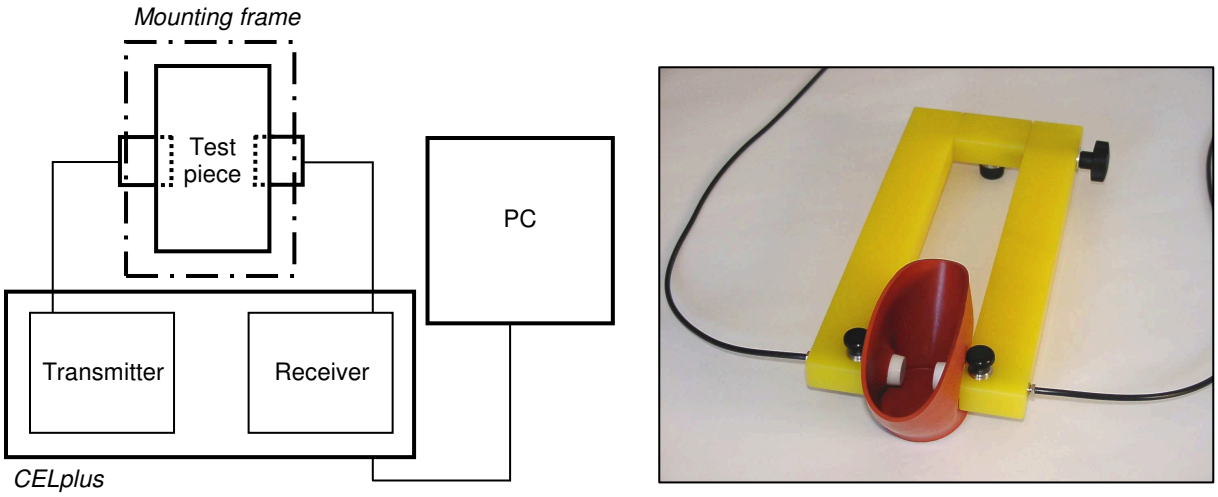

Figure 3.8: Block diagram of the apparatus for pulse velocity measurement (to the left) and the main part of CELplus® equipment as arranged for test (to the right).

The instrument operates according to so-called ultrasonic pulse velocity (UPV) method, a special type of stress wave propagation method also called direct transmission method. In accordance with type of transducers used and their arrangement (Figure 3.8), it allows primary P-waves, a fastest type of mechanical/stress wave called interchangeably longitudinal or compressional waves, to be transmitted most directly which is through sample. This guarantees that high sensitivity of measurement could be obtained at simultaneous provision of possible maximum energy of emitted signal transmitted. Both transmitter and receiver can operate in the middle resonant frequency range between 10 and 200 kHz, which was important for few reasons as following: i) it tuned out to be sufficient for reliable measurement of the P-wave velocity, ii) it fell in typical range used in field of testing cement-based materials, iii) in the study at hand it provided wavelength larger than aggregate size. Other relevant technical information was impulse strength and rate of change, reported by the producer to be approximately 2 kV and 0.3 μs/kV, respectively.

Prior to each experiment, transducers were fixed with the frame's screws. Once the rubbery and highly damping mould had been situated in place as well, silicon jelly/grease chosen as couplant was distributed over the exposed area of sensors. Such step was necessary to enhance contact between the transducers and the material as well as to secure that the sensors could be easily removed after testing without damaging. The next preparation step was then executed by pouring the concrete into the mould and sealing it, taking place not later than 10 minutes from mixing finalization. From this moment, transducers were in direct and full face contact with the specimen under study and the measurement started. At command, the instrument in general and transmitter in particular transmitted pulses of longitudinal wave. After travelling though material, the signal was automatically picked up by receiver. Knowing the distance between transducers (being fixed at constant 2.5 cm) and the time delay between start of transmission and the start of receiving the signal (based on threshold onset picking algorithm), P-wave velocity was calculated as the ratio between the two. Particular and other signal parameters captured, this including e.g. root mean square voltage (i.e. measure of relative energy and complex waveforms resultant from pulses transmitted), were provided in real time of experiment by the attached software. Preliminary tests showed that the monitoring intervals could be limited to range of 1 to 5 minutes, which was held throughout the tests. If not mentioned otherwise, these were continued until approximately 24^{th} hour of age and were processed under quasi-constant temperature 20 ± 1 °C and RH of ambient of 65 %. Regrettably, no measurement on coarse-grained UHPC could be taken owing to early stage of ultrasonic apparatus development when producing the mixes.

The destructive testing of a setting concrete followed a well-known penetration resistance test according to the DIN EN 480-2 standard, in literature being sometimes referred to as Vicat test for mortars and concrete. In this test, a steel right cylinder (i.e. the needle) having diameter of 1.13 ± 0.05 mm and the length of 50 ± 1 mm is lowered into sample-filled frustum 40 mm in height and the penetration depth is measured. Final setting time as counted from the addition of water, being the only setting phenomena aimed at, is when needle penetration is less than 2.5 mm. In the standard, maintaining 90 % of relative humidity is required. However, since the result was nearly identical for sample kept sealed, and, furthermore, such condition corresponded to one met is concrete shrinking autogenously, the latter was chosen and was commonly used. Eventually, more testing samples were produced at once for coarse-grained UHPC to provide sufficiency of measuring points. This step was necessary to ensure that no aggregate grain is hit and needle movement isn't stopped by the

interlocked steel fibres, signs of which would be remarkable change of needle immersion depth at different locations. The ambient temperature was 20 ± 1 °C.

Changes of concrete's in-situ temperature were recorded by means of thermocouple PT100 embedded in the sample of interest. The sensor had a protective hybrid cover to facilitate its extraction after test finalization and further reuse. This cover showed however to have no influence on results as proved/validated in preliminary studies. Experiments themselves involved usage of specimens from parallel measurement of other variables (shrinkage deformation under free or restrained conditions, ultrasonic measurement) or casting of individual specimen of identical boundary conditions from selfsame mix batch. In doing so, selfsame material characteristics and curing conditions have been always maintained. Frequency of data collection by the data acquisition system and, for some tests, its duration was similar if not identical to measurement being validated, substantiated or compared to. The ambient temperature was 20 ± 1 °C.

3.3.4 Free and restrained shrinkage

Figure 3.9: Apparatus used in autogenous shrinkage measurement for small tubes (left) and for big tube (right).

Autogenous shrinkage free of external restraint was measured using two similar set-ups based on corrugated tube method developed by Jensen and co-workers [Jen 95][Qia 08] and, for smaller one, being standardized in ASTM C1698–09. The main differences between the apparatus to be followed in Figure 3.9 regarded the size of the tubes (diameter x length: approximately 30 x 400 vs. 80 x 380 mm x mm), solution for sealing the moulds from their ends (plastic end plugs vs. steel ones), presence of anchorage and fixing (none vs. mounted screws and springs) and finally the number of specimens measured and evaluated at once (three vs. one tube).

In gist in common to both, the special design of the measuring device (dilatometer) and the use of corrugated, tube-shaped polyethylene moulds enable continuous monitoring of the concrete deformations beginning immediately after the filling and encapsulating of the tubes. Having executed small modification to regulation of original ASTM proposal, the autogenous strain of sample at time t was calculated according to Eq. 3.4:

$$\varepsilon_{autogenous} = \frac{L(t) - L(t_0)}{L(t_0)} \cdot 10^6 = \frac{L_{ref} + R(t) - 2 \cdot L_{plug} - L(t_0)}{L(t_0)} \tag{3.4}$$

where L(t) is the length of sample at time t (in mm), $L(t_0)$ is the length of sample at time-zero (in mm), L_{ref} is the set-up associated length of reference bar (in mm), R(t) is the reading of gauge with sample in dilatometer (in mm) and L_{plug} is the set-up associated length (thickness) of one end plug (in mm).

Time-zero needed in Eq. 3.4 was acquired by applying the method described Section 4.3.1.

To better understand relation between changes in courses of autogenous shrinkage and hydration process, **temperature evolution** was monitored for some mixtures. A small hole was drilled in the middle of both types of corrugated tubes and, subsequently, was sealed. After specimen of interest was prepared and placed in the measurement position, the tiny gap was freed from the cover and PT100 temperature sensor was inserted. Having connection with data acquisition system, actual temperatures were recorded for the first 24 hours at minimum. The data were collected when the temperature changed more than 0.5 °C or, but not rarer than, every 5 minutes.

Autogenous shrinkage combined with the effect of drying to ambient, often described as **total shrinkage**, was measured using improved protocol of DIN 52450. The main modification was automatization of testing procedure and extension to more hardened concrete samples measured at once, see Figure 3.10.

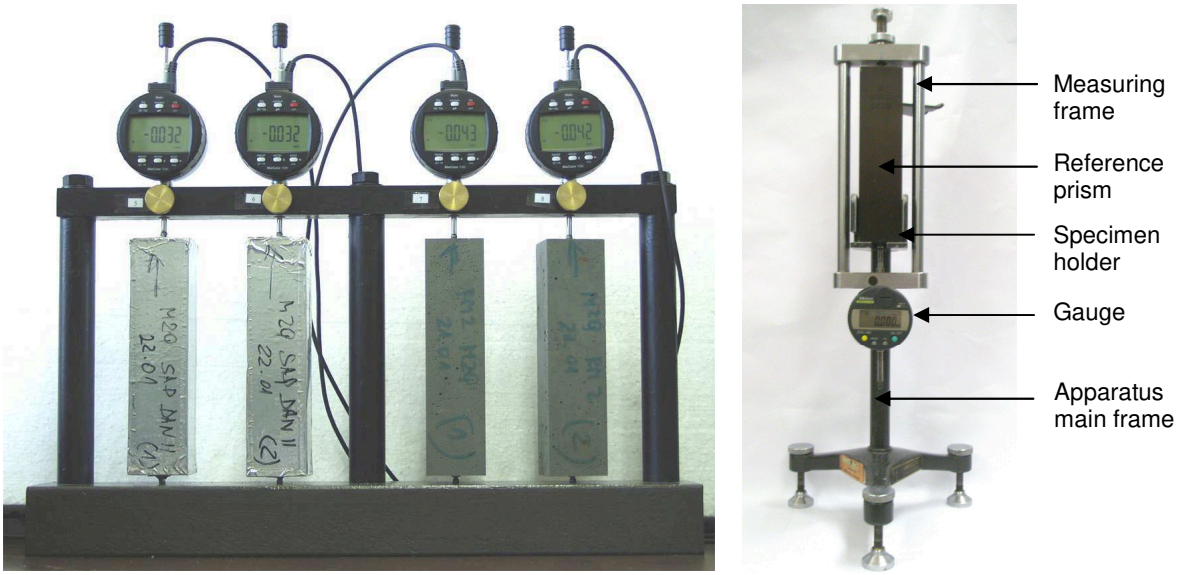

Figure 3.10: Apparatus used in total shrinkage measurement: custom-built device for automatic data recording (to the left) and Graf-Kaufmann set-up for manual records (to the right).

The examination was performed on small beams having cross-section of 40x40 mm² and length of 160 mm, hereafter referred to as prism. Prior to casting, two measuring pins were fixed in every mould compartment, and thus becoming part of test specimen. The sealed configuration followed after the concrete had been poured. At age of demoulding of 1 day, the specimens were either transported to the measuring device or wrapped in thick plastic foil to avoid moisture loss until examination day (additional age of 7 days presented in work at hand; for other demoulding ages, please see e.g. [Dud 10a]). During test, automatic data collection was processed under temperature of 20 °C and 65 % of relative humidity. To limit amount of data acquired, the measuring intervals of 5 to 30 minutes were adapted based on current deformation rate recorded. Depending on measuring place availability, three and exceptionally two nominally identical specimens were produced and the average value is presented. Each specimen removed from automatic device underwent immediate manual measurement on original Graf-Kaufmann set-up and the manual measurement continued with few days intervals.

Additionally, some extra prisms though deposed of measuring pins were produced from the selfsame batch of concrete as the shrinkage prisms and the **mass loss** was recorded. Whenever total shrinkage-mass loss relationship knowledge was aimed at, automatic data acquisition was executed. This involved using balance with accuracy of 0.01 g connected to data acquisition system and record intervals similar to ones set in shrinkage measurements. One specimen could be tested at once; however, as manual control of mass changes using selfsame balance and more samples showed (results will not be presented), the difference between

replicates is negligible, i.e. one specimen was sufficient for this kind of measurement. Mass loss measurements on samples with other geometries than prisms were executed as well, see discussion of Section 4.6.3 for details. Given manual control and number of samples (minimum three per mix and each testing age), less frequent data collection was possible in this case.

The measurement of deformations due to shrinkage under external restraint was carried out using the instrumented ring test in two various set-ups: One as prepared acc. to ASTM C1581 – 04 and another one built by a project partner, Dr. Eppers (formerly German Cement Works Association) [Epp 09][Epp 10]. The smaller geometry of the latter set-up showed in Figure 3.11 allowed favourable hydration heat dissipation and thus minimising of temperature effects.

Figure 3.11: Apparatus used in instrumented ring test measurements: C1581-04 based set-up (to the left) and Dr. Eppers' adapted apparatus (to the right).

Addressing idea of test, a annulus made of fresh cementitious material is cast around a steel ring. As the cement hydration progresses and material transforms from fluid to solid, the annulus starts to shrink. In turn, the concrete ring is pressurized by the steel one, resulting in development of tensile stresses in the former (in circumferential direction). The main quantitative outcome of the test is the steel ring strain change measured on its inner surface which, using appropriate analytical solution, can be translated into the corresponding tensile stresses in concrete.

Until age of 24 hours, a sealed configuration was always applied. This typically involved covering the rings with saturated burlap and/or few layers of plastic foil. Some minimal distance between the cover and concrete surface was however maintained. This was found

necessary to ensure that the cracking, if occurred, was strictly attributed to restraining of shrinkage and not stress concentration around uneven surface area, for instance. To maintain sealed conditions during measurement in following days, the assistance of the outer steel ring was preferred; meanwhile, the top surfaces of the concrete annuli were protected by a dual layer of self-gluing aluminium tape. Sometimes, when new concrete rings were to be cast, the outer rings had to be however removed. In such case, exposed surfaces were immediately sealed in selfsame manner as the top. The outer mould elements were eliminated intentionally only when **measurement of combined effect of restraint and drying from top and bottom or, alternatively, from circumference** was planned (age of 1 day and, for some mixtures, also 7, 14 and 28 days; for most important results see e.g. [Dud 14]). The conditions during examinations were identical: 20 °C and 65 % RH.

At maximum, three concrete rings could be produced from selfsame concrete batch, including two for identical and one for contrary curing condition. To increase reliability of the result, however, some mix repetitions were done as well. The data were collected from the four strain gauges glued to inner surface of the inner steel ring and the average for each ring is reported. To limit amount of data acquired, the measuring intervals of 5 to 30 minutes were adapted based on current deformation rate recorded. The measurement continued until through-cracking appeared (signalized by abrupt drop of strain to approx. zero), the strain approached asymptotic value or both outer and inner steel rings had to be reused in next experiments.

To assess **tensile stresses** developed due to restrained deformations and hence to be able to estimate quantitatively the tendency of these concretes to crack, computation based on strains recorded in ring measurements (case of big IRT) was performed acc. to Eq. 3.5 [Hos 04][Yoo 14]:

$$\sigma_{Actual-Max} = -\varepsilon_{Steel}(t) \cdot E_S \cdot \frac{R_{OS}^2 + R_{OC}^2}{R_{OC}^2 - R_{OS}^2} \cdot \frac{R_{OS}^2 - R_{IS}^2}{2 \cdot R_{OS}^2} \tag{3.5}$$

where $\sigma_{Actual-Max}$ is the maximum residual tensile stress (i.e. theoretical elastic stress minus relaxed stress) in the circumferential direction, $\varepsilon_{Steel}(t)$ is the measured strain at time t, R_{OS} is the outer radius of the steel ring (= 165 mm), R_{IS} is the inner radius of the steel ring (= 152.5

mm), R_{OC} is the outer radius of concrete ring (= 203 mm) and E_S is the Young's modulus of steel ring. For most important results, please see Chapter 4 and Appendix I.

Cracking potential, i.e. indication of how close the uncracked concrete is to cracking, was determined according to Eq. 3.6:

$$\Theta_{CR} = \frac{\sigma_{Actual-Max}}{f_t(t)} \tag{3.6}$$

where Θ_{CR} is cracking potential estimated at time of interest t, $\sigma_{Actual\text{-}Max}$ is the maximum residual tensile stress in the circumferential direction at time of interest t and $f_t(t)$ is the splitting tensile strength at time of interest t, which in own study replaced by corresponding flexural strength.

For sake of correct interpretation of results, it should be pointed out that the tensile strength of unloaded concrete (short-term tensile strength) is typically higher than that of subjected to sustained loading [ref. 8, 10, 11 *Ibid*. Sch 02]. In the instrumented ring tests, this load will be present and will result from tensile stresses generated due to restraining autogenous shrinkage deformations. Simultaneously, measurement of flexural strength should give higher values of tensile strength than one measured in tests of splitting tensile strength, as confirmed, e.g. average of 10.3 MPa (Appendix I) vs. approx. 7 MPa [Epp 10] recorded for concretes of very similar compositions at the age of 1 day. That is to say, by using Eq. 3.6 and input data as declared, cracking potential would be underestimated. Nonetheless, the results were used for different purpose, in particular for assessment of relative changes enabling evaluation of IC effect also under the influence of external restraint. For most important results and ages at which concretes cracked, please see Appendix I.

Pressure transducers RVAP015GV from SensorTechnics allowing measurement in the vacuum range were used to monitor the **capillary pressure evolution** in concrete. The equipment was arranged in such way so that sensors were protected from destructive action of pore solution while entrance of fine concrete components (air, tiny aggregates) was prohibited. For this reason, beside the transducer, one full test set-up consisted of a tube (3 mm inner diameter), sponge-like membrane, sealant, sample mould (analogous to that used in ultrasonic measurement, although made of a stiffer material) and connection to data logging system. In principle of measurement, the vacuum created by the self-desiccation of the matrix is replaced by the de-aired water passing from the tube though the membrane to

concrete. This causes a depression in tube which is measured by the pressure sensor connected to the data logging system.

For sake of accurate measurements, special preparation protocol was followed. First, the transducer and attached sealant, i.e. flexible 2 cm-long rubber hose, was filled with de-aired distilled water. A medical syringe equipped with needle smaller than transducer opening was used for this purpose, allowing injection of liquid from the sensor's bottom. This action continued until sensor contained nothing but water and only water filled the volume of the transparent sealant. As next step, the same procedure was repeated for the translucent stiff tube, however, using rubber hose instead of needle for the syringe ending. When no air bubbles remained in the tube and a drop of water covered its tip, both water-filled elements were connected with each other. Finally, after disconnecting of syringe and removal of air from the tube, if any, the other free end was closed with wet sponge underwater using needle as help.

Such prepared measuring element was inserted into a hole in the mould drilled beforehand and its horizontal position was fixed at height identical to that used in ultrasonic or temperature measurements. In subsequence, concrete was poured, followed by very gentle vibration of sample by own hands. When this finished, the top surface of sample was covered with few layers of plastic foil to ensure that sealed conditions are maintained and the measurement began. It was deduced that the apparatus operated correctly when the pressure record was slightly positive, approx. 2 kPa. Four samples were examined for each mixture, with automatic records being taken with interval of 5 min. For collection of data, software written for Labview® was utilized. The ambient temperature was 20 ± 1 °C.

3.3.5 Mechanical properties

To understand the behaviour of concrete in both free and restrained conditions, some further properties were studied as well including compressive strength, which is a basic engineering property. Owing to multiple purpose: 1) to unify the sample geometry, 2) to avoid size effect when using the results for further evaluation, 3) to provide basis for comparison with other geometry results, and finally 4) to provide geometry allowing possibly fast removal of entrapped air and, in case of simultaneous exposure to ambient, water from concrete, **the main type of specimen used for analysis of mechanical performance of concrete was the**

prism, see Section 3.3.4. All specimens were taken from single batch, however, mix repetition was applied as well.

Compressive strength and indirect measure of resistance to tension, namely flexural strength, were assessed according to two-step procedure described in DIN EN 1015-11. At the age of interest, this being 1, 3, 7, 28, and (whenever possible) 90 days, a three-point bend test on prisms was performed first. In gist, the entire load is applied at the centre span and the maximum stress is present at the centre of the beam. Subsequently, the halves obtained were examined in compression. For the purposes, two different machines were engaged viz. the ZD10/90 apparatus from VEB Thüringer Industriewerk Rauenstein and the DB300 model from VEB Werkzeugmaschinen Kombinat „Fritz Heckert" Karl-Marx-Stadt, respectively. Three beams were prepared per each age considered. However, since more results after mix repetitions were obtained, unless mentioned otherwise, the result reported is an average from all tests per particular age. The calculation of flexural strength followed Eq. 3.7:

$$f = 1.5 \cdot \frac{F \cdot l}{b \cdot d^2} \tag{3.7}$$

where F is force measured [N], l is span length, 100 mm, b is width of test specimen [mm] and d is height of test specimen [mm].

To acquire **indicative of structure formation**, the quasi-static Young's modulus was tested in compliance with DIN EN 1048-5. The measurement is based on three consecutive loading and unloading cycles. The lower loading stress was 0.5 MPa; meanwhile the upper stress equalled to 33 % of the actual resistance to compressive load but exceptionally measured in the prism's longitudinal direction. The specimens' preparation for both measurements involved grinding. Only so, the contact surfaces were possible to be made even and plane-parallel. The strains were collected by two Linear Variable Differential Transformers (shortly LVDTs) mounted on parallel sides of the specimen. The data so obtained were finally used to calculate the Young's modulus acc. to Eq. 3.8:

$$E = \frac{\Delta\sigma}{\Delta\varepsilon} = \frac{\sigma_o - \sigma_u}{\varepsilon_o - \varepsilon_u} \tag{3.8}$$

where E is Young's modulus, σ_o is the upper compressive stress during 3rd loading, σ_u is the lower compressive stress prior to 3rd loading, ε_o is the strain measured at the end of third compression cycle and ε_u is the strain measured until the initiation of 3rd loading.

To account for in fact two-step procedure, six specimens per concrete age of 28 days and earlier ones (1, 3, 7 and 90 days, although tested less regularly) were prepared and tested. Whenever possible, however, average from results on more concrete batches was taken.

Eventually, **to evaluate effect of curing conditions as well as verify IC effect observations made on main specimen geometry**, some additional tests were performed as well. Acknowledging the limit load of apparatus possessed (DB300), behaviour under compression was additionally examined on cubes with side length of 100 mm following DIN EN 12390-3. Until day of examination set at concrete age of 28 days and, for limited number of mixtures, additionally 1, 3, and 7 days, the samples remained subjected to one of curing conditions: 1) sealing with foil (majority of cases), 2) immersion in water until age of 7 days or 3) loss of original moisture to ambient (20 °C, 65 % relative humidity). At least two specimens per parameter were produced and the average was taken. The only exception concerned sealed conditions, where more batches of one composition were produced and tested, the average result of which was eventually reported.

Direct measurement of tensile strength, on the other hand, was taken on specimens which underwent sealed curing only. These however received new shape and in new arrangement had appearance of dumbbell-shaped concrete prisms with cross-section of 40x24 mm² and length of the narrow part of 80 mm. Prior testing, each specimen matured to age of 3, 7 or 28 days was glued with X60 from HBM company, in subsequence of hardening of which deformation controlled test with non-rotatable loading plates was executed. Two and maximum three specimens per age could be tested and the average is presented.

For most important results of all tests, please see Appendix I.

3.3.6 Microstructural investigations

To investigate **accessible porosity in range of capillary forces up to largest capillary size** as well as the corresponding pore size distributions, Mercury Intrusion Porosimetry tests were carried out following DIN 66133. Two fully automated porosimeters, one called Pascal 140 from Fisons Instruments and another one called Pascal 440 from Thermo Electron corporation, enabling operating pressure of maximum 300 kPa and 400 MPa, respectively, were used for the purpose. The necessary samples were obtained from small beams cured in standard manner. At the chosen ages of 1, 3 and 28 days, the big specimens were shattered

and afterwards the hydration of much smaller test pieces sieved to size 4-8 mm was stopped. Typically, gentle oven drying at the temperature of 40 °C was applied until the mass became constant. For comparison reasons, however, other methods of hydration cessation were applied as well, including freeze-drying and combined method, i.e. treatment with isopropanol under vacuum in the first 24 hours and subsequent oven drying at 40 °C until mass constancy. Approx. five grams of so prepared material were finally used for each measurement. While simplifying that pores are cylindrical in shape, the pore entry diameter was calculated using Washburn's equation (Eq. 3.9):

$$D = -\frac{4 \cdot \gamma_{Hg} \cdot \cos\theta_{Hg}}{p_{Hg}} \tag{3.9}$$

where D is pore entry diameter, γ_{Hg} is surface tension of mercury (considered as 0.48 N/m), θ_{Hg} is contact angle of the mercury on the solids (assumed to be 140°) and p is applied, (intrusion) pressure

To characterize porosity of materials even better, the MIP data obtained including pore sizes and corresponding intruded volumes was used to determine characteristic parameters. The found median pore diameter yielded pore diameter at which 50 % intruded pore volume was observed. Critical pore diameter, to be addressed hereafter as modal pore diameter, was second parameter concerned. It was obtained from maximum of the derivative of the pore distribution curve. It was understood to demonstrate the smallest pore size diameter of the subset of the largest pores which creates connected path through sample, after [Hal 95]. Eventually, threshold diameter above which there was comparatively little intrusion in the pore system became known as well. Yet, since regularly having similar values compared to those of modal pore, results will not be presented in this thesis.

Analysis of pores having size of air bubbles and larger was performed by the so-called pore count method in compliance with DIN EN 480-11, although on somewhat smaller specimen size. The RapidAir 457 Automated-Air-Void-Analyzer employed in tests comprised of computerized control unit, a high-resolution video camera and a microscope objective mounted on moving stage.

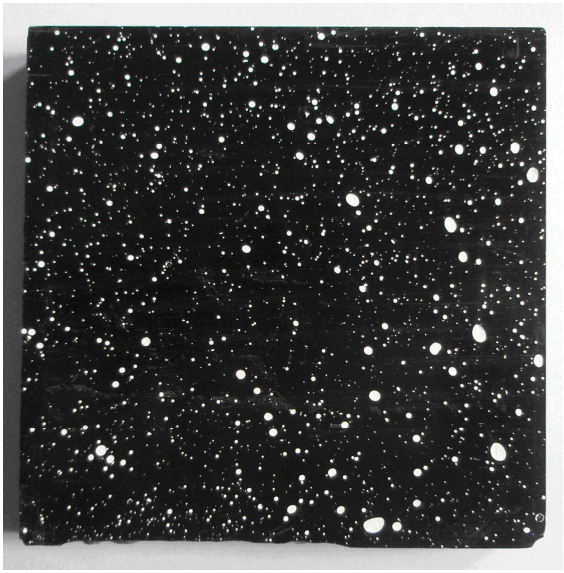

Figure 3.12: Sample for pore count measurement and appearance of lapped surface after white-and-black contrast enhancement.

One cube with side length of 100 mm was manufactured for each test and was maintained sealed until concrete age of 28 days. On examination date, the specimen was sectioned by use of water-cooled concrete saw. One or maximum two disks having thickness of approx. 20 mm were obtained from central part of the member and provided for grinding and polishing until cut surface was removed and surface appeared even. Subsequently, hydration was cessed using oven drying. Afterwards, a contrast enhancement by darkening of specimen, followed by filling the voids with fine powder of barium sulphate, took place. In result of the procedure, the voids appeared bright white and the rest was black (Figure 3.12), facilitating void detection/identification in the measurement and its maximum precision. After the plane section was mounted onto the moving stage situated under the camera, the measurement started. Each specimen was tested twice, with the second scan being run on surface rotated by 90°. The total measuring length approached 2400 mm. Information on air content, pore distribution, specific surface area and spacing factor were calculated automatically by the software.

Total porosity was determined based on true and bulk density of materials matured to age between 1 and 28 days, for assessment of which two tests were necessarily conducted. **Helium pycnometry** was engaged to quantify true density. The apparatus model AccuPyc 1330 Pycnometer from Micrometrics company was used, where two chamber arrangement and gas displacement technique is applied to yield pore-free density. The bulk density was assessed based on ratio between known mass of dry material and its volume found by **hydrostatic weighing method** or, in other words, test based on Archimedes' principle. Prior to each measurement, sample from specimen shattered to pieces of 4 to 8 mm and obtained from selfsame concrete batch as MIP test pieces were dried in oven until mass constancy. Gentle drying at the temperature of 40 °C was executed. For the estimation of true density, the milling process was applied in addition.

The total pore volume content was calculated from Eq. 3.10:

$$V_{pore,total} = \left(1 - \frac{\rho_{bulk}}{\rho_{skeleton}}\right) \cdot 100 \tag{3.10}$$

where $V_{pore,total}$ is total pore content [%], ρ_{bulk} is the bulk density [g/mm³] and $\rho_{skeleton}$ is the true density [g/mm³].

Vicinity of important transition zones as well as both physical and chemical features of large pores were investigated by means of Environmental Scanning Electron Microscopy (ESEM) coupled with Energy-dispersive X-ray spectroscopy (EDX). In the tests, ESEM XL30 apparatus from Philips company was used.

The idea of experiment is based on gas ionization principle. Measurement involved several steps. The chamber was vented first. Afterwards, the doors of chamber were opened and piece of material under study was placed on the stage. Subsequently, chamber's doors were closed and the wet mode was applied. No measurements were performed until destined pressure of 2.0 Torr was reached. This was followed by adjusting the position of sample and setting relevant measurement features, i.e. value of condenser, value of beam and scan rate. Some adjustments of first images obtained were necessary as well (brightness, contrast, focus). Eventually, at location of interest, the sample was measured and the pictures taken were saved. Unless mentioned otherwise, samples at the age of 28 days were studied to provide sufficient strength and thus resistance to high vacuum and to the aggressive electron beam. Some microstructural damage was expected to take place for younger specimens.

3.4 Summary and concluding remarks

Two very different UHPC matrices having various w/c ratio, silica fume content and aggregate graining were chosen for modification with IC. Introduction of IC variables followed ‘on top’ method as it was proved to be the most appropriate solution, securing preferable sorption behaviour of IC agent in concrete, among other arguments. Some further modifications followed, e.g. varying presence of fibres, all leading to tests on twenty four compositions in total. The mix regimes differed, being dictated by different times needed for making the mixtures flowable as dependent on composition and mixer used. If not mentioned or requiring otherwise, the samples casted were sealed and cured at temperature of 20 °C. Both destructive and non-destructive tests were then performed during and after hardening at different concrete ages. Criteria obtained from different literature sources were used to classify behaviour of concrete in fresh state, for which various empirical and rheological tests were employed. The further group of investigations were focused on SAP material itself, alone or after implementation in concrete. Additionally, some tests helpful in defining particular characteristic of SAP and hardly used in context of IC before were carried out.

4 Results and discussions

4.1 Introduction

In this chapter the results of all experimental investigations performed in frames of the thesis are presented. The chapter consists of five main parts (Sections 4.2-4.6) being recognized as crucial to discussion of action of IC. These are:

- Characterization of material properties in terms of IC applicability (Section 4.2)
- Extent of mix modification by IC (Section 4.3)
- Determination of time-zero (Section 4.4)
- Early age hydration aspects (Section 4.5)
- Shrinkage reduction and its mechanisms (Section 4.6).

Each topic concerned and in-depth discussion of associated results is preceded by short introduction to the subject, or alternatively, by preliminary remarks and the goal setting, and finishes with individual summary and conclusions. Whenever found necessary, new solutions to the problem concerned are proposed and validated experimentally or are otherwise analysed theoretically. General summary derived from the results and discussions delivered here is shifted elsewhere and is presented along with the outlook, see Chapter 6.

4.2 Characterization of material properties in terms of IC applicability

4.2.1 Preliminary remarks

Choice of appropriate SAP type is, next to precise curing fluid-IC agent ratio match (Section 4.3) as well as possession of favourable water transport-associated properties by the cement-based material, a precondition to high efficiency of mitigation strategy chosen. In past, many different SAP types have been tested; however, most of the studies did not truly treat about properties of the hydrogel useful for IC purpose. In fact, whether SAP provided the success to greater or lower extent, this was typically related to geometrical particularities (product size, shape) and production method and obviously amount of IC agent used. Meanwhile, hydrogels can be very different in terms of their structural properties and response to different stimuli, see Section 2.5.1. Implication of these particularities which, potentially or upon experimental validation, contributed to the success of IC or at least governed regulation of water content stored by the IC agent would be important step towards recommendation of products fit for the methodology purposes.

To fill this lingering gap to some extent, beside general characterization of SAP material used, certain chemical and physical features of the product that are typically ignored in studies on

IC are investigated in this section. Speaking about details, the pure SAP material was characterized in respect to shape, particle size distribution, composition, and robustness only somewhat in addition to estimation of sol fraction content and identification of porosity, cracking potential and skin formation. Only well-accepted or otherwise simplified test methods derived from polymer science were used for these purposes. In concrete, pores emerges from accommodation of SAP were inspected for growth of hydrates and robustness of SAP material at different stages of concrete life using computer tomography. Eventually, the observations made were confronted with pore structure of UHPCs under investigation, starting from air content estimation. Since ink-bottle effect could not be accounted for in Mercury Intrusion Porosimetry (MIP) measurements due to technical limitations, in particular inability to execute specific MIP testing sequence as required for overcoming so-called 'accessibility effect' (e.g. [Zho 10]), the effect of drying method i.e. another critical parameter affecting results of porosity estimation was in focus. For further information obtained from computer tomography as well as results of some additional tests on pure SAP material enabling comprehension of its behaviour in concrete even better, please also see Sections 5.3 and 5.4.

4.2.2 IC agent

i. Observations on pure SAP

The SAP selected for IC application is demonstrated in Figure 4.1. In dry (= collapsed) state, the IC agent had appearance of white stiff granules. The particles were characterized by regular round shape, this being confirmed under ESEM (Figure 4.2). While implying that SAP was truly a product of inverse suspension polymerization, an important particular advantage was obtained. Since the shape maintained after the polymer swelled in concrete, only spherical pores from accommodation and subsequent deswelling of SAP particles were observed in the IC-modified material matrix (see also the following part of this section). This presents the most favourable condition from perspective of effect on strength and inherent stress concentration under load.

Granules large enough to be captured by eye were separated easily. This indicated low cohesion of material chosen. Such feature was wanted given the aim of uniform distribution of IC agent over concrete volume. The likelihood of this to take effect increases when also the SAP cohesion is not a concern.

Figure 4.1: Appearance of SAP under investigation.

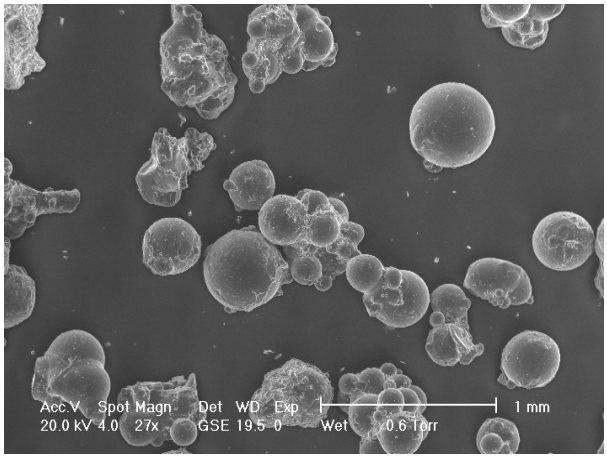

Figure 4.2: ESEM micrograph of SAP in dry/collapsed state.

Based on ESEM investigations, it was expected for IC agent to yield broad particle size range. The result of the laser granulometry is presented in Figure 4.3. The size of SAP microspheres spread from few tens to hundreds of micrometers, with only 10 % being larger than 695 µm. After swelling in fresh concrete, due to accommodation of the fluid, the particles of polymer became obviously bigger.

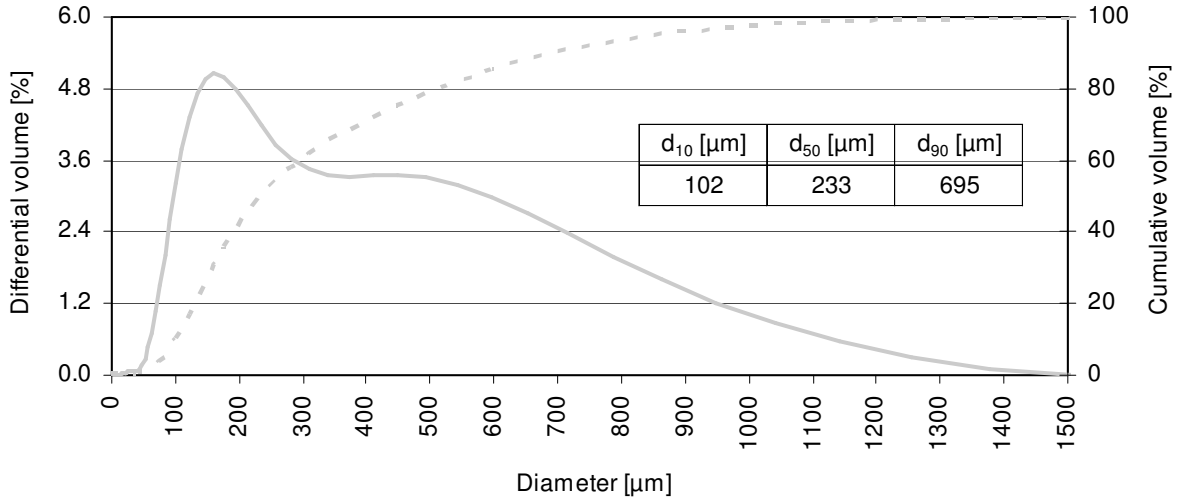

Figure 4.3: Particle size distribution of SAP studied and characteristic threshold values.

Whether the size range of SAP studied included the diameter most effective for internal curing, this cannot be answered in straightforward manner. According to Jensen and Hansen [Jen 02], SAP optimum strictly from perspective of autogenous shrinkage minimization should be small enough to absorb water in most effective manner in order to, subsequently, supply it to every part of cement paste. On the other hand, though potentially conflicting with other goals of curing (e.g. improving concrete properties by promoting cement hydration [TC

196-ICC]), it should be large enough to counteract filling with hydration products and, simultaneously, to eliminate the less active surface zone compared to the bulk. The smallest impact on strength (and thus highest likelihood of hydration front progress into space occupied by SAP) has been showed to occur for SAP that in saturated state obtained diameter of approximately 220 µm [Moe 09]. Indicating somewhat similar, SAP with particle sizes ranging between 100 and 140 µm in dry state used in UHPC, where diameters could be hypothesised to increase by not more than 2-3 times, was reported to have only limited effect on autogenous shrinkage despite high content of IC agent used (with 0.6 % SAP, reduction of 7 day AS measured since final set by 24 % at 20 °C) [Sol 10][Sol 11]. Typically larger inclusions (hundreds of µm) were necessary to effectively reduce this shrinkage type in low w/c concrete/mortar, e.g. [Gor 11][Sch 12c]. Comparing these observations with PSD of SAP under investigation and acknowledging particle size increase by approx. 2-3 times to be expected due to absorption, searched if not optimum size of SAP for purpose of mitigating AS was found. Size of SAP tested was less satisfying in terms of effect on mechanical properties, as validated in preliminary test series as well (see Section 3.2.3 and Appendix I for more details).

An important supplement finding of study by Gorges et al. [Gor 11][Sch 12c] yielded that, with other parameter being equal (i.e. material under modification, amount or even particle size of SAP used), sorption properties in highly alkaline environment may appear the more critical factor in the shrinkage mitigation goal, as equally to w/c of modified material itself [Zhu 13]. This SAP feature notably could be coupled with characteristic of the polymer structure, tested in following.

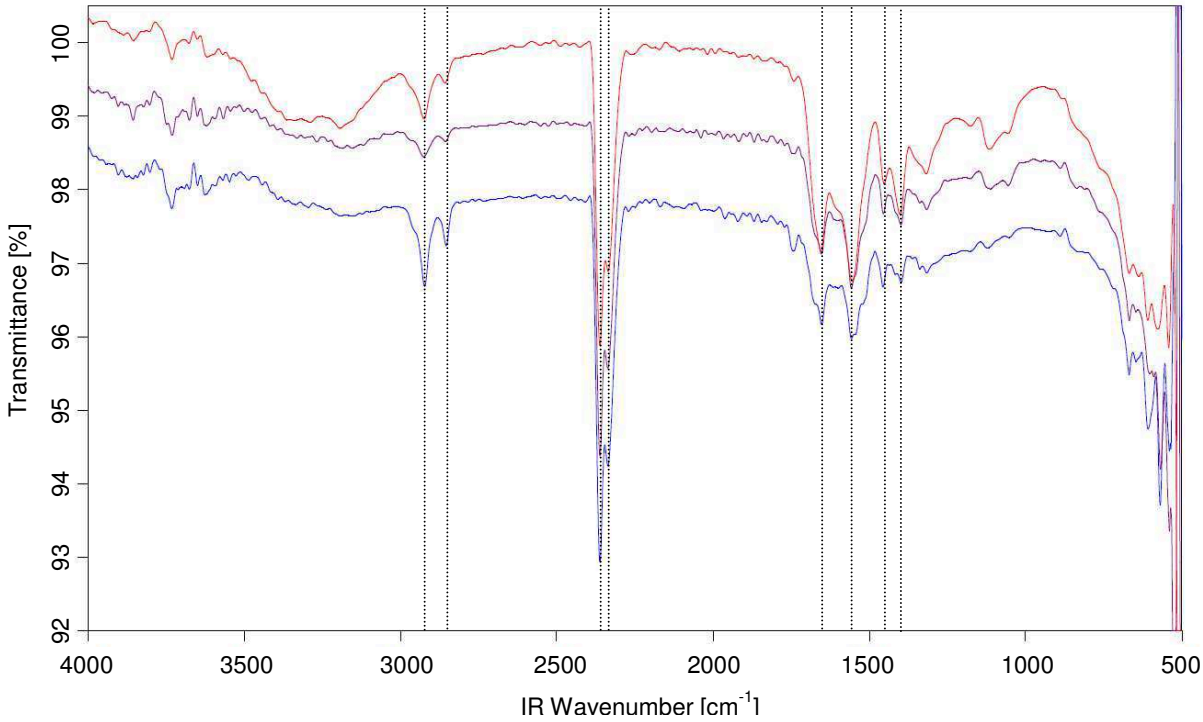

Figure 4.4: FT-IR spectra of dry SAP.

Figure 4.4 gives results of the infrared spectroscopy studies (FT-IR) where each curve is standing for an individual test on dry polymeric material. Few main peaks are to be observed. Some are characteristic for acrylamide group/unit (> 3000, 1653, 1558, 1400 cm^{-1}) while other mainly represent the acrylate group i.e. the derivative of acrylic acid (2924, 1558, 1455, 1317 cm^{-1}) including ones somewhat ascribed/associated with carboxylic group/unit/anion (2361, 1400 cm^{-1}). However, only some bands could be truly attributed to one specific unit e.g. 2333 cm^{-1} to be linked with CO_2 or 2855 cm^{-1} related to -CH_2- symmetric stretching vibration and likely implying usage of surfactant/stabilizer in production process [Pó 94], e.g. for stabilizing suspension and subsequently for reducing stickiness of resultant product (note here the low cohesiveness recorded in ESEM investigation). That is to say, some frequencies/bands in the spectra (especially > 3000, 1653, 1558, 1400 cm^{-1}) were likely assigned to more than one element, e.g., wavenumber ~3300 cm^{-1} which beside being hint of acrylamide monomer presence is commonly associated with OH of adsorbed water. The latter was investigated for own IC agent and was quantified as approx. 7.3 % by mass of the polymer. It is acceptable value for commercial SAP products which, due to negligible fraction, has been ignored when studying the polymer absorption (Section 4.3.3).

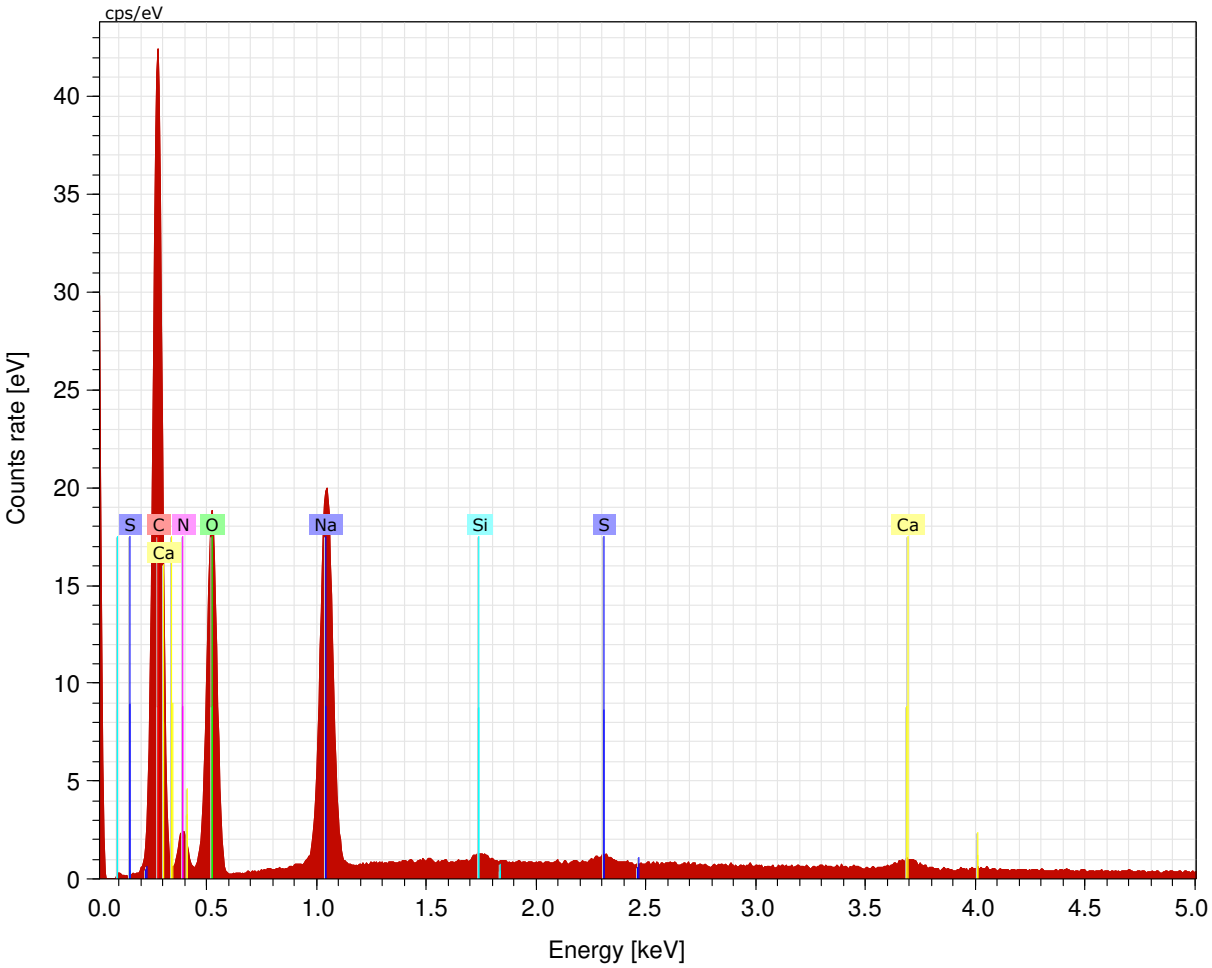

Figure 4.5: Energy-dispersive X-ray spectrum of dry SAP under investigation.

In the EDX measurements, results of which are reported in Figure 4.5, it was furthermore found that the SAP salt was likely partially neutralized, this being reflected by existence of Na^+ peak. Another peak characteristic for nitrogen (N) content and in the copolymer likely standing for acrylamide content has been also observed, but in comparison, it was pronouncedly less intense compared to ones ascribed to elements of the COONa and COOH groups.

Concluding, the IC agent under investigation was recognized to be of anionic type. Taking review from Section 2.5.1 additionally into account, this kind of SAP was expected to be responsive to various stimuli including change of pH, ionic strength and temperature, these being validated in different experiments, in particular tea-bag tests (presented in the following part of this section) and CT investigation (Section 5.4). This indicated, for instance, that water withdrawal from the swollen SAP needn't strictly result from underpressure to evolve in concrete. In fact, control over water carried and changes (positive or negative) could be governed by, among others, pore solution composition and hydration temperature. Still,

another reason for SAP volume changes took effect, as will become clear in the following subsection.

ii. Observations on SAP treated in different fluids

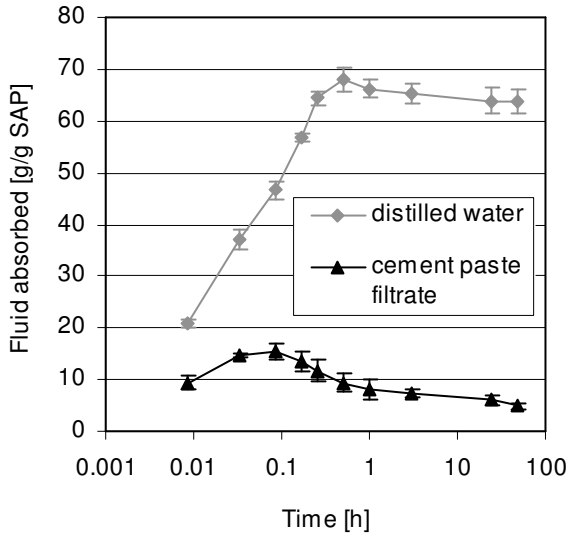

Figure 4.6: Evolution of the absorption capacity of SAP as measured by tea-bag method. The studied fluids were distilled water and filtrate from cement paste based on selfsame binder as used for producing UHPCs, i.e. CEM I 52.5 R-HS/NA.

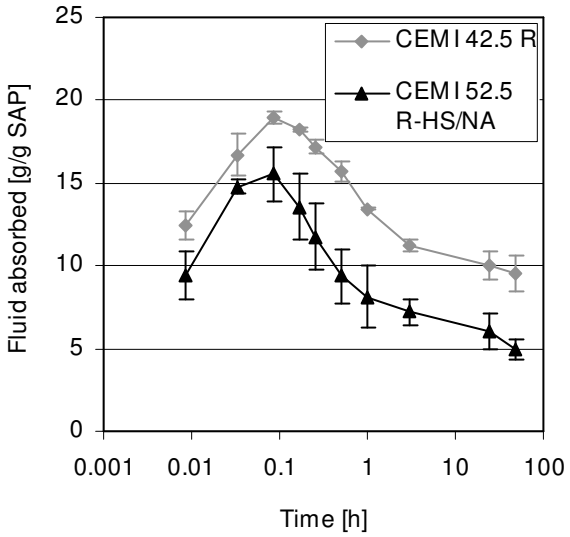

Figure 4.7: Effect of changing CEM I binder in the produced cement paste filtrate on absorption capacity of SAP under investigation. Cement CEM I 42.5 R used as alternative binder is product produced by Schwenk, Bernburg/Germany.

Swelling kinetics of SAP after immersion in one of the fluids having either neutral pH (distilled water) or one closer to that of concrete (cement paste filtrate) is illustrated in Figure 4.6. In both cases, the maximum uptake occurred very soon, in fact within few minutes from contact of polymer with the fluid of interest. As expected, earlier occurrence of maximum absorption and lower absorption limit value was attained in the cement paste filtrate, which could be traced back to shielding of the electric charge and/or new cross-link formation by ions present in the solution. Be that as it may, whatever the fluid absorbed or cement type used for production of filtrate, very similar trends in sorption behaviour of SAP were observed (Figure 4.7): After absorption attained the maximum, it levelled off to a slightly lower value without reaching equilibrium value within testing period. All reasons combined led to finding that behaviour of SAP could not be associated with any of swelling kinetics models known from hydrogel science, see Table 4.1. Pourjavadi et al. [Pou 13] noted similar behaviour, however, only when the immersion fluid was cement paste filtrate. And although the behaviour was proposed in [Pou 13] to be linked to production of white flocs, such explanation fails to explain behaviour of own SAP under investigation in distilled water.

Table 4.1: Results of fitting behaviour of SAP to existent models of swelling/deswelling kinetics.

Model [Reference]	Result of application-distilled water	Result of application-pore solution
• (1) Voigt-based viscoelastic model representing 1st order diffusion (swelling) kinetics [Shu 11][Tha 11] introduced by Castel et al.: $S = S_{eq}(1-e^{-t/\tau})$ where S − degree of swelling (mass of solvent absorbed/imbibed) at any time t (g/g), S_{eq} − degree of swelling at equilibrium or maximum water-holding capacity (= power parameter, g/g), t − time (h), τ − swelling characteristic time (= rate parameter = time required that a sample absorbs 0.63 of its ultimate/equilibrium swelling, h)	• Ad (1) Poor fitting above maximum capacity	• Ad (1) Poor fitting above maximum capacity
• (2) Schott's model representing 2nd order diffusion (swelling) kinetics [Gan 10][Tha 11]: $t/S = A+Bt$ where S − degree of swelling at time t (g/g), A and B − constants having specific physical meaning and being (A and B determined from the intersection and slope of the line t/S vs. time, respectively)	• Ad (2) Fails to describe given that A and B vary with time and while A becomes < 0 above 3h measurement	• Ad (2) Fails to describe given that A and B vary with time while A becomes < 0 above 5 min measurement
• (3) Fick's law based model [Gan 10][Tha 11] applicable until 60 % of water uptake: $S/S_{eq} = kt^n$ where S and S_{eq} − as in models (1) and (2), k-characteristic swelling constant, n − the diffusional exponent characterizing the mechanism of diffusion of solvent into the polymer network (k and n determined from the slope and intercept of line in plot S/S_{eq} versus t on log-log scale)	• Ad (3) Could not be applied given 60 % uptake occurred before 3nd measurement (very rapid uptake process!)	• Ad (3) Could not be applied given 60 % uptake occurred before 2nd measurement (very rapid uptake process!)
• (4) Berens-Hopfenberg model applicable after 60 % water uptake [Gan 10]: $S/S_{eq} = (1-Ae^{-k2t})$ where k_2 − the relaxation rate constant, A − a constant (A and k_2 calculated from the slope and intercept of the plot of $\ln(1-S/S_{eq})$ versus time t at times longer than those corresponding to $S/S_{eq} = 0.60$)	• Ad (4) Cannot be applied to data acquired	• Ad (4) Cannot be applied to data acquired
• (5) Peppas-Sahlin model for solute release fit for first 60 % [Gan 10]: $S/S_{eq} = k_1t^m+k_2t^{2m}$ where k_1 and k_2 − constants, m − diffusion, polymer shape-ascribed exponent	• Ad (5) Selfsame drawback as in case (3)	• Ad (5) Selfsame drawback as in case (3)

To comprehend the specific behaviour, one important characteristic of SAP should be recalled from the literature review, in particular possession of sol fraction i.e. a certain number of the polymer chains which have not been covalently linked to the network structure. This part of every polymer network often addressed as extractables can be minimized to some minimum value by increase of cross-linking degree, for instance. The loose fraction remained however becomes removed from the polymer structure when immersion in aqueous environment continues for appreciable time, this being hours [Buc 05] or even days [Hug 86]. As assessed for own polymer, the extractable material constituted 14.3 % of polymer mass on average, as

quantified in distilled water. Should the water-soluble species be extracted, lower load carriage must result bringing about fluid release-like effect. The effect can be presented by Eq. 4.1, addressing true water content for which fraction of extractables equals 0, after [Hug 86]:

$$\frac{m_t - m_{SAP,dry}}{m_t} = 1 - \left(1 - \frac{m_{eq} - m_{SAP,dry}}{m_{eq}}\right) \cdot (1 - S) \tag{4.1}$$

where m_t is the mass of swollen polymer, $m_{SAP,dry}$ is the mass of SAP before absorption, m_{eq} is the mass of polymer at equilibrium, and S is the fractional loss in mass of gel by release of extractables.

It should be acknowledged that in highly alkaline environment of pore solution the abovementioned effect was plausibly accompanied by additional and direct solvent release to be linked to new chain junction (= ionic bridges, physical cross-links) formation. This result of the complexation of multivalent cations such as Ca^{2+} ions with carboxylic groups in polymeric gel [Jen 11][Sch 12c] however could not be validated in own tests. The difficulty relates to the fact that on binding of ions, the mass of the weighted composite changed as well, thus masking the other effect. Finally, certain role played by extractables-related deswelling stress exerted on the gel phase [Buc 05] is not excluded.

The specific features viz. level of fluid absorbed and sorption behaviour could be used to state preliminary, empirically-based criterion for choice of IC agent. In particular, in agreement with [Sch 12c], it could be deduced that in group of SAP based on two monomers (acrylic acid, acrylamide), polymeric material as tested yields as preferable if not the optimum candidate for purpose of IC, especially when task of reduction of autogenous shrinkage is concerned. Before this statement attains validity, however, two questions had to be answered:
(1) Since sol fraction was incorporated in the particles, did it impact the integrity of SAP structure?
(2) Since none of the models describing swelling could be fit to behaviour of SAP studied, what were apparent pros and cons of its microstructure as far as transport mechanisms are concerned?

To answer the first question, qualitative assessment was performed. As can be partly observed in Figure 4.8, SAP tested revealed high robustness and remarkable gel strength. This was

indicated by shape of individual particles which remained unchanged and small though evident resistance against compression as exerted by human finger.

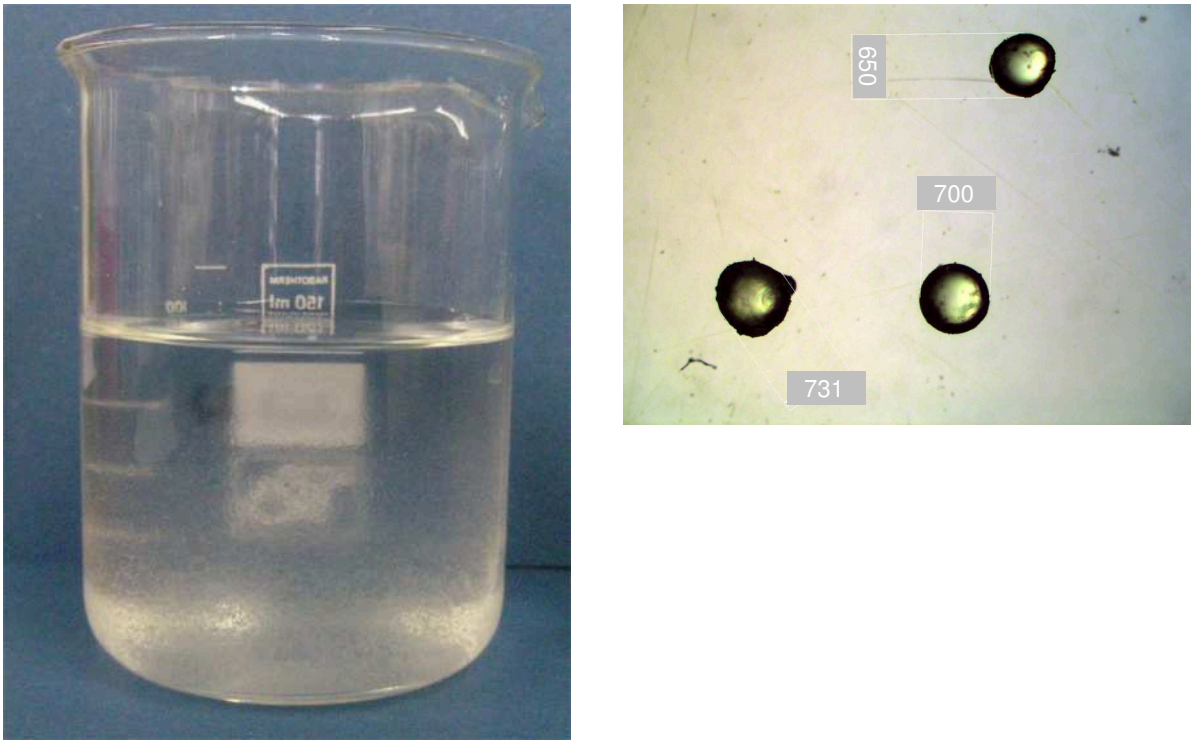

Figure 4.8: Appearance of SAP after many hours of contact with pore solution as revealed in the swelling test (to the left) and under light microscope (to the right). No signs of polymer deterioration observed.

While characteristic behaviour much likely prevented from occurrence of loosening, mushy, or slimy state, which can be used to discriminate SAP from other hydrogels [Zoh 08], another fact became apparent. It was evidenced that characteristic of SAP fulfilled one of oldest requirements for use of other polymers types in concrete, in particular, very high chemical stability towards the extremely active cations such as calcium ions (Ca^{2+}) and aluminium ions (Al^{3+}) liberated during cement hydration [Ram 96]. As the condition has been successfully applied to inhibit the so-called dry-out phenomenon[22] with less high-tech polymeric aids, it must be expected that the same basic requirement is demanded for SAP though working mechanism needn't be alike. In author's opinion, this could be basic recommendation for choice of SAP for IC by practitioners.

To analyse the second issue of interest, the surface morphology was investigated. In hydrogel science, the goal-oriented tests are typically performed under ESEM either using swollen polymer [Ghi 97] or, which is more common, after the polymer swollen to equilibrium (or

[22] Note that in the thesis the same phenomenon is referred to as self-desiccation.

maximum capacity) has been dried to the mass constancy [Tha 11]. Having applied the second solution, it was found that depending on manner of moisture removal, very different appearance of own polymer occurred. When freeze-drying was applied, not only the loss of polymer shape took place, but also various surface modification having certain relation with swelling degree or medium being contacted with emerged, see Figure 4.9 and 4.10. However, as soon as the collapsed state of polymer was approached with alternative method, none of the two changes could be visualized, see Figure 4.11 and 4.12. The difference in appearance was to extent expected given the significant impact which specific drying methods have on gels, e.g. [Sch 90][San 04][Tha 11]. Since from the two exposure to high temperature was main drying procedure used in thesis and is furthermore condition to be met in concrete practice, while all shrinkage measurement are performed at room temperature, only the samples of particular after oven drying treatment were further concerned.

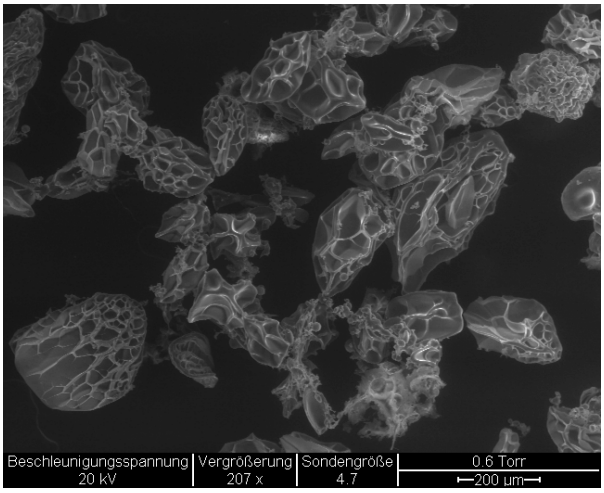

Figure 4.9: ESEM micrograph of freeze-dried SAP previously swollen in distilled water.

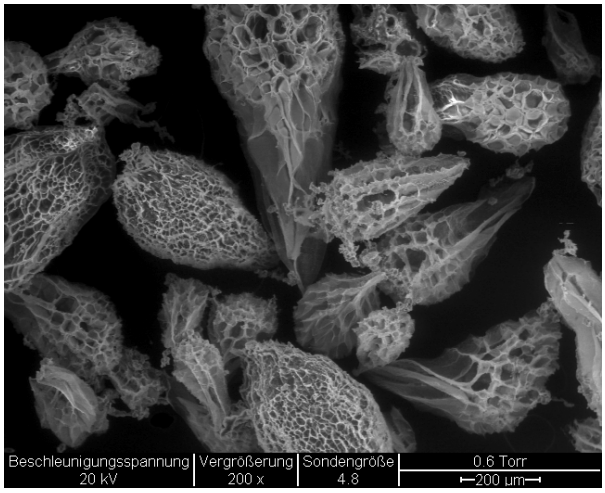

Figure 4.10: ESEM micrograph of freeze-dried SAP previously swollen in pore solution.

As can be seen in Figures 4.11-4.13, regardless whether SAP swelled in distilled water or in pore solution, polymers particles always returned to the virgin spherical, or in worst case scenario (Figure 4.13), quasi-spherical shape. Volume change behind this phase transition took place without visible traces of alternative routes for water transfer (porosity[23], cracks) but also without its limitation (film formation). This means that osmosis, or in other words diffusion across a semi-permeable membrane of polymer, was truly the main mechanism for fluid transport and storage. Virtual lack of pores is also characteristic of solid rigid hydrogel, for which water absorbed in/attached to the hydrogel structure is mostly bound [Omi 05][Gan

[23] Note the same feature was expected based on density of material which was 1450 kg/m³ therefore far from one attained for porous products and amounting typically few hundreds kg/m³.

10], i.e. cannot be removed unless high pressure is applied. Plausibly, all these features decided about favourable thermodynamic and kinetic availability of IC water, which will be verified experimentally in the following sections, especially Section 5.2 and 5.3.

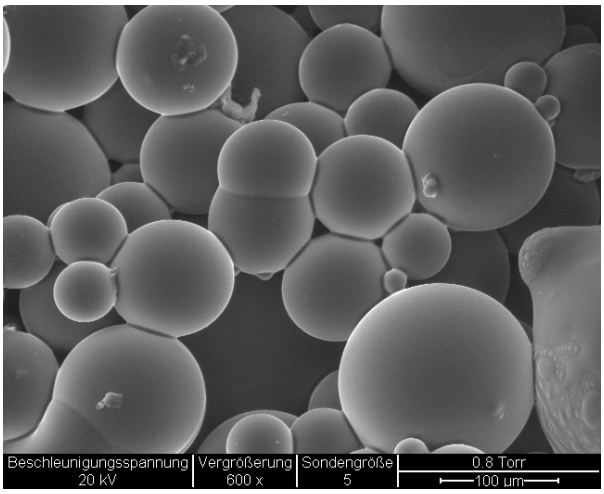

Figure 4.11: ESEM micrograph of oven-dried SAP previously swollen in distilled water.

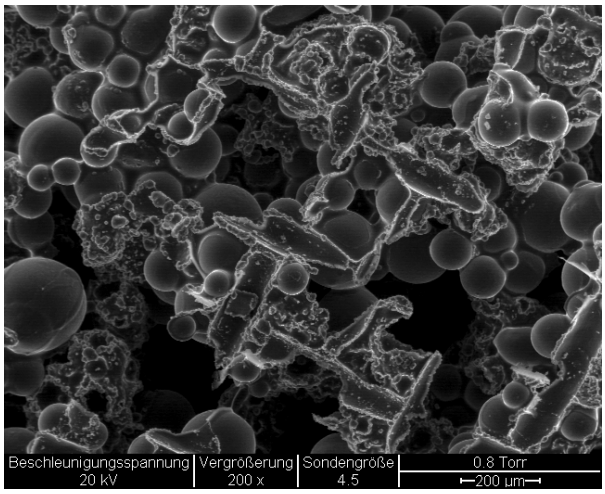

Figure 4.12: ESEM micrograph of oven-dried SAP previously swollen in pore solution.

Another important property finally resulted from anionic nature of the SAP under investigation. As found from combined ESEM-EDX investigation, the material acted as ionic filter when contacted with pore solution. In extreme case, this led to precipitation of calcium carbonate on the surface of SAP particles, see Figure 4.12 and 4.14. It is an important observation given changes in pore solution composition can be used to comprehend various processes and phenomena taking place in concrete, including shrinkage [San 12] and its mitigation [San 11].

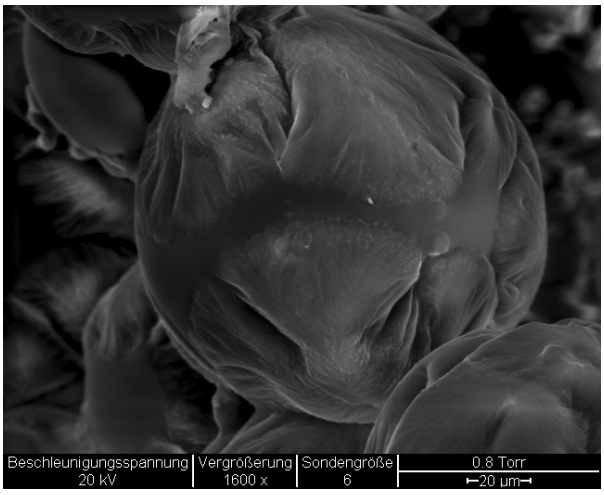

Figure 4.13: ESEM micrograph of wrinkles appeared on surface of oven-dried SAP previously swollen in pore solution.

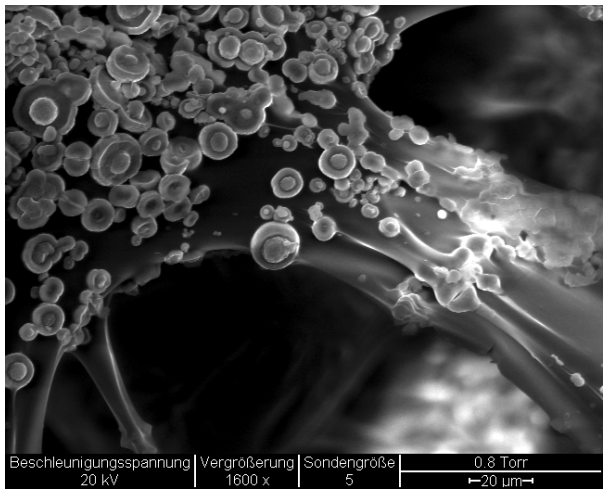

Figure 4.14: ESEM micrograph of calcium carbonate precipitated on surface of oven-dried SAP previously swollen in pore solution.

iii. Observations on SAP as applied in concrete

In order to validate observations made in previous subsections and thus to complete the idea about applicability of SAP as IC agent, it was necessary to test its behaviour in application of interest. Figures 4.15 and 4.16 present fragments of slices as obtained from the CT measurement at two different concrete ages. Depicted are the most common mode of changes and exemplary one appearing in minority, respectively.

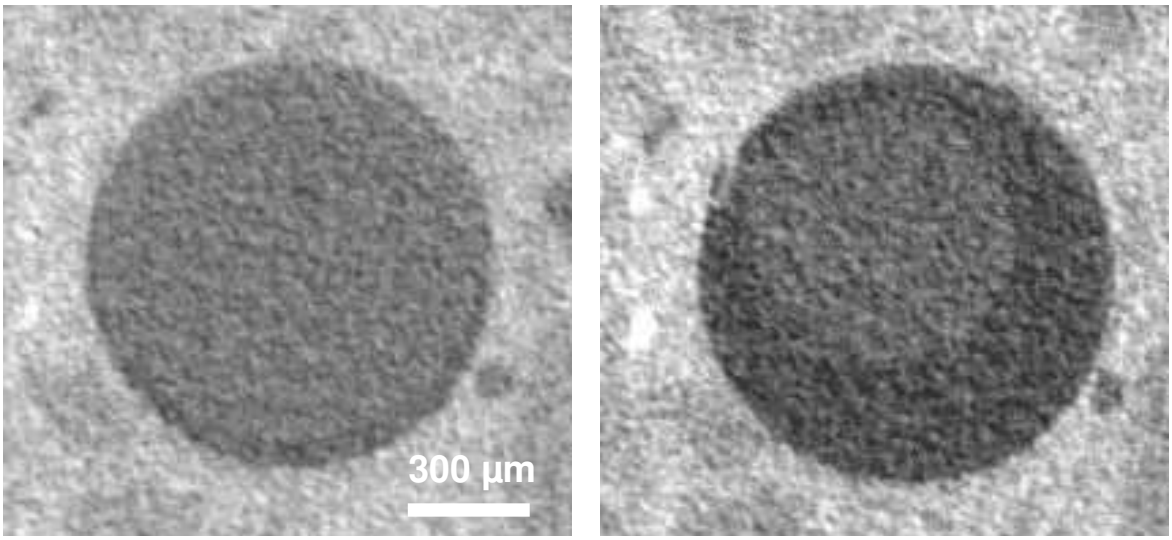

Figure 4.15: Appearance of SAP particle in the accommodating pore in UHPC matrix at concrete age of 10.5 h (to the left) and 34.5 h (to the right).

In both cases, the shape of the pores corresponded to the geometry of the SAP particles applied. That is to say, the material accomplished another demand expected from use of polymers in concrete, in particular very high mechanical stability under severe actions, especially high shear in mortar and concrete mixing [Ram 96]. As the first pictures of each mode yield, the high robustness remained in concrete for many hours, thus confirming observation made previously in free conditions. Why in some cases the integrity was compromised within testing time (Figure 4.16, to the right) is not understood yet. Note however that this scenario and specific behaviour of SAP was less frequent than 'regular' changes, see Section 5.3-5.4 and Appendix H for more details.

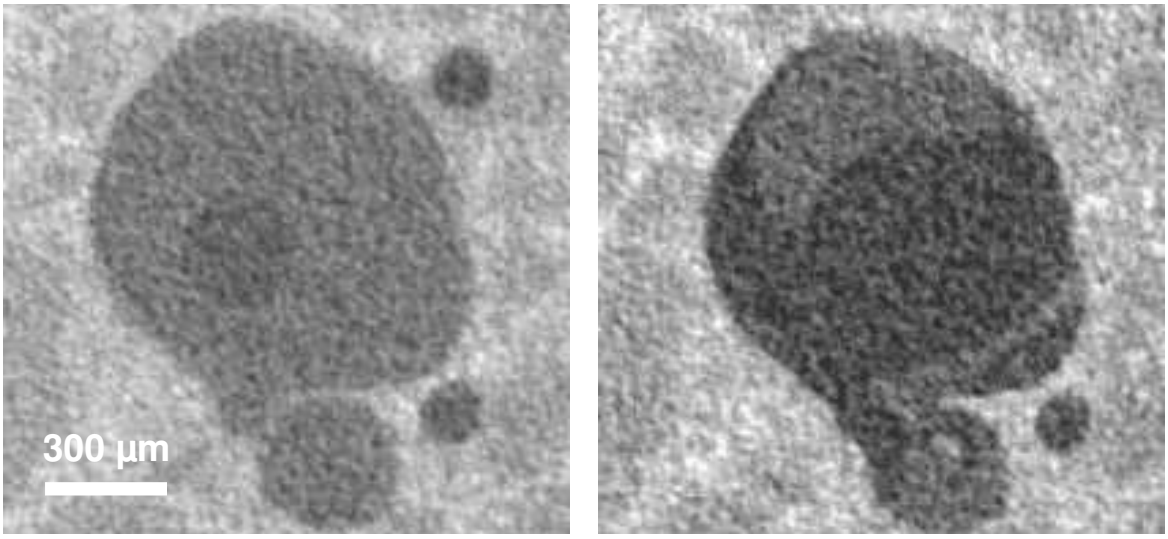

Figure 4.16: Appearance of another SAP particle in the accommodating pore in UHPC matrix at concrete age of 10.5 h (to the left) and 34.5 h (to the right). The specific behaviour of SAP – splitting – is here evident.

4.2.3 UHPC matrix

i. Air content aspect

As acknowledged in many studies [Sch 04][Ma 04], air voids may constitute important part of the UHPC's pore structure. From fresh viscous UHPC mix, the bubbles cannot escape easily and can only be removed when special production conditions (mixing with vacuum, compaction with very specific range of vibrations [Sch 04]) are applied. Usage of polymeric admixture may increase the concern. In fact, past experience with rival polymer types (i.e. polymer latexes [Ram 96] but also PCE [Laz 13]) showed necessity of the use of suitable antifoaming agents during mortar or concrete mixing for securing low entraining action of polymer. SAP may not be different in this respect given that in mixtures containing this IC agent content of air often increases too, e.g. [Pié 06][Moe 09].

Bubbles of any source, if remained in matrix, may affect numerous hardened concrete properties, some of which could be decisive for IC effectiveness, e.g. permeability [Hal 95]. Therefore, air void content was investigated as first.

Figure 4.17 shows the volume fraction of air bubbles as derived from measuring fresh concrete densities of fibre-free finely grained UHPC mixtures without and with modification by IC. The values represent the averages from all test performed for particular composition, name of which is given next to markers. Standard deviations which typically appeared small are not presented. To demonstrate the existing tendencies, the results obtained for identical

total w/c ratios are connected by lines. The reference value of control mix (F-R) is presented as well as is marked in the diagram with dark, dotted line.

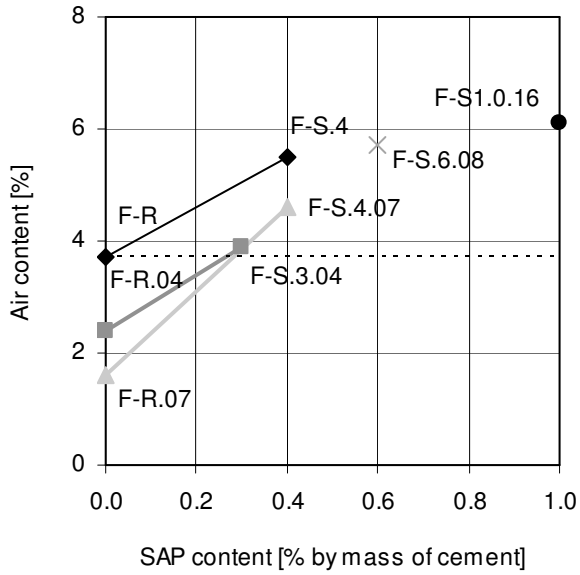

Figure 4.17: Average air content of fresh finely grained UHPC mixtures in dependence on the content of SAP and extra water.

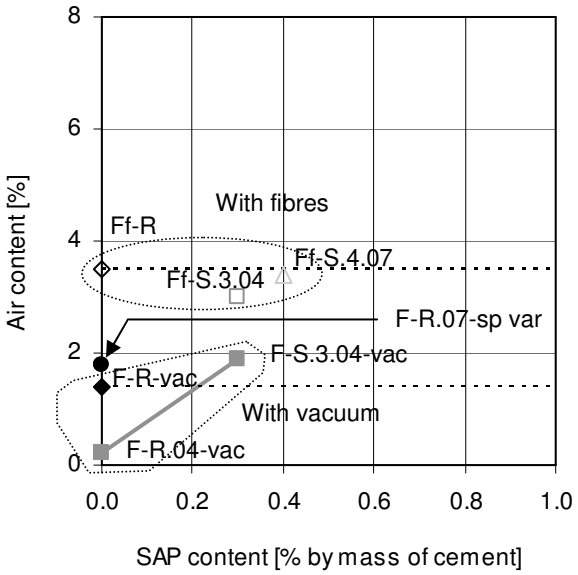

Figure 4.18: Effect of vacuum mixing, addition of steel fibres and superplasticizer reduction on air content of finely grained UHPC mixture.

Although the results showed some deviation from ones obtained using pressure method (see [Dud 10b][Dud 10c]), selfsame clear trend was observed. In particular, among all combinations of the UHPC without coarse aggregates, the mixtures which contained both pure addition of SAP and conjunction of both IC variables yielded increase in air content. This attribute matches the observations made on various cement-based materials by Piérard et al. (case of HPC, [Pié 06]) and, for some SAP types, by Moennig (case of ordinary mortars and concretes, [Moe 09]). Still, taking all combinations tested into account, it could be stated precisely that the effect was more dependent on the SAP material used and dramatic reduction in effective w/c (standing behind unfavourable changes of workability, e.g. special case of F-S.4) that on content of superplasticizer[24], e.g. the case of mix F-S.4 sp var with air content of 3.9 % (not shown in Figure 4.17).

As visualized at present, the increase in volume occupied in the SAP-incorporating UHPCs by air was relatively low when compared to the control mix (F-R), but became pronounced when reference was done to the mix with equivalent amount of extra water (i.e. equivalent total w/c). When considering the amounts of IC agent used and the resultant changes in property

[24] Note that the last two factors are in general the same ones which control behaviour of mixes without SAP addition, see e.g. result obtained for F-R.07 and F-R.07 sp var in Figures 4.17 and 4.18, respectively, and result obtained for the control mix (3.7 %, Figure 4.17).

obtained in first scenario, at first glance, the effect caused by IC appeared somewhat limited. Indeed, with increasing content of SAP, there was only little increase in the magnitude of the air content. To make effect understood, specific way of IC variables introduction and related alterations in composition had to be taken into account, particularly a volumetric reduction that was forced with regard to original ingredients content and, in turn, their complexes i.e. paste and mortar fraction. In applying so, the effect of IC although still evident became somewhat concealed and found only partial reflection in the values obtained.

As can be seen from Figure 4.18, where special cases of finely grained mixtures are presented, regardless introducing IC, air amount was reduced in both cases viz. when applying vacuum mixing and when maintaining steel fibres in original composition. The latter occurred rather unexpectedly and could be likely ascribed to little mixtures tested within one composition, mixing time extension and/or some additional hidden phenomenon emerged.

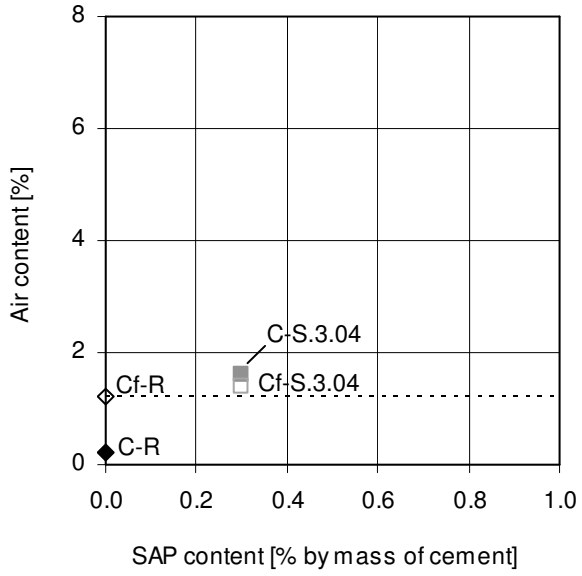

Figure 4.19: Average air content of coarse grained UHPC mixtures.

The effect of IC on air content of coarse-grained UHPC gave results as presented in Figure 4.19. A consequent impact of the modification by IC occurred in case of both fibre-free (full markers) and as well as compositions with steel fibres (empty markers). Smaller value of void content compared to finely grained UHPC compositions in all cases may be traced back to numerous changes introduced on stages of original mix design and the mix production. This may include, although needn't to be limited to: decrease of mortar fraction and less dense aggregate packing (the favourable to effect occurrence acc. to [Kli 52][Ram 96] and [Pow 68a]), less charging mixing energy as assessed based on power consumption of the mixer as well as generally shorter mixing time (in agreement with [Ma 04]), as well as usage of large particles with rough surface appearance. In view of different experience with novel superplasticizer [Laz 13], application of another superplasticizer was assumed as important modification too. Yet, neither these facts and reasons speculated nor other changes in composition (this including variation of cement and silica fume content, as

well as type of the latter) yet prohibited from the main effect i.e. acquiring higher air content in concrete with IC.

As such, in any concrete, air can have different origins and furthermore can undergo various changes (dimensional, structural) [Pow 68a][Mie 58][Du 05][Ley 09]. Meanwhile numerous factors related to mix components or mixing particularities may decide about the phenomenon extent [Bru 55]. In case of concretes containing PCE superplasticizers, however, air entrainment can be assumed to result from decrease of the surface tension of the liquid phase in the paste [Mor 01], a dissolving medium for this admixture. At high surfactant concentration (example of which PCE superplasticizers are), reduced surface tension can motivate foam production, a side effect and one underlying reason for air-entrainment provided by some although not all PCE-based admixtures [Laz 13]. Once due to change of the surface tension a partition of pores is achieved, the rate of coalescence of bubbles decreases and so does the void release in accordance with Stoke's law[25]. Meanwhile, with the surface tension of interstitial fluid being reduced, bubbles become stabilized against mechanical deformation and rupture [NCHRP 06].

The abovementioned mechanism takes place presumably somewhat simultaneously to the so-called 'champagne effect' or 'bubbling' phenomenon [Ram 96], occurring when the superplasticizer dosage used is higher than recommended (case of finely grained UHPCs). As generally agreed, the associated bubbles regenerate on mixing as easily as they are removed from the concrete mix (sparkling out like champagne bubbles); however, in low w/c 'sticky' mixtures some bubbles always remain entrapped and cannot be removed even if heavy vibration is applied. This apparent difficulty is to be perhaps related to the so-called 'cushion effect' existing in high viscosity concretes [Du 05][Laz 13], therefore UHPC as well, and which secures bubbles from rupturing and coalescence. Both viscosity and void content in UHPC without IC become reduced only when using higher basic w/c and/or when reducing superplasticizer content, see Figure 4.17 and 4.18, respectively.

Assuming like e.g. in [Laz 13] that superplasticizers (after adsorption on cement particles) act in process of air entrainment strictly as bubbles stabilizers, generation of voids could be

[25] Alternative explanations of mechanism behind air entrainment by PCE can be found. E.g. Morin et al. [Mor 01] attributed formation of a greater number of bubbles and/or a lower bubbles radii to larger air-liquid surface, which, important enough, was assumed to result from lowering of surface tension, the action induced by PCE-alike superplasticizer.

alternatively related with vortex action and existence of 'three dimensional screen', following theory originally put forward by [Pow 68a], see also [Du 05]. On mixing, much air is likely being infolded by mix equipment operating on the fresh mass, adding to amount of bubble existent e.g. from dissolution in mixing water [Mie 58]. Such mass must fall and cascade onto itself. Since in material containing fine aggregates the solids provide interstices that constrain paste and air bubbles, numerous air bubbles become trapped. According to Mielenz et al. [Mie 58], the most efficient aggregate graining playing primary role in the process is sand ranging between 150 and 600 µm. This fully explains more air entrapped in finely grained compositions compared to UHPC with coarse aggregates.

The engagement of SAP in any of the processes bringing about further air entrainment remains unclear. On one hand, for better absorption characteristic in terms of kinetics and capacity, some SAP compositions can be enriched with foaming aids and blowing/foaming agents without or with foam stabilizer (i.e. surfactant) [Omi 05]. Sign of such components was indeed revealed in own case, see Section 4.2.2. On the other hand, these are typically intended to make the SAP structure more porous, making the final product less rigid which did not match the characteristic of the material tested. Therefore the effect of SAP should be more likely traced back to ability of chelating the calcium ions [Lam 05], apparent component of pore fluid which can alter foaming and stabilizing property of surfactants of ionic type [Du 05], example of which are both PCE superplasticizers used.

Eventually, the values reported in this section were used to assess which of the mixtures tested were self-compacting according to air content criterion presented in Table F.1, see Appendix F. It appeared that unless vacuum mixing is applied, only some finely grained UHPC with IC succeeded to fulfil this requirement, being among goals intrinsic to UHPC. Even so, in the other group, the critical air content value acceptable for self-compacting concrete turned out to be exceeded insignificantly whereas the difference was small compared to space needed to accommodate the SAP pores. Also, it should be respected that optimum air content is only a tool and added value on way to acquire defined properties in hardened state. In fact, as can be followed based on results presented in Appendix I, the effect on compressive strength was to negligible extent decided by air content unlike content of IC variables, i.e. SAP and extra water added for IC; meanwhile, neither positive nor negative effect of IC on the very high freeze-thaw resistance of UHPC tested was recorded (presentation of results omitted), as expected. Thus results were found very satisfying.

ii. Finalizing characterization of pore structure

As several relationships have been successfully obtained in different studies while showing excellent correlation degree, the rule of thumb says that permeability could be linked to one of many porosity/physical characteristics as determined by the MIP method. These being median pore diameter, modal pore diameter and threshold diameter were obtained from the resultant MIP data including pore size distribution and cumulative intruded volume curve.

Table 4.2 demonstrates the change of these parameters and detected MIP porosity prior and after enriching the UHPC mixes with IC in dependence on age and specimen conditioning. Additionally, total porosity results are listed in the same table as well. Only three most relevant finely grained mixtures, in particular studied repeatedly within one composition or otherwise tested for influence of sample preparation method or mixing under vacuum, are concerned.

Table 4.2: Pore characteristic parameters of finely grained UHPC.

Batch No.	Mix (drying and cessation method)	Cumulative volume, total and *for D < 10 µm* [mm³/g]			Volume median / Modal (neck, pore-throat) pore diameter [nm]			MIP / Total porosity [%]		
		1d	3d	28d	1d	3d	28d	1d	3d	28d
1	F-R (oven dry)	54.3 *52.0*	39.3 *37.8*	29.6 *27.3*	26.6 / 26.8	20.4 / 20.0	11.3 / 9.5	12.5 / -	9.1 / -	6.9 / -
	F-R (iso + vac)	54.2 *51.6*	37.0 *34.7*	29.5 *27.7*	20.6 / 21.1	13.9 / 13.5	9.4 / 8.0	12.5 / -	8.6 / -	6.9 / -
	F-S.4.07 (oven dry)	92.0 *85.7*	69.2 *63.8*	49.7 *44.9*	30.1 / 29.3	21.4 / 20.9	11.1 / 9.0	19.4 / -	15.0 / -	10.9 / -
	F-S.4.07 (iso + vac)	94.2 *88.4*	67.2 *61.8*	51.3 *46.6*	27.5 / 27.4	14.7 / 13.7	10.0 / 8.2	19.9 / -	14.5 / -	11.2 / -
2	F-R (oven dry)	50.7 *48.6*	38.6 *35.3*	19.4 *17.0*	26.9 / 27.4	20.6 / 20.4	7.9 / 4.1	11.7 / 13.8	9.0 / 12.5	4.6 / -
	F-R (fr-dry)	57.7 *55.7*	38.8 *36.6*	22.7 *20.9*	25.3 / 26.7	13.6 / 13.3	14.7 / 3.7	13.2 / 16.3	9.0 / 12.7	5.4 / -
	F-S.4.07 (oven dry)	71.5 *65.4*	54.7 *49.9*	37.8 *33.3*	28.7 / 28.3	21.0 / 20.1	9.8 / 4.5	15.6 /-	12.1 / -	8.5 / -
	F-S.4.07 (fr-dry)	81.8 *78.0*	55.1 *51.0*	37.7 *34.4*	37.1 / 31.6	14.1 / 12.9	11.5 / 5.9	17.8 / -	12.2 / -	8.5 / -
3	F-R-vac (oven dry)	44.7 *42.5*	36.1 *33.4*	24.1 *22.6*	26.8 / 27.2	25.1 / 25.3	16.8 / 15.3	10.5 / 14.9	8.5 / 11.8	6.2 / 10.1*
	F-S.3.04-vac (oven dry)	66.7 *62.5*	50.4 *46.9*	33.5 *31.2*	28.0 / 27.5	24.9 / 24.7	15.6 / 15.3	14.8 / 18.5	11.3 / 15.6	7.7 / 12.0

* included approx. 1% of porosity not captured by MIP (> 140 µm)

(continued on the following page)

Table 4.2: Pore characteristic parameters of finely grained UHPC *(continued)*.

Batch No.	Mix (drying and cessation method)	Cumulative volume, total and *for D < 10 µm* [mm³/g]			Volume median / Modal (neck, pore-throat) pore diameter [nm]			MIP / Total porosity [%]		
		1d	3d	28d	1d	3d	28d	1d	3d	28d
All tested	F-R (oven dry)	53.7 (3.5) *51.7 (3.4)*	38.3 (1.3) *36.3 (1.3)*	24.8 (3.1) *22.9 (3.2)*	28.4 (3.1) / 28.6 (3.1)	20.8 (1.1) / 20.4 (1.4)	11.2 (2.0) / 8.4 (2.7)	12.4 (0.7) / 15.9 (1.3)	9.0 (0.2) / 13.2 (0.8)	5.8 (0.7) / 10.4 (1.8)
	F-S.3.04 (oven dry)	72.0 (4.3) *67.6 (3.5)*	47.8 (2.5) *45.3 (2.2)*	30.9 (1.5) *28.3 (1.6)*	33.0 (4.6) / 32.0 (4.0)	21.3 (0.7) / 21.0 (1.2)	11.1 (1.4) / 9.7 (1.7)	16.0 (0.9) / 19.2 (0.8)	10.9 (0.5)/ 15.3 (0.8)	7.1 (0.5) / 11.9 (0.7)
	F-S.4.07 (oven dry)	81.5 (8.2) *75.5 (8.8)*	60.7 (6.1) *56.0 (5.5)*	41.6 (5.0) *38.1 (4.6)*	32.9 (4.7) / 32.4 (4.8)	22.6 (1.4) / 21.9 (1.4)	12.2 (2.2) / 10.4 (3.8)	17.6 (1.5) / 22.0 (0.8)	13.2 (1.1) / 17.3 (0.2)	9.4 (1.0) / 13.5 (1.5)

Generally speaking, certain regularity can be seen in results obtained. E.g. irrespectively of modification by IC, the selfsame effect resulted from change of sample conditioning before testing, bringing about negligible and certain increase in cumulative volume of pores as well as total MIP porosity captured after switching from oven drying to combined method (iso + vac) and freeze-drying (fr-dry), respectively. This effect typically disappeared until later ages. In comparison, change of production conditions to vacuum mixing showed the opposite trend, but again it did not depend on IC. Some small value differences between selfsame mix repetitions and for samples conditioned in the most basic way (oven drying, 40 °C), although present, were only attributed to change of basic ingredient batch and, important enough, fell in range of standard deviation or otherwise in direct vicinity of it. Notably, the first pronounced increase in cumulative pore volume and MIP porosity therefore occurred when enriching the UHPC with IC constituents, the result to be related to accommodating of SAP particles and, supposing some contribution, increasing air content in matrix.

Despite the effect caused by IC, a unimodal-like pore size distribution remained in all cases (for details, see [Dud 10c][Moe 10]). The few exceptions were stated typically at later ages, at which bimodal-like picture was occasionally observed, with or without renewed increase in content of pores in size approaching the limit one (3.4 nm). Far more surprising, however, expected effect of IC variables on characteristic pore sizes and linked to increased degree of hydration (see Section 4.5.4) was lacking. In fact, the median and modal pore diameters

remained very similar to control mix or even, especially at young ages, amounted to higher values.

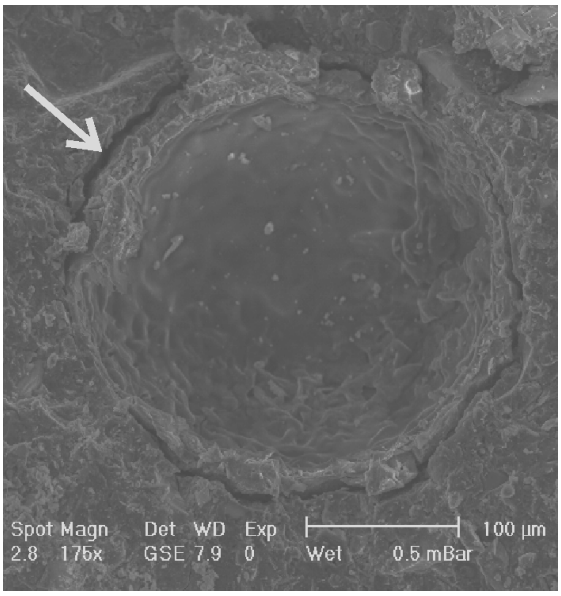

Figure 4.20: ESEM image giving appearance of pore left after SAP in subsequence to sample crushing and drying in oven.

As comparison of UHPC without and with IC demonstrated, this could not be explained as simply as by change of sample conditioning method. It is suggested that this could be masked effect of IC and outcome of competition between favourable hydration conditions in mix with IC (bringing about finer porosity) and autogenous swelling (triggered by crystallization pressure, for instance, likely bringing about pore coarsening). If so and to be validated later on in this work, it was clearly won by the latter. One additional reason for pore coarsening could be also related to premature release of water from SAP. Since potentially taking place when concrete is in fresh state, it could be bringing about additional capillaries, or, as believed at present, increase of diameter of ones already being formed in the matrix. Last but not least, existence of gap between SAP pore and the rest of UHPC matrix (Figure 4.20) as well as increased air porosity (see the following section) with potential access to intrusion could have paid important contribution to observation as well.

When performing MIP experiment, it shouldn't be forgotten that result can be charged with numerous errors somewhat in addition to input parameters (surface tension, contact angle and pore shape definition). Using standard method of intruding mercury in own case meant, for instance, that only dimensions of pore necks connected to bigger chambers (i.e. open pore entry sizes) were in fact measured. Beside issue of ink-bottle type porosity, demonstrated to potentially exist in UHPC of interest as well (Figure 4.22), the material was furthermore expected to possess isolated porosity as well as entrapped air porosity. Ways to detect and characterize either of last two are limited while particularly the entrapped porosity, if accessible for mercury and intruded, can have dramatic effect on amount and size of MIP porosity measured. Nonetheless, such porosity was largely eliminated upon mixing under vacuum.

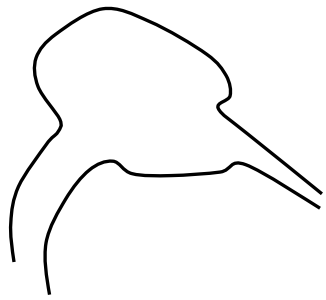

Figure 4.21: Schematic picture of an exemplary ink-bottle shaped pore with entrances having different and, compared to the 'bottle', smaller radii, after [Esp 06].

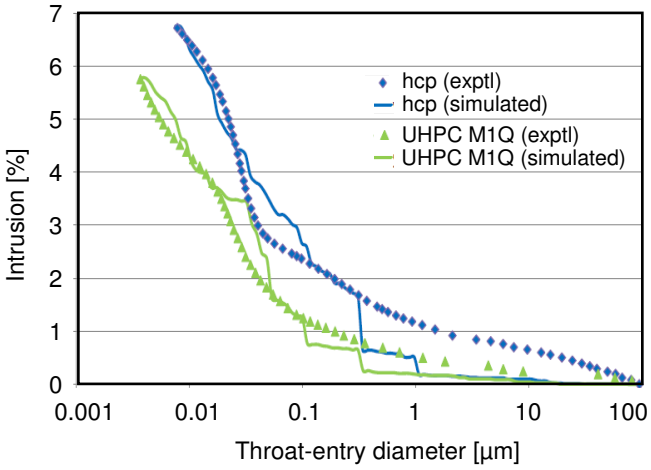

Figure 4.22: Simulated mercury intrusion curves of hardened cement paste (original data are squares) and 28-day-old finely grained UHPC M1Q (original data are triangles) using simulation software Pore-Cor [Mat 08]. Existence of ink-bottles is found as compatible with the shape of the MIP curve.

Looking back at Table 4.2, it could be deduced based on difference between total and MIP porosity obtained for F-R-vac that isolated porosity other than air voids or some other pore group (e.g. part of porosity which could not be intruded by mercury like voids having diameters smaller than 3.4 nm) was truly part of the finely grained UHPC microstructure. At any age considered, it amounted to 20-30 % of total porosity that was not captured in MIP test. Consequently, this put in question sense of employing improved intrusion technique for finding realistic pore structure of UHPC that would facilitate discussion on transport properties of this material[26].

To overcome apparent difficulty but also in order to remain scientifically correct when addressing pore size distribution of UHPC, literature review has been performed. A very similar porosity range to one determined in MIP test was revealed. E.g. after engaging combination of non-destructive methods, Morin et al. [Mor 02] predicted evolution of capillary network in finely grained UHPC of composition similar to tested. They found

[26] According to Ekaputri et al. [Eka 09], the water trapped in the ink-bottle type porosity cannot be released until high curing temperatures such as 60 °C are applied. This may suggest that oven drying at lower temperatures might provide insufficient condition to fully desiccate the test sample. On the other hand, starting from temperature of 50 °C, changes are noted in the water phase distribution as being related to the variations in fluid bound by hydrates formed [Han 01]. Simultaneously, apparent pore coarsening takes place (results of oven drying in 105 °C not shown) which puts in question usage of higher drying temperatures. By using oven drying and 40 °C for own sample conditioning condition, it was assumed that none of these effects was decisive for observations made.

diameter of 40 nm to be attained once solid particles percolated in all three directions[27]. Once hydration progressed, the pore width continued to decrease to reach, at final testing age of approx. 3 days, the size of 2 nm i.e. value characteristic for internal porosity of hydrates. Philipot et al. [Phi 98] testing another kind of what is called Reactive Powder Concrete made similar observation. The main difference was, however, demonstrating porosity as being distributed in more classes at once, in particular ones associated with widths of 56, 17.8, 5.8 and 1.4 nm. Concurrent studies of Bonneau et al. [Bon 00] and Tam et al. [Tam 12] again supplemented information on microstructure of UHPC. As found by former researchers, few hydration days and degree of hydration of minimum 0.20 were required for different finely grained UHPCs to attain capillary depercolation [Bon 00]. About the same time was sufficient for similar material to maintain permeability characteristic rather for concrete of w/c of 0.4, even if in somewhat difficult dependence on superplasticizer (and consequently entrapped air) content [Tam 12]. Eventually, despite the well-known effect of size [Ack 04a], Soliman and Nehdi [Sol 11][Sol 12] testing finely grained UHPC after final set found immediate, remarkable and long lasting effect on deformation of this material in response to submergence in water, consequently showing pronounced permeability of this material to curing fluid holding true for 75x75 mm² cross-section used[28].

Concluding, since depercolation is likely to be continuous process, only final stage of which is reaching the characteristic threshold, porosity of finely grained UHPC studied is likely to remain continuous for many hours. Judging purely based on pore diameter detected by MIP (see Table 4.2), the largest fraction of interconnected pores was of magnitude associated with capillary pores in hydrates [Lou 99] or, being more specific, representing residual space located between the C-S-H clusters [Mor 02][29]. On one hand, the associated size is distant from the MIP pore size range 100-1000 nm that acc. to [Bág 97] may be predominantly related to permeability for some cement-based materials. This held true also upon introduction of IC, although size of pores and their content somewhat increased in comparison to control mix and so did the MIP range 10-1000 nm which, however, still constituted only minor part

[27] Note that radii have been converted into pore widths by multiplying the referenced values by 2

[28] Though UHPC is conceptually very dense material of very low permeability/diffusivity, water migration especially if occurring in early ages may be imagined to be result of delayed and little extent of pozzolanic reaction. This observation has been also made for the studied M2Q matrix [Pfe 10]. Related to existence of silica fume agglomerates or other, this means postponing pozzolanic C-S-H gel production, to which overall reduction of porosity and reduced permeability/diffusivity can be ascribed to.

[29] The general knowledge is that drying and intrusion with mercury as such contributes to coarser pore size distribution and higher connectivity of the pores, respectively. In contrast, because of ink-bottle effect, a smaller pore size distribution is always measured. This means that, to some extent, these effects could equalize and provide satisfying precision of MIP measurement. Studies showing successful usage of MIP data in modelling various properties and phenomena are indeed present, e.g. [Li 14][Che 13].

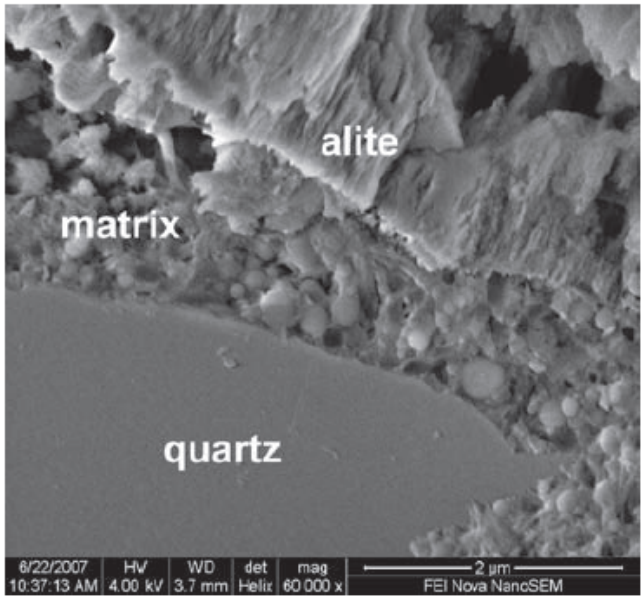

Figure 4.23: Interfacial transition zone as occurred in studied M2Q matrix after 2d curing time in moulds and at room temperature, after [Moe 08].

of MIP porosity (see [Dud 10c][Moe 10] for full MIP curves and results). In any case i.e. irrespectively of IC, this should be related with lack of Interfacial Transition Zone at the contact of aggregate with paste in UHPC (Figure 4.23) that otherwise largely contributes to pore connectivity, e.g. [Hal 95]. On the other hand, pore sizes as detected for IC-incorporating UHPCs using MIP are still in the range where capillary pressure operates [Li 14], which would be important from perspective of enhancing the drainage of water out of SAP, for instance.

Important enough, the mass transport dominance by regarded pores maintains for appreciable amount of time. This could be likely explained by late initiation and poor progress of pozzolanic reactions at room temperatures (Figure 4.24), otherwise paying contribution to pore depercolation [Fel 85]. It is exceptional feature common to Reactive Powder Concretes [Bon 00] which is different from the case of pure cement-silica systems [Est 09]. As currently assessed, nearly half (i.e. 0.21, for the chosen w/c = 0.225 and silica fume content of 15 % [Ben 91]) of the maximum attainable degree of cement hydration (0.44, calculated by modified Powers' model, see Appendix D) would be needed for capillary depercolation to occur, given no delay of pozzolanic reaction start occurred. As will be seen later on, it took 3-4 days for hydration to acquire state close to maximum attainable progress (see UPV investigation in Section 4.5). Practice with UHPC shows that this time can easily extend to few weeks after small change of RPC composition [Mat 00]. The picture is finally consistent with results of Morin et al. [Mor 02] who claimed no progress in capillary pore segmentation of UHPC until pore diameter reaches 20 nm, currently measured only after approaching age of 28 days.

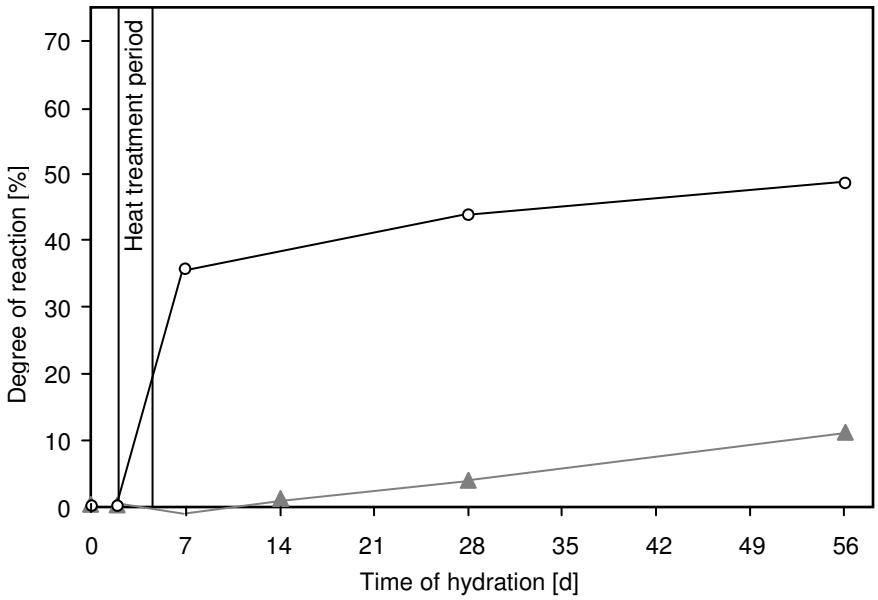

Figure 4.24: Reaction degree of silica fume in M2Q after water storage (full triangles) in comparison to one after heat treatment (empty circles), after [Pfe 10].

In terms of mass transport, role of shrinkage microcracking potentially taking place in young finely grained UHPC [Fey 01] even despite likelihood of high relaxation rates [Sch 07a][Epp 10] can only be speculated upon. The experience shows that this artefact type may easily originate from Young's modulus difference between matrix components [Hea 99] and reasons forcing their propagation from air voids [Kus 05] (decreased fracture toughness and increased heterogeneity around the voids); meanwhile, microcracking can be evidenced even when relative humidity is very high [Cha 82][Tam 00]. When being result of shrinkage, the occurrence of microcracks is typically accompanied by permeability increase [Hea 99]. In finely grained UHPC, however, some change in permeability is expected from usage of superplasticizer in content other than some optimum [Tam 12]. The reason needn't be though entirely different given the control the concrete admixture has over air content (see beginning of Section 4.2.3 Section) and the close relationship of latter to cracking phenomenon[30].

[30] According to Kustermann [Kus 05], the area of microcracks in concrete exposed to autogenous shrinkage increases with increase of air void content. In contrast, Grassl et al. [Gra 10] find number of microcracks as independent of number of the voids but again confirm appearance of cracks around air voids. In any case, the effect of IC bringing about air content increase and its potential role in mass transport must be considered.

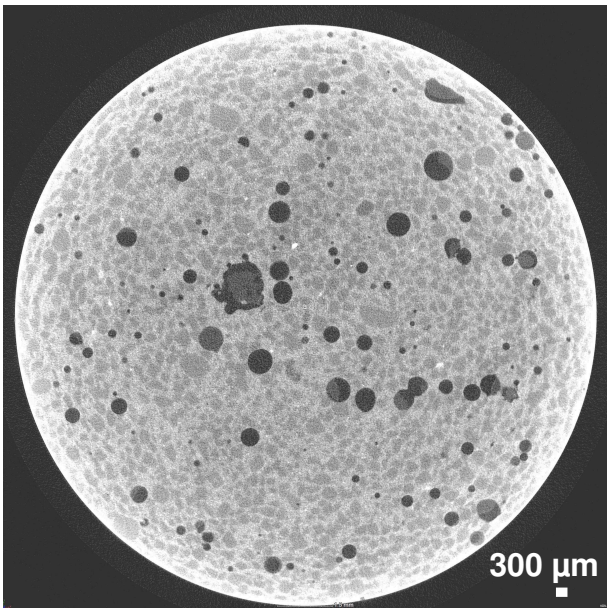

Figure 4.25: Cross-section of UHPC and 2D image as obtained from a computer tomography scan at concrete age of 34.5 hours.

As can be seen from Figure 4.25, signs of microcracking were absent until the test finish age of approx. 34.5 hours, the time otherwise sufficient for major part of autogenous shrinkage of unmodified UHPC mix to develop. On one hand, this well agrees with results of the MIP tests, where evidence of large cavities was indeed missing. On the other hand, width of microcracks could have been smaller than 7 µm, i.e. the best resolution attained with CT. E.g. nanocracks having width of 100 nm have been observed by Kjellsen and Jennings in a low w/c cement-silica fume paste system [Kje 96]. Furthermore, since UHPC material exhibits high chemical activity especially in early ages, some cracks could have healed like expected in UHPC [Fey 01] before measurement was performed. Restated, microcracks could have appeared unnoticed. Obviously, this issue requires in depth studies in future e.g. using acoustic emission.

The contribution of air to internal transport network as such, without judging whether it leads to microcracking or not, is vague. This aspect especially of interest taking into account the amount of air voids in mixes with IC produced without vacuum that increased with increase in SAP addition and percentage of air voids in total porosity (even approx. 1/3 in early ages as noted in experiments!). The general opinion yields that air voids contribute to development of capillary pores [Koe 12] or at least are interconnected by them [Won 11]. This is reasonable given that the only deposition place could be water-filled space, turning into capillary porosity. However, whether they act as conductors or insulators, implying they have been enabled to be fully (or at least partially) filled with water or not, respectively, this already depends on more factors. Examples are moisture state and transport property/mechanism under consideration; in sorptivity case, the effect is non-consistent [Won 11]. Some authors [Pow 53] put doubt in saturation of air voids with water, opposite to others, e.g. [Yan 04]. In optimistic scenario, i.e. water enters voids, early stage of hydration would obviously be the time expected for the phenomenon to happen. In other case, particular voids would be expected to contribute to so-called self-sealing mechanism [Hea 98], which would add

complexity to distribution of water from SAP and, simultaneously, would increase likelihood of microcracking. This issue will be further addressed in Sections 4.6.3 and 5.5.

Last but not least, role of hollow shells hydration grains (Hadley grains) observed in UHPC of interest in early ages [Moe 10] should be concerned. On hydration, these may either develop in completely hollows shells (i.e. with no remnant anhydrous core inside) or they may refill with fresh hydration products. In other words, in the latter scenario, when water is delivered due to connection with pore system, hydration proceeds. However, since existence of this pore type on the hydration progress was reported as continuous, its participation in mass transport appears unlikely.

To which extent the change in UHPC composition affected porosity can be traced in Table 4.3. In general, a very similar picture to that observed previously for finely grained UHPC was revealed.

Table 4.3: Pore characteristic parameters of coarse grained UHPC.

Batch No.	Mix (cessation method)	Cumulative volume, total and *for D < 10 µm* [mm³/g]			Volume median / Modal (neck, pore-throat) pore diameter [nm]			MIP / Total porosity [%]		
		1d	**3d**	**28d**	**1d**	**3d**	**28d**	**1d**	**3d**	**28d**
All tested	C-R (40 °C)	43.2 (-) *41.3 (-)*	34.6 (-) *32.3 (-)*	23.4 (-) *20.9 (-)*	30.8 (-) / 31.9 (-)	23.4 (-) / 22.9 (-)	7.8 (-) / 5.2 (-)	10.6 (-) / 15.3 (-)	8.4 (-) / 13.9 (-)	5.7 (-) / 10.5 (-)
	C-S.3.04 (40 °C)	56.8 (3.0) *53.2 (3.0)*	41.1 (3.4) *39.3 (4.0)*	25.8 (-) *23.6 (-)*	32.6 (1.2) / 31.7 (2.1)	24.7 (0.8) / 24.0 (1.8)	8.8 (-) / 7.6 (-)	13.2 (0.6) / 16.8 (0.9)	9.8 (0.7) / 14.1 (0.6)	6.1 (-) / 10.8 (-)

4.2.4 Summary and concluding remarks

In this section, both the SAP material chosen in preliminary investigations (see Section 3.2.3 for more details) and the two main UHPC matrices provided for modification with IC were characterized. Investigations focused on the properties which could be decisive for successful applicability of IC, especially in terms of autogenous shrinkage reduction. For gaining more in-depth knowledge, SAP was tested in different conditions, viz. in concrete and alone, under varied treatment with different fluids. Drying method choice turned out to be decisive for some results as well.

ESEM (for studying morphology), laser granulometry (particle size distribution), FTIR and EDX measurements (chemical composition) as well as other tests including ones requiring contact with distilled water or pore solution (absorption capacity, robustness) and the eventually computer tomography (appearance in concrete) were the investigation techniques applied. It was found that the SAP material dealt with was product composed of discrete round particles synthesised by the inverse suspension polymerization and existing in relative wide range of sizes. The characteristics were favourable to IC according to literature. E.g. for given size and content of SAP used for IC, it is typically expected for the spherical product to match the role of IC agent better [Est 09], even if absorption of suspension-polymerized SAP (and thus amount of curing fluid being stored by them for curing) is, as a rule of thumb, lower compared to gel/bulk-polymerized one [Est 09][Sir 10][Ass 13], this holding true especially when monomer composition is similar [Sir 10][Gor 11][Sch 12c].

The key to success of the IC agent under investigation was related to three additional observations, viz. 1) common maintenance of structural integrity (confirmed in concrete and in simplified tests with cement paste filtrate), 2) lack of hydrates growing in the SAP pores until latest testing ages (with exception observed only in tests with filtrate, and limited to precipitation of $CaCO_3$, to be further discussed in Section 4.5.6), and 3) relatively slow deswelling of SAP in alkaline environment of concrete after some early release of water carried by IC agent (to be further elaborated in Sections 5.3-5.4 and Section 4.3.4+4.5.5, respectively).

The following argumentation can be given:

- Ad (1) There was favourable IC agent appearance after absorption of pore fluid and upon exposure to load, independent of exposure time. It was noted to be a direct fulfilment of basic requirements for use of any polymers in concrete [Ram 06]. Although from new perspective, the demands originally put forward by Ohama and Ramachandran and presented in [Ram 06] must be obviously matched by any SAP to be fit for IC purposes. The arguments supporting favourable behaviour (robustness) in own study were presumably low sol fraction of the polymeric material used and no specific surface modification otherwise governing speed of water release, see Table 4.4.
- Ad (2) With no hydration front progressing, the hydrates precipitate in capillaries originally formed in system irrespectively of SAP and extra water addition. This limits potential formation of ‘ink-bottles’ or even closed porosity by the SAPs [Kle 13], and

accordingly prevents from loss of curing ability or the effect offsetting expected in such case [Jen 02], this being otherwise revealed as the reduction in the relative humidity despite IC agent presence [Jus 15].

- Ad (3) The absorption capacity and sorption kinetics recorded for SAP under investigation validate the behaviour of anionic SAPs most suitable for IC purpose [Gor 11][Sch 12c].

Table 4.4: Predicted outcome of material characteristics in terms of autogenous shrinkage mitigation.

Characteristic provided	Effect on sorption property or mass transport		Effect in terms of autogenous shrinkage reduction	
	Positive	**Negative**	**Positive**	**Negative**
SAP material				
High robustness	Straightforward		Straightforward	
Anionic nature	Could be responding to changes in pore solution composition		Additional mechanism by which IC water is withdrawn; meanwhile binding ions driving the shrinkage	Water can be lost prematurely
Low sol fraction	Straighforward		Additional mechanism by which IC water is withdrawn	
No porosity	Likely leading to relatively low deswelling rate		Straightforward	
No cracks	Likely leading to relatively low deswelling rate		Straightforward	
No skin formation		Likely leading to relatively high deswelling rate	There is ease of IC water withdrawal	Some fraction of water can be lost prematurely
UHPC matrix				
High air content	When acting as conductors	When acting as insulators	Depends on effect on mass transport	
Porosity in range of capillary force activity	Straightforward		Straightforward	
Potential microcracking	Straightforward in case of shrinkage cracks		Straightforward in case of shrinkage cracks	

Important enough, the SAP under investigation was confirmed as being composed of two monomers, in agreement with original information obtained from the distributor. The specific composition makes such material sensitive to changes in pH, ionic composition of fluid contacted with and temperature, which may consequently provoke it to undergo further

volume changes in response to any alteration in either of factors in concrete. New look on IC work mechanisms may be thus needed. This issue in more depth is discussed in Section 5.4.

Air content investigations, MIP tests, other tests to determine specific densities (and thus total porosity), and eventually ESEM investigations, computer tomography and the additional information collected from project partners were needed to describe IC-relevant properties of UHPC. Before the materials became truly dense and little permeable following expectations, some properties clearly spoke for sufficient moisture transport specifically in early ages. For the finely grained UHPC, allowing good water suction in early ages also in opinion of Soliman [Sol 11][Sol 12], this was attributed to delayed pozzolanic reactions, tens of hours needed to achieve capillary depercolation and perhaps prohibited growth of hydrates in the air pores. For further discussion on role and favourable aspects of UHPC matrix, also see Table 4.4 and Section 4.6.3.

4.3 Extent of mix modification by IC

4.3.1 Introduction

This section comprises own experimental investigations on the assessment of absorption capacity of SAP, being another relevant piece of puzzle as to IC effectiveness. The second associated task being dealt with is verification whether the polymeric material carries all the extra fluid added for the reasons of IC. The presentation is preceded by a short critical review of some of the methods having very different level of usefulness for finding absorption capacity of SAP under conditions to be met in concrete (changing composition of pore fluid, load). One of the gravimetric methods, tea-bag test in particular, is chosen for further analysis. The capabilities and limitations of the test, the influence of factors deriving from concrete production on its results, and most importantly, the new interpretation of results of tea-bag test ('window of absorption') are outlined. On this basis, the assessment of IC water carried is limited to estimation of maximum SAP absorption in concrete by means of empirical test. Mixtures having identical or at least comparable slump flow to that of control UHPC (i.e. without modification by IC or extra water) are eventually tested by rheometer to capture the potential and expected water release. In addition, reasons for classifying investigated UHPC mixtures as self-compacting, based on fresh rheological properties, are depicted.

4.3.2 Absorption determination method

i. Possibilities and limitations

An important piece of the puzzle in evaluating effect of IC is to assess absorption capacity of SAP and thus to verify whether the material carries all the fluid added for IC reasons. The task is not new. To date, however, mainly because of complex sorptivity behaviour of SAP as well as limited number of methods to test SAP absorption which underwent critical review, with only few in concrete [Ass 13][Ass 14], it remains chink in armour for successful internal curing optimization.

Many of methods known mainly from industrial experiences as being summarized in Appendix E cannot be implemented for the goals of this study. This relates to the fact that either no load is or can be applied during measurement or provision of the required and often changeable conditions during absorption is not feasible. Furthermore, testing multiple samples differentiated by size and where the load would be distributed uniformly or the opposite (e.g. as on exposure to shear) also appears to be the apparent difficulty of the methods proposed.

Concluding, knowing absorption capacity of IC agent after it has been already introduced into concrete would be an advantage of solution found. Only in such conditions all factors controlling sorption behaviour of SAP (i.e. exposure to one or more modes of shear/compression as well as varying composition and ionic strength of pore solution) would be in play.

With this in mind, some non-destructive methods and stereology-based approaches could become of interest. Summary of various methods including Neutron Tomography, Nuclear Magnetic Resonance, Computer Tomography, calorimetry tests and evaluation of cross-section of hardened samples has been recently made in [TC 225-SAP]. All other disadvantages of particular approaches aside, their utilization though mostly scientifically correct would not be handy if numerous tests were to be performed. This becomes understood when acknowledging that with amount and type of SAP being held constant, absorption changes with variation of concrete composition, see Section 4.3.3 for example. Another argument against some method application is yielded in case when both shape and size of pores ascribed to air and accommodated SAP particles are similar (the present case!), therefore where demand of production with vacuum appears as necessity to run the estimation e.g. the case of stereology-based approaches. Still, some of the methods could be applied for other as important purpose, viz. tracing behaviour of IC agent in concrete and thus for verifying its applicability for IC, see Section 5.3-5.4 and Appendix H.

As alternative, it has been suggested [TC 196-ICC] that empirical tests on fresh concrete could be a useful tool for the purpose of absorption capacity estimation. Both Mönnig [Moe 09] and Assmann [Ass 13] including group work [Ass 14] carried out comparison of slump flow as measured at different ages for cement-based mixtures without and with IC. A certain difficulty of the method proposed yet considered as necessary to avoid formation of clumps was using additional mixing time within the intervals between the measurements. If applied especially to viscous UHPC, it could mean possibility of introducing extra amounts of technological air[31], impacting workability in similar manner to clumps, i.e. rather negatively that positively. Furthermore, when mixing (and thus shearing of particles) is continued, some water could be potentially lost from SAP (due to solvent release, solvent detachment e.g. [Ver 03]) leading to increase of effective w/c. This adding to specific behaviour of SAP, which

[31] It is recalled that SAP-enriched mixtures did generally contain higher content of air compared to control mixes, see Section 4.1.2. Using extended mixing in the intervals between measurements would therefore increase the concern.

might be releasing water prematurely and independently of load, a resultant increase of slump flow could be expected. That is all to say, there is no guarantee that test for absorption capacity is finished within reasonable frame of time. E.g. fluidity loss was followed for UHPC without and with IC in study of Huang and Wang [Hua 12]. In contrast to control mix, lack of stable trend in slump flow changes until the age of 120 minutes (i.e. the end of test) was reported for one of tested mixtures with SAP.

It was thus concluded that in cases like present only the maximum absorption capacity and not equilibrium swelling of SAP could be assessed from the slump flow measurement. In stating so, it is also assumed that any changes occurred subsequently to time of obtaining the characteristic value is to be interpreted as premature effect of IC, having impact e.g. on capillary porosity that forms.

ii. Solution, establishments and comments

Approach based on test of consistency was applied in own study. Consistency of mixtures containing the IC agent was adjusted by using extra water during mix production but only in amount strictly needed for SAP to attain its maximum absorption capacity. Experimentally, this meant that slump flow comparable to that of F-R was aimed at for IC-incorporating mixtures. The choice to follow particular approach (with only one measurement of consistency per composition) was made having knowledge of both: specific sorption characteristic of SAP under investigation and earliest possible times of the spread record. Both of them and the comparison of their results revealed to be very favourable for the goal of finding maximum absorption capacity of SAP under investigation.

Firstly, the tea-bag test results (Figure 4.26) have been analysed. The investigation for which cement paste filtrate had been used yielded information about shortest swelling time until attaining the maximum absorption for particular SAP. This is in contrast to tea-bag tests with distilled water which, as can be followed based on Section 2.5.1, should lead to revealing the longest swelling time. With some further adjustment in the interpretation of results (e.g. arbitrary shifting of absorption peak to nearest maximum value since having similar value to that of peak)[32,33], important observation was made: It was revealed that despite some changes

[32] It should be pointed out that maximum of absorption when the concrete is already being mixed is likely to be acquired later than in free conditions due to exposure to shear loading, otherwise leading to at least partial water release from polymer at any stage of its absorption [Zan 02]. This implies that further limitation of left 'window of absorption' borderline but being ascribed to swelling in pore solution should result purely from behaviour of SAP itself. Please see later discussion in the Section.

in absorption depending on solvent type, maximum absorption for SAP studied falls into very limited time-frame, which herein is proposed to be referred to as 'window of absorption'. This 'window of absorption' should be expected to differ from one IC agent to another.

Secondly, realistic times of the spread records were assessed. This time was comprised of mixing times ('wet mixing'; changing with mixture type, see Section 3.2.6), extra time taken to start the slump flow measurement and one needed for fresh concrete to flow until stop. After new information was obtained, comparison of both pictures regarding time was made.

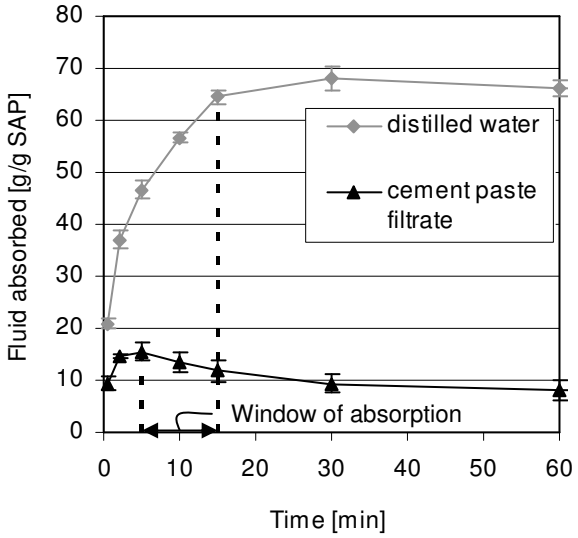

Figure 4.26: Determination of 'window of absorption' from tea-bag test results.

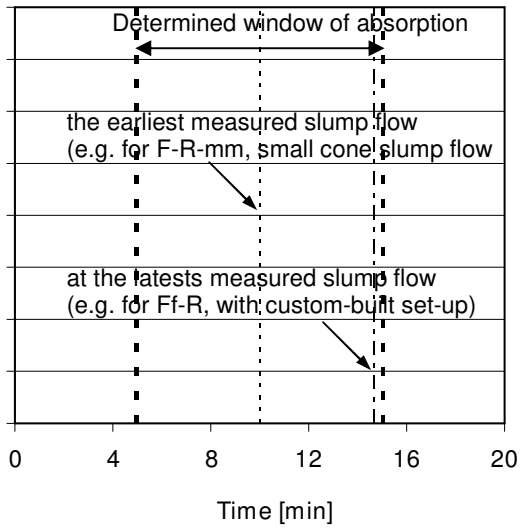

Figure 4.27: Comparison between slump flow testing times and time range ('window of absorption') in which studied SAP attained maximum absorption.

Figure 4.27 shows results of regarded comparison. A clear overlap was found. This meant that estimation of maximum absorption capacity in particular conditions could be performed in first measurement after mixing. This protocol was applied in Section 4.3.3. It is belief of the author that in future 'window of absorption' could be a very useful method for making the choice about slump flow record time or otherwise to decide whether method itself is fit for assessing the absorption in case of rival SAP material chosen.

The remaining question is the role of two simplifications made in the approach with regards to the tea-bag result viz. lack of externally applied load and other pore solution composition. For the moment, the following assumptions can be made with respect to issues not accounted for in measurement:

[33] Absorption rate of SAP in artificial pore solution (i.e. similar to that met in concrete) has been showed to be higher than in cement paste filtrate [Pou 13], the latter being used for own measurements. This again limits the 'window of absorption' and makes the estimation more precise.

- the role of the load

In concrete, this term should be associated with impacts related to mixing as well as the outcomes of gravity, and/or perhaps compaction, if applied [Lee 10]. Such processes bring about added stresses on polymer phase, this including shearing and compressive stresses. Should they be present, there will be shift of the (Gibbs) free energy minimum in SAP towards a new position, see Figure 4.28. It is the type of load as well as state of swelling [Buc 05] which decides about/determines the course of this change and the point in time when the new equilibrium is attained.

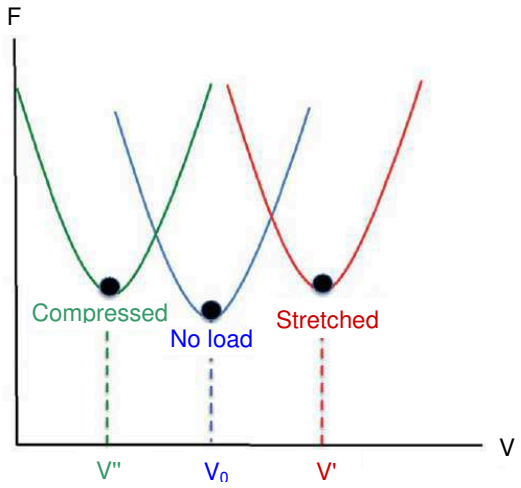

Figure 4.28: Schematic of a shift of the minimum of the free energy (F) caused by imposed deformation, and the resultant change in volume (V) [Ura 12].

Purely theoretically, effect of exposure to shear and compression on volume can be expected as negative i.e. the size of SAP should be smaller compared to case without load. Applied to own case, however, some details regarding extent of exposure and the exposure time clearly differ the individual impacts.

In case of shear, the outcome depends on loading rate applied and theoretically can result in more phenomena [Zan 02][Ver 03]. Ones being relevant in respect to absorption include reversible slow release of solvent (being hindered by simultaneous molecule attraction) and permanent release of liquid once absorbed for the low and high strains applied, respectively. However, these were also reported to hold true after SAP has already swollen and carried appreciable amounts of liquid (in trend: the higher the swelling the higher potential solvent release) [Zan 02][Ver 03]. This is different for the case of mixed UHPC with IC. Considering that: 1) absorption takes place in pore solution, meaning relatively small amount of fluid absorbed by the IC agent, 2) uptake proceeds at appreciable rate for SAP under investigation while 3) passage of time until slump flow record is sufficient to cover any loss of fluid since 'wet mixing', low likelihood of effect or otherwise its negligible impact on maximum absorption capacity as well as time required for it could be hypothesized.

In comparison, the effect of compressive load on swelling of ionic gel (polyelectrolyte) could be addressed using chemical potentials (= pressures) instead of energy acc. to Eq. 4.2:

$$\pi_{gel} = (\pi_{net} + \pi_{ion}) - \pi_{ext} = (\pi_{mix} + \pi_{el} + \pi_{ion}) - \pi_{ext} \quad (4.2)$$

where π_{mix} is the osmotic pressure difference due to entropy and enthalpy of the mixing of the polymer network and water (i.e. osmotic contribution reflecting polymer-solvent interactions), π_{el} is the osmotic pressure difference due to rubber elasticity of the polymer network (i.e. elastic contribution associated with chain deformations in the network and determined by the chain conformation properties) and π_{ion} is the osmotic pressure difference due to counterions of the polymer (i.e. contribution from ion-solvent mixing and electrostatic effects).

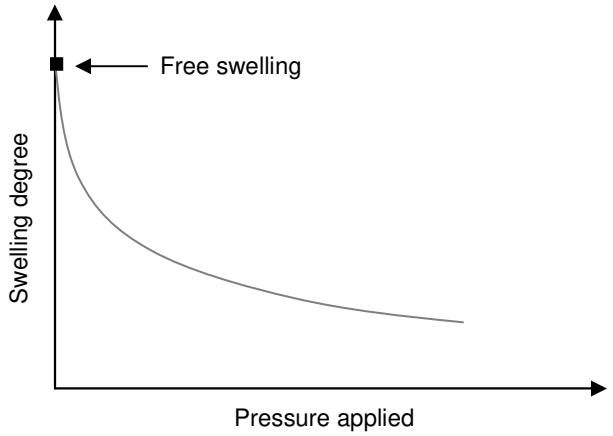

Figure 4.29: Predicted effect of external load on degree of swelling. Based on [Dub 94][San 04].

Based on equation, it is evident that exposure to compressive load makes the static pressure inside gel to increase in contrast to osmotic pressure (of counterions [Ver 05][Gan 10]), undergoing the opposite change. This is accompanied by decrease in entropy and, as stated in [Gan 10], reduced repulsion between monomers caused by van der Waals interactions. The result is reduced volume and diminished sorption capability, see Figure 4.29.

Last information implies that when compression is applied at least some difference in the rates of swelling compared to behaviour without load could plausibly result as well. However, whether this turns into delay of absorption capacity approach time, this is known to be decided by more factors. The rule of thumb is it is network porosity which governs the main absorption mechanism [Gan 10], and consequently decides about the absorption rate as well [Zoh 08][Omi 12]. In fact, any limitation of transport pathways would be disadvantageous from perspective of the latter[34]. On the other hand, substantial difference in sorption behaviour presumably emerges also from mode of swelling allowed that can be either uniaxial

[34] It should be pointed out that the longer the SAP absorption in concrete lasts, the lower likelihood that capacity attains the maximum which could be attributed to competition for water molecules (diminishing potential of absorbing fluid free of any interactions) and/or their entrapment. This follows the hypothesis of Jensen and Hansen [Jen 02] claiming restricted absorption of large SAP particles. It is another argument why according to present author the load effect is insignificant when SAP absorption determination time is concerned.

or three-dimensional [Dub 94]. Among other reasons (e.g. particle size distribution and density of functional groups being another pieces of puzzle), these could be used to explain why both lack of effect [Bud 97] and, presenting the worst case scenario, pronounced delay [Sal 10] of equilibrium swelling acquire time have been reported.

In respect to last aspect, it should be recalled that tested SAP were characterized with low functional group density, leading to much lower absorption in distilled water compared to SAP of [Sal 10]. For such SAP, osmotic compression might be as important, if not more, as external load. Therefore, the delay that in [Sal 10] related to attaining small percentage of total achievable absorption capacity (less or much less than 25 %) was considered as being too little to change the picture observed in swelling measurements. Since in mixing of UHPC with IC load is also exerted from mixing start[35], impact of compressive load is highly unlikely to have retardation effect.

- the role of the ionic concentration

It is recalled that tested SAP is a polyelectrolyte. This means that, among other contributions, the swelling pressure constitutes of additional ionic component (see Eq. 4.2) that strongly depends on the ionic composition of solution. The rule of thumb is swelling pressure will rapidly decrease in response to increase in the concentration of ions, e.g. [Dub 94].

In fresh concrete the pore solution produced from gradual dissolution of reactive components, regardless whether modified by chemical admixture of not, undergoes continues changes. Still, at any stage of development, its ionic concentration can be assumed to be of lower magnitude compared to that of the cement filtrate as used in tea-bag tests. This should be attributed to the low w/c of UHPC (bringing about lower concentration of e.g. Ca^{2+} per g of cement [Hos 09]) and presence of PCE as well as silica fume ('capturing' Ca^{2+} ions present in pore solution, see [Cha 81][Pla 09] and [Oga 80][Pla 09], respectively). It directly translates into lower artificial, isotropic compressive load [Hor 88][Dub 94], also known as osmotic compression. On one hand, the consequence is that peak of absorption appears somewhat later than that recorded in cement paste filtrate and narrower 'window of absorption'. On the other

[35] It should be pointed out that swelling under load of equal magnitude may [Dub 90] but needn't be [Hor 88] affected depending whether three- or one-dimensional mode of network swelling is allowed. The decisive factors for observation are, among others, size of polymeric sample [Dub 89], and, assumed by present author, the state of swelling when loading is applied as well as type of change considered (e.g. volume and not absorption time!). This would set another new challenge in accounting for the effect of load in concrete. For simplicity, this effect is not discussed further.

hand, because chelating of ions still present takes place, thus restricting absorption, importance of shearing and compression in selfsame respect becomes diminished. Again, this would be apparent advantage for the IC water estimation proposed.

4.3.3 Investigations on consistency of fresh concrete

i. Finely grained compositions

In Figures 4.30 and 4.31, the results from the slump flow tests recorded for the most relevant of fibre-free finely grained UHPC mixtures and being produced by means of high-intensity mixer without vacuum unit are presented. The values represent the averages from all test performed on particular composition under moist condition and with usage of larger version of the test set-ups. In case of Figure 4.30, the same mode of presentation as used previously in Figures 4.17 and 4.18 is applied. The standard deviations for two mixes studied repeatedly i.e. F-R and F-S.3.04 are given in Figure 4.31.

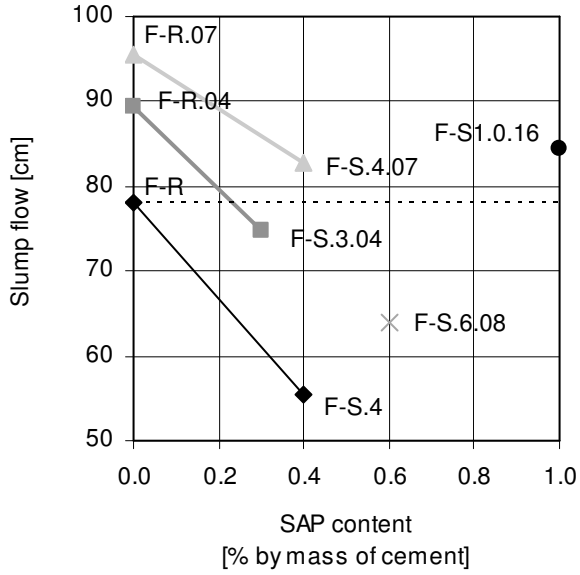

Figure 4.30: Average slump flows of fresh finely grained UHPC mixtures in dependence on the content of SAP and extra water.

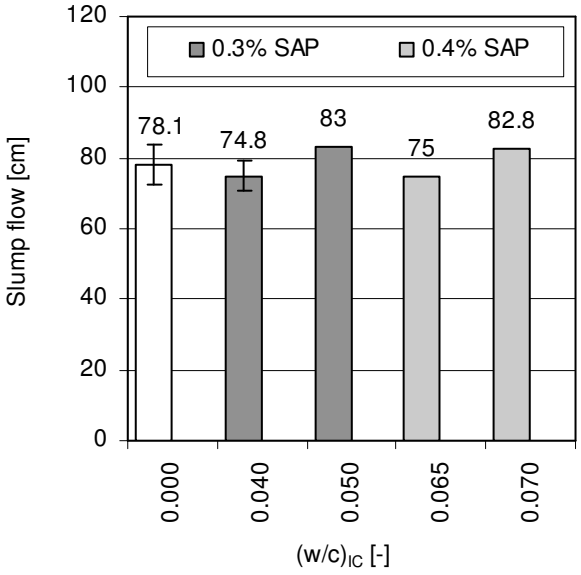

Figure 4.31: Detailed effect of extra (curing) water variation on consistence of finely grained UHPC mixtures with two dosages of SAP as compared to the control mix.

It can be seen that despite some consistence change, nearly all SAP-enriched mixtures exhibited a consistence of excellent self-compacting concrete. Indeed, their spreads alike that of control concrete F-R, fell into range suggested for concrete requiring no additional compaction, see Table F.1 in Appendix F. This is in clear contrast to mixtures with pure

addition of water, for which, simultaneously, bleeding phenomenon[36] turned out to be a concern unless superplasticizer content was reduced (F-R.07-sp var, not shown).

Another exceptional case is UHPC F-S.4, i.e. mixture with SAP but without extra water. At first glance, the effect of SAP observed here resembled the one observed in case of other IC agent-incorporating mixes. In particular, it was observed a loss of workability relative to the control mix with the selfsame water-to-cement ratio. This confirmed absorptive nature of the polymeric admixture added and showed that the well-known Lyse's rule[37] applies on addition of polymers in UHPC. Differently compared to cases, however, for the mix F-S.4, not solely the target flow spread was not reached, also change of consistence was pronounced enough to stop the mix from acquiring the self-compaction.

The unfavourable change of workability continued until the foreseen and empirically verified amount of extra water added[38] was sufficient to reach saturation threshold of the SAP used. Estimating based on proportions of SAP and extra water used (note: being given in the mix designations), it can be read that the solution uptake by SAP was about 15-16 g/g SAP. On one hand, this value was similar to that determined in tea-bag test with cement paste filtrate. It cannot be interpreted other than a coincidence given that no optimization was made when producing the pore solution. On the other hand, this correspondence was not very surprising considering that in both cases load was applied. The main difference was the artificial character of the load in case of tea-bag test, which was clarified in the foregoing section. It might be eventually usage of other polymeric admixture such as superplasticizer in concrete which brought the values closer together, to be traced back to control over the pore solution composition.

The prediction made in concrete using 'on top' approach when introducing IC variables could be assumed as more precise (and therefore also closer to tea-bag result) in comparison to the rival way of IC implementation, i.e. where part of aggregate fraction is removed in order to accommodate swollen SAP particles. The argument behind this statement relates to the fact that coating thickness of paste around particle and thus water film remain unchanged. Without

[36] Bleeding phenomenon is treated as taking place if observing ring of bleeding water surrounding the mortar/concrete cake formed.
[37] Lyse's rule was founded in 1932 and states that 'for given materials consistency of fresh cement concrete is determined exclusively by the free water content of the mix'.
[38] As alternative, more superplasticizer has been used as well. However, this solution required enormous increase of admixture content whereas benefit from mitigation of autogenous shrinkage was only little, see Section 4. for more details.

'on top approach', some water is otherwise released and, if not taken into account and not absorbed by SAP, increases the effective w/c. This leads to a consequent error of absorption estimate[39]. The concern vanished with 'on top' method.

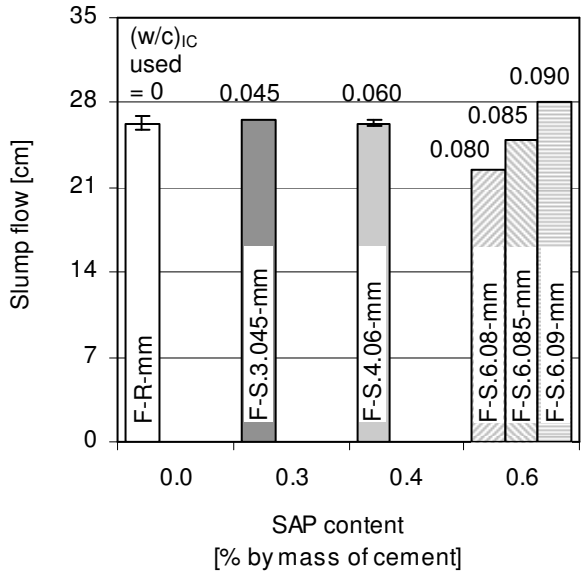

Figure 4.32: Small cone slump flow values of finely grained UHPC produced by using mortar mixer (-mm) with exclusion of basic ingredients properties effect.

Note that the above-derived value was reconfirmed and fixed as precisely 15 g/g SAP after the more systematic test programme had been performed. In Figure 4.32, consistence of mixtures produced with change of mixing details but, important enough, from the selfsame batch of premix of dry ingredients and in identical laboratory conditions is presented. Standard deviations are given for mixtures studied more than twice.

Somewhat similar in comparison to tests with high-intensity mixer (see Figure 4.30 and especially Figure 4.31), a significant role played by extra water variation was evidenced. In fact, even when the rate of over- or underestimation of the SAP uptake was relatively small, it still led to pronounced change of flowability. However, the main benefit of conducting additional tests was reduction of factors otherwise impacting slump flow value. One source of such impact is so-called batching error i.e. phenomenon related to change of physical properties of concrete component and found for material batches from different production dates. Should it be present especially in case of cement, it may lead to change of more concrete properties including slump flow and rheology [Sch 08] or even shrinkage [Bra 02][Epp 09]. Hence, usage of premix facilitated and allowed more precise prediction of the maximum SAP absorption.

[39] On one hand, the excess water gained on replacement of aggregate by the IC variables needn't be expected large. For instance, removal of quartz sand having adsorption of 1 % in amount of 6 vol.-% would increase the effective w/c by about 0.0025 [Won 09]. On the other hand, the replacement needn't concern one aggregate only, e.g. [Mec 06][Dud 08b] or will be restricted to removal of very fine aggregate like in finely grained concrete. Should the diameter of aggregate removed be decreasing, more water would become available in system. A change of any aggregate fraction could furthermore change tortuosity (including microcracks, …), consequently affecting all transport properties [Won 09]. This means that two systems theoretically differing only by presence IC would be in fact even harder to compare. This is not the case for manner of IC variables implementation used.

The small deviation from the prediction withdrawn based on Figure 4.32 was noticeable for one mix with highest amount of SAP but nonetheless was not decisive for the claims put forward. Evidently, because IC/SAP modified other properties in fresh state, secondary contribution cannot be excluded e.g. insignificant but negative outcome of air entrainment on workability, cf. Appendix F. In any case, this deviation only appeared for the largest content of IC variables (0.6 % SAP, extra w/c = 0.09), and a mix which was tested only once. In such scenario, slump flow change can be attributed also to other reasons, e.g. formation of polymer assemblies due to high content of the admixture.

As signalized above, because the mixtures could not be always prepared from single batch of cement and other ingredients, execution of mix repetitions appeared as necessity. In this respect, the results collected in Appendix F yielded that neither the change of test conditions nor the testing set-up provided overall any significant change to the information obtained to this point for the fibre-free UHPCs. In contrast, the results obtained for fibre-incorporating mixtures were inconclusive due usage of different dry ingredients batches and owing to insufficient amount of mixtures tested.

ii. Coarse grained compositions

To which extent the change of UHPC composition, small changes in mixing regime and varied presence of fibres affected the behaviour of SAP-enriched mixtures with extra water is to be followed based on Figure 4.33.

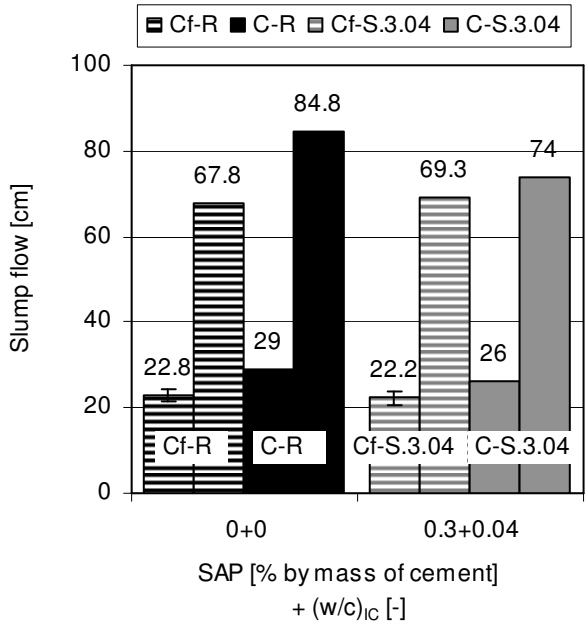

Figure 4.33: Effect of IC and fibres on small and big slump flow of coarse grained UHPC, average values.

While all mixtures showed consistence of self-compacting concrete or very close to one, implementation of internal curing occurred to provide two contradicting results. Once the IC components were added to fibre-containing mixture, very similar concrete flowability of so created Cf-S.3.04 in comparison to that of control mix (Cf-R) was obtained. This means that for regarded mixtures the selfsame type of polymer and being in identical concentration appeared to absorb less than yielded for the case of

finely grained UHPC, i.e. about 13.3 g/g SAP (if having the very small change of flowability neglected) versus 15 g/g SAP, respectively. In contrast, the polymers commenced to uptake remarkably much more when the fibres are removed. Indeed, in terms of big slump flow value obtained the difference was remarkable: over 11 cm between mixtures C-R and C-S.3.04 in comparison to only 3 cm in case of finely grained mixtures F-R and F-S.3.04 (see Figures 4.33 and 4.31, respectively).

The more dramatic loss of consistence compared to the other matrix clearly suggests increased absorption of the IC agent. The underlying reasoning is however other than IC variables' content applied, which was maintained constant. Load factor aside, the belief is this could be attributed to other mixture proportioning of B5Q: increase of silica fume content, more superplasticizer added whereas only insignificant increase in w/c (simplification made here: change of pozzolan and superplasticizer product and, given SAP-to-cement mass proportion, cement content considered of secondary importance). As experience shows, in pure cement-based system with a particular kind of binder, it is, among others, the w/c applied [Ass 13] which decides about initial composition of pore solution including concentration of Ca^{2+} ions, therefore the parameter limiting absorption of SAP. On the other hand, part of the ions released should be adsorbed by pozzolan [Oga 80] and/or the rival polymeric admixture present [Cha 81][Pla 09], from which overriding the former effect likely resulted. These contributions were apparently masked when the fibres were added, which may be explained with increased tendency of fibres to interlock in presence of coarse aggregates.

4.3.4 Rheological tests

In Figure 4.34, the evolutions of flow curves obtained during first and second rotational mode of testing two finely grained UHPCs, one without and one with IC, are demonstrated. The mixtures are characterized by nearly identical slump flow after mixing. As indicated by the number of curves, each composition was examined repeatedly, three times in particular.

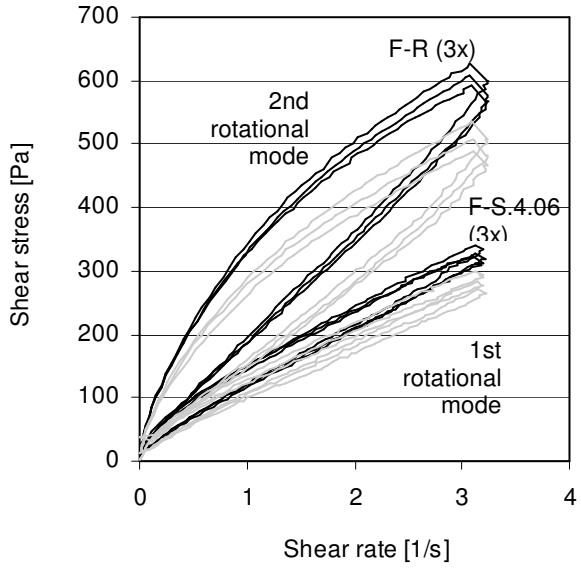

Figure 4.34: Flow curves (shear stress as a function of shear rate) for mix without and with IC in two separated rotational modes.

In response to IC implementation, a noticeable change in rheological behaviour of concrete was observed. Speaking about details, for any given shear rate, the mix with IC presented lower value of shear stress compared to the control mix (F-R). This finding held true prior to and after the oscillatory test i.e. in both rotational modes.

Notably, in the second rotational mode the IC effect became even more pronounced. It was time when both mixes presented a well-recognizable hysteresis loop ascribed to thixotropic behaviour. While in accordance with [Cas 09] smaller hysteresis area may imply many favourable attributes for the IC-incorporating mix, overall rheological response to shearing appeared to be somewhat similar. In particular, no shear-thickening behaviour as expected for plasticized mixes of high flowability [Fey 09] was observed. Yet possibly, this effect was masked by usage of lower shear rates than needed to acknowledge this phenomenon.

Studies on additional mixtures involving other IC combinations, results of which are presented in Figures 4.35 and 4.36, revealed an expected relationship, viz. a strong dependency of system response on precision of extra water assessment. Clearly, on condition that any IC-incorporating mixture had slump-flow at least not worse than that of control mix, only positive effect on rheological behaviour of IC was yielded. In the opposite case, the addition of IC variables led to higher shear stress at any given shear rate. The extreme case was combination of 0.6 % SAP and 0.08 of extra w/c (mix F-S.6.08) where the change was dramatic enough to eliminate the measurement during second rotational mode. Paiva et al. [Pai 09] who studied the effect of SAP on rheological behaviour showed agreeing results i.e. pronounced increase in torque (herein translated into shear stress) upon reduction of original effective w/c by the polymer.

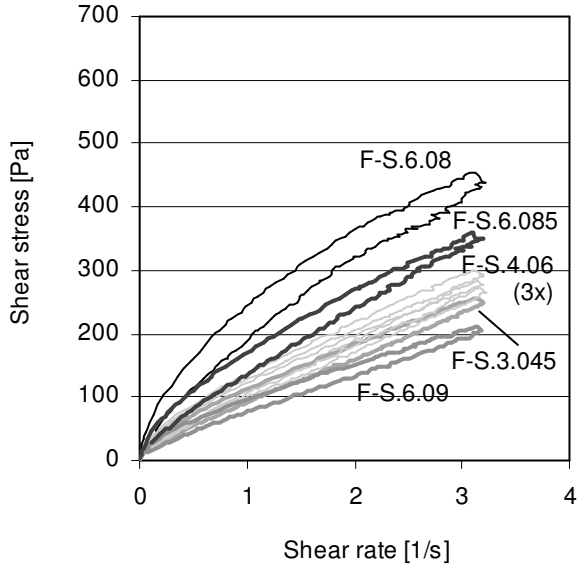

Figure 4.35: Flow curves for all IC-incorporating mixes tested in first rotational mode.

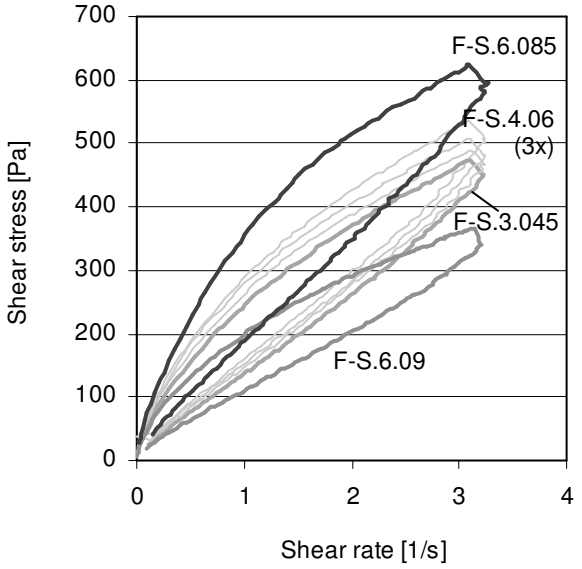

Figure 4.36: Flow curves for all IC-incorporating mixes tested in second rotational mode.

All abovementioned effects found input in evolution of the Bingham constants, see Table 4.5. For instance, in both first and second rotational modes, only the mixtures with well matched proportions between SAP and extra water presented the yield stress and plastic viscosity low enough to be accepted for self-compacting concrete (criteria see in Table F.1 in Appendix F). For other mixtures, this including control mix and some of IC-incorporating UHPCs, rather limit values were obtained, in some cases already at the stage of first rotational mode. This implies that the first group remained workable for time period much longer than laboratory-required 20 min (condition: down-curves taken into account in analysis!)[40,41].

[40] As such, derivation of Bingham constants can be done from analysis of either down- or up-curves obtained in rotational mode. The one carried out on the down-curves showed generally higher correlation factor, detailed presentation of which is omitted here.

[41] It is signalized that V-funnel flow times measured in parallel presented more complex behaviour of the mixes, yet again confirmed benefit of implementing IC.

Table 4.5: Regression analysis of results of the rotational measurements in respect to Bingham constants.

Mix	Yield stress [Pa]		Plastic viscosity [Pa·s]	
	1st mode	2nd mode	1st mode	2nd mode
From analysis of the up-curves:				
F-R	39.0 (2.9)	102.5 (1.3)	98.6 (2.6)	184.1 (6.1)
F-S.3.045	28.4 (-)	71.4 (-)	76.0 (-)	142.7 (-)
F-S.4.06	34.2 (1.7)	86.0 (4.0)	84.5 (4.4)	152.5 (7.3)
F-S.6.08	78.9 (-)	-	134.2 (-)	-
F-S.6.085	47.9 (-)	112.3 (-)	106.8 (-)	187.6 (-)
F-S.6.09	27.2 (-)	65.7 (-)	61.2 (-)	107.1 (-)
From analysis of the down-curves:				
F-R	23.3 (2.7)	20.5 (2.6)	93.5 (2.7)	168.3 (5.6)
F-S.3.045	16.9 (-)	5.1 (-)	71.9 (-)	132.3 (-)
F-S.4.06	20.6 (1.0)	12.3 (1.0)	80.0 (4.6)	140.3 (5.5)
F-S.6.08	63.1 (-)	-	121.1 (-)	-
F-S.6.085	30.1 (-)	14.6 (-)	103.2 (-)	171.3 (-)
F-S.6.09	15.5 (-)	11.0 (-)	59.0 (-)	98.6 (-)

Figure 4.37, which demonstrates the result of oscillation tests, provides some additional information. It can be seen that after some structural reconstruction and result of foregoing rotational mode, the increment of viscosity was more remarkable for the control mix (F-R) than for mixtures with both IC variables. This explains larger differences in the Bingham constants between the two rotational modes which could be traced based on results depicted in Table 4.5. The only exception was again mix F-S.6.08; its dramatic increase of complex viscosity provided the final proof of inability of the mix testing in the subsequent rotational mode.

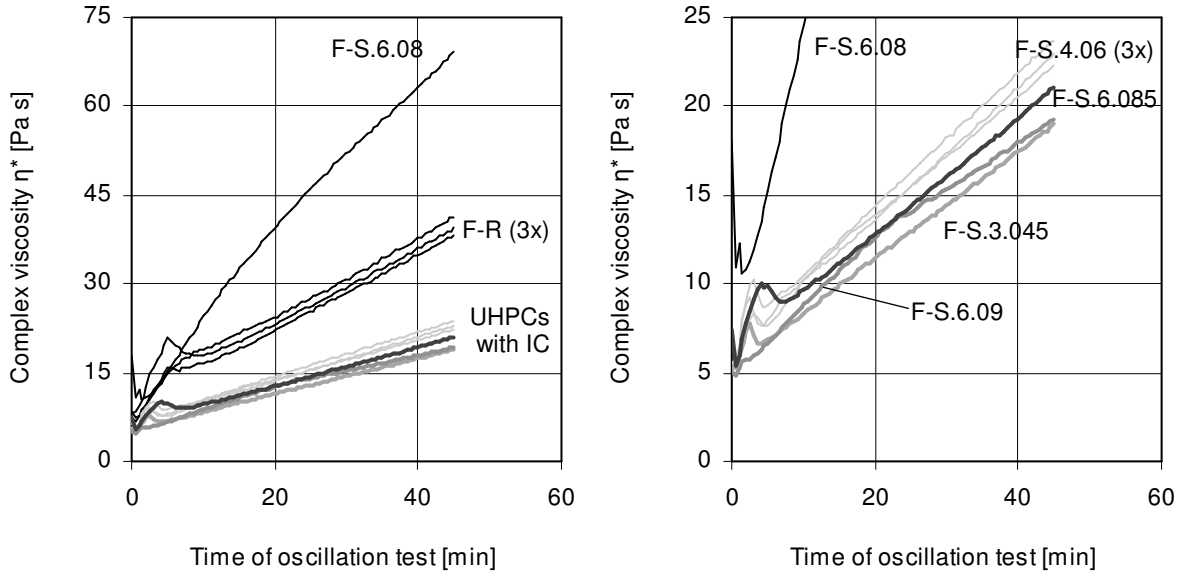

Figure 4.37: Results of oscillation test for all mixtures (to the left) and UHPCs incorporating IC (to the right).

Although both testing modes suggest fundamental role of IC variables, it could be expected that more parameters must be considered as decisive for the complex rheological behaviour. The study of Secrieru [Sec 12] who examined, among other, polymer somewhat similar

compared to tested in this work and low w/c concretes with identical type of silica fume and superplasticizer is especially interesting in this respect. It can be read that besides the extra water content, rheological characteristic will be governed by particle size of the polymer and, to high extent, the testing method, especially if in combination with change of testing modes. Investigation of these aspects was outside the scope of this thesis, although a twofold analysis of rotational mode data was performed, see results in Table 4.5.

As far as own study is concerned, when to acknowledge engagement of two different modes during rheological testing, new and very interesting finding is revealed. It is observed that although each UHPC became stiffer, the differences between mixtures without and with IC became more and more distinguishable with elapse time, in fact even after the shearing stoped. Notably, from knowledge gathered in [Zan 02][Ver 03], it would be expected some solvent could follow shearing of hydrogel, thus contributing to more favourable behaviour of UHPC with IC. However, with no shear present, it was surprising that not only the water was likely not absorbed back during the oscillation mode, also the favourable modification of rheological behaviour by IC continued and consequently resulted in much more pronounced differences in mixes behaviour compared to first rotational mode. Clearly, other reason than simply the shear-induced solvent release contributed to this change. This could be traced back to possession of the sol fraction; presumably, since removal of extractable polymer occurred mostly after swelling, fluid absorbed prior to polymer leaching was released from the hydrogel during the leaching process. Note that this confirms observation made previously in tea-bag tests, see Section 4.2.2.

4.3.5 Summary and concluding remarks

Following acknowledgement of advantages and disadvantages of tea-bag method as well as analysis of the impacting factors, a combined approach based on the introduced ‘window of absorption’ and the slump flow test was successfully used to determine maximum absorption capacity of the SAP in concrete. It was proved that the maximum absorption is the only variable related to sorption behaviour of SAP which could be truly read from simple tests on fresh concrete. It was revealed that its value very likely differs depending on UHPC matrix under modification with IC. The subsequent changes in effective w/c may require other approach to be tested in future. Additional tests on fresh finely grained UHPC using rheometer showed general improvement of rheological behaviour however strictly on condition that absorption capacity of SAP was satisfied. It appeared that small but certain

premature fluid release was taking place, giving reasons to believe that 1) modification of pore system (due to modification of water-filled spaces from which is emerges) starts very early, and 2) retardation might be expected when both SAP and extra water were added, to be further investigated in Section 4.5 (note it could be one potential reason for pore coarsening effect found in Section 4.2, although other causes have been suggested as well, see Sections 4.6.3 and 4.8.2). Last but not least, nearly all mixtures were found to be self-compacting, with very few exceptions e.g. when no extra water was added to SAP-containing mix.

4.4 Determination of time-zero

4.4.1 Introduction

Experimental series were performed in order to find time-zero required for evaluation of shrinkage measurements and estimation of IC effectiveness to be presented in Section 4.6. First, suitability of existing criteria is examined. From critical review of the time-zero criteria proposals further investigation turns to the own partly practical and partly phenomenological approach. The time-zero is determined using shrinkage deformation-time curve, temperature measurement, restrained ring test, and computer tomography, with some additional theoretical argumentation being provided as well. Both advantages and limitations of new approach are outlined. Eventually, the physical significance of time-zero is assessed by means of non-destructive and destructive test with support of literature review.

4.4.2 Time-zero criterion

i. Possibilities and limitations

As has been signalized in the literature review, keeping the test object and conditions constant and, additionally to this, having thermal effects due to hydration heat excluded, the magnitude of autogenous shrinkage will vary depending on concrete age chosen as the starting point for AS data evaluation. This reference point has been commonly referred to as time-zero and it is of major importance as far as assessment of curing method efficiency is concerned. Indeed, unjustified choice of time-zero could lead to large under- or overestimation of real autogenous shrinkage while affecting interpretation of IC effect.

Despite the fact that this issue has attracted much attention including debates performed in the framework of three RILEM Technical Committees (TC-181 EAS, TC-196 ICC and TC-225 SAP) with extension to many separate, goal-oriented studies (among others [Jus 00][Med 06][Cha 07][Cus 07][Ima 07][Epp 09][Kaz 10][Dar 11][Med 11b][Yoo 13]), the choice of time-zero and its determination method is still vague. To date, the most popular procedure being in accordance with the standardized protocol [ASTM C1698-09] is evaluating autogenous shrinkage from final set in accordance with one of the specified penetration tests. When comparing it to an early publication of the method developers [Jen 95], one immediately acknowledges that the viewpoint, for reasons that can be only speculated (e.g. some experimental observations [Tia 08] and general need of limitation of deformation to the part which can actually generate tensile stresses leading to cracking), has changed; in particular, it is found that the final set replaced time of setting, which in [Jen 95] had been

used as time-zero. This alteration was likely necessary given that the latter ascription has been often interpreted as initial set/initial setting time [Igarashi and Watanabe, p.77 in RILEM pro052]. Nonetheless, because very few authors have ever attempted to justify the choice of the time-zero without depending on arbitrary chosen setting-related points only, with exceptions regarding mainly the case of studies on cement paste (e.g. [Sant et al., p. 375 in RILEM pro052][San 09]) and very rare ones on concrete (e.g. [Epp 09][Dar 11]), evaluation of autogenous shrinkage results starts with this important aspect.

Establishing a definition/criterion of time-zero is challenging especially if both phenomenological and practical aspects of the deformation are concerned at once. For instance, it is evident that autogenous shrinkage origins very early, on contact of cement with water, without [Mou 06] or with [Cha 07][Mou 06] accompanying contribution of self-desiccation. A logical step is therefore to begin with the measurements as early as possible, best directly after mixing, in order to record the entire history of early age deformation. Notably and as further showed in references [Dud 10b][Gor 11], only so important changes which start much before final set and are attributed to IC can be captured (see also discussion part in Section 4.6.3) . As will be shown in short, some criteria for finding time-zero are in fact based on this knowledge. On contrary, it is generally understood that production of effective autogenous shrinkage i.e. part of deformation which could actually lead to stresses and potentially cracking, starts much later than mixing. This could be traced back to regaining the tensile strain capacity (after the sharp drop began in the plastic state) [Med 11b] on one hand, and development of mechanical properties, especially Young's modulus, on the other hand. Both of these events as a rule of thumb have been associated with material that has already undergone the complex fluid-solid transition and falls in the time-period when it is considered to be in the semi-solid state. This shows why starting point of autogenous shrinkage measurement and being possible from sample casting itself cannot be considered as time-zero, the initiation point of effective autogenous shrinkage.

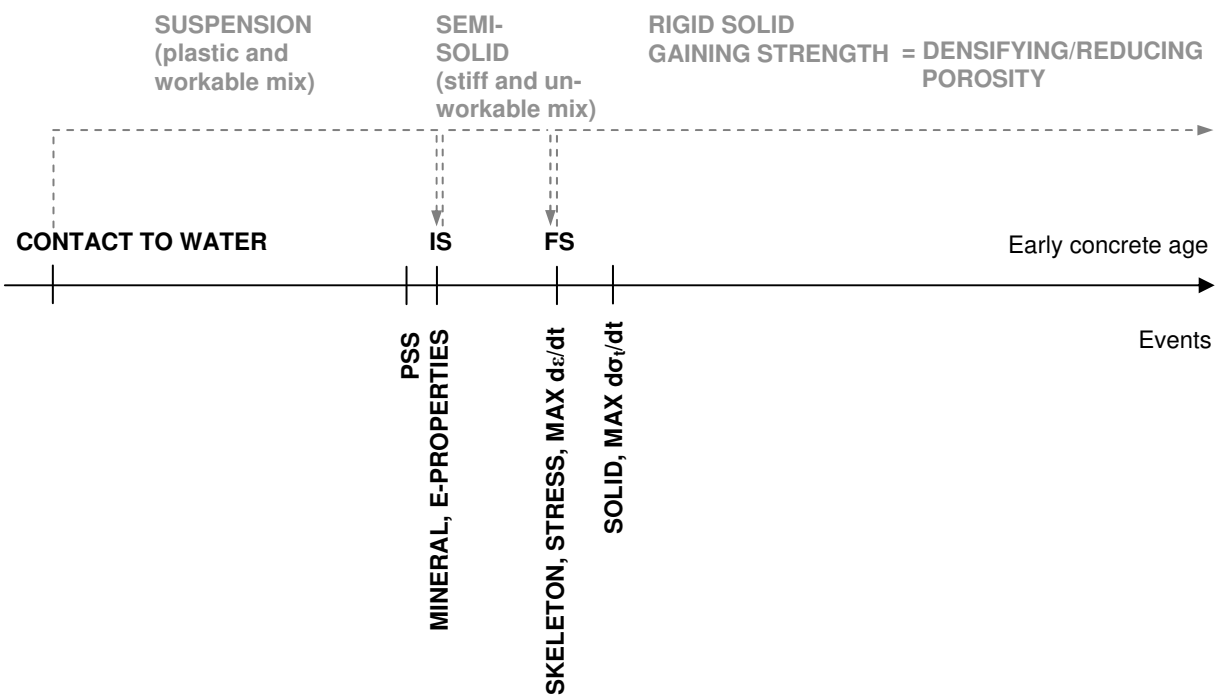

Where:
IS, FS – initial set, final set, respectively
PSS – point of self-support [Ham 06b]
MINERAL – mineral percolation threshold [Bar 01]
E-PROPERTIES – development of elastic properties (low w/c paste) [San 09]
SKELETON – formation/development of load-resisting skeleton in case of pastes [San 09]; event sometimes shifted to later ages after setting, e.g. [Zhu 08]
STRESS – onset of tensile stress generation under external restraint in some UHPC [Epp 09]; takes place earlier for other UHPC [Epp 09] and later for pastes [San 09]
MAX $d\varepsilon/dt$ – max deformation rate change (maximum velocity) in some UHPC [Epp 09] and paste without additives [Ass 13]; taking place later in some UHPC [Epp 09], other concretes [Med 11b], and paste/mortar with mineral additions [Pir 06]
SOLID – threshold of solidification and vicinity of maximum thermal flux (= max rate of temperature change) [Med 06][Med 11b]
MAX $d\sigma_t/dt$ – maximum rate of electrical conductivity change in UHPC [Bon 00]; in pastes = FS [San 09].

Without identified occurrence in respect to setting points:

P point – percolation point [Fey 01]; occurs when shrinkage is impaired by agglomeration of the sample as whole
I point – 'isostatic' point; related to locking of solid skeleton and end of global freedom to largest particles of the medium (small interstitial particles however still remain mechanically uncoupled inside the frame) [Fey 01]; giving rise to rapid evolution of Young's modulus and bulk modulus (at this stage: bulk modulus > Young's modulus) as well as decrease of Poisson's ratio [Fey 01]
H point – hyperstatic (mechanical) point; takes place when all particles of the material are linked together ([Fey 01] to the main framework) = material is totally connected [Mor 02] and no degree of freedom remains for any particle [Mor 01]; Young's modulus becomes higher than the bulk one [Fey 01][Mor 02] and degree of hydration is approx. 3 %.

Figure 4.38: Events associated with time-zero definition and their real or likely appearance in respect to setting points.

As such, the fluid-solid transition is complex process and covers multitude of events happening about very close time vicinity, see Figure 4.38. While this notably masks the

borderline between plastic shrinkage and effective autogenous shrinkage, more criteria for finding time-zero have been proposed (based on physical and chemical aspects of autogenous deformation development) which are necessarily to be taken into account.

The criteria can be arbitrary divided into two main groups including priority criteria and secondary criteria, see Table 4.6. Priority criteria/defintions (PC) are defined hereafter as ones according to which development of effective autogenous shrinkage is accompanied by the onset of stress build-up or events at the origin of (micro)cracking. Secondary criteria (SC) represent the rest of the proposals, majority of which are based on the belief that distinct changes in variables (or their derivatives) can be indicating formation of load-bearing structure or otherwise the unverified expert knowledge. The criteria which cannot be applied due to technological limitations or originated from outdated standards for AS measurement are not considered in the discussion.

Table 4.6: Review of criteria proposed for time-zero determination, in general order of increasing concrete age.

Nb.	Cate-gory	Proposed definition/implication of time-zero	Potential event accompanied or argumentation for usage	Refe-rence(s)
1	SC/PC	Before initial set [Aït 99b] e.g. moment at which penetration equals 1.5 MPa and UPV is 621 m/s [Yoo 13][Yoo 14] or at the solid phase percolation (percolation threshold) [Pic 07][1]	Self-desiccation likely starting before setting [Mou 06] therefore immediate character of autogenous shrinkage development and need of curing before initial set [Aït 99b]; at this time restrained shrinkage stress development begins while AS captured by embedded strain gauge of nearly zero stiffness is buiding-up [Yoo 13][Yoo 14]; very early age (2h) cracking in the ITZ of mortar found in simulations [Sch 07b]	[Aït 99b] [Yoo 13] [Pic 07]
2	SC/PC	Initial set	Beginning of strength gain around this time-point or after [Min 81] while material considered as a porous elastic solid with non-zero bulk and shear moduli and with water in pores [Pop 94]; initiation of shrinkage as measured by embedded strain gauges [Kad 02]; temperature onset and very close vicinity of final set [Sch 02]	In JCI defintion of AS; used e.g. by [JCI 99] [Kad 02]
3	PC	End of swelling [Hab 06a]/ Maximum swelling [Gra 04] (if occurred and if, acc. to [Med 06][Kam 08] due to causes other than hydration heat); otherwise final set [Dar 11]	End of dormant period [Gra 04][Med 11b]; initial set [Hab 06a] (apparent stiffness > 1 GPa [Hab 06b]); the temperature rapidly increases [Kam 08] while the stresses under restraint begin to be produced [Hab 06a][Kam 08]	[Gra 04] [Hab 06a] [Dar 11]
4	PC	Onset [Sch 02] or rapid rise [Zha 03] in temperature of concrete	Initiation of shrinkage as measured by embedded strain gauges [Zha 03]; generation of tensile stresses begins [Ima 07]; shrinkage rate increases for the second time, this taking place in close time vicinity of initial and final set [Sch 02]	[Sch 02] [Zha 03]
5	PC	Rate of temperature starts to increase sharply	End of dormant period/initial setting; axial force is developed in restrained specimen	[Cus 07]

(continued on the following page)

Table 4.6: Review of criteria proposed for time-zero determination, in general order of increasing concrete age (*continued*).

Nb.	Cate-gory	Proposed definition/implication of time-zero	Potential event accompanied or argumentation for usage	Refe-rence(s)
6	SC	Maximum rate of temperature change (threshold of solidification)	Plastic shrinkage stops and thermal expansion begins; solid structure counteracting deformations is formed	[Med 06]
7	PC	(Second) Maximum rate of deformation (maximum velocity of deformation = inflection point of deformation curve)	Close vicinity of or, more likely after final set [Pir 06][Med 11b]; microcracking occurs shortly after this time-zero [Pir 06][San 09]	[Pir 06] [Med 11b]
8	SC	Rates of deformation (vertical and horizontal) become equal	Deformation becomes isotropic since dead weight no longer contributes to volume change	[Bel 02]
9	SC	Maximum temperature (second temperature peak) [Ma 03][Ma 04] unless no swelling [Gra 04] and measurement cannot be performed in isothermal conditions (otherwise initial set [Ma 04])	Similarly to final set criterion, CTE is assumed constant [Ma 03]; approximity of final set [Cus 07]	[Ma 03] [Gra 04]
10	SC/PC	Final set	Physical manifestation of complete solidification of plastic cement paste [Cha 07]; coefficient of thermal expansion is stabilized and remains constant (in subsequent period Kad 02]); corresponds to UPV of about 1165 m/s [Yoo 13]; corresponds to hydration heat-related onset of temperature rise and initiation of dynamic elastic modulus development [Kaz 10]	[ASTM C1698-09] [Kaz 10] [Dar 11]
11	PC	Abrupt change of capillary pressure (in the so-called transition zone [Cha 07]) or pure onset of pressure build-up	Physical significance of time-zero (formation of the solid structure [Cha 07]); possesses no strict ascription to setting process (from comparison of studies [Hol 01][Cha 07][Zhu 08])	[Cha 07] [Zhu 08]
12	PC	Onset of restrained shrinkage strain (stress) given no separation of AS from thermal effects [Ima 07] or the shift from compressive stresses towards tensile stresses	Former corresponds to start of heat evolution [Min 81][Ima 07] (deviation point [Yoo 13]) and, if swelling occurs, initial set [Hab 06a], but it is always subjective empirical judgement according to [Ima 07]	[Ima 07] [Yoo 13]
13	SC	Some hours after final set	Pure result of self-desiccation in subsequent period	[Hol 01] [Zhu 08]

[1] It should be understood that setting of cement paste results from percolation of the particles. Consequently, event called (mineral/solid) percolation threshold, i.e. when first solid path is formed within material [Bar 01], should generally occur earlier than first of important setting points measured by destructive methods and referred to as initial set [Mou 06]. This is different especially when the w/c is low, for which percolation threshold is expected to situate in very close vicinity of initial set, e.g. [Zha 12b]. As such, percolation threshold therefore delivers a rigorous theoretical definition of the set point of cement paste.

While making decision about time-zero, applicability of old criteria was proved so as to exclude necessity for a new criterion definition. To date, ignoring this step has in fact led and is still leading to new proposals, without final agreement on one time-zero criterion useful for cement-based materials. Numerous criteria collected in Table 4.6 should be also noted to be regarding materials with low w/c but typically less advanced in terms of composition than UHPC, with few exceptions [Sch 02][Ma 03][Ma 04][Hab 06a][Kam 08][Yoo 13]. Combined

with imprecise sound of some of criteria offered, especially ones referring to temperature increase and current practical needs (such as reading time-zero directly from deformation curve), this urge becomes apparent.

ii. Solution and establishments

The main demand considered in search for time-zero was finding evaluation point of the part of deformation which could be responsible for generation of stresses under restraint. Simultaneously, it was set to be easily identifiable using pure free deformation curve for all UHPC mix combinations, or otherwise the underlying causes hindering this aim were meant to be recognized. Eventually, some phenomenological issues were taken into account too when making final choice about this time-point.

In-depth analysis of all collected data has been performed. It was concluded that time-zero related in best manner with one of the local extrema in the deformation curve as measured using corrugated tube protocol. The corresponding graphical solution of this issue is demonstrated in Figure 4.39. In the graph, for finding the point of interest, deformation curve as plotted in time was first fit to the best curve with help of FindGraph software [UNIPHIZ] and rationals type of function[42]. Subsequently, the first and second derivatives already in their best, smoothed appearance were derived using derivative calculator [MATHPORTAL]. Finally, the inflection point of deformation curve that matches new time-zero was found either from the former by evaluating the local maximum (assumption: deformation is presented in negative values) or directly using the second derivative of deformation (intersection point with X-axis).

[42] With free version of the software, the model based on rationals function had to be used instead of applying the more commonly preferred multi-logistic or more-parameter exponential models, e.g. based on Boltzmann equation. Whereas the rival solutions generally present the more appropriate scientific approach (better description of quantities that grow exponentially), own solution allowed to determine points of interest and was as reliable as guaranteed very high precision of fit with $R^2 > 0.999$ for the polynomial degree of fitting of minimum 8. Another advantage was also that it could be used for more purposes, e.g. when fitting other complicated curves meanwhile always ensured possibility of in-depth inspection of the curve.

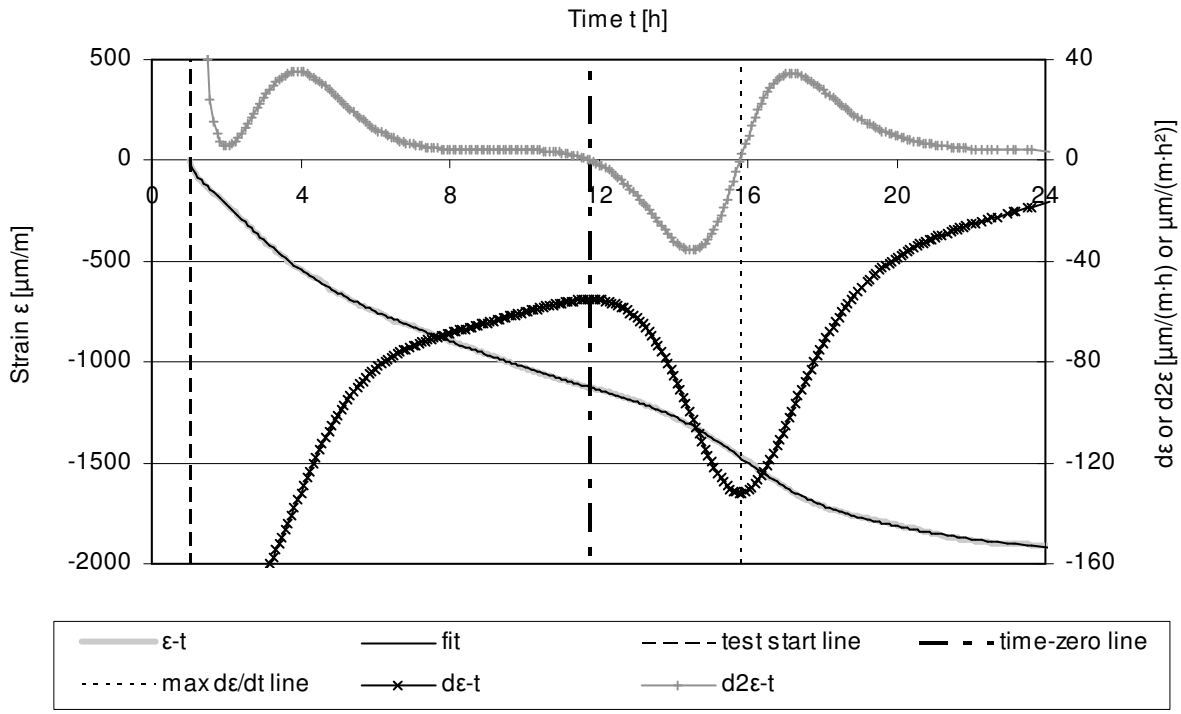

Figure 4.39: New method of determining time-zero.

It was noticed that the new time-zero was best defined as the first minimum absolute value of the strain rate or, in other words, the last extremum before the attaining maximum (negative) strain rate. Starting from this point the rate of deformation started to increase rapidly, in some hours achieving the maximum of deformation velocity. Its manifestation confirmed possibility of finding time-zero directly from deformation-versus-time curves as suggested by Bentz et al. [Ben 01c] and therefore remarkably facilitated evaluation of results.

Whether the selected time-point had any relation to setting as being the case of 'abrupt change in slope in deformation-versus-time' [Ben 01c], this will be discussed in the following Section 4.4.3. However, what is more remarkable is the number of other events having start or otherwise important stage found as coinciding with time-zero. These events or coincidences could be treated as arguments for particular time-zero selection and can be summarized along with a single counter-argument as follows:

- argument 1

In Figure 4.40, a representative picture of evolution of deformation rate is compared with that of temperature and the latter's change in time.

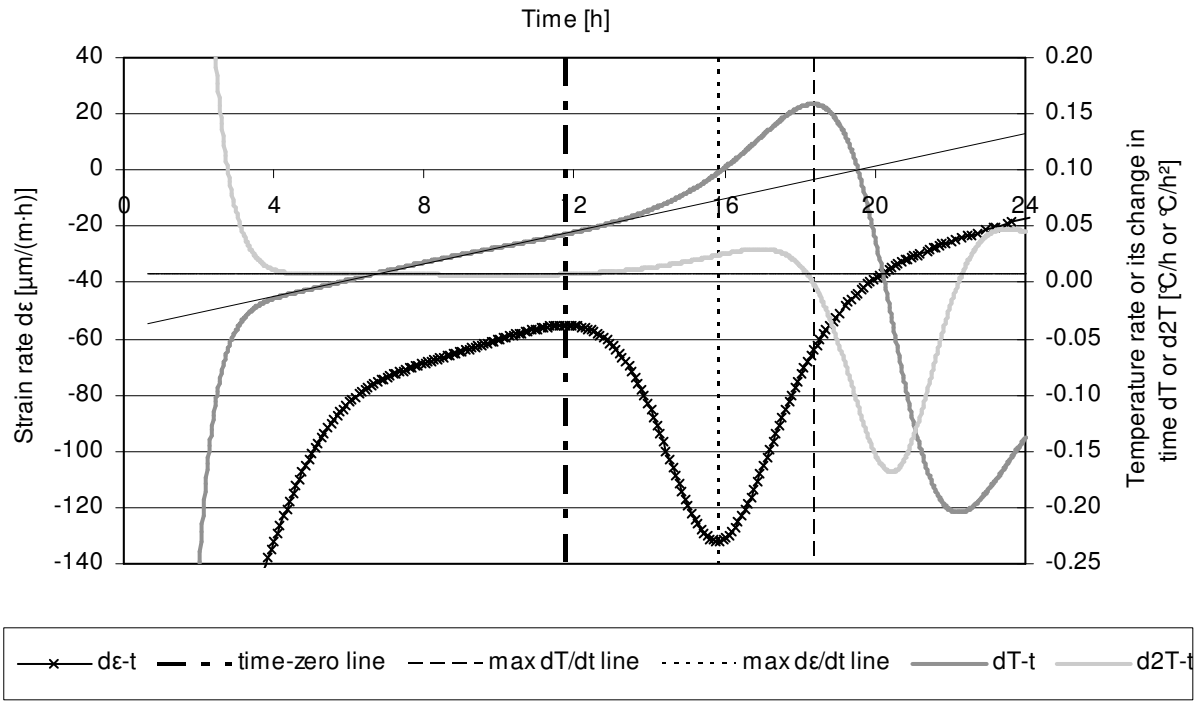

Figure 4.40: Time evolution of rate of free deformation and corresponding sample temperature in the first and second derivative.

It could be observed that time-zero chosen corresponded to end of period between start of 'wet mixing' and moment when temperature did not increase any more. In other words, starting from particular time-point rather pronounced gain in hydration heat took place. In this way, time-zero validates the chemical nature of autogenous shrinkage. Meanwhile, the criterion received more precise sound when compared to some temperature-based definitions of time-zero reported previously in Table 4.6.

An important comment to be made regards the fact that part of hydration heat was clearly used to heat up the sample over the ambient temperature, thus providing more favourable conditions for hydration. In theory, this could result in shifting of the time-zero towards other concrete age and certain effect on magnitude of autogenous shrinkage, e.g. [Zha 03][Tia 08][Med 11b]. However, since the geometry of the element measured, particularly the cross-section of the tube, was small, the extra heat produced in the small sample dissipated easily and fast, owing to which increase of sample temperature remained negligible. This implies that autogenous shrinkage overtook the thermal expansion/swelling quite rapidly, leading to negative strain development. Due to this or another reason, both time-zero defined and maximum deformation rate were obtained before the temperature reached its maximum rate.

Although not demonstrated here, the observation held true in case of bigger tubes as well, that if used in measurement yielded closely settled extrema of deformation and maximum temperature rate compared to ones determined from small tubes. That is to say, it seemed that from the two, age associated with time-zero and autogenous shrinkage magnitude developed after time-zero, only the latter required certain correction on the scale of investigation performed. As in interest of finding effectiveness of IC the temperature aspect was avoided by using always the same sample size while small tubes could be used for finding temperature effect-free AS, further in-depth investigation of the aspect has been abandoned.

- argument 2

Looking back at Table 4.6, no additional evidence is required to show that new evaluation point better applies as time-zero than maximum deformation rate. Indeed, since microcracking has been reported to start around the latter [Pir 06], the former event seemed to provide an appropriate basis for deriving the time-zero at the first glance. From this perspective, the new definition of time-zero could be better representing the moment the structure is resistant enough to carry the force causing the cracking. Reference to some earlier time-points than the maximum rate of deformation should not be excluded also in opinion of Meddah and Tagnit-Hamou [Med 11b], who although widespread maximum deformation rate criterion as well as delivered theoretical background standing behind this choice, but did not support it with other than free shrinkage and temperature measurements.

- argument 3

Other tests comprehensively confirmed particular engineering significance of the new time-zero. This is demonstrated in Figure 4.41, where the time-point determined is compared with start of stresses build-up in both types of rings i.e. ones subjected to temperature effect and ones where increase in temperature due to hydration heat was as negligible as in small tubes[43].

[43] Under restraint of uniform shrinkage, example of which autogenous shrinkage is, wall thickness of the steel as well as concrete ring become parameters decisive for level of stresses generated, relaxed and, holding true only for former, measured, e.g. [Hos 06]. In comparison, no impact of the onset time of stress generation is typically recorded on changing walls thickness of steel ring at a constant thickness of the concrete ring; meanwhile, change of diameter of the steel ring is showed to be of secondary importance, see [Yoo 14]. This implies that effect of changing the set-up on time-zero could only be attributed to change of concrete wall thickness and height, leading to main underlying consequence of different time-zero situation, i.e. increase of concrete temperature due to non-dissipated heat of hydration. It will provide better conditions for hydration, thus faster development of Young's modulus and autogenous shrinkage, with expansion being hindered by stiff sand aggregates.

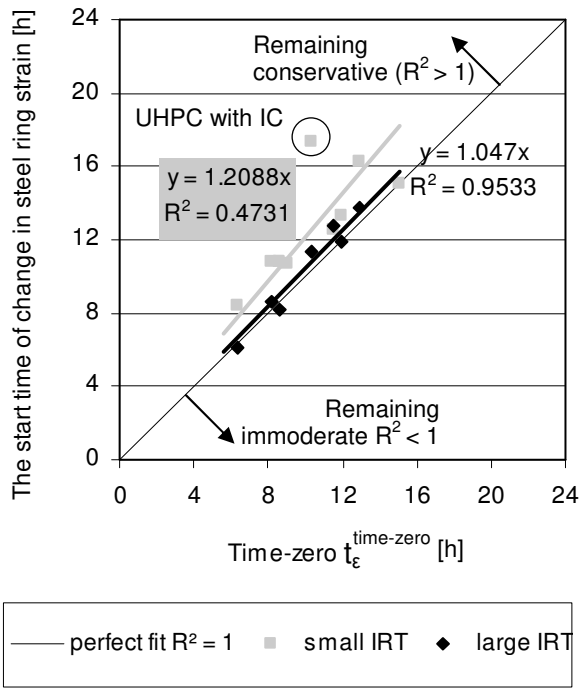

Figure 4.41: Relation between time-zero and important change recorded in IRT, with trends.

With regards to former case, it could be followed that new time-zero either very well matches initiation of restrained shrinkage stress development or, as alternatively considered, is in good agreement with change of course from compressive towards tensile stresses. In comparison, having effect of temperature largely limited, the delay of stress generation was about two hours as compared to the time-zero (in excellent agreement with Eppers and Mueller [Epp 09] [44] where alternative measuring system was used for capturing the free AS changes). This implies that usage of newly defined evaluation point of the begin of autogenous shrinkage represented rather a conservative approach from engineering viewpoint. But considering that the stress generation start always fell in-between the time-zero and maximum deformation rate (e.g. approximately in the middle of regarded period for UHPC without IC), it could be concluded that former was still better suited as evaluation point of autogenous shrinkage than the latter.

It should be pointed out that Figure 4.41 only partially includes the results recorded for mixtures with IC. Their elimination turned out to be necessary given that for mixtures incorporating IC finding the point of interest more pronouncedly than in rival cases (i.e. control UHPC, mixes with extra water) depended on subjective empirical judgement. In fact, when IC was incorporated, lack of one clear time-point of stress initiation was noticed. This could lead to building a puzzling picture instead of scientifically-supported one. Exemplary outcome of this uncertainty is appearance of apparent outliner from trend based on results of instrumented ring tests involving smaller of the set-up geometries used (large IRT) and in Figure 4.41 referred to as UHPC with IC.

[44] With importance to the results, it has been showed in supplementary studies of Eppers [Epp 10] that both Young's modulus and tensile strength develop before onset of stress build-up in the instrumented ring tests and the final set in reference to the 2009 [Epp 09] results. This again validates using another definition of time-zero as proposed at present.

The origin of the particular inconvenience could be currently only speculated upon. On one hand, it could be linked to the fact that, for reasons still to be revealed, mixtures with IC generally presented much smoother transition between states of suspension and solid. For this reason, reading of extrema (and thus time-zero) already at the stage of free deformation required much better inspection of its curve, in some instances giving no result at all, see Figure 4.43 and 4.44 and the corresponding discussion. On the other hand, the rule of thumb is that in IRT, the free strain variable does speak only for one of contribution to the final result obtained, with other as important influences being the strength development and tensile creep characteristic. Whatever the true underlying cause was, given that one solution was intended to be used for all mixtures, the evaluation approach proposed and having applicability confirmed for UPHC without IC was maintained in the whole study.

- argument 4

An additional argument has been delivered on occasion of performing the computer tomography scans. Various concrete ages were considered for the test, with fist age corresponding to time-zero. As has been preliminary visualized in Figure 4.15 and will become even clearer in Section 5.3, until this concrete age, some volume loss of SAP occurred, but without corresponding change in the matrix. This would only be possible if solid skeleton was already formed. Important enough, the fact that SAP showed particular behaviour also meant that IC effect had been already initiated. Thus two additional reasons supported the choice of time-zero made, currently from phenomenological viewpoint.

- argument 5

Review of studies presented in Table 4.6 even with limitation to ones focusing on UHPC indicated a clear conflict of rival criteria proposed. E.g. while the work performed by Schachinger et al. [Sch 02] indicated final set as nearly equivalent to time-zero, Yoo and co-workers [Yoo 13] noted its two hour delay compared to what they consider as the true evaluation point. Latter study in fact is an example presenting the most extreme criterion: not only the time-zero was fixed before setting started, also temperature began to increase at more remarkable rate later, i.e. around final set. On one hand, this difference could be forced by usage of different standards for evaluation of the setting behaviour. Indeed, the destructive penetration tests could give different values of reference points of setting, especially final set

[Gra 06c] given their relation to different levels of shear/yield stress [Loo 09][45]. Pronounced impact is furthermore sometimes related to the curing conditions used [Yoo 13], despite the fact it is not shared opinion for materials other than UHPC, e.g. [Jus 00]. Altogether, there exists argumentation why time-zero could be sometimes ascribed to hours before or after final set, as presented in verification by ring test [Epp 09] and capillary pressure measurement [Hol 01], respectively. However, even if picture of restrained strain is scientifically convincing, the conflict could be resulting from little number of tests performed and consequent hidden metrological issue not noted by Yoo et al.

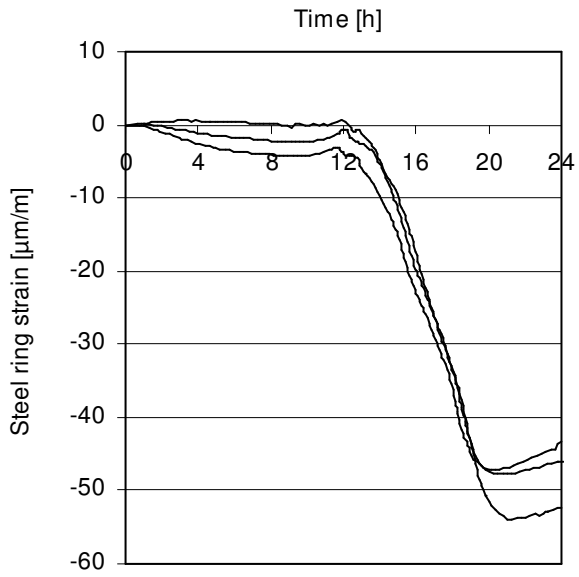

Figure 4.42: Exemplary time evolution of restrained shrinkage strain in instrumented ring tests.

Staying critical to own work, instance of metrological issue should be pointed out. In Figure 4.42, the development of strain in restrained ring test is presented for three samples produced from selfsame concrete batch. It is visualized that when, for appreciable time span, the inner rings of two restrained test set-ups deformed despite concrete ring still remaining in plastic state, the third average strain remained positive. At certain point, however, all concrete rings started to gain in strain rather abruptly, leaving a pronounced mark of important event in all curves, which was believed to reflect development of structure able to carry the shrinkage stress. Since in the maximum level of negative strain developed was nearly alike for all, particular metrological issue appeared to be concern of early period and time-zero evaluation. Note that alternative explanation, i.e. charge with thermal effects, is excluded. Two arguments supporting this statement are relative constant value of α_T of UHPC [Viv 07], on one hand, and no reflection of temperature changes in shape of curve until critical point, on the other hand.

[45] It is important to note that time at which penetration resistance measured on UHPC equals 1.5 MPa corresponds to earliest age at which the cement paste would start to set, if at all acc. to [Chu 10] who used the selfsame standard ASTM C403 in tests on pastes. This makes the alternative definition of time-zero of Yoo et al. [Yoo 13] to that of stress development onset truly exceptional and never observed before.

- counter-argument

Two examples can be named where picture of evaluating new time-zero from the shrinkage was less clear, both referring to mixtures with IC. To demonstrate this, Figures 4.43 and 4.44 give examples of deformation curves for the finely grained UHPC with IC being differentiated by presence of fibres and tube size.

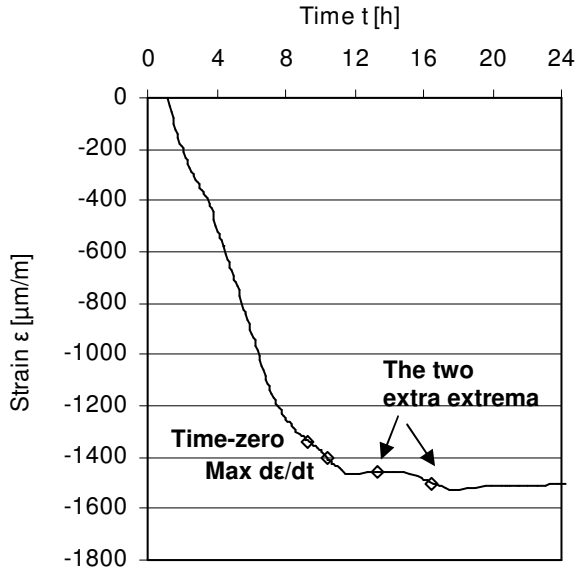

Figure 4.43: Time evolution of free shrinkage for finely grained UHPC with IC as measured using small tubes.

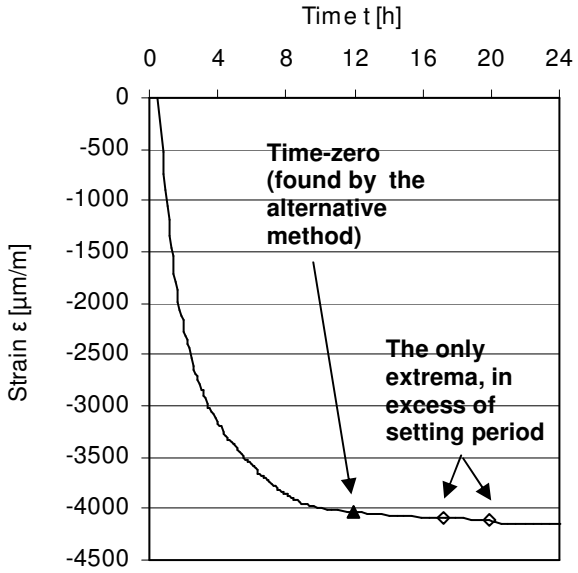

Figure 4.44: Time evolution of free shrinkage for finely grained fibre reinforced UHPC with IC as measured using large tubes.

In the first scenario (Figure 4.43), one observes an additional change in curve taking place some hours after new time-zero, and contributing to curve pattern nearly identical to one observed before by Esping [Esp 07]. It held true for small and large tubes which excluded any influence from changing the test set-up on event occurrence. Obviously, an additional shrinkage mitigating mechanism is likely existed. E.g. if related to crystallization pressure of portlandite, being one important example, it would be expected to take place within first 2 days, i.e. when formation of particular crystals in paste of UHPC is highest and almost no pozzolanic reaction in fine-grained UHPC occurs [Pfe 10]. To explain an analogous case, i.e. when the rate of deformation did not decrease monotonically after obtaining the peak, another cause has been suggested (cf. ref. 11 *Ibid.* [San 11]) and evidenced [San 11] in the past, in particular a shrinkage-balancing chemical reaction, e.g. formation of ettringite.

In the second case (Figure 4.44), where larger samples had to be used owing to problems with pouring the fibre-incorporating mix into smaller size tubes, the extra change in course of

deformation represented the only distinguishable point of reference. This hardly means that additional events observed in deformation curve better identify with time-zero, rather it is interpreted that its occurrence becomes masked by the fibres. Presumably, since the bond strength between fibres and matrix is not abrupt and requires hydration time [Yoo 13], the mechanism of deformation resistance is engaged gradually just like it is in case of solid skeleton formation. It seems that for some yet unknown reason the former overrode the latter.

The single counter-argument implied there was clear need of assessing physical significance of new time-zero and finding alternative for the case when the new criterion fails to describe it, discussion on which is continued in following section.

4.4.3 Assessing physical significance of the suggested time-zero

The starting point of the following discussion is the assumption that new time-zero has certain relation to setting, especially to one of its limiting points, i.e. final set. This hypothesis has been based on experimental results provided by Tian and Jensen [Tia 08]. In present author's opinion, these researchers were first to show, although without commenting, that regarded set point appears in deformation curve of non-bleeding concrete at similar moment as deduced in foregoing section. This viewpoint, interestingly enough, does also agree with study of Pease et al. [Pea 04] who independently revealed beginning of intermediate phase that separated two stages of shrinkage evolution, and being caused either by expansion or physical response, to be matching the time of final set. Whether any relation like this existed between time-zero and final set in own studies (or not), this was verified using Vicat test for mortars/concretes [DIN EN 480-2] as well as the P-wave ultrasonic method (see Section 3.3.3 for more details).

The first experiments performed on the subject with the destructive method gave promising results, but did not confirm fully the relation between the extremum of deformation curve and setting. The expectation was better correspondence of a rival test method which, following [Gra 06c], should give a wider time spectrum for regarded event given no uniformity of setting criteria. Indeed, it could be pointed out that while in tests acc. to DIN EN 480-2 one needle size is used to measure shear resistance, for a different constant load acc. to ASTM C403 requires application of set of needles of different contact area in dependence on degree of hydration. The latter solution was imagined to be advantageous from perspective of usage for high and gradually increasing viscosity of UHPC. However, in case that the destructive

test would not give answer as expected, main attention was finally devoted to the non-destructive measurement as it also allowed continuous monitoring of concrete hydration.

i. Approach based on UPV

- theoretical

Among many variables one can measure using ultrasonic method, the velocity of ultrasonic longitudinal wave (that is alternatively referred to as P-wave velocity, UPV or compression(al) wave velocity) is most basic but, simultaneously, one of paramount importance. Indeed, this variable finds relation to changes of fundamental microstructure parameters such as the solid percolation (i.e. the microstructure parameter most related to the setting, e.g. [Ye 03]), degree of cement hydration (i.e. parameter in common to development of mechanical properties, e.g. [Kra 06][Yoo 13]), as well as formation of different hydration products, all being validated in work of Robeyst et al. [Rob 11].

The main disadvantage of using UPV is that its value is not unique and varies depending on many factors, these being sometimes subcategorized in two groups including ones simultaneously affecting concrete properties (i.e. aggregate size, graining, type and content; cement type; w/c; air entrainment and admixtures; compaction degree; curing conditions and age of concrete) and ones with no effect on the properties of concrete (i.e. acoustical contact; temperature of concrete; moisture condition of concrete; path length; size and shape of specimen, presence of steel) [Mal 91][46]. The main outcome this results in is lack of one criterion of UPV-particular setting event type useful for all cement-based materials[47].

From another perspective, this variable also possesses rather complex linkage to different elastic constants depending on state of material appearance [Kea 89]. E.g. in a solid, being of major interest here, it combines knowledge about K and G, i.e. bulk modulus of compressibility and modulus of rigidity (also known as shear modulus), respectively, in their

[46] Classification presented by Malhotra and Carino [Mal 91] can only be taken as somewhat arbitrary, yet still greatly reviewing the fundamental impact list. Additional results could be imagined to result e.g. from shrinkage cracks [Hea 99] or technical particularities, e.g. frequency of the pulse sent [Haa 75]. More detailed classifications are also possible, e.g. distinguishing between main impacts (paste content, aggregate size) and secondary parameters (w/c), e.g. [Rei 96][Lee 04].

[47] As a rule of thumb, one specific value of UPV will never reflect the exact selfsame hydration progress for mix of incomparable mix proportions [Pes 88]. This could be explained by referring to underlying relations. The general knowledge is that degree of hydration at which particles become interconnected and mix attains setting could be considered as function of the interparticle distances (e.g. [Bou 96][San 09]). In turn, given that UPV and degree of hydration are related as well, one specific value cannot represent setting times for mixes after change of mix proportions. Analogously, other UPV value must furthermore result unless limits of solidification are not judged based on the selfsame reference, e.g. destructive penetration test following a particular standard.

relation to material's density. The rule of thumb is that from the two only shear modulus G can serve information about level of the microstructure build-up. Without separation possibility of G from K, i.e. without simultaneous transverse shear wave velocity measurements, for instance, P-wave at any stage of microstructural development must be therefore considered as characteristic to particular group of mixtures of similar composition. The corresponding threshold value will be always derived based on another setting evaluation method, e.g. penetration test[48].

- experimental

To best author's knowledge, only one study has been ever performed on setting behaviour of UHPC using both destructive penetration test and ultrasonic measurement. For finely grained mix of very similar composition to studied M2Q, Yoo et al. [Yoo 13] experienced initial and final set as according to standard ASTM C 403 to be coinciding with UPV of 621 and 1165 m/s, respectively. As this standard presented rival reference compared to the test standard used in own investigations, comparison was made between time of acquiring one of the UPVs and new time-zero as derived from deformation curves. In result, the correlation to initial set was immediately excluded (corresponding graph not shown).

[48] According to [Pop 94], neither consistency measurements such as penetration tests nor the non-destructive ultrasonic measurement based on P-waves can provide the direct insight into internal structure development of the setting and hardening material. However, since not only the former represents rough measure of shear modulus changes [San 08][Sub 10] and kinetics of stiffening [Pop 94], also the latter accurately approximates other established indicators of cement setting (including penetration test result, e.g. [Dom 91]), a comparison is fully justified.

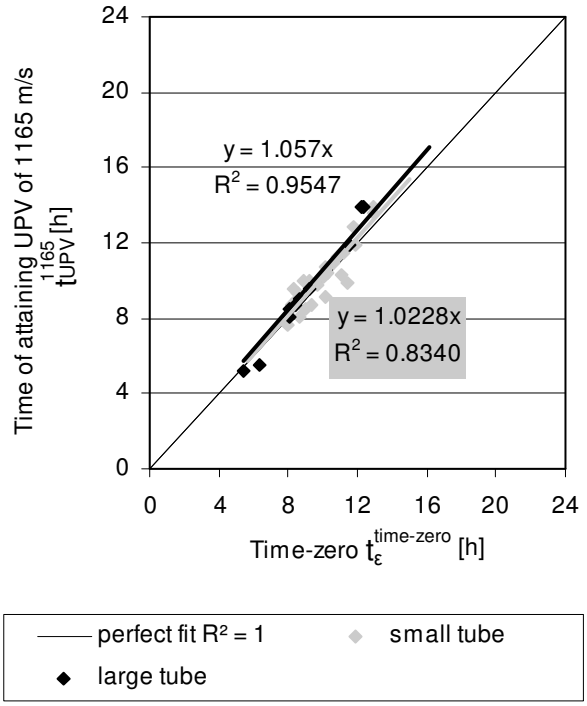

Figure 4.45: Relation between time-zero and time when UHPC reaches UPV of 1165 m/s including trend lines.

Evaluation of potential linkage of time-zero to final set is presented in Figure 4.45. A very satisfying match [49] was found. For mixtures of similar composition, this correspondence could mean acquiring selfsame state of hydration advancement.

Interestingly enough, the correlation held true despite the fact that a potential impact on UPV could not be fully omitted in mixtures without IC or SAP. The plausible loss of contact of tested object with transducers due to autogenous shrinkage and resultant creation of air-pockets, being technical error impossible to exclude within equipment used, is believed however to have little if any impact on UPV. It is recalled that the rate of deformation in mixtures of interest was only decreasing until time-zero (see again Figure 4.39), meaning it was mainly driven by settlement (or similar process) of material still remaining in fluid state. This implies that the particles would rather rearrange than follow horizontal shrinkage, if any occurred. Furthermore, usage of silicon gel as couplant plausibly reduced these imperfections by providing enhanced contact between transducers and material.

Important to acknowledge, correspondence of new time-zero to the UPV criterion increased once large tubes were used in measurement of autogenous shrinkage. In particular, the R^2 increased from a value of 0.834 to 0.955 at very similar slope of the line which indicates that a perfect match was obtained. This finding is yet to be expected considering the more corresponding conditions of microstructural development of sample in the larger tube to that in the cone (i.e. sample volumetrically equal to UPV test). In Figure 4.46, temperature rates and their corresponding changes in time are plotted. The comparison regards three different samples used in tests including the cone, both types of corrugated tube and larger of the two

[49] The success of the match found could be decided in terms of slope of the line and correlation coefficient. Both were taken into account while making judgement about precision of correlation found, with latter being considered as important as the former.

IRT[50]. It could be pointed out that although some differences remained (e.g. level of maximum temperature rate), being a reason for finding closer relations between certain samples, some features were clearly in common for all specimens. This includes still relative small temperature rate change in time as attributed to curing conditions chosen and, except for big IRT, nearly identical time-point of acquiring the maximum temperature velocity. These reasons could be finally used to explain why both the time-zero and maximum deformation rate − despite measurement in varied Jensen's set-ups − were attained at similar time (somewhat correspondingly to observations made by Meddah and Tagnit-Hamou [Med 11b]) while relation to UPV test result was always high.

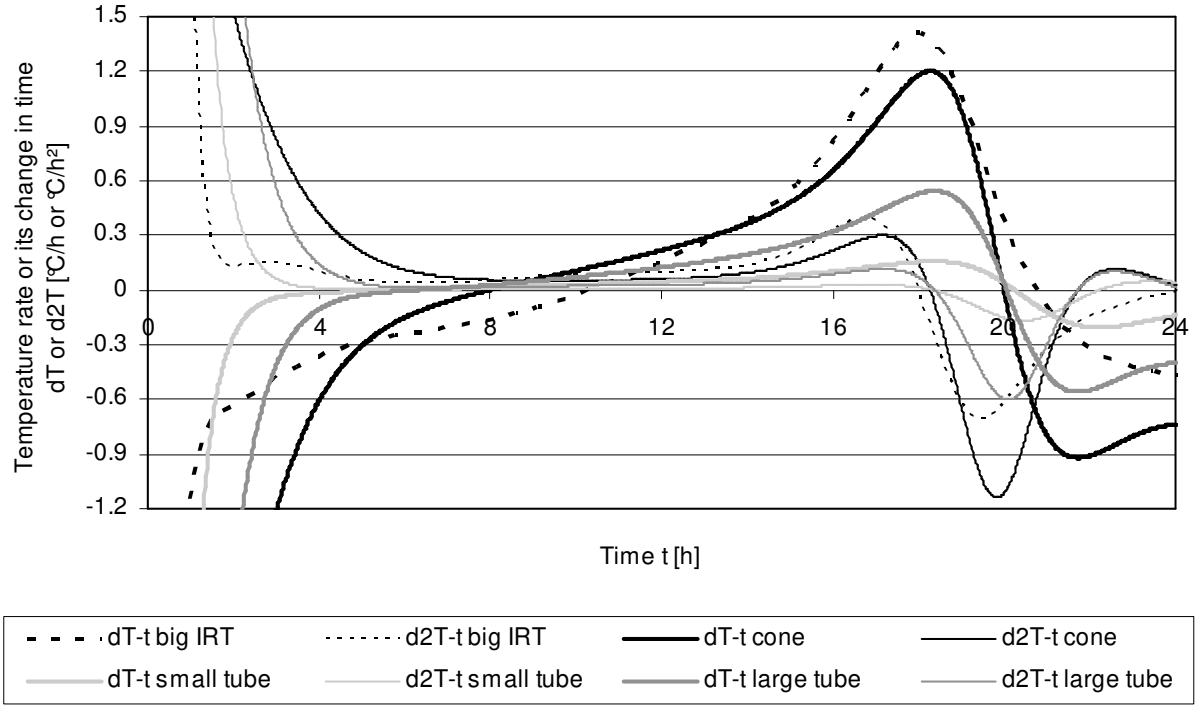

Figure 4.46: Representative time evolution of temperature rates in different samples of one of the finely grained UHPCs after fitting and smoothening.

Interesting enough, and to be observed when looking back at Figure 4.43, the match with UHPC containing IC/SAP appeared to be little affected[51] by the higher air content that these mixtures presented, see Section 4.2.3. While negative effect of air voids on UPV at low

[50] Differences in non-dissipated hydration heat as measured in the small IRT were comparable to that in small tube. Thus, for sake of clarity, their presentation has been omitted in the graph.

[51] It is worth pointing out in comparison between time-zero (as read from deformation curve) with UPV of 1165 m/s a better correspondence was found for UPHCs without than ones with IC incorporation. In other words, for the latter mix type it is revealed that time-zero is sometimes more shifted towards maximum deformation rate than in rival cases. Consequently, it means that impact of air (or some concurrent factor) cannot be entirely excluded and implies that for mixes with IC time-zero occurs at lower UPV values. Yet, since this does not affect the choice of time-zero, further investigation of the aspect was abandoned.

frequencies is well known [Kea 89][Zhu 11a], it is plausible that some threshold of critical volume of technological voids has been attained before original mix modification with IC and SAP. E.g. air volume of 2 % (1.1 % by the cement paste volume) has been shown to be the bottom limit of range in excess of which UPV remains almost equally sensitive to the gas presence in case of cement paste, cf. [Zhu 11a]. If so, the extra content of bubbles in UHPC with IC or SAP alone would not be influencing UPV to a further extent. This explanation regrettably fails in application for mixtures with pure addition of water without IC agent. For most of these UHPCs having reduced air content compared to F-R (but, simultaneously, containing void volume still close to the threshold value), much higher UPV values than 1165 m/s were recorded at time-zero. In fact, P-wave propagation was often faster than one in water (approx. 1500 m/s) already from the beginning of ultrasonic measurement, see Section 4.5.2. Therefore, to eliminate dependence on particular value of the ultrasonic wave transmission speed, another source of reference was quested for.

ii. Other approaches

- possibilities, limitations and theoretical

As UPV is not the only parameter characterizing the ultrasonic pulses transmitted through concrete (signal received), other ways of determining setting points and based on entire received signal could be concerned. Following opinion of Teodoru [Teo 89], information of interest could be as successfully determined from change of parameters related to damping/attenuation and measured as amplitude, energy and conductivity. In practice, this choice has been typically narrowed down to analysis of relative energy and/or frequency spectrum, one recent refinement of which is translation of the latter into parameter labelled TG parameter [Trt 13a], see also Table G.2 in Appendix G.

Usage of any of these information sources about signals would appear attractive since, compared to UPV, other underlying phenomena (affecting the pulse transmission) decide about particular variables' evolution. However, the short review performed showed that although the changes can be well correlated with at least one of setting points and result in number of criteria, many of approaches are charged with clear shortcomings. Indeed, unlike hypothesized by Teodoru [Teo 89] that setting points could be matched with abrupt change in one of the variables, it is observed that some do present purely informative character of correlation found, while suffer from lack of physical meaning/basis, e.g. one of alternative energy-based criteria put forward by Robeyst et al. [Rob 09] and reviewed in Appendix G.

Own example of such criterion is demonstrated in Figure 4.47, where a match near perfection was found between time-zero and change of amplitude range of the data acquisition unit from 50 to 100 mV[52].

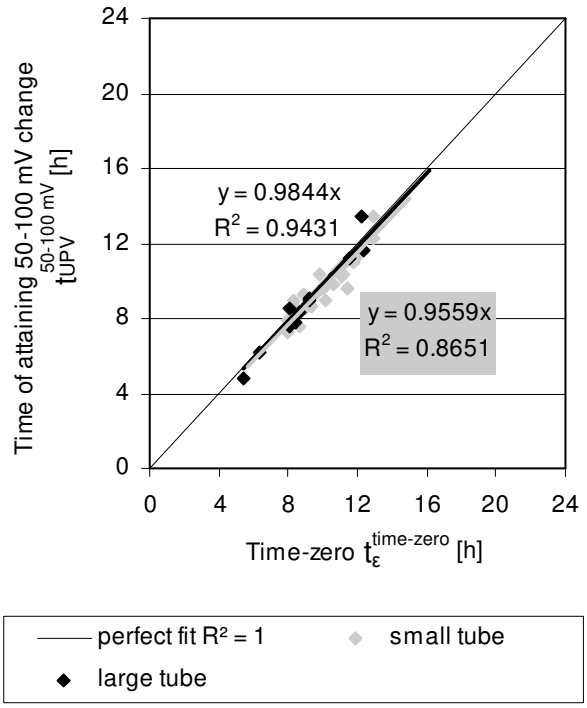

Figure 4.47: Correspondence between time-zero and change of amplitude range.

An important alternative could be application of criteria based on inspection of frequency spectrum or certain acoustic emission parameters. In fact, variables like TG parameter allow overcoming necessity of specifying threshold values related to setting points. Simultaneously, they typically possess physical meaning and give strong argumentation for finding important events in microstructural development, without need of providing additional test reference for criterion statement. Regrettably, these are solutions that for further data processing require access to waveform of every received signal in its purest form (i.e. record without encoding), being often limited for some ultrasonic devices as that used in the study at present[53]. For these reasons, and since development of own criteria failed in view of data restriction by equipment producer, evaluation according to particular approach was abandoned.

iii. Approach based on inflection point

Taking above discussion into account, another very important conclusion is drawn. In particular, it could be fixed that a perfect criterion needs not only to be based on physical changes happening in the cement paste but also, for practical reasons, it should allow final set to be determined as accurately and as unambiguously as possible, desirably using basic ultrasonic data set. Luckily enough, the basis for the former is delivered within particular

[52] For the type of equipment used, a parameter called preamplifier-degree (Vorverstärker-Stufe) is used in order to guarantee description of signal received in terms of transmission time as precise as possible. This parameter depends on signal strength and describes sensitivity of the hardware based on run regulating steps. It could be expected to alter automatically given changes of the measured material characteristic, being related to state transition of concrete, for instance.

[53] Encoding of the received ultrasonic signals record will be often used for commercial purposes. It cannot be overcome without changes in original software, similarly to manual withdrawal of every signal in the version given. In comparison, graphical illustration was found too imprecise for determining information of interest.

UPV-t pattern evolution (see Section 4.5.2) which, to its advantage, allows being further subject to mathematic description. In doing so, characteristic points could be determined such as inflection point or tangent lines. The latter, on the other hand, allows limitation of numerous criteria of mostly imprecise sound as given in Appendix G to two solutions, with one proposed by Herb [Her 03] and the other addressed as inflection point, originally proposed by Neisecke [Nei 74]. Neisecke's approach was chosen given its more revealed validity in field of low w/c materials [Lee 04][Zha 12b], no input of supplementary experiments needed and, as believed [Lee 04], better reflection of microstructural changes than in UPV.

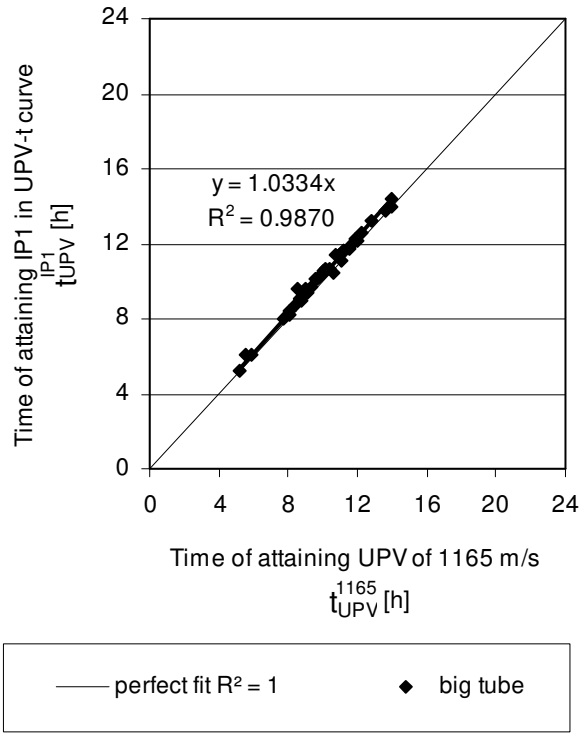

Figure 4.48: Relation between the time when UHPC reaches UPV of 1165 m/s and first inflection point on UPV-t curve including trend line.

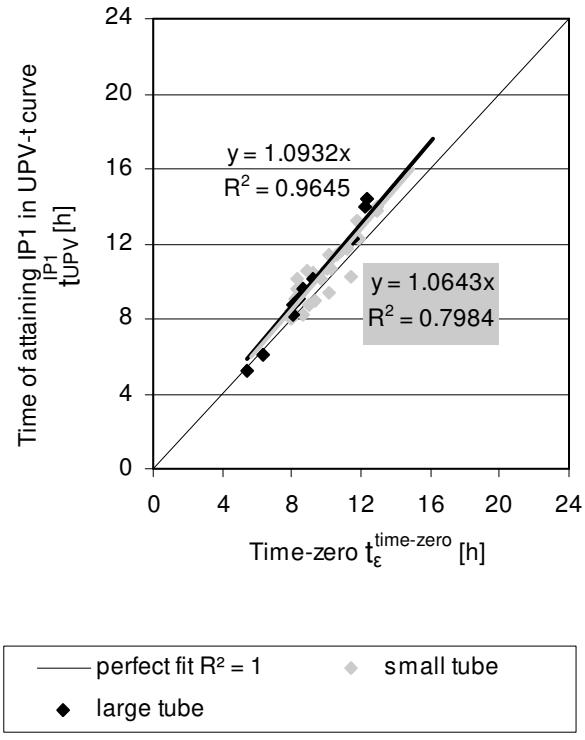

Figure 4.49: Relation between time-zero and time when UHPC reaches first inflection point on the UPV-t curve including trend lines.

Application of abovementioned theory to own research is illustrated in Figure 4.48 and 4.49. Given there was excellent agreement between the UPV velocity of 1165 m/s and first inflection point in UPV curve (Figure 4.48), satisfying and, as for bigger tubes, very good match between new time-zero and the characteristic point in UPV curve was recorded (Figure 4.49), as expected. In general, more time was needed to obtain maximum of first velocity derivative than to attain UPV of 1165 m/s, but the difference between the two events did not typically exceed 0.5 h. Again, this shows why the correspondence between IP1 and new time-zero is as close as in case of UPV of 1165 m/s (Figure 4.45).

The results of alternative match require yet another look and can be further interpreted as following. In particular, any match of setting points to UPV curve could be shown to be material-dependent, especially acknowledging its w/c. For instance, while currently the UPV inflection point most likely coincided with final set for UHPC of very low w/c, it yields initial set for concrete of high w/c given the selfsame setting measurement procedure (ASTM C403) is used, see [Rob 08][54]. On the other hand, since this study demonstrates independent ascription to UPV curve, adding to fact that according to [Zha 12b] it can be associated with final set as per ASTM C403 too[55], other evidence supporting the selfsame meaning of new time-zero is obtained.

In conclusion, the characteristic point observed in the deformation curve has confirmation in being important event in setting evolution corresponding to complete solidification (final set). A strong support to the hypothesis set at the discussion beginning has been therefore delivered.

It is finally worth to acknowledge that the procedure of finding meaning of time-zero incorporated one important simplification. In particular, it was assumed that autogenous shrinkage is not critical for shape of the curve obtained and resultant time-point of inflection point occurrence. This belief was based on inspection of the energy measure (the RMS Signal parameter), showing that no contact was lost between the mix and the transducers. Consequently, it was also possible to assume that the technical limitation associated with ultrasonic set-up used had only secondary input in results obtained, if any. As showed by Gabrijel et al. [Gab 11], under fulfilling of such condition, the estimation of final set using

[54] For different cement-based materials, i.e. a cement paste and mortar/concrete, using rival measuring standards for the destructive test of setting being referenced to (EN 196-3 vs. ASTM C403), systematization of the relation has been approached by Trtnik et al. [Trt 08] and Lee et al. [Lee 04], respectively. Although a clear conflict in conclusion about trends was reported, altogether these studies revealed the success of finding correspondence of setting points and first inflection point to depend on aggregate size, w/c (or w/cm), binder fineness and composition as well as curing temperature. In contrast, change of measuring standard can be found to be of no impact provided it is applied as intended i.e. ASTM C191 (equivalent to EN 196-3) to cementitious pastes and ASTM C403 to mortars acc. to opinion of Zhang et al. [Zha 12b]. In consequence, given satisfying correspondence of finely grained UHPC compositions of present study to mortars of [Zha 12b] (i.e. very low w/cm, high binder content, only fine aggregate used), validation of the criterion choice and the matching was enabled.

[55] The study of Lee et al. [Lee 04] regarding tests on low w/cm materials and involving usage of ASTM C403 standard is another example presenting general agreement in terms of event matching. Although some difference in UPV corresponding to final set and inflection point is shown to exist in that study, it is also found that important points in the UPV development curves are more trustworthy and giving better reflection of microstructural changes. This is also because final set typically falls into stage where UPV is strongly increasing, meaning small time difference in capturing final set will lead to pronounced change in reading of respective UPV. That is to say, time and not attaining specific UPV value would better describe moment of final set and inflection point occurrence, and some event coincidence, although not observed in [Lee 04], needn't be surprising too (observed in own case, see Figure 4.48).

active ultrasonic technique (example of which is the set-up used in the present study) is excellent and, important enough, finds confirmation upon using non-destructive testing alternatives being free of such shrinkage impact. This fact and the fact that the group of UHPC with IC largely (if not fully) free of AS effect showed great use of criterion was used for making decision about its further application to all mixtures. The validity of particular choice needs to be finally verified in future in one of the tests unavailable during this work and proposed in the work's outlook.

4.4.4 Final comments on time-zero

The fact that time-zero likely matches final set might be important for numerous reasons, discussion on which reader may find in Appendix G. Nonetheless, one final remark should be made on coincidence of time-zero as read from deformation curve and final set. In comparison to study of Assmann [Ass 13], who matched the end of setting with maximum deformation rate, earlier occurrence of the final set and its particular coincide with first minimum absolute value of the strain rate is revealed in own study. Since the comparable measuring system and curing conditions have been used, whereas impact of setting behaviour testing method could be excluded (based on study of [Zha 12b] and discussion in the previous section), this difference in opinion could be reasonably linked to configuration of material under investigation (UHPC vs. cement paste of w/c = 0.3 and CEM I 42.5 R as binder).

Two different aspects of the regarded impact are likely necessary to be considered here. One could be directly referred to incorporation of extra ingredients to the paste of UHPC as well as change in the effective w/c and the cement class/composition. Evidently, when the content of hydrating material is reduced, and so does effective w/c (also due to unintended adsorption mechanism of aggregates), other conditions for hydration process must result. This especially involves less paste which binder will be packed more dense and which, owing to higher fineness, can interact/dissolute faster (relative to cement in paste) in lower particle spaces after dormant/induction period ends. Under such circumstances, the particle-to-particle bridges and the shear-rigid bonds develop earlier, leading to faster rate of/more abrupt shear modulus development in UHPC than in the paste. It will be supplemented by effect owed to presence of aggregates which by provision of global mechanical effect, abrasive effect and the effect of site [Mou 11] will contribute to more favourable development of Young's modulus

too. The manifestation of these changes is observed shift in deformation curve[56]. This effect finds clear validation in literature, where different composition changes are shown to affect time-ascription of time-zero in reference to setting and/or shrinkage rate, this including cement type [Epp 09], w/c or incorporation of pozzolans [Cha 07] (although for some reasons and in respect to w/c not agreeing with opinion of [Zhu 08]). It is furthermore analogous to similar factors affecting correlation between knee-point or TG parameter and setting, this typically revealed to be both cement type and w/c [Jus 00] as well as w/c and aggregate incorporation (from comparison of [Gam 13] and [Trt 13a]), respectively. In comparison, the change of mix composition could plausibly trigger other phenomena. Strictly speaking, in paste that possesses higher basic w/c, contains no aggregates or binder other than cement, meanwhile has to be vibrated during casting (which is assumption based on own experience with pastes), the likelihood of bleeding is typically higher compared to UHPC. Thus, given the bleeding affects the shape of deformation curve [Tia 08], other coincidence of two discussed points should result, as observed. Eventually, different viscosity of mixes is not concerned, although it is admitted that for penetration tests this could be important issue to consider as well, e.g. [Med 11b].

It could be concluded that deformation curve cannot be fully trusted in respect to time-zero determination whenever change of mix configuration and/or bleeding takes place.

4.4.5 Summary and concluding remarks

New criterion for determination of time-zero directly from strain-time curve was proposed in subsequence to analysis of alternative assessment approaches. According to the proposal, time-zero is experimentally defined as the last extremum before the maximum deformation rate is attained. It is far before a flattening of the autogenous shrinkage curve occurs and being often considered as mark of transition between chemical shrinkage and self-desiccation shrinkage [Justnes et al. 1996 *Ibid*. Che 10 or Jus 00]. The big advantage of new approach is support in other important changes taking place in concrete around the time when the fluid-to-

[56] Comment 1: Why end of setting and not some other point is manifested as characteristic point in the shrinkage curve, this could only be speculated. However, taking into account that development of Young's modulus is close to this time-point, in deformation curve it should be manifested as first, like observed. It follows that rate of deformation reduces after end of settlement and on advancing the stage of shear-rigid bonds development (increasing stiffness of material); meanwhile, shrinkage can be regained only to certain degree afterwards provided that self-desiccation is pronounced enough. The reason for reduction of shrinkage rate in subsequence of the second maximum (which has been referred to maximum rate of deformation) is different, and could be likely attributed to resistance to the contraction of volume provided by the negative pressure in the internal voids [Yoo 14], changes in pore-size distribution [Hab 06a][Med 11b], crystallization processes and topochemical reactions of inner C-S-H [Hab 06a]. These could be as important, if not more, as self-restraining of chemical shrinkage by hardening, paying certain contribution as well [Hab 06a][Yoo 14].

solid transition is noted in low w/c systems. Another purely practical pro is obviously the handiness. On the other hand, some disadvantage found was the fact of remaining somewhat conservative as to stress generation onset or initiation of the compressive stresses reduction when using new time-zero. Decision of putting forward new description of time-zero was finally dictated by other observations made, in particular the difficulty of tracing stress generation in case of mixes with IC, producing very little free (Section 4.6.3) and simultaneously restrained autogenous shrinkage (Appendix I) as well as presence of SAP volume changes without accompanying changes in pore structure before, e.g., maximum deformation rate in shrinkage curve was recorded. Subsequently, the meaning of time-zero was analysed with support of destructive and non-destructive methods, having done additional review regarding detection possibilities and particular definitions of setting points or other for the latter (Appendix G). Both specific value of ultrasonic pulse velocity (UPV = 1165 m/s) as well as the first inflection point in UPV-t curve showed as coinciding with time-zero, and, simultaneously, as corresponding to final setting time although strictly according to American standard ASTM C403. Since results depended on norm and not the meaning behind occurrence of particular setting point as such (in theory: rapid strength development), it was concluded that matching time-zero with final set done to date on regular basis is incorrect and should be investigated in more depth in future.

4.5 Early hydration aspects

4.5.1 Introduction

Autogenous shrinkage is closely linked to hydration, as described in literature review (Section 2.3). Inspired additionally by results of rheological testing (Section 4.3.4), this section aims at evaluation of all potential hydration-related effects the IC variables (and pure SAP) expectedly induce at age corresponding to development of the major part of autogenous shrinkage. For the purpose, the non-destructive measurement used previously for assessing meaning of time-zero (Section 4.4.3) is extended and is supplemented by the temperature measurements. First, interpretation of representative results is performed for each method with reference to important literature studies. Then characteristic points are depicted and the match between methods is analysed. This knowledge is subsequently utilized to assess effect of IC/SAP exerted at different stages of early hydration, with the last age being the moment when rate of hydration slows down to negligible level. Eventually, based on different theories regarding hydration and behaviour of polymeric materials in ionic solutions, hypothesises explaining the role of IC and SAP as such in the hydration process are presented.

4.5.2 A combined UPV-temperature approach

i. Approach based on UPV

- theoretical (stages in evolution of P-wave velocity)

The most common curve of P-wave velocity (UPV) in function of time as obtained from ultrasonic testing is presented in Figure 4.50. It could be observed that the curve possessed S-shaped pattern, a typical for this kind of measurement and recorded before e.g. by [Rei 96][Lee 04][Zha 12b]. In agreement with [Smi 02], that pattern is picturing well microstructural evolution of low w/c material at the curing temperature of 20 °C. On this condition, the evolution could be characterized by at least 4 main stages in analogy to [Lee 04][Zha 12b].

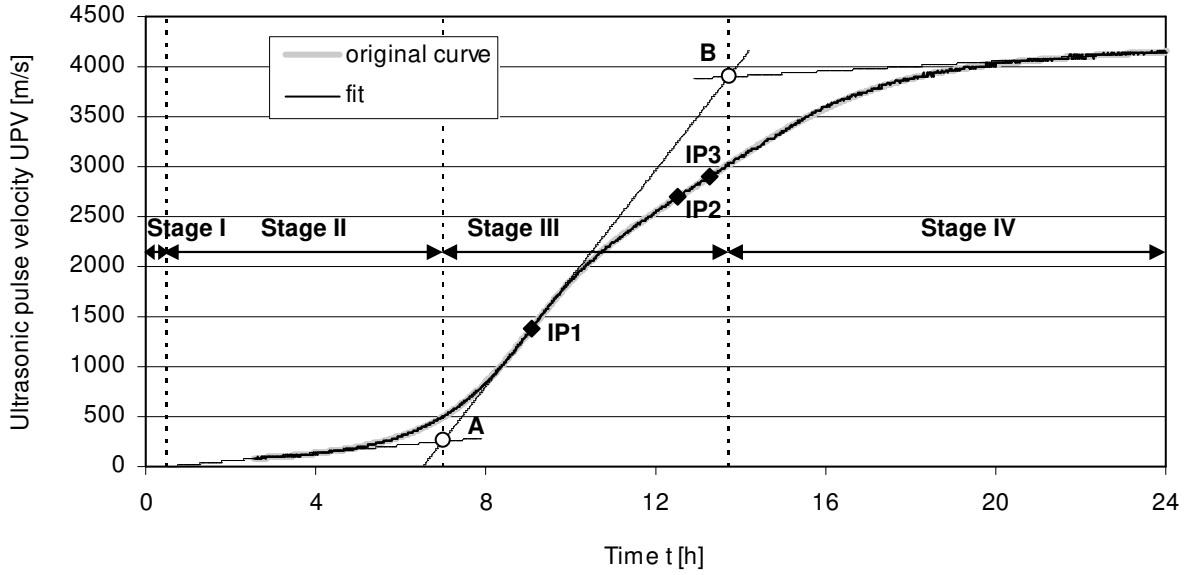

Figure 4.50: Stages in evolution of UPV-time curve and the corresponding characteristic events.

Microstructural development of hydrating paste and related to it behaviour of pulses in concrete as well as meaning of stages could be interpreted as follows:

During **stage 1**, typically no signal was received, resulting in UPV equal to nil[57]. For mixtures that contain high amount of entrapped voids as being currently the case of finely grained UPC with only few exceptions (see Section 4.2.3), this effect could be attributed to high attenuation capability these internal discontinuities possess [Kea 89]. In low frequency range of measurement[58], they likely dominated the scattering mechanism in wave propagation over the fine quartz aggregates, even if latter may be playing similar role as well [Agg 05][Zha 12b]. This impact lasts from minutes to hours and finishes at random time which, as a rule of thumb, is always before setting.

When **stage 2** commenced, the first values recorded were relatively small irrespectively of mix combination, in fact falling below UPV in water (around 1500 m/s) or even air (340 m/s). It implies that the role played by the scatterers was most likely continued though this period as well but new reasoning appeared as plausible[59]. Be that as it may, given that cement grains were suspended in still fluid-like material state and no connected passage (of solids) existed,

[57] In some cases, a considerable scatter of values with no defined trend has been observed during the stage 1. This confirms results of Pessiki and Carino [Pes 88] and yields generally larger signal attenuation ability compared to more advanced stage of hydration.

[58] High frequencies can be assumed to be completely damped until set.

[59] It could be assumed, for instance, that low velocities were alternatively generated in result of solution process of cement in water and consequent change of internal viscous forces [Haa 75], they alternatively occurred as sign of insufficient coupling of cement particles with water [Fey 01] and/or, more generally, were result of the fact that in fresh UHPC the wave transfer media were all three: liquid, solid and gas, although restricted to fluid phase before initial set [Zhu 11a].

oscillation and motion of emulsion phase rather than propagation took place [Rei 96], leading to elongation of the wave-path length and low UPV.

As stage 2 progressed, the UPV increased only insignificantly to a higher value but of unchangeably low level. This indicated general high sensitivity of UPV to (massive) hydrate formation [Smi 02], likely ettringite [Moe 10], as well as to relative density variation [Cho 01]. None of the reasons behind it[60], however, could yet pay a direct contribution to connectivity/integrity of solids and resultant construction of load-bearing structure at this hydration moment.

The so-called solid percolation threshold[61] (point 'A' in the graph) put an end to stage 2 and gave rise to **stage 3**. From this important event (found mathematically as the intersection point of two straight lines tangent to data in stage 2 and 3 acc. to [Smi 02][Lee 04]) onwards, the UPV increased rapidly. The appearance of first event informed that new propagation path became available, in particular the wave propagation was granted through the solid phase[62]. The latter, on the other hand, yielded its network and linkage of which was gradually increasing due to silicate hydrate formation and especially C-S-H phase [Moe 10]. Soon, the advancement of connectivity brought about stiffening, including phenomenon ascribed to first inflection point in UPV curve and time-zero (or its vicinity) in this thesis. Additional events were also recorded but their meaning remained vague, see Section 4.5.3 for more details.

Eventually, **stage 4** took place with a mathematically specified start point (point 'B' in the graph) defined as intersection point of two straight lines tangent to curve in stage 3 and stage 4. During this stage, UPV curve did not show significant increment any more and rather levelled off, to reach plateau within few days time. Such dramatic change of course indicated acquirement of fully connected solid frame, approaching the final stiffness by slid skeleton

[60] Examples of former and the latter are ettringite formation [Voi 05] and declining rate of gravitational setting [Voi 05], respectively. Another school of thought presented by Popovics [Pop 94], however excludes increase in velocity due to formation of large quantities of solid hydration products if having no interconnections, or when the interconnected solid frame is tenuous (i.e. still non-rigid, non-elastic. Therefore other explanations appear plausible such as increase in viscosity of liquid phase [Pop 94], air bubble migration and workability loss [Rob 11], chemical shrinkage [Cho 01], and/or in general- increasing number of physical contacts between particles [Fey 01].

[61] It is moment describing finalization of processing of isolated events between cement grains, their clustering and mutual building up bridges. The event is often ascribed to phenomena such as creation of first interconnected solid phase and creation of first interparticle bonds.

[62] The solid phase is preferable path of ultrasonic wave propagation. It can be assumed to be attained at critical quantity of hydration product and inter-particle bonds between solids. The structure receives certain stiffness.

and filling up of last remaining pores by hydration. Only part of this so-called hardening phase could be followed due to reasons discussed in Section 4.5.4.

- *experimental*

Summarizing the foregoing section, the transitions points A and B as well as important changes in the UPV rate reflected as inflection points IP1, IP2, IP3, all taking place during stage 3, could be considered as important events in microstructural development in early age. Since falling in the period when the connectivity is generally only increasing, they seem good points of reference to be taken into account when analysing moment of strength build-up, setting and especially effect of IC.

The same statement cannot be applied to case of some UHPC with highest amount of extra water but containing no SAP. Examples are shown in Figure 4.51.

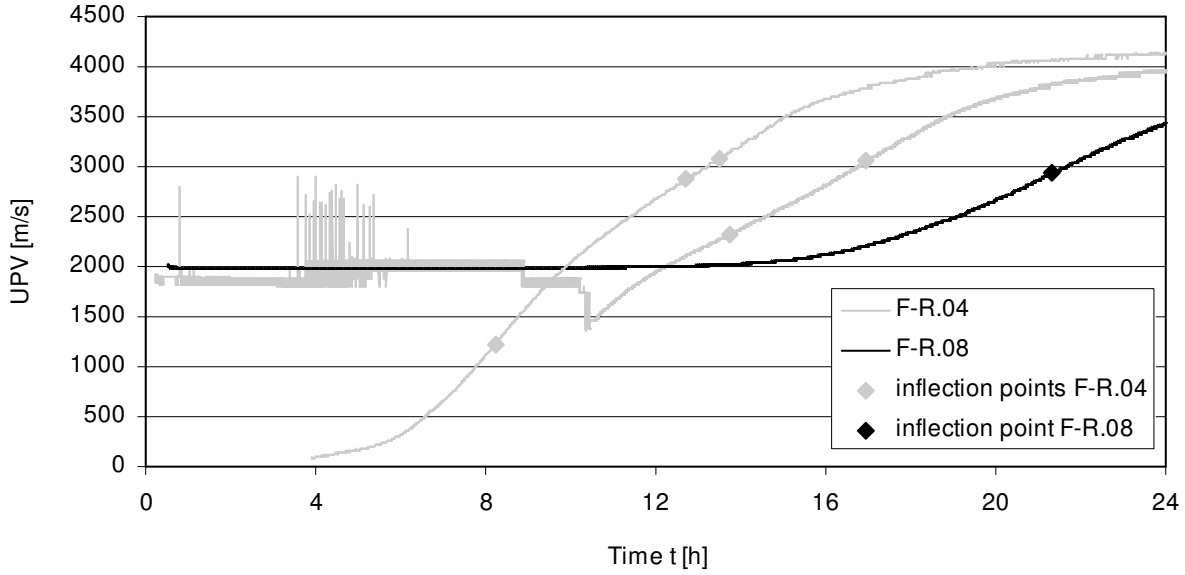

Figure 4.51: Evolution of UPV in time for mixtures with extra amount of water, but no addition of SAP.

Compared to other mixtures, the curve picture for mixtures F-R.04 and F-R.08 was different and only sometimes the S-shaped pattern was recorded. This was very much likely triggered by pronounced viscosity reduction due to increase of basic w/c by extra water bringing about increasingly lower content of entrapped air, see trend in Section 4.2.3. Air is well known as major modifier of UPV curve [Zhu 11] similarly to curing temperature [Smi 02] and superplasticizer type [Trt 13b], which were maintained constant in own tests. In some cases, it brings about picture like recorded for mix F-R.08, being picture characteristic for the air void-

free mixtures of low w/c [Cho 01][63]. In other cases, for certain low values of air entrapped, this modifier appeared mainly to perturb the curve evolution built in stages 1, 2 and partly 3, even when the selfsame composition was concerned and the only difference being different production dates. In consequence of apparent modification, important events to report appeared to be alteration of UPV which changes from constant or quasi-constant value higher than longitudinal velocity in water towards much lower one or just the opposite, i.e. UPV increase starts. However, to maintain regularity of data evaluation, only the well definable inflection points were concerned in the following.

ii. Approach based on temperature

To understand changes occurred in early ages even better while also to examine meaning of infection points, changes in the in-situ temperature evolution were examined in addition to ultrasonic test. In principle, referring to a measure of heat of hydration and comparing it to a tool of monitoring mechanical processes is fully justified given possibility of translation of both results into degree of hydration or reaction, see examples in [Moe 09] and [Rob 11], respectively.

- theoretical (stages in evolution of temperature curve)

For assessing exothermic output of hydration reactions typically diverse calorimetric methods are used where the heat produced is expressed after taking binder quantity into account[64]. More recently, however, it has been showed that this step might not be necessary. According to Trtnik and Turk [Trt 13b], a platform for correlation between results of in-situ temperature (in °C) and P-wave velocity should also exist when referring to important changes in their evolution, example being their rate maxima[65]. Other researchers [Özt 06][Gab 11] go even

[63] UPV higher than in water for concrete that has not set yet is rare but has been sometimes recorded for low w/c materials that contained theoretically no air entrapped. It has been ascribed to low quantity of water [Cho 01], although other underlying reasons might be imagined as plausible, e.g. higher concentration of solid phase at low w/c or presence of agglomerates.

[64] Calorimetric measurements (or in other words heat of hydration investigations) can be generally performed under three different conditions, i.e. isothermal (in the so-called conduction calorimetry), where it is the ambient temperature that is maintained constant, semiadiabatic/adiabatic, where heat exchange is prohibited due to insulation of different level of efficiency or according to heat of solution method where heat of hydration is assessed by measuring the temperature rise when the cement is decomposed in an acidic solution. Of these three, the method used at present (i.e. in-situ temperature record of a sealed sample) most resembles isothermal/conduction calorimetric method and possesses similar advantages including allowance of early measurement start. On contrary, relatively large specimen made of low conductivity material could be tested at present, which should be borne in mind as a step towards overcoming the major drawback of the isothermal conduction calorimetry, i.e. lack of realistic and repeatable results owing to small sample size.

[65] As a rule of thumb, measurements of temperature on the same batch of concrete but cured under different conditions (with respect to heat insulation measures and similarly to curing temperature) are likely to give different time association of important evolution events, an issue also verified in this work, see Section 4.3.2 and

further in simplifying the comparison but without loosing the scientific correctness. In particular, instead of performing the measurements in semi-adiabatic conditions or similar (e.g. those following which temperature rise in test samples is more than extra 20 °C over room temperature) they suggest less severe test conditions, these being isothermal or ones in which temperature of sample increases only by few degrees relative to ambient. Experience showed that following them, sufficient reflection of hydration process resembling that in calorimetric conditions is found [Özt 06] while changes in both variables, P-wave velocity and in-situ temperature, are very likely to be connected when they follow similar trend [Voi 05]. This should apply especially to period between end of induction/dormant period or beginning of resistance test and maximum of the temperature, i.e. of main interest currently.

- *experimental*

A typical temperature vs. time curve as obtained from tests on selfsame batch of exemplary concrete as in P-wave velocity measurement is shown in Figure 4.52. It can be seen that, as expected, evolution of temperature followed the classic heat of hydration curve and the characteristic stages of its progress. This involves pre-induction period (also known as initial exothermic reaction period) when heat only reduces, induction/dormant period when temperature stabilizes, acceleration period (also called as nucleation and growth period) when heat production regains on strength again, and, eventually, deceleration period when the temperature reduces for the second time after attaining the maximum (2^{nd} peak).

4.3.3. The effect will be similar if not identical when the sample size changes alone or simultaneously too and no variation in the binder content has been acknowledged. Therefore, only under specific set of conditions the two may equalize the effect exerted on other properties, one of examples being presented in [Med 11b]. In this work, by using the samples of identical size and their exposure to the selfsame curing conditions during UPV and temperature measurements as well as with temperature sensor being embedded at exactly the selfsame position, the potential sources of errors were eliminated.

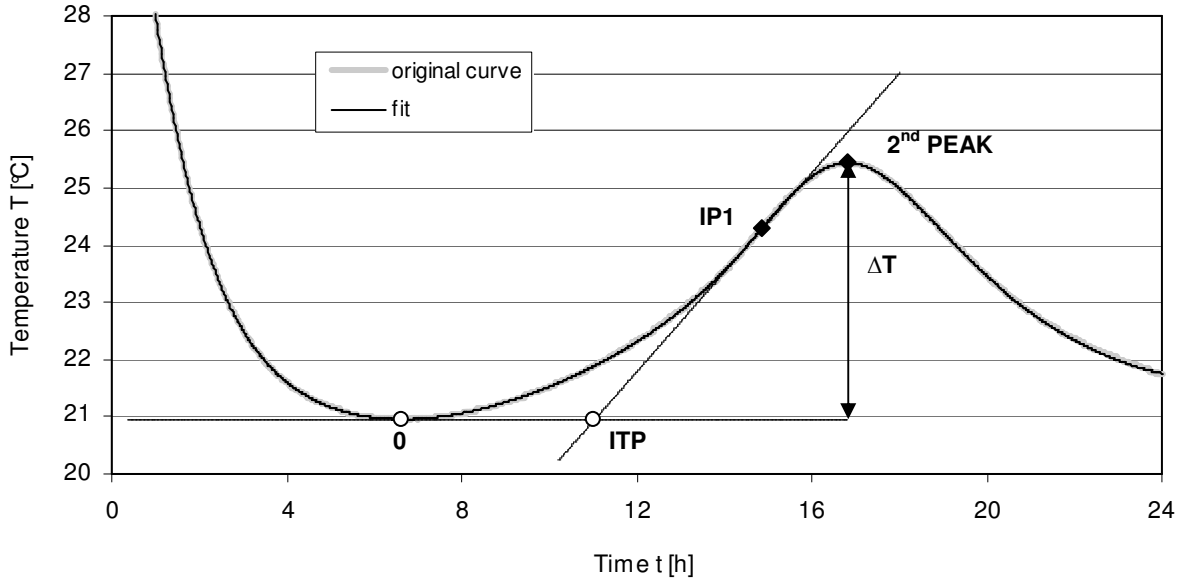

Figure 4.52: Characteristic events in temperature-time curve and their determination.

Among the stages, one important event is beginning of the temperature rise [Smi 02] or, in other words, start of accelerated exothermic reactions of cement [Özt 06] which could be defined as minimum on temperature curve [Özt 99]. The singularity is assumed to coincide with the end of induction period and the beginning of stiffening process that is also bringing about coalescence of stable skeleton of cement matrix [Özt 99][66]. It is different to intersection point (ITP) of two straight lines tangent at point of minimum temperature and first inflection point of temperature curve; here another relevant event is addressed, in particular the moment when temperature after initial slow increase started to rise at incomparably higher rate, as already seen in Figure 4.38[67]. Yet, since preliminary data analysis showed that inflection points in UPV-t curves appeared at later ages, other characteristic points in temperature evolution were taken into account as well, this including maximum temperature rate, i.e. first inflection point on T-t curve (IP1) and second peak temperature (2^{nd} PEAK). Evaluation finally involved parameter important from engineering viewpoint and referring to measure of heat developed (ΔT).

[66] Differences in monitoring systems used as well as in mix compositions could be named as underlying reasons for significant change in slope of UPV-t curve (point A in Figure 4.50) to occur earlier than one in case of in-situ temperature (ITP in Figure 4.52) as opposite to [Cho 01][Smi 02] but in agreement with [Voi 05][Gab 11][Trt 13b]. Still, the meaning of the event referred to as beginning of temperature rise could be somewhat similar, e.g. start of formation of minimum hydrates content or otherwise modification of nature of the bridges being the prerequisite towards the abrupt rise in UPV.

[67] Note that both points mentioned could be highly important for UHPC, since low w/c materials set soon after the end of dormant period [Özt 06][San 09], i.e. when the temperature of sample due to increasing hydration heat starts to increase, having confirmation for UHPC provided e.g. in [Sch 02b][Yoo 13].

4.5.3 Results of the approach

The characteristic parameters recognized in Section 4.5.2 have been determined from data of all experiments performed and results are listed in Table 4.8, first for the ultrasonic tests. Labels t_{UPV}^{1165}, t_{UPV}^{IP1}, t_{UPV}^{A}, t_{UPV}^{IP2}, t_{UPV}^{IP3}, t_{UPV}^{B} are used to define time of attaining UPV velocity of 1165 m/s, first inflection point in UPV-t curve or otherwise point A, second inflection point, third inflection point and point B, respectively. Unless UPV is defined, each time column is followed by a column with corresponding velocities.

Table 4.8: Information from interpretation of ultrasonic data (standard deviation is given in parentheses).

Mix	Time-zero related criteria			Other important events on UPV-t curve							
	t_{UPV}^{1165} [h]	t_{UPV}^{IP1} [h]	UPV at t_{UPV}^{IP1} [m/s]	t_{UPV}^{A} [h]	UPV at t_{UPV}^{A} [m/s]	t_{UPV}^{IP2} [h]	UPV at t_{UPV}^{IP2} [m/s]	t_{UPV}^{IP3} [h]	UPV at t_{UPV}^{IP3} [m/s]	t_{UPV}^{B} [h]	UPV at t_{UPV}^{B} [m/s]
F-R	9.6 (1.3)	10.1 (1.3)	1374 (43)	8.1 (1.1)	544 (52)	13.3 (1.5)	2636 (111)	14.4 (1.3)	2963 (101)	-*	-*
F-S.4	8.6 (-)	9.7 (-)	1573 (-)	7.4 (-)	846 (-)	-	-	-	-	-	-
Ff-R	8.5 (-)	8.7 (-)	1296 (-)	6.7 (-)	464 (-)	11.9 (-)	2517 (-)	13.6 (-)	2990 (-)	-	-
F-R.04	8.1 (-)	8.2 (-)	1222 (-)	6.4 (-)	431 (-)	13.2 (-)	2602 (-)	15.2 (-)	3072 (-)	-	-
F-S.3.04	9.7 (-)	10.1 (-)	1357 (-)	7.8 (-)	540 (-)	13.6 (-)	2441 (-)	15.1 (-)	2828 (-)	-	-
F-S.3.05	10.7 (-)	11.4 (-)	1430 (-)	8.2 (-)	470 (-)	14.6 (-)	2367 (-)	16.4 (-)	2815 (-)	-	-
F-R.07	13.9 (-)	14.0 (-)	1185 (-)	11.2 (-)	348 (-)	15.7 (-)	2209 (-)	18.4 (-)	2876 (-)	-	-
F-S.4.07	11.6 (1.2)	12.0 (1.3)	1309 (56)	9.7 (-)	492 (25)	13.9 (0.4)	2279 (108)	16.0 (0.7)	2893 (109)	-*	-*
Ff-S.4.07	11.5 (-)	11.7 (-)	1222 (-)	8.9 (-)	419 (-)	15.2 (-)	2250 (-)	16.8 (-)	2621 (-)	-	-
F-R.08	Not occurred	21.3 (-)	2934 (-)			Not occurred	-	Not occurred	-	-	-
F-S.6.08	-	-	-	-	-	-	-	-	-	-	-
F-S1.0.16	13.6 (-)	13.7 (-)	1197 (-)	11.3 (-)	559 (-)	Not occurred	-	Not occurred	-	-	-

*- not determined due to little data recorded beyond 24 hours = imprecise estimation

All parameters seemed to be ascribed to reasonably constant values of UPV for a particular composition. E.g. mixtures F-R and F-S.4.07 that were studied repeatedly for any event reported, obtained differences of UPV which were lower that 5 %. It is an excellent agreement for this kind of test. This indicated that the characteristic events (on UPV measurements) are consistent for different repetitions. The time at which characteristic events occurred varied with standard deviation of approx. 1.3 h for most parameters studied. However, this was

expected given usage of more batches of basic constituents during repetitions. Overall, it was possible to validate the ability and accuracy of ultrasonic method to trace the microstructural changes regardless of IC presence.

Speaking about the selfsame attribute, very much the same precision was maintained for parameters based on T-t curves once expressed in corresponding values of UPV. These are summarized in Table 4.9 where the additional labels t_T^0, t_T^{ITP}, t_T^{IP1}, $t_T^{2.PEAK}$ and ΔT in the foregoing columns are applied to indicate time of attaining minimum temperature, intersection point, first inflection point, second peak (= the only maximum recorded) and maximum temperature difference, respectively. No information on UPV at t_T^0 is presented in this table given lower reliability of the UPV parameter in view of varying air contents for each composition and overshadowing true correspondence of temperature results.

Table 4.9: Information from interpretation of temperature data and the corresponding UPV (standard deviation is given in parentheses).

Mix	**Event on T-t considered**							
	t_T^0	t_T^{ITP}	**UPV at** t_T^{ITP}	t_T^{IP1}	**UPV at** t_T^{IP1}	$t_T^{2.PEAK}$	**UPV at** $t_T^{2.PEAK}$	ΔT
	[h]	**[h]**	**[m/s]**	**[h]**	**[m/s]**	**[h]**	**[m/s]**	**[°C]**
F-R	7.1 (0.8)	12.4 (1.4)	2356 (122)	15.9 (1.4)	3423 (95)	17.7 (1.5)	3830 (64)	5.3 (1.0)
F-S.4	6.8 (-)	10.6 (-)	1923 (-)	15.7 (-)	3397 (-)	19.3 (-)	4058 (-)	3.0 (-)
Ff-R	-	-	-	-	-	-	-	-
F-R.04	7.4 (-)	12.5 (-)	2377 (-)	15.8 (-)	3208 (-)	17.8 (-)	3646 (-)	4.0 (-)
F-S.3.04	8.2 (-)	12.8 (-)	2232 (-)	16.3 (-)	3157 (-)	18.5 (-)	3655 (-)	5.6 (-)
F-S.3.05	9.2 (-)	14.0 (-)	2216 (-)	17.9 (-)	3189 (-)	20.2 (-)	3634 (-)	5.2 (-)
F-R.07	8.6 (1.8)	15.6 (1.6)	2245 (32)	18.8 (1.6)	2953 (49)	20.8 (1.5)	3435 (-)	5.2 (0.8)
F-S.4.07	8.1 (0.5)	14.7 (0.9)	2317 (166)	17.9 (1.0)	3203 (115)	19.8 (1.0)	3622 (102)	5.9 (1.0)
Ff-S.4.07	-	-	-	-	-	-	-	-
F-R.08	-	-	-	-	-	-	-	-
F-S.6.08	7.5 (-)	14.0 (-)	-	18.5 (-)	-	20.9 (-)	-	2.9 (-)
F-S1.0.16	10.1 (-)	16.7 (-)	2003 (-)	21.2 (-)	2976 (-)	23.9 (-)	3378 (-)	3.3 (-)

Having compared data presented in Tables 4.8 and 4.9, Figure 4.53 was created where times of acquiring the extrema on the UPV-t curve are compared with times of maximum rate of temperature rise. Only in one case a reasonably strong linear correlation and high correlation coefficient could be observed, this being the case of third inflection point on UPV-t curve and temperature extremum in reference to time. Having it further analysed, however, it was noticed that ideal match was solely limited to mixtures that lost appreciable amount of entrained air i.e. UHPCs with extra water and no SAP. Adding to this random appearance of the two extra inflection points on UPV-t curve (resulting in IP1 existence alone or along with both IP2 and IP3, not obvious from Figure 4.53), meaning of the new events could be claimed as vague.

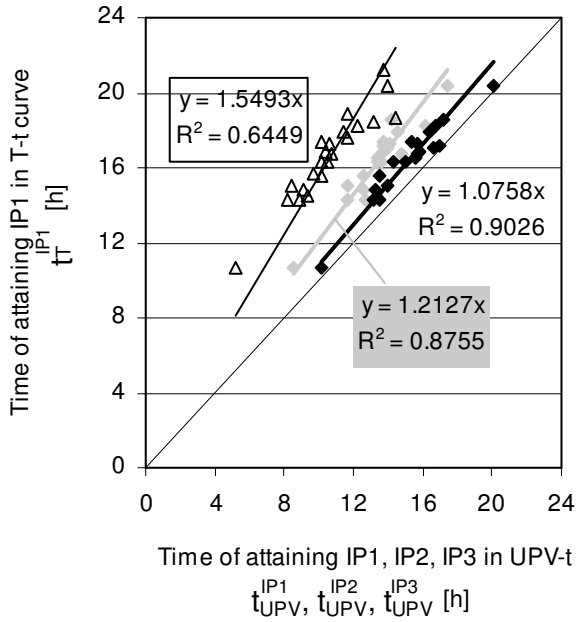

Figure 4.53: Correspondence between inflection points on UPV-t curve and inflection point on temperature-t curve.

Last conclusion is in clear contrast to that made by Trtnik and Turk [Trt 13b] who found the time of appearing the additional extremum in the evolution of UPV-t curve to be matching that in T-t curve in a perfect way. In other words, it was hypothesized before that the two variables are very likely related and common ground responsible for changes and appearance of extrema is hydration progress. Presently, it could be only speculated whether this is somewhat related to test particularities (usage of curing conditions hardly forcing high heat production in this study; employing other measuring system) or other (e.g. composition, air content). The fact is however that the UPV-t shape/pattern in each case is typical for material studied i.e. the arch-type one for low w/c cement paste with more inflection points, e.g. [Gab 11] and the S-shaped one for low w/b mortar or concrete with one main inflection point [Lee 04][Zha 12b]. Further study would be needed in future to recognize whether additional extrema are important or not.

Being far more important for goals of this study, many alternative arguments can be given proving meaningfulness of the comparison between two variables (UPV, t) for building picture about early hydration and effect of IC. One that has been already addressed is

excellent translation of characteristic events in temperature evolution into values of UPV. Relevant enough, this important feature held true before and especially after the velocity followed connectivity of solid phase. Simultaneously, another as relevant observation is remarkably high mutual correspondence of the events regardless if the translation has been performed or not (i.e. the time scale is still being referenced to). Indeed, if expressed via UPV and time, the ratios between intersection point and inflection point of temperature curve to the peak were found to be nearly constant and were recorded to be 0.62 ± 0.03, 0.71 ± 0.04, 0.89 ± 0.01, and 0.90 ± 0.01, respectively. This implies no difference between mixtures without or with SAP, the only exception being UHPC with pure SAP addition and no extra water for which ratios become 0.47, 0.55, 0.84, and 0.81, respectively to yet unknown reasons. Presenting another perspective of the apparent correlation, comparison of both parameter evolutions for exemplary mixture (Figures 4.50 and 4.52) also revealed that the time at the maximum of temperature corresponded quite well with time at which UPV approached the asymptotic value. In fact, once the intensity of chemical reactions reflected by temperature reduced to the level close to that met in dormant period, UPV responded largely correspondingly, i.e. increased slowly and insignificantly. Last but not least, there is well-definable regularity of IC effect on level of UPV noted, again to be traced in Tables 4.8 and 4.9.

When taking all these into account, the results clearly validate the ability and accuracy of both methods to detect the influence of IC/SAP on the hydration process and formation of structure of the materials. In turn, for estimation of the IC (or pure SAP addition) effect on hydration, two different measures could be theoretically considered. On one hand, this issue could be analysed based on P-wave velocity which describes the absolute amount of the total and connected solid phase developed during hydration process [Trt 13b]. Thus, given that condition for microstructural development has occurred (i.e. about the time solid phase begins to form and UPV starts to increase abruptly), its value compared for mixtures at any given concrete age (or, alternatively, the opposite solution) could be used to follow the hydration advancement. On the other hand, since original composition underwent more acknowledgeable modification every time the content of IC variables was increased, focusing on the important events declared in Tables 4.8 and 4.9 in their time scaling seemed more appropriate and was applied[68].

[68] In cement-based materials, the value of UPV is, as a rule of thumb, related to concentration of solid phase, in turn changing accordingly with increasing extent of hydration. This applies to UHPC as well, where apparent linkage between UPV and degree of hydration or mechanical development (Young's modulus, tensile strength)

4.5.4 Effect of IC and SAP on early hydration

The results listed in Tables 4.8 and 4.9 indicate that all mixtures incorporating both IC variables exhibited retardation at every stage of early microstructural development especially when compared to control mix F-R. The trend followed the amount of IC variables, i.e. the more SAP and extra water was added, the more pronounced was the effect. This held true provided that there was no loss of workability (= no significant modification of effective w/c), implying the maximum IC-agent absorption had been attained, see Section 4.3.3 for details. In opposite case, microstructural changes appeared sooner, in particular making the less workable UHPC F-S.3.04 to behave somewhat similar to the reference F-R. No extra water added for curing in mix F-S.4 presented obviously the most extreme conditions for hydration among SAP-incorporating mixtures.

Be that as it may, neither presence of IC nor, interestingly, incorporating SAP alone resulted in the increase of maximum (peak) temperature. In fact, particular measure of hydration heat was seen to reduce on occasion of mix with highest IC variables content tested (F-S1.0.16) as well as F-S.4 containing no extra water at all, see ΔT in Table 4.9. The source of lower UPV values of IC-incorporating mixtures at the regarded events could be finally related to diminished composite elastic modulus (as attributed to lowering paste and aggregate phases on addition of IC variables), their higher porosity and/or tortuosity.

Concluding, if IC was to enhance hydration as commonly believed, this was expected to happen at ages not sooner than by end of setting or even later for the UHPC tested at present. To investigate this aspect in greater detail, ultrasonic measurements were extended until the age of 96 hours for some of the finely grained mixtures including F-R (control mix) and F-S.4.07. The result is presented in Figure 4.54 showing evolution of mixtures' UPV values with the corresponding UPV rate changes. For sake of better view on effect, the comparison start was situated at first inflection point of the corresponding T-t curve.

---

could be judged, e.g. based on empirically-derived relationships that mechanical properties have with degree of hydration and UPV [Yoo 13]. These are likely not unique since, as importantly acknowledged by Pessiki and Carino [Pes 88], mixtures being compared to but varied by mix proportions could be at different hydration stages and accordingly possess different elastic moduli even if the same velocity is reached. Evaluation of time-zero criteria showed that this does not necessarily concern UHPC after incorporation of any content of IC variables and underwent air content variation, since similar P-wave velocity at time-zero was obtained. Therefore by referring to evolution of events in time, and only thereafter to corresponding values of velocity, the conservative approach was maintained.

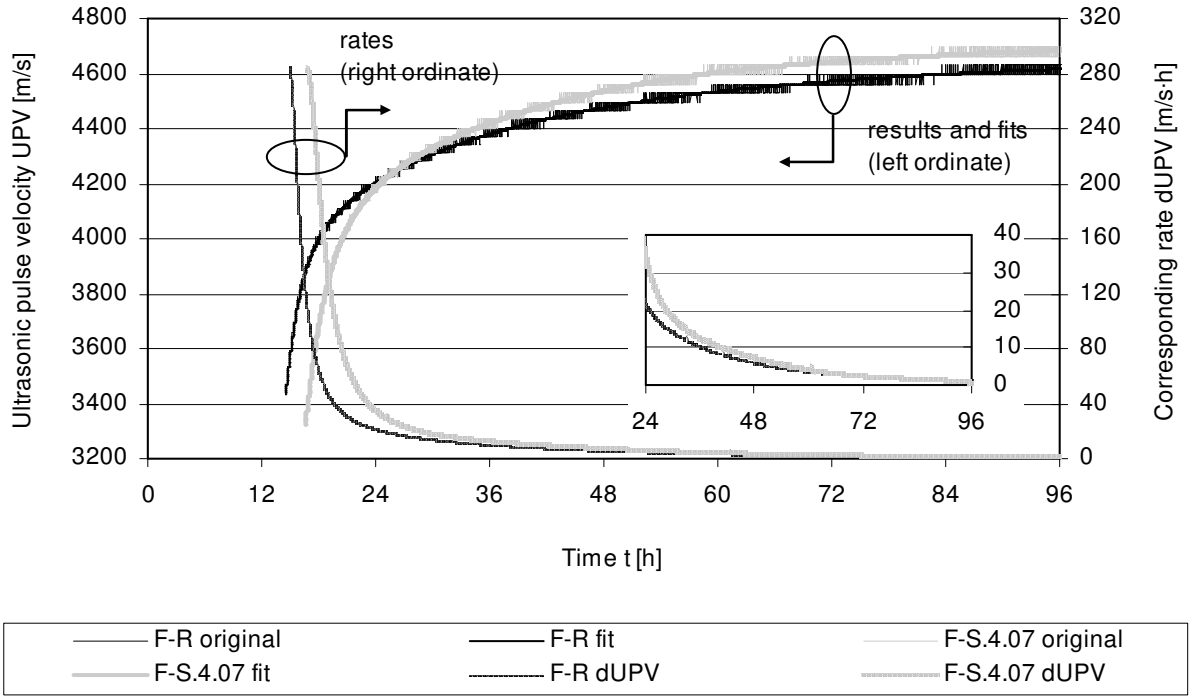

Figure 4.54: Evolution of UPV and rate of UPV change from inflection point in corresponding T-t curve for control mix F-R and mix with IC F-S.4.07. Magnification of UPV rates for concrete ages above 24 h.

It is seen that until regarded event occurred, i.e. some hours after hypothesized final set and time-zero considered in this work, the rates of UPV change have already equalized. Subsequently, the first derivative of UPV became reduced less pronouncedly and accordingly maintained on higher level for mix with IC compared to that of F-R. This forced the UPV to be no different once a certain stage of hydration was reached and its value to grow increasingly faster for mix with IC thereafter. This continued until the age of approximately 3 days, after which no distinct changes of UPV were noted anymore due to reduction of changes' rate value to a very low level. Obviously, this implies significant progress of hydration until regarded time as expected for UHPC and, more importantly, exact period of the IC activity that is bringing about higher total solid volume fraction. In other words, it was confirmed that higher hydration degree can be truly expected when the IC is applied in UHPC, even though the extent of changes was limited to early age[69]. The prediction of the IC effect using Powers' model as demonstrated in Figure 4.55 and based on calculation delivered in Appendix D could be therefore evidenced on new much more important level being real concrete situation[70].

[69] It could be hypothesized that higher IC variables' quantities applied would lead to further increase of degree of hydration or otherwise shortage of time required to bring hydration to a higher level. However, this issue could not be finally verified due to high shrinkage of the reference UHPC F-R and, related to this fact, difficulty in removing the transducers after long-term ultrasonic measurement on particular mix.

[70] It should be emphasized that Powers' model including the modified version is based on set of equation of simplified establishments. For instance, in this model it is assumed that all entrained water carried by IC-agent is

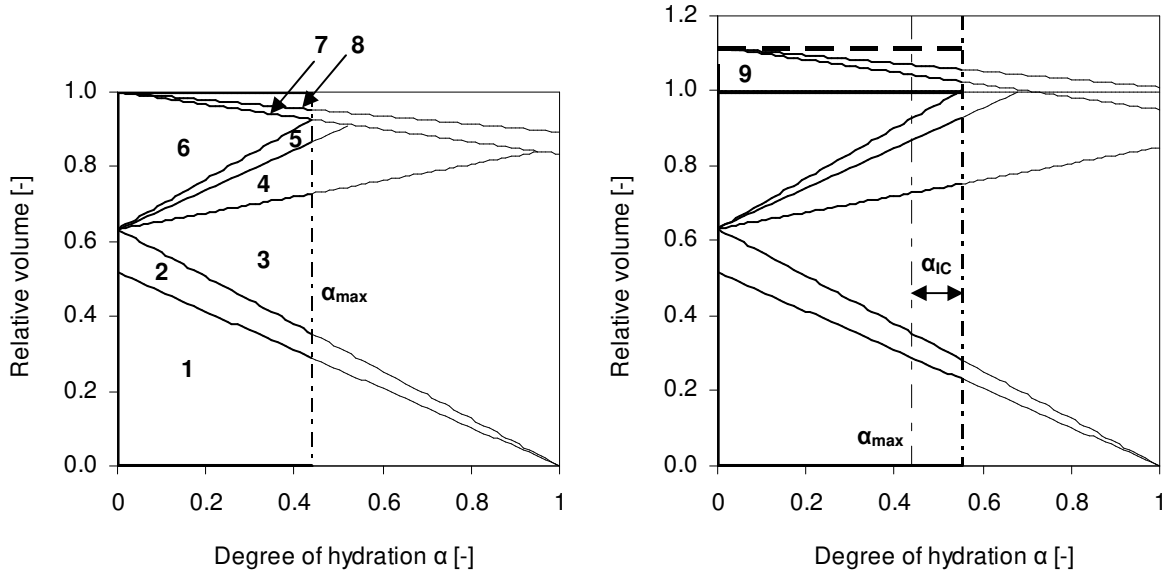

1 - Unhydrated cement 2 - Unreacted silica fume 3 - Gel solid 4 - Gel water (cement) 5 - Gel water (silica fume) 6 - Capillary water 7 - Chemical shrinkage/Empty pores (silica fume) 8 - Chemical shrinkage/Empty pores (cement) 9 - Entrained water/Pores α_{max} - maximum degree of hydration α_{IC} - extra α due to IC

Figure 4.55: Powers' model in adaptation for phase distribution of the paste of the control mix F-R (to the left) and IC-incorporating F-S.4.07 (to the right). The potential input to effective w/c due to overestimation of IC agent absorption is ignored.

4.5.5 Further on effect of IC and SAP on early hydration

The fact that no adverse influence on cement hydration occurred with exception for initial retardation means that important requirement for use of polymeric admixtures in concrete postulated in [Ram 06] has been fulfilled by the IC agent tested at present. Combined with potential temperature reduction, this would only add to number of advantages of SAP recognized before and after usage in concrete, see Section 4.2.2 for details.

Experience gained in field of early hydration to date does not allow presenting uniform viewpoint on effect of IC. For instance, contrary to results of present investigation, rival study on low w/c (= 0.25) finely grained UHPC with IC by Soliman [Sol 10][Sol 11] yielded both earlier attaining of setting limits (following higher degree of hydration from the ages before setting) and lower peak temperature in the semi-adiabatic conditions. A higher and earlier heat production, therefore plausibly sooner acquiring of setting times (although one equal

freely available to hydrating system when needed, so that it could be prevented from self-desiccation and hydration can continue. Such establishment is however proved to be unrealistic also in this work. Among other limitations (e.g. disregarding changes in time, disregarding that not all capillary water can be used for hydration, disregarding possibility of retarded pozzolanic reaction), Powers' model as operating on relative volumes also disregards possibility of absolute binder volume changes upon modification with IC (unlike in case of pure SAP addition, cf. [Moe 09]), which currently is reported to lead to small changes of UPV values. In this respect, ultrasonic testing proves to be the more attractive tool for tracing the effect of IC/SAP on degree of hydration.

percolation threshold being claimed by authors to be the time-zero irrespectively of IC presence), was already the attributes of internally cured HPC of basic w/c of 0.32 tested in adiabatic conditions [Cra 11]. Both examples are therefore in clear contrast to other studies on IC, which, similarly to present one, show retardation of setting limits (e.g., final setting time in case of HPC with basic w/c = 0.35 [Pié 06], initial and final set time in case of very low [Dud 10b] and low w/c (= 0.3) cement pastes [Wyr 11]) as well as retardation and less advanced evolution of temperature of cement pastes [Dud 10b].

Some reasons for the differences appear clearer than other. Precision of the SAP absorption capacity estimate could be assumed an important one [Has 12]. E.g. in a study on similar finely grained UHPC by Soliman [Sol 10][Sol 11], some underestimation of IC agent absorption could be expected. Arguments to support this hypothesis are: the selfsame SAP material used except for its fineness which was higher (resulting in higher absorption acc. to [Dud 14]), usage of twice as much of silica fume in mix without and with IC compared to that used in matrix M2Q (meaning greater rivalry for the ions controlling the SAP absorption, as analogously to introduction of SAP to B5Q) and finally picture of temperature evolution very close to that of F-S.4. In other instances, downsizing w/c to threshold value of 0.3 [Zhu 13], overestimating the polymer absorption or varying the content of the superplasticizer, i.e. rival polymeric admixture for control of workability, might be of importance as well. Still, this does not explain the effect observed in this work.

Table 4.10 presents compilation of most attractive hypothesises which could be used to explain effect of IC/SAP on early hydration. These were put forward by analyzing different theories from various fields of science including concrete technology and by making logical analogies in respect to application of SAP in cement-based materials. Three groups could be distinguished, either directly or indirectly related to introduction of IC. Already at first glance, it is seen that one mechanism is insufficient to explain all aspects of retardation observed. In fact, one finds that not only is the list long, also ease of separating the contribution of each parameter/each contribution is very likely low. Due to multithreading of the task, only platform was delivered while verification was left for future studies with more SAP types.

Table 4.10: Claims for explanation of effect of IC and SAP on early hydration.

Factor responsible for effect	Main outcome
• Introduction of IC (remark: presence of both IC variables i.e. SAP and extra water)	• (1) Higher/Increased (specific) heat capacity of UHPC • (2) Dilution effect • (3) Supersaturation (state/level) control
• Introduction of hydrogel (remark: no presence of IC water necessary)	• (4) Nucleation control (Ca-sink role) • (5) Secondary Ca^{2+} concentration control and primary to alkali • (6) Complexation/precipitation control (general ionic sink role) • (7) Adsorption/Nucleation control • (8) Secondary supersaturation (state) control • (9) Hydration cessation conditions delivery
• Introduction of changes in properties of concrete in fresh state and in role played by concrete components due to IC/SAP	• (10) Worsening of hydration conditions • (11) Secondary control over silica fume reactivity and hydration rate (formation of sorption/protective layer)

4.5.6 Analysis and interpretation of results

On way to understanding the mechanism behind/theories proposed in the foregoing section, the following explanations could be given:

- Ad (1)(2) With IC introduction method used (see Section 3.2.4 for more details), some portion of concrete ingredients including binder becomes substituted with the gel-like containers. The main constituent of the latter is weakly bound water, especially when compared to state the same fluid would present in contact with cement. This fact is important for two reasons: a very high heat capacity of water [Ben 08a] and dependence of (specific) heat capacity of hardening concrete on unbound water content in concrete [Sch 05]. Taking both into account, a clear benefit from implementation of IC is therefore yielded especially in terms of concrete temperature evolution and is additional to dilution effect.

- Ad (3) The extra water for curing that is first separated from hydrating system will be subsequently released when favourable condition or trigger occurs, plausibly prior to setting. Should the concentration of hydration-relevant species (especially Ca^{2+}) undergo decrease due to water migration from the water tanks to bulk/pore solution, greater amount of C_3S must dissolve to precipitate hydrates and thus to give impulse to hydration restart. In other words, there will be delay in time of attaining supersaturation level and thus hydrate formation. The general knowledge is that setting time is closely associated with concentration of Ca^{2+} in liquid phase [Uch 92]. Similarly, it is the ionic concentration in pores which governs the rate of heat evolution acc. to [Scr 11]. Thereby, upon reduction in the calcium concentration and

increasing distances between hydrating particles due to increase in effective w/c, prolongation of dormant period and retarded setting may be postulated based on [Lan 02] and [Uch 92][Ben 08a], respectively. On the other hand, the increase in water content may be useful in later stages of hydration as more particles may react. Past experience indeed shows more intense hydration (from which higher heat release may result) and higher degree of hydration upon increase of w/cm [Sch 05]. Important in respect to IC, for system of given total w/cm, retention of certain water amount and its gradual delivery instead of unrestricted availability to hydration may be the condition sufficient enough for considerably lower heat of hydration evolved acc. to Korpa et al. [Kor 08].

- Ad (4) Before hydration gains in velocity/rate and hydration truly restarts after period of negligible reactivity, the main process underway until supersaturation state is achieved is diffusion of calcium ions. Important in selfsame respect, many polymeric materials in general and hydrogels of ionic type in particular tend to bind various ionic species in presence of dissociated ionic functional groups e.g. K^+ and Ca^{2+} in case of anionic SAP [Lam 05]. Hence, with SAP in concrete, there will be removal of calcium ions leading to their concentration depression in the liquid phase, from which a consequent hindered solid phase nucleation and growth/crystallization (C-S-H, portlandite, ettringite, e.g. [Lar 90]) and thereby retarded setting would result. This effect would be consistent with delay of setting caused by chelate production through the interaction of Ca^{2+} with the unadsorbed admixture remaining in the liquid phase as postulated by Uchikawa et al. [Uch 92][71]. Upon binding of Ca^{2+} by polymeric admixtures, more time would be needed for the formation of protective membrane coating [Tho 81] (sometimes appearing as Ca-rich hydrate/surface layer on the clinker minerals [Wei et al., ref. 20 *Ibid*. Lan 02]), resulting in longer induction period. This interpretation and mechanism alone may still appear somewhat insufficient in view of potentially greater penetrability/permeability of retarding hydrate layer formed on surface of C_3S in environment of decreased Ca^{2+} concentration [Kor 08].

  Why resultant reduction of Ca^{2+} concentration does not promote acceleration of C_3S hydration and therefore hydration as such (including the process of diffusion) which,

[71] It should be mentioned though that occurrence of complex formation phenomenon for PCE [Sow 15] has been doubted by some researchers [Lot 07][Wit 07].

with exceptions [Qin 07][72], is typically expected for low w/cm systems modified by Ca^{2+} consumers like silica fume and superplasticizer [Pin 99], this could be linked with specificity of SAP's Ca-sink role. When anionic hydrogel contacts free calcium ions, there will be ionic bonding with carboxylate ions of polymer or an interaction with free atom valences. The additional cross-link formation and one of potential consequences leaves no or otherwise only few free valences of Ca^{2+} available. Adding to this little content of admixture, this implies that possibility of SAP to act as nucleation/precipitation site[73] would be very limited. It may be plausibly restricted[74] to formation/precipitation of calcium carbonate crystals ($CaCO_3$) [Sno 12][Pou 13] which as result of very early carbonation may imply initially accelerated hydration, as similarly to effect of $CaCO_3$-containing admixture [Ram 96]. However, for good efficiency of the process, carbonation also requires numerous favourable conditions to be fulfilled first, which is impossible, at least difficult, to imagine in sealed low w/c system with IC at early hydration stage, e.g. presence of well dissolved CO_2, intermediate relative humidity, and other [Ber 04]. Furthermore, on reestablishment of free calcium level in solution, a thicker and heavier protective coating around cement grains may form [Tho 81]. For hydration followed based on osmotic membrane model, this gives argument for retarded cement hydration.

Alternative explanation of the effect could be related to formation of multilayer assemblage of PCE on solid surfaces [Sow 15] but to reason other than conformation suggested in the reference. In gist, since the process of Ca^{2+} concentration regaining to level of system without modifying admixtures could be very rapid [Tho 81], after the first adsorption of PCE (and perhaps extractables), the hydration proceeds further: front of the hydrate products progresses from surface towards aqueous solution and covers the polymeric coating[75]. This delivers new solid surfaces/interfaces on which polymeric admixtures could adsorb, leading to reinitiating steric hindrance effect and extension of time needed to attain the percolation, setting etc.

[72] Similar exception exists in system without superplasticizer, see Langan et al. [Lan 02], for instance.
[73] Potential role of nucleation site e.g. for the C-S-H phase from solution [Sil 06] has been reported for many polymers. On the other hand, this role is typically common to much smaller polymers, perhaps only of size of extractables or smaller (< 1 μm).
[74] Because both SAP and superplasticizer are carrying functional groups, complexing effect of Al^{3+} is possible (see also discussion of theory 6). This can result in precipitates of an amorphous solid, in agreement with effect of organic admixtures by Diamond [Dia 72]. Therefore, a certain simplification might be made.
[75] Although first hydrates after precipitation on solid surfaces could be subsequently dispersed in the aqueous phase [Zin 08][Sow 15], this phenomena is considered as not critical for mechanism to occur.

- Ad (5) Not only gain of water (see theory 3), but also its early loss may constitute of composition of bulk solution/pore solution. By absorbing portion of mixing water by the hydrophilic polymer, notably less water can directly contribute to hydration process of cement. This consequently results in less cement taking part in hydration process, meaning limited hydrolysis of cement phases [Kor 08] and dissolution of supplementary cement ingredients such as free lime or gypsum [Uch 92] which are decisive for the concentration of Ca^{2+}. In turn, and similarly to important adsorption property of silica fume in low w/cm system [Lan 02], some delay in hydration may be expected, particularly prolongation of dormant period and reduced rate of hydration heat during acceleration period.

  Similar explanation should be also applied to concentration of alkalis present in pore solution. In agreement with [Dan 62], on lowering the basic w/c, the amount of alkali released from calcium silicates (and likely other sources) notably decreases, thereby limiting rate of heat of hydration and related hydration-acceleration effect. The counterargument in own study is however little amount of alkalis as such as related to cement used.

- Ad (6) Owing to high concentration of Ca^{2+} ions, the content of SAP complexing them must be also sufficiently high. In mixtures with IC, this is unlikely the case given that for IC only small amount of polymeric agent is needed. On the other hand, chelate formation in the presence of carboxylic acid groups needn't be only limited to calcium species but should be also extended for various especially multivalent cations including aluminate, ferrite and silicate ions [You 72]. Studies on SAP showed in fact that some of the ionic crosslinks between certain ions and anionic groups in the polymer network e.g. caused by Al^{3+} [Zhu 15] can be much stronger or even replace the one already formed due to complexing of Ca^{2+}. Should the action between IC agent and the species take place, early precipitation of hydration products may be prevented. This could lead to more time required before hydration barriers are set up and consequently hydration delay, in accordance with hypothesis of Young [You 72]. On the other hand, Al^{3+} can exert poisoning effect on growth of C-S-H nuclei [Scr 11], meaning its removal will lead to earlier start of acceleration period of alite. This relates to the fact that Al-free C-S-H can readily grow unlike the calcium alumino-

silicate hydrate which precipitates rivalry when Al^{3+} is available, see ref. 37 *ibid.* [Scr 11] for more details.

Important to point out/acknowledge, as own EDX investigations on pure SAP treated with pore solutions of various compositions showed, other ions including potassium (K^+) and sulphate ions (SO_4^{2-}) can be adsorbed simultaneously by the polymer to form a complex on its surface and perhaps inside the polymer network. During hydration process, this may decrease their already low concentration in pore solution, and if so, affect the progress of chemical reactions. By complexing the former, many phenomena otherwise accompanying their presence and in detail reviewed in [Jaw 78] would not occur. This would be unfavourable in view of C_3S and C_3A early hydration acceleration potential of alkalis. In comparison, by complexing the latter, there will be decreasing concentration of sulphate ions in pore solution, without or with limitation of their adsorption on the reactive sites [Scr 11], causing faster dissolution of both-sulphate carriers (gypsum, …) and C_3A [Jan 13]. In theory, the resultant higher availability of Ca^{2+} concentration, either due to induced higher rate of alite dissolution or simply from dissolution of sulphate carriers, may trigger faster activation of start of silicate reactions, i.e. acceleration effect. However, this fails on presence of superplasticizer which, when dissolved in mixing water, is readily adsorbed, unlike the release of SO_4^{2-} into liquid solution being more gradual process. That is to say, the rate-controlling effect of sulphate ions on hydration of C_3A [Jol 98] is likely overtaken by the superplasticizer. In view of additional role − complexation of Ca^{2+} − the retardation is a result to be awaited.

Larbi and Bijen [Lar 90] found increased amount of K^+ and SO_4^{2-} in liquid phase of system with organic admixtures which was proposed to be related to interaction between polymers' charged groups and ions released by cement during hydration, including Ca^{2+} and OH^-. Similarly, in agreement with rule of optimum SO_3 content described in [Jaw 98], for given C_3A content and gypsum in cement but simultaneously upon decreasing alkali content in system with IC/SAP, it may be expected that excessive SO_4^{2-} content becomes available. Different than in [Lar 90] is however that in system with IC/SAP this content may yet undergo changes due to potential chelate formation phenomenon as discussed above. The overall effect of the alkali and SO_4^{2-} seems therefore very complex and depends likely on more parameters

(type of polymer, testing conditions) and thus requires further studies on particular polymers. For the moment, low alkali and C_3A content in the cement at hand may be claimed as the limiting factors for any related/plausible impact on hydration to take effect.

- Ad (7) In environment saturated with Ca^{2+}, negatively charged surface of C-S-H converts into positive one [Zin 08][76]. In turn, given the presence of free valences of atom chelated and providing free bonding sites available on crystals/nucleation sites, a new type of cross-linkage can form, particularly between carboxylate groups of polymer particle and the surface of nucleating hydrate particles. This phenomenon could be compared to ionic bonding via electrostatic forces from interaction between (other) organic compounds and solid $Ca(OH)_2$ [Cha 81] or its nuclei [You 73]. As under particular circumstances the growth of calcium nuclei would be inhibited[77], and nucleus/nuclei cannot achieve a minimum critical size (so as to form stable nuclei), C_3S dissolution and C-S-H formation slow down and eventually cease. Taking into account the extra time required for concentration of $Ca(OH)_2$ to become high enough to overcome the restraint (i.e. fairly high level of supersaturation needed), a reason for retarded end of induction stage and onset of acceleration period becomes thus manifested, in agreement with hydration progress theories [Bul 11]. The resultant effect could be named poisoning effect acknowledging similar phenomenon caused by adsorbing soluble silicate species [You 72]. Banfill and Saunders [Ban 86] found similar behaviour occurring in case of sorption of different organic compounds on calcium hydroxide.

  On one hand, since in mixtures with IC and one with pure SAP lower heat output is often followed the retardation[78], it could be assumed that very limited amounts of new hydrate products are formed during dormant period. This argument could indeed speak for the poisoning effect. On the other hand, since the accompanying effect occurred randomly for other mixtures with IC, additional mechanisms must be likely engaged. These should be furthermore expected due to geometrical restraints provided by the

[76] Similar surface charge could be expected for calcium hydroxide, e.g. after dissociation or after the conversion. However, hardly any portlandite forms is very early age in UHPC according to opinion of Moeser et al. [Moe 10][Pfe 10].
[77] Note that on inhibited growth of hydrate phases (C-S-H, CH), the heat evolution will decrease too, being a common knowledge, e.g. reference 9 *ibid.* [Sil 06].
[78] It should be pointed out that the temperature of concretes with IC was controlled and was lower during and immediately after mixing (results not showed).

large SAP particles, making poisoning effect for the studied material to be limited to work of extractables (see explanation to theory 8) and PCE[79].

- Ad (8) SAP could be considered as material in composition analogous to water-soluble polymers, except for presence of cross-links. Still, it is expected for every SAP material to consist of certain sol fraction (e.g. [Shu 11]) which, according to [Hug 86][Jen 02][Qi 08], is capable of leaching out of the network. The outcomes could be twofold. Should soluble parts of the polymer enter into the surrounding solution, the event which could initiate as early as within first hour of hydration (see Section 4.3.4), potential overflow of deposited solute from hydrogel to that solution may follow [Hug 86][Qi 08]. This would deliver a strong argument for changes in calcium concentration, the consequences of which have been discussed above (theory 3).

  From different perspective, a new deposition place for the tiny polymeric pieces will be quested for. This could be rapidly formed protective coating upon surface of hydrating cement grains, on which extractables are adsorbed or become part of, or the hydrates' structure as such. According to first scenario, there may be modifications of the membrane's permeability triggered by the organic admixture. In opinion of Thomas and Double [Tho 81] as well as that of Banfill and Saunders [Ban 86], such change provides sine qua non for retardation or acceleration of hydration, course of which will finally depend on type of permeability change exerted. E.g. for combination of retarder and water retention agent, Recalde Lummer and Plank [Rec 12] noted enhanced retardation effect initiated by low permeability polymer layer formation on cement particles.

  According to second but generally supplementary scenario, there may be structural alteration due to incorporation of polymeric admixture into the hydration products (so-called intercalation phenomenon) and/or changes in morphology of hydrate particle [Jol 98]. Silva and Monteiro [Sil 06] using soft X-ray microscopy observed in fact great changes in morphology of hydrates accompanying the hydration retardation, although different water-soluble polymers governed the effect differently. Irrespectively whether polymeric admixture acted as accelerator or retarder, modified morphology of C-S-H and calcium hydroxide was also observed in study by Young et

[79] PCE should be seen as water-soluble organic polymers bearing ionisable groups. Accordingly, making any comparison between PCE and especially extractable seems fully justified.

al. [You 73]. More recently, similar alterations regarding morphology and density of hydrate layer covering the clinker grains during hydration were also found after usage of PCE and were postulated as one of potential reasons for retarded hydration [Win 07]. Owing to certain structure similarities between water-soluble polymers or ones of PCE and SAP, it seems reasonable to believe that analogous changes are exerted by extractables too.

- Ad (9) Without full compensation of water absorbed by SAP within minutes after contact with water, there will be less fluid remaining in the suspension-like hydrating medium. Given the ability of the medium to convert, this results in either shorter distances between hydrating cement grains or, even though more like in case of non-uniform SAP distribution, reduced capillary content but without dimensional changes of remaining porosity. The rule of thumb is that interparticle spacing governs extent of reaction needed to develop the solid structure [San 09]. Meanwhile, both space and sufficient water are demanded so that hydration can progress (and generate heat) without cessation [Pow 48][Han 86]. Accordingly, mix with IC water underestimation or without its incorporation should demonstrate earlier setting approaching time and lower hydration heat, the best example being a mixture with pure SAP addition (F-S.4). Since the reduction in already very low w/c system could be dramatic, example again being mix F-S.4 which likely looses 1/3 of the effective w/c relative to F-R, particular mechanism should be dominating one in early ages and outweigh other mechanisms proposed to explain effect on hydration.

- Ad (10) Increase of the air content in UHPC with IC/SAP as evidenced in Section 4.2.3 leads to an increase of the internal surface area. As cement particles are further apart, adding to this no hydrates growing in the interior of SAP and the air voids, more time is required to attain percolation and erect solid skeleton, turning into reduced early stiffening potential. When considering physical and not chemical aspects of the mechanism, this effect would be similar to increasing system's w/c for which more hydration is needed to achieve set as the initial interparticle spacing is larger.

- Ad (11) Owing to Ca-sink role (4) and gradual formation of additional cross-links in polymer network, being accompanied by capturing Ca^{2+} by unadsorbed PCE, the increase of particular ion (concentration) in bulk solution is delayed. Still, adsorption

of negatively charged backbone of PCE may only occur on positively charged surfaces, the action which requires interaction with Ca^{2+} as the mediation element in case of clinker compound C_3S [Zin 08], hydrates like C-S-H [Zin 08] as well as silica fume [Pla 09]. With this being hindered, there could be a remarkable reorganization of superplasticizer adsorption sites and/or, upon exceeding adsorption possibilities (due to low w/c and thus little Ca^{2+} ions available, and furthermore limited availability of preferential adsorption sites due to low C_3A in cement) higher content of admixture remaining in the bulk/pore solution in comparison to systems without IC/SAP.

In the first scenario, according to the positive charge of solid surfaces contacted with and rapidity of adsorption process as such, more PCE is likely adsorbed on C_3A and C_4AF [Lot 07] and their hydration products like ettringite [Zin 08]. While this is unlikely to hinder aluminate phase dissolution and precipitation of ettringite, being nearly independent of PCE [Lot 07], compared to mix without IC/SAP, thicker coating of undispersed particles of silica fume surrounds cement grains. As this layer inhibits the diffusion of water to the cement surface, delay in hydration could be expected, similarly to lowering w/c effect [Lan 02], i.e. effect which in a system with IC/SAP also takes place under conditions discussed in theory 5.

The fact that re-establishment of free calcium level in solution may require time and no PCE adsorbs immediately on certain surfaces like C_3S also implies longer hydration of particular clinker phase. This change may turn into formation of thicker and heavier protective coating with or without changes in chemical composition, in agreement with theory of Thomas and Double [Tho 81]. As the modified membrane seals off and prevents attack from water to further extent while simultaneously screens off hydrating particles from each other, delay in reaching the supersaturation level will be forced giving way to induction period extension.

Both behaviours of binders will continue and perhaps supplement each other unless delayed PCE adsorption kinetics occurs, which presents another reason for the retardation effect.

In the second scenario, owed to diminished dispersive effect, more (or larger) cement particles clusters incorporating restrained water would form, the phenomenon existent

also for mixtures with superplasticizer compatible with cement [Sak 06]. Using the analogy to silica fume, this might be negative in respect to hydration speed [Lan 02] although favourable as far as hydration heat distribution is concerned [Kor 08]. In addition to this, oxygen atoms of the many ether bonds of the PCE side chains and water molecules in the liquid phase are likely to form hydrogen bonds [Sak 03]. With this plausibly happening also in case of unadsorbed PCE admixture but without simultaneous provision of dispersive effect, and for which admixture adsorption would be generally required/necessary[80], some hindrance to water movement could be expected. Thus given somewhat similar input from presence of water-soluble polymers [Kna 07] (note: to which SAP extractables could be compared to) and bringing about increase of the pore solution viscosity, the result will be restricted ion mobility to be attributed to diffusion barrier induced and diffusion coefficient decrease [Ben 08b]. As this decreases dissolution rate of the anhydrous phases, and translates in decreased precipitation of hydrates, hydration retardation is awaited. The theory explaining negative changes on hydration process based of ions diffusion barrier hypothesis is not new, although, especially in field of organic admixtures, is still of secondary importance in opinion of some researchers [Pou 06].

In supplement to mechanisms discussed above, it should be borne in mind that many hydration-ascribed physico-chemical phenomena can change strictly depending on dispersive ability of superplasticizer, that is, the amount of PCE not remaining in liquid phase. Beside changes in growth kinetics and morphology, this could also involve alterations in bonding of hydrates and ability to fill capillaries with the hydration products [Leg 94]. With poorly dispersed structure, because of poorer distribution of cement particles than in deflocculated one, first but generally weak connections between particles may appear very soon. On the other hand, the filling of pores will be harder due to increased size of largest pores which, in turn, increases degree of hydration needed to attain the same true (= strong) percolation threshold. Thus another potential reason for retardation likely exists and strengthens outcome of

[80] For sake of scientific correctness it should be pointed out that best workability and perhaps best dispersing effect is produced when some admixture is adsorbed on solid particle while other part remains in the pore solution, a conclusion to be derived from studies of Bonneau et al. [Bon 97] on finely grained UHPC. This however only applies to optimum content of superplasticizer, attaining which is unlike in regarded case. For mechanism behind the former, being outside scope of this thesis, reader is addressed to Lange with Hirata and Plank Special Publication 288.30 of American Concrete Institute from 2012.

decreased surface area of cement particle (= smaller area of water interaction) in system suffering from imperfect dispersion.

4.5.7 Summary and concluding remarks

The non-destructive ultrasonic investigations initiated in Section 4.4 were extended and were supplemented with concrete temperature tests to study effect of IC and SAP on early hydration. In subsequence to analysis and interpretation of individual exemplary results being performed first, a combined approach was utilized to all finely grained mixtures (remark: compositions based on UHPC with coarse aggregates, i.e. B5Q, could not be tested at the moment of topic investigation due to technical issues). Early retardation effect exceeding time-zero occurrence time followed by acceleration/extension of hydration relative to control concrete, both taking effect in first 24 hours, were identified for mixture containing most optimal amount of IC variables (F-S.4.07). Of the two, the latter was as expected and was in full agreement with the modified Powers' model prediction applied. Some of the potential reasons for existing differences in opinions on effect of IC were presented; these were mainly attributed to specificity of implementing IC to mixtures of incomparable compositions. Eventually, a discussion on both effects observed followed. It is hypothesized that either UPV rate or temperature changes may be attributed to specific role of SAP (ability to control pore solution as well as effective w/c), on one hand, and secondary effect introduced by either IC or SAP itself, on the other hand.

Overall, the study revealed great potential of using non-destructive measurement to study of effects of IC or SAP on early hydration. Although in own investigations this issue has been studied only qualitatively, the next step would be to match the UPV with degree of hydration, shown as possible e.g. by [Rob 11]. With the conversion known and since total non-evaporable water is hardly a good estimate of the degree of hydration in systems with silica fume, e.g. acc. to [Yog 91], measurement of UPV could become an important alternative to assessment of degree of hydration from chemically bound water content typically used, e.g. by [Sol 11]. Nonetheless, usage of other devices seems desired in case of UHPC mixtures shrinking strongly (i.e. without IC) in sealed conditions due to potential loss of contact of transducers with the mix. The emergence of characteristic gap was not captured in own study due to unknown reasons.

4.6 Shrinkage reduction and the mechanisms

4.6.1 Introduction

This section addresses investigations of free autogenous shrinkage, i.e. endogenous volume change free of external restraints. The tests are performed by means of two versions of corrugated tubes method set-ups, with supplementary validation by one of the traditional testing method. Before turning to main topic, i.e. evaluation of the effect of water entrainment, in which both IC variables (SAP, extra water) are used, the first focus (Section 4.6.2) is on alternative implementations of SAP. The argumentation for involving concurrent introduction manner being specifically attractive for UHPC is presented first; in subsequence, and following presentation of results, analysis of reasons of failure and discussion of potential mechanisms are presented. The main objective of the analysis finally answers what happens if some underestimation of water absorption occurs and whether this affects mitigation mechanisms. The parameters varied in research part devoted to water entrainment effect (Section 4.6.3) are the amount of IC variables and type of UHPC matrices. In-depth discussion and analysis are performed after the presentation of results, starting with the influence resultant from the UHPC matrix change. Whenever found necessary, additional tests are performed and observations made in foregoing sections are recalled, all aiming at possibly best understanding of phenomena which, although strictly indirectly, can be derived from the shrinkage deformation-time curves. The knowledge gained will serve as the starting point to further investigations and discussions on IC working mechanisms being presented in the following sections.

4.6.2 IC method specification

i. Preliminary remarks

Since water is inherent component of every hydration-related reaction, application of water entrainment, i.e. implementation of both IC agent and extra water, seems a logical step in curing concrete. Yet still, it is categorization of internal curing [TC 196-ICC][TC 225-SAP] that allows SAP to be applied without extra water, that is, as water-reducing/water-retaining agent. Undoubtedly, such solution should not be excluded also from perspective of enhancement of concrete strength that in UHPC which, among other fundamental steps, is gained by reducing effective w/c (and thus capillary fraction) and not by promotion of hydration as such. Initially, the expected loss of workability of UHPC due to the addition of SAP was compensated by using extra superplasticizer and compared to effect of IC and pure SAP addition (the only mixture with intense compaction applied).

ii. Autogenous shrinkage investigations – results

The measured development of autogenous shrinkage in time is shown in Figure 4.56. In the graph, time-zero, i.e. time-point at which the strains are zeroed, is determined as described in Section 4.4.

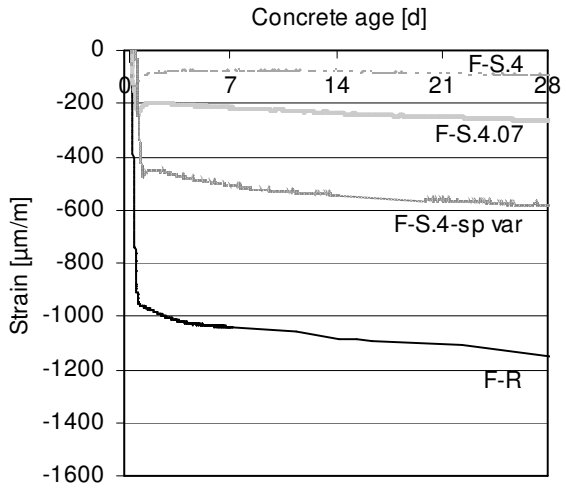

Figure 4.56: Autogenous shrinkage of UHPCs with 0.4 % SAP without or with addition of extra water or PCE compared to control concrete.

All the mixtures containing SAP demonstrated pronounced reductions in deformation due to autogenous shrinkage. Nonetheless, considering entire test period of 28 days, the best effect was obtained for mixture F-S.4 being modified only by SAP. It involved a significant reduction of autogenous shrinkage in some hours after the time-zero, and then only a moderate increase in strain level in the days onward. However, in contrast to water entrainment (F-S.4.07), these IC alternatives that excluded extra water addition (F-S.4, but also F-S.4-sp var containing additionally extra amount of superplasticizer) regrettably led to other, mostly unfavourable, changes in UHPC properties. The clear one reported for pure SAP addition was workability loss, see Section 4.3.3. In comparison, for SAP applied with more PCE, increase in viscosity was noted, resulting also in increase in amount of entrapped air relative to control mix. Also for this mixture, a pronounced delay in hydration process in its early stage was observed (time-zero = 15.3 h >> F-S.4.07 > F-S.4, see Section 4.5). Adding to this finally the highest strength reduction (24.4 % compressive strength loss in comparison to 14.6 % and 17.7 % for UHPC with pure SAP and SAP plus extra water, respectively[81]), it could be concluded the addition of SAP without extra water is not meaningful option of IC in case of UHPC mixtures.

Owing to the threefold motivation inspired by: 1) unexpectedly pronounced reduction of autogenous shrinkage case of mix F-S.4 which simultaneously reflects extreme case of underestimation of SAP absorption capacity easily to take place in work with IC (note: own cases of mixes F-S.3.04 and especially F-S.6.08 to be tested in the following), 2) as interesting result revealed for F-S.4-sp var being representative to all cases where superplasticizer (and not extra water) content is varied while its separate effect on autogenous

[81] Strengths were measured at the age of 90 days on small beams halves. The reference is made to control mixture having a compressive strength fcm,prism halves of 164 MPa, see Appendix I for more details.

shrinkage is neglected (e.g. [Pié 06]), and, finally, 3) for general better insight into potential self-curing mechanisms (as strictly attributed to SAP) and, if so, being rival to IC (i.e. SAP plus extra water), the result obtained for the IC alternatives are interpreted and analysed in the following.

iii. Analysis and interpretation of results

- the discussion of pure SAP addition effect

Because SAP attracts water, the positive effect on autogenous shrinkage owed to addition of pure SAP should be primarily attributed to changes in the forming pore system and, related to it, alterations of mechanical properties. In gist, because changing the way how water is further available for hydration and the shifting of its part to SAP particles is taking place in suspension-like state, early reorganization of system's elements occurs: initially water-filled spaces are partially eliminated in favour of SAP cavities whereas the remaining part, if not all spaces of already very small dimensions, undergoes some geometrical reduction. By bringing hydrating particles closer and simultaneously minimising the amount of hydration needed to 'glue' dense clinker particles together, the connectivity of particles[82,83] is thus approached earlier and consequently much stiffer load-bearing structure develops, particularly owing to reinforcement of the granular skeleton with unhydrated cement/residual clinker having Young's modulus of about 120 GPa (note: much higher than that of hydrates or aggregates!). In consequence, compression in the solid phase – one that pushes voids e.g. in the C-S-H closer – may be opposed more efficiently and generally sooner, turning into reduced autogenous shrinkage and earlier setting (the latter as observed in Sections 4.5.3 and 4.5.4). Shortly, it is speculated that in cases like presented, the shrinkage stresses, although much likely more pronounced due to basic w/c reduction by SAP, do not fully override the balancing effect of restraint, in result of which autogenous shrinkage decreases.

Notably, particular mechanism falls into picture of strengthening/stiffening effect associated with the unhydrated clinker grains (e.g. [Bea 85][Lou 99]) which has been recently renewed

[82] It is assumed that elastic moduli (Young's (bulk), shear) are governed primarily by the connectivity of the cement particles (and solid phase in general), unlike compressive strength, which is assumed to be more closely related to the filling of pores with hydration products, after Boumiz et al. [Bou 96]. Contact point will transmit the pressure that induces the compressive stress on the solid phase and generated by emptying of capillary pores. Therefore if their amount and/or the contact area increases, so will the resistance ability to volume changes [Sol 11].

[83] Although connectivity and the underlying change of contact points is referred to, other mechanism could be imagined as paying supplementary contribution to the changed occurred e.g. mechanical interlocking of cement particles. It may be seen an analogy to the mechanical interlocking of the cement hydration products with the rough aggregate surface proposed e.g. by Tasong et al.

both by modelling and experimentally by Pichler et al. [Pic 13] and was shown to increase with decreasing w/c[84]. The same indication, in particular more mechanical than chemical origin of mitigation mechanism, seems to be directly evidenced in the shrinkage-time curve where after first SAP impact (exhibited soon after time-zero), it is seen no significant deformation change, as expected. Following expectations, similar observation was made in the measurements on prisms from concrete age of 1 day (Figure 4.57).

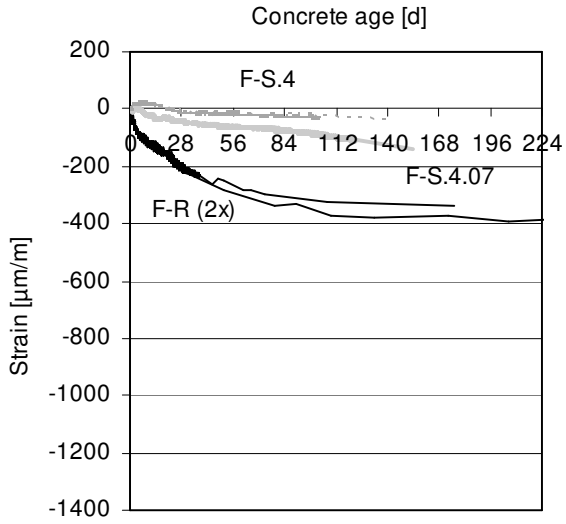

Figure 4.57: Autogenous shrinkage of control UHPC and mixes with 0.4 % SAP as measured on prisms.

The encountered big difference in volume change developed between mixtures F-R and F-S.4, despite both having equal total w/c, may require yet additional explanation. In theory, both mixtures should be attaining similar if not identical degree of hydration, in line with [Jen 01b][Ass 13]. Irrespectively whether this holds true for UHPC or not, however, the competition between self-desiccation and hydration can be expected to differ and, depending on SAP presence, may proceed in one of scenarios as following. With capillaries occupying bigger volume in case of control mix F-R compared to F-S.4 (UHPC with SAP), more hydrates form in the initially water-filled space. This is immediately followed by filling the same space with self-desiccation 'product', particularly empty porosity, which concurrently to deposition of hydrates limits the space accessible (to growing hydration products) to further extent. As no extra source of curing fluid exists or its withdrawal from any remaining water-rich zones is limited, if not impossible, increasingly more pronounced self-desiccation develops which, somewhat rivalry to pore size reduction effect [Pow 47], is setting vapour pressure to very low level. In consequence, since relevant shrinkage trigger is delivered forcing, for instance, capillary tension, very high autogenous shrinkage must result.

[84] Not that supplementary explanation can be given and regards inapplicability of gel-space ratio concept for low w/c systems. It has reported, for instance, that for similar hydration degree, the Young's modulus is higher for the lower w/c [Bou 97], be it to due to less capillaries, more favourable particle spacing and connectivity or other. If the w/c is furthermore lower than needed for hydration, the stiffness is expected to grow along with parameter decrease provided no capillaries present, the important positive contribution being attributed to anhydrous clinker [Bou 97].

On contrary, in system with SAP, only little self-desiccation can develop as water is efficiently withdrawn from the tiny water containers. The response could be very pronounced given the reduced pore size in F-S.4 in comparison to control mix F-R (see [Dud 10c][Moe 10] for more details) and its main consequence, i.e. generation of increased suction power in accordance with Laplace and Kelvin laws. In addition to this, or alternatively, there may be earlier partial segmentation of the global capillary network, being favourable condition to limitation of chemical activity [Mor 02], therefore chemical shrinkage. When partial capillary segmentation occurs, being early event for UHPC [Mor 02] and to be imagined even faster when with SAP, the (active) capillary network is perhaps entirely concentrated inside the C-S-H hydrates. In response, the rate of hydration, the extent of which is already relatively smaller compared to system without SAP owed to reduced number water-filled capillaries, slows down. Thus as the ratio of hydration degree to the restraint at any given time might be lowered compared to system without SAP, the material is macroscopically shrinking less despite no changes to total water content as such.

Other important contribution could be linked with the specific ion-sink role played by SAP that was subject of discussion in Section 4.5.6 (see comments on theory 6). High alkali content leads to C-S-H structure which is more deformable [Bel 05], whether related to changed morphology of the hydrate [Bel 08] or other. By limiting their content in pore solution, and thereby making the structure stronger compared to concrete with 'normal' availability of alkali, it may be awaited that the autogenous shrinkage of mix with SAP is resisted even better. Similar positive outcome (related to formation of C-S-H of improved mechanical properties evidenced in higher micro-strength/stiffness) may be also expected on lowering w/c [Haa 75]. This change in UHPC with SAP results from hydrophilic nature of SAP and could bring about few effect-favourable modifications in C-S-H, creation of new chemical bonds [Ben 06] and rearrangement/consolidation of C-S-H layers [Bea 85] being two important instances. On the other hand, because some mixing water is being stored by SAP and thus some water migration within C-S-H nanostructure may still occur, new look on the effect might be required, see Section 4.6.3 and part of discussion to follow.

It is believed that the abovementioned effects are very likely to offset the original reduction in elastic modulus caused by small increase in total porosity content and larger pores in comparison to F-R, and to be associated with more technological air entrapped (see Section 4.2.3) as well as accommodation of hydrogel as such. There could be yet imagined other ways

leading to formation of stronger load-bearing structure and being rival to strengthening mechanism of the residual clinker, especially if to follow excellent review of Beaudoin and Feldman [Bea 85]. One hypothesised example is impregnation of C-S-H pores with PCE and extractables, e.g. by intercalation within the structure of hydrates according to mechanisms described in Section 4.5.6. If adding to this the fact of uniformly shaped and spaced SAP/air pores and much less capillaries (generally treated as kind of artificial cracks!) being changes favourable with respect to stress field [Bea 85], many reasons for outweighing the negative aspects of SAP incorporation seem to exist.

Whether and how much of the fluid carried is released by SAP, these remain open questions. In theory, earlier depercolation likely to occur due to modification by SAP should be advantageous with regards to time of water release, however, only provided that the phenomenon truly coincides with water movement from SAP, as anticipated in [Sol 12]. If wetting at humidities higher than 50 % occurs, it would lead to significant stiffening [Ser 67] and thereby further limit the negative effect resulting from increased porosity. On the other hand, because the basic w/c is decreased by SAP, there will be much smaller need for curing fluid, in agreement with Powers' model, meaning most of water initially absorbed by SAP will be retained by the IC agent. Again, this could be an upside to having pure SAP added to UHPC. By absorbing energy during deformation of the composite by the swelled SAP and furthermore by bonding with hydrated cement, elastic behaviour can be likely improved too. This hypothesis being based on speculations of Manning and Hope [Man 71] however requires further studies, being outside the scope of this thesis.

To stay on the safe side, also a case should be considered when no release of fluid carried by SAP occurs. In fact, the changes related to reducing the w/c, including densifying the UHPC matrix as well as reduction of capillary porosity and currently induced by SAP, might be critical to moisture transfer from the IC agent. This results from potential reduction in suction power (despite its initial increase due to decreasing pore sizes!) and reduced diffusion coefficient [Sol 11][Sol 12]. If so, and assuming the amount of water migrated from SAP is insufficient for hydration to proceed, the process may be ceased, thus stopping further autogenous shrinkage development[85]. It is apparently more likely to happen for low w/c

[85] Note that in sealed system the volume of empty porosity i.e. measure of self-desiccation occurred is directly proportion to degree of hydration [Pow 47][Ben 01c]. This means that any interference into hydration process should be generally favourable in respect to autogenous shrinkage reduction, observed also under additional drying to ambient [Sol 11][Soliman and Nehdi, ref. 17 *Ibid*. Sol 12].

systems given the lower original w/c, the lower mixing water loss needed to stop hydration [Pow 47]. It should be however considered that applicability of the effect may be restricted to long-term changes given that more vanishing rate of the strength-gain compared to mix with IC which would validate such effect. Interesting enough, reasoning of somewhat similar hydration-related basis could stand for shrinkage mitigation extent difference existing between mixtures F-S.4 and F-S.4.07: because lower degree of hydration occurs for the former, and translates into less self-desiccation, lower autogenous shrinkage can only develop.

Although not confirmed in MIP measurement owed to testing methodology limitations, also a supplementary explanation could be put forward for effect of pure SAP addition. In a plausible scenario, some pores may be diminished to size being outside the range of capillary forces. If so, and assuming capillary pressure is operative shrinkage mechanism, new change adds to reduction of capillaries fraction making the very low water content in system as such less critical factor. This explanation is in apparent agreement with results of Cheyrezy and Behloul [Che 01] who observed decreasing autogenous shrinkage of finely grained UHPC after lowering its w/c below the level of 0.23. It may be though behaviour intrinsic only to UHPC material and its fine tuning given existence of other past experiences, and demonstrating autogenous shrinkage increase on decreasing w/c to very low values.

Eventually, given the creep-shrinkage couplings, the potential influence of SAP on visco-elastic behaviour should be considered. For concrete containing SAP and characterizing with strength higher than the reference concrete despite no changes in total w/c, which important enough reflects the case of F-S.4 and the reference F-R mixes studied at present (see Appendix I for corresponding mechanical properties in early age), Assmann and Reinhardt [Ass 14b] observed reduced basic creep[86]. In agreement with [Ben 01c], it could be interpreted that for smaller capillary stresses and higher elastic modulus longer time lapse is required for any stress relaxation and creep to manifest themselves. This argumentation apparently matches the finding regarding application of pure SAP in the finely grained UHPC, for which reduced creep factor up to an age of 24 h was recorded [Epp 10]. Since creep can vary appreciably especially in early ages and, furthermore, since creep is expected

[86] It should be borne in mind that matrix changes exerted by pure SAP addition include initial reduction of effective w/c but, on the other hand, increased moisture content, i.e. especially increased relative humidity in the pore system, in the later ages. Acc. to Soroka [Sor 79], the former brings about reduction of basic creep in contrast to effect of the latter. That is to say, changes in w/c as triggered by SAP might be considered as overriding parameter in terms of final effect on basic creep.

to be governing long-term autogenous shrinkage only [Ulm 00][Lur 03], other explanation must exist for changes occurring in autogenous shrinkage during early ages. This subject will be further explored when discussing effect of water entrainment on autogenous shrinkage, see Section 4.6.3.

- the discussion of effect of SAP combined with extra superplasticizer

Since in mixture F-S.4-sp var the total content of superplasticizer including that present in original composition of the finely grained UHPC, and in particular case exceptionally increased, was very high, and, furthermore, since no significant workability changes were observed on increasing admixture until dosage level finally used, it could be assumed that saturation (adsorption) point [87] was acquired if not exceeded. This implies no sense of invoking the outcomes of further, if any, increase of viscosity of pore solution as well as decreasing surface tension of the pore fluid upon increasing superplasticizer dosage, irrespectively how pronounced their final and still controversial/debated effect on shrinkage is. More important to acknowledge, other clearly disadvantageous reasons existed and in presence of more fluidising admixture limited positive outcome brought from addition of SAP without extra water.

Accounting for individual impacts of admixtures, i.e. assuming initially no interaction between the two polymeric admixtures, various phenomena associated with application of excessive superplasticizer contents [88] and admixture introduction as such should be considered. They include chemical incompatibility [Tam 12], segregation [Tam 12] and bleeding [Moh 10]. Experience shows the first two could result in increased permeability and a similar change may be expected from increasing w/c [Tam 12] given the high fluid content in superplasticizer used. This would counteract increasing density, and thus lowering matrix permeability, as associated with lowering the effective w/c by SAP. On the other hand, the extent of such effect might be insufficient to override the output of latter. In fact, the matrix densification partially counterbalanced by PCE could be intensified by bleeding [Tia 08] as well as presence of entrapped air, especially considering complex effect the latter exhibits in concrete [Mor 01][Ham 06b]. Since finally none of the visually detectable phenomena (segregation, bleeding) was truly evident (Figure 4.58) and, furthermore, since neither high

[87] It could be distinguished between more characteristic dosages of superplasticizer, often related to obtaining most favourable concrete behaviour/property in fresh or hardened state. These are: saturation (adsorption) point, segregation point and, less reported, permeability-optimal content [Tam 12]. Referring to one is certain simplification made to the complex matter.

[88] Excessive content is understood as overdosage beyond the saturation point.

permeability (assumption: lack of permeability-optimum content of PCE [Tam 12] used in mix that could bring about such property) nor 'overshadowing' effect due to bleeding reported in [Moh 10] could speak for the increase of autogenous shrinkage in F-S.4-sp var compared to SAP-incorporating mix with no PCE content change (F-S.4), a new reasoning was quested for.

Figure 4.58: The final shape of F-S.4-sp var "cake".

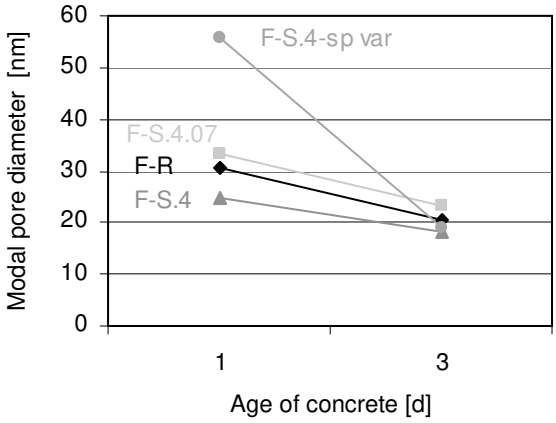

Figure 4.59: Trends of changes in the most frequent neck pore diameter of mixtures with 0.4 % SAP as compared to control mix (F-R).

As seen from Figure 4.59, which demonstrates the results from MIP tests, the modal neck-pore diameter in system F-S.4-sp var undergoes dramatic reduction between age of 1 and 3 days. This change is less pronounced for other mixtures. It shows that superplasticizer, despite initial negative effect on hydration and prolongation of the dormant period, causes more favourable process progress at later ages, as expected from [Rid 13] and [ref. 14 *Ibid.* Rid 13].

Combining views of Legrand and Wirquin [ref. 1 *Ibid.* Leg 94] with Zhou et al. [Zho 08] on work of superplasticizer leads to an attractive interpretation of the effect: At low PCE dosages, the polymer disperses the flocculent structure of cement particles, thereby increasing contact between the liquid and solid phase. Thus even though dispersion is still insignificant, dissolution/solution process accelerates, owing to which hydration speeds up. The more PCE is added though, the more molecules adsorb on the surface of particles to form hydrophilic steric film, hence inhibiting further contact of the two and decreasing hydration rate of cement. In parallel, large portion of free water is released out and dispersion of cement particles becomes more and more marked. Therefore when the hydration barrier eventually ceases, chemical reactions are run under much different (and likely improved) conditions. In the best case scenario, i.e. no bleeding and especially segregation occurred, more homogenous

microstructure is thus generated and is yielded, for instance, by improved distribution of hydrates around sand grains [Che 10].

From abovementioned mechanism both advantages and disadvantages result and could be used to explain magnitude of the shrinkage developed. On one hand, the specific matrix improvement (or other, still hidden reason) gives way to higher Young's modulus of UHPC relative to the same system but with lower superplasticizer dosage [Che 10]. Submitted to an identical internal capillary tension, UHPC with extra PCE would be therefore shrinking less. On the other hand, such benefit might be perhaps obtained only in longer time perspective, e.g. 28 days age tested in [Che 10]; meanwhile it will be easily overwhelmed by strengthening/stiffening effect taking more pronounced effect in case of F-S.4 and less at present. Better dispersion of cement particles occurring due to higher PCE dosage also means formation of more bridges of hydration products between cement particles, bringing about more hydration even in respect to F-R. Since the process cannot be completed before fluid-to-solid transitions occurs (despite higher deformation developing also in this period, earlier observed in [Che 10]), autogenous shrinkage is high as expected, although still lower than that of F-R.

Because the working mechanism of superplasticizer is not limited strictly to adsorption on cement and silica fume, another as important factor affecting concrete strength (and likely stiffness too) and acting opposite/inversely to dispersion effect could be linked with the physico-chemical action of superplasticizer. According to [Leg 94], changes triggered by admixture may involve modification of growth, the morphology and bonding of the hydrates. All of them concern especially ettringite, crystallization and growth rate of which is very likely to be affected negatively in presence of admixture [ref. 32 *Ibid.* Jol 98], until cessation in most extreme case [Leg 94]. As a consequence or maybe attributed to other reason, addition of superplasticizer results in formation of smaller[89] [ref. 7 *Ibid.* Bon 97][ref. 30 and 32 *Ibid.* Jol 98] and, particularly in case of PCE[90], thinner ettringite crystals [Gey 04]. Its content is also typically less [ref. 32 *Ibid.* Jol 98] or even the hydrate undergoes substitution by organo-mineral composite/compound/complex [Leg 94][Bon 97]. Therefore, if shrinkage reduction mechanism truly benefits from ettringite formation (or other hydrate phase like

[89] According to some literature sources [ref. 19 Ibid. Coh 83], production of smaller crystals needn't be always disadvantageous. In fact, it could lead to higher degree of expansion being triggered by crystallization pressure increase or other. This fact is considered as secondary, although it might be a certain simplification.
[90] According to Uchikawa et al. [Uch 92], distinction of superplasticizer type is important since different admixtures lead to different morphological changes of ettringite.

portlandite, being perhaps produced in extra content due to release of water stored in SAP) and the crystallization pressure accompanying its growth, this contribution is likely outweighed. Overall, the smallest shrinkage mitigation efficiency among mixtures with 0.4 % SAP presented particularly by F-S.4-sp var would result from less water used for formation of ettringite (note: the highest value of c in Eq. 4.3, discussed next).

Alternatively, the reasoning behind changing SAP effect on autogenous shrinkage in dependence on superplasticizer amount should be traced back to potential changes in course of hydration. In another study on finely grained UHPC, it has been noted that increased dosage of superplasticizer may induce abnormal progress of chemical reactions, particularly earlier hydration of belite [Cou 13]. As short-term autogenous shrinkage is property originating from hydration, and assuming applicability of abnormal behaviour to own case, this would bring about lower shrinkage magnitude. Such claim could be supported by Eq. 4.3, which shows a relation between autogenous shrinkage and advancement of hydration of clinker compounds at any given time t, originally proposed by Tazawa and Miyazawa [JCI 99] for cement pastes:

$$\varepsilon_{as} = a \cdot \alpha_{C3S}(t) \cdot (C_3S\%) + b \cdot \alpha_{C2S}(t) \cdot (C_2S\%) + c \cdot \alpha_{C3A}(t) \cdot (C_3A\%) + d \cdot \alpha_{C4AF}(t) \cdot (C_4AF\%) + e \cdot (Blaine) + f \quad (4.3)$$

where

ε_{as} – autogenous shrinkage of cement paste at age t

$\alpha_i(t)$ – degree of hydration of compound at age t

(i %) – content of clinker compound i

Blaine – Blaine fineness of cement

a, b, c, d, e, f - constants determined for multiple regression analysis of chemical compositions of cement with the autogenous shrinkage measured for respective cements at respective ages.

Abovementioned study showed that a, b < 0, i.e. as if C_3S and C_2S contribute more to autogenous swelling than to shrinkage, and that c, d > 0 and, simultaneously, c > d >> a, b (note: for absolute values). While this suggests that for alite and belite, respectively, the crystallization pressure of portlandite likely compensates the volume reduction due to chemical shrinkage, reduction of autogenous strain (though of relatively small magnitude) can be expected upon hydration of belite, being currently assumed to apply for increased dosage

of superplasticizer. Without detailed knowledge of constants for own system, requiring new studies, the explanation may be presented in a simplified manner: Because each cement grain hydrates more, the unhydrated core becomes smaller, leading to lower shrinkage restraining ability.

From the discussion performed above, it seems evident that PCE could itself lead to higher shrinkage, this strictly depending on content used. This claim is in fact also supported by the two observations made in similar studies: shrinkage evidenced from moment of flattening of the autogenous shrinkage curve (i.e. from fluid-solid transition) as well as occurrence of unhealed microcracking in finely grained UHPC, the extent of which increased with increasing dosages of superplasticizer according to Cherkaoui et al. [Che 10] and Morin et al. [Mor 01], respectively. Still, synergistic effects from application of both SAP and extra superplasticizer cannot be excluded.

When accounting for the structure of both (carriage dissociated anionic groups) and geometrical details (SAP >> cement grain > PCE molecule), however, it is immediately recognized that the mechanism can only partly, if at all, resemble that known from combined effect of concurrent water-retaining agents and superplasticizer [Sar 03][Rec 12][Rid 13]. For this reason, the following inputs and potential mechanism elements could be imagined as triggering shrinkage occurred:

- *Hypothesis 1: Change of C-S-H morphology (due to single/individual or combined/synergistic impact of admixtures)*

Since working mechanism of certain viscosity modifiers often resembles that of SAP, this being the case of e.g. some cellulose derivatives [Ale 04], it may be assumed that less dense structure of C-S-H gel, e.g. of laminar features or otherwise less fibrils in favour of foil-like/sheet-like C-S-H morphology of good interconnectivity, forms also in presence of water regulator studied. Although observed in presence of prehydrated water carrier too [Ale 04][ref. 15 *Ibid.* Rid 13], in this respect, the incorporation of admixture needn't appear critical for the change to occur; in fact, the phenomenon was noted to keep effective also when superplasticizer is combined with water retaining agent [Sar 03] as well as in singular PCE application [ref. 14 *Ibid.* Rid 13], in case of which PCE may also lead to the extension of the silicate chains in C-S-H [Cap 13]. Hence, in presence of any of polymeric admixtures, unless re-saturation of the emptied pore space takes place, higher specific surface area of hydrates as

well as the low density C-S-H formation and their generally higher dispersion provide critical conditions in which high shrinkage would develop on drying.

- Hypothesis 2: Complexation-induced changes to stored water content and its release

Owing to hydrophilic nature of SAP, some original mixing water with or without that from liquid/aqueous part of superplasticizer is being shifted to new storage location. Depending on extent of changes in effective w/c exerted, if any, this could be leading preliminary to numerous consequences which were already discussed on occasion of interpreting pure SAP effect, see foregoing parts of current subsection. Differently in new arrangement though, with more PCE added, there is higher likelihood that interaction and synergistic effect between the two polyelectrolytes are experienced. Upon great amount of superplasticizer presumably remaining unadsorbed[91] but also due to geometrical restrictions (size of SAP >> cement particle), these phenomena would need to take place in the liquid phase, and not after adsorption on cement particles as in case of other interacting admixtures [Rec 12].

Although some weak and in principle indirect interaction/complexation between polyelectrolyte and surfactant having equal charge cannot be excluded [Phi 96][ref. 24 *Ibid.* Phi 96][Tia 02], in the highly alkaline environment, an obvious, strong and direct one presumably results from metal cat(ion)-induced mediation/interaction between the two polyelectrolytes and the resultant ternary complex formation[92]. The bridging element giving rise to the attractive forces can be speculated to be Ca^{2+} (Figure 4.60) or, because of low stability constant of complexes formed with Ca^{2+} [Win 07] as well as stronger binding ability (due to entropic effects) [Bur 10], some cations of higher valency and especially Al^{3+}, presence of which in pore solution in early ages is at least acknowledgeable. Seen from perspective of SAP, binding of (charged) PCE anions occurs in potential scenario as follows: after using up of first ions released to create the additional cross-links, i.e. after first intramolecular interactions in SAP, or perhaps in parallel to this event, any further liberation contributes to ruling out of electrostatic repulsion between similarly charged network units

[91] The author is aware that superplasticizer sorption may proceed in more stages, see e.g. [ref. 32 *Ibid.* Jol 98]. This aspect is not concerned currently for simplification of already complex matter.

[92] Note that, with some simplification, PCE is surfactant. The admixture generally consists of two different parts: a main chain molecule that includes the surfactant portion (negative charged acrylic backbone which is adsorbing) and side chains (not charged and nonadsorbing). On the other hand, both SAP and PCE incorporating carboxylic polymer are weak polyelectrolytes, the latter being additionally referred to as grafted polyelectrolyte. For this reason, knowledge about potential complexation between anionic polyelectrolyte and anionic surfactant as well as between two anionic polyelectrolytes should be taken into account.

and surfactant ions, and by charge reversal of one of the sites, triggers/promotes adsorption of PCE onto/into particles of former.

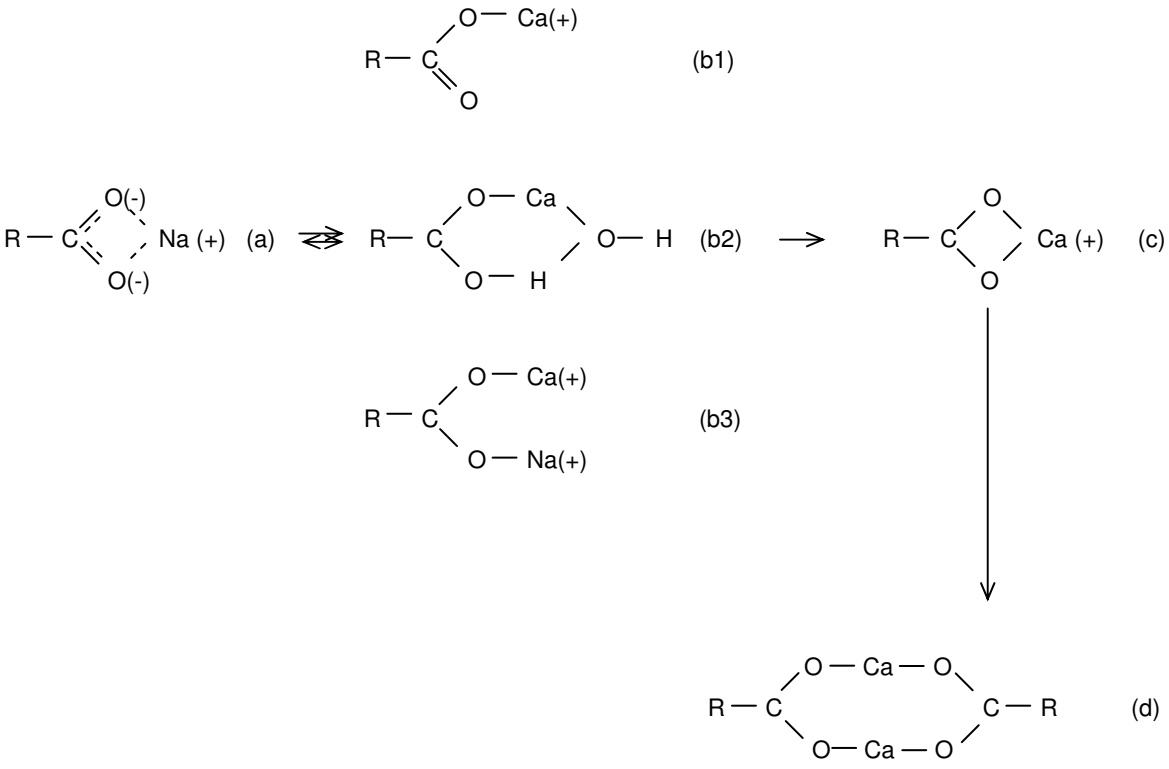

Figure 4.60: Scheme of potential Ca^{2+}-provoked reactions within own structure of polymers (a-c, based on example of polyacrylate [ref. 31 Ibid. [Win 07]) and the final complex/structure type (d).

The resultant consequences of the complex formation may become new factors decisive for magnitude of shrinkage developed. It is hypothesized that the remarkable loss of shrinkage reduction ability in presence of extra superplasticizer compared to system with IC results from lower amount of liquid stored by the curing agent as well as its suppressed release.

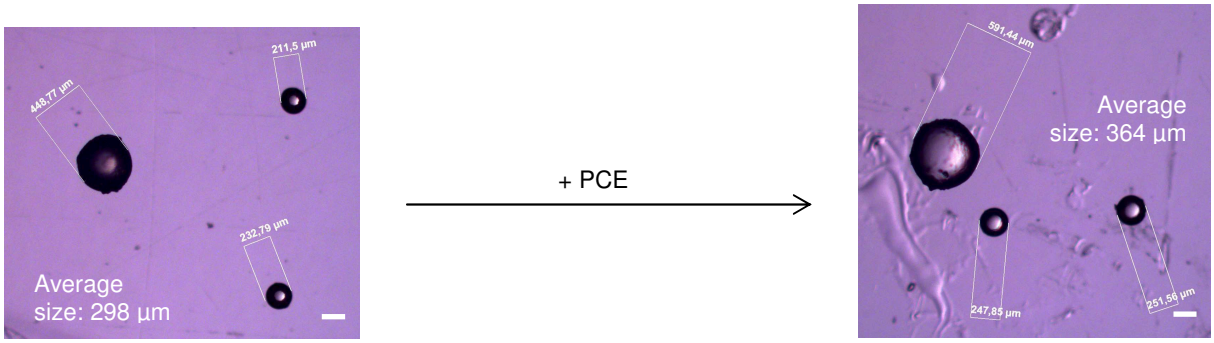

Figure 4.61: Appearance of SAP before (to the left) and after 180 min contact with superplasticizer (to the right) as recorded under light microscope. The scale is 200 µm.

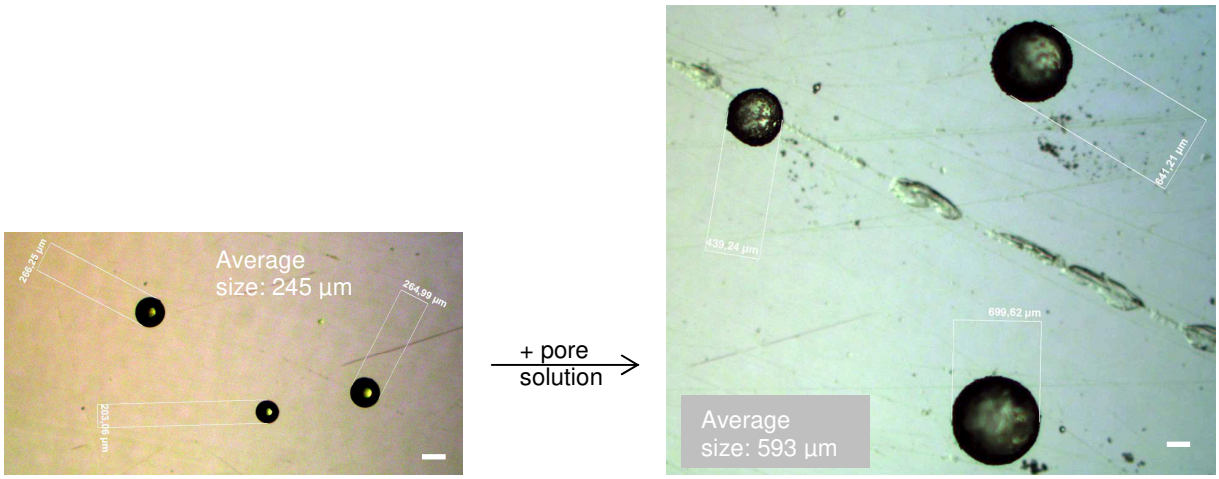

Figure 4.62: Appearance of SAP before (to the left) and after 180 min contact with cement filtrate (to the right) as recorded under light microscope. The scale is 200 µm.

The former was investigated and was validated by two means: light microscopy tests which showed less amount of maximum liquid adsorbed by SAP in presence of PCE compared to absorption in pore solution-alike fluid (see results in Figure 4.61 and 4.62, respectively) and pore counting tests which yielded less porosity in nearly entire pore range corresponding to swelled SAP in the same comparison (Figure 4.63). These observations appear in good accord with studies of Tian et al. [Tia 02] who demonstrated decreasing swelling ratio of chemically cross-linked poly(acrylic acid)-based gel on substitution of solution contacted with from pure water to solution containing increasing concentration of surfactant of equal charge. Also currently, such an effect could be attributed to lack of hydrophobic interactions between the two admixtures and, related to it, incapability for PCE to obtain energy to penetrate the SAP network. That is to say, superplasticizer after dissociation of carboxylic groups will plausibly act as salt, thus increasing ionic strength of medium external to SAP, dictating changes in its swelling behaviour. The latter of consequences, on the other hand, could be compared to formation of transport rate-controlling 'skin', in analogy to adsorption of PCE on cement. Because each SAP particle becomes densely covered by shell of PCE, its interior is practically 'fenced off' from the bulk solution or at least water migration pathway becomes somewhat more tortuous. This increases time required to release given water content, which in turn could be critical for effective counteraction of the shrinkage origin.

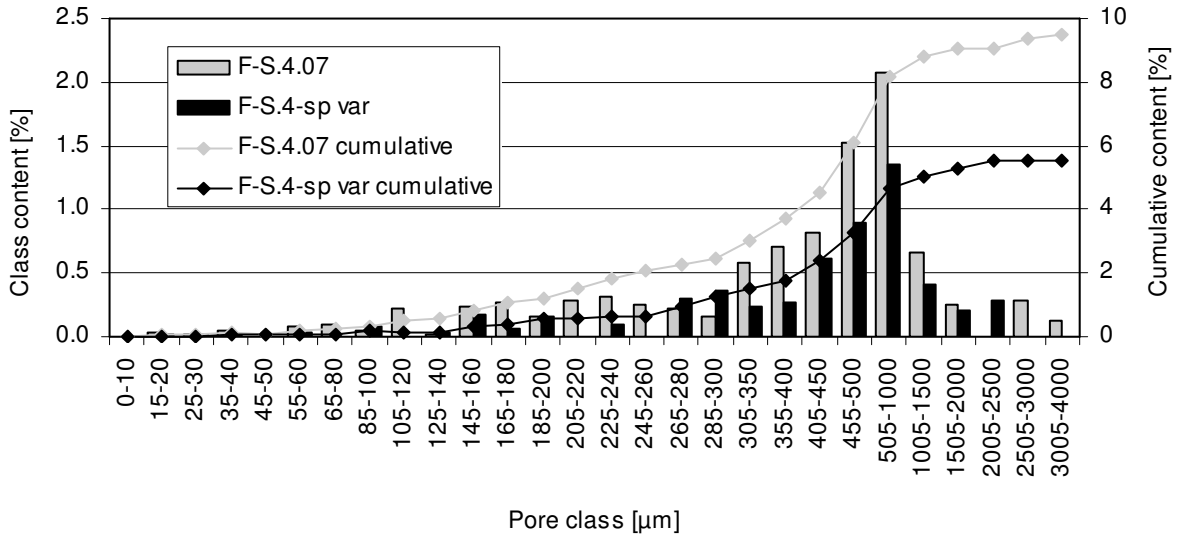

Figure 4.63: Pore size distribution of mixtures with 0.4 % SAP in range above 1 µm as measured by computerized pore counting method using RapidAir system at the age of 28 days.

Eventually, assuming bridging polymers by Ca^{2+} takes place, as well as hydrate formation occurs also in pore solution (as rivalry to dispersion of first C-S-H phases [Sow 15] and ettringite [Zin 08] by PCE), one could speculate about alteration in stability of hydrates precipitated and embedded in the complex, depending strictly on superplasticizer content, see [Win 07] and [ref. 34 *Ibid.* Win 07]. Taking into account extra added PCE without and with complexation with SAP, it could be imagined that all hydrate precursors have been covered with polymer, and stable hydrates are formed to greater extent. Also Ridi et al. [Rid 13] noted similarly: increased hydration efficiency in the acceleration period after initial retardation of reactions and resultant extension of induction period in presence of water-retaining agent, added dryly, and superplasticizer. Without curing effect occurred, the phenomenon would notably enhance shrinkage potential. On the other hand, it should be borne in mind that the complexation process as such could proceed in somewhat more complex manner than can be currently deduced from information available and therefore requires more studies in future. Beside the dosage-dependent phenomena (possibility of aggregation, saturation with surfactant etc.), this also concerns the potential role of dehydration (i.e. liberation of coordinated water molecules from the hydration shells/spheres of Ca^{2+} and Al^{3+} due to ion binding [Bur 10]) and intercalation phenomenon in respect to shrinkage.

4.6.3 Effect of water entrainment on free autogenous shrinkage

i. Finely grained compositions – results

The results of the free autogenous shrinkage investigations as obtained for the most relevant of fibre-free finely grained UHPC mixtures using smaller version of test set-ups are presented in Figures 4.64 and 4.65 for the first 28 days and until virtual stop of shrinking of the IC-unmodified material, respectively. The standard deviation is given in Figure 4.64 for those UHPCs which were studied repeatedly, viz. F-R, F-S.3.04 and F-S.4.07. Dictated by limited number of long-term measurements (mostly manual readings) as well as for sake of clearer presentation, however, the statistical evaluation was reduced to concrete ages of 1, 3, 7, 14, 21 and 28 days.

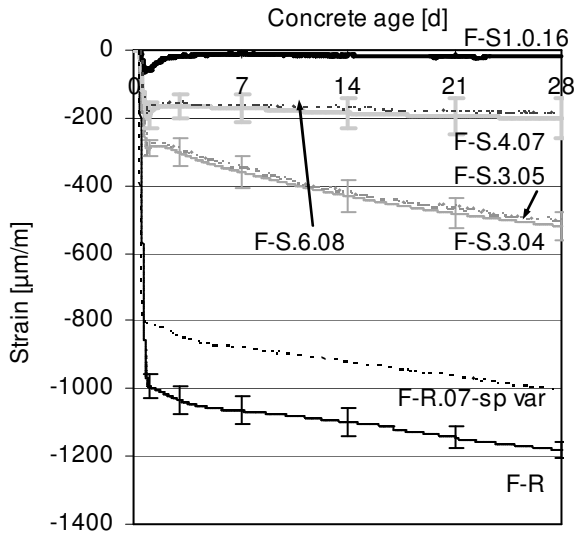

Figure 4.64: Evolution of free autogenous shrinkage of finely grained UHPCs without and with IC during first 28 days and the corresponding standard deviations at selected concrete ages. Concrete age for which strain equals zero corresponding to time-zero.

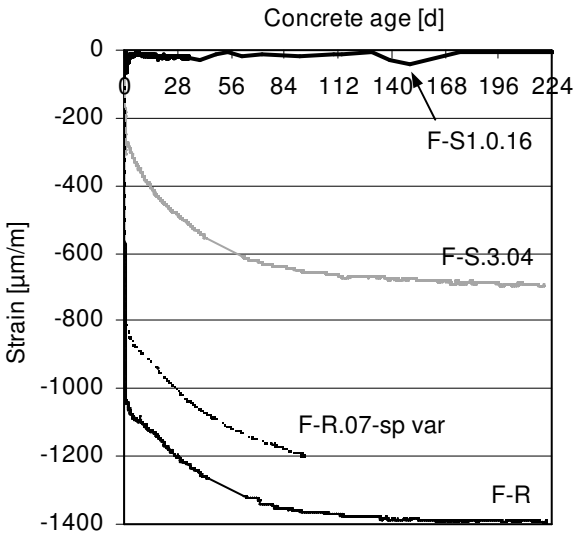

Figure 4.65: Long-term and partly manually captured evolution of free autogenous shrinkage for most important finely grained UHPC compositions tested.

The autogenous shrinkage of the control UHPC (F-R) was found to be very high, as anticipated from the specific material design. It reached nearly 1.5 mm/m within 120 days though it was needed only some tens of hours for major part (approx. 2/3) of shrinkage deformation to develop. It is notably faster shrinkage evolution than reported in study on UHPC material of similar finely grained composition to examined one [Sol 11][Sol 12], likely to be attributed to finer cement used triggering faster hydration process and thus higher autogenous shrinkage [Far 07] or perhaps some other hidden reason. On the other hand, the level of volume change is comparable to that recorded for quasi-identical matrix by Eppers [Epp 09] using, among other possibilities investigated, similar time-zero definition though

other measuring equipment. Overall all, a very strong contributor to cracking likelihood is revealed.

Investigated property of material changed only insignificantly after increasing water content and, simultaneously, reducing superplasticizer content for production of bleeding-free mix F-R.07-sp var. With no PCE reduction, very high shrinkage developed for UHPCs F-R.04, F-R.07, F-R.08 and was comparable with that recorded for F-R (presentation of curves was finally omitted for sake of graph clarity). Although bleeding could be important aspect of the difference occurred (note the indirect evidence in the results of ultrasonic investigations in Section 4.5.2 and values of slump in Section 4.3.3, for instance), it should be also considered a potential outcome of competition between increase of w/c and entrapped air bubble release. The former leads to coarsening of pore structure, therefore also permeability increase, being favourable in respect to reduction of autogenous shrinkage. On the other hand, opposite changes were likely caused by the latter, and if dominating, could thus become decisive for the final result recorded. This finding and its validity requires yet more studies given the differences in opinion on role of air in autogenous shrinkage and the potential complex work and role of air bubbles in concrete, see [Mor 01][Ham 06b][Est 09][Tam 12].

In big contrast to this picture, all the mixtures incorporating both IC components viz. water-retaining agent and extra water showed pronounced reductions in shrinkage deformations. These reductions were particularly dramatic at a very early age, in fact the first IC impact allowed limiting the respected volume change to nearly null although never for expansion, also noted in [Hua 12]. This means change of efficiency of water addition to factor of about 4 in case of mixtures of equivalent amount of extra water used (F-S.4.07 and F-R.07-sp var) which was only due to simultaneous implementation of SAP. Positive effect of maintaining original PCE content in case of the former could be obviously doubted based on foregoing discussions, see Section 4.6.2.

How pronounced the first IC impact exerted was and how the behaviour in its excess changed, this clearly depended on the content of the IC variables. E.g. the addition of 0.3 % SAP by mass of cement plus extra water (mixes F-S.3.04 and F-S.3.05) resulted in a decrease in autogenous shrinkage from approximately 993 μm/m (F-R) to approximately 290 μm/m at the concrete approached the age of 1 day. The IC efficiency was however somewhat lost in the following days and the property development followed in general the course of the

corresponding curves for UHPC without SAP addition. In fact, approximately the same increase in autogenous shrinkage over time was experienced for the control UHPC and mixtures with 0.3 % SAP. In comparison, UHPC with 0.4 % SAP and especially 1.0 % SAP having further increased extra water contents demonstrated highest reduction of autogenous shrinkage in early age and only minor, if any, changes in property with increasing age. The general trend is therefore yielded and it can be stated: the more IC variables added, the more efficient reduction of deformations due to autogenous shrinkage and the effect maintenance over time. In current study, this held true at least until development rate of autogenous shrinkage in case of control mix (F-R) dropped to very low value.

ii. Aspect of changing the test set-up and incorporating fibres

Owing to presence of coarse aggregates in the composition, volume changes of four UHPC mixtures (Cf-R, C-R, Cf-S.3.04, C-S.3.04) based on the second of the matrices tested, in particular B5Q, could be measured solely with bigger of the test set-ups. Accordingly, to make comparison valid when changing the matrix type, the impact resulting from increasing the sample's cross-section and other arrangements dictated by the new set-up had to be established first. Tests focused on this topic were performed on the M2Q matrix without and with fibres since it allowed easy encapsulation in both types of tubes. The results for mixtures devoid of and incorporating IC are demonstrated in Figure 4.66 and Figure 4.67 for the standardized, i.e. smaller tubes, and the tubes fitting large scale dilatometer, respectively.

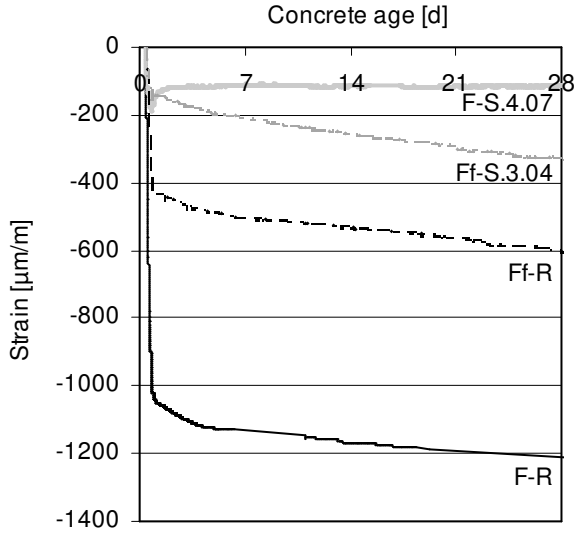

Figure 4.66: Free autogenous shrinkage of finely grained UHPCs without and with IC as recorded using standardized method. Concrete age for which strain equals zero corresponding to time-zero.

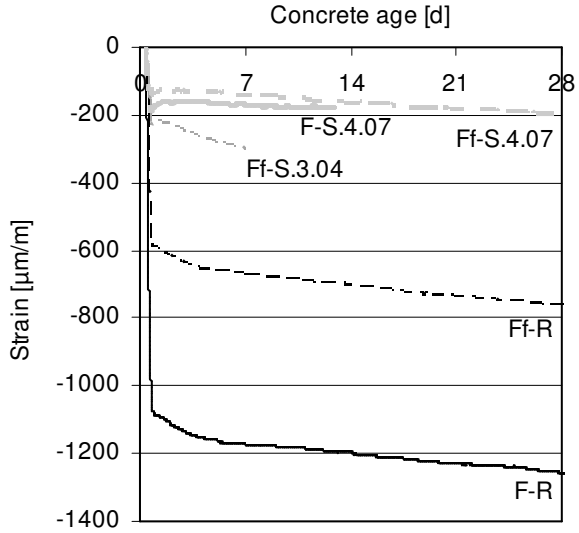

Figure 4.67: Changes in free autogenous shrinkage evolution when using large-scale dilatometer. The same time-zero applied as in case of the standardized method.

It can be seen that the autogenous shrinkage has somewhat higher magnitude for the thicker specimens irrespectively whether IC is present or not. Given that the large portion of this change occurs within first 24 hours, one explanation could be traced back to hydration heat developing in sample under measurement. As signalized in Section 4.4.3, hydration heat as translated into temperature is higher for larger cross-sections/volumes. Since the heat cannot dissipate easily, it will lead to delay in attaining the equilibrium between the core of sample and that of ambient compared to smaller cross-section. That is to say, higher strains measured on big tubes may be result of more favourable conditions when autogenous shrinkage develops i.e. temperature is actually favouring chemical reactions and development of initially denser microstructure. Once particular impact diminishes and concrete's temperature approaches that of the ambient, there is approximately the same increase in autogenous shrinkage over time. Such result is in full agreement with study of Tian and Jensen [Tia 08] who also proposed changes in extent of 'wall effect' phenomenon as alternative reason for behaviour occurred.

The comparison made could be also used to deduce the effect of steel fibres on autogenous shrinkage. A remarkable benefit from incorporation of the ingredient is observed. It was succeeded to reduce autogenous shrinkage by 40-60 % which is better than 10-20 % previously reported for similar trial in case of one UHPC [Che 01] and, simultaneously, effect close to that found for another, again finely grained UHPC [Far 07]. Some difference occurred could be plausibly traced back to potential usage of different fibre type (other aspect ratio, surface appearance/geometry, or other physical property, which could easily translate into significant impact on mitigation extent, as reviewed in Appendix B), their specific alignment in sample or by other still unknown reason. The favourable alignment of fibres in the longitudinal dimension of the specimen and expected to be more evident in case of casting smaller tubes could be finally the reason for greater reduction of autogenous shrinkage even when the selfsame composition was tested, see e.g. result for F-R in Figures 4.66 and 4.67.

In general, because compositions without coarse aggregates, contrary to coarse grained UHPCs [Cwi 08], should be free from fibre interlocking phenomenon, the contribution of steel fibres to reduction of autogenous shrinkage may result from three different functions: restraining mechanism due to very high stiffness of steel fibre, creation of channels at the interface between fibre and paste and promoting higher permeability of UHPC without [CONCRETEPORTAL] as well as with coarse aggregates [Sch 12a] at room temperatures,

and, finally, reduction of microcracking that otherwise leads to the excess deformation[93] that is observed for concrete that is restrained and drying [Lan 03]. Whatever true origin of effect is, however, benefit with respect to autogenous shrinkage and brought about from fibre incorporation appears rather secondary in comparison to effect obtained by using IC. That is to conclude, addition of fibres similarly to addition of pure extra water cannot be considered as alternative mitigation strategy, although especially the former, via permeability changes or in other way, obviously influences IC efficiency, see Figures 4.66 and 4.67.

iii. Coarse grained compositions – results

To which extent the change of UHPC composition, varied presence of IC and the steel fibres affected the shrinkage behaviour of the B5Q-based UHPC mixtures is shown in Figures 4.68 and 4.69, along with statistical evaluation in case of former.

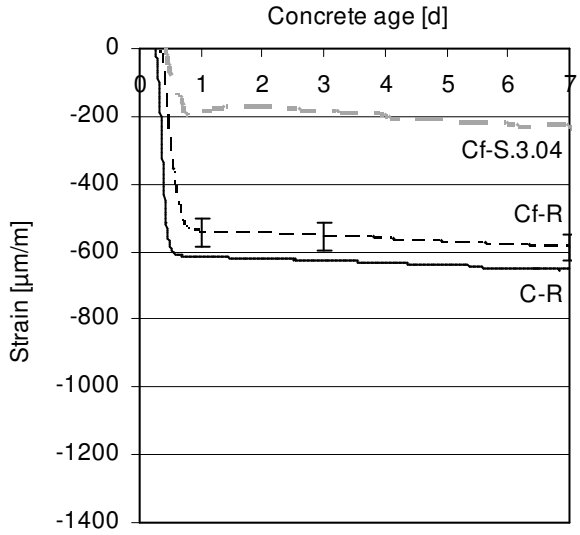

Figure 4.68: Evolution of free autogenous shrinkage of coarse-grained UHPCs without and with IC and fibres until concrete age of seven days and the standard deviation at selected concrete ages for Cf-R. Concrete age for which strain equals zero corresponding to time-zero.

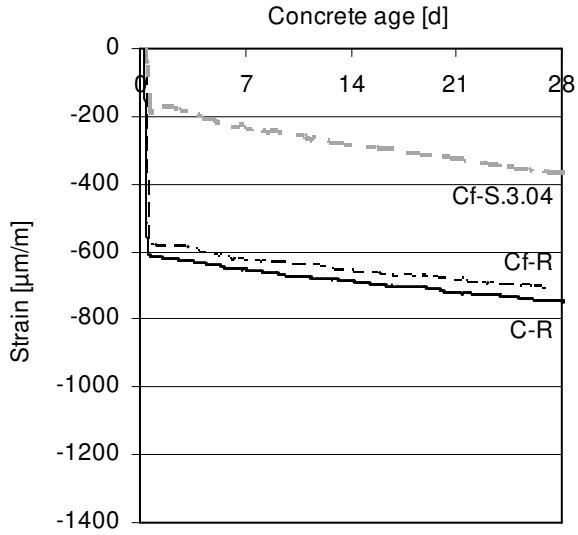

Figure 4.69: Extended 28 days evolution of free autogenous shrinkage for the coarse aggregate-incorporating UHPC compositions tested. Individual curves.

[93] It could hypothesised that microcracking is one of the mechanisms behind basic (tensile) creep, e.g. after [Lan 03][Ass 14b]. Furthermore, one also finds appropriate to ascribe at least part of autogenous deformation to the basic creep, e.g. [Lur 03]. Eventually, load that could lead finely grained matrix of UHPC to creep is likely to be present too, to be linked to internal stresses resulting e.g. from capillary pressure. That is to say, by reducing microcracking with fibres, evolution of AS will be positively affected too, a result of creep reduction. Still, it must be admitted this scenario is charged with certain simplifications. In fact, both microcracking and creep could pay positive role in terms of AS reduction. The contribution of former will be discussed in the following part of this section. As far as contribution of creep is concerned, however, note that it could lead to relaxation of shrinkage stresses [Gra 06a], the extent of which will be finally decided by numerous factors, especially degree of internal restraint. Which components truly constitute the restraint in case of finely grained UHPC is still under debate.

At any considered age, the absolute autogenous shrinkage values of the concrete mixtures with coarse aggregate and without (C-R) or with fibres (Cf-R) were lower in comparison to corresponding mixtures free of large aggregates (see results for F-R and Ff-R, respectively, in Figure 4.67). At first glance, such improvement could be coupled with higher w/c (therefore also higher w/b) at simultaneously reduced binder volume, as well as with the presence of coarse stiff aggregates, all adding up to less finer tuning of the UHPC matrix with coarse aggregates, and thus lower autogenous shrinkage. In addition to that, similar positive output plausibly resulted from improved connectivity of capillary pores and locally increased porosity in the B5Q-based UHPCs, with latter being speculated to be attributed to local microbleeding [Cwi 08] (note importantly: taking effect even if the coarse aggregate-matrix ITZ as such appears limited [Sch 12a] or non-existent [Cwi 08]), and perhaps (without fibres [Sch 12a] and as far as parts of matrix far from the fibre assemblies are concerned) microcracking. With coarser porosity and higher likelihood of free water presence or its redistribution, the chance of mitigating autogenous shrinkage autogenously obviously increases. On the other hand, this interpretation is still charged with some simplifications[94], as analysed in-depth and discussed in the following subsections.

Far more important, despite certain possibility of regulating the level of volume change by the UHPC design, the benefit of incorporating of IC remained evident. The autogenous shrinkage of Cf-S.3.04 was remarkably reduced compared to Cf-R. Still, when to compare mixes containing selfsame amount of IC variables and tested by the same method (Cf-S.3.04 with Ff-S.3.04 in Figures 4.68/4.69 and 4.67, respectively), rather unexpectedly only little difference is noted upon modification of both matrices with IC. This concerns especially the main IC effect occurred within few hours after time-zero, which is very similar in both cases. Going even further, from the selfsame comparison with respective fibre-free control mixes C-R and F-R, it becomes also evident that addition of fibres along with IC led to more pronounced changes in the autogenous shrinkage value in case of UHPC without coarse aggregate than one containing it. This effect can be only partially explained by role of fibres; owed to local formation of fibre assemblies leading to lack of the restraint in other parts of

[94] Note preliminary that two very different functions of the potential microcracking often exist. Microcracking, if occurred, which will be finally decided by many factors related to both matrix under modification and fibre used (product properties, actual alignment [Far 07], activation time [Yoo 13]), commonly facilitates penetration by aggressive media. On the other hand, it needn't [Lou 99] but may also coincide with reduction of shrinkage [Pow 59][Mou 11] due to dilation effect [Mou 11], production of new pathways facilitating water transport, and probably other. Likelihood that microcracking first occurs in UHPC matrix is obviously larger when coarse aggregates are present. E.g. bleeding that increases chance for phenomenon occurrence by the contribution to matrix defects production as well as fibre interlocking were indeed observed during testing of fresh B5Q-based mixtures.

matrix and related poorer fibres bonding, as well as the coarse matrix porosity as such, fibres only little contributed to shrinkage mitigation after upgrading C-R (control, without fibres) to Cf-R (incorporating fibres). Nonetheless, it should be also pointed out that the contents of IC variables relative to mass of cement in mixtures Cf-S.3.04 and Ff-S.3.04 were identical. As will become even clearer from subsections to follow, this yields dependency of curing efficiency on both: satisfying the particular need for curing fluid as well as important role of matrix itself in controlling efficiency of IC.

iv. Time-zero-related aspect of changing the test set-up

Although in limited range compared to dilatometer tests, some of the compositions of finely and coarse-grained UHPCs were also investigated on prisms. The results acquired are demonstrated in Figures 4.70 and 4.71, respectively.

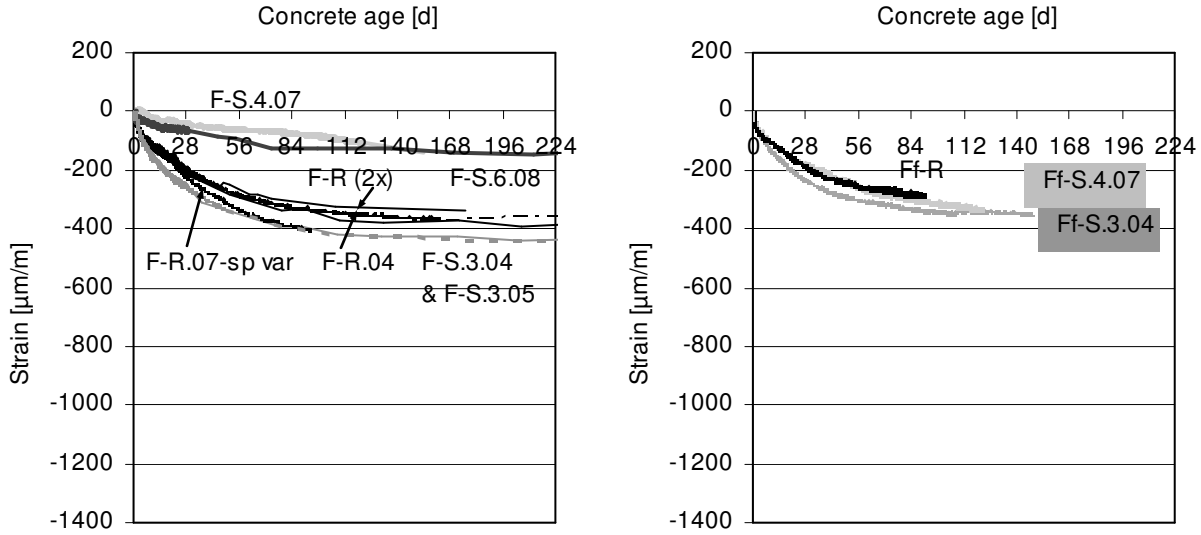

Figure 4.70: Free autogenous shrinkage of finely grained UHPCs without and with IC as measured on prisms starting after demoulding at a concrete age of one day and regarding mixtures with no fibres (to the left) and fibre-incorporating UHPCs (to the right).

When to account for the change of concrete age at first measurement, most if not all trends recorded before on tubes became confirmed for the M2Q matrix-based (Figure 4.70) as well as B5Q matrix-based UHPCs (Figure 4.71), as expected. Rather surprising though, no big differences were noted between Ff-R and Ff-S.4.07 likely due to unique role of tunnels around fibres or other. Damaging of prism sealing was excluded as being the underlying reason based on mass loss results.

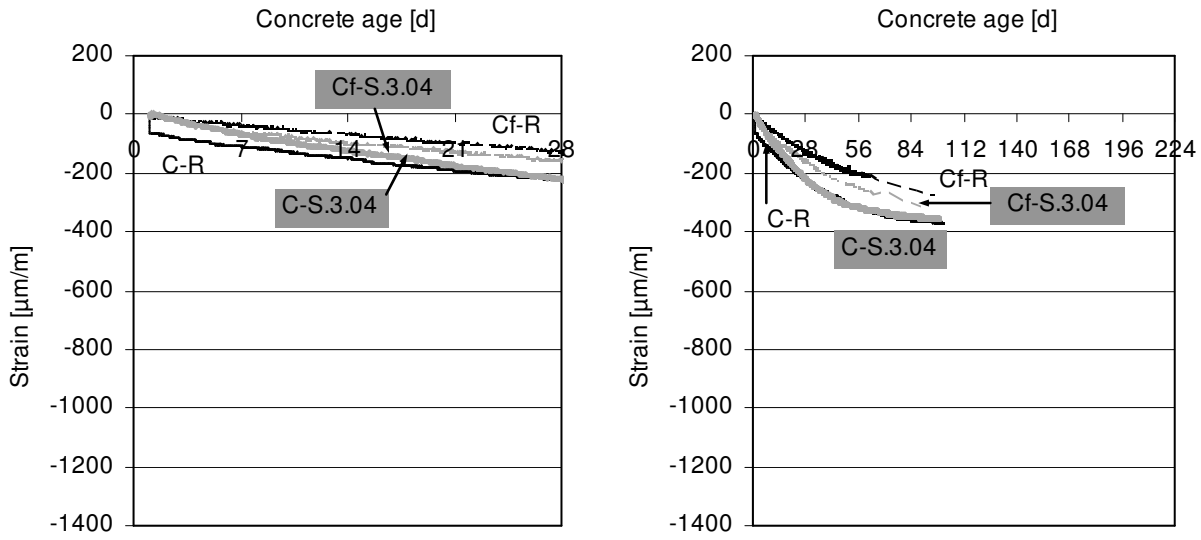

Figure 4.71: Free autogenous shrinkage of coarse-grained UHPCs without and with IC as measured on prisms starting after demoulding at a concrete age of one day and regarding evolution during first 28 days (to the left) and until the test end (to the right).

v. Analysis and interpretation of results

- the discussion of the general matrix-shrinkage relationship/correlation

The specificity of the UHPC design induces necessity of new look on role played by main phases in the concrete composite. This especially regards the paste. The rule of thumb is that when w/c is lower than approx. 0.4 as in considered case of UHPC, not only distances between cement grains are small (having straightforward negative effect on shrinkage, to be linked to e.g. higher capillary stress generated on drying), also only some cement becomes converted into hydrate phase. Another fact is that especially in finely grained matrix M2Q the cement content is very high, at least double the amount that is typically used for production of e.g. conventional concrete. In consequence, the forming solid skeleton is constituted of relatively more and potentially larger residual/unhydrated/anhydrous cement/clinker grains, which given no fibres present become the stiffest element among all ingredients of UHPC (approx. 125 GPa). By making use of this unique property, when capillaries de-saturate and the pressure (to be transmitted through contact points between solid phase particles of the paste) becomes produced/exerted, these elements actively participate in restraining autogenous shrinkage. The final effect on shrinkage very likely, and similarly to effect of strength [Pic 13], depends on w/c used and hydration degree, increasing with the decrease of former and the lower the latter maintains.

The supporting evidence of high restraint provided by the anhydrous cement is the microcracking phenomenon observed in rival study on low w/c cement pastes as well as

mortars [Pir 06], the extent of which increased on exposure to additional restraint. This unfavourable phenomenon is speculated to be taking place in case of finely grained UHPC as well [Fey 01] despite high relaxation rate being inherent to UHPC [Sch 02][Sch 07a][Epp 10] and mortars in general [Pir 06]. Important enough, microcracking may be induced by shrinkage plausibly at any time, even when the RH is high [Cha 82][ref. 3 and 20 *Ibid*. Tam 00].

In view of presented fact, the extent of restraint provided by the two matrices was analysed first. The calculation of the average Young's moduli of solid phases was performed and the results acquired are presented in Table 4.11. Despite some simplifications made and accompanying usage of modified Power's model (e.g. assumption that pozzolanic reaction takes place from very early ages, which is hardly the case especially for M2Q matrix, see Section 4.2.3 or [Pfe 10]), it can be seen that stiffness-related parameters for both UHPC matrices were much alike. Still, at the age of 7 days, magnitude of autogenous shrinkage was higher, particularly by factor of 1.8, in favour of the control finely grained UHPC mix (F-R), see Figure 4.67 and Figure 4.68/4.69. This was obtained despite M2Q matrix being characterized with more anhydrous cement grains and, as mentioned, having confirmed little pozzolanic activity due to formation of silica agglomerates or other reasons.

The observation brings about two important conclusions. Firstly, it shows that benefit brought about from non-reacted cement presence shouldn't be overestimated and perhaps cannot be made use of for manipulation of the stiffness and/or counteracting the shrinkage force unless w/c is very low (as speculated in case of pure SAP addition). It is plausible that, similarly to case of aggregate [Bis 01][Bis 02], for given Young's modulus of the solid sufficiently large diameter has to be attained (and more precisely for the case of cement: maintained) in order to provide remarkable restraining effect, currently obtainable only by modifying w/c parameter. This idea would be somewhat supplementary to that known e.g. from Alexander and Wardlaw [Ale 59] where lower hygral volume changes were associated with coarser aggregate allowing earlier restraining effect as well as other more favourable from perspective of shrinkage reduction distribution of tensile/compressive stresses. Secondly, it can be concluded that reasons other than presence of fibres and temperature effect existed and led to the different levels of autogenous shrinkage observed. Obviously, one source of differences should be related to w/c (Table 4.11) while the other to incomparability of binder compositions, to be discussed in the following.

Table 4.11: Stiffness-related particularities of the tested matrices. Fibres are not concerned.

Binder component or the resultant property [unit][1]	Considered matrix@time-point studied			
	M2Q@0	**M2Q@α_{max}**	**B5Q@0**	**B5Q@α_{max}**
All binder components, concrete volume fraction [-]	0.514	0.514	0.471	0.471
Unhydrated cement, relative volume [-]	0.517	0.289	0.438	0.223
Unreacted silica fume, relative volume [-]	0.116	0.065	0.175	0.089
Gel solid, relative volume [-]	0	0.374	0	0.374
Gel water (cement), relative volume [-]	0	0.140	0	0.132
Gel water (silica fume), relative volume [-]	0	0.060	0	0.094
Capillary water, relative volume [-]	0.367	0	0.387	0
Chemical shrinkage (cement), relative volume [-]	0	0.047	0	0.044
Chemical shrinkage (silica fume), relative volume [-]	0	0.026	0	0.042
All binder components, relative volume [-]	1.0	1.0	1.0	1.0
Average Young's modulus of binder solid phase (in parenthesis- value including quartz powder W12) [GPa]	72.7 (69.4)	**57.9 (56.6)**	67.0 (63.0)	**52.1 (51.3)**
Average Young's modulus of aggregates [GPa]	66.2	66.2	65.3	65.3
Average Young's modulus of concrete solid phase (without entrapped voids and PCE solid part) [GPa]	69.6	61.8	66.1	59.0
Measured Young's modulus of entire composite at 28d (bulk modulus) [GPa]	-	48.8	-	54.7 (with fibres)

[1] the literature-based and averaged values used for calculations of Young's moduli: unhydrated cement E = 125 GPa, silica fume E = 70 GPa, hydration products E = 30 GPa, quartz powder E = 48 GPa, quartz sand E = 70 GPa, basalt E = 77 GPa. The hydration products are also considered as being comprised by hydrated cement and the gel water (also from reaction of cement and silica fume).

Because shrinkage mechanisms of any solid material are typically closely related with its specific surface area, associated properties of the paste and aggregate were taken into account[95]. One acknowledges that the compositions of both matrices in general and their particle graining as well as the w/c ratios in particular were clearly different. It could be deduced, for instance, that although M2Q contained less silica fume (reminder: not reactive until later ages!), the total specific surface area of the paste was higher compared to B5Q matrix (Table 4.12). This value diminished and became only insignificantly smaller when the very fine quartz powder Millisil W12 was treated as reactive material which could be yet certain simplification. On the other hand, the amount of mixing water introduced to the mix was clearly less. It furthermore had to be spread over similar amount of aggregate solid particles which, important enough, fineness and specific surface area was higher for the finely

[95] In the following discussion, it is imagined that all solid particles (cement, silica fume, aggregates) become coated with (excess) water film i.e. consisting of water in excess to one needed to fill the voids. Furthermore, it is considered that thin film of paste lubricates each aggregate grain, except for the finest quartz powder (entire fraction of Millisil W12). In this regard, it is assumed that this material due to very fine appearance can be intermixed with the cement and water to become inseparable part of paste and, simultaneously, can be stimulator of early hydration (certain physico-chemical interaction).

grained UHPC. Adding to this smaller paste thickness coating, values for which are also reported in Table 4.12, this led to critical changes in the centre of bulk paste in between the aggregates, especially further w/c reduction from the initial w/c of 0.22.

The final consequence of abovementioned contributions was the very high autogenous shrinkage of M2Q. Herein, the limitation of paste thickness by the aggregate was obviously not favourable to shrinkage reduction which is in contrast to general knowledge. This effect can be well explained by occupation of aggregate fraction of M2Q with particles of diameter < 1 mm, which has low restraining capability according to some sources [Bis 01][Bis 02]. Plausibly, as explained by Alexander and Wardlaw [Ale 59], great compressive stresses must be exerted onto small aggregate particles first to activate them in the restraining mechanism or any other mechanism bringing about the shrinkage reduction. Very fine quartz aggregate could be contrary involved in chemical reaction with the cement paste, which analogously to limestone [Zha 13] may be restraining the free water mass movement, the content of which as mentioned earlier was much smaller than in B5Q matrix; particular activation/stimulation may yet require delivery of additional heat above room temperature according to some literature sources. Larger aggregates, on the other hand, for a given aggregate fraction have lower surface area to bond with the paste, so shrinkage produces larger stresses at the interface [Won 09] and the restraint is used better to reduce the shrinkage magnitude.

Table 4.12: Results of calculation of specific surface area of solids and the average paste layer thickness.

	Parameter determined			
Parameter estimated	**(Total, specific) surface area of solid reactive particles [m²/m³ mortar or concrete][1]**	**Total aggregate content [kg/m³ mortar or concrete] (relative volume of aggregate < 1 mm [-])**	**Total specific surface area of aggregates [m²/m³ mortar or concrete][2]**	**Averaged (excess) paste film thickness [µm][2]**
M2Q	**689972** (783881)	1212.4 (1.00) / without W12: **1000.1 (1.00)**	8676.0	48.2
B5Q	685453 (832824)	1442.5 (0.60) / without W12: 1109.3 (0.48)	6746.5	89.5
B5Q (with fibres)	**668600** (812348)	1407.0 (0.60) / without W12: **1082.0 (0.48)**	not determined	not determined

[1] Finer of the two quartz flours used for producing UHPCs, in particular Millisil W12, treated as reactive powder
[2] Quartz flour Millisil W12 not included in calculation

Interesting enough, the picture presented above and explaining reasons for greater shrinkage recorded in case of M2Q resembles to a high extent that applicable for comprehension of the

rock volume changes. In agreement with theory originally proposed by Fujiwara [Fuj 84], changes in the surface energy and disjoining pressure, therefore phenomena closely associated with changes in the specific surface area of the aggregate as well as its water saturation state, could provoke the volume changes of the solid on its drying or rewetting (assumption: RH < 100 %). This is schematically showed in Figure 4.72. The possibility that the same mechanisms apply for concrete or even some hydrates appears more alike given the confirmed existence of certain linear relationships, especially between aggregate shrinkage strain or aggregate specific surface area and the hygral volume change of concrete [Ima 08][Zha 13]. On the other hand, in Section 4.2.3, it was observed that M2Q had finer porosity, owing to which larger capillary depression could have developed in the material in agreement with Kelvin and Laplace laws. That is to say, capillary pressure could be considered as the rival potential mechanism standing behind the volume change developed.

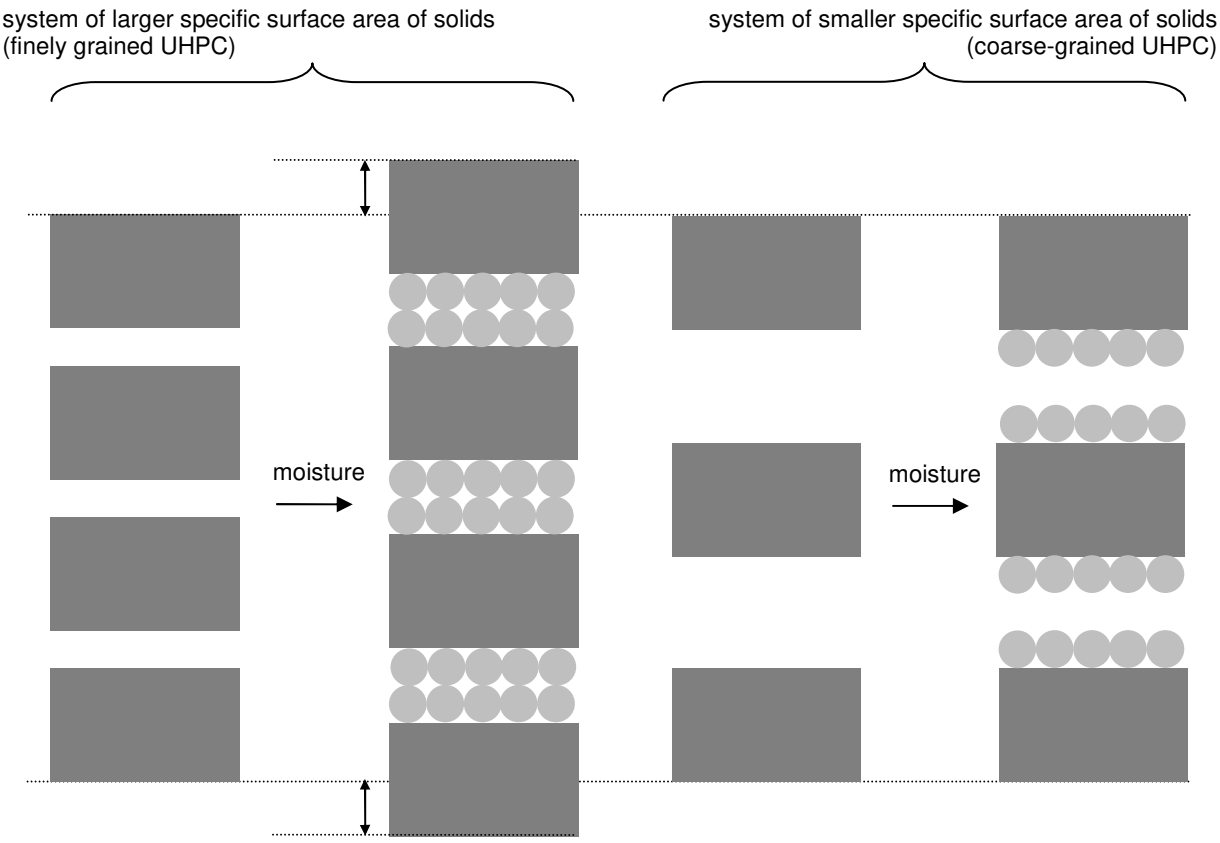

Figure 4.72: Effect of moisture sorption (disjoining pressure) on volume changes of system having larger and smaller specific surface area of solids, to the left and to the right, respectively. Note that the schematic drawing can be used to explain more pronounced reduction of autogenous shrinkage of M2Q-based UHPCs compared to B5Q matrix-based mixes for selfsame amount of SAP and extra water content used. However, it could be also used to understand greater shrinkage of former compared to latter. Inspired by the influence of aggregate on drying shrinkage [Ima 08].

In order to be able to support/indicate true mechanism(s) triggering autogenous shrinkage in case of UHPC, the capillary pressure (i.e. quasi-directly measurable variable unlike the

disjoining pressure) was determined. The result and discussion of particular test will be subject of presentation in Section 5.2.

- the discussion on role of the UHPC matrix in controlling internal sealing and IC efficiency

It was demonstrated in Section 4.6.3 that a small amount of IC variables used, viz. 0.3 % SAP plus 0.04 of extra w/c, was sufficient for pronounced reduction in autogenous shrinkage of M2Q and B5Q matrices (mixtures F-S.3.04 and Cf-S.3.04, respectively). Still, the extent of the first major IC impact being recorded within first 24 hours was observed to be somewhat composition-dependent. Indeed, relative to corresponding control UHPCs, less shrinkage was enabled to develop in case of finely grained mix (UHPC F-S.3.04). This could imply higher efficiency of IC in the finely grained matrix compared to one with coarse aggregates. It appears even more interesting finding when to acknowledge like contribution of shrinkage microcracks to opening up of porosity and resultant permeability increase [Hea 99], the phenomenon which in case of B5Q should be specifically more remarkable given the presence of coarse aggregate.

Table 4.13: Comparison of IC variables content used in relation to the IC shrinkage reduction effectiveness without and with accounting for the silica fume presence.

Mix	Powers' model		Modified Powers' model		Relative autogenous shrinkage reduction at 1 / 3 / 28 days [%]
	$(w/c)_{IC,req}$ [1]	$(w/c)_{IC,used}$ / $(w/c)_{IC,req}$ [%] [2]	$(w/c)_{IC,req}$ [1]	$(w/c)_{IC,used}$ / $(w/c)_{IC,req}$ [%] [2]	
F-S.3.04	0.040	100	0.055	73	-71 / -71 / -56
Ff-S.3.04	0.040	100	0.055	73	-66 / -64 / -46
F-S.3.05	0.040	125	0.055	91	-71 / -72 / -58
F-S.4.07	0.040	175	0.055	127	-81 / -84 / -83
F-S.6.08	0.040	200	0.055	145	-82 / -85 / -84
F-S1.0.16	0.040	400	0.055	291	-94 / -98 / -98
Cf-S.3.04*	0.049	81	0.078	51	-67 / -67 / -48

[1] the quantity of entrained water necessary to avoid self-desiccation acc. to Powers' model
[2] estimate of fulfilment of curing water requirement for avoiding self-desiccation (simplification made: all extra water added is spent on internal curing)
[*] relative to Cf-R

At first glance, particular efficiency change must be related with the amount of extra water provided for IC. Taking into account information given in Table 4.13, it could be acknowledged that the added extra w/c of 0.04 balanced 73 % and 51 % of theoretical water amount needed to avoid self-desiccation in M2Q and B5Q, respectively. This difference becomes even more pronounced when accounting for the delayed pozzolanic reaction in case of M2Q [Pfe 10], the phenomenon bringing about less chemical shrinkage occurred and thus

lower curing water demand than predicted by the modified Powers' model from cement-silica systems. In none of the considered cases, however, does the amount of curing fluid used allow full mitigation of autogenous shrinkage or, which would be expected, turning the negative strain into positive one i.e. expansion, being yet in agreement with similar studies [Sol 11][Hua 12][Jus 15].

It is thus obvious that transport properties of the matrix under modification must be the particular critical factor controlling efficiency of IC. Important in this respect, it should be recalled that the relationship between the content of extra water used and absorption capacity of the IC agent was different and, as consistency investigations showed (Section 4.3.3), depended on UHPC composition under modification. For instance, mix F-S.3.04 incorporated nearly as much free water as to maintain the workability of F-R; given so, the pore percolation of the mix with SAP could be expected to be much alike the one of the corresponding control mix F-R. This is in big contrast to modifying B5Q with selfsame IC variables amount which obviously resulted in deficit of extra water in relation to SAP absorption capability. The consequence of the change was spending part of fraction of mixing water originally present in the mix, bringing about less capillaries (affecting shrinkage reduction much likely positively e.g. lower curing water demand) but simultaneously decreasing degree of hydration needed for capillaries depercolation (thus earlier pore depercolation) compared to the respective control mix. In author's opinion, the latter may be overriding factor in terms of final curing efficiency.

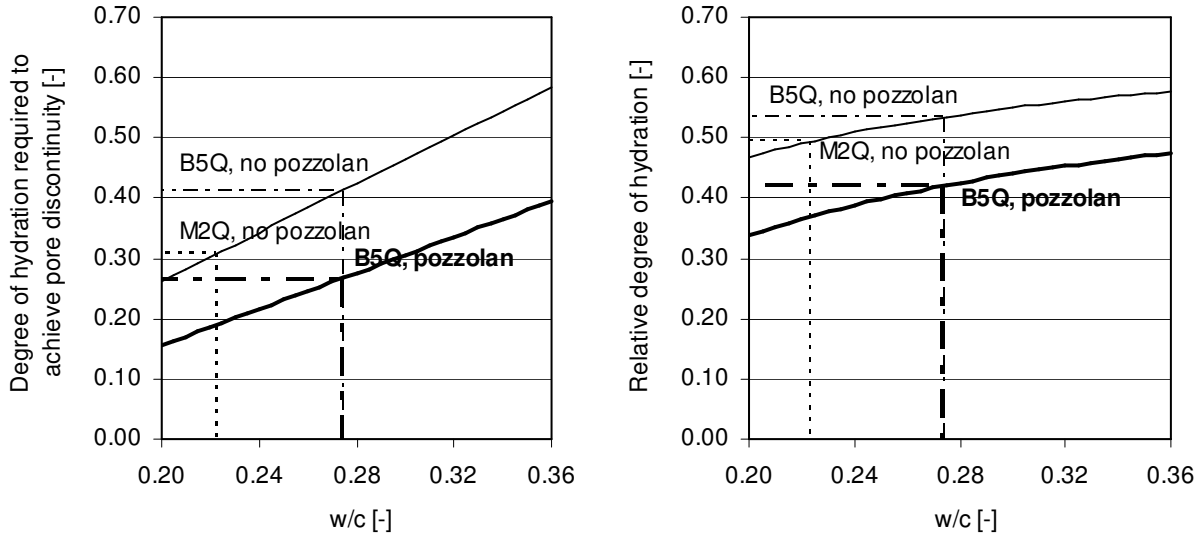

Figure 4.73: Degree of hydration required to achieve capillary pores discontinuity of UHPC pastes following indicatives of the Bentz and Garboczi simulation model [Ben 91] for the pure clinker reaction and, optionally for B5Q, total pozzolanic reaction (to the left) and relation of the critical degree determined to maximal attainable degree of hydration for corresponding systems assuming perfect curing (to the right).

It should be borne in mind that the distance of how far water can travel will much depend on pore percolation, which is parameter being decided, among others, by w/c (Figure 4.73). The length of concrete life until the critical moment of attaining the transport system discontinuity will be one of decisive parameters for the curing efficiency. From the perspective of the matrix under modification, the associated input related to matrix could be thus anticipated as twofold: direct one resulting from particular mix design and an indirect one related to absorption behaviour of SAP in given conditions. Plausibly, the combination of these two contributions eventually led to observed change of IC efficiency on changing UHPC matrix.

Assuming existence of some relation between the capillary suction and water release from SAP, another look on efficiency of IC from the material perspective can be presented. Because B5Q porosity was characterized with larger pores (see Section 4.2.3), on self-desiccation much lower capillary pressure was generated compared to M2Q. In turn, less curing water could be delivered to the matrix before depercolation occurred. This relation may presumably change on reduction of original w/c of B5Q by SAP provided that IC agent changes capillaries' size and not their content as such. However, even in this case, there might be insufficient time left to remove the curing fluid, amount of which is more compared to M2Q as confirmed in pore counting investigations, see Figure 4.74, from the SAP pores.

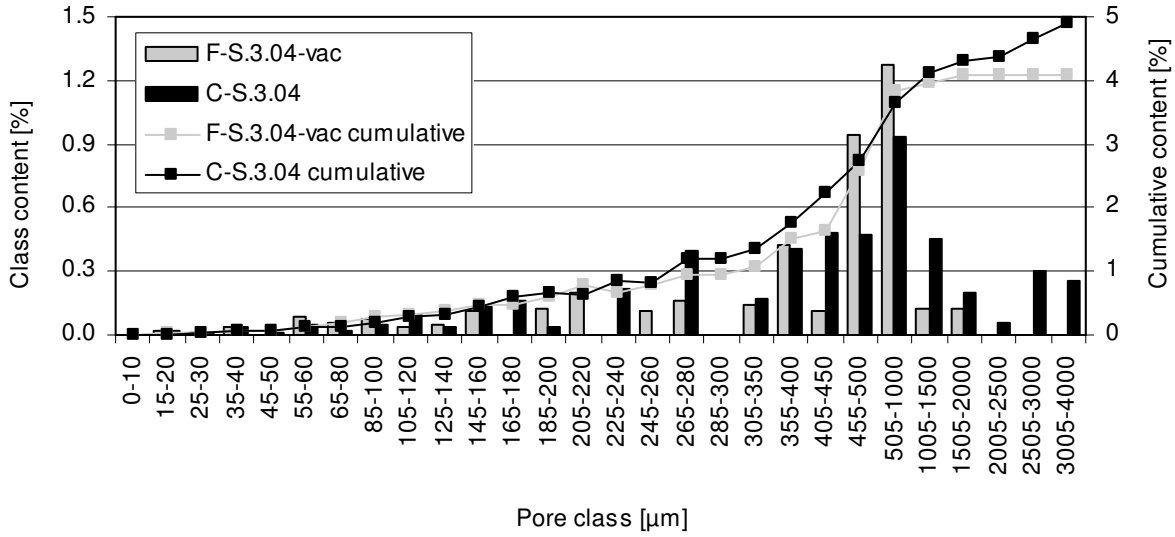

Figure 4.74: Pore size distribution in finely and coarse-grained UHPC modified with 0.3 % SAP and having similar initial entrapped air content as measured by pore counting method at the age of 28 days.

It is worthy to note that analogous explanation likely applies to changing the size of SAP in frames of the same matrix [Lur 06][Dud 14]. In this case, the absorption capacity of finer IC agent of selfsame type in total is more but curing ability is less due to manipulation of pore

system combined with water release ability from SAP, the final effect of which is less autogenous shrinkage reduced or, in favourable case, less expansion produced. This should be investigated in more details in future, also to account for difference in water release from SAP of different particle sizes (see also Sections 5.3 and 5.4 and Appendix H).

- the discussion of the matrix changes behind IC effect

It was demonstrated in Section 4.6.3 that autogenous shrinkage can be mitigated to very high extent by means of IC. The effect is notably linked with amount of IC variables used. In particular, the more curing fluid smartly delivered by the IC agent and, more importantly, the better satisfaction of the curing water requirement (Table 4.13), the greater the reduction of autogenous shrinkage observed even if presenting non-linear relationship. When accounting for factors governing curing efficiency in cement-based materials, this suggest preferable access to free water centres in system enriched with IC variables though it can be argued that additional favourable effect could result from the extended dilution effect[96] which in the considered UHPC systems had two sources: the IC presence-associated air content increase (Section 4.2.3) and, accompanying introduction of IC, the original concrete volume decrease (Section 3.2.4 and Appendix C).

Since the major IC impact occurred within first 24 hours and not much later (note: rather the first IC effect maintenance in later ages), it was awaited spending most of the free water to counteract the origin of autogenous shrinkage to this age especially given not much shrinkage developing onwards, see again result obtained for F-R in Figure 4.64 and 4.65. To test this hypothesis the mass loss was examined. Specimens were made of UHPC without and with IC, particularly F-R and F-S.4.07, and were casted in different sizes assuming very limited moisture influential depth. At testing ages (1, 3, 7, 14 and 28 d), some were unwrapped from the foil cover and, after any necessary preparation (e.g. shattering of the prism sample for the conversion into small test pieces sieved to final size of 4-8 mm, i.e. MIP size-like samples), were exposed to oven drying. Temperature level of 40 °C was chosen for the drying to facilitate free water removal speed but without simultaneous encouraging microcracking or hydrate decomposition to be expected at somewhat higher temperatures. In next step, the relative ratios of the mass lost to theoretical total water mass possessed by the samples before

[96] Dilution in traditional understanding refers to replacement of reactive concrete components and especially cement by non-reactive one, be it knowingly (e.g. using higher aggregate fraction) or unknowingly (e.g. entrapment of technological air). By extended dilution effect, it is meant substitution of all original concrete ingredients with IC variables, while remaining the mutual proportions of the former.

the oven drying were calculated. The results obtained for some ages tested are presented in Figure 4.75.

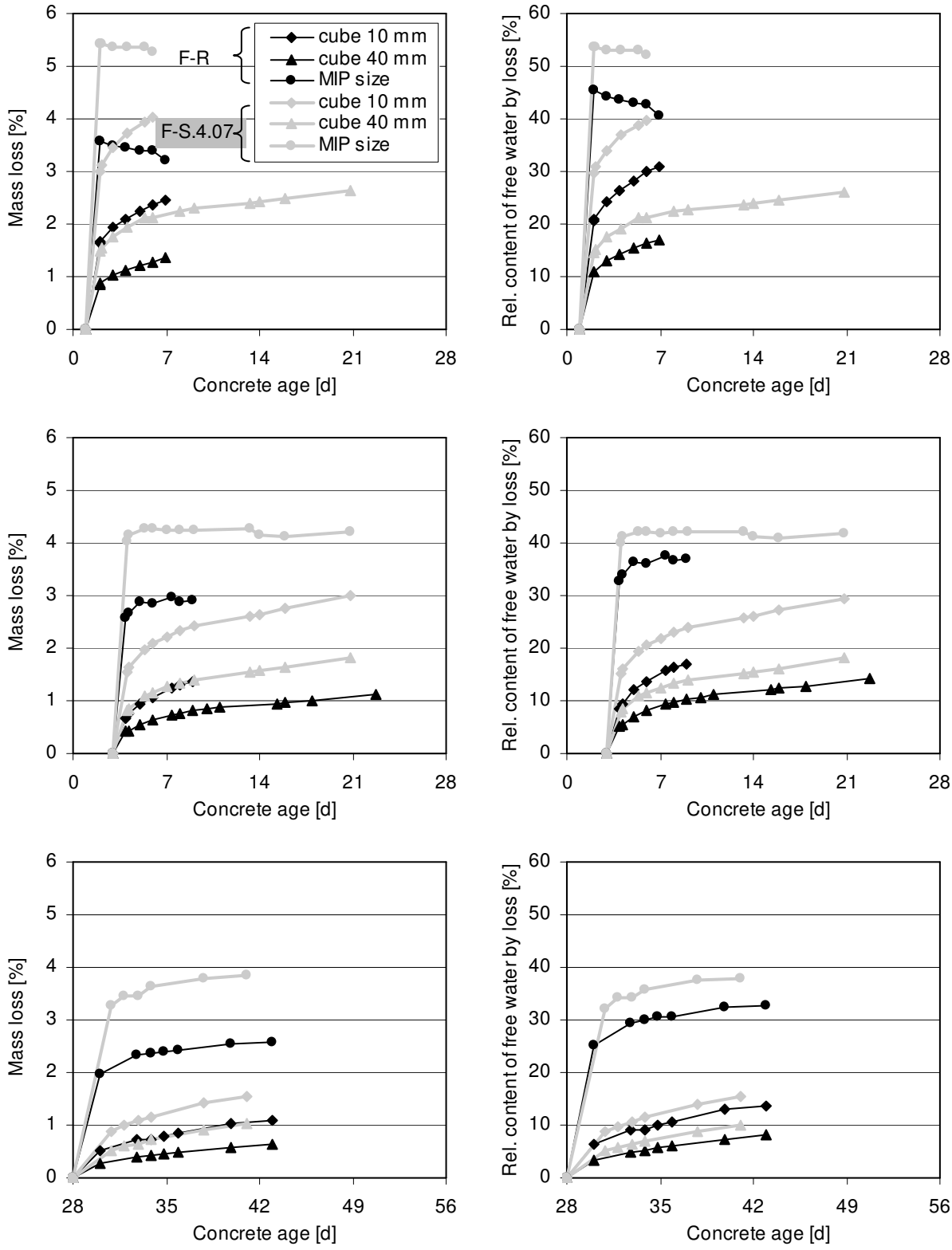

Figure 4.75: Mass losses (to the left) and the corresponding relative contents of free water remained (to the right) as determined for control mix and exemplary mix with IC after initiation of drying to ambient at concrete ages of 1 (top row), 3 (middle row) and 28 days (bottom row). The same legend applies to all graphs.

It can be seen that at any testing age both mixtures types, i.e. without and with IC, exhibited presence of unbounded water[97]. Its content captured clearly depended on specimen size, in trend: the smaller the sample piece, the better free water withdrawal and thus higher moisture loss for a given time until associated maximum was reached[98]. As expected, in each case, the content of ingredient needed to sustain hydration as well as curing (including self-curing) was higher for mixture incorporating IC which can be traced back to higher total water contents used for this mix. Even so, in both cases, the main finding could be interpreted very similarly, particularly as insufficient utilization of any of available water resources for mitigation of autogenous shrinkage. The causes of such behaviour are different for each case.

Free water existence in the control mix, which for finely grained UHPC has been also observed by Vernet et al. [Ver 98], could be likely attributed to greater content of ink-bottle porosity or their creation in UHPC as such. The specific pore type is inherent to non-cured systems of low w/c [Odl 72b], and becomes produced especially on severe drying [Esp 06]. Translated into current situation, ink-bottle porosity, existence of which in M2Q-alike UHPC was also hypothesized by Matthews et al. [Mat 08], could be induced by the self-desiccation. In course of hydration, as the necks of the ink-bottle pores become narrower, the availability of evaporable water is increasingly more restricted, hindering its transfer from the water-rich zones to ones lacking of the moisture to further extent. This situation and phenomenon comparable (if not equivalent) to pore blocking [Jen 13] maintains unless some favourable change occurs.

Important enough, as being implied indirectly by results of shrinkage, the microcracking phenomenon if occurred in UHPC as suggested by past experience [Fey 01] is not a sufficient condition for a change. This may be due to the fact that, on one hand, microcracking affects permeability[99] more than diffusivity or sorptivity [Won 09][100]. Diffusion i.e. process, to which

[97] Mobile and evaporable water can be associated with several pore categories, including interlayer, gel and capillary [Jen 13]. According to same classification source, the gel pores are small open space between particles or some defect regions where solid C-S-H particles come into imperfect contact. Capillary pores are, on the other hand, remaining larger pores and initially consisting of mentioned fluid. This distinction of porosity will be important for further discussions, especially disjoining pressure theory.

[98] Note that the observation plausibly gives a new insight into overestimation error related to determination of autogenous shrinkage under drying conditions. This should be validated in the future.

[99] It should be borne in mind another reason why higher permeability should exist for system without IC and having restricted availability of evaporable water, particularly collapse of C-S-H gel layers [Hea 96]. Some bonds will be permanent therefore leading to irreversible shrinkage.

[100] In the study referred to [Won 09], the transport properties measured and determined for effect of microcracking were: oxygen diffusivity, oxygen permeability and water sorptivity. Although certain findings should also apply for other masses e.g. microcracking indeed influencing water permeability (e.g. [Hea 96][Hea 99]), it could be some simplification involved as far as the properties relation is concerned. Consider here

both hygral shrinkage/swelling [Tam 00] and moisture movement through the pore necks [Odl 72b] may be linked to, on the other hand, requires another trigger. This could be for instance curing under elevated temperatures as high as 60 °C, bringing about activated diffusion process [Odl 72b] (or other) and thus increase of RH in pore system [Eka 09] which, assuming capillary pressure is operative shrinkage mechanism, would mean lowering of autogenous shrinkage. The opposite changes may be awaited at room temperatures alike used in current study or even small elevated ones, observed also for UHPC [Sol 11][Soliman and Nehdi 2011, ref. 17 *Ibid.* Sol 12]. Other experiences concerning maturing at hot environments and changes of RH are also known showing this subject still requires attention in future.

Obviously, the underlying reasoning that finally dictated the shrinkage behaviour of UHPC before modification with IC could be more complex and be affected by more factors. E.g. it could be originating from higher tortuosity (regarding both microcracks and cement paste in mortar) and/or more complex microgeometry of pore system compared to system with IC, involving perhaps higher content of isolated pores as well. These aspects should be investigated in future.

What is clear, the case of UHPC with IC presents itself somewhat differently compared to the system before the modification. At any given age, some amount of free water is present and in fact must remain given that curing is demanded to be long-term process. For high amounts of IC variables applied in considered case of mix F-S.4.07 (investigated for mass loss) it did in fact allowed maintenance of the first IC impact. On the other hand, despite using in some instances more extra water than theoretically needed to counteract self-desiccation (Table 4.13), it was still not possible to eliminate particular type of volume change completely (Figures 4.64-4.67). Similar conclusion does in fact result from another study on UHPC [Hua 12] where more types of SAP and very high contents of extra water as for IC reasons were used and where the efficiency of the method was proved again somewhat limited.

Since in UHPC reversal of volume change into expansion can be attained when using submerged curing condition from early hardening stage [Sol 12] and furthermore since

---

likelihood of physical and chemical reaction between water and cement structure, for instance. On the other hand, the rule of thumb is that permeability better scales with (critical) pore size than the two other properties [Hal 95][Mar 97], and for which any relation might be actually missing, especially in case of larger pores [Won 09].

depercolation manifest itself not sooner than after tens of hours [Ver 98][Bon 00][Sol 12][Tam 12], the restrained removal of curing water from SAP must be considered as the critical factor. E.g. in case of highest amount of IC agent used (1.0 % SAP in mix F-S1.0.16), the difficulty likely reflects the high relative humidity attained, which induces insufficient osmosis effect (due to lowered ion concentration) or capillary suction[101] for the water withdrawal from the tiny water reservoirs. In some cases, limited water migration was also a result of underestimation of SAP absorption capacity, bringing about locally occurred self-desiccation and formation of ink-bottle porosity. Although little understood, curing fluid release from SAP may be however also dependent on matrix development state and for some IC agent type taking place after depercolation occurs [Sol 12]. These events should be visualized in capillary pressure measurement which will be investigated in Section 5.2.

One way to force the water migration from SAP and water movement as such is production of moisture gradient. This can be obtained when empowering the effect of drying due to hydration origin with effect of drying to ambient on condition that the relative humidity of new environment is lower compared to that of sealed concrete. The tests performed at 20 °C and approx. 60 % RH were finally combined with record of the shrinkage strain acquired from the drying initiation moment, which served as additional and indirect information on potential matrix changes the mass loss has caused.

[101] In theory, capillary suction could be considered as the driving force for water diffusion into the porous material [Sol 12]. On the other hand, it is recognized that in material with SAP other more effective way of water release from the IC agent might be taking effect. One proposal is to consider IC as 'demand-supply' mechanism [Wyr 11], acc. to which internal reservoirs supply water that instantaneously and completely fills empty pore volume created due to the hydration process (i.e., the chemical shrinkage) until all water stored by SAP is withdrawn. Acc. to own judgement, self-release of IC fluid like that observed in behaviour of own SAP in cement filtrate (Sections 4.2.2 + 4.3.2), changes in pore solution composition, as well as water release due to changes in disjoining pressure should be considered as important parts of effective IC working mechanism.

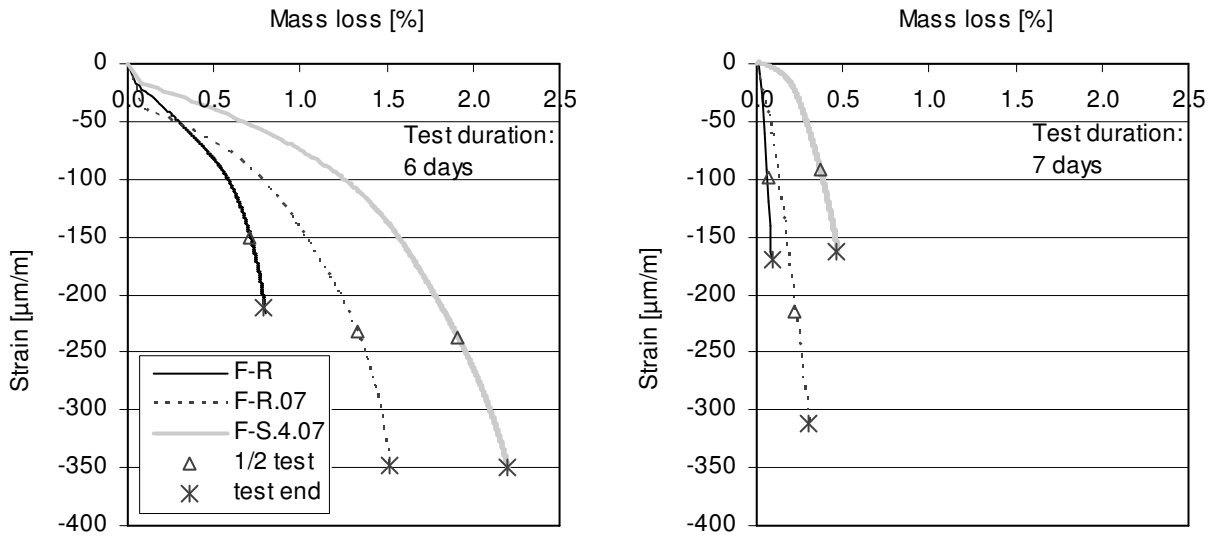

Figure 4.76: Mass loss-total shrinkage relationship for control mix and exemplary UHPC incorporating IC as well as concrete with equivalent amount of extra water after the exposure to ambient at concrete age of 1 day (to the left) and 7 days (to the right). The same legend applies to both graphs.

Figure 4.76 shows the obtained mass loss-strain relationships for the 6 and 7 subsequent days following initiation of drying at concrete ages of 1, 7, respectively. The new mixture in comparison is UHPC F-R.07 (containing the same amount of extra water as mix F-S.4.07) which was investigated to exclude differences in hydration degree attained due to varying w/c between mixes F-R and F-S.4.07.

It can be seen in course of each curve development, having somewhat bi-linear character especially in case of earlier drying initiation, that mass loss changes were accompanied by increasingly more pronounced changes of strain. This is logical relation given that gradually smaller/finer pores are being emptied in each system due to drying, resulting in more shrinkage developed for less mass lost. The exceptional attribute of UHPC with IC is however that although it exhibited highest mass losses, with or without simultaneous changes of shrinkage magnitude compared to control mix (for drying from age of 1 day and 7 days, respectively), the shrinkage increment per water loss was clearly the smallest among all mixtures tested.

The rule of thumb is that pore size distribution can be used to explain differences in shrinkage, indeed sometimes better than the mass loss [Bel 11] which is solely secondary information especially in system with water absorber [Sol 12][102]. In this spirit, as far as early

[102] In current discussion, porosity is considered to be common factor to changes in variables occurred. In general, if not related to change of surface-to-volume ratio of concrete element and the relative humidity of ambient air,

ages are concerned, the finding/result presented above could be interpreted as possession of coarser pore structure by the material with IC, whatever the mixture it is being referenced to (without or with extra water). Such understanding of matter is apparently in agreement with opinion of Kovler and Bentur [Kov 09] who associated the higher shrinkage for a given mass loss with water withdrawal from finer pores, here reflecting the concurrent to IC cases of F-R and F-R.07.

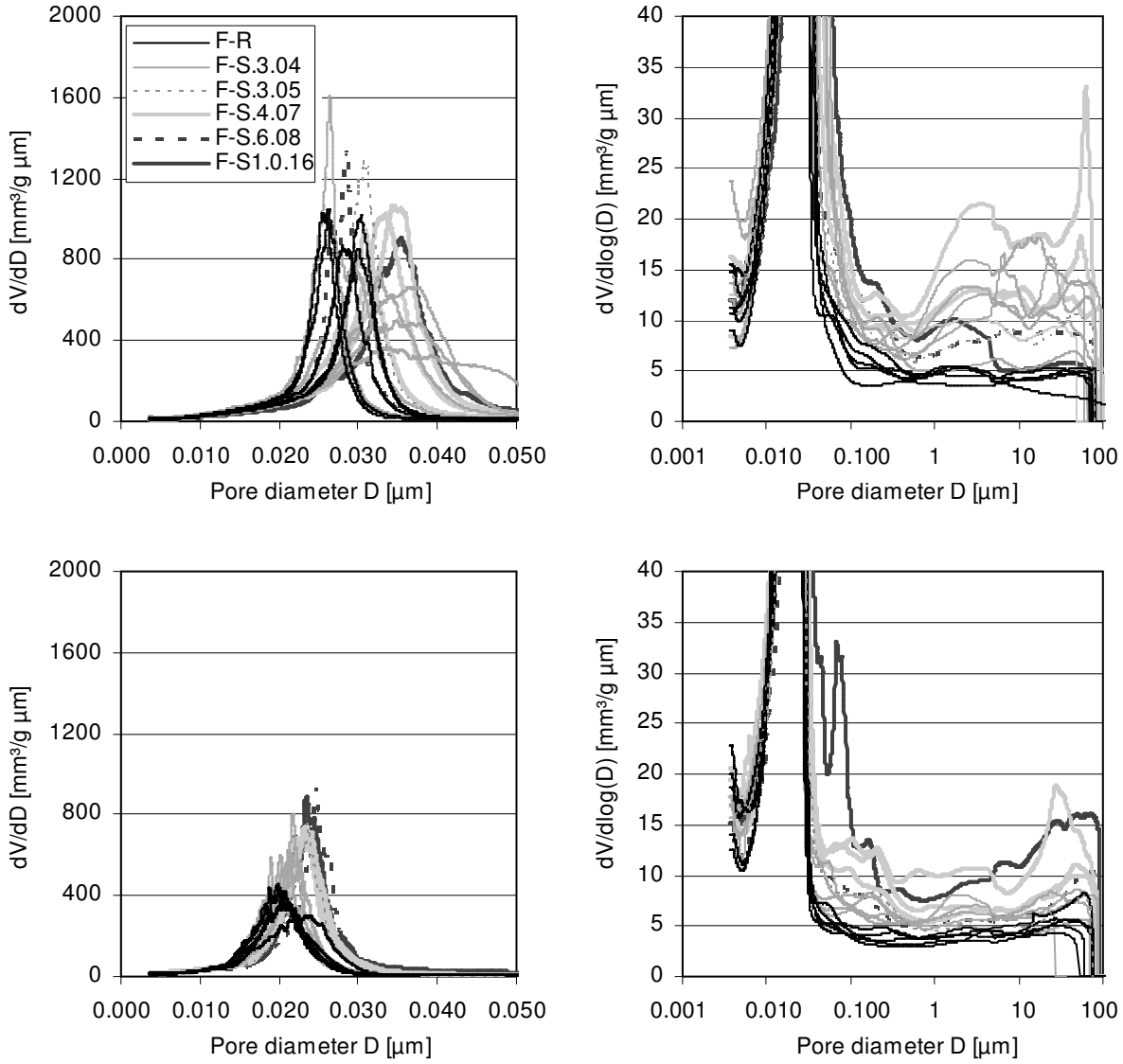

Figure 4.77: MIP pore size distribution for selected, sealed-stored UHPC mixtures at concrete ages of 1 day (top row) and 3 days (bottom row) with focus on small pore diameters (to the left) and entire measured pore range (to the right, logarithmic scale). The same legend applies to all graphs.

the mass loss is governed by porosity of concrete and characteristics of capillary pore system such as size and shape of the pores and their continuity (i.e. percolation), e.g. [Aït 97]. Similarly, both autogenous and drying shrinkage are influenced by the quantity and state of moisture in concrete, as well as pore structure characteristics, e.g. [Yan 05].

The microstructural change caused by IC, the extent of which notably increased with increasing amount of IC variables under sealed conditions (Figure 4.77), thus excluding the likelihood of overriding input of additional drying[103], is truly surprising given that the basic (effective) w/c of any of UHPC with IC was closer to that of F-R and always lower compared to that of F-R.07. The origin of this change will be discussed in the following subsection. Important enough though, particular finding compliments the observations made in Section 4.2.3 and apparently yields new contribution of IC to shrinkage reduction which is lowering the capillary stress according to well-known inverse relationship of variable to pore diameter and/or larger distancing of the solid phase in UHPC with IC (the idea visualized in Figure 4.72), being as favourable change if capillaries participation in shrinkage is negligible as hypothesized [Bel 11].

Looking again at Figures 4.76 and 4.77, the feeling is that 'coarsening' pore structure of system with IC holds true also for later ages. This especially regards the comparison case of UHPCs F-S.4.07 and F-R.07 where the advantage of modifying the system with IC became somewhat more pronounced than in younger ages. Nonetheless, when the mix being referenced to is F-R, the effect is seen to loose on strength and to vanish around the concrete age of 3-10 days, the exact age strictly depending on curing/test conditions.

Notably, as the hydration progresses with time and gains in rate due to presence of IC (Section 4.5.4), much denser internal microstructure develops limiting exchange of moisture with surrounding environment (i.e. reduced influential depth) as well as lowering diffusion characteristics. Still, another observation is that some difference in behaviour remains between the same systems tested under sealed conditions (see Figures 4.64-4.67) compared to additional drying to ambient (Figure 4.76) for equivalent periods, with the effect of IC being evidenced only in case of former. That is to say, coarsening of pore structure could be considered as solely one mechanism leading to reduction of hygral shrinkage, which was taken into account when comprehending mechanisms behind autogenous shrinkage in the following subsections. E.g. in presented case, owing to further limitation of moisture influential depth by the relatively large geometry of tested specimen (i.e. second main finding to be read from Figure 4.75), this could be linked with particular effect of IC on autogenous

[103] Note that drying to ambient can affect the degree of hydration and consequently autogenous shrinkage, leading to autogenous shrinkage overestimation error that was discussed previously. However, since the same change due to IC is observed under sealed conditions, the importance of drying to ambient can be considered as only secondary.

shrinkage. It may be the single type of hygral volume change that the core of the specimen undergoes (in analogy to interior of large concrete mass [Aït 97]) and it is reduced by IC. In doing so, IC reduces total shrinkage of UHPC as well, be it due to otherwise significant contribution of autogenous shrinkage to total shrinkage and/or owed to the effect of self-restraint.

Finally, some limitation of the coarsening phenomenon in general should be noted. While it may be the effect triggered by particular SAP used (copolymer of acrylamide and acrylic acid), and be perhaps empowered by inability of hydration front to progress into the pore created by particular absorbent material (meaning that more hydration products are preferably formed in the UHPC capillaries), other IC agents may behave differently in line with results of recent studies [Siramanont et al. 2010 *Ibid*. Sir 12][Kle 13].

- the discussion on the origin of pore structure changes and parameters decisive for underlying phenomenon

In view of findings just presented, it is important to point out an apparent paradox evidenced in case of mixture F-S.4.07, in particular larger capillary pores' size in system that finally, as also evidenced by Soliman [Sol 11] as in own tests (Section 4.5.4), is hydrated more than IC-unmodified one. The paradox is however only virtual. Both alterations regard different ages, except for the short overlapping stage. Indeed, larger capillary pores' sizes are specific mainly until age of 1 day and undergo significant reduction beyond this time-point, see Table 4.2 or Figures 4.76 and 4.77, for instance. This extra time is needed so the greater changes in hydration process start to manifest themselves for mixture with IC.

Although input from early modification of the pore system by premature release of curing fluid cannot be entirely excluded (Section 4.3.4), much more plausible explanation of such behaviour could be related to autogenous swelling phenomenon. Its overall contribution to shrinkage opposition may be explained on the basis of two competing influences suggested for low porosity systems [Odl 72a] and some further input which in investigated materials results from IC. Note that unlike in UHPC without modification by IC, where the surface tension of the water (or other phenomenon) pulls the pore walls inward causing the concrete to shrink [Tam 12], size of porosity does not decrease immediately. Indeed, in UHPC with IC, empty porosity created due to the hydration process and the capillaries as such are likely to be instantaneously filled with curing water coming from SAP, e.g. [Wyr 11]. This means

relatively more hydrates filling water-filled pores, except for the spaces where SAP is accommodated (excluded in own case, see Section 4.2.2). On one hand, the consequence of this action is accumulation of hydrates having larger volume than that of unhydrated cement. This leads to the pore volume reduction. On the other hand, given that the size of pores is small and their volume is limited (the effect of low w/c of UHPC produced), internal pressure (crystallization pressure) builds up. If stiffness of the paste and restriction of pore walls to the crystal growth (confining pressure) are still low, microscopic swelling and consequently increase of the pore volume available for hydration are allowed. That is to say, the effect of IC on porosity is likely to be complex function and depends on concrete age as well. In early ages, microscopic swelling might be contributing to pore volume/size increase and be prevailing over pore volume/size decrease due to filling of capillaries with hydrates, the net result of which is reflected in e.g. increased average pore size when IC is present (see Table 4.2). This means no direct evidence for expected increase of degree of hydration (Section 4.5.4), perhaps not even at 3 days and upon increase of IC variables to very high contents (see Figure 4.77 and [Dud 10c][Moe 10] for details of results for 28 days).

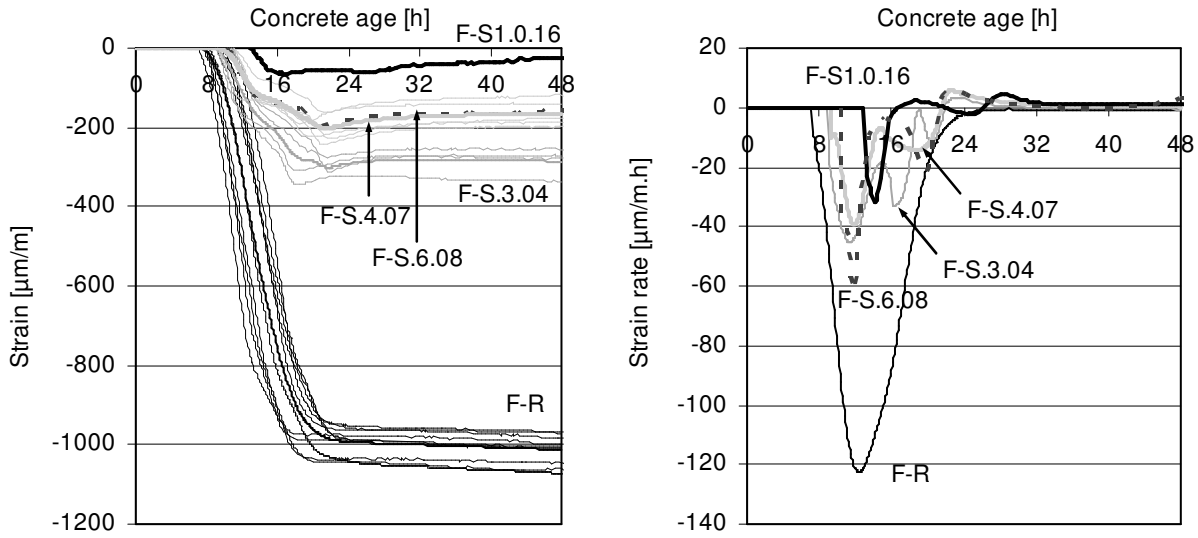

Figure 4.78: Evolution of free autogenous shrinkage of selected UHPC mixtures during first 48 hours (to the left) and corresponding strain rates as derived from singular measurement or the average responses (to the right).

Potential shrinkage compensation mechanism related to the crystallization pressure (which with high likelihood was evidenced in shrinkage-time curves, see Figures 4.43, 4.44 and, for more mixtures with IC, Figure 4.78) can be associated with two hydration products, viz. ettringite and portlandite [San 11]. The first hydrate type is being produced in UHPC under study from very early ages [Moe 10] and perhaps involves C_4AF phase in the production process similarly to case of some systems with low C_3A content in the binder component [Ben

01c]. Validating the input to further extent, it is recognized that the size of crystals of the specific hydrate is small [Moe 10], in fact much smaller than one observed in more conventional concrete which is however advantageous property from perspective of crystallization pressure exerted and the final the expansive behaviour exhibited [Okushima et al. *Ibid*. Coh 83]. In comparison, in the selfsame system portlandite nucleates and grows mostly within first 2 days [Pfe 10] starting presumably around setting time (being strictly attributed to usage of new generation superplasticizer [Ron 02]) and this also coincides with the critical period of shrinkage compensation observed. That is all to say, there can be more than one contribution related with crystallization pressure in the shrinkage compensation mechanism.

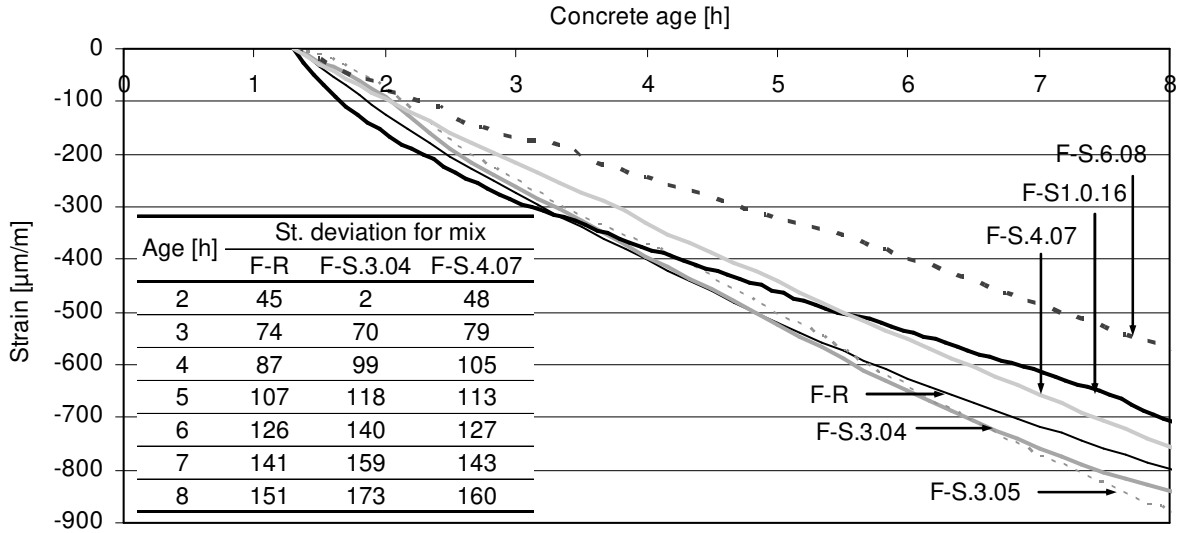

Age [h]	St. deviation for mix		
	F-R	F-S.3.04	F-S.4.07
2	45	2	48
3	74	70	79
4	87	99	105
5	107	118	113
6	126	140	127
7	141	159	143
8	151	173	160

Figure 4.79: Evolution of free autogenous shrinkage of selected UHPC mixtures before setting.

The evidence of expansive stresses or other mechanism governing phenomenon in the preceding fluid state can be indicated as well. Figure 4.79 presents average autogenous shrinkage deformation curves for mixtures incorporating IC as well as control mix. Evaluation point was the shrinkage measurement start, i.e. after encapsulation and tube transportation to testing device but, simultaneously, excluding any time differences occurred between performing individual tests. For UHPCs containing highest amounts of IC variables (0.4, 0.6 and 1.0 % SAP), strains decreased either immediately or with only some delay, with the latter being attributed to retardation effect of IC (responsible for extension of dormant/induction period, see Sections 4.5.3 and 4.5.4) or otherwise limited number of shrinkage data for mixes F-S.6.08 and F-S1.0.16. Also here effect of IC could be related with ease of access to greater amount of free water. Its supply very likely reduces moisture gradients and the resulting differential expansion given local character of ettringite-triggered phenomenon [Ben 01c].

Phenomenon occurrence may thus validate well-known ability of some UHPCs to demonstrate positive strain before solidification [Hab 06a][Kam 08] just like during and after it [Sol 12], for which sealing curing condition applied needn't be hampering factor. Given the smooth change of shrinkage rate accompanying transition from fluid to solid, the effect provided could be also treated as renewed indication of the lack of the induction period during formation of ettringite [Odl 99].

The missing piece of puzzle in understanding the role of the mechanism in the shrinkage compensation process is the level of autogenous swelling produced in UHPC. When to perform brief literature study, an observation easy to make is that after hardening the positive impact resulting from the swelling must be balanced more in the material studied than in other IC-incorporating systems. This is evidenced by the lack of positive strains production in UHPC which is contrary to case of rival mortar-like silica fume-containing system [Gor 11][Sch 12c] (showing though very low AS of unmodified system!), and especially cement pastes [Lur 06][Ass 13] as well as aggregate-free cement-silica fume systems [Est 09] (both having higher AS of reference mixes than exhibited by the finely grained UHPC!). It could be interpret that after expansive stresses reach certain maximum, depending on IC variables used, the magnitude remains quasi-constant or tends to decline despite formation of additional amounts of specific hydrate phases. It is hardly a singular tendency for cement-based systems [Sub 02]. The high degree of restraint present in UHPC (from solid skeleton, aggregates, …), high stiffness (though lowered on application of IC!) as well as high relaxation rate of the material studied [Epp 10] could be forcing such behaviour.

Other as negative factors for the expansive behaviour could be still pointed out with linkage to the properties of reactive components used and specificity of the mix design. In compliance with review of Mather [Mat 70] and reasoning presented by that researcher in-depth, potential candidates are: high cement fineness, low aluminate phase fraction, insufficient (relative to large water consumption by ettringite!) quantity of free water, very high superplasticizer content and, although little understood even to date, specific stiffness, size, shape and surface texture of aggregate. Similar effect may be finally expected from the little hydration level experienced in the UHPC system.

- the discussion on specific matrix parameters affecting expansion and/or shrinkage reduction

A special attention should be devoted to specific changes occurred in the UHPC matrix. The rule of thumb is that for sufficiently high content of aggregate irrespectively of small [Win 94], intermediate [Est 09], or even high [Sch 12a] additions of silica fume, the Interfacial Transition Zones (ITZ) forms around aggregate grains as well as steel fibres (if present) [Sch 12a]. While occupying a very high faction of the total pore volume, these matrix regions can interconnect/percolate and in turn deliver new pathway through which the water, initially deposited at ITZ, can flow without restrictions e.g. in response to underpressure. It would be important benefit from shrinkage compensation perspective as migration of water from particular water-rich zones, with their percolation or not, might reactivate the hydration process in the surrounding bulk cement paste of the mortar.

The consequence of enhanced water migration would be swelling extent increase. However, while the true and complex ITZ effect on transport properties being still under debate [Mar 97][Won 09], this scenario from principle fails for any of the UHPCs tested especially if based on M2Q matrix. Indeed, upon very fine tuning and production of very small paste thickness (to be followed based on foregoing discussions in this section), the ITZ has been largely eliminated already in early ages as verified under microscope, see Section 4.2.3 and Figure 4.23. It means that in UHPC there could be another reason for the autogenous swelling phenomenon limitation compared to traditional mortar or concrete.

Given the substantial participation in matrix of UHPC, influence of air on same phenomenon must be concerned too. It is better known that depending on the size of bubbles or some other property, air can be potentially involved in modification of the shrinkage course at different stages of concrete life, beginning from plastic stage [Mor 01][Ham 06b]. This contribution could be originating from menisci formed by air voids [Mor 01][Ham 06b], their expansion/relaxation ability (buffer effect) [Ham 06b], changing concrete permeability [Won 11][Tam 12] or general functioning as conductor or insulator [Won 11], with last role being closely related to the potential self-sealing ability [Hea 98] (note: phenomenon rival to depercolation!) and depending on void saturation level [Won 11][104]. Simultaneously, because of its specific properties and sometimes accompanying transition zone with matrix [Won 09], the air-associated cavities initiate microcracking [Kus 05][Gra 10][Sch 02][Tam 12] which for

[104] Another important role of air bubbles should be recalled, viz. diluting of paste matrix. However, in view of other potential impacts, it is believed that the relevance of particular effect is secondary, but obviously requiring further analysis in future.

high-performance materials isn't excluded even at high relative humidity [Cha 82][Tam 00]. This suggests role of air to be also of restraint-type, being another factor to diminish swelling potential especially on increasing IC variables content which is noted to increase the entrapped air volume, see Section 4.2.3. Further studies are required though. E.g. upon introduction of very tiny air bubbles, Esteves [Est 09] observed autogenous shrinkage reduction. Surprisingly, the same outcome was observed for UHPC (Figures 4.64 and 4.65) when combining extra water addition with superplasticizer (and thus, as Figure 4.18 yielded, air content) reduction.

What present study importantly revealed, although indirectly (consider here the non-linear relationship demonstrated in Figure 4.17), on exceeding absorption capacity of SAP, reduction in air content may be plausibly expected too, somewhat similarly to addition of extra water without the IC agent [Dud 10b]. That is to say, overestimation of the extra water to be added to 'satisfy' SAP absorption ability, beside the obvious effect of pore continuity, may be another way to impact autogenous swelling extent.

It should be finally borne in mind that concrete volume could increase and thus diminish the effect of autogenous shrinkage due to reasons other than autogenous swelling. E.g. once concentration of shrinkage stresses occurs in vicinity of air bubbles or anhydrous cement grains (contents of both of which in UHPC are very high), and the tensile strength (insufficiently high, on the other hand) is exceeded, microcracking will take place, see [Kus 05][Gra 10][Tam 12] and [Hearn and Morley *Ibid*. Hea 98][Hea 99], respectively. While giving another potential reason for pore coarsening (via combination with ink-bottle effect, for instance), the unfavourable phenomenon would actually decrease the negative volume change occurred in agreement with [Pow 59][Mou 11]. Going even further, it would imply more microcracking occurred in system with IC to obtain any shrinkage difference. This opportunity shouldn't be excluded given e.g. more air entrapped in the IC-modified matrix (which may [Kus 05] although needn't be [Gra 10] coinciding with crack area/number increase), lower relaxation ability of UHPC with SAP[105] [Epp 10] and, owing to improved hydration and thus healing ability in UHPC with IC, intense filling of microcracks with hydrates stopping their closure. However, it would be also expected the curing fluid to be

[105] Studies can be found (e.g. [Ham 07]) showing the opposite effect of SAP/IC, i.e. increase of stress relaxation, although for different cement-based material under modification with SAP/IC. On the other hand, Assmann and Reinhardt [Ass 14b] found recently reduced tensile creep (note: to which stress relaxation could be related to) due to implementation of IC, again for different material than UHPC. They explained this by reduced microcracking due to IC This shows that related topic still requires further investigations in future.

released from SAP to counteract self-desiccation and thus lower cracking likelihood, which will be the subject of investigation in Chapter 5.

4.6.4 Summary and concluding remarks

Free autogenous shrinkage of two main UHPC matrices under modification with different amounts of IC variables and the SAP alone and furthermore varied by the steel fibres presence and addition of extra PCE amount (only in latter case) was studied. Measurements were carried out using two main test set-ups based on corrugated tube method developed by Prof. Jensen, with bigger one showing higher strain developed at early ages due to less efficient liberation of hydration heat from the centre of sample or other reasons. Third apparatus was used for validation of autogenous shrinkage results after first 24 hours and for additional purpose, in particular examination of total shrinkage, to be further combined with mass loss measurement in the discussion part.

Unless IC or SAP alone was implemented, the autogenous shrinkage of UHPC was very high and higher for finely grained (M2Q) matrix. Still, of the two, the former appeared more favourable solution to use as to extent of changes exerted in other concrete properties. Evaluation of operative IC mechanisms standing behind all combinations tested, i.e. implementation of both IC variable, pure SAP addition and adding SAP along with extra superplasticizer content, was finally aimed at as relevant argumentation existed, in particular underestimation of extra water with respect to SAP absorption capacity often met in practice with IC.

The reduction of autogenous shrinkage when SAP is added alone could be associated with strengthening effect due to limitation of hydration, reduction of shrinkage-operative porosity or higher suction (and thus curing water withdrawal) power, to be followed by changes in pore solution and potential favourable effect on C-S-H structure. Adding more superplasticizer and cancelling most of positive impact exerted by SAP alone was explained differently. Small reduction relative to control mix was preliminary attributed to potential early reactivity of belite, having positive impact with respect to autogenous shrinkage evolution according to Tazawa et al. [JCI 99]. Main downside of combining SAP and extra superplasticizer was possibility of building complexes (with hydrates, with SAP) and somewhat related limitation of absorption of IC agent, as validated on SAP material alone and in concrete.

Mechanisms related to water entrainment effect were analysed next. In view of curing water release failing to explain the changes occurred and being issue set for further investigation (Chapter 5), other theories were accounted for. Based on shrinkage-time curve, a potential positive contribution resulting from hydrate growth was found. It was supported by the finding of characteristic pore structure changes as derived from results from MIP (sealed specimens) and the total shrinkage-mass loss graphs. The influence resulting from matrix under modification with IC was eventually concerned too and was related to change of SAP absorption that affected capillary depercolation moment. It was concluded that other particularities of matrices e.g. higher content of air in case of M2Q-based UHPCs and lack of ITZ (Section 4.2.3) could have been decisive for the obtained results as well.

Overall, the results revealed little dependence of autogenous shrinkage on Young's modulus of concrete and the limitation of paste thickness to smaller value in case of M2Q matrix. The conclusion is that other mechanisms concurrent to capillary pressure could be effective, validation of which was among scopes of the Chapter to follow.

5 Mechanisms of IC

5.1 Introduction

Development of capillary suction can be one although needn't be the only way curing fluid is provoked to move from the tiny containers created by SAP, as stated in the literature review (Section 2.5.1 and 2.5.2). The capillary suction as driving force notably contrasts with very high relative humidity typically claimed upon modification of cement-based material with IC, i.e. as if only insignificant capillary pressure is needed to withdrawn the moisture out of the IC agent or from pore in which it has been accommodated.

In this section capillary pressure measurements are carried out to find whether it is the operative mechanism behind autogenous shrinkage, on one hand, and whether and, if so, when it undergoes expected reduction due to IC. As the investigation results do not give straightforward answers, the computer tomography investigation is performed and the findings are analysed in more detail, involving supplementary tests on SAP material. Eventually discussion on potential mechanisms of IC is continued using observations made and findings from Sections 4.6. Three starting points for putting forward the hypothesises are the close relationship between hygral volume change and the specific surface of aggregates, increase of pore sizes concerning different ranges of the pore size distribution, and eventually high likelihood of secondary contribution of capillary pressure mechanism to autogenous shrinkage. Presented mechanisms cannot be currently excluded due to experimental restrictions whereas present important value for future studies.

5.2 Capillary pressure investigation

Figure 5.1 shows the typical results of capillary pressure evolution until age of 1 day as obtained for both UHPC mixtures chosen, one without and one with IC, i.e. control mix (F-R) and mix with 0.4 % SAP and 0.07 of extra w/c (F-S.4.07), respectively. Some of the averaged results are presented together with the standard deviations. Time-points being selected for statistical evaluation from the whole testing period (note: to be continued in Figure 5.4) correspond either to characteristic events (peak pressure, end of individual tests) or pressures acquired at equal concrete age and appeared between these time-points.

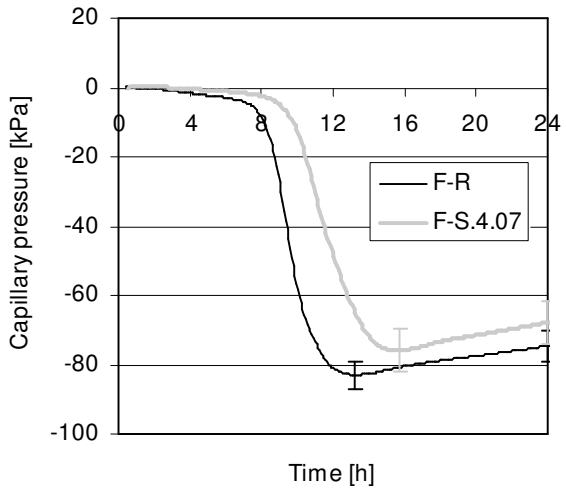

Figure 5.1: Evolution of capillary pressure for the control mix and UHPC with IC during first 24 hours.

It can be seen that both curves exhibited very much the same evolution pattern, irrespectively whether IC was applied or not. In fact, a straightforward segmentation of variable development into three well-recognizable stages is possible. The division includes: i) a phase of a constant pressure close to zero, ii) a phase of abrupt capillary pressure build-up, with acquirement of the negative pressure maximum, and eventually iii) a phase of further (though less critical from the shrinkage perspective) changes in the variable. Altogether, a pattern largely similar to that known for different cement-based materials of various w/c [Hab 06b][Mou 11] is confirmed. More complex patterns are yet acknowledged to exist too, e.g. [Kha 09][Bra 02].

Of the stages named certain ones can be ascribed to some characteristic phenomenon and hydration-relevant (therefore shrinkage as well!) event. E.g. end of phase one and onset of phase two well corresponded to concrete age when time-zero occurred and final setting time according to one of the standards (see Section 4.4.3) was noted. It is particular concrete age until which settlement has progressed to a very high extent (maximum, in general) and from dominating it became minor component of total volume change irrespective of IC. Interestingly enough, such an observation also justifies the choice of time-zero while explaining first main cessation moment in the shrinkage curve evolution. The phenomenological interpretation of the event could be: transition from a continuous to a discontinued water system which is reflected by development of gas-filled spaces, after [Mou 11]. Other correlations of the events may be yet found in literature, e.g. ascribing the moment of the abrupt rise in the variable to age beyond final setting time acc. to studies [Hol 01][Zhu 08][Ham 06b][Mou 11]. The matter as such is indeed very complex and always requires individual analysis[106]. The absolute capillary pressure values are lager than those in the

[106] The transition time, i.e. time when meniscus depression abruptly increases from zero, or non-zero value and its situation vs. setting points can be found to depend, among others, on w/c, presence of pozzolans [Cha 07], aggregate addition [Mou 11] and bleeding [Cha 07][Tia 14], if any. Being visualized in Section 4.3.2, standard chosen for measuring setting of concrete mixture might play here additional role as well [Gra 06c]. Similar concerns could be addressed for other analyses, e.g. the pressure-strain relationship, where efficiency of overcoming adhesive forces in the shrinkage set-up could be the most important masking effect (problem

studies being referred to. However, this also needn't be surprising given very fine tuning and very low w/c of the M2Q matrix tested.

The stage of major IC effect observed is stage ii. Upon modification with IC, it starts at a later concrete age compared to control mix. The changes exerted by IC/SAP in early hydration and discussed in Section 4.5.4 obviously played a role here. Plausibly for same reasons, and especially due to continued or otherwise newly initiated release of water from SAP, evident reduction in rate of capillary pressure development is observed (Figure 5.2). The finding is particularly important with regard to autogenous shrinkage that develops. In fact, by the time the selfsame capillary stress is generated, meaning comparable to F-R 'fine' water menisci appear in microstructure, the connectivity and thus stiffness of load-bearing skeletal structure is likely more advanced in case of mix with IC (F-S.4.07), with some evidence in ultrasonic measurements (Section 4.5.4). The resultant improved resistance to contraction force as well as the primary and secondary countermeasures (viz. water release and more pronounced stress relaxation due to extension of pressure development time, respectively) could thus effectively contribute to minimizing autogenous shrinkage. This is validated in Figure 5.3 showing the respective shrinkage curves (recorded on selfsame production date to exclude batch effect) and exhibiting clearly less volume changes occurred for F-S.4.07.

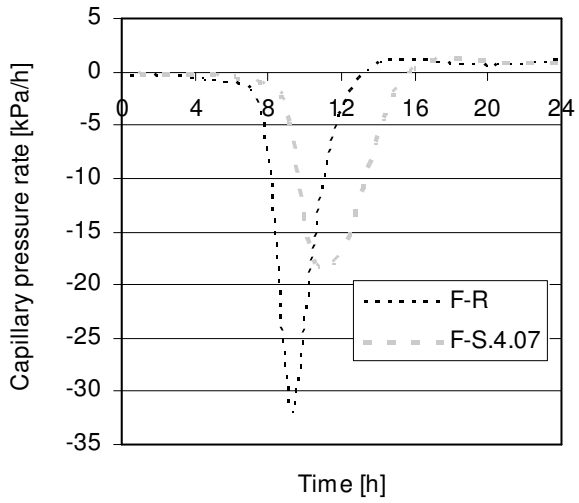

Figure 5.2: Rates of capillary pressure development for the control mix and UHPC with IC during first 24 hours.

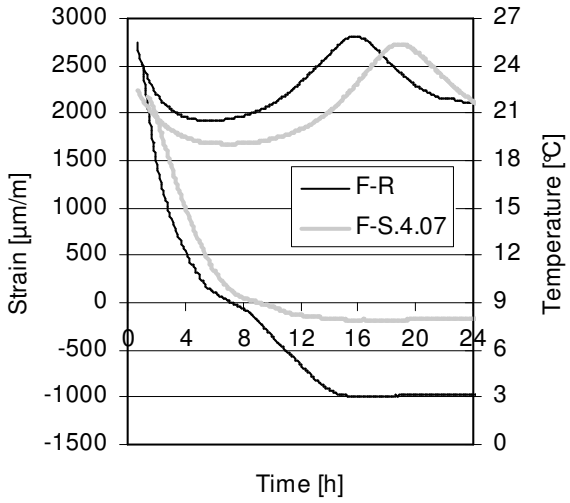

Figure 5.3: Evolution of shrinkage for the control mix and UHPC with IC during first 24 hours.

resolved in own study by using corrugated tube protocol for the AS measurements). That is to say, other correlations and situation of especially setting points with respect to capillary pressure evolution than the presented one seems plausible.

In view of observations made, however, it is rather surprising to acknowledge very similar values of the maximum negative pressure in both mixtures tested. On one hand, as suggested by the small standard deviation of results at this peak pressure (sometimes called breakthrough pressure, e.g. [Esp 07]), the precision of measurement remains very high even if solely local changes occurred in capillary network are finally captured within test [Bra 02][Geo 10a]. The extreme values of pressure recorded do indeed appear relatively far from the limits of operating range (0 to -103.4 kPa, with proof pressure of 206.8 kPa) and the boiling point of water (approx. 20 mbar = 2 kPa which corresponds to the gauge reading of -99.325 kPa at applied room temperature), both being relevant conditions for successful measurement. Any change occurring thereafter and especially the characteristic switch in variable evolution is again recorded systematically, with insignificant change of the value within same composition or even in comparison (Figure 5.4). Furthermore, the reduction of the absolute values spreads over period of few days. This means that during measurements pressure transducers were continuously in contact with the liquid phase of the capillary water and no percolation of air either in the tube (if any present) or in pore solution (tap water used!) at high negative pressure took place.

Some loss/collapse of pressure or even measurement stoppage at random times appears often unavoidable, e.g. [Hol 01][Esp 07]. This, on the other hand, may imply other reasoning for the findings. If not of phenomenological nature (for example: due to either local destruction of meniscus [Bra 02] potentially by cavitation [Ham 02] or bubble percolation and/or growth [Ham 02] in pore fluid (or tube) under negative pore pressure and less likely due to hydration heat-related changes), there could be an experimental reason involved.

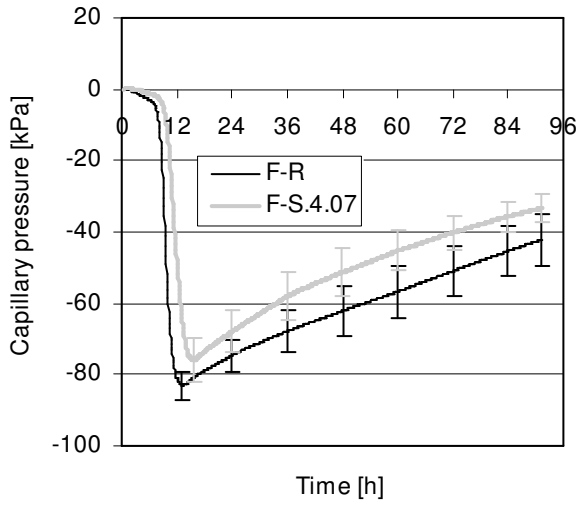

Figure 5.4: Evolution of capillary pressure for the control mix and UHPC with IC including later ages.

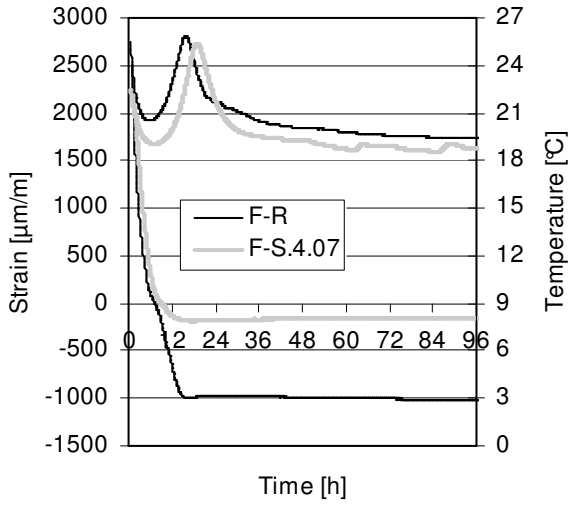

Figure 5.5: Evolution of shrinkage and hydration heat-related temperature for the control mix and UHPC with IC including later ages.

Acceptance of either interpretation would notably have crucial consequence with regard to role of capillary pressure. If to compare Figure 5.3 with Figure 5.1 or Figure 5.2, it is seen that main part of the autogenous shrinkage developed within first 24 h for the mix with IC (F-S.4.07) is recorded already before occurrence of breakthrough pressure. That is, evolutions of both variables seem to coincide very well for many hours after time-zero. However, this doesn't hold true for the control mix (F-R), for which deformation continued to develop mainly after the capillary pressure peak was reached. That is also to say, for particular mix, good match between the two regarded variables was lost in first hours after time-zero. As expected, in both cases, the variables' correlation appears vaguer in later ages when either no significant shrinkage develops (F-S.4.07) or only autogenous deformation is observed to increase for the mix without IC, see Figures 5.4 and 5.5.

The conclusion to be drawn from the experiments is that capillary pressure is not the main operative shrinkage mechanism in UHPC and, simultaneously, complex way of emptying SAP from water (other than suction at very low pore pressure) exists. Alternatively, it could be assumed that the measurement itself and especially in presented set-up arrangement is not fit for usage for finely grained materials like the tested M2Q matrix and study of IC effect. Both hypothesises receive a strong argumentation, see Table 5.1.

Table 5.1: Critical summary of arguments for and against accepting the hypotheses related to capillary pressure measurements.

Hypothesis	Argument	Counterargument
Negligible role of capillary pressure	• Direct translation of results obtained in very high RH range (> 99 %) maintained for several hours and big size of capillaries remaining water-filled in both systems, i.e. as if pressure only little depends on modification with IC. • In other studies: Necessity of including additional mechanism is AS modelling due to existence of stage with RH≈100 % few hours after setting [Zha 12a]. Also observed by Han et al. [Han 14].	• Very low capillary depression argued as being sufficient of triggering large deformation even for some hours after final set [Zhu 08]. • 'Buffer' role played by the air bubbles in pore fluid is possible in system irrespectively of IC introduction, in line with [Ham 06b].
	• Very little experimental support validating existence of straightforward relationship between shrinkage and pressure variable as derived from RH measurement in the first 24 hours, with exceptions [Jen 96][Ben 02][Zhu 08]. This is in contrast to later ages [Han 14], including UHPC [Lou 99]. • Furthermore, often very little differences in RH between systems without and with modification with IC are reported, e.g. [Est 09][Han 14][Jus 15].	• Every measurement being charged with some error. E.g. shortcoming of using certain sensors in RH measurement that is leading to readings of RH > 100 % (observed in case of UHPC too, e.g. [Ma 03]) is indicated and eliminated in [Gra 06a][Eka 09].
Specificity of the measurement in the test set-up used/Potential source of error	• Much lower values of capillary pressure are measured with pressure sensors compared to ones obtained using rival approach (RH measurement) and expected from pore size developed in typical microstructure (10-100 MPa).	• Due to osmotic effect and usage of semi-permeable filter (sponge-like membrane) in measurement preventing from effect of dissolved salts in the pore fluid, otherwise affecting RH reading [Lur 03]. • Satisfactory, if not very good, conversion of sensor-measured pressure into effective pore pressure, at least for the beginning of self-desiccation [Geo 10a]. • 'Buffer' role played by the air bubbles in pore fluid is possible in system irrespectively of IC introduction, in line with [Ham 06b].
	• In hardened concrete, experimental errors in sensor measurement very likely derive from very high autogenous shrinkage exerted on the tube (case of the control UHPC mix) as well as general and gradual clogging of the protection membrane with hydrates at concrete-contacted tube tip (both mixtures tested). Sealing water in tube off from concrete possible!	• Clearly less studies validating applicability of capillary pressure measurement beyond semi-liquid state, with very few exceptions, e.g. bleeding cement-based materials [Tia 14]. • High stiffness of the tube used in own set-up, confirmed qualitatively, e.g. no deformation in funnel drawn in concrete and associated with the tube.
	• Confirmed influence of sensor preparation protocol on results, see Figure 5.6.	• Obvious change observed in values but not in tendencies. E.g. similar value of negative pressure is captured for mixes without and with IC using rival protocol.

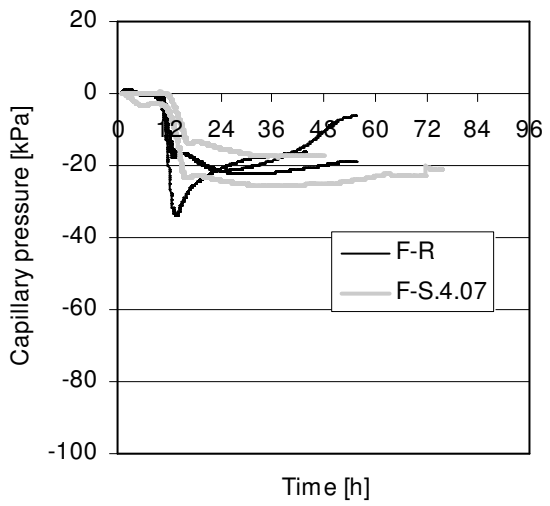

Figure 5.6: Results of the preliminary studies of capillary pressure using the finally rejected sensor preparation protocol. Usage of another batch of concrete components is acknowledged as well.

The true reason for observation might be of secondary importance given the ability of swelling (see mechanism for shrinkage reduction discussed in Section 4.6.3) to occur after setting even in presence of negative pore pressure [Ham 02]. Nonetheless, to obtain more comprehensive view, and particularly to follow sensitivity of water release to pressure changes, supplementary experiment, in particular Computer Tomography investigation, was conducted and the results are presented in the following section.

5.3 Computer Tomography investigation

- distinction between porosity created by SAP and air voids

It has been experienced in preceding parts of present study (Section 4.2.3) that the finely grained UHPC examined may contain few percent of air. It was further noted its entrapment solely increased with application of IC. Therefore, important preliminary step towards analysis of CT results obtained was recognition of the porosity emerged specifically from accommodation of IC agent particles in the matrix of UHPC.

Hereafter addressed as SAP porosity, voids formed by swelled SAP particles were imagined to be initially water-filled in accordance with hydrophilic nature of polymeric material used. On one hand, this forced difference in densities between concrete components as expressed by the change of gray scale; the sine qua non for successful applying CT measurement was therefore fulfilled. On the other hand, the density variation was assumed as being relatively small in comparison to that associated with entrapped air.

The verification of particular issue can be based on Figure 4.25 which was presented in Section 4.2.2. However, beside limitation to one time capture, the scaling applied in regarded case was relatively small making overall picture somewhat blurry and trustworthy only to limited extent. More detailed analysis could be therefore made based on another image (Figure 5.7) demonstrating two major insertions in exemplary piece of the M2Q matrix, including an air void and a SAP-induced pore. Here and for all analogous CT results to follow

(including those presented in Appendix H), sequence of images addressed by letters a to d in alphabetic order yields increasing concrete ages as chosen for scan execution. Four scans were performed in total: at 10.5, 13.5, 18.5, and 34.5 hours, starting from age corresponding to time-zero for the tested UHPC with IC (F-S.4.07), see Figure H.9 in Appendix H. The test ended when no significant mitigation input from IC could be observed, this being assessed based on evolution of shrinkage curves for control mix and that modified with IC in time. The time intervals between the scans were finally adjusted taking into account working hours given the necessity of each scan to be initiated manually.

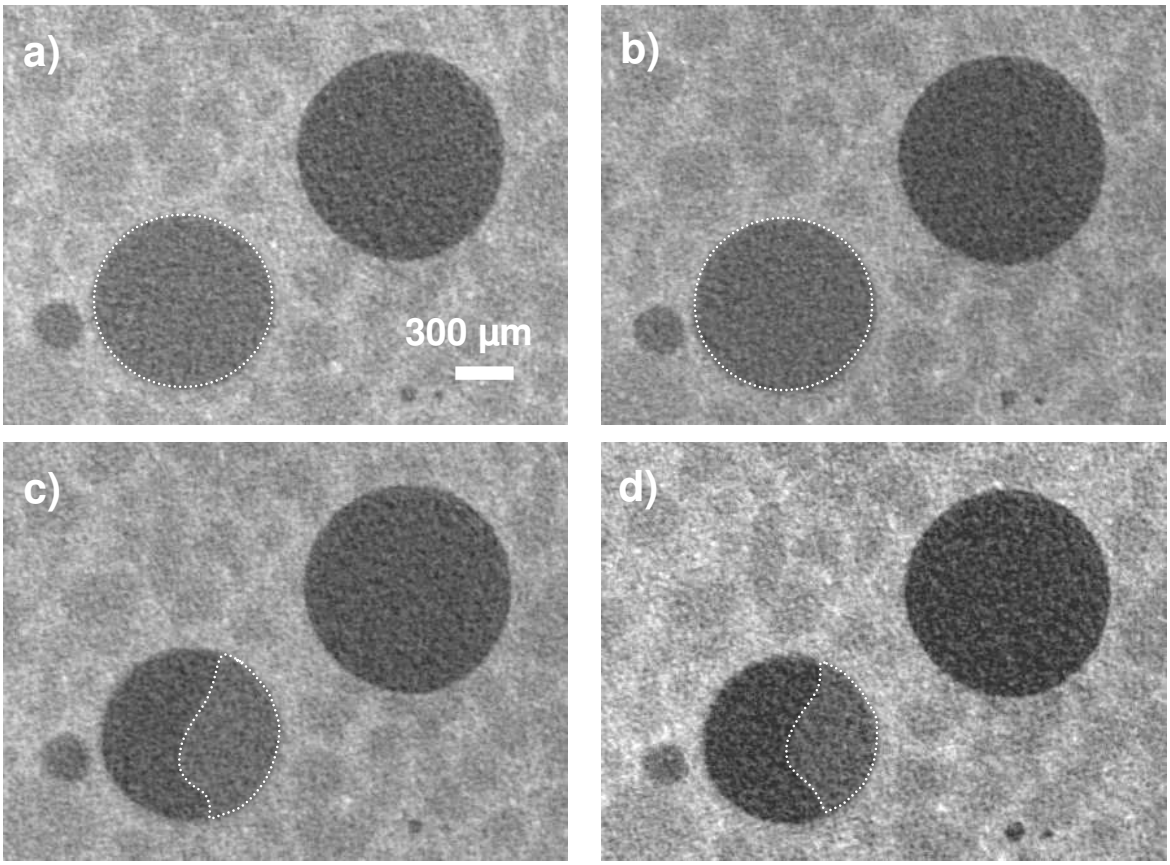

Figure 5.7: Exemplary modes of changes in pores created from accommodation of entrapped air and SAP in the concrete matrix. Each of the pictures shows piece of one particular slice focusing on the selfsame place of interest and being obtained at identical sample height. The growing alphabetical labelling reflects the following increasing concrete ages at which the CT scans were carried out: a) 10.5 hours, b) 13.5 hours, c) 18.5 hours, d) 34.5 hours. The same scale given in case a) applies to all pictures.

Although geometrical appearance of both types of voids was similar (i.e. identical spherical shape of pores, often similar size), one feature clearly differentiated the inclusions. In particular, only in the case of SAP porosity, the void was intruded by extraneous object. As was signalized before in Figures 4.15 and 4.16, is visualized in Figure 5.7 and will become ever clearer in the following section and extended by Appendix H, this object underwent certain geometry alterations. This excluded occupying the void by hydrate phase and implied

water content fluctuations likely due to response to change of boundary conditions in hydrating medium or other. Such behaviour could be only associated with that specific for IC agent particle. In contrast, constitution of the gas-filled porosity remained free of any deposits, the observation which held true throughout the whole measurement. On this basis, distinction between porosity created by SAP and technologically entrapped voids was made possible.

Because particularities of IC particles volume changes in other slices differed depending on part of concrete studied, it was decided to investigate particular aspect in greater detail, as discussed in the following.

- modes of changes in SAP porosity

Assuming amount of fluid carried by the IC agent is sufficient for the purpose of IC (meaning also SAP is stable enough for the purpose, see Section 4.2.2), effectiveness of the process will depend on two further conditions which need to be fulfilled first. This includes ability of IC agent to release the curing fluid when it is needed and capability of the concrete's matrix to allow its transport to the water-poor areas, i.e. ones suffering from self-desiccation. Although to different degree, all three could be followed indirectly based on observations of SAP volume changes in the corresponding porosity.

Selection of the most common mode of alterations occurred in fragment of exemplary but representative slice is exhibited in Figure 5.8. The trend only partly expected from the role of IC in mitigation of autogenous shrinkage and clearly in contrast with capillary pressure test implications was revealed. In particular, after first two stages of the fluid dispatch (scans a and b), as reflected in decreasing size of SAP and partial detachment from pore wall and to be interpret as counter-response to self-desiccation or other, a restart of fluid absorption was observed (scan c). After this process terminated, polymer resumed shrinking again (scan d). It was characteristic behaviour that repeated on more occasions. In fact, this trend did not change neither when SAP lost portion of fluid carried while maintaining quasi-full or only partial attachment to the pore walls, nor when SAP underwent some fracture or even when assemblies of the small IC agent particles appeared, see corresponding Figures H.2-H.5 in Appendix H. To best author's knowledge, because of the interruption moment occurred, this is new, unreported SAP behaviour in concrete which without adequate mitigation measure is susceptible to high autogenous shrinkage.

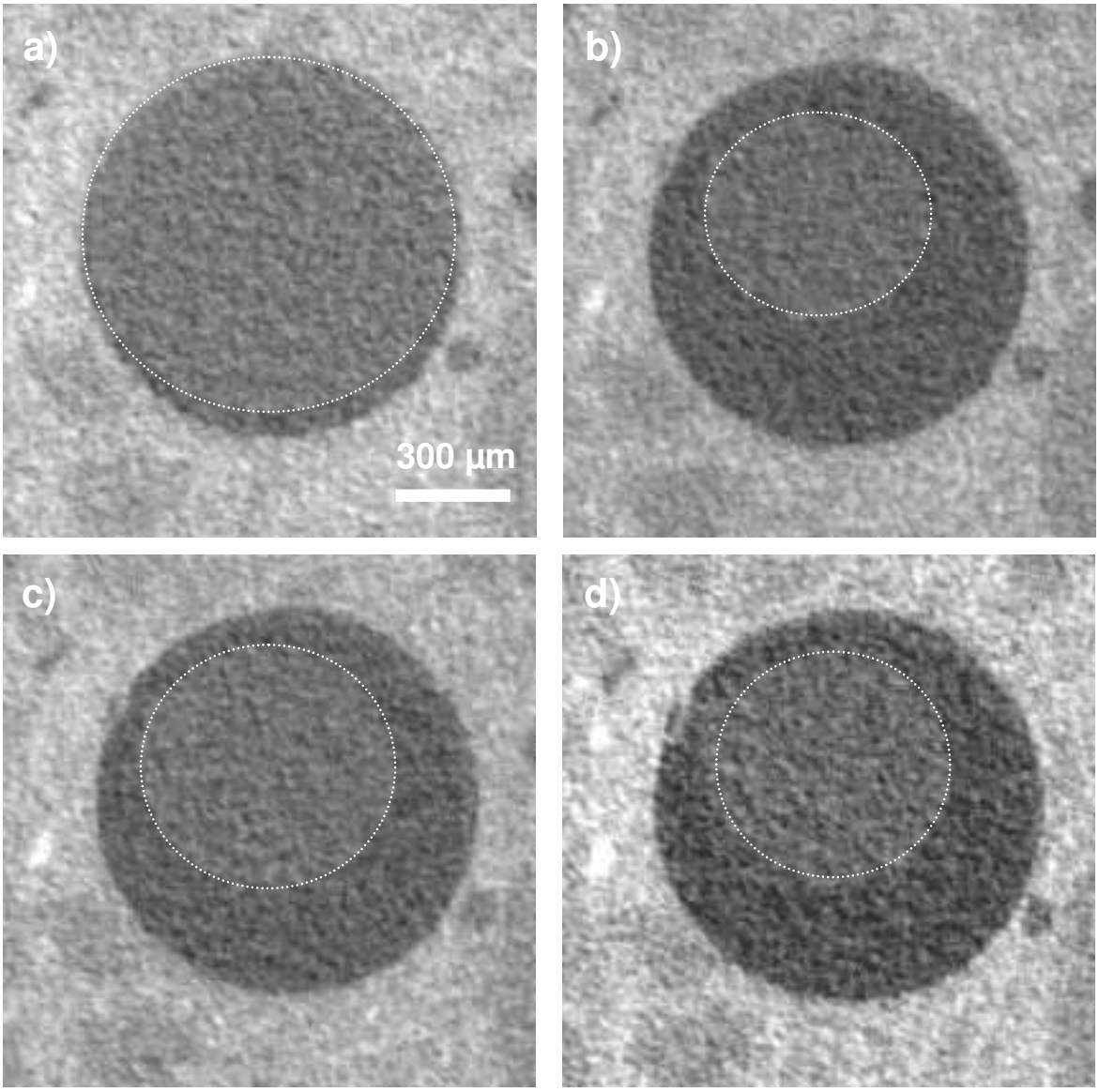

Figure 5.8: The main mode of changes in pore created from accommodation of SAP particle in the concrete matrix. Each of the pictures shows piece of one particular slice focusing on the selfsame place of interest and being obtained at identical sample height. The growing alphabetical labelling reflects the following increasing concrete ages at which the CT scans were carried out: a) 10.5 hours, b) 13.5 hours, c) 18.5 hours, d) 34.5 hours. The same scale given in case a) applies to all pictures.

Notably, the SAP behaviour recognized in general and reverse of the water migration in particular has one important implication in terms of role of IC in mitigation of autogenous shrinkage. Figure 5.9 addresses another characteristic mode of changes in SAP porosity[107]. Apparently, it was noted that a different particle of SAP didn't undergo the negative volume transition in the associated pore, at least not until concrete age was many hours (scan d). It could mean that in preceding time, only some insignificant amount of curing water was transported from SAP to shrinking matrix, if any. The SAP particles showing similar behaviour were in fact numerous, see e.g. Figures H.6 and H.7 in Appendix H. In presented

[107] It is author's belief that Figure 5.9 combined with Figure H.4 yields one manner of changes in the SAP structure. This requires however further tests.

case, however, also a period occurred, this being intermediate stage of testing period (scans b and c), when IC agent tended to gain more water. And although this observation was initially stated based on subjective judgement (following changes in the intensity of grey), it seemed to confirm existence of selfsame trigger which in Figure 5.8 led to SAP volume increase[108].

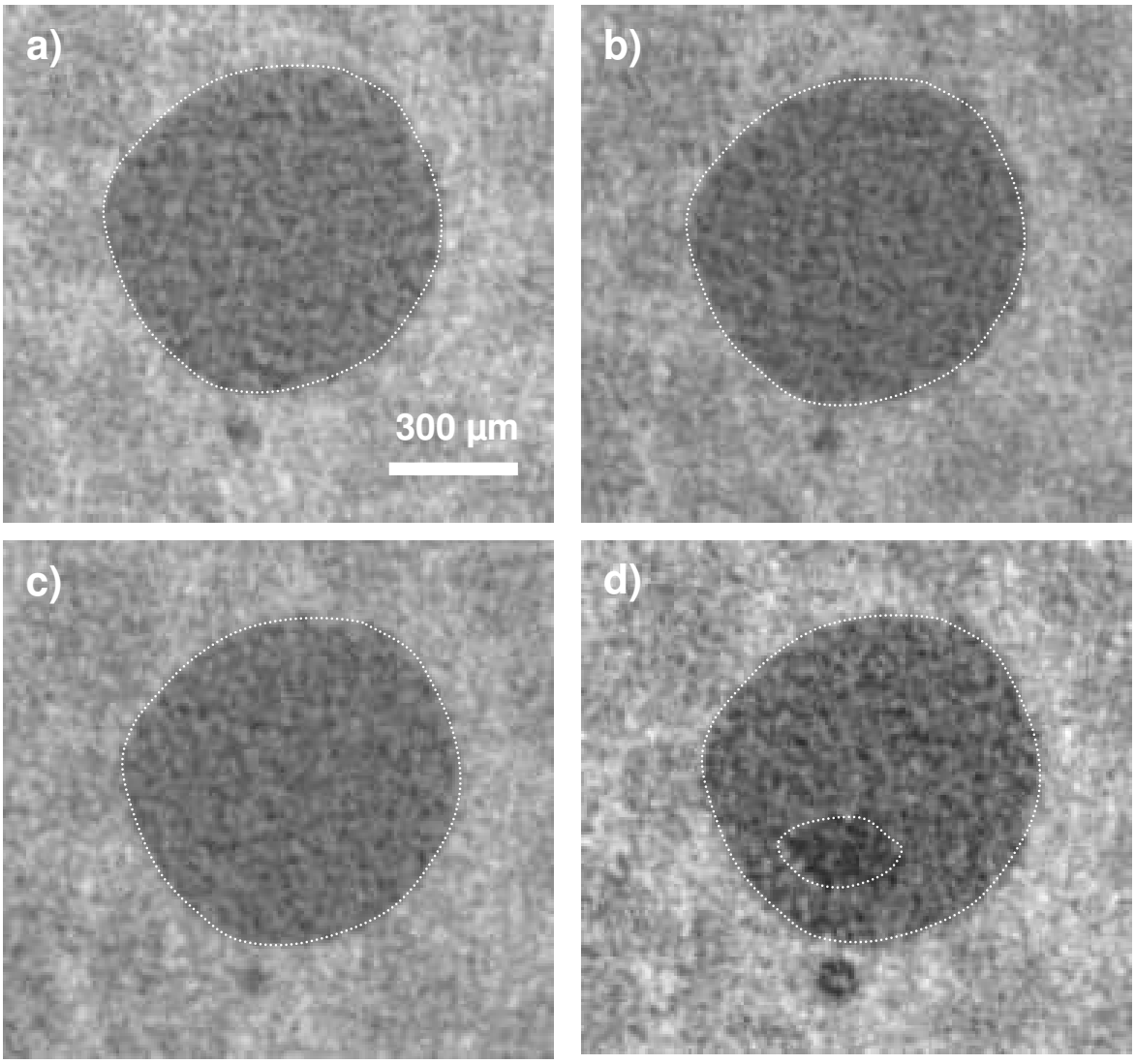

Figure 5.9: Rival mode of changes in pore created from accommodation of SAP particle in the concrete matrix. Each of the pictures shows piece of one particular slice focusing on the selfsame place of interest and being obtained at identical sample height. The growing alphabetical labelling reflects the following increasing concrete ages at which the CT scans were carried out: a) 10.5 hours, b) 13.5 hours, c) 18.5 hours, d) 34.5 hours. The same scale given in case a) applies to all pictures. Comparing scans b) and c), potential intensification in the grey scale can be observed although no differential pictures could be obtained to verify this due to limitations of the method. First very clear loss of water from SAP (the dark spot) is to be observed in scan d).

It should be taken into account that in environment of concrete, all SAP particles are swollen only to limited extent. In fact, due to load acting on IC agent and upon specificity of fluid that is being absorbed (pore solution), not only swelling volume (swelling ratio) is far from the

[108] Please note that production of another evidence to support the statement – differential grey picture – turned out to be inconclusive due to particularities of the CT measurement.

maximum, also it is hardly stable one. Should certain favourable changes in pore solution composition be experienced owing to ongoing hydration (to be further discussed in Section 5.4), SAP volume increase may be provoked. In case of situation presented in Figure 5.9, however, the conditions during these changes are very special. Firstly, the increase of water content inside SAP is recorded when the matrix of concrete with IC still undergoes some shrinkage (see Figure H.9 in Appendix H for more details). Secondly and more importantly, potential swelling of the SAP particle takes place in cavity, particularly pore, constraining its volume. Therefore, given no growth of the size of the pore, external compression becomes induced on the swelling gel particle, meaning between scans b and c SAP reswells under load. The result is occurrence of and then increase in the swelling pressure, which is a phenomenon being successfully used e.g. in design of self-repairing sealing materials' concept based on SAP [Wac 07]. This pressure may reach up to few MPa acc. to [Wac 07][San 04] and, if so, effectively contribute to the resistance against contraction forces otherwise leading to autogenous shrinkage[109].

Scenario as described above could be interpreted as other, rival mitigation mechanism to one put forward by Soliman and Nehdi [Sol 12] who claimed likelihood of SAP particle swelling and, consequently, exertion of UHPC expansion yet strictly on access to extra water source. Both findings highlight important role of shrinkage balancing mechanisms in evolution of the autogenous volume change. Although the source of the pore fluid to be absorbed by SAP under investigation in the intermediate stage is not very clear, it is reasonable to believe that some free water may become available due to its sudden release from other neighbouring SAP particle (like one to be presented in Figure 5.10).

5.4 Triggers to water release mode changes

- discussion of triggers of renewed fluid uptake by SAP

The cause of renewed fluid uptake by SAP is not straightforward. At least two very different reasonings appear as plausible.

Taking into account observations made in [Bow 91][Sir 12], it could be assumed that the phenomenon is brought about by exchange of the counter ions in polymer part associated with polyacrylamide as triggered by hydration-ascribed changes in pore solution composition. To

[109] The effect of locally observed phenomenon might be, to some extent, compared to the microscopic swelling that is induced by the swelling gel product of the alkali-silica reaction, and appearance of which in UHPC of composition similar to the tested one was in past recorded as well [Pfe 09].

test this hypothesis, preliminary EDX tests were conducted on oven-dried SAP previously swollen for 20 minutes in cement paste filtrate, composition of which was additionally varied by the presence of silica fume and PCE (added in proportion to cement identical to that used in M2Q matrix). For comparison, pure SAP material and one after contact with distilled water for identical time of 20 minutes followed by oven drying were examined as well. All obtained results are presented in Table 5.2. For appearance of materials after the treatment, please also see Figures 4.11-4.14 in Section 4.2.2.

Table 5.2: EDX test results for pure SAP material and one treated with different fluids simulating behaviour in concrete with subsequent drying to constant mass.

Material tested	Content [mass %]									
	C	**N**	**O**	**Na**	**Al**	**S**	**Cl**	**K**	**Ca**	**Cu**
Pure SAP, dry	45.4	9.4	35.3	9.4	-	0.1	-	-	**0.3**	-
SAP + distilled water, dried	45.2	10.6	37.1	6.9	-	0.2	-	-	-	-
SAP + pore solution with PCE, dried	23.1-59.8	-	34.3-49.6	0.6-9.0	0-0.2	0.3-5.9	0-1.3	**0.7-3.3**	**1.6-10.3**	0-0.1

It was found that monovalent ions of potassium were absent in the SAP product as delivered. However, they become present as soon as contact of polymeric material with any of filtrates tested was made. In fact, complexation of cations with carboxylate groups seemed to be as clear for K^+ as for Ca^{2+}, even if the former species tended to bind to polymer network less intensively likely due to low content of alkalis in cement used in study and not due to lower ion valence. It yields comparable observation to that made by Lam and Hooton [Lam 05] for SAP in concrete, which for own IC agent was again confirmed with combined ESEM/EDX test. As known, the bond provided by Ca^{2+} is relatively weak one [Zhu 15] and can be broken down in favour of pure charge screening effect, e.g. that related to monovalent ions [Bow 91][Sir 12]. The likelihood of this mechanism to happen increases in light of gradual early initiated release of alkali (from the dissolution of the alkali sulphates) leading to their concentration increase in pore solution of ordinary Portland cement as well as simultaneous calcium ion presence decrease (due to hydrate formation) in pore solution of ordinary Portland cement, see Figure 2.7. Should the cation substitution take place, there would be weakening of the swelling restriction set by the additional ionic cross-links. The resultant volume change would be analogous to behaviour of SAP after transferring from calcium-rich solution to sodium-dominated one as presented in [Sir 12].

Important in other respect, the cations once absorbed, the action which apparently can take even when water is being released from SAP [Shu 11] and thus theoretically already during initial stage of distributing IC water (case a and b in Figure 5.8), remain trapped within polymer structure [Sir 12]. This is another one reason why effectiveness of IC remains on very high level. In particular, when some mixing water is 'lost' from pore system and enters SAP causing it to re-swell, some alkalis have been already or are being removed from the pore solution. This fact is important since alkalis like potassium can be at the origin of numerous changes in concrete microstructure, e.g. [Ben 06][Bel 08]. In particular, when some alkalis are removed from pore solution, fewer cations being surrounded by so-called solvation or hydration shells [Bel 05][Bel 08][Wit 09] and having, important enough, smaller ionic radius compared to K^+ cations, e.g. Ca^{2+} [Ben 06], remain in space between the hydrates. Simultaneously, correlations among divalent counterions undergo strengthening, irrespectively whether the content of these ions changes in response to occurred diminution of K+ concentration, or not. Lower disjoining pressure attributed to both leads to a smaller equilibrium distance between C-S-H gel particles (= gel with lower total water content = smaller degree of swelling) resulting in lower macroscopic deformation of cementitious material once self-desiccation occurs, if any[110].

Other important influences attributed to alkalis commonly involve changes in C-S-H gel morphology, molar volume as well as an acceleration effect on early age hydration, e.g. [Ben 06]. Accordingly, as some alkalis are removed from the pore solution and their concentration decreases, de-percolation of the capillary pores in system with IC/SAP is expected to occur at higher degree of hydration and lower porosity. This means later hydration age as compared to system without IC. Given that the transport properties, i.e. permeability, sorptivity and diffusion, depend on the interconnected pores, movement of water from neighbouring water-rich zones might be more efficient and thus in favour of lower autogenous shrinkage when IC is present. Finally, by reducing negative effect alkalis have on water activity of the pore fluid and the Kelvin's component of RH [San 12], development of lower shrinkage inducing (capillary) stresses is expected in system with IC; this and potentially higher stiffness/strength in systems being less alkali-rich [San 12] are another two arguments speaking for no negative outcome of occurred SAP reswelling in terms of autogenous shrinkage[111].

[110] The mechanism may be more complex than described, see Section 5.5 for more details.

[111] The effect of alkalis on shrinkage should not be underestimated. On one hand, the specific cement type used in own investigation suggests presence of alkalis in pore fluid in low concentration. On the other hand, the cement content used in production of UHPC is much higher than in case of ordinary concrete, meaning alkalis'

Another understanding of the renewed fluid uptake by SAP could be theoretically invoked. Notably, since SAP of composition and production details analogous to tested is recognized as thermo-sensitive [Zho 03][Ech 09], some influence on swelling degree as resultant from temperature variation during CT experiment appears plausible. For copolymers based on acrylic acid and acrylamide, associated responsiveness was reported as positive or, in other words, so-called UCST-type behaviour was exhibited. This means that given the presence of permanent cross-links in own network SAP should undergo discontinuous volume phase transition (particularly: swelling) once heating above respective temperature threshold. Acknowledging that temperature during CT measurement was above 30 °C as adding up from ambient conditions and the additional hydration heat liberated inside sample, the minimum transition temperature, i.e. UCST, of approximately 30 °C is needed [Ech 09] or likely less due to pH effect [Zho 03] as determined for similar polymers was indeed exceeded. On the other hand, the rule of thumb is that stimulus-responsiveness is a complex property/phenomenon of variety of controlling factors somewhat in addition to application temperature, with some being related to polymer structure (e.g. ratio and especially charge type of monomers used) and others to properties of aqueous solution present (composition, quality and especially pH) or any other contribution affecting polymer-polymer interaction, see [Ech 09] and excellent recent review in [Seu 12]. These factors determine the threshold value or decide about switching to opposite temperature effect or even particular trigger effect vanishing. Highly alkaline environment, i.e. one of pH like met in concrete, is an evident example of such parameter [Zho 03]; as carboxylate groups in SAP (acrylic acid groups) dissociate provoking electrostatic repulsion between polymer chains, breakage/weakening of thermally reversible hydrogen bonds between two types of polymer segments (acrylic acid, acrylamide) stops to dominate swelling. Accordingly, UCST-like behaviour becomes suppressed and does not recover unless favourable screening/shielding of the functional groups occurs [Sue 12].

Although optimistic scenario can be speculated, experience shows that the recovery of transition temperature to the selfsame value might be not plausible. This can be linked with fact of the exchange of the interaction type between polymer chains/segments from, in the matter of dissociation, weak hydrogen bonding to relatively stronger hydrophobic polymer-polymer interaction [Gan 01] and apparently ionic (electrostatic cross-link) bridging [Sue 12], i.e. two of effects to be caused by dissolved salt presence in pore solution. This means that

content is with likelihood significant. Still, further in-depth studies should be performed in future to verify the mechanisms proposed.

well-documented argumentation exists and it speaks against temperature effect. A support to this claim is delivered within recent experiments by Schröfl et al. [Sch 15] who tested absorption of different copolymers of similar composition in cement paste filtrates heated to temperature of 20, 30 and 40 °C and found no noteworthy changes in swelling behaviour of SAP. That is to say, underlying reasoning of the swelling restart might be very different and seems much more likely to be related to alkali effect.

- discussion of different deswelling regimes of IC agent

The experience gained from polymer science and studies on pure SAP material allows to state that given kinetics of (de-)swelling is typically governed by diffusion-limited transport, response of SAP to any stimuli must be expected as a polymer size-dependent property, the subject being in attention of numerous studies e.g. [Mat 88][Vas 98][Moe 09][Shu 11]. This means that if particle size distribution of SAP in concrete was broad (as occurred in present case), there would be different time of emptying of SAP related to their swollen size and overlapping that triggered by self-desiccation phenomenon itself.

Having analysed more data including those presented in Appendix H, the evidence to abovementioned relation was not found. In general, deswelling process was noted to last some hours, 'success' of which could be likely related to lack of porosity and cracks in structure and on surface of SAP, respectively, see Figure 4.11 and 4.13 in Section 4.2.2. According to Ganji et al. [Gan 10], without extra pathways through which fluid could travel, its transport in hydrogel could be only due to diffusion (through free volumes), which in any material is known to be a very slow process. As such, some hindrance to abrupt water release from SAP as attributed to IC agent type used was plausibly in favour of successful mitigation of autogenous shrinkage.

When following subsequent records, different rates of water release were observed in individual cases. Such fact is yet hardly surprising given high complexity of deswelling process which could be driven by inhomogenous network structure generated during polymerization process (or other), and for general case has been described e.g. by Vasilevskaya et al. [Vas 98]. However, what appeared unexpected were the two different behaviours of SAP in associated porosity of comparable size, see Figure 5.8 and Figure 5.10. Since this observation could not be explained by distribution of polymer particles in matrix, other reasoning was considered as plausible.

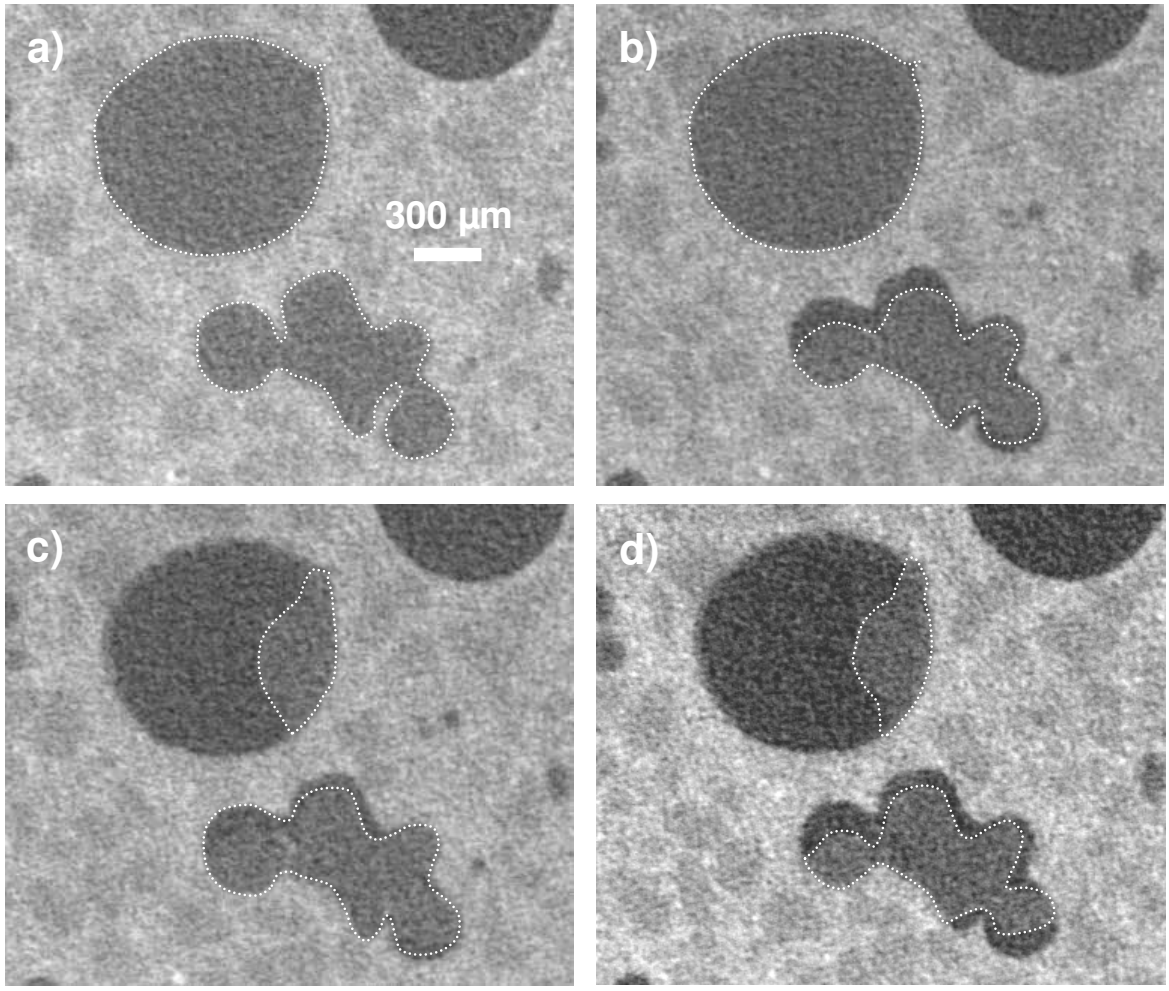

Figure 5.10: Modes of changes in pores created from accommodation of one SAP particle (full top pore) and the assembly of IC agent particles (bottom pore) in the concrete matrix. Each of the pictures shows piece of one particular slice focusing on the selfsame place of interest and being obtained at identical sample height. The growing alphabetical labelling reflects the following increasing concrete ages at which the CT scans were carried out: a) 10.5 hours, b) 13.5 hours, c) 18.5 hours, d) 34.5 hours. The same scale given in case a) applies to all pictures. Two very different behaviours of SAPs are revealed. Only in one case, this regarding SAP assembly (in the bottom pore), the main mode of changes including stage of SAP reswelling appears to be demonstrated again.

The rule of thumb is that if absorption takes place under influence of different stimuli including load (from shearing/compression, for instance) and, furthermore, when some competition for water molecules is effective, larger SAP could be inhibited to attain their potential maximum capacity. This implies that two SAP particles having different virgin size in concrete may exhibit similar swelling ratio although organization of the chains and thus mesh size (i.e. the size of interstitial space created between chain junctions) needn't be the same. Should this be evidenced when condition for curing fluid extraction occurs, the release rate will vary depending how freely water can travel.

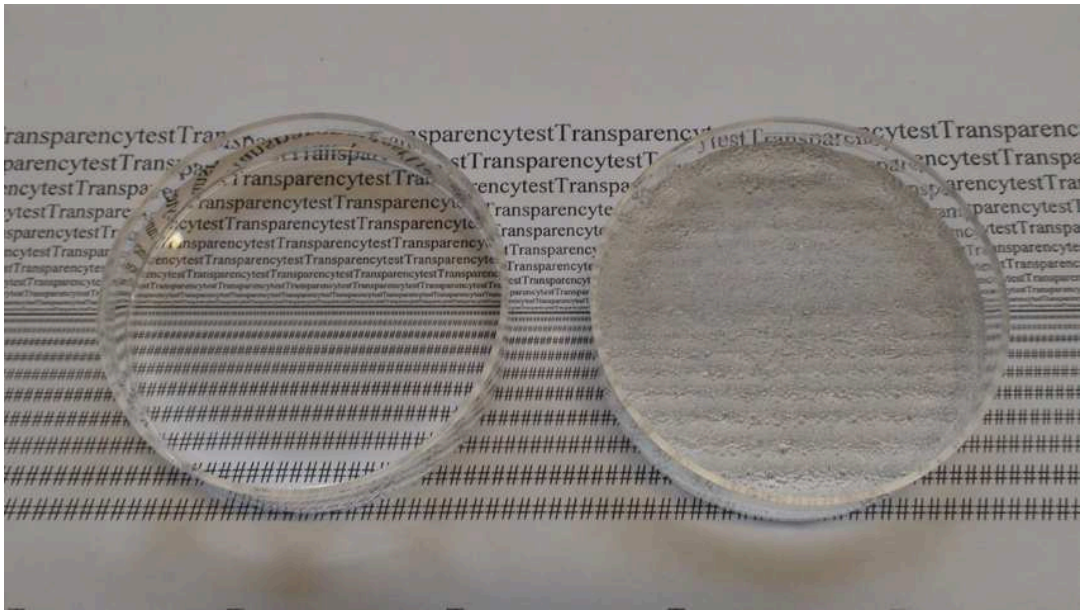

Figure 5.11: Traces of spatial inhomogeneity as determined from investigating the optical transparency by simplified engineering method. Comparison is made between pure distilled water (sample to the left) and one layer of swelled SAP particles after absorption of this fluid (sample to the right). The possibility to see the text despite the 'filter' put on the top of paper sheet is only noted for the sample to the left and implies excellent transparency.

The fact that loss of solution absorbed in one of cases considered was additionally accompanied by loss of the regular shape, being observation similar to that made by Trtik et al. [Trt 10], becomes understood after optical transparency of SAP studied in the swollen state is taken into account. Figure 14 shows the appearances of two samples: distilled water (sample to the left) and the swelled SAP bed (sample to the right). Only in latter case, very weak optical clarity (transparency) was evidenced, this being attributed to presence of SAP and storage of fluid in the interior of the polymer particles.

Since swelled SAP particles forming the bed consist of water in nearly 100 % and, furthermore, have size >> than in virgin (dry/collapsed) state, special attention must be paid to specificity of polymer construction that held obviously responsible for the blurry picture. As polymer science shows, unless the production of SAP follows certain, non-standard procedure of stabilizing the three-dimensional polymeric structure, the chemically cross-linked hydrogel is expected to be charged with spatial/structural (morphological) inhomogeneities. These imperfections originate, among others, from non-uniform distribution of cross-links, e.g. [Oka 10]. The feature, while governing mechanical and optical [Har 02][Oka 10] properties of gel, also leads to randomization of the inter-crosslinking molecular weight, i.e. the chains lengths between cross-linking points. It increases likelihood that more than one of diffusion coefficients are detected for SAP [Yam 04] in view of which hydrogel can loose its shape on

drying in scenario as following: A stimulus for dehydration occurs and localized mechanical stresses emerge. Without possibility of stress equalization and upon differences in network transport properties due to stresses, some regions in polymer are forced shrink while other swell, both taking place upon poor shape memory ability of chemically non-crosslinked parts of poly(acrylamide-co-acrylic acid) [Don 13]. This gives route to reconfiguration of the structure and arisen change of shape bringing about the stresses relief. Such hypothesis is in line with experimental finding of Deo et al. [Deo 10] who suggested non-uniform dehydration in presence of salt solution as reason for hydrogel loosing its spherical shape. Considering that spatial inhomogeneities do not always appear or govern shape memory loss of SAP on polymer deswelling as indicated in other studies, e.g. [Hir 08], implies however a more complex character of the phenomenon, which should be further investigated in future.

5.5 More on mechanisms of IC

- disjoining pressure-based hypothesis

In foregoing investigations, a lack of consistency has been experienced between evolution of capillary pressure (being the most commonly postulated mechanism behind hygral volume change) and the available shrinkage data. This was noted on double occasion viz. when determining the variable by pressure sensors (Section 5.2) and, what was anticipated[112], when testing UHPC F-S.4 (Section 4.6.2). For this mix deposed of extra water for IC and having lower effective w/c as well as capillaries content, in fact no changes in shrinkage behaviour were observed in comparison to UHPC with IC (F-S.4.07). In comparison, the latter demonstrated capillary tension evolution resembling that of unmodified UHPC (F-R), see Section 5.2. Taking both findings into account, an immediate analogy to result obtained by Beltzung [Bel 11] and earlier by Wittmann [Wit 09] comes in mind, in particular secondary contribution of large pore spaces in which capillary force operate to the volume changes triggered by water fluctuations.

From another standpoint, it is a fundamental conclusion that macroscopically recorded autogenous strain of UHPC with IC must be considered as an outcome from two separate inputs, i.e. autogenous shrinkage and autogenous swelling, see Figure 4.78 and e.g. [Bar 05] for other evidence. The likelihood that the shrinkage balancing phenomenon takes place is especially high in the early phase of UHPC hardening [Sol 12], although, as own study showed (Figure 4.79) and was furthermore depicted in [Hab 06a][Kam 08], could also

[112] In further deliberations, it is considered that the final result of IC work might be the result of the competition between several processes taking place at once.

account for the period before fluid-to-solid transition occurs. The origin is however still controversial. While it has been preliminary ascribed to crystallization pressure, studies could be named questioning growth of ettringite [Mou 06][ref. 82 *Ibid.* San 11] and portlandite [Fey 01] as causes of the expansion[113]. In view of another argument, particularly IC effect observed also in a system virtually deposed of capillaries (F-S.4), consideration of possibility of other reasons behind swelling may be in order.

As experimentally evidenced for finely grained UHPCs similar to the tested M2Q, age of few tens of hours [Ver 98][Bon 00][Sol 12] has to be acquired for capillary pore space discontinuity to occur. Attaining the characteristic threshold, however, is solely the final stage of longer pore segmentation process, which could be imaginary compared to percolation process occurring and bringing about setting. During the intermediate phases, the order of magnitude of permeability of the finely grained UHPC remains as high as in system of much higher w/c [Tam 12]. On the other hand, partial segmentation of capillary network is taking effect in UHPC [Mor 02] as C-S-H phases are gradually filling and resultantly blocking the very few capillary pores. In system with IC segmentation could be also facilitated by the fact that SAP like other water retaining agents plausibly cuts the capillary network[114] [Pai 09] or at least in some cases plays role of a buffer [Cer 09]. Once attaining the critical degree of hydration, transport pathways will switch from the capillary pore network to porous C-S-H network and transport will be controlled by characteristics of the latter.

A goal-oriented literature review was performed. It was revealed that segmentation of capillaries needn't be critical factor inhibiting swelling in cement-based system to occur. E.g. UHPCs without and with coarse aggregate were noted to swell in response to storage at high relative humidity after previous maturing and shrinking for many days [Cwi 08]. The cause of such behaviour can be deduced from other sources:
- Having treated 18-months-old oven dried mortar (w/c = 0.485) with water, Hearn [Hea 96] observed significant permeability reduction relative to first measurement made, being

[113] Another reason for microscopic swelling and thus autogenous shrinkage reduction should be considered which is related to specific role played by silica fume. Before pozzolanic reaction occurs (which is not until concrete age is approx. 7 days in case of tested finely grained UHPC, see Figure 4.24), silica fume is likely to accelerate the rate of hydration of calcium aluminium phase [Lob 93]. In doing so, and due to invoking accompanying events further discussed in [Lob 93], lower degree of hydration is required to produce expansion by ettringite. This means that autogenous shrinkage may be reduced more effectively. When pozzolanic reaction takes effect, the new products produced surely occupy extra volume [Ben 91]. On the other hand, this second positive outcome of silica fume presence is unlikely to overcome the negative effect brought about from chemical shrinkage which increases on silica fume reaction, e.g. [Ben 04].

[114] It should be borne in mind that unsaturated entrapped air bubbles may lead to self-sealing effect, thus, provide similar effect to SAP.

simultaneously in contrast to saturation with propan-2-ol. The apparent blocking and segmentation of flow passage of the otherwise interconnected shrinkage microcracks was explained as a consequence of wedging C-S-H layers apart from their fully or partially collapsed state (induced by the oven drying), being another after Robertson and Mills [Rob 85] extension of Bangham's idea and alternative to Kovler's [Kov 96] understanding of wedging effect.

- In similar spirit, but for somewhat lower w/c of 0.35, Chemmi et al. [Che 15] using conductivity measurement concluded that networks of micro- and mesopores of cement paste matured 2 years in endogenous humidity must be involved in and stay efficient for moisture transport on macroscale. This opinion is found consistent with results of Martys and Ferraris [Mar 97] who attributed the second, less rapid stage of moisture ingress to capillary transport through the gel pores or moisture diffusion in the capillary and gel pores.
- Eventually, after considering possibility of moisture transport through C-S-H gel grains as well water in motion within inter-particle spaces of hydrate microproducts, the predictions of short- and long-term creep were improved pronouncedly in study of Asamoto et al. [Asa 06]. In the same study, drying shrinkage could be realistically predicted as well.

The general knowledge is that water occupies and can penetrate the whole size spectrum of pores within the hardened cement paste. This includes the smallest pore spaces where surface forces play a dominant role and where non-water liquids such as mercury cannot infiltrate. The special ability could be linked to water small molecular size and high dipole moment [Odl 72b][Tam 00]. It is important given that C-S-H being main binding phase in hydrated cement paste indicates significant sensitivity of morphology to moisture changes [Gar 99]. In particular, owed to specific nature and (upon) attraction and adsorption of water molecules, the hydrated phase tends to swell, which may be explained by breaking the weak bonds between the layers of C-S-H by cleavage or adsorption of water or other polar liquid [Bea 10], being finally result of kind of 'molecular bombardment at sharp re-entrant angles at surface' [Rob 85][115]. To which extent C-S-H swells, however, this finally depends on type of the structure created and especially degree of restraint related to the solid phase nanostructure.

In any cement-based system, different types of C-S-H phase may form depending on advancement of the hydration process, matrix design and curing conditions. In UHPC of

[115] Note another important fact in this respect and observation made for low w/c systems, in particular potential fractal/rough structure of the surface of the capillary pores, the fact that the walls of these pores are essentially formed of C-S-H compounds, which themselves have a fractal porous structure [Ack 04a].

finely grained matrix like the tested M2Q, owing to application of PCE superplasticizer [ref. 14 *Ibid.* Rid 13] and likely other reasons, e.g. low w/c [Bea 85], the C-S-H structure can be claimed though to be sheet- or lamellar-like [Ado 04]. Given the past experience, similar appearance can be also assumed to exist in systems additionally enriched with water absorber [Sar 03][Ale 04][ref. 15 *Ibid.* Rid 13]. This implies nanostructure of C-S-H in UHPC without or with modification by IC behaves as layered silicate and not as colloidal gel, with importance in terms of difficulty for water entrance: in between the lamellae there will be room for water molecules and exchangeable ions [Bel 11].

Cohesion is, among others, given by Ca^{2+} ions acting as bridges [Bel 11], which however simultaneously reduces the repulsive component of disjoining pressure [Bel 08]. On the other hand, the attractive ion-ion correlation forces between the C-S-H surfaces and controlling the equilibrium gap in UHPC may plausibly be cancelled by the superplasticizer adsorption in agreement with recent findings of Flatt et al. [Fla 09]. Under new circumstance supported by the admixture[116], more of structured water surrounding Ca^{2+} can exist in the C-S-H interlayer space, triggering larger basal spacing of C-S-H at higher RH.

The output being advantageous from perspective of shrinkage reduction might be still empowered by other properties of UHPC microstructure formed. Firstly, it should be recalled that the basic (effective) w/c especially of M2Q matrix was low, and it further reduced on underestimation on SAP absorption capacity. Given so, this means more calcium ions incorporated in the nanostructure of C-S-H [Mul 12] and thus higher likelihood of more water entering the hydrate, although finally opposed by changes in density of both matrix and C-S-H (increases and decreases, respectively). Secondly, the benefits from the delay of pozzolanic reaction in UHPC until later ages presented in Section 4.2.3 must be accounted for too. Initially, only conventional C-S-H forms, meaning high C/S (i.e. Ca/Si atomic ratio) as well as higher porosity compared to pozzolanic C-S-H (approx. 28 % vs. 19 %). These attributes however enhance swelling: former property provides the better response to humidity changes acc. to [Mar 15] despite having potentially lower specific surface area of water vapour; meanwhile, the latter supports the percolation/connectivity of the C-S-H pore network when occurred and thus higher transport rates, including (tritiated) water diffusion [Ben 00b][117].

[116] It could be imagined that same benefit results from intercalation of both superplasticizer and sol fraction of SAP.

[117] It is assumed that until pozzolanic reaction occurs, connected pore network is more likely to consist of capillary pores and open gel hydration products (filling the entryways of capillaries) instead of dense gel formation using pore categorization proposed by Bentz and Stutzman [Ben 06].

Overall, many favourable conditions for application of disjoining pressure theory supported by Beltzung [Bel 05][Bel 11], Wittmann [Wit 09] and Beaudoin et al. [Bea 10] as well as its derivative, i.e. hydration pressure theory put forward by Maruyama [Mar 10] and refined with co-workers [Mar 15] seem to exist for UHPC. The mechanism could be finally compared to Bazant's microprestress theory (with review e.g. in [Tam 00][Ulm 00][Ulm et al. 1999 *Ibid*. Ulm 00]) explaining the creep as being generated by disjoining pressure of the hindered adsorbed water and/or the pressure associated with interlayer hydrate water.

It has been a long belief that diffusion process may be responsible for both hygral volume changes and swelling of the cement paste [Tam 00], being currently extended to autogenous shrinkage and mechanism behind IC in UHPC. In theory, water migration rate may be still facilitated by osmosis (due to changing concentration of dissolved species in the pore fluid on desiccation), convection due to gravity effect and, given existence of numerous pores in vicinity of C-S-H phase (Figure 2.8), capillary suction. The remaining question is however the period in which the mechanism operates.

In principle, when a repulsive force is produced on adsorption of water on surface of a narrow gap, stress is exerted on the solid surfaces forming the gap when thickness of adsorbent remains constant [Mar 10]. In cement-based system, this means balancing the force with mechanical stress of the skeleton. The resistance provided by the solid skeleton will notably increase with maturing of concrete. Meanwhile, as the time elapses, C-S-H will undergo chemical aging rendering it less susceptible to deformation [Tho 08] while the pozzolanic reaction in UHPC, after the initial delay, will initiate. It could be thus concluded that earlier ages might be particular ones when abovementioned mechanism will be activated. One important time threshold, specifically for mechanism activation, could be, for instance, moment when diffusion of water through layers of hydrates is supposed to become the rate-determining process of the hydration kinetics. A piece of evidence can be though presented indicating potentially more pronounced time-spreading, as presented in the following.

Figure 5.12 presents the results of long-term shrinkage measurements conducted on prisms made of two finely grained UHPCs of identical total w/c, one without (F-R.04) and one with IC (F-S.3.04). Each curve represents a record started at concrete age of 1 day without or with additional exogenous desiccation, the new condition being obtained by removal of sealing and exposure of all sample faces to ambient environment of lower RH. Only mixtures which in

frames of particular mixture group had relatively high autogenous shrinkage developed in excess of 1 day are chosen for better effect clarification.

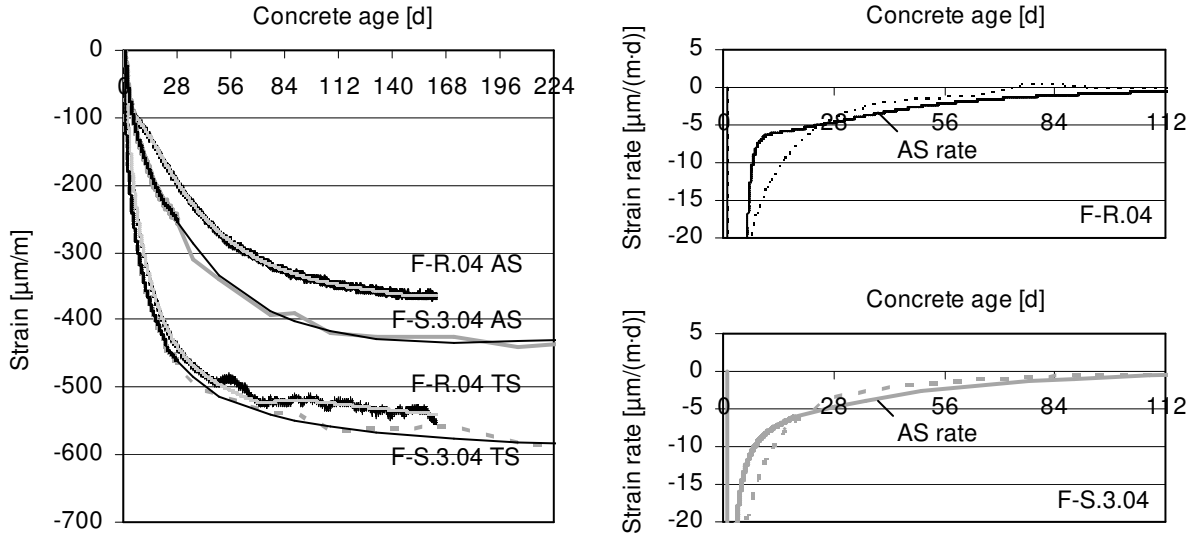

Figure 5.12: Autogenous and total shrinkage of finely grained UHPCs with varied presence of IC as developed from demoulding age of 1 day (to the left) and the corresponding strain rates after the shrinkage curves fit (to the right).

For the presented cases, a certain age existed at which rate of autogenous shrinkage became higher than that of total shrinkage. Applying the well-known superposition principle, this could be interpreted as a decrease of UHPC's drying shrinkage (i.e. concrete swelling) within drying time and its fluctuation on any further changes of the shrinkage rates. Such picture is nonetheless illusive and it could be traced back to overestimation error related to measurement of autogenous shrinkage under drying condition [Yan 05]. This unfavourable impact was originally proposed to originate from concrete member moisture loss to outside [Ish 99] which, given relatively fast decreasing permeability of UHPC [Tam 12], concerns mainly early ages and members with high exposed surface/volume ratios (Figure 4.75). As the system is still in process of rapid changes in pore structure and formation of increasingly stronger solid skeleton, and given depercolation is only in perspective, evaporative water has certain ease of redistribution and rearrangement due to capillary forces or other. While initial drying may induce sharp drying front progressing inward from the exposed surfaces depending on member thickness [Ben 00a], some water is notably lost from hydrating system. In turn, the hydration process is disturbed, especially at the surface. The consequence is lower bound water content (= lower degree of hydration) and coarser porosity, leading in result to lower autogenous shrinkage.

In UHPC as tested, this situation must undergo some changes after material maturing for 3 to 7 days as deduced based on dramatic reduction of UPV change rate, cf. Figure 4.54. At this moment, hydration progress is only little and thus cannot be governing long term autogenous shrinkage which in case of delaying age at initiation of drying contributes more and more to the total strain [Yan 05]. While this means better sealing off of concrete member and lower moisture loss to ambient (confirmed in mass loss data, see Figure 4.75), the overestimation error becomes expectedly limited, however, it does not disappear completely. In fact, at later ages, higher rate of autogenous shrinkage compared to one of total shrinkage becomes yielded directly in the shrinkage data (Figure 5.12), being important enough in agreement with Yang et al. study results [Yan 05]. Eventually, taking into account 1) moisture loss record details (still acknowledgeable mass loss from UHPC at later ages; the variable difference when changing the sample size; extension of time needed to remove all free fluid at room temperature upon delaying drying initiation age), 2) complex response of the system to slow diffusion of available fluid [Mar 15], and 3) inconsistency between mass loss data and the overestimation ratio observed in rival study on UHPC with IC [Sol 11][Soliman and Nehdi 2011, ref. 17 *Ibid*. Sol 12], one explanation hypothesized and reason for the autogenous shrinkage decrease when under exhibition of ambient could be swelling of C-S-H. In author's opinion, the phenomenon is likely taking place somewhat in parallel to matrix creep [Lur 03] being noting but a response to (internal) hygral stress applied by the liquid phase on the pore surface [Ulm 00][Ulm et al. 1999 *Ibid*. Ulm 00] and exerted predominantly in the tinniest micropores (gel pores) [Ulm et al. 1999 *Ibid*. Ulm 00]. Although mechanism requires further in-depth investigation, the known calculations based on adsorption thermodynamics reveal level of pressures like disjoining pressure to be enormous[118].

- *(the above menisci) vapour pressure change-based hypothesis*

It is worth considering another reason for swelling occurrence in UHPC, especially considering the case of system modification with IC. It should be borne in mind that upon water release[119] in vicinity of individual SAP particles and/or potential cutting of capillary network by the IC agent as well as air bubbles, high likelihood exists that the vapour pressure above the water menisci will locally increase. Under the new circumstance, the menisci

[118] A possibility exists that the behaviour of concrete under drying to ambient becomes affected by carbonation. Powers' [Pow 62] suggestion is that as the calcium carbonate replaces the portlandite, concrete shrinkage will be resisted more effectively given higher stiffness of the former. This cause however was not considered as primary one in own cause and could be some simplification.

[119] It is considered that release of moisture initially stored by SAP might be in form of both liquid and vapour. Any further moisture transport might be then taking place in form of liquid and vapour, e.g. due to humidity gradient.

curvature should flatten [Kov 96], releasing surface tension of capillary water that consequently allows free water rise along walls of capillaries. Shape of capillaries needn't be cylindrical one. Thus, in view of potential wedging effect, displacement of capillary walls becomes provoked. In the final result, given the complex control gained over both capillary pressure and disjoining pressure (note: the pressure will attain its potential maximum due to saturation), swelling deformation (expansion) must take place, all being in line with swelling theory originally proposed by Kovler [Kov 96].

- repercolation-based hypothesis

In-depth analysis of data collected and presented in foregoing sections allows putting forward another potential mechanism of the IC work. In general belief, by using internal curing, saturated curing conditions should maintain in systems with IC. As experienced in present study, this might not be always the case. Given that not all SAP particles release the stored water immediately (see Sections 5.3-5.4 and Appendix H), and which in UHPC with sufficiently small SAP particles of identical type as tested may be in fact postponed until depercolation is exhibited [Sol 12], locally, rise of capillary pressure takes place. The development of the variable however is not continuous and stops to be finally reversed within elapse of time. It is similar to case of control UHPC, however, the course reversal is likely to be to different reason, this being distribution of required liquid directly from the SAP or other neighbouring water-rich zone rather than microcracking, being very likely case of control UHPC mix [Fey 01][120]. That is to conclude, after the period of drying, in some volume segments of concrete with IC there will be subsequent period of resaturation. As such scenario could lead to reopening the originally closed pore entryways (so-called necks) after the foregoing depercolation [Ben 06], coarse connected pores including open gel and capillary pores may reappear, leading to water permeability increase and thus more easy transfer of curing medium from water container to refill the empty pores, finally bringing about the autogenous shrinkage reduction.

Abovementioned phenomenon known as repercolation and likely involving complex aging process [Ben 06] may be considered to be taking place in UHPC with IC earlier than expected for any other cement-based material. This could result from the mentioned long-term

[120] To stay scientifically correct, another scenario should be considered, i.e. micro- or at least nanocracking taking place also in system with IC. Also in this case the presence of the water containers turns favourable. As the crack passes through SAP particle or at least delivers additional route for moisture migration as observed sometimes for SAP [Hem 10], moisture will start to be transported very rapidly. Crack healing phenomenon may occur [Hua 10].

saturation provided by IC after the initial (local) drying of material as well the alkalis-sink function of SAP. The course of latter could be as following: due to binding the alkalis by SAP and thus reducing their content in pore solution, the forces otherwise stabilizing the C-S-H [Ben 06b] (somewhat in addition to those provided by Ca^{2+}) become weakened. This will lead to easier rearrangement of particular hydrate phase in response to forces originating repercolation, i.e. shrinkage stresses and strains imposed on C-S-H gel as well as its local shrinkage within a basically non-shrinking 3D framework [Ben 06]. In the same respect, the very low w/c of UHPC will be as important, given that with lowering the parameter, repercolation will intensify too [Ben 06], with some or little influence on repercolation occurrence moment.

The arguments which could validate occurrence of the phenomenon in UHPC and supported by different porosity-related changes are numerous. For instance, repercolation could be used to explain pore coarsening (rivalry to crystallization pressure hypothesis) as well as little reduction in porosity despite maturing of concrete and/or smaller increase of strength of UHPC with IC sometimes observed compared to control mix, with presentation in Appendix I. On the other hand, given the phenomenon involves C-S-H gel shrinking (perhaps somewhat in addition to its creeping and local matrix microcracking), a collision with IC working mechanism previously proposed and based on disjoining pressure theory appears as plausible. It is preliminary assumed that each of mechanisms operates in rival region(s) of the UHPC matrix and the two take effect somewhat in parallel. For final acceptance of mechanism more studies are obviously needed to explain some of the remaining paradoxes, e.g. later depercolation of system with less alkalis in analogy to [Ben 06b] which would be favouring better permeability of UHPC with IC (note: positive change in terms of IC efficiency), on one hand, but consequently also later staging of repercolation (note: negative change in respect to the 'efficiency'), on the other hand.

- IC agent's ion sink function role-based hypothesis

During hydration in concrete like UHPC, release and dissolution of alkalis in pore solution takes place, having different sources of the component withdrawal including cement ingredients, silica fume or even superplasticizer (5 % for the used Glenium 51 acc. to technical data!). Content of each of these ingredients in the tested material was very high and so is the expected level of alkalis. By exerting larger shrinkage inducing stresses (so-called effective pressure) as well as due to provoking higher porosity development [San 12], alkalis

limit material's capability to resist shrinkage deformation while simultaneously forcing it to creep more [Bel 08]. This could be accompanied by negligible [ref. 52 and 53 *Ibid*. San 12] or some [Ben 06b][Bel 05][Bel 08] change of C-S-H structure and no changes or some [San 12] increase of surface tension of pore solution due to alkalis, again unfavourable in respect to the volume change level.

The behaviour becomes affected on modification with IC (due to specific role of SAP, see Section 4.5.6) and the resultant change is favourable in respect to autogenous shrinkage development course. The scenario behind could be presented as following: As fewer alkalis remain in the pore solution, the concentration of Ca^{2+} increases [Bel 08] compared to system without IC/SAP. These cations become immediately surrounded by hydration/solvation shells which are simultaneously larger than ones forming around alkalis given higher electric charge of calcium ions as well as greater water availability ('released' by alkalis, extra water due to IC). With Ca^{2+} being preferably distributed in respect to disjoining pressure induction, in which the primary role is attributed to accompanying hydration/solvation shells [Bel 08], gaps widths between C-S-H surfaces attain their maximum, leading to reduction in autogenous shrinkage in response to IC. This is assuming water release occurs and RH remains on high level, as found in capillary pressure investigation, see Section 5.2.

5.6 Summary and concluding remarks

Pressure changes in the capillaries of UHPC were measured by means of pressure sensors. The advantage over relative humidity investigation, from which capillary pressure can be alternatively read too, was avoiding condensation problem. This made the measurement results more reliable compared to the other and commonly used approach, employed e.g. in [Ben 02][Jen 02][Est 09][Ass 13] and which misses that attribute, with exceptions e.g. [Gra 06b][Eka 09].

The patterns of capillary pressure developed in UHPC were very similar independent on IC, except for rates of development being much smaller for mix with IC. This was a clear improvement attributed to IC. However, the final picture built in the measurements could not be fully accepted due to different potential reasons behind the final results, with only some being related to work of IC. The focus on IC work was therefore approached by alternative method, particularly X-ray computed tomography. The main modes of changes, involving both shrinkage and reswelling of polymer, as well as less typical modes, some of which being

truly favourable in respect to reduction of autogenous shrinkage, were captured. These allowed themselves to be partly explained on basis of tests performed on pure SAP material. Ionic exchange inside SAP and the cross-link inhomogeneities present within polymeric structure rather than IC agent reaction to temperature stimuli seemed effective in dictating different modes of changes. These should be investigated in more detail in future.

Eventually, on basis of different results of this work, discussion of other potential IC mechanisms followed. It seems that the reduction of autogenous shrinkage, beside positive effect on negative pressure development rate, could be also attributed due to one or more of the processes such as swelling of C-S-H/disjoining pressure, change of menisci curvature, wedge effect, repercolation, and the benefits of SAP acting as ion-sink. These should be investigated more in-depth in future with some other phenomena suggested in Outlook, see Section 6.3.

6 Summary, conclusions and outlook

6.1 Introduction

The treatise at hand dealt with different aspects related to the topic of mitigating autogenous shrinkage of UHPC by means of internal curing using SAP. This chapter summarizes all principal findings which result from the work. The order of the presentation corresponds to the order of Sections. Whenever found necessary though, integration between individual parts is performed as well. Some important conclusions are drawn from this knowledge. Finally, in the Section Outlook (6.3) the lingering gaps in comprehension of IC mechanisms or the autogenous shrinkage itself are pointed out. This is followed by provision of suggestions for further research as well as means of extending the information gathered.

6.2 Summary and conclusions

Autogenous shrinkage is the main driving force for deformations of cement-based materials with low w/c and, unless thermal changes occur, is main reason for their proneness to early-age cracking under restraint. This also concerns the two UHPCs that were focused upon herein and which for tailoring the mechanical properties required the respective water-to-cement ratios to be brought to very low value.

A way of eliminating this 'Achilles' heel' of such high-tech materials is internal curing. The method involves introduction of a hydrophilic component of high water storage capacity. The additive absorbs potentially a particular amount of extra water incorporated in the mixing water and subsequently releases it, ideally when the internal dry-out process initiates. Superabsorbent Polymer appears perfect choice in this respect. However, as being indicated by the literature review, every polymeric material is characterized with specific physical and chemical properties and responsiveness to various stimuli. This constitutes a challenge in terms of estimation of the IC effectiveness and or even defining the periods of IC work in concrete life.

As the urge for in-depth characterization of SAP became apparent, the properties of the material being important from IC perspective were analysed first, together with the two UHPCs under modification with IC (Section 4.1). Only one SAP material was chosen for testing; important though, the IC agent was very effective in minimizing autogenous shrinkage as exhibited in preliminary studies and Section 4.6. By using simplified tests that were necessarily further extended in Section 5.4, it was possible to identify these properties

and external stimuli which surely affected water transport from the IC agent and its water carriage in general. Although some further research efforts are still needed, it is author's belief that with only some additional testing (see Outlook) this could serve as blueprint for choice of appropriate SAP in future. The high early-age permeability of UHPC which made it applicable to effective IC notably related to other events occurred, namely delay in the start of pozzolanic reaction and sufficiently late manifestation of the depercolation threshold, which were judged based on material-oriented literature review.

The tea-bag tests as well as investigations using rheometer did not provide clear evidence that exact amount of the extra water added is maintained inside SAP until self-desiccation initiation. This finally shaped the experimental programme and enabled to precise these properties worthy for investigation which are influenced by IC, on one hand, and affect evolution of autogenous shrinkage, on the other hand. It also made clear that in own case maximum absorption capacity and not equilibrium swelling could be read from consistency tests for SAP as chosen.

Effect of IC on hydration (Section 4.5) was approached in non-destructive manner by performing ultrasonic investigations in combination with temperature measurements. While showing excellent correspondence between methods despite individual limitations, it was possible to trace the effect of IC on hydration with simultaneous avoidance of error that accompanies derivation of degree of hydration either from relative non-evaporable water or from portlandite content in two binder systems. Earlier (Section 4.4), the same methods but additionally supported with results of instrumented ring tests, X-ray computed tomography and shrinkage data from casting the samples were successfully used in definition of time-zero. In both cases, the premature release of water from the IC agent served as one among many potential reasons behind the effect observed, with other being related with e.g. SAP type under investigation and especially its interaction with pore solution.

Free autogenous shrinkage of mixtures without and with coarse aggregates as well as under varied presence of IC was investigated in Section 4.6. The apparatus engaged in testing were two set-ups of the corrugated tube method developed by Prof. Jensen. Encouraged by difficulty of estimating the water absorption of SAP and different workability compensation approaches used by other researchers, it was possible to account for all different potential working mechanisms of IC and SAP itself. When both matrices were internally cured, it

became clear that output by SAP for satisfying the demand for curing fluid was as important as effect of UHPC matrix on absorption by SAP. The reading of latter was partly masked by addition of fibres, acknowledged earlier in consistency tests (Section 4.3.3).

Again in Section 4.6, a closer look was taken at the basic compositions of UHPCs as well at the shrinkage curves. It allowed drawing important conclusions with regards to operating shrinkage mechanism and reasons of IC efficiency other than simple release of water. Further analysis in this concern was continued in Sections 5.2 - 5.4 and was supported by the capillary pressure and X-ray computer tomography investigations. The most appealing finding and the biggest paradox revealed was high efficiency of IC in mitigating autogenous shrinkage and simultaneously appearance of stage where very clear reverse in mode of polymer volume change was observed. This suggests partial reabsorption of water initially released and puts interpretation of operative shrinkage mechanisms and ones standing behind IC effect in a new perspective. The final remarks on other mechanisms of IC are finally made in Section 5.5.

Based on results of the investigation the following conclusions could be drawn:

- Internal curing can mitigate autogenous shrinkage of Ultra-High Performance Concrete to very high extent irrespectively of differences in the concrete composition and low permeability expected for the well-aged concrete. This success was notably attributed to sufficient porosity of the material at early ages and connectivity of the pores, allowing transport of curing water in critical period of highest autogenous shrinkage development rates and hydration activity.
- The important precondition for the high efficiency of IC attained was adequately selected Superabsorbent Polymer (SAP). The basic property demanded and exhibited by the SAP was its ability to survive rigorous production regime of UHPC without loosing ability to store the curing water. Some premature loss of water carried by the IC agent although occurred as confirmed in rheometer tests was indecisive for the high effectiveness attained.
- The behaviour of SAP in alkaline environment and/or under load and its usefulness for IC depended on chemistry of SAP as well as on production details. Undoubtedly and more particularly, fit of particular SAP for IC results from its water transport-related properties and responsiveness to stimuli. Still, as important observation made in selfsame respect was lack of hydrates growing inside of SAP pore (i.e. pore accommodating SAP particle) disabling its conversion into ink-bottle type pore.

- Single consistency tests (slump flow measurements) on concrete without and with IC served as reliable indicator of maximum absorption capacity of SAP, the latter being deduced from tea-bag test. This, and not equilibrium swelling value, was the only measurable sorption-related characteristic of the IC agent tested given certain loss of water prior to self-desiccation.
- The absorption capacity of selfsame SAP but implemented into concrete of other composition differed. Underestimation of extra water content needed also to 'satisfy' the absorption capacity of SAP led to usage of original mixing water of mixture under modification with IC. This affected, among other influences, the pore percolation and thus effectiveness of IC.
- The effect of IC on hydration process was showed as depended not only on state of SAP absorption (or in other words: effective water-to-cement ratio of the mix at the concrete age concerned), but also on type of SAP used, since determining specific ability of polymer to undergo interaction with pore solution. Overall, retardation and acceleration of chemical processes was observed already within first 24 hours.
- The mode of emptying SAP from curing fluid was revealed to be very complex, to possess several stages and to differ from one SAP particle to another. The size of SAP particles in swollen state was hardly the determinant for SAP behaviour.
- As expected from theoretical considerations and verified to acknowledgeable extent experimentally, the capillary suction was neither the main operative shrinkage mechanism nor the main mechanism governing migration of curing fluid from IC agent into surrounding matrix. Important contributions to reducing autogenous shrinkage, on the other hand, notably resulted from autogenous swelling and restraining effect of water-filled SAP. The latter effect increased in case of reversal in the mode of SAP particle volume change.
- Potential origins of the autogenous swelling were associated with crystallization pressure and movement of water through pores of non-rigid, volume changing C-S-H. This type of C-S-H was the main hydrate that forms in UHPC matrix before pozzolanic reactions initiated. Positive outcome of wedging effect and other secondary mechanisms' could not be excluded though.

6.3 Outlook

This thesis does not close discussion on mechanisms governing autogenous volume change and the mechanisms of IC as well as related topics treated herein. Potential improvements are possible especially with regard to measuring techniques and appeared very clear in course of the experimental programme. They should be introduced in future for further argumentation of the claims put forward and more comprehensive understanding of phenomena occurred. The suggestions are as following:

- SAP material characterization − basic and specific for understanding applicability for IC

To characterize SAP material in own work, numerous methods commonly used in the field of construction materials rather than specific for study of polymers have been used. Some tests could yet still find further use. The biggest challenge acknowledged to date is estimation of absorption capacity of polymer with its kinetics for polymer under load and in alkaline environment as inherent to concrete. Although usage of some methods reviewed in Appendix E seems feasible after small alterations, further engagement of rheometer should not be excluded. It is author's belief that mixing of SAP with glass beads of concrete solid components' size and the representative pore fluid in the rotational mode (as simulation of mixing) and subsequent monitoring evolution of storage and loss moduli in oscillation mode would help in finding solid-like behaviour of SAP (sign of maximum or equilibrium swelling accomplished). If not, result could be utilized to confirm the sol fraction influence hypothesis and/or favourable mechanical properties possessed by the IC agent in conditions much closer to real application. In such case, the absorption of SAP should be read from fresh cement-based material after quenching and demoulding its small casted piece in liquid nitrogen and subsequently inspection by means of low temperature SEM (LTSEM) or cryo-TEM at different concrete ages.

A next step forward to be made for any SAP tested would be applying some alternative and generally more precise methods for evaluation of various important particularities of the polymeric structure. Chemical analysis of polymer could be improved by engaging Energy Disperse Spectrometry and Electron Spectrometry (XPS). Structural homogeneities could be analysed by combination of small-angle neutron (SANS), small-angle X-ray (SAXS) and static light scattering (SLS) techniques. Information on porosity may be derived from examination based on solvent replacement method with help of cryo-TEM. The morphology and structure characterization with special focus on potential fracture and skin layer formation

in case of SAP (see references in Section 2.5.1) especially under varied temperature is preferably to be analysed by atomic force microscopy (AFM) and Transmission Electron Microscopy (TEM) rather then under ESEM only. This would result in better spatial resolution and greater level of detail for surface topography that are enabled by the first and the second tool mentioned, respectively. Eventually, detection of upper critical solution temperature (UCST) behaviour transition temperature and behaviour of SAP as such under concrete specific pH of pore solution should be associated with changes in transmittance as measured by visible spectrophotometer and/or to be detected with high impedance multimeter.

- UHPC characterization − basic and specific for understanding applicability for IC

Because of existence of ink-bottle and isolated porosity, UHPC − more than any other cement-based material known − requires new approaches for characterization of porosity and the water exchange within. It could be as advanced as proposed by J.-P. Korb [Kor 09] and involve the following nuclear magnetic relaxation (NMR) techniques: 1D NMR relaxation (to study distribution of average pore sizes), T_1-NMR Spectroscopy MAS (to assess hierarchy of pores), field cycling relaxometry $T_1(\omega_0)$ (to examined progressive setting of microstructure-pore size, surface area) and finally 2D NMR correlation T_1-T_1 T_2-Storage-T_2 (to follow water exchange between connected micropores). The simplified alternative could be combining information derived from low temperature calorimetry (examination of capillary porosity percolation/depercolation/repercolation and relative pore volume [Ben 06a]) with electrical conductivity (study of pore connectivity [Ver 98][Bon 00][San 09]) and combined depleted nitric acid extraction/SEM (investigation of pozzolanic reaction evolution [Pfe 10]) for every UHPC tested, i.e. irrespectively of graining or IC presence.

- source of autogenous deformation and IC-triggered shrinkage reduction mechanisms

Disjoining pressure theory requires further attention given the potential to explain mechanisms behind autogenous shrinkage as well as IC. However, models where the action of disjoining pressure is accounted for are normally empirical and allow (mainly) predicting macroscopic deformation of cement-based materials that are drying to ambient. Furthermore, these models cannot reliably illustrate the internal stresses imposed on the cement paste's solid skeleton nor its corresponding deformation in the microscale. For models to become more powerful, improved experimental measurements are also needed. Preliminary step (to confirm contribution of disjoining pressure) would be testing effect IC using in UHPC system

incorporating much finer cement than used in own experiments to reduce capillaries content to highest possible extent. Alternatively, the cement could be replaced with limestone filler as giving way to discussion of involvement of disjoining pressure too [Esp 07]. The latter could be executed with simultaneous control over the negative pressure (artificial induction) and corresponding volume changes for building even clearer picture.

The fact is though that the number of studies finding support of capillary tension theory in either modelling or at least predicting autogenous shrinkage is still overwhelming. To advantage of the approach, experimentally, no information on the internal surface area or on the pore size distribution of the hardening cement paste is required to fill the purpose, only direct and unsophisticated measurement of the variable or knowledge of the RH evolution, e.g. [Lur 03]. Adding to this the remarkable results of present study, it is clear that capillary pressure measurements should be continued. In this respect, it would be advantageous though to use other more refined tensiometers better known from solid science and enabling measurement of very high suction levels (>> 100 kPa). This typically involves also usage of more advanced saturation procedure of the measuring element like pre-pressurization, i.e. applying high positive water pressures before the test. When executed, measurement should be done under full control over bleeding phenomenon affecting initiation of capillary pressure measurements [Cha 07][Tia 14] and to be judged in manner other than visual observation or slump flow result. Only under fulfilment of such conditions it would be meaningful to compare the result with condensation problem-free measurement of RH and the capillary tension theory to be finally accepted or rejected.

In either case, the results should be confronted with quantitative information on drainage of SAP at different RH/temperatures as well as with the bound state of water/pore solution in individual polymer. The most complete picture would be certainly built if this aim was executed for both SAP in concrete and contacted solely with moisture, since enabling completing the linkage between polymer characteristic and sorption properties. Attractive measurement in this respect seems to be one or more of NMR techniques available in research market. Some types of NMR do in fact allow obtaining additional record on diffusion length [Fri 06] or even kinetics and final value of water uptaken by SAP [Nes 09]. Important enough, the method finds its advanced use in study of hydration/pozzolanic reaction [Sol 11] and yielding more realistic pore size distribution [Fri 06] including UHPC [Phi 98], which would be important supplementary information too. Magnetic resonance imaging (MRI), a special

type of NMR, requires though more fundamental research efforts, although it has been successful in validating absorption of pore fluid by SAP particle in course of early hydration of UHPC, see Figure 6.1. For study on SAP without contacting concrete, because of more common access, FT-IR on collapsed/swollen polymer and, if not available, adiabatic compressibility tests [Kod 94] or usage of temperature/RH controlling thermogravimetric analyzer [Thi 07] are recommended.

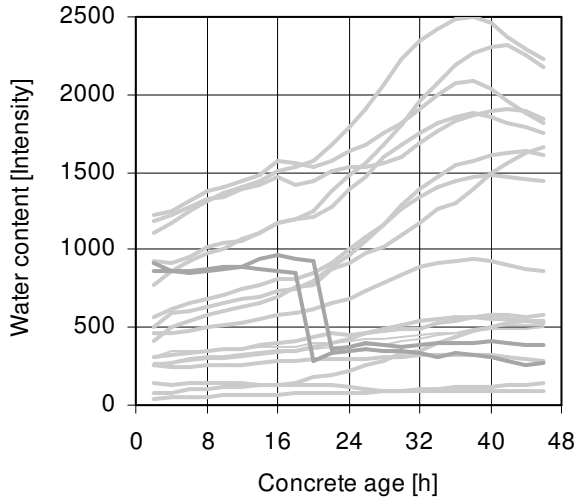

Figure 6.1: Changes of water content in the individual SAP particles as recorded during MRI study for the mix F-S.4.07.

In view of different SAP types available on the market, and given general availability and appealing potential of CT measurements shown, it could be concluded that more tests should follow. The biggest field of improvement is to be related with data evaluation. While SAP behaviour was currently derived from individual slices, ability to separate SAP pores exists. The resultant 3D presentation together with small time intervals between measurements would obviously assist in obtaining more quantitative information. On the other hand, opportunity of reading SAP behaviour means that as soon as modelling thereof in concrete becomes successful (note: necessary for successful modelling of IC), the results of CT measurement could be used for the model validation.

Pore solution extraction being currently enabled also for UHPC [Bon 97] and chemical analysis thereof would be desired for couple of reasons. First it could be used as modern tool for studying contribution of crystallization pressure [San 11] to reduction of autogenous shrinkage which is a phenomenon that cannot be modelled as yet, e.g. [Wyr 11]. To obtain the same goal otherwise and without error due to temperature affecting hydration of two binder system would require application of less handy comparative studies with quantitative X-ray diffraction method, synchrotron microtomography or study of respective chemical reactions behind production of ettringite or portlandite in terms of accompanying volume changes. Second pore solution analysis could be used to determine possibility and, if allowed, kinetics

of different ion migration into polymeric structure. With this knowledge, one could better understand volume changes of SAP particles too, e.g. [Bow 91][Sir 12].

Eventually, it seems evident that the evaluation of shrinkage mechanisms wouldn't be fully comprehended without additional acoustic emission investigation and measurement of tensile basic creep of young UHPC. Further to that, because of moisture still available in SAP for later ages and awaited pozzolanic reaction initiation, more attention should be paid to effect of IC on alkali-silica reaction (argumentation: sufficient amount of alkali present due to high cement content used) and SAP volume changes as triggered by the changes of pH, respectively.

- record and evaluation of shrinkage data

Corrugated tube protocol in form as standardized is attractive for use in every lab. However, it must be borne in mind that it is not free of shortcomings. In fact, neither does the method account for anchorage of the gage-opposite end plug nor enables to remove bleeding, if occurred. The former could be solved by fixing the tube to dilatometer using zip-tie mounted behind last corrugation of the tube. This would be the alternative in case when measurement with two gauges/LVDTs was not an option. The latter requires building rotational device for the tubes like proposed e.g. by Mohr and Hood [Moh 10]. For minimization of the effect, it could be though considered performing measurement with intermediate angle like 45 degrees to counterbalance the respective influences on volume changes otherwise expected in horizontal and vertical position of measuring apparatus [Tia 08].

Some changes are certainly needed to enable even better assessment of the physical significance of time-zero as detected from shrinkage curve. Regrettably, ultrasonic measurement in the set-up used is very limited in this respect. The only improvement possible is in fact supplementing the extension to the device's software to enable encoding the signal record. This may serve as new insight into characteristic of the hardening material with basis such as energy or frequency change. Ideal measuring device should, on the other hand, allow elimination of the gap resulting from autogenous shrinkage of the control UHPC and, simultaneously, record of the shear waves (being more sensitive to solid matrix connectivity) and the P-waves with high frequency transducers. Interesting optional apparatus in this case is one based on echographic method, e.g. [Mor 01][Mor 02]. The former goal could be also

attained with embedded piezoelectric transducers or performing air-coupled ultrasonic measurement. If this turns successful, final linkage to degree of hydration should be made.

To stay on the safe side of the research, and given difficulties in reading time-zero from shrinkage curve of mixtures with IC, another way of determining time-zero might be considered. This opportunity would be given upon application of smart aggregates or, in other words, special multi-functional sensors recently developed for concrete structures. It is feasible to use associated technique for monitoring early strength/Young's modulus development and, important enough, microcracking and thus to set criteria for defining time-zero. Such solution seems more effective than the engineering approach i.e. embedding strain gauges and conduction of destructive strength measurements at very early ages using special equipment, e.g. ones customized by Yoo et al. [Yoo 13] or Sika-modified penetration resistance method acc. to EN 14488-2, which would involve surely higher experimental costs or at least more research efforts. Also in this case, sample volumetrically equal to that of formed by corrugated tubes could be used which would be important change for increasing precision of the assessment too.

- Other

During experiments, new possibility was found, in particular assessment of coefficient of thermal expansion (α_T) from combined shrinkage-temperature measurements performed with two set-ups based on corrugates tube protocol. It is author's belief that with certain adjustments, the double record could be used as tool for derivation of this important parameter of high variability in early age in future.

References

[ACI 207.2R-95] ACI 207.2R-95. *Effect of Restraint, Volume Change, and Reinforcement on Cracking of Mass Concrete*, 2002

[ACI 308R-01] ACI 308R-01. *Guide to Curing Concrete*, 2001

[ACI 224R-01] ACI 224R-01. *Control of Cracking of Concrete Structures*, 2001 (Reapproved 2008)

[Ack 04a] Acker, P.: Swelling, shrinkage and creep: a mechanical approach to cement hydration. *Materials and Structures*, 37(4), 2004, 237-243

[Ack 04b] Acker, P.: Why does Ultrahigh-Performance Concrete (UHPC) exhibit such low shrinkage and such low creep? In: Jensen, O.M.; Bentz, D.P.; Lura, P.; ACI Committee 236 (Eds.): *SP-220: Autogenous Deformation of Concrete*, Special publication, Vol. 220, 2004, pp. 141-154

[Ado 04] Adolphs, J.; Schreiber, A.: Microstructural characterisation of Ultra-High Performance Concrete. In: Schmidt, M.; Fehling, E.; Geisenhansluke, C. (Eds.): *Ultra High Performance Concrete*, kassel university press: University of Kassel, 2004, pp. 265-271

[Agg 05] Aggelis, D.G.; Polyzos, D.; Philippidis, T.P.: Wave dispersion and attenuation in fresh mortar: theoretical predictions vs. experimental results. *Journal of the Mechanics and Physics of Solids*, 53(4), 2005, 857-883

[Aït 97] Aïtcin, P.-C.; Neville, A.M.; Acker, P.: Integrated view of shrinkage deformation. *Concrete International*, 19(9), 1997, 35-41

[Aït 99a] Aïtcin, P.-C.: Does concrete shrink or does it swell? *Concrete International*, 21(12), 1999, 77-80

[Aït 99b] Aïtcin, P.-C.: Demystifying autogenous shrinkage. *Concrete International*, 21(11), 1999, 54-56

[Ale 04] Alesiani, M.; Capuani, S.; Giorgi, R.; Maraviglia, B.; Pirazzoli, I.; Ridi, F.; Baglioni, P.: Influence of cellulosic additives on tricalcium silicate hydration: Nuclear Magnetic Resonance relaxation time analysis. *Journal of Physical Chemistry B*, 108(15), 2004, 4869-4874

[Ale 05] Alexander, M.G.; Mindess, S.: *Aggregates in concrete*. Taylor & Francis, London and New York, 2005

[Ale 59] Alexander, K.M.; Wardlaw, J.: Effect of powdered minerals and fine aggregates on the drying shrinkage of Portland cement paste. *Journal of the American Concrete Institute*, 55(6), 1959, 1303-1316

[Asa 06] Asamoto, S.; Ishida, T.; Maekawa, K.: Time-dependent constitutive model of solidifying concrete based on thermodynamic state of moisture in fine pores. *Journal of Advanced Concrete Technology*, 4(2), 2006, 301-323

[Ass 13] Assmann, A.: *Physical properties of concrete modified with superabsorbent polymers*. Doctoral Thesis, University Stuttgart, 2013

[Ass 14a] Assmann, A.; Mazanec, O.; Eissmann, D.: Study of macroscopic viscosity for prediction of the swelling capacity of salt-insensitive superabsorbent polymers in cementitious materials. In: Mechtcherine, V.; Schroefl, Ch. (Eds.): *Application of Superabsorbent Polymers in Concrete Construction*, Dresden, Germany, RILEM Proceedings pro095, RILEM Publications S.A.R.L., 2014, pp. 105-114

[Ass 14b] Assmann, A.; Reinhardt, H.W.: Tensile creep and shrinkage of SAP modified concrete. *Cement and Concrete Research*, 58, 2014, 179-185

[Bac 81] Bache, H.H.: Densified cement/ultra fine particle based materials. In: *Superplasticizers in Concrete*. Ottawa, Canada, 1981, pp. 185-213

[Bág 97] Bágel, L.; Živica, V.: Relationship between pore structure and permeability of hardened cement mortars: On the choice of effective pore structure parameter. *Cement and Concrete Research*, 27(8), 1997, 1225-1235

[Ban 86] Banfill, P.F.G.; Saunders, D.C.: The relationship between the sorption of organic compounds on cement and the retardation effect of hydration. *Cement and Concrete Research*, 16(3), 1986, 399-410

[Bar 01] Barcelo, L.; Boivin, S.; Acker, P.; Toupin, J.; Clavaud, B.: Early age shrinkage of concrete: back to physical mechanisms. *Concrete Science and Engineering*, 3(10), 2001, 85-91

[Bar 05] Barcelo, L.; Moranville, M.; Clavaud, B.: Autogenous shrinkage of concrete: a balance between autogenous swelling and self-desiccation. *Cement and Concrete Research*, 35(1), 2005, 177-183

[Baž 72] Bažant, Z.P.: Thermodynamics of interacting continua with surfaces and creep analysis of concrete structures. *Nuclear Engineering and Design*, 20(2), 1972, 477-505

[Bea 85] Beaudoin, J.J.; Feldman, R.F.: High-strength cement pastes- A critical appraisal. *Cement and Concrete Research*, 15(1), 1985, 105-116

[Bea 10] Beaudoin, J.J.; Raki, L.; Alizadeh, R.; Mitchell, L.: Dimensional change and elastic behaviour of palyered silicates and Portland cement paste. *Cement and Concrete Composites*, 32(1), 2010, 25-33

[Bel 02] Beltzung, F.; Wittmann, F.: Influence of cement compositions on endogenous shrinkage. In: Persson, B.; Fagerlund, G. (Eds.): *Self-desiccation and Its Importance in Concrete Technology*, Division of Building Materials, Lund University, 2002, pp. 113-126

[Bel 05] Beltzung, F.; Wittmann, F.H.: Role of disjoining pressure in cement based materials. *Cement and Concrete Research*, 35(12), 2005, 2364-2370

[Bel 08] Beltzung, F.; Wittmann, F.H.; Wan, X.: Influence of alkali content on creep and shrinkage of cement-based materials. In: Sun, W.; Van Breugel, K.; Miao, C.; Ye, G.; Chen, H. (Eds.): *Microstructure Related Durability of Cementitious Composites*, RILEM Proceedings pro061, RILEM Publications, 2008, pp. 905-915

[Bel 11] Beltzung, F.: On hygral shrinkage mechanisms of hardened cement paste. *Restoration of Buildings and Monuments*, 17(6), 2011, 359-2011

[Ben 07] Benboudjema, F.; Meftah, F.; Torrenti, J.-M.: A viscoelastic approach for the assessment of the drying shrinkage behaviour of cementitious materials. *Materials and Structures*, 40, 2007, 163-174

[Ben 01a] Bentur, A.: Early-age shrinkage and cracking in cementitious systems. *Concrete Science and Engineering*, 3, 2001, 3-12

[Ben 91] Bentz, D.P.; Garboczi, E.J.: Percolation of phases in a three-dimensional cement paste microstructural model. *Cement and Concrete Research*, 21(2-3), 1991, 325-344

[Ben 99] Bentz, D.P.: Effects of cement psd on porosity percolation and self-desiccation. In: Persson, B.; Fagerlund, G. (Eds.): *Self-desiccation and Its Importance in Concrete Technology*, Division of Building Materials, Lund University, 1999, pp. 127- 134

[Ben 00a] Bentz, D.P.; Hansen, K.K.: Preliminary observations of water movement in cement pastes during curing using X-ray absorption. *Cement and Concrete Research*, 30, 2000, 1157-1168

[Ben 00b] Bentz, D.P.; Jensen, O.M.; Coats, A.M.; Glasser, F.P.: Influence of silica fume on diffusivity in cement-based materials I. Experimental and computer modeling studies on cement pastes. *Cement and Concrete Research*, 30(6), 2000, 953-962

[Ben 01c] Bentz, D.P.; Jensen, O.M.; Hansen, K.K.; Olesen, J.F.; Stang, H.; Haecker C.-J.: Influence of cement particle-size distribution on early age autogenous strains and stresses in cement-based materials. *Journal of the American Ceramic Society*, 84(1), 2001, 129-135

[Ben 02] Bentz, D.P.; Geiker, M.; Jensen, O.M.: On the mitigation of early age cracking. In: Persson, B.; Fagerlund, G. (Eds.): *Self-desiccation and Its Importance in Concrete Technology*, Division of Building Materials, Lund University, 2002, pp. 195-203

[Ben 04] Bentz, D.P.; Jensen, O.M.: Mitigation strategies for autogenous shrinkage cracking. *Cement and Concrete Composites*, 26(6), 2004, 677-685

[Ben 06] Bentz: D.P.: Lithium, potassium and sodium additions to cement pastes. *Advances in Cement Research*, 18(2), 2006, 65-70

[Ben 06a] Bentz, D.P.; Stutzman, P.E.: Curing, hydration, and microstructure of cement paste. *ACI Materials Journal*, 103(5), 2006, 348-356 with supplementary information on the mixtures and subject in: Bentz, D.P.: Capillary porosity depercolation/repercolation in hydrating cement pastes via low-temperature calorimetry measurements and CEMHYD3D modelling. *Journal of American Ceramic Society*, 89(8), 2006, 2606-2611

[Ben 06b] Bentz: D.P.: Lithium, potassium and sodium additions to cement pastes. *Advances in Cement Research*, 18(2), 2006, 65-70

[Ben 08a] Bentz, D.P.: A review of early-age properties of cement-based materials. *Cement and Concrete Research*, 38(2), 2008, 196-204

[Ben 08b] Bentz, D.P.; Snyder, K.A.; Cass, L.C.; Peltz, M.A.: Doubling the service life of concrete structures. I: Reducing ion mobility using nanoscale viscosity modifiers. *Cement and Concrete Composites*, 30(8), 2008, 674-678

[Ber 04] Bertos, M.F.; Simons, S.J.R.; Hills, C.D.; Carey, P.J.: A review of accelerated carbonation technology in the treatment of cement-based materials and sequestration of CO_2. *Journal of Hazardous Materials B*, 112(3), 2004, 193-205

[Bis 01] Bisschop, J.; Lura, P.; Van Mier, J.G.M.: Shrinkage microcracking in cement-based materials with low water-cement ratio. *Concrete Science and Engineering*, 3(11), 2001, 151-156

[Bis 02] Bisschop, J.: *Drying shrinkage microcracking in cement-based materials*. PhD Thesis, Delft University of Technology, 2002

[Blo 93] Blodgett, A.M.; Beattie, D.J.; White, J.W.; Elliott, G.C.: Hydrophilic polymers and wetting agents affect absorption and evaporative water loss. *HortScience*, 28(6), 1993, 633-635

[Bon 97] Bonneau, O.; Vernet, C.; Moranville, M. ; Moindrot, L. : Rheological monitoring of superplasticizers adsorption on reactive powder concrete (RPC). In : Nonat, A. (Ed.): *Hydration and Setting*, Lyngby, Denmark, RILEM Proceedings pro074, RILEM Publications S.A.R.L., 1997, pp. 339-351

[Bon 00] Bonneau, O.; Vernet, Ch.; Moranville, M. ; Aïtcin, P.-C. : Characterization of the granular packing and percolation threshold of reactive powder concrete. *Cement and Concrete Research*, 30(12), 2000, 1861-1867

[Bor 01] Bornemann, R.; Schmidt, M.; Fehling, E.; Middendorf, B.: Ultra-Hochleistungsbeton UHPC: Herstellung, Eigenschaften und Anwendungsmöglichkeiten. *Beton- und Stahlbetonbau*, 96(7), 2001, 458-467

[Bou 96] Boumiz, A.; Vernet, C.; Tenoudji, F.C.: Mechanical properties of cement pastes and mortars at early ages. *Advanced Cement Based Materials*, 3(3-4), 1996, 94-106

[Bou 97] Boumiz, A.; Sorrentino, D.; Vernet, C.; Cohen Tenoudji, F.: Modelling the development of the elastic moduli as a function of the hydration degree of cement pastes and mortars. In : Nonat, A. (Ed.): *Hydration and Setting*, RILEM Proceedings pro013, RILEM Publications S.A.R.L., 1997, pp. 295-316

[Bow 91] Bowman, D.C.; Evans, R.Y.: Calcium inhibition of polyacrylamide gel hydration is partially reversible by potassium. *HortScience*, 26(8), 1991, 1063-1065

[Bra 02] Branch, J.; Hannant, D.J.; Mulheron, M.: Factors affecting the plastic shrinkage cracking of high-strength concrete. *Magazine of Concrete Research*, 54(5), 2002, 347–354

[Bra 94] Brazel, Ch.; Peppas, N.A.: Temperature- and pH- Sensitive Hydrogels for Controlled Release of Antithrombotic Agents. Mater. Res. Soc. Symp. Proc. 331 (1994) 211–216

[Bru 55] Bruere, G.M.: Air entrainment in cement and silica pastes. *ACI Materials Journal*, 51(5), 1955, 905-919

[Buc 05] Buchholz, F.L.; Pesce, S.R.; Powell, C.L.: Deswelling stresses and reduced swelling of superabsorbent polymer in composites of fiber and superabsorbent polymers. *Journal of Applied Polymer Science*, 98(6), 2005, 2943-2507

[Bud 97] Budtova, T.; Suleimenov, I.: Swelling behaviour of a polyelectrolyte network under load. *Polymer*, 38(24), 1997, 5947-5952

[Bul 11] Bullard, J.W.; Jennings, H.M.; Livingston, R.A.; Nonat, A.; Scherer, G.W.; Schweitzer, J.S.; Scrivener, K.L.; Thomas, J.J.: Mechanisms of cement hydration. *Cement and Concrete Research*, 41(12), 2011, 1208–1223

[Bur 08] Burkart, I.; Mueller, H.S.: Creep and shrinkage characteristics of ultra high strength concrete (UHPC). In: Fehling, E.; Schmidt, M.; Stuerwald, S. (Eds.): *Ultra High Performance Concrete*, kassel university press: University of Kassel, 2008, pp. 469-476

[Bur 10] Burrows, H.D.; Chimamkpam, T.O.; Encarnação, T.; Fonseca, S.M.; Pereira, R.F.P.: Ramos, M.L.; Valente, A.J.M.: Trivalent metal ion binding to surfactants and polyelectrolytes: A Review. *Journal of Surface Science and Technology*, 26(3-4), 2010, 1-16

[Cap 13] Cappelletto, E.; Borsacchi, S.; Geppi, M.; Ridi, F.; Fratini, E.; Baglioni, P.: Comb-shaped polymers as nanostructure modifiers of calcium silicate hydrate: A ^{29}Si solid-state NMR investigation. *Journal of Physical Chemistry C*, 117(44), 2013, 22947-22953

[Car 39] Carlson, R.W.: Remarks on durability of concrete. *ACI Materials Journal*, 35(4), 1939, 359-364

[Cas 09] Castro, A.L.; Liborio, J.B.L.; Pandolfelli, V.C.: Evaluation of fresh high performance concrete behaviour by rheometer assistance. *Ibracon Structures and Materials Journal*, 2(4), 2009, 282-305

[Cer 09] Cerolini, S.; D'Orazio, M.; Di Perna, C.; Stazi, A.: Moisture buffering capacity. *Energy and Buildings*, 41(2), 2009, 164-168

[Cha 81] Chandra, S.; Berntsson, L.; Flodin, P.: Behaviour of calcium hydroxide with styrene-methacrylate polymer dispersion. *Cement and Concrete Research*, 11(1), 1981, 125-129

[Cha 07] Chang-wen, M.; Qian, T.; Wei, S.; Jia-ping, L.: Water consumption of the early-age paste and the determination of 'time-zero' of self-desiccation shrinkage. *Cement and Concrete Research*, 37(11), 2007, 1496-1501

[Che 15] Chemmi, H.; Petit, D.; Tariel, V.; Korb, J.-P.; Denoyel, R.; Bouchet, R.; Levitz, P.: A comprehensive multiscale moisture transport analysis: From porous reference silicates to cement-based materials. *The European Physical Journal Special Topics*, 224(9), 2015, 1749-1768

[Che 07] Chen, D.-P.; Qian, Ch.-X. ; Gao, G.-B. ; Zhao, H.-K.: Mechanism and effect of SAP for reducing shrinkage and cracking of concrete. *Journal of Functional Materials*, 38(3), 2007, 475-478 (in Chinese)

[Che 13] Chen, H.; Wyrzykowski, M.; Scrivener, K.; Lura, P.: Prediction of self-desiccation in low water-to-cement ratio pastes based on pore structure evolution. *Cement and Concrete Research*, 49, 2013, 38-47

[Che 10] Cherkaoui, K.; Courtial, M.; Dunstetter, F.; Khelidj, A.; Mounanga, P.; De Noirfontaine, M.-N.: Early-age volume changes of extrudable reactive powder concrete. In: Brémand, F. (Ed.): *Experimental Mechanics*, EPJ Web of Conferences, Volume 6, id.23005, Poitiers, France, 2010

[Che 01] Cheyrezy, M.; Behloul, M.: Creep and shrinkage of Ultra-High Performance Concrete. In: Ulm, F.-J.; Bažant, Z.P.; Wittmann, F.H. (Eds.): *Creep, Shrinkage and Durability Mechanics of Concrete and other Quasi-Brittle Materials*, Elsevier Science, 2001, pp. 527-538

[Cho 01] Chotard, T.; Gimet-Breart, N.; Smith, A.; Fargeot, D.; Bonnet, J.P.; Gault, C.: Application of ultrasonic testing to described hydration of calcium aluminate cements. *Cement and Concrete Research*, 31(3), 2001, 405-412

[Coh 83] Cohen, M.D.: Theories of expansion in sulfoaluminate - type expansive cements: Schools of thought. *Cement and Concrete Research*, 13(6), 1983, 809-818

[CONCRETEPORTAL] The Concrete Portal, Reactive Powder Concrete. www.theconcreteportal.com/reac_pow.html, accessed for the last time: 2016

[Cha 64] Chahal, R.S.: Effect of temperature and trapped air on the energy status of water in porous media. *Soil Science*, 98(2), 1964, 107-112

[Chu 10] Chung, Ch.-W.; Mroczek, M.; Park, I.-Y.; Struble, L.J.: On the evaluation of setting time of cement paste based on ASTM C403 Penetration Resistance Test. *Journal of Testing and Evaluation*, 38(5), 2010, 527-533

[Cou 13] Courtial, M.; De Noirfontaine, M.-N.; Dunstetter, F.; Signes-Frehel, M.; Mounanga, P.; Cherkaoui, K.; Khelidj, A.: Effect of polycarboxylate and crushed quartz in UHPC: Microstructural investigation. *Construction and Building Materials*, 44, 2013, 699-705

[Cra 11] Craeye, B.; Geinaert, M.; De Schutter, G.: Super absorbing polymers as an internal curing agent for mitigation of early-age cracking of high-performance concrete bridge decks. *Construction and Building Materials*, 25(1), 2011, 1-13

[Cus 07] Cusson, D.; Hoogeveen, T.: An experimental approach for the analysis of early-age behaviour of high-performance concrete structures under restrained shrinkage. *Cement and Concrete Research*, 37(2), 2007, 200-209

[Cwi 08] Cwirzen, A.; Penttala, V.; Vornanen, C.: Reactive power based concretes: Mechanical properties, durability and hybrid use with OPC. *Cement and Concrete Research*, 38(10), 2008, 1217-1226

[Dan 62] Danielson, U.: Heat of hydration of cement as affected by water-cement ratio. In: *Chemistry of Cement*, Washington DC, USA, National Bureau of Standards, Monograph 43, Volume 1, 1962, Paper IV-S7, pp. 519-526

[Dar 11] Darquennes, A.; Staquet, S.; Espion, B.: Determination of time-zero and its effect on autogenous deformation evolution. *European Journal of Environmental and Civil Engineering*, 15(7), 2011, 1017-1029

[Deo 10] Deo, N.; Ruetsch, S.; Ramaprasad, K.R.: Stable environmentally sensitive cationic hydrogels for controlled delivery applications. *Journal of Cosmetic Science*, 61(6), 2010, 421-437

[Der 87] Derjaguin, B.V.; Churaev, N.V.; Muller, V.M.: *Surface forces*. Consultants Bureau, New York, 1987

[Dia 72] Diamond, S.: Interactions between cement minerals and hydroxycarboxylic-acid retarders: III. Infrared spectral identification of the aluminosalicylate complex. *Journal of American Ceramic Society*, 55(8), 1972, 405-408

[Dom 91] Domone, P.L.; Thurairatnam, H.: The relationship between early age property measurements on cement pastes. In: Banfill, P.F.G. (Ed.): *Rheology of Fresh Cement and Concrete*, E&FN SPON, 1991, pp. 181-191

[Don 13] Dong, J.; Ding, J.; Dai, L.: Graphene enhances the shape memory of poly(acrylamide-co-acrylic acid) grafted on graphene. *Macromolecular Rapid Communications*, 34(8), 2013, 659-664

[Don 91] Dong, L.-Ch.; Hoffman, A.S.: A novel approach for preparation of pH- sensitive hydrogels for enteric drug delivery. *Journal of Controlled Release*, 15(2), 1991, 141-152

[Du 05] Du, L.; Folliard, K.J.: Mechanisms of air entrainment in concrete. *Cement and Concrete Research*, 35(8), 2005, 1463-1471

[Dub 90] Dubrovskii, S.A.; Afanas'eva, M.V.; Lagutina, M.A.; Kazanskii, K.S.: Comprehensive characterization of superabsorbent polymer hydrogels. *Polymer Bulletin*, 24(1), 1990, 107-113

[Dub 94] Dubrovskii, S.A.; Lagutina, M.A.; Kazanskii, K.S.: Method of measuring the swelling pressure of superabsorbent gels. *Polymer Gels and Networks*, 2(1), 1994, 49-58

[Duc 09] Duckheim, C.; Setzer, M.J.: Drying shrinkage mechanisms of hardened cement paste. In: Tanabe, T.; Sakata, K.; Mihashi, H.; Sato, R.; Maekawa, K.; Nakamura, H. (Eds.): *Creep, Shrinkage and Durability Mechanisms of Concrete and Concrete Structures*, Ise-Shima, Japan, CRC Press, Taylor&Franics Group, London, 2009, pp. 49-55

[Dud 08a] Dudziak, L.; Goetze, M.; Schiekel, M.: *Characterization of SAP material*. Internal paper

[Dud 08b] Dudziak, L.; Mechtcherine, V.: Mitigation of volume changes of Ultra-High Performance Concrete (UHPC) by using Super Absorbent Polymers. In: Fehling, E.; Schmidt, M.; Stuerwald, S. (Eds.): *Ultra High Performance Concrete (UHPC)*, kassel university press: University of Kassel, 2008, pp. 425-432

[Dud 10a] Dudziak, L.; Mechtcherine, V.: Deliberations on kinetics of internal curing water migration and consumption based on experimental studies on SAP-enriched UHPC. In: Jensen, O.M.; Hasholt, M.T.; Laustsen, S. (Eds.): *Use of Superabsorbent Polymers and Other New Additives in Concrete*, Lyngby, Denmark, RILEM Proceedings pro074, RILEM Publications S.A.R.L., 2010, pp. 33-43

[Dud 10b] Dudziak, L.; Mechtcherine, V.: Enhancing early-age resistance to cracking in high-strength cement-based materials by means of internal curing using Super Absorbent Polymers. In: Brameshuber, W. (Ed.): *Material Science*, Aachen, Germany, RILEM Proceedings pro077, RILEM Publications S.A.R.L., 2010, pp. 129-139

[Dud 10c] Dudziak, L.; Mechtcherine, V.: Reducing the cracking potential of Ultra-High Performance Concrete by using Super Absorbent Polymers (SAP). In: Van Zijl, G.P.A.G. and Boshoff, W.P. (Eds.): *Advances in Cement-Based Materials*, Stellenbosch, South Africa, Taylor & Francis Group, London, 2010, pp. 11-19

[Dud 14] Dudziak, L.; Mechtcherine, V.: On challenges of interpreting the internal curing (IC) effect on autogenous shrinkage of concrete when using SAP as IC agent. In: Mechtcherine, V.; Schröfl, Ch. (Eds.): *Application of Superabsorbent Polymers and Other New Admixtures in Concrete Construction*, Dresden, Germany, RILEM Proceedings pro095, RILEM Publications S.A.R.L., 2014, pp. 221-232

[Ech 09] Echeverria, C.; López, D.; Mijangos, C.: UCST responsive microgels of poly(acrylamide-acrylic acid) copolymers: Structure and viscoelastic properties. *Macromolecules*, 42(22), 2009, 9118-9123

[Eka 09] Ekaputri, J.J.; Bongochgetsakul, A.; Ishida, T.; Maekawa, K.: Internal relative humidity measurement on moisture distribution of mortar considering self-desiccation at early ages. JCI Annual Conference, 31 no 1, 2009, pp. 643-648

[Ell] Elliott, M.: *Superabsorbent Polymers*. Paper of Product Development Scientist for SAP, BASF Aktiengesellschaft, http://chimianet.zefat.ac.il/download/super-absorbant_polymers.pdf, 2012

[Epp 09] Eppers, S.; Mueller, C.: Autogenous shrinkage and time-zero of UHPC determined with the shrinkage cone. In: Tanabe, T.; Sakata, K.; Mihashi, H.; Sato, R.; Maekawa, K.; Nakamura, H. (Eds.): *Creep, Shrinkage and Durability Mechanics of Concrete and Concrete Structures*, Taylor & Francis Group, London, 2009, pp. 709-714

[Epp 10] Eppers, S.: *Assessing the autogenous shrinkage cracking propensity of concrete by means of the restrained ring test*. Doctoral Thesis, TU Dresden, 2010

[Esp 06] Espinosa, R.M.; Franke, L.: Influence of the age and drying process on pore structure and sorption isotherms of hardened cement paste. *Cement and Concrete Research*, 36(10), 2006, 1969-1984

[Esp 07] Esping, O.: *Early age properties of self-compacting concrete – Effects of fine aggregate and limestone filler*. PhD Thesis, Chalmers University of Technology, 2007

[Est 09] Esteves, L.P.: *Internal curing in cement-based materials*. PhD Thesis, Universidade de Aveiro, 2009

[Far 07] Farhat, F.A.; Nicolaides, D.; Kannellopoulos, A.; Karihaloo, B.L.: High performance fibre-reinforced cementitious composite (CARDIFRC) – Performance and application to retrofitting. *Engineering Fracture Mechanics*, 74(1-2), 2007, 151-167

[Feh 05] Fehling, E.; Schmidt, M.; Teichmann, T.; Bunje, K.; Bornemann, R.; Middendorf, B.: *Entwicklung, Dauerfestigkeit und Berechnung Ultra-Hochfester Betone (UHPC).* Forschungsbericht, Schriftenreihe Baustoffe und Massivbau, Heft 1, Kassel, 2004

[Fei 92] Feil, H.; Bae, Y.H.; Feijen, J.; Kim, S.W.: Mutual influence of pH and temperature on the swelling of ionizable and thermosensitive hydrogels. *Macromolecules*, 25(20), 1992, 5528-5530

[Fel 70] Feldman, R.F.; Sereda, P.J.: A new model for hydrated Portland cement and its practical implications. *Engineering Journal*, 53(8/9), 1970, 53-59

[Fel 85] Feldman, R.F.; Cheng-yi, H.: Properties of Portland cement-silica fume pastes I. Porosity and surface properties. *Cement and Concrete Research*, 15(5), 1985, 765-774

[Fer 87] Ferraris, C.F.; Wittmann, F.H.: Shrinkage mechanisms of hardened cement paste. *Cement and Concrete Research*, 17(3), 1987, 453-464

[Fey 01] Feylessoufi, A. ; Tenoudji, F.C.; Morin, V.; Richard, P.: Early ages shrinkage mechanisms of ultra-high-performance cement-based materials. *Cement and Concrete Research*, 31(11), 2001, 1573-1579

[Fey 09] Feys, D.; Verhoeven, R.; De Schutter, G.: Why is fresh self-compacting concrete shear thickening? *Cement and Concrete Research*, 39(6), 2009, 510-523

[Fla 09] Flatt, R.J.; Schober, I.; Raphael, E.; Plassard, C.; Lesniewska, E.: Conformation of adsorbed comb copolymer dispersants. *Langmuir*, 25(2), 2009, 845-855

[Fra 02] Frank, M.: Superabsorbents. In: *Ullmann's Encyclopedia of Industrial Chemistry*. 2002

[Fri 06] Friedemann, K.; Stallmach, F.; Kärger, J.: NMR diffusion and relaxation studies during cement hydration – A non-destructive approach for clarification of the mechanism of internal post curing of cementitious materials. *Cement and Concrete Research*, 36(5), 2006, 817-826

[Fuj 84] Fujiwara, T.: Change in length of aggregates due to drying. *Bulletin of the International Association of Engineering Geology - Bulletin de l'Association Internationale de Géologie de l'Ingénieur*, 30(1), 1984, 225-227

[Gab 11] Gabrijel, I.; Mikulic, D.; Milovanovic, B.: Application of ultrasonic measurements for determination of setting and hardening in cement paste. *Journal of Civil Engineering*, 5(3), 2011, 278-283

[Gam 04] Gambhir, M.L.: *Concrete technology*. Tata McGraw-Hill Education, New Delhi, India, 2004

[Gam 13] Gams, M.; Trtnik, G.: A new US procedure to determine setting period of cement pastes, mortars, and concrete. *Cement and Concrete Research*, 53, 2013, 9-17

[Gan 01] Gan, L.-H.; Cai, W.; Tam, K.C.: Studies of phase transition of aqueous solution of poly(N,N-diethylacrylamide-co-acrylic acid) by differential scanning calorimetry and spectrophotometry. *European Polymer Journal*, 37(9), 2001, 1773-1778

[Gan 10] Ganji, F.; Vasheghani-Farahani, S.; Vasheghani-Farahani, E.: Theoretical description of hydrogel swelling: A review. *Iranian Polymer Journal*, 19(5), 2010, 375-398

[Gar 99] Garci, M.C.G.: *Quantifying microstructural variations in cement pastes: Implications on drying shrinkage*. PhD Thesis, Northwestern University, 1999

[Gar 95] Garnier, V.; Corneloup, G.; Sprauel, J.M.; Perfumo, J.C.: Setting time study of roller compacted concrete by spectral analysis of transmitted ultrasonic signals. *NDT&E International*, 28(1), 1995, 15-22

[Geo 10a] Georgin, J.F.; Le Bihan, T.; Amroise, J.; Pera, J.: Early-age behaviour of materials with a cement matrix. *Cement and Concrete Research*, 40(7), 2010, 997-1008

[Geo 10b] Georgy, A.; Tejaswi, M.P.: *Effect of internal curing using SAP on plastic shrinkage of UHPC*. Student Project, TU Dresden, 2010

[Gey 04] Geyer, M.; Trettin, R.; Böttger, K.G.; Thieme, J.; Becker, S.: Sorption von definierten Polycarboxylaten an synthetischen Hydratphasen. In: Neubauer, J. (Ed.): Tagung Bauchemie, Erlangen, 2004, pp. 206-209

[Ghi 97] Ghi, P.Y.; Hill, D.J.T. ; Maillet,D.; Whittaker, A.K.: N.M.R. Imaging of the diffusion of water into poly(tetrahydrofurfuryl methacrylate-co-hydroxyethyl methacrylate). *Polymer*, 38(15), 1997, 3985-3989

[Gon 12] Gong, J.P.; Hong, W.: Mechanics and physics of hydrogels. *Soft Matter*, 8(31), 2012, 8006-8007

[Gor 11] Gorges, M.: *Entwicklung von Methoden zur Charakterisierung des Wirkmechanismus von Super-Absorbierenden Polymeren als Zusatzmittel für innere Nachbehandlung in Beton*. Project report, TU Dresden, 2011

[Gra 04] Granju, J.-L.; Sarkis, M.; Arnaud, M.; Escadeillas, G.: A relevant origin-time for shrinkage measurements. *Materials and Structures*, 37(271), 2004, 449-455

[Gra 06a] Grasley, Z.C.: *Measuring and modelling the time-dependent response of cementitious materials to internal stresses*. PhD Thesis, University of Illinois at Urbana-Champaign, 2006

[Gra 06b] Grasley, Z.C.; Lange, D.A.; D'Ambrosia, M.D.; Villalobos-Chapa, S.: Relative humidity in concrete: What does it mean? *Concrete International*, 28(10), 2006, 51-57

[Gra 06c] Graubner, C.-A.; Kaiser, H.-U.; Proske, T.: Erstarrungsverhalten von SVB – Analyse von Prüfverfahren (Setting of Self-Compacting Concrete – Evaluation of test methods). Darmstadt Concrete 21, 2006

[Gra 10] Grassl, P.; Wong, H.S.; Buenfeld, N.R.: Influence of entrained air and aggregates on shrinkage induced micro-cracking of concrete. In: *Concrete Modelling ConMod '10*, Lausanne, Switzerland, 2010, pp. 207-210

[Haa 75] De Haas, G.D.; Kreijger, P.C.; Niël, E.M.M.G.; Slagter J.C.; Stein, H.N.; Theissing, E.M.; Van Wallendael, M.: The shrinkage of hardening cement paste and mortar. *Cement and Concrete Research*, 5(4), 1975, 295-319

[Hab 06a] Habel, K.; Charron, J.-P.; Denarié, E.; Brühwiler, E.: Autogenous deformations and viscoelasticity of UHPFRC in structures. Part I: Experimental results. *Magazine of Concrete Research*, 58(3), 2006, 135-145

[Hab 06b] Habel, K.; Viviani, M.; Denarié, E.; Brühwiler, E.: Development of the mechanical properties of an Ultra-High Performance Fiber Reinforced Concrete (UHPFRC). *Cement and Concrete Research*, 36(7), 2006, 1362-1370

[Hal 95] Halamickova, P.; Detwiler, R.J.; Bentz, D.P.; Garboczi, E.J.: Water permeability and chloride diffusion in Portland cement mortars: Relationship to sand content and critical pore diameter. *Cement and Concrete Research*, 25(4), 1995, 790-802

[Ham 02] Hammer, T.A.: Is there relationship between pore water pressure and autogenous shrinkage before and during setting. In: Persson, B.; Fagerlund, G. (Eds.): *Self-desiccation and Its Importance in Concrete Technology*, Division of Building Materials, Lund University, 2002, pp. 27-38

[Ham 06a] Hammer, T.A.; Bjøntegaard, Ø.: Testing of autogenous deformation (AD) and thermal dilation (TD) of early age mortar and concrete - Recommended test procedure. In: Jensen, O.M.; (Eds.): *Volume Changes of Hardening Concrete: Testing and Mitigation*, RILEM Proceedings pro052, RILEM Publications S.A.R.L., 2006, pp. 341-346

[Ham 06b] Hammer, T.A.; Fosså, K.T.: Influence of entrained air voids on pore water pressure and volume change of concrete before and during setting. *Materials and Structures*, 39(9), 2006, 801-808

[Ham 07] Van der Ham, H.W.M.; Koenders, E.A.B.; Van Breugel, K.: Mitigating autogenous shrinkage of hardening concrete. In: Carpinteri, A.; Corrado, M.; Paggi, M.; Mancini, G. (Eds.): *Fracture Mechanics for Concrete and Concrete Structures (FRAMCOS-6)*, Catania, Italy, Taylor & Francis, London, 2007, pp. 1319-1325

[Han 14] Han, Y.; Zhang, J.; Luosun, Y.; Hao, T.: Effect of internal curing on the internal relative humidity and shrinkage of high strength concrete slabs. *Construction and Building Materials*, 61, 2014, 41-49

[Han 86] Hansen, T.C.: Physical structure of hardened cement paste. A classical approach. *Materials and Structures*, 19(6), 1986, 423-436

[Han 87] Hansen, W.: Drying shrinkage mechanisms in Portland cement paste. *Journal of the American Ceramic Society*, 70(5), 1987, 323-328

[Han 01] Hansen, T.B.: Temperature dependency of the hydration of dense cement paste systems containing micro silica and fly ash. *Nordic Concrete Research*, 27, 2001, 27-34

[Har 02] Haraguchi, K.; Takehisa, T.: Nanocomposite hydrogels: A unique organic-inorganic network structure with extraordinary mechanical, optical, and swelling/deswelling properties. *Advanced Materials*, 14(16), 2002, 1120-1124

[Has 10] Hasholt, M.T.; Jespersen, M.H.S.; Jensen, O.M.: Mechanical properties of concrete with SAP part I: Development of compressive strength. In: Jensen, O.M.; Hasholt, M.T.; Laustsen, S. (Eds.): *Use of Superabsorbent Polymers and Other New Additives in Concrete*, Lyngby, Denmark, RILEM Proceedings pro074, RILEM Publications S.A.R.L., 2010, 117-126

[Has 12] Hasholt, M.T.; Jensen, O.M.; Kovler, K.; Zhutovsky, S.: Can superabsorent polymers mitigate autogenous shrinkage of internally cured concrete without compromising the strength? *Construction and Building Materials*, 31, 2012, 226-230

[Has 89] Hasuo, K.; Okamoto, T.: High-strength concrete using water-absorbent polymer. In: Igata, N.; Kimpara, I. (Eds.): *New Materials and Processes for the future*, Chiba, Japan, Society for Advancement of Material and Process Engineering, Tokyo, 1989, pp. 1570-1575

[Hea 96] Hearn, N.: Comparison of water and propan-2-ol permeability in mortar specimens. *Advances in Cement Research*, 8(30), 1996, 81-86

[Hea 98] Hearn, N.: Self-sealing, autogenous healing and continued hydration: What is the difference? *Materials and Structures*, 31(8), 1998, 563-567

[Hea 99] Hearn, N.: Effect of shrinkage and load-induced cracking on water permeability of concrete. *ACI Materials Journal*, 96(2), 1999, 234-242

[Hem 10] Hempel, S.: Personal communication, 2010

[Hir 84] Hirokawa, Y.; Tanaka, T.: Volume phase transition in a nonionic gel. The *Journal of Chemical Physics*, 81(12), 1984, 6379-6380

[Hir 08] Hirokawa, Y.; Okamoto, T.; Kimishima, K.; Jinnai, H.; Koizumi, S.; Aizawa, K.; Hashimoto, T.: Sponge-like heterogeonous gels: Hierarchical structures in poly(N-isopropylacrylamide) chemical gels as observed by combined scattering and confocal microscopy method. *Macromolecules*, 41(21), 2008, 8210-8219

[Hol 01] Holt. E.: *Early age autogenous shrinkage of concrete*. PhD Thesis, Technical Research Centre of Finland (VTT), 2001

[Hor 88] Horkay, F.; Zrinyi, M.: Studies on mechanical and swelling behaviour of polymer networks on the basis of the scaling concept. 7. Effect of deformation on the swelling equilibrium concentration of gels. *Macromolecules*, 21(11), 1988, 3260-3266

[Hos 04] Hossain, A.B.; Weiss, J.: Assessing residual stress development and stress relaxation in restrained concrete ring specimens. *Cement and Concrete Composites*, 26(5), 2004, 531-540

[Hos 06] Hossain, A.B.; Weiss, J.: The role of specimen geometry and boundary conditions on stress development and cracking in the restrained ring test. *Cement and Concrete Research*, 36(1), 2006, 189-199

[Hoš 09] Hošková, Š.; Tichá, P.; Demo, P.: Determination of Ca^{2+} ions at early stage of hydrating cement paste. *Ceramics – Silikáty*, 53(2), 2009, 76-80

[Hu 96] Hu, Ch.; De Lerrard, F.: The rheology of fresh high-performance concrete. *Cement and Concrete Research*, 26(2), 1996, 283-294

[Hua 95] Hua, C.; Acker, P.; Ehrlacher, A.: Analyses and models of the autogenous shrinkage of hardening paste. Modelling at macroscopic scale. *Cement and Concrete Research*, 25(7), 1995, 1457-1468

[Hua 10], Huang, H.; Ye, G.; Van Breugel, K.: Numerical simulation on moisture transport from super absorbent polymers to concrete. In: Van Breugel, K.; Ye, G.; Yuan, Y. (Eds.): *Service Life Design for Infrastructures*, RILEM Proceedings pro070, RILEM Publications S.A.R.L., 2010, pp. 185-194

[Hua 12] Huang, Z.-Y.; Wang, J.: Effect of SAP on the performance of UHPC. *Bulltetin of the Chinese Ceramic Society*, 31(3), 2012, 539-544 (in Chinese)

[Hug 86] Huglin, M.B.; Zakaria, M.B.: Swelling properties of copolymeric hydrogels prepared by gamma irradiation. *Journal of Applied Polymer Science*, 31(2), 1986, 457-475

[Hyo 13] Hyodo, H.; Tanimura, M.; Sato, R.; Kawai, K.: Evaluation of effect of aggregate properties on drying shrinkage of concrete. In: *Sustainable Construction Materials and Technologies*, Kyoto, 2013, T2-82

[Iga 10] Igarashi, S.-I.; Aragane, N.; Koike, Y.: Effects of spatial structure of superabsorbent polymer particles on autogenous shrinkage behavior of cement paste. In: Jensen, O.M.; Hasholt, M.T.; Laustsen, S. (Eds.): *Use of Superabsorbent Polymers and Other New Additives in Concrete*, Lyngby, Denmark, RILEM Proceedings pro074, RILEM Publications S.A.R.L., 2010, pp. 137-147

[Ima 07] Imamoto, K.: An old approach to determine ‚time zero' (T0) in SCC and its variance in self-stress evaluations. In: De Schutter, G.; Boel, V. (Eds.): *Self-Compacting Concrete*, RILEM Proceedings pro54, RILEM Publications S.A.R.L., 2007, pp. 533-538

[Ima 08] Imamoto, K.; Arai, M.: Specific surface area of aggregate and its relation to concrete drying shrinkage. *Materials and Structures*, 41(2), 2008, 323-333

[Ish 99] Ishida, T.; Chaube, R.P.; Kishi, T.; Maekawa, K.: Micro-physical approach to coupled autogenous shrinkage and drying shrinkage of concrete. In: Tazawa, E.-i. (Ed): *Autogenous Shrinkage of Concrete*, E & FN Spon, London, 1999, pp. 301-312

[Ish 07] Ishida, T.; Maekawa, K.; Kishi, T.: Enhanced modeling of moisture equilibrium and transport in cementitious materials under arbitrary temperature and relative humidity history. *Cement and Concrete Research*, 37(4), 2007, 565-578

[Ito 94] Itou, Y.; Tsuji, M.; Kubo, M.: A study on concrete with cooled high absorption polymer. *Doboku Gakkai Ronbunshu*, 490(23), 1994, 71-80

[Jan 13] Jansen, D.; Goetz-Neunhoeffer, F.; Neubauer, J.; Haerzschel, R.; Hergeth, W.-D.: Effect of polymers on cement hydration: A case study using substituted PDADMA. *Cement and Concrete Composites*, 35(1), 2013, 71-77

[Jaw 78] Jawed, I.; Skalny, J.: Alkalies in cement: A review II. Effects of alkalies on hydration and performance of Portland cement. *Cement and Concrete Research*, 8(1), 1978, 37-52

[JCI 99] Technical Committee on Autogenous Shrinkage of Concrete, Japan Concrete Institute: Terminology. Autogenous shrinkage and its mechanism. Autogenous shrinkage stress and its estimation. Testing method. In: Tazawa, E.-i. (Ed.): *Autogenous Shrinkage of Concrete*, Hiroshima, Japan, E&FN Spon, London, 1999, pp. 3-62

[Jen 13] Jennings, H.M.; Masoero, E.; Pinson, M.B.; Strekalova, E.G.; Bonnaud, P.A.; Manzano, H.; Ji, Q.; Thomas, J.J.; Pellenq, R.J.-M.; Ulm, F.-J.; Bazant, M.Z.; Van Vliet, K.J: Water isotherms, shrinkage and creep of cement paste: Hypotheses, models and experiments.

In: Ulm, F.-J.; Jennings, M.H.; Pellenq, R.J.-M. (Eds.): *Mechanics and Physics of Creep, Shrinkage, and Durability of Concrete: A Tribute to Zdenek P. Bazant*, ASCE Publications, pp. 134-141

[Jen 93] Jensen, O.M.: *Autogenous deformation and RH-change-self-desiccation and self-desiccation shrinkage*. PhD thesis with notes, Technical University of Denmark, 1993

[Jen 95] Jensen, O.M.; Hansen, P.F.: A dilatometer for measuring autogenous deformation in hardening Portland cement paste. *Materials and Structures*, 28(7), 1995, 406-409

[Jen 96] Jensen, O.M.; Hansen, P.F.: Autogenous deformation and change of the relative humidity in silica fume-modified cement paste. *ACI Materials Journal*, 93(6), 1996, 539-543

[Jen 01a] Jensen, O.M.; Hansen, P.F.: Autogenous deformation and RH-change in perspective. *Cement and Concrete Research*, 31(12), 2001, 1859-1865

[Jen 01b] Jensen, O.M.; Hansen, P.F.: Water-entrained cement-based materials: I. Principles and theoretical background. *Cement and Concrete Research*, 31(4), 2001, 647-654

[Jen 02] Jensen, O.M.; Hansen, P.F.: Water-entrained cement-based materials: II. Experimental observations. *Cement and Concrete Research*, 32(6), 2002, 973-978

[Joh 84] Johnson, M.S.: Effect of soluble salts on water absorption by gel-forming soil conditioners. *Journal of the Science of Food and Agriculture* , 35(10), 1984, 1063-1066

[Jol 98] Jolicoeur, C.; Simard, M.-A.: Chemical admixture-cement interactions: Phenomenology and physico-chemical concepts. *Cement and Concrete Composites*, 20(2-3), 1998, 87-101

[Jus 00] Justnes, H.; Clemmens, F.; Sellevold, E.J.: Correlating the deviation point between external and total chemical shrinkage with setting time and other characteristics of hydrating cement paste. In: Baroghel-Bouny, V.; Aïtcin, P.-C. (Eds.): *Shrinkage of Concrete*, RILEM Proceedings pro17, RILEM Publications S.A.R.L., 2000, pp. 57-73

[Jus 15] Justs, J.; Wyrzykowski, M.; Lura, P.: Internal curing by superabsorbent polymers in ultra-high performance concrete. *Cement and Concrete Research*, 76, 2015, 82-90

[Kad 02] Kada, H.; Lachemi, M.; Petrov, N.; Bonneau, O.; Aïtcin, P.-C.: Determination of the coefficient of thermal expansion of high performance concrete from initial setting. *Materials and Structures*, 35(1), 2002, 35-41

[Kam 08] Kamen, A.; Denarié, E.; Sadouki, H.; Bruehwiler, E.: Thermo-mechanical response of UHPFRC at early age – Experimental study and numerical simulation. *Cement and Concrete Research*, 38(6), 2008, 822-831

[Kaz 10] Kazemi-Kamyab, H.; Denarié, E.; Brühwiler, E.: Very early age stiffness development of UHPFRC matrices in low temperatures. Proc. of 8th fib Symposium, Lyngby, Denmark, 2010

[Kea 89] Keating, J.; Hannant, D.J.; Hibbert, A.P.: Comparison of shear modulus and pulse velocity techniques to measure the build-up of structure in fresh cement pastes used in oil well cementing. *Cement and Concrete Research*, 19(4), 1989, 554-566

[Kha 09] Khairallah, R.: *Analysis of autogenous and drying shrinkage of concrete*. Msc Thesis, McMaster University, 2009

[Kim 04] Kim, S.J.; Park, S.J.; Kim, S.I.: Properties of smart hydrogels composed of polyacrylic acid/poly(vinyl sulfonic acid) responsive to external stimuli. *Smart Materials and Structures*, 13(2), 2004, 317–322

[Kje 96] Kjellsen, K.O.; Jennings, H.M.: Observations of microcracking in cement paste upon drying and rewetting by Environmental Scanning Electron Microscopy. *Advanced cement based materials*, 3(1), 1996,14-19

[Kle 13] Klemm, A.; Sikora, K.: The effect of Superabsorbent Polymers (SAP) on microstructure and mechanical properties of fly ash cementitious mortars. *Construction and Building Materials*, 49, 2013, 134-143

[Kli 52] Klieger, P.: Studies of the effect of entrained air on the strength and durability of concrete made with various maximum sizes of aggregate. *Research Department Bulletin*, 40, Portland Cement Association, 1952

[Kna 07] Knapen, E.: *Microstructure formation in cement mortars modified with water-soluble polymers*. PhD Thesis, Katholieke Universiteit Leuven, 2007

[Kod 94] Koda, S.; Yamashita, K.; Iwai, S.; Nomura, H.; Iwata, M.: Ultrasonic investigation of the states of water in hydrogels. *Polymer*, 35(26), 1994, 5626-5629

[Koe 97] Koenders, E.A.B.; Van Breugel, K.: Numerical modelling of autogenous shrinkage of hardening cement paste. *Cement and Concrete Research*, 27(10), 1997, 1489-1499 and Koenders, E.A.B.; Van Breugel, K.: Modelling dimensional changes in low water/cement ratio pastes. In: Persson, B.; Fagerlund, G. (Eds.): *Self-desiccation and Its Importance in Concrete Technology*, Division of Building Materials, Lund University, 1997, pp. 158-173

[Kor 09] Korb, J.-P.: Nuclear magnetic relaxation in cement-based materials. Summer School on field-cycling NMR relaxometry, Mede, 1-3 June 2009. www.ffcrelax.com/schoolNMR/school2009/download/pdf/Korb/cement.pdf

[Kor 08] Korpa, A.; Kowald, T.; Trettin, R.: Hydration behaviour, structure and morphology of hydration phases in advanced cement-based systems containing micro and nanoscale pozzolanic additives. *Cement and Concrete Research*, 38(7), 2008, 955-962

[Kov 96] Kovler, K.: Why sealed concrete swells. *ACI Materials Journal*, 93(4), 1996, 334-339

[Kov 06] Kovler, K.; Zhutovsky, S.: Overview and future trends of shrinkage research. *Materials and Structures*, 39(9), 2006, 827-847

[Kov 09] Kovler, K.; Bentur, A.: Cracking sensitivity of normal- and high-strength concretes. *ACI Materials Journal*, 106(6), 537-542

[Kra 06] Krauss, M.; Hariri, K.: Determination on initial degree of hydration for improvement of early-age properties of concrete using ultrasonic wave propagation. *Cement and Concrete Composites*, 28(4), 2006, 299-306

[Kus 05] Kustermann, A.: *Einflüsse auf die Bildung von Mikrorissen im Betongefüge*. Doctoral Thesis, Universität der Bundeswehr München, 2005

[Lam 05] Lam, H.; Hooton, R.D.: Effects of internal curing methods on restrained shrinkage and permeability. In: Persson, B.; Bentz, D.; Nilsson, L.-O. (Eds.): *Self-desiccation and Its Importance in Concrete Technology*, Gaithersburg, Maryland, USA, June 2005, pp. 210-228

[Lan 02] Langan, B.W.; Weng, K.; Ward, M.A.: Effect of silica fume and fly ash on heat of hydration of Portland cement. *Cement and Concrete Research*, 32(7), 2002, 1045-1051

[Lan 03] Lange, D.; Altoubat, S.A.: Early age creep. In: Bentur, A. (Ed.): *Early Age Cracking in Cementitious Systems*, RILEM Publications S.A.R.L., 2003, pp. 57-62

[Lan 83] Langer, R.; Peppas, N.: Chemical and physical structure of polymers as carriers for controlled release of bioactive agents: A review. *Journal of Macromolecular Science, Part C*, 23(1), 1983, 61-126

[Lar 90] Larbi, J.A.; Bijen, J.M.J.M.: Interaction of polymers with Portland cement during hydration: A study of chemistry of the pore solution of polymer-modifed cement systems. *Cement and Concrete Research*, 20(1), 1990, 139-147

[Laz 10] Łaźniewska-Piekarczyk, B.: Influence of anti-foaming admixture and superplasticizer on fresh and hardened properties of self-compacting mortar. *Architecture Civil Engineering Environment*, 3(4), 2010, 61-72

[Laz 13] Łaźniewska-Piekarczyk, B.: The influence of admixtures type on the air-voids parameters of non-air-entrained and air-entrained high performance SCC. *Construction and Building Materials*, 41, 2013, 109-124

[Lee 97] Lee, W.-F.; Yeh, P.-L.: Superabsorbent polymeric materials. III. Effect of initial total monomer concentration on the swelling behavior of crosslinked poly(sodium acrylate) in aqueous salt solution. *Journal of Applied Polymer Science*, 64(12), 1997, 2371-2380

[Lee 01] Lee, W.-F.; Huang, Y.-L.: Superabsorbent polymeric materials X: Effect of degree of neutralization on swelling behaviour of crosslinked poly(sodium acrylate) in aqueous salts solutions. *Journal of Polymer Research*, 8(1), 2001, 9-15

[Lee 90] Lee, K.K.; Cussler, E.L.: Pressure-dependent phase transitions in hydrogels. *Chemical Engineering Science*, 45(3), 1990, 766-767

[Lee 04] Lee, H.K.; Lee, K.M.; Kim, Y.H.; Kim, H.; Bae, D.B.: Ultrasonic in-situ monitoring of setting process of high-performance concrete. *Cement and Concrete Research*, 34(4), 2004, 631-640

[Lee 05] Lee, N.P.; Chisholm, D.H.: *Reactive Powder Concrete*. Study Report SR 146, BRANZ Ltd, Judgeford, New Zealand

[Leg 94] Legrand, C.; Wirquin, E.: Influence of superplasticizer dosage on the quantity of hydrates needed to obtain a given strength for very young concrete. *Materials and Structures*, 27(3), 1994, 135-137

[Ley 09] Ley, M.T.; Folliard, K.J.; Hover, K.C.: Observations of air-bubbles escaped from fresh cement paste. *Cement and Concrete Research*, 39(5), 2009, 409-416; also study continuation by Ley, M.T.; Chancey, R.; Juenger, M.C.G.; Folliard, K.J.: The physical and chemical characteristics of the shell of air-entrained bubbles in cement paste. *Cement and Concrete Research*, 39(5), 2009, 417-425

[Li 90] Li, Y.; Tanaka, T.: Kinetics of swelling and shrinking of gels. *The Journal of Chemical Physics*, 92(2), 1990, 1365-1371

[Li 07] Li, Z.; Xiao, L.; Wie, X.: Determination of concrete setting time using electrical resistivity measurement. *Journal of Materials in Civil Engineering*, 19(5), 2007, 423-427

[Li 14] Li, Y.; Li, J.: Capillary tension theory for prediction of early autogenous shrinkage of self-consolidating concrete. *Construction and Building Materials*, 53(28), 2014, 511-516

[Lin 06] Lin, Ch-Ch.; Metters, A.T.: Hydrogels in controlled release formulations: Network design and mathematical modelling. *Advanced Drug Delivery Reviews*, 58(12-13), 2006, 1379-1408

[Lob 93] Lobo, C.; Cohen, M.: Hydration of type K expansive cement paste and the effect of silica fume: II. Pore solution analysis and proposed hydration mechanism. *Cement and Concrete Research*, 23(1), 1993, 104-114

[Loo 09] Lootens, D.; Jousset, P.; Martinie, L.; Roussel, N.; Flatt, R.J.: Yield stress during setting of cement pastes from penetration tests. *Cement and Concrete Research*, 39(5), 2009, 401-408

[Lot 07] Lothenbach, B.; Winnefeld, F.; Figi, R.: The influence of superplasticizers on the hydration of Portland cement. In: Beaudoin, J.J.; Makar, J.M.; Raki, L. (Eds.): *Chemistry of Cement*, Montreal, Canada, 2007, pp. W1-5.03

[Lou 99] Loukili, A.; Khelidj, A.; Richard, P.: Hydration kinetics, change of relative humidity, and autogenous shrinkage of ultra-high-strength concrete. *Cement and Concrete Research*, 29(4), 1999, 577-584

[Lur 03] Lura, P.; Jensen, O.M.; Van Breugel, K.: Autogenous shrinkage in high-performance cement paste: An evaluation of basic mechanisms. *Cement and Concrete Research*, 33(2), 2003, 223-232

[Lur 06] Lura, P.; Durand, F.; Jensen, O.M. : Autogenous strain of cement pastes with Superabsorbent Polymers. In : Jensen, O.M.; Lura, P.; Kovler, K. (Eds.): *Volume Changes of Hardening Concrete: Testing and Mitigation*, Lyngby, Denmark, RILEM Proceedings pro52, RILEM Publications S.A.R.L., 2006, pp. 57-65

[Lur 08a] Lura, P.; Ye, G.; Cnudde, V.; Jacobs, P.: Preliminary results about 3D distribution of Superabsorbent Polymers in mortars. In: Miao, C.; Ye, G.; Chen, H. (Eds.): *The 50-year Teaching and Research Anniversary of Prof. Sun Wei on Advances in Civil Engineering Materials*, Nanjing, China, RILEM Proceedings pro71, RILEM Publications S.A.R.L., 2008, pp. 1341-1348

[Lur 08b] Lura, P.; Lothenbach, B.: Influence of pore solution chemistry on shrinkage of cement paste. In: Miao, C.; Ye, G.; Chen, H. (Eds.): *The 50-year Teaching and Research Anniversary of Prof. Sun Wei on Advances in Civil Engineering Materials*, Nanjing, China, RILEM Proceedings pro71, RILEM Publications S.A.R.L., 2008, pp. 191-200

[Lur 14] Lura, P.; Wyrzykowski, M.: Internal-curing water distribution in concrete at early ages: Experiments and modelling. In: Mechtcherine, V.; Schröfl, Ch. (Eds.): *Application of Superabsorbent Polymers and Other New Admixtures in Concrete* Construction, Dresden, Germany, RILEM Proceedings pro095, RILEM Publications S.A.R.L., 2014, pp.71-80

[Ma 03] Ma, J.; Dehn, F.; Koenig, G.: Autogenous shrinkage of self-compacting ultra-high performance concrete (UHPC). In: Ying-shu Yuan, Y-s.; Shah, S.P.; Lü, H-l. (Eds.): *Advances in Concrete and Structures*, RILEM Proceedings pro032, RILEM Publications S.A.R.L., 2003, pp. 255-262

[Ma 04] Ma, J.; Orgass, M.: Comparative investigations on Ultra-High Performance Concrete with and without coarse aggregates. Leipzig Annual Civil Engineering Report (LACER), No. 9, 2004,
Also continued as:
Ma, J.; Orgass, M.; Dehn, F.; Schmidt, D.; Tue, N.V.: Comparative investigations on Ultra-High Performance Concrete with and without coarse aggregates. In: Schmidt, M.; Fehling, E.; Geisenhansluke, C. (Eds.): *Ultra High Performance Concrete*, kassel university press: University of Kassel, 2004, pp. 205-212
[Mal 91] Malhotra, V.M.; Carino, N.J.: *Handbook of non-destructive testing of concrete*. CRC Press, Florida, United States, 1991
[Man 71] Manning, D.G.; Hope, B.B.: The effect of porosity on the compressive strength and elastic modulus of polymer impregnated concrete. *Cement and Concrete Research*, 1(6), 1971, 631-644
[Mar 97] Martys, N.S.; Ferraris, Ch.F.: Capillary transport in mortars and concrete. *Cement and Concrete Research*, 27(5), 1997, 747-760
[Mar 10] Maruyama, I.: Origin of drying shrinkage of hardened cement paste: Hydration pressure. *Journal of Advanced Concrete Technology*, 8(2), 2010, 187-200
[Mar 15] Maruyama, I.; Igarashi, G.; Nishioka, Y.: Bimodal behavior of C-S-H interpreted from short-term length change and water vapor sorption isotherms of hardened cement paste. *Cement and Concrete Research*, 73, 2015, 158-168
[Mas 14] Masuda, F.; Ueda, Y.: Superabsorbent Polymers. In: Encyclopedia of Polymeric Nanomaterials, Springer-Verlag Berlin Heidelberg, 2014, pp. 1-18
[Mat 70] Mather, B.: *Expansive cements*. US Army Engineer Waterways Experiment Station, 1970, 34 pp.
[Mat 88] Matsuo, E.S.; Tanaka, T.: Kinetics of discontinuous volume–phase transition of gels. *The Journal of Chemical Physics*, 89(3), 1988, 1695-1703
[Mat 00] Matte, V.; Moranville, M.; Adenot, F.; Richet, C.; Torrenti, J.M.: Simulated microstructure and transport properties of ultra-high performance cement-based materials. *Cement and Concrete Research*, 30(12), 2000, 1947-1954
[Mat 08] Matthews, P.; Gribble, Ch.; Lucarelli, L.; Schreiber, A.; Adolphs, J.: Analysis of ink bottle pores from MIP data with the Pore-Cor model. Porotec Workshop, 2008. http://www.pore-cor.com/downloads_41/COPS_2008_Pore-Cor-Adolphs-Matthews-Poster.pdf; http://www.pore-cor.com/downloads_41/cement%20ink%20bottle%20pores.pdf

(the pages like simulation software Pore-Cor does not exist any more and have been replaced by www.porexpert.com and PoreXpert, respectively)

[Mec 06] Mechtcherine, V.; Dudziak, L.; Schulze, J.; Staehr, H.: Internal curing by super absorbent polymers (SAP) – effects on material properties of self-compacting fibre-reinforced high performance concrete. In: Jensen, O.M.; Lura, P.; Kovler, K. (Eds.): *Volume Changes of Hardening Concrete: Testing and Mitigation*, RILEM Proceedings pro052, RILEM Publication S.A.R.L., 2006, pp. 87-96

[Mec 09] Mechtcherine, V.; Dudziak, L.; Hempel S.: Mitigating early age shrinkage of Ultra-High Performance Concrete by using Super Absorbent Polymers (SAP). In: Tanabe, T.; Sakata, K.; Mihashi, H.; Sato, R.; Maekawa, K.; Nakamura, H. (Eds.): *Creep, Shrinkage and Durability Mechanics of Concrete and Concrete Structures*, Taylor & Francis Group, London, 2009, pp. 847-853

[Mec 11] Mechtcherine, V.; Dudziak, L.; Brüdern, A.-E.; Hempel, S.; Schroefl, Ch.: Superabsorbierende Polymere (SAP): Innovative multifunktionale Betonzusatzmittel. *Beton*, 3, 2011, 68-72

[Mec 14] Mechtcherine, V.; Gorges, M.; Schroefl, Ch.; Brameshuber, W.; Ribeiro, A.B.; Cusson, D.; Toledo, R.D., Filho; Ichimiya, K.; Igarashi, S.-i.; Kovler, K.; Lura, P.; Reinhardt, H.-W.; Da Silva, E.F.; Weiss, J.; Ye, G.: *Effect of internal curing by using Superabsorbent Polymers (SAP) on autogenous shrinkage and other properties of high-performance fine-grained concrete: Results of a RILEM Round-robin Test, TC 225-SAP. Materials and Structures*, 47(3), 2014, 541-562

[Med 06] Meddah, M.S.; Aïtcin, P.-C.; Petrov, N.: A new approach for the determination of the starting point of autogenous shrinkage strains. American Concrete Institute, Special Publication 234, Paper No. 29, 2006, 473-484

[Med 11a] Meddah, M.S.; Suzuki, M.; Sato, R.: Influence of a combination of expansive and shrinkage-reducing admixture on autogenous deformation and self-stress of silica fume high-performance concrete. *Construction and Building Materials*, 25(1), 2011, 239-250

[Med 11b] Meddah, M.S.; Tagnit-Hamou, A.: Evaluation of rate of deformation for early-age concrete shrinkage analysis and time zero determination. *Journal of Materials in Civil Engineering*, 23(7), 2011, 1076-1086

[Mee 99] Meeks, K.W.; Carino, N.J.: *Curing of High-Performance Concrete: Report of the State-of-the-Art*. Publication No. NISTIR 6295, Building and Fire Research Laboratory, Gaithersburg, MD, 1999

[Mie 58] Mielenz, R.C.; Wolkodoff, V.E.; Backstrom, J.E.; Flack, H.L.: Origin, evolution, and effects of the air void system in concrete. Part 1 - Entrained air in unhardened concrete. *ACI Materials Journal*, 55(7), 1958, 95-121

[Min 81] Mindess, S.; Young, J.F.: *Concrete*. Prentice-Hall, Englewood Cliffs, New Jersey, 1981

[Min 95] Min, D.; Dongwen, H.; Xianghui, L.; Mingshu T.: Mechanism of expansion in hardened cement pastes with hard-burnt free lime. *Cement and Concrete Research*, 25(2), 1995, 440-448

[Miy 01] Miyazawa, S.; Tazawa, E.-I.: Influence of specimen size and relative humidity on shrinkage of high-strength concrete. *Concrete Science and Engineering*, 3(9), 2001, 39-46

[Moe 09] Moennig, S.: *Superabsorbing additions in concrete – applications, modelling and comparison of different internal water sources*. Doctoral Thesis, University Stuttgart, 2009

[Moe 08] Moeser, B.; Pfeifer, C.: Microstructure and durability of Ultra-High Performance Concrete. In: Fehling, E.; Schmidt, M.; Stuerwald, S. (Eds.): *Ultra High Performance Concrete (UHPC)*, kassel university press: University of Kassel, 2008, pp. 417-424

[Moe 10] Moeser, B.; Pfeifer, C.; Heinz, D.; Gerlicher, T.; Mechtcherine, V.; Dudziak, L.: Investigations on the workability and microstructure development of UHPC; part 2: Influence of admixtures and curing on the microstructure of ultra-high strength concretes. *Cement International*, 8(6), 2010, 74-85

[Moh 10] Mohr, B.J.; Hood, K.L.: Influence of bleed water reabsorption on cement paste autogenous deformation. *Cement and Concrete Research*, 40(2), 2010, 220-225

[Mor 01] Morin, V; Tenoudji, F.C.; Feylessoufi, A.; Richard, P.: Superplasticizer effects on setting and structuration mechanisms of ultra high-performance concrete. *Cement and Concrete Research*, 31(1), 2001, 63-71

[Mor 02] Morin, V.; Cohen-Tenoudji, F.; Feylessoufi, A.; Richard, P.: Evolution of the capillary network in a reactive powder concrete during hydration process. *Cement and Concrete Research*, 32(12), 2002, 1907-1914

[Mou 06] Mounanga, P.; Baroghel-Bouny, V.; Loukili, A.; Khelidj. A.: Autogenous deformations of cement pastes: Part I. Temperature effects at early age and micro–macro correlations. *Cement and Concrete Research*, 36(1), 2006, 110-122

[Mou 11] Mounanga, P.; Bouasker, M.; Pertue, A.; Perronnet, A.; Khelidj, A.: Early-age autogenous cracking of cementitious matrices: physico-chemical analysis and micro/macro investigations. *Materials and Structures*, 44(4), 2011, 749-772 with images and supplementary information in-depth discussed in: Grondin, F.; Bouasker, M.; Mounanga, P.;

Khelidj, A.; Perronnet, A.: Physico-chemical deformations of solidifying cementitious systems: multiscale modelling. *Materials and Structures*, 43(1-2), 2010, 151-165

[Mue 10] Mueller, H.S.; Burkart, I.; Budelmann, H.; Ewert, J.; Mechtcherine, V.; Dudziak, L.; Mueller, Ch.; Eppers, S.: Time-dependent behaviour of Ultra High Performance Concrete (UHPC). In: *fib Congress and Exhibition and PCI Annual Convention and Bridge Conference*, Washington D.C., USA, Proceedings disc, 2010

[Mul 12] Muller, A.C.A.; Scrivener, K.L.; Gajewicz, A.M.; McDonald, P.J.: Densification of C-S-H measured by 1H NMR Relaxometry. *The Journal of Physical Chemistry*, 117(1), 2012, 403–412

[NCHRP 06] National Cooperative Highway Research Program: Procedures for Evaluating Air Entraining Admixtures for Highway Concrete, Appendix A. Construction Technology Laboratories Inc., Skokie, IL, 2006, http://onlinepubs.trb.org/onlinepubs/nchrp/nchrp_rpt_578.pdf

[Neh 98] Nehdi, M.; Mindess, S.; Aïtcin, P.-C.: Rheology of High-Performance Concrete: Effect of ultrafine particles. *Cement and Concrete Research*, 28(5), 687-697

[Nei 74] Neisecke, J.: *Ein dreiparametriges, komplexes Ulraschall-Prüfverffahren für die zerstörungsfreie Materialprüfung im Bauwesen*. Doctoral Thesis, TU Braunschweig, 1974

[Nes 09] Nestle, N.; Kühn, A.; Friedemann, K.; Horch, C.; Stallmach, F.; Herth, G.: Water balance and pore structure development in cementitious materials in internal curing with modified superabsorbent polymer studied by NMR. *Microporous and Mesoporous Materials*, 125(1-2), 2009, 51-57

[Nev 96] Neville, A.M.: *Properties of Concrete*. John Wiley & Sons, New York, 1996

[Odl 72a] Odler, I.; Yudenfreund, M.; Skalny, J.; Brunauer, S.: Hardened Portland cement pastes of low porosity. III. Degree of hydration. Expansion of paste. Total porosity. *Cement and Concrete Research*, 2(4), 1972, 463-480

[Odl 72b] Odler, I.; Hagymassy, J., Jr.; Bodor, E.E.; Yudenfreund, M.; Brunauer, S.: Hardened Portland cement pastes of low porosity. IV. Surface area and pore structure. *Cement and Concrete Research*, 2(5), 1972, 577-589

[Odl 99] Odler, I.; Colán-Subauste, J.: Investigations of cement expansion associated with ettringite formation. *Cement and Concrete Research*, 29(5), 1999, 731-735

[Oga 80] Ogawa, K.; Uchikawa, H.; Takemoto, K.: The mechanism of hydration in the system C_3S-pozzolana. *Cement and Concrete Research*, 10(5), 1980, 683-696

[Oka 10] Okay, O.: General properties of hydrogels. In: Gerlach, G.; Arndt, K.-F. (Eds.): *Hydrogel Sensors and Actuators Engineering and Technology*. Springer, Berlin/Heidelberg, 2010, pp. 1-14

[Omi 05] Omidian, H.; Rocca, J.G.; Park, K.: Advances in superporous hydrogels. *Journal of Controlled Release*, 102(1), 2005, 3-12

[Omi 10] Omidian, H.; Park, K.: Introduction to hydrogels. In: Park, K.; Okano, T. (Eds.): *Biomedical applications of hydrogels Handbook*. Springer, 2010, pp. 1-16

[Omi 12] Omidian, H.; Park, K.: Hydrogels. In: Siepmann, J.; Siegel, R.; Rathbone, M. (Eds.): *Fundamentals and Applications of Controlled Release Drug Delivery*. Springer, New York, 2012, pp. 75-106

[Øst 01] Østergaard, T.; Bentz, D.P.: *Measurements on water-entrained cement paste at NIST*. GNI Newsletter, 2001, http://www.gni.dk/files/August%202001.PDF

[Özt 06] Öztürk, T.; Kroggel, O.; Grübl, P.; Popovics, J.S.: Improved ultrasonic wave reflection technique to monitor setting of cement-based materials. *NDT&E International*, 39(4), 2006, 258-263

[Pai 89] Paillère, A.M.; Buil, M.; Serrano, J.J.: Effect of fiber addition on the autogenous shrinkage of silica fume concrete. *ACI Materials Journal*, 86 (2), 1989, 139-144

[Pai 09] Paiva, H.; Esteves, L.P.; Cachim, P.B.; Ferreira V.M.: Rheology and hardened properties of single-coat render mortars with different types of water retaining agents. *Construction and Building Materials*, 23(2), 2009, 1141-1146

[Pau 94] Paulini, P.: A through solution model for volume changes of cement hydration. *Cement and Concrete Research*, 24(3), 1994, 488-496

[Pea 04] Pease, B.; Hossain, A.B.; Weiss, J.: Quantifying volume change, stress development and cracking due to early-age autogenous shrinkage. In: Jensen, O.M.; Bentz, D.P.; Lura, P. (Eds.): *Autogenous Deformation of Concrete*, ACI Special Publication No. 220, 2004, 23-39

[Pes 88] Pessiki, S.P.; Carino, N.J.: Setting time and strength of concrete using the impact-echo method. *ACI Materials Journal*, 85(5), 1988, 389-399

[Pfe 09] Pfeifer, C.; Moeser, B.; Giebson, C.; Stark, J.: Durability of Ultra-High Performance Concrete. In: Gupta, P.; Holland, T.C.; Malhotra, V.M. (Eds.): *Recent Advances in Concrete Technology and Sustainability Issues*, ACI Special Publication vol. 261, paper no. 1 (SP-261–1), 2009, pp. 1-16

[Pfe 10] Pfeifer, C.; Moeser, B.; Weber, C.; Stark, J.: Investigations of the pozzolanic reaction of silica fume in Ultra High Performance Concrete (UHPC). In: Brameshuber, W. (Ed.):

Material Science, Aachen, Germany, RILEM Proceedings pro077, RILEM Publications S.A.R.L., 2010, pp. 287-298

[Phi 98] Phillipot, S.; Korb, J.P.; Petit, D.; Zanni, H.: Analysis of microporosity and setting of Reactive Powder Concrete by proton nuclear relaxation. *Magnetic Resonance Imaging*, 16 (5/6), 1998, 515-519

[Phi 96] Philippova, O.E.; Hourdet, D.; Audebert, R.; Khokhlov, A.R.: Interaction of hydrophobically modified poly(acrylic acid) hydrogels with ionic surfactants. *Macromolecules*, 29(8), 1996, 2822-2830

[Pic 07] Pichler, Ch.; Lackner, R.; Mang, H.A.: A multiscale micromechanics model for tha autogenous-shrinkage deformation of early-age cement-based materials. *Engineering Fracture Mechanics*, 74(1-2), 2007, 34-58

[Pic 13] Pichler, B.; Hellmich, Ch.; Eberhardsteiner, J.; Wasserbauer, J.; Termkhajornkit, P.; Barbarulo, R.; Chanvillard, G.: Effect of gel-space ratio and microstructure on strength of hydrating cementitious materials: An engineering micromechanics approach. *Cement and Concrete Research*, 45, 2013, 55-68

[Pié 06] Piérard, J.; Pollet, V.; Cauberg, N.: Mitigating autogenous shrinkage in HPC by internal curing using superabsorbent polymers. In: Jensen, O.M.; Lura, P.; Kovler, K. (Eds.): *Volume Changes of Hardening Concrete: Testing and Mitigation*, Lyngby, Denmark, RILEM Proceedings pro52, RILEM Publications S.A.R.L., 2006, 97-106

[Pié 09] Piérard, J.; Cauberg, N.; Remy O.: Evaluation of durability and cracking tendency of Ultra High Performance Concrete. In: Tanabe, T.; Sakata, K.; Mihashi, H.; Sato, R.; Maekawa, K.; Nakamura, H. (Eds.): *Creep, Shrinkage and Durability Mechanics of Concrete and Concrete Structures*, Taylor and Francis Group, London, 2009, pp. 695-700

[Pin 99] Pinto, R.C.A.; Hover, K.C.: Superplasticizer and silica fume addition effects on heat of hydration of mortar mixtures with low water-cementitious ratio. *ACI Materials Journal*, 96(5),1999, 600-605

[Pir 06] Pirskawetz, S.; Weise, F.; Fontana, P.: Detection of early-age cracking using acoustic emission. In: Jensen, O.M.; Lura, P.; Kovler, K. (Eds.): *Volume Changes of Hardening Concrete: Testing and Mitigation*, Lyngby, Denmark, RILEM Proceedings pro52, RILEM Publications S.A.R.L., 2006, pp. 385-392

[Pla 09] Plank, J.; Schroefl, Ch.; Gruber, M.; Lesti, M.; Sieber, R.: Effectiveness of polycarboxylate superplasticizers in ultra-high strength concrete: the importance of PCE compatibility with silica fume. *Journal of Advanced Concrete Technology*, 7(1), 2009, 5-12

[Pó 94] Pó, R.: Water-absorbent polymers: A patent survey. *Journal of Macromolecular Science*, Part C, 34(4), 1994, 607-662

[Pop 94] Popovics, S.; Silva-Rodrigez, R.; Popovics, J.S.; Martucci, V.: Behavior of ultrasonic pulses in fresh concrete. In: Stevens, D.J.; Issa, M.A. (Eds.): New Experimental techniques for evaluating concrete material and structural performance. ACI Special Publication SP-143, American Concrete Institute, Detroit, pp. 207-225

[Pou 06] Pourchez, J.; Grosseau, P.; Guyonnet, R.; Ruot, B.: HEC influence on cement hydration measured by conductometry. *Cement and Concrete Research*, 36(9), 2006, 1777-1780

[Pou 13] Pourjavadi. A.; Fakoorpoor, S.M.; Hosseini. P.; Khaloo, A.: Interactions between superabsorbent polymers and cement-based composites incorporating colloidal silica nanoparticles. *Cement and Concrete Composites*, 37, 2013, 196-204

[Pow 47] Powers, T.C.: A discussion of cement hydration in relation to the curing of concrete. *Research Department Bulletin*, 25, Portland Cement Association, 1947, http://cement.org/pdf_files/RX025.pdf

[Pow 47/48] Powers, T.C.; Brownyard, T.L.: Studies of the physical properties of hardened Portland cement paste. *Research Department Bulletin*, 22, Portland Cement Association, 1948, http://cement.org/pdf_files/RX022.pdf

[Pow 53] Powers, T.C.; Helmuth, R.A.: Theory of volume changes in hardened Portland cement paste during freezing. Bulletin no. 46, Research and Developments Laboratories of the Portland Cement Association, reprinted from Proceedings of the Highway Research Board, 32, 285, 1953, 285-297

[Pow 59] Powers, T.C.: Causes and control of volume change. *Journal of the PCA Research and Development Laboratories*, 1959, 29-39

[Pow 68a] Powers, T.C.: *The Properties of Fresh Concrete*. John Wiley & Sons, New York, 1968 with supplementary discussion in paper: Topics in Concrete Technology, http://cement.org/pdf_files/rx174.pdf

[Pow 68b] Powers, T.C.: The thermodynamics of volume change and creep. *Materials and Structures*, 1(6), 1968, 487-507

[Pyt] Pytlik, E.; Molino, D.; Moritz, J.: Superabsorbent Polymers, http://www.eng.buffalo.edu/Courses/ce435/Diapers/Diapers.html, 2012

[Qi 08] Qi, X.; Liu, M.; Chen, Z.; Zhang, F.: Study on the swelling kinetics of superabsorbent using open circuit potential measurement. *European Polymer Journal*, 44, 2008, 743-754

[Qia 01] Qian, X.; Li, Z.: The relationships between stress and strain for high-performance concrete with metakaolin. *Cement and Concrete Research*, 31(11), 2001, 1607-1611

[Qin 08] Qing, Y.; Zenan, Z.; Deyu, K.; Rongshen, Ch.: Influence of nano-SiO_2 addition on properties of hardened cement paste as compared with silica fume. *Construction and Building Materials*, 21(3), 2007, 539-545

[Rah 12] Rahhal, V.; Bonavetti, V.; Trusilewicz, L.; Pedrajas, C.; Talero, R.: Role of the filler on Portland cement hydration at early ages. *Construction and Building Materials*, 27(1), 2012, 82-90

[Rah 82] Rahman, A.A.; Double, D.D.: Dilation of Portland cement grains during early hydration and the effect of applied hydrostatic pressure on hydration. *Cement and Concrete Research*, 12(1), 1982, 33-38

[Ram 96] Ramachandran, V.S.: *Concrete Admixtures Handbook. Properties, Science, and Technology*. 2nd Edition. William Andrew Publishing, 1996

[Rec 12] Recalde Lummer, N.; Plank, J.: Combination of lignosulfonate and AMPS®-co-NNDMA water retention agent – An example for dual synergistic interaction between admixtures in cement. *Cement and Concrete Research*, 42(5), 2012, 728-735

[Rei 96] Reinhardt, H.-W.; Grosse, Ch.; Weiler, B.; Bohnert, J.; Windisch, N.: P-wave propagation in setting and hardening concrete. *Otto-Graf-Journal*, 7, 1996, 181-189

[Ric 95] Richard, P.; Cheyrezy, M.: Composition of Reactive Powder Concretes. *Cement and Concrete Research*, 25(7), 1995, 1501-1511

[Rid 13] Ridi, F.; Fratini, E.; Alfani, R.; Baglioni, P.: Influence of acrylic superplasticizer and cellulose-ether on the kinetics of tricalcium silicate hydration mechanism. *Journal of Colloid and Interface Science*, 395(1 April), 2013, 68-74

[RILEM pro052] Jensen, O.M.; Lura, P.; Kovler, K. (Eds.): *Volume Changes of Hardening Concrete: Testing and Mitigation*, Lyngby, Denmark, RILEM Proceedings pro52, RILEM Publications S.A.R.L., 2006

[RILEM pro074] Jensen, O.M.; Hasholt, M.T.; Laustsen, S. (Eds.): *Use of Superabsorbent Polymers and Other New Additives in Concrete*, Lyngby, Denmark, RILEM Proceedings pro074, RILEM Publications S.A.R.L., 2010

[Rob 85] Robertson, B.; Mills, R.H.: Influence of sorbed fluids on compressive strength of cement paste. *Cement and Concrete Research*, 15(2), 1985, 225-232

[Rob 08] Robeyst, N.; Gruyaert, E.; Grosse, C.U.; De Belie, N.: Monitoring the setting of concrete containing blast-furnace slag by measuring the ultrasonic p-wave velocity. *Cement and Concrete Research*, 38(10), 2008, 1169-1176

[Rob 09] Robeyst, N.; Grosse, Ch.U.; De Belie, N.: Measuring the change in ultrasonic p-wave energy transmitted in fresh mortar with additives to monitor the setting. *Cement and Concrete Research*, 39(10), 2009, 868-875

[Rob 11] Robeyst, N.; Grosse, Ch.U.; De Belie, N.: Relating ultrasonic measurements on fresh concrete with mineral additions to the microstructure development simulated by CEMHYD 3D. *Cement and Concrete Composites*, 33(6), 2011, 680-693

[Roe 85] Roessler, M.; Odler, I.: Investigations on the relationship between porosity, structure and strength of hydrated Portland cement pastes. I. Effect of porosity. *Cement and Concrete Research*, 15(3), 1985, 320-330

[Ron 02] Roncero, J.; Valls, S.; Gettu, R.: Study of the influence of superplasticizers on the hydration of cement paste using nuclear magnetic resonance and X-ray diffraction techniques. *Cement and Concrete Research*, 32(1), 2002, 103-108

[Roo 94] Roorda, W.: Do hydrogels contain different classes of water? *Journal of Biomaterials Science, Polymer Edition*, 5(5), 1994, 381-395

[Ros 82] Rossetti, V.A.; Chiocchio, G.; Paolini, A.E.: Expansive properties of the mixture C4A$\bar{S}$H12 - 2C$\bar{S}$ I. An hypothesis on the expansion mechanism. *Cement and Concrete Research*, 12(5), 1982, 577-585

[Ros 87] Rossi, P.; Acker, P.; Malier, Y.: Effect of steel fibers at two stages: The material and the structure. *Materials and Structures*, 20(6), 1987, 436-439

[Sak 03] Sakai, E.; Yamada, K.; Ohta, A.: Molecular structure and dispersion-adsorption mechanisms of comb-type superplasticizers used in Japan. *Journal of Advanced Concrete Technology*, 1(1), 2003, 16-25

[Sak 06] Sakai, E.; Kasuga, T.; Sugiyama, T.; Asaga, K.; Daimon, M.: Influence of superplasticizers on the hydration of cement and pore structure of hardened cement. *Cement and Concrete Research*, 36(11), 2006, 2049-2053

[Sak 04] Sakata, K.; Shimomura, T.: Recent progress in research on and code evaluation of concrete creep and shrinkage in Japan. *Journal of Advanced Concrete Technology*, 2(2), 2004, 133-140

[San 04] Sannino, A.; Mensitieri, G.; Nicolais, L.: Water and synthetic urine sorption capacity of cellulose-based hydrogels under a compressive stress field. *Journal of Applied Polymer Science*, 91(6), 2004, 3791-3796

[San 06] Sant, G.; Lura, P.; Weiss, J: A discussion of analysis approaches for determining 'time-zero' from chemical shrinkage and autogenous strain measurements in cement paste. In: Jensen, O.M.; Lura, P.; Kovler, K. (Eds.): *Volume Changes of Hardening Concrete: Testing*

and Mitigation, Lyngby, Denmark, RILEM Proceedings pro52, RILEM Publications S.A.R.L., 2006, pp. 375-383

[San 08] Sant, G.; Ferraris, Ch.F.; Weiss, J.: Rheological properties of cement pastes: A discussion of structure formation and mechanical property development. *Cement and Concrete Research*, 38(1), 2008, 1286-1296

[San 09] Sant, G.; Dehadrai, M.; Bentz, D.; Lura, P.; Ferraris, Ch. F.; Bullard, J.W.; Weiss, J.: Detecting the fluid-to-solid transition in cement pastes. *Concrete International*, 31(6), 2009, 53-58

[San 11] Sant, G.; Lothenbach,B.; Juilland, P.; Le Saout, G.; Weiss, J.; Scrivener, K.: The origin of early age expansions induced in cementitious materials containing shrinkage reducing admixtures. *Cement and Concrete Research*, 41(3), 2011, 218-229

[San 12] Sant, G.; Kumar, A.; Patapy, C.; Le Saout, G.; Scrivener, K.: The influence of sodium and potassium hydroxide on volume changes in cementitious materials. *Cement and Concrete Research*, 42(11), 2012, 1447–1455

[Sar 03] Saric-Coric, M.; Khayat, K.H.; Tagnit-Hamou, A.: Performance characteristics of cement grouts made with various combinations of high-range water reducer and cellulose-based viscosity modifier. *Cement and Concrete Research*, 33(12), 2003, 1999-2008

[Sas 97] Sasaki, S.; Maeda, H.: Effect of Donnan osmotic pressure on the volume phase transition of hydrated gels. *The Journal of Chemical Physics*, 107(3), 1997, 1028-1029

[Sch 90] Scherer, G.W.: Theory of drying. *Journal of the American Ceramic Society*, 73(1), 1990, 3-14

[Sch 02] Schachinger, I.; Schmidt, K.; Heinz, D.; Schiessl, P.: Early-age cracking risk and relaxation by restrained autogenous deformation of Ultra High Performance Concrete. In: Dehn, F.; Faust, T.; Koenig, G. (Eds.): *6th International Symposium on Utilization of High Strength/High Performance Concrete*, Universitaet Leipzig Pressestelle, Leipzig, 2002, vol. 2, pp. 1341-1354

[Sch 04] Schachinger, I.; Schubert, J.; Mazanec, O.: Effect of mixing and placement methods on fresh and hardened Ultra High Performance Concrete (UHPC). In: Schmidt, M.; Fehling, E.; Geisenhansluke, C. (Eds.): *Ultra High Performance Concrete*, kassel university press: University of Kassel, 2004, pp. 575-586

[Sch 05] Schindler, A.K.; Folliard, K.J.: Heat of hydration models for cementitious materials. *ACI Materials Journal*, 102(1), 2005, 24-33

[Sch 07a] Schachinger, A.I.: *Massnahmen zur Herstellung von rissefreien Bauteilen aus ultrahochfestem Beton mit höher Duktalität*. Doctoral Thesis, TU München, 2007

[Sch 07b] Schlangen, E.; Koenders, E.A.B.; Van Breugel, K.: Influence of internal dilation on the fracture behaviour of multi-phase materials. *Engineering Fracture Mechanics*, 74(1-2), 2007, 18-33

[Sch 08] Scheydt, J.C.; Herold, G.; Mueller, H.S; Kuhnt, M.: Development and application of UHPC convenience blends. In: Fehling, E.; Schmidt, M.; Stuerwald, S. (Eds.): *Ultra High Performance* Concrete, kassel university press: University of Kassel, 2008, pp. 69-76

[Sch 12a] Scheydt, J.C.; Mueller, H.S.: Microstructure of Ultra High Performance Concrete (UHPC) and its impact on durability. In: Fehling, E.; Schmidt, M.; Glotzbach, C.; Froehlich, S.; Piotrowski, S. (Eds.): *Ultra High Performance Concrete and Nanotechnology in Construction*, kassel university press: University of Kassel, 2012, pp. 349-356

[Sch 14] Schmidt, M.; Fehling, E.; Fröhlich, S.; Thiemicke, J. (Eds.): *Sustainable Building with Ultra-High Performance Concrete*. Kassel University Press, 2014

[Sch 12b] Schroefl, Ch.; Gruber, M.; Plank, J.: Preferential adsorption of polycarboxylate superplasticizers on cement and silica fume in ultra-high performance concrete (UHPC). *Cement and Concrete Research*, 42(11), 2012, 1401-1408

[Sch 12c] Schroefl, Ch.; Mechtcherine, V.; Gorges, M.: Relation between the molecular structure and the efficiency of superabsorbent polymers (SAP) as concrete admixture to mitigate autogenous shrinkage. *Cement and Concrete Research*, 42(6), 2012, 865-873

[Sch 15] Schröfl, Ch., Secrieru, E.: Personal communication, 2015

[Scr 11] Scrivener, K.L.; Nonat, A.: Hydration of cementitious materials, present and future. *Cement and Concrete Research*, 41(7), 2011, 651–665

[Sec 12] Secrieru, E.: *Rheometric characterisation of fresh mortars modified with different superabsorbent polymers (SAP)*. Master Thesis, TU Dresden, 2012

[Ser 67] Sereda, P.J.; Feldman, R.F.; Swenson, E.G.: *Effect of sorbed water on some mechanical properties of hydrated Portland cement pastes and compacts*. National Research Council of Canada, Division of Building Research, Research Paper No. 308, 1967

[Seu 12] Seuring, J.; Agarwal, S.: Polymers with upper critical solution temperature. *Macromolecular Rapid Communications*, 33(22), 2012, 1898-1920

[Shu 11] Shukla, N.B.; Madras, G.: Reversible swelling/deswelling characteristics of ethylene glycol dimethacrylate cross-linked poly(acrylic acid-co-sodium acrylate-co-acrylamide) superabsorbents. *Industrial and Engineering Chemistry Research*, 50(19), 2011, 10918-10927

[Sil 06] Silva, D.A.; Monteiro, P.J.M.: The influence of polymers on the hydration of Portland cement phases analyzed by soft X-ray transmission microscopy. *Cement and Concrete Research*, 36(8), 2006, 1501-1507

[Sir 12] Siriwatwechakul, W.; Siramanont, J.; Vichit-Vadakan, W.: Behavior of Superabsorbent Polymers in calcium- and sodium rich solution. *Journal of Materials in Civil Engineering*, 24(8), 2012, 976-980

[Siv 12] Sivaprakasam, K.; Mawilmada, P.; Schoess, J.N.; Schaeffer, L.; Lee, Y.H.; Ramakrishnan, L.; Mandell, M.: Rapid deswelling of poly(n-isopropyl acrylamide-co-acrylic acid) hydrogels in response to temperature changes. *World Research Journal of Biomaterials*, 1(1), 2012, 12-15

[Smi 02] Smith, A.; Chotard, T.; Gimet-Breart, N.; Fargeot, D.: Correlation between hydration mechanism and ultrasonic measurements in an aluminious cement: effect of setting time and temperature on the early hydration. *Journal of European Ceramic Society*, 22(12), 2002, 1947-1958

[Sno 12] Snoeck, D.; Van Tittelboom, K.; De Belie, N.; Steuperaert, S.; Dubruel, P.: The use of superabsorbent polymers as a crack sealing and crack healing mechanism in cementitious materials. In: Alexander, M.G.; Beushausen, H.-D.; Dehn, F.; Moyo, P. (Eds.): *Concrete Repair, Rehabilitation and Retrofitting III (ICCRRR -2012)*, 2012, Cape Town, South Africa, CRC Press, pp. 152-157

[Soh 03] Sohn, O.; Kim, D.: Theoretical and experimental investigation of the swelling behavior of sodium polyacrylate superabsorbent. *Journal of Applied Polymer Science*, 87(2), 2003, 252-257

[Sol 11] Soliman, A.M.: *Early-age shrinkage of Ultra High-Performance Concrete: Mitigation and compensating mechanisms*. PhD Thesis, The University of Western Ontario, 2011

[Sol 12] Soliman, A.; Nehdi, M.: Early-age shrinkage of Ultra-High-Performance Concrete under drying/wetting cycles and submerged conditions. *ACI Materials Journal*, 109(2), 2012, 131-139

[Sol 14] Soliman, A.; Nehdi, M.L.: Effects of shrinkage reducing admixture and wollastonite microfiber on early-age behaviour of ultra-high performance concrete. *Cement and Concrete Composites*, 46, 2014, 81-89

[Sow 15] Sowoidnich, Th.; Rachowski, T.; Rößler, Ch.; Völkel, A.; Ludwig, H.-M.: Calcium complexation and cluster formation as principal modes of action of polymers used as superplasticizer in cement systems. *Cement and Concrete Research*, 73, 2015, 42-50

[Sta 02] Staples, T.L.; Chatterjee, P.K.: Synthetic Superabsorbents. In: Chatterjee, P.K.; Gupta, B.S. (Eds.): *Absorbent Technology*, Elsevier Science B.V., 2002, pp. 283-322

[Sta 04a] Staehli, P.; Mier, J.G.M.: Rheological properties and fracture processes of HFC. In: Di Prisco, M.; Felicetti, R.; Plizzari, G.A. (Eds.): *Fibre-Reinforced Concretes (BEFIB 2004)*, Varenna, Italy, 2004, pp. 299-308

[Sta 04b] Staehli, P.; Mier, J.G.M.: Three fiber type Hybrid Fiber Concrete. In: Li, V.C.; Leung, C.K.Y.; Willam, K.J.; Billington, S.L. (Eds): *Fracture Mechanics of Concrete and Concrete Structures*, Vail, USA, 2004, pp. 1105-1112

[Sub 02] Subauste, J.C.; Odler, I.: Stresses generated in expansive reactions of cementitious systems. *Cement and Concrete Research*, 32(1), 2002, 117-122

[Sub 10] Subramaniam, K.V.; Wang, X.: An investigation of microstructure evolution in cement paste through setting using ultrasonic and rheological measurements. *Cement and Concrete Research*, 40(1), 2010, 33-44

[Tak 91] Takeuchi, H.; Okamoto, T.; Demura, K.; Ohama, Y.: Fundamental research on superabsorbent polymer as a concrete admixture. *Transactions of The Japan Concrete Institute*, 13, 1991, 17-24

[Tam 12] Tam, C.M.; Tam, V.W.Y.; Ng, K.M.: Assessing drying and water permeability of reactive powder concrete produced in Hong Kong. *Construction and Building Materials*, 26(1), 2012, 79-89

[Tam 00] Tamtsia, B.T.; Beaudoin, J.J.: Basic creep of hardened cement paste. A re-examination of the role of water. *Cement and Concrete Research*, 30(9), 2000, 1465-1475

[Tan 87] Tanaka T.; Sun, S.; Hirokawa, Y.; Katayama, S.; Kucera, J.; Hirose, Y.; Amiya, T.: Mechanical instability of gels at the phase transition. *Nature*, 325, 1987, 796-797

[Tas 98] Tasong, W.A.; Cripps, J.C.; Lynsdale, C.J.: Aggregate-cement chemical interactions. *Cement and Concrete Research*, 28(7), 1998, 1037-1048

[Tay 97] Taylor, H.F.W.: *Cement chemistry, Second Edition*. Thomas Telford, London, 1997

[TC 196-ICC] Kovler, K.; Jensen, O.M. (Eds.): *RILEM State of the Art Reports, Internal Curing of Concrete*. RILEM Publications S.A.R.L., 2007

[TC 225-SAP] Mechtcherine, V.; Reinhardt, H.-W. (Eds.): *RILEM State of the Art Reports, Application of Superabsorbent Polymers (SAP) in concrete construction*. Springer, 2012

[Teo 89] Teodoru, G.: *Zerstörungsfreie Betonprüfungen. Inbesondere Anwendung von Ultraschall. Kritische Betrachtungen*. Beton-Verlag, Düsseldorf, 1989

[Tha 11] Thakur, A.; Wanchoo, R.K.; Singh, P.: Structural parameters and swelling behavior of pH sensitive poly(acrylamide-co-acrylic acid) hydrogels. *Chemical and Biochemical Engineering Quarterly*, 25(2), 2011, 181-194

[Thi 07] Thijs, H.M.L.; Becer, C.R.; Guerrero-Sachez, C.; Fournier, D.; Hoogenboom, R.; Schubert, U.S.: Water uptake of hydrophilic polymers determined by a thermal gravimetric analyzer with a controlled humidity chamber. *Journal of Materials Chemistry*, 17(46), 2007, 4864-4871

[Tho 08] Thomas, J.J.; Allen, A.J.; Jennings, H.M.: Structural changes to the calcium-silicate-hydrate gel phase of hydrated cement with age, drying, and resaturation. *Journal of the American Ceramic Society*, 91(10), 2008, 1-8

[Tho 81] Thomas, N.L.; Double, D.D.: Calcium and silicon concentrations in solution during the early hydration of Portland cement and tricalcium silicate. *Cement and Concrete Research*, 11(5-6), 1981, 675-687

[Tia 02] Tian, Q.; Tang, X.-Z.; Zhuang, D.-Q.; Zhang, Y.-X.: Synthesis of hydrophobically modified poly(acrylic acid) gels and interaction of the gels with cationic/anionic surfactants. *Chinese Journal of Chemistry*, 20(10), 2002, 1088-1096

[Tia 08] Tian, Q.; Jensen, O.M.: Measuring autogenous strain of concrete with corrugated moulds. In: Sun, W.; Van Breugel, K.; Miao, C.; Ye, G.; Chen, H. (Eds.): *Microstructure Related Durability of Cementitious Composites*, RILEM Proceedings pro061, RILEM Publications S.A.R.L., 2008, pp. 1501-1511

[Tia 14] Tian, Q.; Liu, J.; Zhang, H.; Wang, Y.; Guo, F.; Zhang, J.: *Method for testing setting time of cement-based material*. Patent Application Publication, US2014/0130620 A1, 2014

[Trt 10] Trtik, P.; Muench, B.; Weiss, W.J.; Herth, G.; Kaestner, A.; Lehmann, E.; Lura, P.: Neutron Tomography measurements of water release from Superabsorbent Polymers in cement paste. In: Brameshuber, W. (Ed.): *Material Science*, Aachen, Germany, RILEM Proceedings pro077, RILEM Publications S.A.R.L., 2010, pp. 175-185

[Trt 08] Trtnik, G.; Turk, G.; Kavčič, F.; Bosiljkov, V.B.: Possibilities of using the ultrasonic wave transmission method to estimate initial setting time of cement paste. *Cement and Concrete Research*, 38(11), 2008, 1336-1342

[Trt 13a] Trtnik, G.; Gams, M.: The use of frequency spectrum of ultrasonic P-waves to monitor setting process of cement pastes. *Cement and Concrete Research*, 43, 2013, 1-11

[Trt 13b] Trtnik, G.; Turk, G.: Influence of superplasticizers on the evolution of ultrasonic P-wave velocity through cement pastes at early age. *Cement and Concrete Research*, 51, 2013, 22-31

[Tsu 99] Tsuji, M.; Shimata, K.; Isobe, D.: Basic studies on simplified curing technique, and prevention of initial cracking and leakage of water through cracks of concrete by applying

superabsorbent polymers as new concrete admixture. *Journal of the Society of Material Science Japan*, 48(11), 1999, 1308-1315 (in Japanese)

[Tsu 97] Tsukida, N.; Muranka, H.; Die, M.; Maeda, Y.; Kitano, H.: Effect of neutralization of poly(acrylic acid) on the structure of water examined by Raman Spectroscopy. *The Journal of Physical Chemistry*, 101(34), 1997, 6676-6679

[Tua 10] Tuan, N.V.; Ye, G.; Van Breugel, K.: Effect of rice husk ash on autogenous shrinkage of Ultra High Performance Concrete. In: Jensen, O.M.; Hasholt, M.T.; Laustsen, S. (Eds.): *Use of Superabsorbent Polymers and Other New Additives in Concrete*, Lyngby, Denmark, RILEM Proceedings pro074, RILEM Publications S.A.R.L., 2010, pp. 293-304

[Uch 92] Uchikawa, H.; Hanehara, S.; Shirasaka, T.; Sawaki. D.: Effect of admixture on hydration of cement, adsorption behaviour of admixture and fluidity and setting of fresh cement paste. *Cement and Concrete Research*, 22(6), 1992, 1115-1129

[Ulm 00] Ulm, F.-J.; Le Maou, F.; Boulay, C.: Creep and shrinkage of concrete- Kinetics approach. In: Al-Manaseer, A. (Ed.): *Creep and Shrinkage-Structural Design Effects*, SP194-04, American Concrete Institute, 2000, pp. 135-154

[Ura 12] Urayama, K.; Takigawa, T.: Volume of polymer gels coupled to deformation. *Soft Materials*, 8(31), 2012, 8017-8029

[Var 97] De Varennes, A.; Balsinhas, A.; Carqueja, M.J.: Effect of two Na polyacrylate polymers on the hydrophysical and chemical properties of a sandy soil, and on plant growth and water economy. *Revista de Ciéncias Agrárias*, 20(4), 1997, 13-27

[Var 99] De Varennes, A.; Torres, M.O.; Conceição, E.; Vasconcelos, E.: Effect of polyacrylate polymers with different counter ions on the growth and mineral composition of perennial ryegrass. *Journal of Plant Nutrition*, 22(1), 1999, 33-43

[Vas 90] Vasheghani-Farahani, E.; Vera, J.H.; Cooper, D.G.; Weber, M.E.: Swelling of ionic gels in electrolyte solutions. *Industrial & Engineering Chemistry Research*, 29(4), 1990, 554-560

[Vas 98] Vasilevskaya, V.V.; Men'shikova, L.V.: Kinetics of polyelectrolyte network swelling and collapse: Effect of ion association-dissociation. *Polymer Gels and Networks*, 6(2), 1998, 149-161

[Ver 98] Vernet, Ch.; Lukasik, J.; Prat, E.: Nanostructure, porosity, permeability, and diffusivity of Ultra High Performance Concrete (UHPC). In: *High Performance and Reactive Powder Concretes*, Sherbrooke, Canada, 1998, pp. 17-35

[Ver 03] Vervoort, S.; Budtova, T.: Evidence of shear-induced polymer release from a swollen gel particle. *Polymer International*, 52(4), 2003, 553-558

[Ver 05] Vervoort, S.; Partazhan, S.; Weyts, J.; Budtova, T.: Solvent release from highly swollen gels under compression. *Polymer*, 46(1), 2005, 121-127

[Viv 07] Viviani, M.; Glisic, B.; Smith, I.F.C.: Separation of thermal and autogenous deformation at varying temperatures using optical fiber sensors. *Cement and Concrete Composites*, 29(6), 2007, 435-447

[Voi 05] Voigt, Th.; Grosse, Ch.U.; Sun, Z.; Shah, S.P.; Reinhardt, H.-W.: Comparison of ultrasonic wave transmission and reflection measurements with P-wave and S-waves on early age mortar and concrete. *Materials and Structures*, 38(8), 2005, 729-738

[Wac 07] Wack, H.; Bertling, J.: Water swellable materials – Application in self-healing sealing systems. In: Schmets, A.J.M.; Van der Zwaag, S. (Eds.): *Self Healing Materials*, Noordwijk aan Zee, The Netherlands, Springer, 2007, pp. 1-9

[Wan 09] Wang, F.; Zhou, Y.; Peng, B.; Liu, Z.; Hu, S.: Autogenous shrinkage of concrete with Super-Absorbent Polymer. *ACI Materials Journal*, 106(2), 2009, 123-127

[Wei 99] Weiss, W.J.: *Prediction of early age shrinkage cracking in concrete*. PhD Thesis, Northwestern University, 1999

[Wei 03] Weiss, J.; Berke, N.: Admixtures for reduction of shrinkage and cracking. In: Bentur, A. (Ed.): *Early Age Cracking in Cementitious Systems*, Report of RILEM Technical Committee 181-EAS - Early age shrinkage induced stresses and cracking in cementitious systems, RILEM Publications S.A.R.L., 2003, pp. 323-335

[Win 07] Winnefeld, F.; Zingg, A.; Holzer, L.; Figi, R.; Pakusch, J.; Becker, S.: Interaction of polycarboxylate-based superplasticizers and cements: Influence of polymer structure and C3A-content of cement. In: Beaudoin, J.J.; Makar, J.M.; Raki, L. (Eds.): *Chemistry of Cement*, Montreal, Canada, 2007, pp. M6-03.2

[Win 94] Winslow, D.N.; Cohen, M.D.; Bentz, D.P.; Snyder, K.A.; Garboczi, E.J.: Percolation and pore structure in mortars and concrete. *Cement and Concrete Research*, 24(1), 1994, 25-37

[Wit 14] Witono, J.R.; Noordergraaf, I.W.; Heeres, H.J.; Janssen, L.P.B.M.: Water absorption, retention and the swelling characteristics of cassava starch grafted with polyacrylic acid. *Carbohydrate Polymers*, 103, 2014, 325-332

[Wit 09] Wittmann, F.H.: Heresies on shrinkage and creep mechanisms. In: Tanabe, T.; Sakata, K.; Mihashi, H.; Sato, R.; Maekawa, K.; Nakamura, H. (Eds.): *Creep, Shrinkage and Durability Mechanics of Concrete and Concrete Structures*, Taylor and Francis Group, London, 2009, pp. 3-9

[Won 09] Wong, H.S.; Zobel, M.; Buenfeld, N.R.; Zimmerman, R.W.: Influence of the interfacial transition zone and microcracking on the diffusitivity, permeability and sorptivity of cement-based materials after drying. *Magazine of Concrete Research*, 61(8), 2009, 571-589

[Won 11] Wong, H.S.; Pappas, A.M.; Zimmerman, R.W.; Buenfeld, N.R.: Effect of entrained voids on the microstructure and mass transport properties of concrete. *Cement and Concrete Research*, 41(10), 2011, 1067-1077

[Wyr 11] Wyrzykowski, M.; Lura, P.; Pesavento, F.; Gawin, D.: Modelling of internal curing in maturing mortar. *Cement and Concrete Research*, 41(12), 2011, 1349-1356

[Wyr 14] Wyrzykowski, M.; Lura, P.: Effect of self-desiccation and internal curing with superabsorbent polymers on the thermal expansion coefficient of HPC. In: Mechtcherine, V.; Schröfl, Ch. (Eds.): *Application of Superabsorbent Polymers and Other New Admixtures in Concrete* Construction, Dresden, Germany, RILEM Proceedings pro095, RILEM Publications S.A.R.L., 2014, pp. 169-178

[Xu 00] Xu, Y.; Chung, D.D.L.: Reducing the drying shrinkage of cement paste by admixture surface treatments. *Cement and Concrete Research*, 30(2), 2000, 241-245

[Yam 04] Yamane, Y.; Ando, I.; Buchholz, F.L.; Reinhardt, A.R.; Schlick, S.: Detection of spatial inhomogeneity in poly(acrylic acid) gels by measuring time-dependent diffusion coefficient of a probe in NMR experiments: Effect of the degree of cross-linking and degree of swelling. *Macromolecules*, 37(26), 2004, 9841-9849

[Yan 04] Yang, Q-b.; Zhang, S-q.: Self-desiccation mechanism of high performance concrete. *Journal of Zhejian University SCIENCE*, 5(12), 2004, 1517-1523

[Yan 05] Yang, Y.; Sato, R.; Kawai, K.: Autogenous shrinkage of high-strength concrete containing silica fume under drying at early ages. *Cement and Concrete Research*, 35(3), 2005, 449-456

[Ye 03] Ye, G.: *Experimental study and numerical simulation of the development of the microstructure and permeability of cementitious materials*. PhD thesis, Delft University of Technology, 2003

[Yog 91] Yogendran, V.; Langan, B.W.; Ward, M.A.: Hydration of cement and silica fume paste. *Cement and Concrete Research*, 21(5), 1991, 691-708

[Yoo 13] Yoo, D.-Y.; Park, J.-J.; Kim, S.-W.; Yoon, Y.-S.: Early age setting, shrinkage and tensile characteristics of ultra high performance fiber reinforced concrete. *Construction and Building Materials*, 41, 2013, 427-438

[Yoo 14] Yoo, D.-Y.; Park, J.-J.; Kim, S.-W.; Yoon, Y.-S.: Influence of ring size on the restrained shrinkage behaviour of ultra high performance fiber reinforced concrete. *Materials and Structures*, 47(7), 2014, 1161-1174

[Yoo 97] Yoo, M.K.; Sung, Y.K.; Cho, Ch. S.: Effect of polymer complex formation on the cloud-point of poly(N-isopropyl acrylamide) (PNIPAAm) in the poly(NIPAAm-co-acrylic acid):polyelectrolyte complex between poly(acrylic acid) and poly(allylamine). *Polymer*, 38(11), 1997, 2759-2765

[Yoo 00] Yoo, M.K.; Sung, Y.K.; Lee, Y.M.; Cho, C.S.: Effect of polyelectrolyte on the lower critical solution temperature of poly(N-isopropyl acrylamide) in the poly(NIPAAm-co-acrylic acid) hydrogel. *Polymer*, 41(15), 2000, 5713-5719

[You 72] Young, J.F.: A review of mechanisms of set-retardation in Portland cement pastes containing organic admixtures. *Cement and Concrete Research*, 2(4), 1972, 415-433

[You 73] Young, J.F.; Berger, R.L.; Lawrence Jr, F.V.: Studies on the hydration of tricalcium silicate pastes III. Influence of admixtures on hydration and strength development. *Cement and Concrete Research*, 3(6), 1973, 689-700

[Zan 02] Zanina, A.; Budtova, T.: Hydrogel under shear: A rheo-optical study on the particle deformation and solvent release. *Macromolecules*, 35(5), 2002, 1973-1975

[Zha 03] Zhang, M.H.; Tam, C.T.; Loew, M.P.: Effect of water-to-cementitious materials ratio and silica fume on the autogenous shrinkage of concrete. *Cement and Concrete Research*, 33(10), 2003, 1687-1694

[Zha 06] Zhan, B.-g.; Ding, Y.-b.: Effect of super-absorbent polymers on the internal relative humidity in high performance concrete at early ages. *Journal of Hefei University of Technology*, 29(9), 2006, 1151-1155 (in Chinese)

[Zha 12a] Zhang, J.; Hou, D.; Han, Y.: Micromechanical modelling on autogenous and drying shrinkages of concrete. *Construction and Building Materials*, 29(3), 2012, 230-240

[Zha 12b] Zhang, Y.; Zhang, W.; She, W.; Ma, L.; Zhu, W.: Ultrasound monitoring of setting and hardening process of ultra-high performance cementitious materials. *NDT&E International*, 47, 2012, 177-184

[Zha 13] Zhang, W.; Zakaria, M.; Hama, Y.: Influence of aggregate materials characteristics on the drying shrinkage properties of mortar and concrete. *Construction and Building Materials*, 49, 2013, 500-510

[Zho 03] Zhou, X.; Wenig, L.; Chen, Q.; Zhang, J.; Shen, D.; Li, Z.; Shao, M.; Xu, J.: Investigation of pH sensitivity of poly(acrylic acid-co-acrylamide) hydrogel. *Polymer International*, 52(7), 2003, 1153-1157

[Zho 08] Zhou, J.; Xiao, G.; Xu, Z.: Influence of polycarboxylate water reducers on cement hydration. In: Miao, C.; Ye, G.; Chen, H. (Eds.): *The 50-year Teaching and Research Anniversary of Prof. Sun Wei on Advances in Civil Engineering Materials*, Nanjing, China, RILEM Proceedings pro71, RILEM Publications S.A.R.L., 2008, pp. 25-31

[Zhu 15] Zhu, Q.; Barney, Ch.W.; Erk, K.A.: Effect of ionic crosslinking on the swelling and mechanical response of model superabsorbent polymer hydrogels for internally cured concrete. *Materials and Structures*, 48(7), 2015, 2261-2276

[Zhu 08] Zhutovsky, S.; Kovler, K.: Dependence between capillary stress and autogenous shrinkage for high-strength cement pastes. In: Schlangen, E.; De Schutter, G. (Eds.): *Concrete Modelling - ConMod '08*, Delft, The Netherlands, RILEM Proceedings pro58, RILEM Publications S.A.R.L., 2008, pp. 595-602

[Zhu 11a] Zhu, J.; Kee, S.-H.; Han, D.; Tsai, Y.-T.: Effect of air voids on ultrasonic wave propagation in early age cement pastes. *Cement and Concrete Research*, 41(8), 2011, 872-881

[Zhu 11b] Zhutovsky, S.; Kovler, K.; Bentur, A.: Revisiting the protected volume concept for internal curing of high-strength concretes. *Cement and Concrete Research*, 41(9), 2011, 981-986

[Zhu 13] Zhutovsky, S.; Kovler, K.: Hydration kinetics of high-performance cementitious systems under different curing conditions. *Materials and Structures*, 46(10), 2013, 1599-1611

[Zin 08] Zingg, A.; Winnefeld, F.; Holzer, L.; Pakusch, J.; Becker, S.; Gauckler, L.: Adsorption of polyelectrolytes and its influence on the rheology, zeta potential, and microstructure of various cement and hydrate phases. *Journal of Colloid and Interface Science*, 323(2), 2008, 301-312

[Zoh 08] Zohuriaan-Mehr, M.J.; Kabiri, K.: Superabsorbent Polymer Materials: A Review. *Iranian Polymer Journal*, 17(6), 2008, 451-477

[Zoh 10] Zohuriaan-Mehr, M.J.; Omidian, H.; Doroudiani, S.; Kabiri, K.: Advances in non-hygenic applications of superabsorbent hydrogel materials. *Journal of Materials Science*, 45(21), 2010, 5711-5735

Norms, standards, guidelines and other evaluation aids:

[ASTM C 1581-04] ASTM C 1581-04:2004 *Standard test method for determining age at cracking and induced tensile stress characteristics of mortar and concrete under restrained shrinkage*.

[ASTM C1698-09] ASTM C1698-09. *Standard test method for autogenous strain of cement paste and mortar*.

[DAfStb 03] Guideline for Self-Compacting Concrete (DAfStb-Richtlinie für Selbstverdichtenden Beton), German Committee for Reinforced Concrete (Deutscher Ausschuss für Stahlbeton), DAfStb (Hrsg.), Berlin, 2003

[DIN EN 480-02] DIN EN 480-02:2006. *Admixtures for concrete, mortar and grout – Test methods – Part 2: Determination of setting time; German version EN 480-2:2006.*

[DIN EN 480-11] DIN EN 480-11:2005-12. *Admixtures for concrete, mortar and grout - Test methods - Part 11: Determination of air void characteristics in hardened concrete; German version EN 480-11:2005*.

[DIN EN 1015-3] DIN EN 1015-3:2004-06. *Methods of test for mortar for masonry - Part 3: Determination of consistence of fresh mortar (by flow table) (includes amendment A1:2004); German version EN 1015-3:1999 + A1:2004*.

[DIN EN 1015-6] DIN EN 1015-6:1998-12. *Methods of test for mortar for masonry - Part 6: Determination of bulk density of fresh mortar; German version EN 1015-6:1998.*

[DIN EN 1015-7] DIN EN 1015-7:1998-12. *Methods of test for mortar for masonry - Part 7: Determination of air content of fresh mortar; German version EN 1015-7:1998.*

[DIN EN 1015-11] EN 1015-11:1999 + A1:2006 (D). *Methods of test for mortar for masonry - Part 11: Determination of flexural and compressive strength of hardened mortar; German version EN 1015-11:1999+A1:2006*.

[DIN 1045-1] DIN 1045-1:2008-08. *Concrete, reinforced and prestressed concrete structures – Part 1: Design and construction (Tragwerke aus Beton, Stahlbeton und Spannbeton – Teil 1: Bemessung und Konstruktion).* Beuth Verlag GmbH, Berlin, Germany

[DIN 1048-5] DIN 1048-5:1991-06. *Testing methods for concrete; hardened concrete; specially prepared specimens*.

[DIN EN 12350-6] DIN EN 12350-6:2000-03. *Testing fresh concrete - Part 6: Density; German version EN 12350-6:1999*.

[DIN EN 12350-7] DIN EN 12350-7:2000-11. *Testing fresh concrete - Part 7: Air content - Pressure methods; German version EN 12350-7:2000.*

[DIN EN 12350-8] DIN EN 12350-8:2010-12. *Testing fresh concrete - Part 8: Self-compacting concrete - Slump-flow test; German version EN 12350-8:2010*.

[DIN EN 12390-3] EN 12390-3:2001 (D). *Testing hardened concrete - Part 3: Compressive strength of test specimens; German version EN 12390-3:2001*.

[DIN 52450] DIN 52450:1985-08. *Testing of inorganic non-metallic building materials - Determination of shrinking and swelling on small test pieces*.

[DIN 66133] DIN 66133:1993-06. *Determination of pore volume distribution and specific surface area of solids by mercury intrusion*.

[EFNARC 02] EFNARC (The European Federation of Specialist Construction Chemicals and Concrete Systems): *Specification and Guidelines for Self-Compacting Concrete*, 2002

[MATHPORTAL] MathPortal by Miloš Petrović, http://www.mathportal.org/calculators/calculus/derivative-calculator.php, until 2014

[UNIPHIZ] Uniphiz Lab: FindGraph (different versions), www.findgraph.com/download.htm, until 2014

[WSP 11] Standard Test Methods for the Nonwovens Industry, World Strategic Partners recommended test methods for superabsorbent materials: WSP 200.3 (11), WSP 210. 3 (11), WSP 220. 3 (11), WSP 230. 3 (11), WSP 240. 3 (11), WSP 241. 3 (11), WSP 242. 3 (11), WSP 250. 3 (11), WSP 270. 3 (11), 2011

A Abbreviations, symbols, and indices

Abbreviations

x.y % SAP	Percentage of superabsorbent polymer (SAP) in relation to mass of cement
2D/3D	Two-dimensional/three-dimensional
2^{nd} PEAK	Second peak temperature
agg	Sand or other aggregate content
dx	First derivative of variable x
d2x	Second derivative of variable x
fagg	Fine aggregate content
fit	Best fitting curve to the data
fr-dry	One of the applied methods of hydration cessation − freeze-drying
iso + vac	One of the applied methods of hydration cessation − treatment with isopropanol under vacuum in the first 24 hours and subsequent oven drying at 40 °C until sample mass constancy
large tube	Non-standardized AS test [Tia 08] performed using larger corrugated tube and, and correspondingly, other version of test set-up compared with ASTM C 1698-09
i line	Help line indicating moment of phenomenon i occurrence
original	Data as obtained from test
oven dry	One of the applied methods of hydration cessation − drying in oven at the temperature of 40 °C until sample mass constancy
ref. i	Reference number i
sf	Silica fume content
sf/c	Silica fume-to-cement ratio
small tube	AS test performed in accordance with ASTM C 1698-09
sp	Superplasticizer content
vac	Mixture produced with high-intensity mixer equipped with vacuum unit
var	Mixture with varied content of superplasticizer in comparison to reference
vol.-%	Volume fraction
w_{mixing}	Mass proportion of mixing water to cement
w_{total}	Mass proportion of total water to cement
$w_{total,eq}$	Mass proportion of total water to binder

w/c	Water-to-cement ratio
$(w/c)_e$	Ratio (mass proportion) of entrained water needed to avoid self-desiccation to cement
w_{IC} or $(w/c)_{IC}$	Ratio/mass proportion of extra added water (for internal curing) to cement
w/cm or w/b	Water-to-binder ratio
Al^{3+}	Aluminium ion
AE	Acoustic emission
AS	Autogenous shrinkage
C- and Cf-	Coarse-grained UHPC without and with steel fibres, respectively
C_3S	Tricalcium silicate (alite)
C_2S	Dicalcium silicate (belite)
C_3A	Tricalcium aluminate (celite)
C_4AF	Tetracalcium alumino ferrite (ferrite)
Ca^{2+}	Calcium ion
$CaCO_3$	Calcium carbonate
CO_2	Carbon dioxide
COO^- or COOH	Carboxyl (functional) group
C-S-H	Calcium silicate hydrate
CT	X-ray computed tomography
IC	Internal curing
EDX	Energy-dispersive X-ray spectroscopy/emission
ESEM	Environmental Scanning Electron Microscopy
F- and Ff-	Finely grained UHPC without and with steel fibres, respectively
FT-IR	Fourier transform infrared spectroscopy
H^+	Hydrogen ion
Ibid.	Ibidem (*latin*) = the same source in the immediately following reference (note: after change introduced to original meaning!)
IC	Internal curing
IC variables	Certain amount of SAP and extra water used for purpose of internal curing
IPi	Inflection point number i, with i being 1, 2 or 3

IRT	Instrumented ring test(s); small IRT = tests performed with test set-up produced by Dr. Eppers [Epp 10]; big/large IRT = tests performed with test set-up acc. to ASTM C 1581-04
ITP	Intersection point
ITZ	Interfacial Transition Zone
K^+	Potassium ion
LCST	Lower critical solution temperature
LVDT	Linear variable differential transformer
MIP	Mercury intrusion porosimetry
MRI	Magnetic resonance imaging
Na^+	Sodium ion
NMR	Nuclear magnetic relaxation/resonance
OH^-	Hydroxide/hydroxyl ion
PCE	Polycarboxylate ether superplasticizer
PSD	Particle size distribution
RH	Relative humidity
RPC	Reactive Powder Concrete
SAP, SAPs	Superabsorbent polymer(s)
TS	Total shrinkage
UCST	Upper critical solution temperature
UPV	Ultrasonic pulse velocity
UHPC(s)	Ultra-High Performance Concrete(s)

Capital letters

A	Solid percolation threshold
B	Second of the intersections points in the UPV-t graph
C	Concrete age at cracking
D	MIP pore diameter
E	End of instrumented ring test
E_{id}	Young's modulus of UHPC at the concrete age of i days
E_s	Young's modulus of steel

R	Ideal gas constant
R_{IS}	The inner radius of steel ring
R_{OC}	The outer radius of concrete ring
R_{OS}	The outer radius of steel ring
S	SAP content
T	Temperature

Lower case letters

a, b	Equation constants from regression analysis
c	Cement content
d	Diameter of fibre
d	Days
d_{10}	Particle diameter corresponding to 10 % cumulative undersize PSD
d_{50}	Mass median diameter/the medium value of the PSD
d_{90}	Particle diameter corresponding to 90 % cumulative undersize PSD
d_{95}	Particle diameter corresponding to 95 % cumulative undersize PSD
f	Steel fibres type or content
$f_{cf,id}$	Flexural strength at the concrete age of i days
$f_{cm,\ prism\ halves}$	Compression strength measured on halves of beam 40x40x160 mm³
$f_{cm,\ cubes}$	Compression strength measured on cube with side length of 100 mm
k	Artificial constant
p	Initial porosity
p_c	Capillary pore pressure/stress
t	Time/concrete age as counted from contact of cement with water
t_x^y	Time of event “y” occurrence as determined from plot of “x” variable against time
w	Water content

Greek letters

α	Degree of hydration
α_{IC}	Extra degree of hydration attributed to internal curing

α_{max}	Final (= maximum attainable) degree of hydration
α_T	Coefficient of thermal expansion
ΔT	Temperature difference
ΔV_c	Chemical shrinkage (cement)
ΔV_s	Chemical shrinkage (silica fume)
ε	Strain
η^*	Complex viscosity
μ	Plastic viscosity
ρ_c	Density of cement
ρ_{sf}	Density of silica fume
ρ_w	Density of water
$\sigma_{Actual\text{-}Max}$	Maximum residual tensile stress
τ	Shear stress
τ_0	Yield stress

Indices and prefixes

0	Point of attaining minimum temperature
2. PEAK	Second peak temperature
50-100 mV	Change of amplitude range in ultrasound measurement
ε	Strain
c	Cement
sf	Silica fume
total	Total content
w	Water
IC	Internal curing
IPi	Inflection point number i, with i being 1, 2 or 3
ITP	Intersection point
T	Temperature
UPV	Ultrasonic pulse velocity

Symbols and miscellaneous

None

B UHPC mix design vs. autogenous shrinkage mitigation

Table B.1: Comparison between manner of composing UHPC and mitigation strategy for autogenous shrinkage.

Component or parameter	Main attribute	General requirement for UHPC	Role	AS reduction requirement	Manner of mitigation	Solution/ Outcome disadvantage
Cement	Main binder; first or second (after finer pozzolan, if applicable) finest ingredient	**Very high content of fine cement**; preferred CEM I of high early strength; for durability reasons: low shrinkage, high sulphate resistant and of low alkali cements; high C_3A not welcomed [Lar 94][Ric 95] Usage of finer cement for higher strength [Yud 72] and early age strength development [Ben 01c]	• Gluing matter (after combined with water) • Needed as packing agent • Needed for transferring stresses (unhydrated cement particles = solids of very high Young's modulus and higher than that of aggregate)	• **Usage of low cement contents** [Ben 01c], e.g. replacement with different powders [Ma 02][Moe 10] (assumption/simplification made: limitation of chemical shrinkage outweighs removal of the important internal restraint) • Usage of coarse cement [Taz 95b][Ben 99][Ben 01c] (assumption/simplification: long lasting hydration [Che 01][Fah 07] is outweighed) • Cement with appropriate amount of free lime [Bar 05] and low alkalis [Ven 68][San 12] • Low heat/shrinkage (i.e. low aluminate), high belite (C_2S) cement [Taz 95b] • If combined with SAP, usage of CEM II/B-V 32.5 not advised [Klemm and Sikora 2012, ref. 3 *Ibid.* Kle 13]	When using coarser cement [Ben 99][Ben 01c]: • Less rapid hydration progress • More time and larger degree of hydration needed for capillary depercolation = delaying restriction of water movement • Larger pores = lowering capillary stresses • Lower empty porosity fraction = less rapid reduction of relative humidity • Favourable ITZ modification • Promoting autogenous swelling in early ages Furthermore: • More unhydrated cement particles acting as ultra-stiff microaggregate = internal restraint [Han 87][Pic 13] • Secondary role: Less superplasticizer needed	• Negative effect on strength and durability

(continued on following page)

Table B.1: Comparison between manner of composing UHPC and mitigation strategy for autogenous shrinkage (*continued*).

Component or parameter	Main attribute	General requirement for UHPC	Role	AS reduction requirement	Manner of mitigation	Solution/ Outcome disadvantage
Silica fume	Inherent binder ingredient, with exceptions e.g. [Deu 06][Khu 08][Mor 11]; approx. 100 smaller than cement	Optimum content: **around 25%** (in weight of cement) [Ric 95]; lower contents yet economically justified and typically allowing approaching strength of UHPC [Khu 08][Mor 11][Mad 13]; excessive amounts (>15% [Mad 13]) making mix viscous and sticky; product should be of low alkali and carbon content [Lar 94]; best: undensified product or suspension	Various physical and chemical effects: • Filler effect (e.g. [Det 89]) at contents close to optimum [Ric 95][Ma 02] • Pozzolan of importance starting often in later ages [Det 89], of max effectiveness at around 15% for low w/b [Yog 91] • Seeding effect: acting as precipitation/ nucleation sites provider [Oga 80][Sar 87][Det 89][ACI 234R-06]; simultaneously, alite dissolution rate accelerator [Oga 80] • Cohesion increase contributor [Det 89][ACI 234R-06] • Secondary role: lubrication effect [Ric 95] In turn [ACI 234R-06]: • Pore size refinement • ITZ as well as fiber bond improvement (the latter for RPC discussed in [Cha 04]) • Adhesion/bond strength between paste and aggregates improvement • General reduction of structural flaws • Control over alkali-silica reaction	• **Content reduction or, at best complete elimination**, e.g. substitution with less reactive fly ash [Ben 01c] like in case of cement, assuming it possesses definable favourable properties [Ter 05] • Alternatively: partial substitution with quartz powder [Che 10] • Since properties can be engineered [Oer 14], substitution with synthetic products may also present some advantage Rival viewpoint: • Only partial elimination truly required due to low pozzolanic reactivity in UHPC [Pfe 10] likely owed to low w/c [Sar 87], low content of portlandite available for conversion or other reasons	• Decreasing the very high chemical shrinkage of pozzolan [Ben 04] = reduction in amount of empty porosity created • Coarsening of pore structure [Ben 04] = less rapid RH reduction • Lowering water demand = Potential increase in unbound water content • Increased ionic mobility = increased diffusion, in analogy to theory of [Kum 87] • Lower amount of C-S-H produced = less spaces where shrinkage mechanisms are operative as well as no reduction in calcium hydroxide-associated shrinkage restrainer [Jen 96] • Reduction in relative basic creep, although effect finally dependent on sf content [Bro 00]	• Impaired development of concrete strength in case of non-synthetic products • Production of less durable materials

(continued on following page)

Table B.1: Comparison between manner of composing UHPC and mitigation strategy for autogenous shrinkage (*continued*).

Component or parameter	Main attribute	General requirement for UHPC	Role	AS reduction requirement	Manner of mitigation	Outcome disadvantage
w/c; w/b	Basic concrete parameter	**w/c: typically around 0.2** (see Appendix C) and optimum when around 0.18 [Lar 94] w/b: optimum when approx. 0.14 [Lar 94][Ric 95]	On condition that parameters' optima have been attained: • Maximization of density • Securing ease of placement	• **Best: w/c ≥ 0.42** [Jen 01b], with exception for very low w/c ratios [Che 01] (assumption: no other reason for capillary discontinuity)	• Elimination of self-desiccation given the homogenous matrix • Higher connectivity of pores • Improved diffusivity	Impaired mechanical performance and durability, with exceptions e.g. in case of former [Sch 03]
Super-plasticizer	Water-reducer to plasticize the mix	**At least few percent (in weight of cement)** and typically usage advised-excessive amounts of polycarboxylate-type admixture or other new generation superplasticizer; product must have confirmed compatibility with binder [Han 08][Pla 09] [CONCRETEPORTAL2]; favourable chemical structure being recognized [Win 07][Han 08][Hir 08][Pla 09][Sch 12b]; addition timing important as well e.g. stepwise and delayed addition of superplasticizer enhancing workability [Tue 08][Han 08]	• Steric hindrance-dominated [Han 08] dispersion of solid particles i.e. cement, cement hydrate particles and silica fume • Reduction of surface tension of water [Mor 01][Moh 10] • Decrease of frictional resistance or other [CONCRETEPORTAL2] In turn: • Maximal limitation of water restrained/entrapped due to flocculation [Sak 06] • Influence on porosity in terms of both the total porosity and the pore size distribution (effect being likely a function of dosage and air-entraining ability, among others)	• **The lower content, the better** [Mor 01] analogous to effect on drying shrinkage of UHPC [Tam 12] • **Rival opinion**: - though studies majority showing similar trend, **vague view on effect** from past studies on different shrinkage types [Bis 03] - also for each PCE **effect must be analysed individually** given the numerous decisive and varied factors: concrete age referenced to [Mor 01][Che 10][Moh 10], effect of bleeding [Moh 10] and individual ability of air-entrainment by PCE [Laz 13]	Assuming sp is air entraining, and the surface tension reduction effect is outweighed, is still high enough or the mechanism is not operative in shrinkage: • Lower volume of entrained air and/or larger bubbles radii = lower capillary depression [Mor 01] • Stronger paste less prone to deformation [Bro 00] • Additionally: Less pronounced delay in chemical kinetics = higher strength [Mor 01] Without any particular condition specified: • Potentially less rapid relative humidity reduction given the corresponding effect of SP [Jen 93] • Worse dispersion of silica fume [Sar 87] = limited pozzolanic reactivity	Lowering superplasticizer in low w/c concrete signifies: • worsening workability • faster loss of workability

(continued on following page)

Component or parameter	Main attribute	General Requirement	Role	AS reduction requirement	Manner of mitigation	Outcome disadvantage
Aggregate	Important source of internal restraint	**Elimination of coarse aggregates** [Lar 94][Ric 95]; optimization of granular mixture, especially introduction of cocktail of quartz aggregates with **max. size of 600 µm** [Ric 95]; otherwise clean, cubical, angular, 100% crushed aggregate with minimum of flat and elongated particles e.g. bauxite or basalt split [Cwi 06]	Ascribed to usage of fine aggregates: • Enhancement of homogeneity [Ric 95] • **Maximization of packing density** [Ric 95] • Minimising Maximum Paste Thickness [Lar 94] • Additional benefits expected in hydration (especially upon heat treatment)and behaviour under load	• **Best: inclusion of coarse aggregates** • When only **fine aggregate** is used: diameter of **min. 0.5-1 mm** [Bis 01][Bis 02] • Possibly **lowest specific surface area of aggregate** [Mou 11], in analogy to effect on drying shrinkage [Ima 07] • Possibly highest content • Possibly highest stiffness and volumetric stability	Acc. to [Mou 11]: • global mechanical effect • local restraint • dilution effect • "water tank" effect On the other hand: • General increase of chemical shrinkage per g of cement [Mou 11] • Less and smaller unhydrated cement grains	• Potential strength increase limitation (coarse aggregates) due to: - severe stress concentration - decreased reactive components content

(continued on following page)

Table B.1: Comparison between manner of composing UHPC and mitigation strategy for autogenous shrinkage (*continued*).

Component or parameter	Main attribute	General Requirement	Role	AS reduction requirement	Manner of mitigation	Outcome disadvantage
Steel fibres	Largest constituent (in case of finely grained mixes)	Always comprehensive judgement in view of the desired performance [Ros 01] and choice depending on concrete behaviour in both fresh and hardened state; commonly **short, small-sized steel fibres, in amount around 2%** [Ric 95] **like fine straight smooth fibres of (low) aspect ratio of 40 to 60** [Bor 01] or similar, see Appendix C; fibre cocktails or even replacement with other fibre type not excluded [Ros 01][Mad 13]	Owed to potential intervening at different stages [Ros 01] and other: • Enhancement of fracture toughness [Pai 89][Ben 04] • Confinement after cracking [Pai 89] • Ductility, tensile capacity and tensile strength improvement In turn: • At least some enhancement of mechanical performance, with effect extent finally depending on more factors [Cwi 06] • Secure behaviour of concrete structures [Pai 89]	• When geometry is favourable and given Young's modulus is very high: **content as low as 0.25% by volume** [Saj 12] • When some fibre properties unsatisfying and generally **for greater** though limited [Lou 99][Che 01] (with exceptions e.g. [Fah 07]) **shrinkage reduction**: - **higher contents** [Miy 98][Saj 12], with optimum likely around 1 [Bar 03] -2% [Che 89], - **usage of other geometries and surface textures than of straight smooth fibres** [Man 88][Che 89], - choosing more favourable, typically **higher aspect ratios** [Man 88][Pai 89][Che 89][Saj 12], with exceptions [Saj 12]; also **longer fibres** [Pai 89][Che 89][Saj 12] • Favourable orientation [Man 88][Far 07] and even distribution [Far 07] (no fibre balling [Saj 12]) • **Rival opinion: fibre effect as such put in question by some researchers** [Ben 04]	• High stiffness and bearing capacity of fibres [Saj 12] = high moduli ratio between fiber and matrix in early age = force transfer [Saj 12] and early hindrance of free deformation on micro-level [Kam 06] • Increase in the modulus of elasticity of the paste [Che 89][Far 07] • Increasing water permeability [Saj 12] though holding true in dependence on microcracking occurrence [Sch 12a]	• Without heat treatment, increased porosity in vicinity of fibres [Sch 12a] • Commonly observed negative effect on workability, with exceptions, see e.g. [Cwi 06]

References for Appendix B

For [Bar 05], [Ben 01c], [Ben 04], [Bis 01], [Bis 02], [Bor 01], [Che 10], [Che 01], [Far 07], [Jen 93], [Jen 96], [Jen 01b], [Kle 13], [Laz 13], [Lou 99], [Moe 10], [Moh 10], [Mor 01], [Mou 11], [Oga 80], [Pai 89], [Pfe 10], [Pic 13], [Pla 09], [Ric 95], [Sak 06], [San 12], [Sch 12a], [Sch 12b], [Tam 12] and [Yog 91] please see Chapter REFERENCES.

[ACI 234R-06] ACI Committee 234: *Guide for the Use of Silica Fume in Concrete*. American Concrete Institute, Farmington Hills, MI, 2006

[Bar 03] Barr, B.I.G.; El-Baden, A.S.A.: Shrinkage properties of normal and high strength fibre reinforced concrete. *Structures & Buildings*, 156(1), 2003, 15-25

[Ben 99] Bentz, D.P.; Garboczi, E.J.; Haecker, C.J.; Jensen, O.M.: Effects of cement particle size distribution on performance properties of Portland cement-based materials. *Cement and Concrete Research*, 29(10), 1999, 1663-1671

[Bis 03] Bisschop, J.: Drying shrinkage microcracking at early ages. In: Bentur, A. (Ed.): *Early age cracking in cementitious systems*, RILEM Publications S.A.R.L., 2003, pp. 47-55

[Bro 00] Brooks, J.J.: Elasticity, creep, and shrinkage of concretes containing admixtures. In: Al-Manaseer, A. (Ed.): *The Adam Neville Symposium: Creep-Structural Design Effects*, Special Publication 194, Paper No. 10, American Concrete Institute, Farmington Hills, MI, 2000, pp. 283-360

[CONCRETEPORTAL2] The Concrete Portal, Cement-Superplasticizer Compatibility. http://www.theconcreteportal.com/compat.html, 2015

[Che 89] Chern, J.-Ch.; Young, Ch.-H.: Study of factors influencing drying shrinkage of steel fiber reinforced concrete. *ACI Materials Journal*, 87(2), 1989, 123-129

[Cwi 06] Cwirzen, A.; Pentalla, V.: Effect of increased aggregate size on the mechanical and rheological properties of RPC. In: Marchand, J.; Bissonnette, B.; Gagné, R.; Jolin, M.; Paradis, F. (Eds.): *Advances in Concrete through Science and Engineering*, Quebec City, Canada, RILEM Proceedings pro051, RILEM Publications S.A.R.L., 2006, pp. 207-224

[Deu 09] Deuse, T.; Hornung, D.; Möllmann, M.: From Mikrodur to Nanodur technology: Standard cement for practice-oriented manufacture of UHPC. *Betonwerk und Fertigteil-Technik*, 75(5), 2009, 4-15

[Det 89] Detwiler, R.J.; Mehta, P.K.: Chemical and physical effects of silica fume on the mechanical behaviour of concrete. *ACI Material Journal*, 86(6), 1989, 609-614

[Han 87] Hansen, W.: Constitutive model for predicting ultimate drying shrinkage of concrete. *Journal of the American Ceramic Society*, 70(5), 1987, 329-332

[Han 08] Hanehara, S.; Yamada, K.: Rheology and early age properties of cement systems. *Cement and Concrete Research*, 38(2), 2008, 175-195

[Hir 08] Hirschi, Th.; Wombacher, F.: Influence of different superplasticizers on UHPC. In: Fehling, E.; Schmidt, M.; Stuerwald, S. (Eds.): *Ultra High Performance Concrete (UHPC)*, kassel university press: University of Kassel, 2008, pp. 77-84

[Ima 07] Imamoto, K.; Arai, M.: Specific surface area of aggregate and its relation to concrete drying shrinkage. *Materials and Structures*, 41(2), 2008, 323-333

[Kam 06] Kamen, A.: Time dependent behaviour of Ultra High Performance Fibre reinforced Concrete (UHPFRC). In: Vogel, Th.; Mojsilović, N.; Marti, P. (Eds.): 6th International PhD Symposium in Civil Engineering, Zurich, 2006, pp.72-73

[Khu 08] Khurana, R.; Magarotto, R.; Moro, S.: User Friendly Ultra High Performance Concrete. In: (Eds.): *Advances Concrete Technology in the Middle East*, Dubai, November 19-20, 2008

[Kum 87] Kumar, A.; Komarneni, S.; Roy, D.M.: Diffusion of Cs^+ and Cl^- through sealing materials. *Cement and Concrete Research*, 17(1), 1987, 153-160

[Lar 94] De Larrard, F.; Sedran, T.: Optimization of Ultra-High Performance Concrete by the use of a packing model. *Cement and Concrete Research*, 24(6), 1994, 997-1009

[Ma 02] Ma, J.; Schneider, H: Properties of Ultra-High-Performance Concrete. *Lacer*, 7, 2002, 25-32

[Mad 13] Abdulla Taisir Al Madhoun, A.T.: *Mechanical properties of Ultra High Performance Fiber Reinforced Self-Compacting Concrete*. Master Thesis, The Islamic University of Gaza, 2013

[Man 88] Mangat, P.S.; Azari, M.M.: Shrinkage of steel fibre reinforced cement composites. *Materials and Structures*, 21(3), 1988, 163-171

[Miy 98] Miyazawa, S.; Kuroi, T.; Shimomura, H.: Effect of fiber on autogenous srhinkage stress of high-strength cement mortar. In: Cohen, M.; Mindess, S.; Skalny, J.P. (Eds.): *Material Science: The Sidney Diamond Symposium*, Wiley, 1998, pp. 179-190

[Mor 11] Moro, S.; Di Prisco, M.; Barragan, B.; Magarotto, R.; Roncero, J.: Ultra high performance concrete: from material optimization to structural applications. Structural Engineers World Congress (SEWC), 2011, Como, Lombardia, Italy. Accessed online: https://joanaroncero.files.wordpress.com/2011/09/cp40-sewc2011-milan.pdf

[Oer 14] Oertel, T.; Hutter, F.; Helbig, U.; Sextl, G.: Amorphous silica in ultra-high performance concrete: First hour of hydration. *Cement and Concrete Research*, 58, 2014, 131-142

[Ros 01] Rossi, P.: Ultra-High-Performance Fiber-Reinforced Concretes: A French perspective on approaches used to produce high-strength, ductile fiber-reinforced concrete. *Concrete International*, 23(12), 2001, 46-52

[Saj 12] Saje, D.; Bandelj, B.; Šušteršič, J.; Lopatič, J.; Saje, F.: Autogenous and drying shrinkage of fibre reinforced high-performance concrete. *Journal of Advanced Concrete Technology*, 10(2), 2012, 59-73

[Sar 87] Sarkar, S.L.; Aïtcin, C.-P.: Dissolution rate of silica fume in very high strength concrete. *Cement and Concrete Research*, 17(4), 1987, 591-601

[Sch 03] Schmidt, M.; Fehling, E.; Teichmann, T.; Bunje, K.; Bornemann, R.: Ultra-High Performance Concrete: Perspective for the Precast Concrete Industry. *Concrete Precasting Plant and Technology*, 69(3), 2003, 16-29

[Taz 95b] Tazawa, E.-i.; Miyazawa, S.: Influence of cement and admixture on autogenous shrinkage of cement paste. *Cement and Concrete Research*, 25(2), 1995, 281-287

[Ter 05] Termkhajornkit, P.; Nawa, T.; Nakai, M.; Saito, T.: Effect of fly ash on autogenous shrinkage. *Cement and Concrete Research*, 35(3), 2005, 473-482

[Tue 08] Tue, N.V.; Ma, J.; Orgass, M.: Influence of addition method of superplasticizer on the properties of fresh UHPC. In: Fehling, E.; Schmidt, M.; Stuerwald, S. (Eds.): *Ultra High Performance Concrete (UHPC)*, kassel university press: University of Kassel, 2008, pp. 93-100

[Ven 68] Venuat, M.: Influence du ciment sur le retrait hydraulique après prise. Colloque International sur le retrait des bétons hydrauliques, Madrid 1968, Vol. I, I-H

[Win 07] Winefeld, F.; Becker, S.; Pakusch, J.; Götz, Th.: Effects of the molecular architecture of the comb-shaped superplasticizers on their performance in cementitious materials. *Cement and Concrete Composites*, 29(4), 2007, 251-262

[Yud 72] Yudenfreund, M.; Hanna, K.M.; Skalny, J.; Odler, I.; Brunauer, S.: Hardened Portland cement pastes of low porosity V. Compressive strength. *Cement and Concrete Research*, 2(6), 1972, 731-743

C Compositions of UHPC mixtures in rival and own studies

Finely grained UHPC compositions from important rival studies and the patents

Table C.1: Exemplary compositions of UHPC mixes without coarse aggregates from patented products and laboratory materials.

Mix constituent	Mix designation or marketed name [reference]					
	Optimal mortar mix 4 [Lar 94]	**RPC200 [Ric 94]**	**Typical RPC [Ver 98]**	**Ductal®, one of types [Gra 06]**	**CEM-TEC$_{multiscale}$®, type MSCC-NG [Ros 02]**	**CARDIFRC®-mix I [Far 07]**
	Content [kg/m³, otherwise the unit reported]					
Cement (c)	1080.6	955	746	712	1050.1	855
Silica fume (sf)	334.2	229+10	242	231	268.1	214
Fine aggregate (fagg)	813.2	1051	1066+224	1020+211	514.3	470+ 470
Water (w)	198.2	153	142	109	180.3	188
Super-plasticizer (sp)	1.3 % c + 2 % sf (=saturation quantity, in solid content)	13	9	30.7	44	28
Steel fibres (f)	-	191	161	156	858	390 +78
Basic or special ingredient specification: type or type combination	fagg: quartz sand with d >100 µm and < 400 µm; sp: melamine	fagg: quartz sand; sp: polyacrylate; sf: undensified and precipitated; f: l/d=12.5/0.18 mm	fagg: quartz sand and quartz flour; f: l/d= 13/0.2 mm	fagg: fine sand and ground quartz; sp: PCE but also additional accelerator 30 kg/m³ f: l/d=12.7/0.2 mm	f: mix of steel fibres with three different geometries and max length of 20 mm (multi-scale fibre-reinforcement)	fagg: quartz powder (9-300 µm) and sand (250-600 µm); f: 5 vol.-% and 1vol.-% of f with l=6 and 13 mm, respectively
w/c	0.183	0.15	0.20	-	0.201	0.22
sf/c	0.309	0.25	0.32	0.32	0.26	0.25
w/b	0.140	-	Not given	-	0.16	0.18
Air entrained [vol.-%]	2.6 and 2.0 (2nd series)	-	-	-	2.0	-

Finely grained UHPC compositions used in own investigations

In formulation of UHPC with IC, the volume of the pores entraining the water was explicitly considered in the mix design, similar to the customary method used for air pores. It was assumed that water pores have the density of free water, while the SAP itself was, because of its very small proportion, neglected in the calculation. Since the water pores demand a certain share of mix unit volume, the other components of the mixture must be proportionally reduced in the mixtures with SAP and curing water in comparison to the reference mixture without such addition.

Table C.2: Compositions of UHPC mixes without coarse aggregates studied [kg/m³ concrete].

Nb	Mixture	Cement c	Silica fume sf	Mixing water w	Extra water for IC	SAP	Quartz flour I (W12)	Quartz flour II (W3)	Fine aggregate	Coarse aggregate	Steel fibres f	Superplasticizer sp
1	F-R / F-R-mm/ F-R-vac	853.4	138.5	170.3	-	-	212.3	-	1000.1	-	-	30.2
2	Ff-R (=M2Q)	832.0	135.0	166.0	-	-	207.0	-	975.0	-	192.0	29.4
3	F-S.4	853.4	138.5	170.3	-	3.41	212.3	-	1000.1	-	-	30.2
4	F-S.4-sp var	809.7	131.4	161.6	-	3.24	201.5	-	948.9	-	-	83.5
5	F-R.04 / F-R.04-vac	824.5	133.8	197.5	-	-	205.1	-	966.3	-	-	29.1
6	F-S.3.04 / F-S.3.04-vac	824.5	133.8	164.5	33.0	2.47	205.1	-	966.3	-	-	29.1
7	Ff-S.3.04	804.6	130.5	160.5	32.2	2.41	200.1	-	942.9	-	185.7	28.4
8	F-S.3.045-mm	821.1	133.2	163.8	36.9	2.46	204.3	-	962.2	-	-	29.1
9	F-S.3.05	817.6	132.7	163.1	40.9	2.45	203.4	-	958.2	-	-	28.9
10	F-R.07-sp var	817.6	132.7	220.4	-	-	203.4	-	958.1	-	-	11.0
11	F-R.07	804.2	130.5	216.8	-	-	200.1	-	942.4	-	-	28.4
12	F-S.4.06-mm	810.8	131.6	161.8	48.7	3.24	201.7	-	950.2	-	-	28.7
13	F-S.4.065	807.5	131.0	161.1	52.5	3.23	200.9	-	946.3	-	-	28.5
14	F-S.4.07	804.2	130.5	160.5	56.3	3.22	200.1	-	942.4	-	-	28.4
15	Ff-S.4.07	785.2	127.4	156.7	55.0	3.14	195.3	-	920.1	-	181.2	27.7
16	F-R.08	797.6	129.4	222.9	-	-	198.4	-	934.7	-	-	28.2
17	F-S.6.08 / F-S.6.08-mm	797.6	129.4	159.1	63.8	4.79	198.4	-	934.7	-	-	28.2
18	F-S.6.085-mm	794.4	128.9	158.5	67.5	4.77	197.6	-	930.9	-	-	28.1
19	F-S.6.09-mm	791.1	128.4	157.8	71.2	4.75	196.8	-	927.1	-		28.0
20	F-S1.0.16	748.7	121.5	149.4	119.8	7.49	186.3	-	877.3	-	-	26.5

Coarse grained UHPC compositions from important rival studies and the patents

Table C.3: Exemplary compositions of UHPC mixes with coarse aggregates from patented products and laboratory materials.

Mix constituent	Mix designation or marketed name [reference]				
	Compact Reinforced Composite- CRC® [Aar 08] (with binder based on Densit®)	**BSI/Ceracem®, type CERACEM B1M2.5U1D7 [Lap 07]**	**Vicat's Composite Concrete- BCV® [BCV][Tou 11]**	**Contec Secutec®, type S9 [Kap 04] [Bal 11]**	**UHPC2 with coarse aggregates**
	Content [kg/m³, otherwise the unit reported]				
Cement (c)	920-940: premix of cement, silica fume and dry superplasticizer, with exemplary mass percentage 27.2, 6.4 and 0.78, respectively [Lou 99]	1114	2090-2115: premix of binder and aggregates	1100: premix of cement and silica fume	1.0
Silica fume (sf)		169			0.30
Sand or other aggregate (agg)	1300-1350	1072		685+625	0.811 +1.830
Water (w)	145-155	195	160-215	200	0.302
Superplasticizer (sp)	Dry, mass included in the premix	44.6	21.4 or 21.5	Not given	Not given
Steel fibres (f)	150-300	195	79 or 158	200	Not given
Special ingredient attribute (type or combination)	agg: sand 0-2 mm and sand 2-4/5 mm (in content approx. 50%+50%, respectively); sp: condensed napthalene sulfonate [Lou 99] f: typically 2-4 vol.-% (max. 6 vol.-%), l/d=12/0.4 mm	agg: 0-7 mm; sp: PCE; f: 2.5 vol.-%, l/d= 20/ 0.3 mm	agg: 0-3 mm; sp: PCE as applied with or without addition of air reducing agent (1.7-3.4 kg/m³); f: max 2 vol.-% where 2/3 is fibre with l/d=20/0.3 mm and 1/3 is fibre with l/d=13/0.175 mm (otherwise only shorter fibre used)	c: CEM III 52.5; agg: bauxite 0-1 and 5-8 mm; sp: superplasticizer and air detraining agent; f: steel fibres l/d= 12.5/0.4 mm	agg: quartz sand (0.3-0.8 mm) and basalt split (2-5 mm); agg: basalt split sometimes 1-3 (1.13) and 2-5 mm (0.79) [Org 04] sp: PCE; f: steel fibres max. 2 vol.-%, l/d= 13/0.16 mm [Org 04]
w/c	Typically 0.20 [Lou 99]	0.22	0.25	Not given	0.302
sf/c	0.24 [Lou 99]	0.15	Not given	Not given	0.30
w/b	0.16 or lower	Not given	Not given	0.18	0.232
Air entrained [vol.-%]	Not given	Not given	<5	Not given	2.5-3.5

Coarse grained UHPC compositions used in own investigations

Table C.4: Compositions of UHPC mixes with coarse aggregates studied [kg/m³ concrete].

Nb	Mixture	Cement c	Silica fume sf	Mixing water w	Extra water for IC	SAP	Quartz flour I (W12)	Quartz flour II (W3)	Quartz sand	Coarse aggregate	Steel fibres f	Superplasticizer sp
1	C-R	666.4	181.4	162.0	-	-	333.2	134.3	362.9	612.1	-	31.2
2	Cf-R (=B5Q)	650.0	177.0	158.0	-	-	325.0	131.0	354.0	597.0	192	30.4
3	C-S.3.04	649.0	176.7	157.8	26.0	1.95	324.5	130.8	353.5	596.1	-	30.4
4	Cf-S.3.04	633.4	172.5	154.0	25.3	1.90	316.7	127.7	345.0	581.8	187.1	29.6

References for Appendix C

For [Far 07], [Lou 99], [Ma 04] and [Ver 98] please see Chapter REFERENCES.

For [Lar 94] please see Appendix B.

[Aar 08] Aarup, B.: CRC-Structural application of Ultra High Performance Fibre Reinforced Concrete. In: Fehling, E.; Schmidt, M.; Stuerwald, S. (Eds.): *Ultra High Performance* Concrete, kassel university press: University of Kassel, 2008, pp. 831-837

[Bal 11] Balbaid, H.: *Application of Higher Strength Concrete in Tubular Structures*. Master Thesis, Delft University of Technology, 2011

[BCV] BCV - Béton Composite Vicat - Vicat's composite concrete, https://f2fcontinuum.files.wordpress.com/2014/03/notes_vicat.pdf

[Gra 06] Graybeal, B.A.: *Material Property Characterization of Ultra-High Performance Concrete*. Federal Highway Administration, Publication No. FHWA-HRT-06-103, 2006

[Kap 04] Kaptijn, N.; Blom, J.: A new bridge deck for the Kaag bridges- The first CRC (Compact Reinforced Composite) application in civil infrastructure. In: Schmidt, M.; Fehling, E.; Geisenhansluke, C. (Eds.): *Ultra High Performance Concrete*, kassel university press: University of Kassel, 2004, pp. 49-57

[Lap 07] Lappa, E.S.: *High Strength Fibre Reinforced Concrete- Static and fatigue behaviour in bending*. Doctoral Thesis, TU Darmstadt, 2007

[Org 04] Orgass, M.; Klug, Y.: Fibre Reinforced Ultra-High Strength Concretes. In: Schmidt, M.; Fehling, E.; Geisenhansluke, C. (Eds.): *Ultra High Performance Concrete*, kassel university press: University of Kassel, 2004, pp. 637-647

[Ric 94] Richard, P.; Cheyrezy, M.H.: Reactive Powder Concretes with high ductility and 200-800 MPa compressive strength. In: Mehta, P.K. (Ed.): *Concrete Technology: Past, Present and Future*, SP-144, American Concrete Institute, Detroit, 1994, pp. 507-518

[Ros 02] Rossi, P.: Development of new cement composite materials for construction. In: Dhir, R.K.; Hewlett, P.C.; Csetenyi, L.J. (Eds.): *Innovations and Developments in Concrete Materials and Construction*, Thomas Telford Publishing, 2002, pp. 17-29

[Tou 11] Toutlemonde, F.; Resplendino, J. (Eds.): *Designing and Building with UHPFRC – State-of-the-Art and Development*. Wiley & Sons, Inc., 2011

D Modified Powers' model

The phase composition of the UPHC's binder paste

Powers' model as adapted and modified for silica fume addition by Jensen [Jen 93] is used to assess phase composition of the binder's paste in UHPC under investigation. In line with it, assuming closed hydrating system and its freedom from entrapped air, the following set of formulas can be applied to describe distribution of the paste components in terms of relative volume fractions (where the final form of each equation given is eventually as evaluated finely grained UHPC M2Q tested and/or incorporates the constants in common with every cement-based material):

Chemical shrinkage (cement):

$$V_{cs,c} = (1-p)k\rho_c \Delta V_c \alpha$$

For M2Q=B5Q: $V_{cs,c} = (1-p)k0.20672\alpha$

Chemical shrinkage (silica fume):

$$V_{cs,sf} = (1-p)k\rho_c \left(\frac{sf}{c}\right)\rho_{sf}^{-1}\rho_{sf}\Delta V_{sf}\alpha$$

For M2Q=B5Q: $V_{cs,sf} = (1-p)k0.7106\frac{sf}{c}\alpha$

Gel water (cement):

$$V_{gw,c} = (1-p)k\rho_c\rho_w^{-1}W_{gw,c}\alpha$$

For M2Q=B5Q: $V_{gw,c} = (1-p)k0.6137\alpha$

Gel water (silica fume):

$$V_{gw,sf} = (1-p)k\rho_c \left(\frac{sf}{c}\right)\rho_{sf}^{-1}\rho_{sf}\rho_w^{-1}W_{gw,sf}\alpha$$

For M2Q=B5Q: $V_{gw,sf} = (1-p)k1.615\frac{sf}{c}\alpha$

Capillary water:

$$V_{cw} = p-(1-p)k\rho_c\rho_w^{-1}W_n\alpha - V_{gw,c} - V_{gw,sf}$$

For M2Q=B5Q: $V_{cw} = p-(1-p)k\left(1.3566+1.615\frac{sf}{c}\right)\alpha$

Unhydrated cement:

$$V_{uc} = (1-p)k(1-\alpha)$$

Unreacted silica fume:

$$V_{usf} = (1-p)k\rho_c\left(\frac{sf}{c}\right)\rho_{sf}^{-1}(1-\alpha)$$

For M2Q: $V_{usf} = (1-p)k1.38626609\frac{sf}{c}(1-\alpha)$

For B2Q: $V_{usf} = (1-p)k1.46818182\frac{sf}{c}(1-\alpha)$

Gel solid:

$$V_{gs} = 1 - V_{cs,c} - V_{cs,sf} - V_{cw} - V_{gw,c} - V_{gw,sf} - V_{uc} - V_{usf}$$

For M2Q:

$$V_{gs} = (1-p)\left(1 + 1.53618k\alpha + 0.67566609\frac{sf}{c}k\alpha - k - 1.38626609\frac{sf}{c}k\right)$$

considering that: $1 - k - 1.38626609\frac{sf}{c}k = 0 \rightarrow V_{gs} = (1-p)k\left(1.53618 + 0.67566609\frac{sf}{c}\right)\alpha$

For B5Q:

$$V_{gs} = (1-p)\left[1 + 1.53618k\alpha + 0.75758182\frac{sf}{c}k\alpha - k - 1.46818182\frac{sf}{c}k\right]$$

considering that: $1 - k - 1.46818182\frac{sf}{c}k = 0 \rightarrow V_{gs} = (1-p)k\left[1.53618 + 0.75758182\frac{sf}{c}\right]\alpha$

Where:

$\sum_i V_i = 1$ and w, c, s refer to respective masses of water, cement and silica fume and the w/c includes water from superplasticizer; furthermore:

Initial porosity:

$$p = \frac{V_w}{V_{paste,tot}}\frac{m_c^{-1}}{m_c^{-1}} = \frac{\frac{w}{c}\rho_w^{-1}}{\frac{w}{c}\rho_w^{-1} + cc^{-1}\rho_c^{-1} + \frac{sf}{c}\rho_{sf}^{-1}}\frac{\rho_w}{\rho_w} = \frac{\frac{w}{c}}{\frac{w}{c} + \rho_w\rho_c^{-1} + \rho_w\rho_{sf}^{-1}\frac{sf}{c}}$$

For M2Q: p= 0.36975

For B5Q: p= 0.38689

Artificial constant:

$$k = \frac{\rho_c^{-1}}{\rho_c^{-1} + \frac{sf}{c}\rho_{sf}^{-1}} = \frac{1}{1 + \rho_c\rho_{sf}^{-1}\frac{sf}{c}}$$

For M2Q: k= 0.81637

For B5Q: k= 0.71439

Specific constants: ρ_c= 3230 kg/m³; ρ_{sf}= 2330 kg/m³ (for M2Q) and ρ_{sf}= 2200 kg/m³ (for B5Q); ρ_w= 1000 kg/m³

Common constants:

Non-evaporable water: W_n= 0.23 g/g cement reacted

Gel water (cement): $W_{gw,c}$= 0.19 g/g cement reacted

Gel water (silica fume): $W_{gw,sf}$= 0.5 g/g silica fume reacted

Chemical shrinkage (cement): ΔV_c= 6.4 ml / 100 g (= $6.4 \cdot 10^{-5}$ m^3/kg) cement reacted

Chemical shrinkage (silica fume): ΔV_{sf}= 22 ml / 100 g (= $22 \cdot 10^{-5}$ m^3/kg) silica fume reacted

Final (=maximum attainable) degree of hydration for UHPC without IC:

$$\alpha = \alpha_{\max} \text{ for } V_{cs,c} + V_{cs,sf} + V_{gw,c} + V_{gw,sf} + V_{gs} + V_{uc} + V_{usf} = 1 \text{ with } V_{cw} = 0$$

In turn: $$\alpha_{\max} = \frac{p}{(1-p)k\left(1.3566 + 1.615\frac{sf}{c}\right)}$$

For M2Q: $\alpha_{\max} = 0.44$

For B5Q: $\alpha_{\max} = 0.49$

Final (=maximum attainable) degree of hydration for UHPC with IC:

$$\alpha = \alpha_{\max} \text{ for } V_{gw,c} + V_{gw,sf} + V_{gs} + V_{uc} + V_{usf} = 1 \text{ with } V_{cs,c} = 0 \text{ and } V_{cs,sf} = 0 \text{ and } V_{cw} = 0$$

This becomes:

For M2Q: $$(1-p)k\left(1.14988 + 0.9044\frac{sf}{c}\right)\alpha_{\max} = 1 - (1-p)k\left(1 + 1.38626609\frac{sf}{c}\right)$$

Hence given that: $$1 - (1-p)k\left(1 + 1.38626609\frac{sf}{c}\right) = 1 - (1-p) = p$$

In turn: $$\alpha_{\max} = \frac{p}{(1-p)k\left(1.14988 + 0.9044\frac{sf}{c}\right)} = 0.55$$

For B5Q: $$(1-p)k\left(1.14988 + 0.9044\frac{sf}{c}\right)\alpha_{\max} = 1 - (1-p)k\left(1 + 1.46818182\frac{sf}{c}\right)$$

Hence given that: $$1 - (1-p)k\left(1 + 1.46818182\frac{sf}{c}\right) = 1 - (1-p) = p$$

In turn: $\alpha_{\max} = \dfrac{p}{(1-p)k\left(1.14988 + 0.9044\dfrac{sf}{c}\right)} = 0.63$

The quantity of entrained water necessary to avoid self-desiccation can be calculated by assuming it is equal chemical shrinkage of the paste in saturated conditions and assuming maximum degree of hydration. Accordingly, the relative volume of initially entrained water can be assessed from Eq. D.1.

$$V_{ew,0} = (1-p)k\left(0.20672 + 0.7106\frac{sf}{c}\right)\alpha_{\max} = \frac{\left(0.20672 + 0.7106\dfrac{sf}{c}\right)p}{\left(1.14988 + 0.9044\dfrac{sf}{c}\right)} \quad \text{(D.1)}$$

Multiplying each side by $\rho_w \cdot V_{uc,0}^{-1} \cdot \rho_c^{-1}$ and simultaneously assuming $p = V_{cw,0}$ for which $V_{cw,0} \cdot \rho_w \cdot V_{uc,0}^{-1} \cdot \rho_c^{-1}$ becomes = w/c, the formula (Eq. D.2) for entrained water but on the mass basis is obtained.

$$\textit{Entrained water:}\ \left(\frac{w}{c}\right)_e = \frac{V_{ew,0}\rho_w}{V_{c,0}\rho_c} = \frac{\left(0.20672 + 0.7106\dfrac{sf}{c}\right)}{\left(1.14988 + 0.9044\dfrac{sf}{c}\right)}\frac{w}{c} \quad \text{(D.2)}$$

For M2Q: $\left(\dfrac{w}{c}\right)_e = 0.055$

For B5Q: $\left(\dfrac{w}{c}\right)_e = 0.078$

E SAP absorption test methods review

Methods used to test absorption of superabsorbent polymer – free and under load.

A review.

Table E.1: Review of methods for testing the SAP absorption without and with kinetics of the uptake and effect of load. Trials of method comparison regard studies [Oga 93][Lee 97][Lee 01][Cam 03][Che 07][Qi 08].

Property captured	Method	Main advantage(s)	Main disadvantage(s)
Free absorption	• (1) Gravimetric method: tea-bag test [Oga 93] • (2) Optical method [Buc 62] • (3) Microscopic observation/picture analysis [Oga 93], with refinements/alternatives [Bra 88][Est 11] • (4) Calorimetric method [Oga 93] • (5) Jensen's method [Jen 11] • (6) Capillary method, DW method [Mas 83] • (7) (Natural/Gravity) Filtration method [Mas 83] with certain modifications/improvements [Yos 92][Lee 01][Zho 08]	• Ad (1) Method is standardized [JIS K 7223] and gives similar result to that of other method e.g. conductance method studied in [Che 07] or at least in terms of equilibrium swelling arrival time [Qi 08]; appreciably small retardation with regards to latter compared to picture analysis also in [Oga 93] • Ad (1) Easy and widely used • Ad (3) The volume changes of spherical SAP particles being easy to assess ($V= 4/3(d/2)^2$) [Oga 93] • Ad (3) One is able to account for interstitial fluid in the improved test version [Sta 02] • Ad (4) Heat of swelling from interaction of water with SAP is easy to determine [Oga 93] • Ad (7) If suction is applied in procedure, scarcity of the free water between the gel particles, unlike in DW-method [Lee 01]	• Ad (1) Determination of tens of seconds-like swelling kinetics is made impossible [Oga 93]; also some unabsorbed water may be held between the particles by capillary forces [Oga 93][Jen 11] (mistake of about 25% or less in case of distilled water and ionic solutions) • Ad (1) As in any other gravimetric method, correction has to be made for the specific gravity of the swelling medium, the quantity of soluble material extracted by the liquid, and the loss of solvent from the test specimen during final weighing [Har 85] • Ad (2) Non-uniform swelling and problematic light transmission (loss of transmitted light), unless precautions are executed • Ad (3) Big deviation of results and problems with controlling initial humidity [Oga 93] • Ad (3) Has to be extended to many particles if the SAP size varies • Ad (3) Many simplifications to be made for polymers of irregular shape • Ad (3)(5) In case of ionic SAP, uptake of some substances e.g. surfactant of particular charge needn't result in polymer swelling [Phi 96] • Ad (4) Heat of swelling does not incorporate interaction of polymer with free water [Oga 93] • Ad (7) Vacuum filtration can dry the SAP thus leading to poor reproducibility [Sta 02] • Ad (7) As such, error is relatively large, method yields vastly differing results depending on type and particle size

(continued on following page)

Table E.1: Review of methods for testing the SAP absorption without and with kinetics of the uptake and effect of load. Trials of method comparison regard studies [Oga 93][Lee 97][Lee 01][Cam 03][Che 07][Qi 08] (*continued*).

Property captured	Method	Main advantage(s)	Main disadvantage(s)
Free absorption	• (8) Centrifugal dehydration/centrifuge method [Mas 83][Sta 02][Zoh 08] • (9) Sheet method [Mas 83] incl. modifications [Pou 13] • (10) Demand Wettability-based method [Lee 01] • (11) Conductance method [Che 07] • (12) Open circuit potential measurement [Qi 08] • (13) Vortex test [Mas 83] • (14) Methods based on photon-correlation spectroscopy [Bou 00], dynamic light scattering [Ech 09], laser diffraction particle size analysis [Est 15] • (15) Dynamic vapour sorption (DVS) measurement [Sno 12] or similar [Thi 07] • (16) Dielectric (constant) measurement [Fra 06] • (17) Magnetic Resonance Imaging [Bra 03] • (18) Karl-Fischer-titration [Cha 07][Joe 10] • (19) Near-Infrared Spectroscopy [Cam 03] • (20) Thermal Gravimetric Analysis [Cam 03] • (21) Differential Scanning Calorimetry [Cam 03] • (22) Loss on drying method [Cam 03] • (23) Dielectric property-based: Terahertz time-domain spectroscopy [Joe 10] • (24) Gravimetic, volumetric and optical methods (traditional methods) before 1985, review [Har 85], with refinements e.g. [Ric 84] • (25) Proposal: Refractive index or interferometric device (film science) [Har 85]; e.g. former important for solution in laser diffraction method [Est 15]	• Ad (8) Includes advantages of gravity filtration method and tea-bag [Sta 02] • Ad (13) Fit for screening multiple samples [Sta 02] • Ad (17) Excellent for studying dynamic and (spatial) distribution of water [Bra 03] • Ad (18) Exclusive sensitivity to water [Joe 10] unlike spatial information • Ad (19)(21) Rapid • Ad (19) Non-destructive [Cam 03] • Ad (20) Sensitive to water in both free and bound states while allowing to differentiate between them [Joe 10] • Ad (24) Some methods could be used for testing granules/powders	• Ad (8) Method can easily plug up the screen • Ad (11) Nonselective nature and error introduced [Qi 08] • Ad (13) Only fit for measuring rate of absorption • Ad (14) Dynamic light scattering measurement giving only measure of relative swelling volume $(d/d_0)^3$ • Ad (16) For estimation of absorption capacity, empirical derivation of unknowns required • Ad (17) Fit for testing of sample of limited geometry while giving 20-150% error compared to gravimetric method [Bra 03] • Ad (18)(20) Is toxic/hazardous • Ad (18)(20)(21)(22) Involves heating of sample [Cam 03] • Ad (19) Exposure to electromagnetic radiation [Cam 03] • Ad (20) Requires long running times [Cam 03] • Ad (20)(21)(22) Not fit for online analysis [Cam 03] • Ad (20)(22) Time-consuming [Cam 03] • Ad (23) Not tested for sample smaller than discs • Ad (24) Difficulties in quantitative separation of the swollen gel from outer solution, unless refinement is applied

(continued on following page)

Table E.1: Review of methods for testing the SAP absorption without and with kinetics of the uptake and effect of load. Trials of method comparison regard studies [Oga 93][Lee 97][Lee 01][Cam 03][Che 07][Qi 08] (*continued*).

Property captured	Method	Main advantage(s)	Main disadvantage(s)
Absorption under load/pressure (compressor/and shear)	• (1) Using supply tube for a constant head reservoir in various studies, study review [Sta 02] • (2) 'Absorbency against pressure by gravimetric determination' [WSP 11] using petri dish to hold an excess of fluid [Sta 02] • (3) Zohuriaan-Mehr workgroup testing apparatus [Zoh 08] • (4) Various other test arrangements [Bel 96], including combination with recorder [Cut 98] • (5) Custom-built apparatus for exerting isotropic compressive load on single hydrogel particle [San 04] • (6) Self-developed device incorporating moisture content analyzer [Law 09] • (7) Osmotic deswelling technique, study review [Dub 94][San 04] • (8) Mechanical measurements, study review [San 04] and own study- piston technique [Dub 94] • (9) Swelling chamber technique [Dub 94] • (10) Home-made piston-based apparatus [Bud 97] • (11) Osmotic cell [Sur 72] • (12) Demound wettability method, review [Mas 01] • (13) Diffusive absorption ratio method, review [Mas 01]	Ad (3)(4)(5)(6)(10) and piston technique in (8) Apparatus enabling testing microparticles Ad (5) Fit for testing swelling under isotropic compressive stress field; simplicity (swelling in cavity constraining volume) Ad (6) Improved setup in comparison to (3) Ad (7) Isotropic swelling [Dub 94] Ad (8) Some techniques provide possibility of measuring isotropic swelling pressure and can be used for several granules with applicability for free swelling tests as well, e.g. piston technique [Dub 94] Ad (9) Convenient to use Ad (10) Can be used for studying swelling of gel powder with or without load [Bud 97]	Ad (3)(4) Not fit for testing under isotropic compressive load Ad (5) Since test is performed on single particle, application of method doubtful for SAP of (swollen) size used in IC Ad (3)(6) Applicable to spheres of similar size (diameter) Ad (7)(8) Apparatus not fit for testing microspheres [San 04] Ad (7) Not fit for study under varying ionic composition Ad (8) Complicated, inaccurate, slow [Dub 94] Ad (8) In piston technique, alike in tea-bag test- small estimate error due to liquid retained by capillary forces Ad (9) For measuring multiple specimen [Dub 94] but mainly gel plates Ad (11) Difficulty of application for SAP, associated with measurement of small pressures and with the low modulus of elasticity

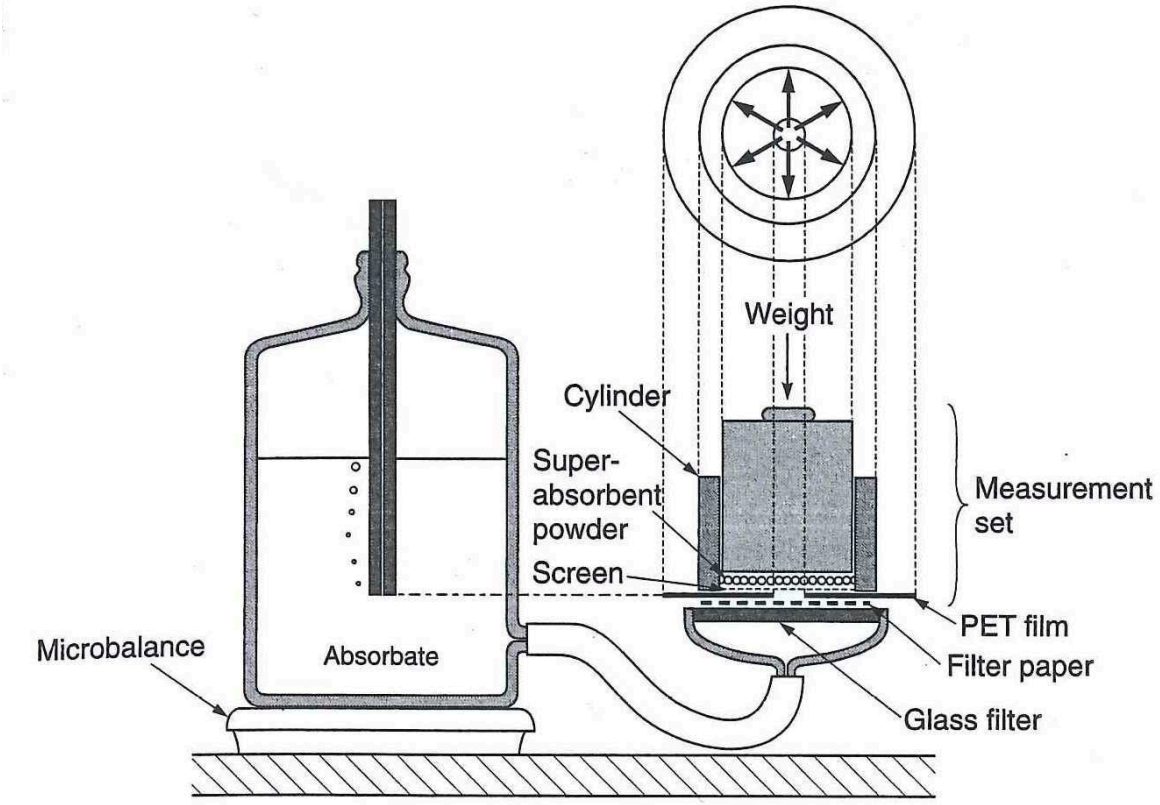

Figure E.1: Apparatus for absorption under load in set-up arranged for diffusive absorption ratio measurement [Mas 01].

References for Appendix E

For [Bud 97], [Dub 94], [Ech 09], [Lee 01], [Qi 08], [San 04], [Sno 12], [Sta 02], [WSP 11] please see Chapter REFERENCES.

[Bel 96] Bell, C.L.; Peppas, N.A.: An apparatus to measure polymer swelling under load. *International Journal of Pharmaceutics*, 134(1-2), 1996, 167-172

[Bou 00] Bouillot, P.; Vincent, B.: A Comparison of the swelling behaviour of the copolymer and interpenetrating network microgel particles. *Colloid and Polymer Science*, 278(1), 2000, 74-79

[Bra 88] Brandt, K.A.; Goldman, S.A.; Inglin, T.A.: Hydrogel-forming polymer compositions for use in absorbent structures. United States Patent, Re. 32,649, 1988

[Bra 03] Braun, J.; Klein, M.O.; Bernarding, J.; Leitner, M.B.; Mika, HD.: Non-destructive, three dimensional monitoring of water absorption in polyurethane foams using magnetic resonance imaging. *Polymer Testing*, 22(7), 2003, 761-767

[Buc 62] Buckley, D.J.; Berger, M.; Poller, D.: The swelling of polymer systems in solvents. I. Method for obtaining complete swelling-time curve. *Journal of Polymer Science*, 56(163), 1962, 163-174

[Cam 03] Camacho, W.; Vallés-Lluch, A.; Ribes-Greus, A.; Karlsson, S.: Determination of moisture content in nylon 6,6 by near-infrared spectroscopy and chemometrics. *Journal of Applied Polymer Science*, 87(13), 2003, 2165-2170

[Cha 07] Chakraborty, S.; Debnath, M.; Bandyopadhyay, S.; Mukhopadhyay, R.; Deuri, S.: Moisture content determination of different polymers by Karl Fischer titration. *Rubber World*, 236(4), 2007, 12-14

[Che 07] Chen, Z.; Liu, M.; Qi, X.; Zhan, F.; Kiu, Z.: Conductance method study on the swelling kinetics of the superabsorbent. *Electrochimica Acta*, 52(5), 2007, 1839-1846

[Cut 98] Cutié, S.S.; Smith, P.B.; Reim, R.E.; Graham, A.T. in: F.L. Buchholz; Graham, A.T. (Eds.): Modern Superabsorbent Polymer Technology, Wiley-VCH, New York, 1998

[Est 11] Esteves, L.P.: Superabsorbent polymers: On their interaction with water and pore fluid. *Cement and Concrete Composites*, 33(7), 2011, 717–724

[Est 15] Esteves, L. P.: Recommended method for measurement of absorbency of superabsorbent polymers in cement-based materials. *Materials and Structures*, 48(8), 2015, 2397-2401

[Fra 06] Fraga, A.N.; Frulloni, E.; De la Osa, O. ; Kenny, J.M. ; Vázquez, A.: Relationship between water absorption and dielectric behaviour of natural fibre composite material. *Polymer Testing*, 25(2), 2006, 181-187

[Har 85] Harrison, D.J.; Yates, W.R.; Johnson, J.F.: Techniques for the analysis of crosslinked polymers. *Journal of Macromolecular Science, Part C*, 25(4), 1985, 481-549

[Jen 11] Jensen, O.M.: Water absorption of superabsorbent polymers in a cementitious environment. In: Leung, Ch.; Wan, K.T. (Eds.): *Advances in Construction Materials*, Hong Kong, China, RILEM Proceedings pro079, RILEM Publications S.A.R.L., pp. 22-35

[JIS K 7223] JIS K 7223:1996 Testing method for water absorption capacity of super absorbent polymers, Japanese Standards Association

[Joe 10] Jördens, C.; Wietzke, S.; Scheller, M.; Koch, M.: Investigation of the water absorption in polyamide and wood plastic composite by terahertz time-domain spectroscopy. *Polymer Testing*, 29(2), 2010, 209-215

[Law 09] Lawal, O.S.; Storz, J.; Storz, H.; Lohmann, D.; Lechner, D.; Kulicke, W.-M.: Hydrogels based on carboxymethyl cassava starch cross-linked with di- or polyfunctional caboxylic acids: Synthesis, water absorbent behavior and rheological characterizations. *European Polymer Journal*, 45(12), 2009, 3399-3408

[Mas 83] Masuda, F.: Super Absorbent Polymers – Characteristics and trends in development of Applications. *Chemical Economy & Engineering Review*, 15(11), 1983, 19-23

[Mas 01] Masuda, Y.: Absorptivity of water (moisture absorptivity and retention of water). Section 1 in: Osada, Y.; Kajiwara, K. (Eds.): Gel Handbook, Vol. 2 - Functions. Academic Press, 2001, 17-45

[Oga 93] Ogawa, I.; Yamano, H.; Miyagawa, K.: Rate of swelling of sodium polyacrylate. *Journal of Applied Polymer Science*, 47(2), 1993, 217-222

[Ric 84] Ricka, J.; Tanaka, T.: Swelling of ionic gels: Quantitative performance of the Donnan theory. *Macromolecules*, 17(12), 1984, 2916-2921

[Sur 72] Surdutovich, L.I.; Tager, A.A.; Ovchinnikova, G.P.; Khomyakova, N.I.; Safonov, Y. A.: An investigation of the swelling pressures of the three-dimensional polymers. Polymer *Science U.S.S.R.*; 14(2), 1972, 360-370

[Yos 92] Yoshinobu, M.; Morita, M.; Sakata, I.: Porous structure and rheological properties of hydrogels of highly waer-absorptive cellulose graft copolymers. *Journal of Applied Polymer Science*, 45(5), 1992, 805-812

F Supplementary test results – Fresh state

The consistency test results

Air content determined vs. slump flow measured with the bigger test set-up

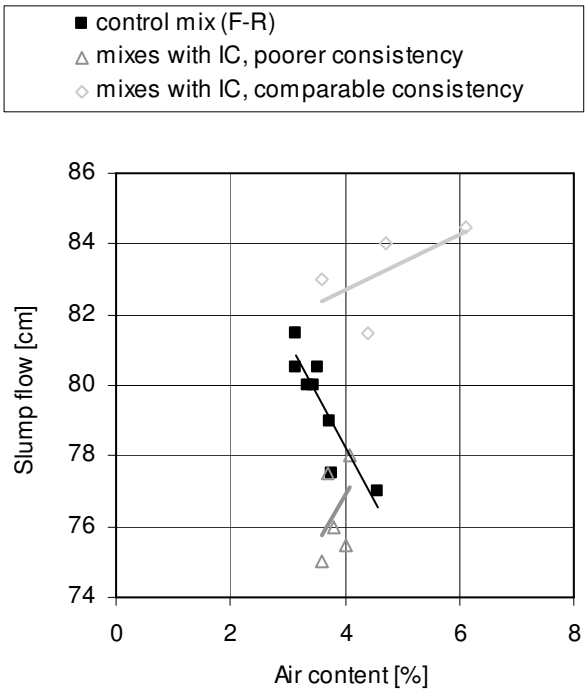

Figure F.1: Correlation between air content and the slump flow measured.

Correlation between slump flow results after varying test conditions or test set-up

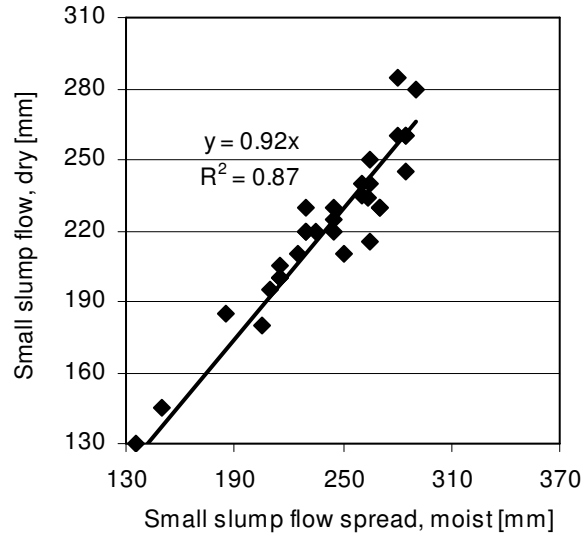

Figure F.2: Correlation between measurements of slump flow in two different test conditions. No distinction between mixtures without or with IC, SAP, extra water made.

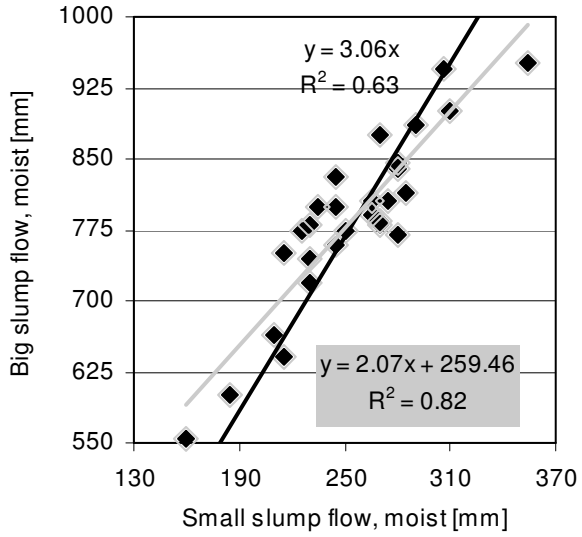

Figure F.3: Correlation between results of slump flow as measured using two different test set-ups in moist condition. No distinction between mixtures without or with IC, SAP, extra water made.

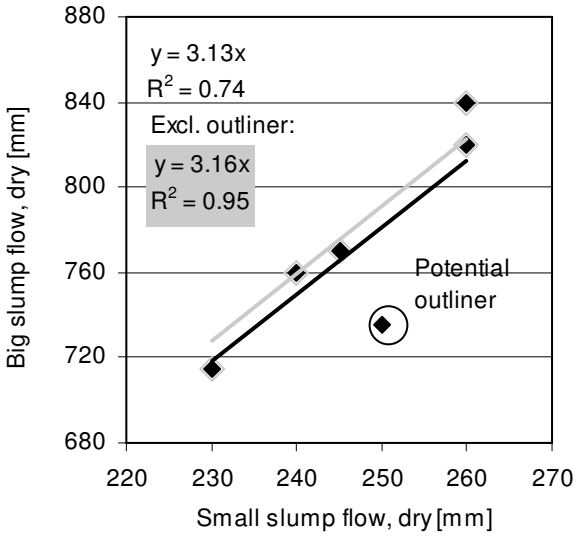

Figure F.4: Correlation between results of slump flow as measured using two different test set-ups in dry condition. No distinction between mixtures without or with IC, SAP, extra water made.

The rheometer test results

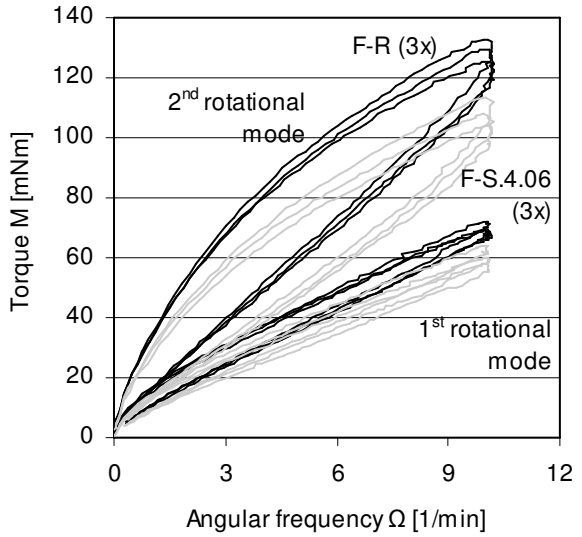

Figure F.5: Original rheometer test results as recorded during two separated rotational modes for F-R and F-S.4.06.

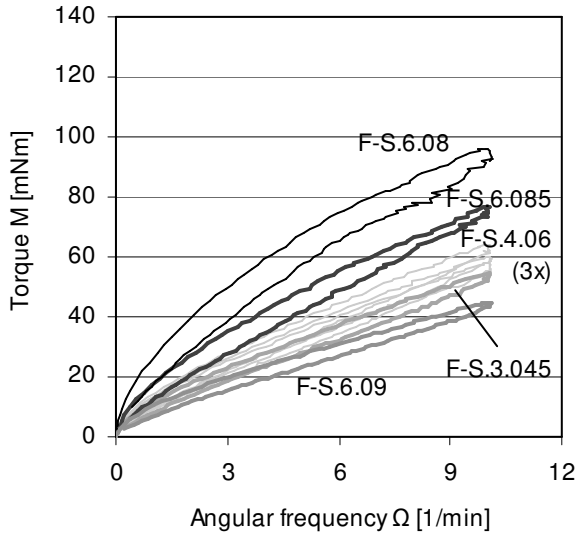

Figure F.6: Original rheometer test results as measured in first of separated rotational modes for mixes with IC.

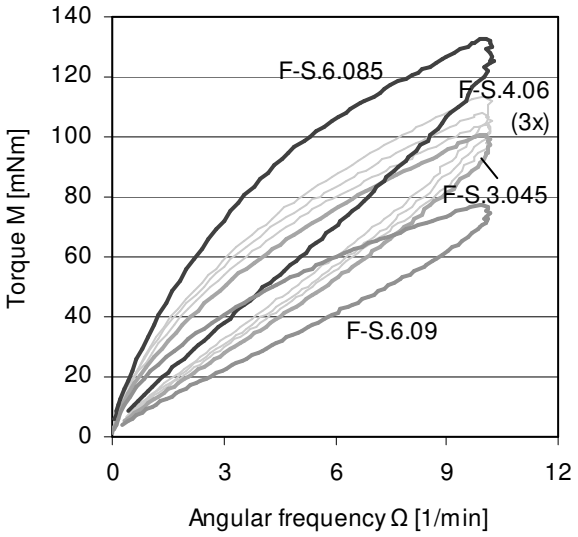

Figure F.7: Original rheometer test results as measured in second of separated rotational modes for mixes with IC.

Acceptance criteria for classifying mix as self-compacting

Table F.1: Typical acceptance criteria for self-compacting concrete.

Property	Typical target value [Reference]
(Small) slump flow	• 240-325 mm, as reviewed in [Bro 05], for which Γ_m = 4.8-9.6 • Relative slump limit Γ_m ($\Gamma_m=(d/d_0)^2-1$, where d_0 is the initial diameter of the cone (= 100 mm), and d is the final diameter of the mortar [EFNARC 02]) = 4.8
(Big/Large) slump flow[1]	• ≥ 700 mm without blocking ring and permissible rotation of the cone [Rei 01], (wider window of workability possible [DAfStb 03]) • 600-800 mm [Sch 08] • 630-800 mm as reviewed in [Bro 05] • 650-800 mm [EFNARC 02]*
Yield stress	• 50-200 Pa [Ban 03] • 0-60 Pa as reviewed by [Wal 03] • 0-100 Pa as reviewed by [Wal 11], although limitation proposed • Slightly above 120 Pa (for HSC SCC) as reviewed by [Wal 03]
Plastic viscosity	• 20-100 Pa·s [Ban 03] • 7-160 Pa·s [Wal 03] • 30-120 Pa·s as reviewed by [Wal 03] • 5-120 Pa·s as reviewed by [Wal 11], although limitation proposed • 100-140 Pa·s (for HSC-SCC) as reviewed by [Wal 03]
Air content	• A_{300} (DIN EN 480-11) < 1.8 % [DAfStb 03] • 4.5 % [JSCE 1999, ref. 2 *Ibid.* Ouc 03]
Workability time	• > 20 min for precast element construction [Rei 01]

* Abrams cone is placed differently to DAfStb; however, acc. to [Ram 03], the result of the test is independent of the cone position (inverted, upright)

References for Appendix F

For [EFNARC 02] please see Chapter REFERENCES.

[Ban 03] Banfill, P.F.G.: The rheology of fresh cement and concrete – A review. Proc. 11th International Cement Chemistry Congress, Durban, May 2003

[Bro 05] Brouwers, H.J.H.; Radix, H.J.: Self-Compacting Concrete: Theoretical and experimental study. *Cement and Concrete Research*, 35(11), 2005, 2116-2136

[Ouc 02] Ouchi, M.; Nakamura, S.-a.; Osterberg, Th.; Hallberg, S.-E.; Lwin, M.: Applications of self-compacting concrete in Japan, Europe and the United States. In: *High Performance Computing (ISHPC)*, Tokyo-Odaiba, Japan, 2003, www.fhwa.dot.gov/bridge/scc.pdf

[Ram 03] Ramsburg, P.: The SCC test: inverted or upright. *The Concrete Producer*, 21(7), 2003, 34-38

[Rei 01] Reinhardt, H.-W.: Self compacting concrete: DAfStb guideline on self compacting concrete. *Beton+Fertigteil-Technik*, 12, 2001, 54-62

[Wal 03] Wallevik, O.H.: Rheology – A scientific approach to develop Self-Compacting Concrete. In: Wallevik, O.; Niellson, I. (Eds.): *Self-Compacting Concrete*, Reykjavik, Iceland, RILEM Proceedings pro33, RILEM Publications S.A.R.L., 2003, pp. 23-32

[Wal 11] Wallevik, O.H.; Wallevik, J.E.: Rheology as a tool in concrete science: The use of rheographs and workability boxes. *Cement and Concrete Research*, 41(12), 2011, 1279-1288

G Supplementary reviews regarding time-zero

Review of time-zero related events

Table G.1: Critical review of advantages for using final set as time-zero.

Argument description	Important remarks
• **Final set gives time-zero a physical/mechanical meaning**: Particles belonging to solid network become highly bridged/connected and hindered in all three directions [Bar 01]. The material is solidified completely [Cha 07]; in other words, by the time of final set, being certainly beyond the percolation threshold of the solid phase [Bou 96], mineral (solid) skeleton developed in 3D is fully self-supportive and, as acknowledged in [Bar 01], the upper bound of the continuous process of suspension-solid transition is attained.	• There is close time proximity of the end of fluid-to-solid transition and final set with lowering of w/c [Bar 01] if setting is determined acc. to EN 196-3. • Alike in case of cement paste [Ben 03], also for concrete, other measuring standards can be and often are applied leading to various time ascription of final set [Gra 06c], to be related to incomparable stresses applied during tests (and thus yields stress captured) [Loo 09], on one hand, and shortcomings of using certain methods especially for concretes having unique attributes, e.g. [Med 11b], on the other hand.
• Due to appearance of 3D network of dimensional products, only isotropic deformation develops from final set [Bel 02].	•
• For low w/c and room temperature, final set coincides with [Ham 06b] or, in worst case scenario, is slightly conservative to [Jus 00][Mou 06] the knee-point i.e. physically manifested change of course in volumetric autogenous shrinkage curve (when it starts flattening out) that is believed to be addressing formation of load-bearing microstructure strong enough to resist the contracting forces created by chemical shrinkage [Jus 00][Mou 06]. It is confirmed by acoustic emission measurements [San 09].	• The success of the match depends on w/c [Jus 00][Mou 06], cement fineness [Bar 01] or other binder characteristic [Jus 00], air content [Ham 06b], differences in mechanism behind the tests [Jus 00], moisture conditions when performing the Vicat needle test [Jus 00], load applied in penetration test (see remarks above) and temperature [Mou 06]. • Occurrence of 'divergence point' (when autogenous shrinkage diverges/bneds from chemical shrinkage curve) itself dependent on initial consistency (stiffness) of the paste [Ham 99]. • It is likely to hold true specifically for buoyancy principle-based method of AS measurement.
• Another 'mechanical' support: (**Dynamic) elastic modulus, being indicative of structure formation [San 09], starts to develop for UHPC** [Kaz 10] similarly to cement paste [San 09]. This implies that percolated network is capable of sustaining increasingly higher loads without plastic deformation i.e. there is load-bearing microstructure developed. Under additional external restraint, development of stresses is expectedly recorded [San 09][Epp 09], with exceptions [Epp 09].	• **Setting time of UHPC determined acc. to ASTM C191** as for paste. This means remaining conservative with regards to final set as captured for mortar/concrete e.g. acc. to ASTM C403. • Following expectations, increase rate of effective stiffness reaching its maximum after attaining the ASTM C403-determined final set for high-performance concrete acc. to Lee et al. [Lee 04]. • Remaining potentially conservative: Development of effective Young's modulus and onset of capillary pressure build-up does sometimes shift towards ages as advanced as final set or even later [Hol 01][Zhu 08], which for materials such as UHPC (for which effect has been observed as well, see Section 5.2) could be attributed to very low w/c and high content of space fillers, in line with [Cha 07]. • Typically earlier recordings of non-destructive methods compared to static ones in the (very) early ages. Meanwhile, no transition between the results [Bou 13], the observation changing to some extent in somewhat later ages [Epp 10] and ages as late as 28 days, especially for concretes having high Young's modulus [Phi 55] and/or strength [Kol 80].

(continued on following page)

Table G.1: Critical review of advantages for using final set as time-zero (*continued*).

Argument description	Important remarks
• **Linkage to chemical changes (reactions, transport)**: Given room temperature or higher, at final set or its close time vicinity of it so-called chemical threshold (portlandite precipitation threshold=chemical indicator of setting) is detected. This event often gives location of knee-point and start of **linear relation between volumetric autogenous shrinkage and degree of hydration** [Mou 06]. In case of latter, there is **certain but more complicated correlation found for UHPC too** [Sol 11].	• Constant value of degree of hydration associated with chemical threshold contrasts with changing value of degree of hydration at setting points, and depending, among others, on system's w/c [Bou 96][San 08][San 09]. • Nucleation and growth of portlandite being only one reason behind onset of acceleration period [Bul 11] that is needed so that setting/solidification occurs.
• Certain relation between the changes occurring in chemical shrinkage (being related to hydration, e.g. [Wei 03] and the autogenous shrinkage curves [San 06] and their corresponding rates [San 09].	• The moment at which chemical shrinkage and (linear) autogenous shrinkage diverge and that is indicating formation of structural skeleton is very likely to occur before stresses could be transferred through concrete [Wei 03].
• Final setting related to distinct changes in electrical conductivity and electrical resistivity for pastes [San 09] and concretes [Li 07][Dar 11], respectively.	• Primary correspondence of electrical measurements to chemical processes and secondary to physical structure formation (mechanical processes), similarly to heat of hydration rate approach [Wei 03].
• **Certain relation between hydration heat-relate temperature evolution and final set for UHPC** [Sch 02][Kaz 10].	• Solidification and thus setting in general doubt as being related to rate of reaction (rate of heat release) [San 09] which can be explained by contradictory dependence of each process on w/c [Ben 09]. The consequence is different occurrence of final set with respect to hydration heat rate [Wei 03] or temperature evolution [Sch 02].

References for Table G.1

For [Bar 01], [Bel 02], [Bou 96], [Cha 07], [Dar 11], [Epp 09], [Gra 06c], [Ham 06b], [Hol 01], [Jus 00], [Kaz 10], [Li 07], [Lee 04], [Loo 09], [Med 11b], [Mou 06], [San 06], [San 08], [San 09], [Sch 02], [Sol 11], [Zhu 08] please see Chapter REFERENCES.

[Ben 03] Bentz, D.P.; Haecker, C.J.; Feng, X.P.; Stutzman, P.E.: Prediction of cement physical properties by virtual testing. In: *Process Technology of Cement Manufacturing*, Düsseldorf, Germany, 2003, pp. 53-63

[Ben 09] Bentz, D.P.; Peltz, M.A.; Winpigler, J.: Early-Age Properties of Cement-Based Materials: II. Influence of Water-to-Cement Ratio. *ASCE Journal of Materials in Civil Engineering*, 21 (9), 512-517, 2009.

[Bou 13] Boulay, C.; Staquet, S.; Azenha, M. ; Deraemaeker, A.; Crespini, M.; Carette, J.; Granja, J.; Dumoulin, C.; Karaiskos, G.: Monitoring elastic properties of concrete since very early age by means of cyclic loadings, ultrasonic measurements, natural resonant frequency of

composite beam (EMM-ARM) and with smart aggregates. In: *Fracture Mechanics of Concrete and Concrete Structures (FraMCoS-8)*, 2013, paper 185

[Ham 99] Hammer, T.A.; Heese, C.: Early age chemical shrinkage and autogenous deformation of cement pastes. In: Persson, B.; Fagerlund, G. (Eds.): *Self-desiccation and Its Importance in Concrete Technology*, Division of Building Materials, Lund University, 1999, pp. 7-13

[Kol 80] Kolias, S.; Williams, R.I.T.: Relationships between the static and the dynamic modulis of elasticity in cement stabilised materials. *Matériaux et Construction*, 13(2), 1980, 99-107

[Phi 55] Philleo, R.E.: Comparison of results of three methods for determining Young's modulus of elasticity of concrete. *Journal of American Concrete Institute*, Proceedings vol. 51, 1955, pp. 461-469

[Wei 03] Weiss, J.: Experimental determination of the 'Time Zero', t0 ('Maturity-Zero', M0). In: Bentur, A. (Ed.): Early Age Cracking in Cementitious Systems – Report of RILEM Technical Committee 181-EAS, RILEM Publications S.A.R.L., 2003, pp. 195-206

Table G.2: Criteria for determination of setting limits applicable to ultrasonic method used other than specifying UPV threshold.

Refe-rence	Material investigated and basic recipe attributes	Setting evaluation method (for criterion statement)	Criterion set		Theoretical basis or other comment
			Point evaluated		
			Initial set/ Time of set	Final set	
[Whi 51]	Concretes		The sudden change of velocity rate to much lower one	Marked change in growth rate of the P-wave velocity	
[Woo 57]	Concretes with w/c = 0.4	Unknown (needle but not Vicat needle)	(1) Time at which rate of change of the velocity decreases suddenly (2) Being mathematical solution for (1): Point of intersection of tangents drawn to the curve immediately prior to and after the period during which the decrease (of rate of change of velocity) occurs	Not given	Advantage: Although criterion hardly referred to, existing criterion modifications, enabling applicability for low w/c materials [Lee 04] Disadvantage: Sound-like criterion existing for concrete containing blast-furnace slag (w/b = 0.5) [Rob 08], in turn implying plausible dependence of criterion success on the UPV-t shape curve (this depending on curing conditions [Smi 02], for instance)
[Doh 69]	Cement pastes	Vicat test	After beginning of increase in velocity curve	Cannot be specified but after maximum rate of velocity = after inflection point	
[Nei 74]	Cement pastes with Portland and blast furnace cement, without and with retarding admixture	DIN 1164	Te same criterion if not applicable to final set determination	Close to maximum rate of P-wave velocity = after inflection point; although match finally dependent on cement and admixture used	

(continued on following page)

Table G.2: Criteria for determination of setting limits applicable to ultrasonic method used other than specifying UPV threshold (*continued*).

Refe-rence	Material investigated and basic recipe attributes	Setting evaluation method (for criterion statement)	Criterion set		Theoretical basis or other comment
			Point evaluated		
			Initial set/ Time of set	Final set	
[Pes 88]	Concretes with w/c = 0.4 or 0.8, incorporating both fine and coarse aggregate in varied presence of admixtures	ASTM C403	P-wave velocity begins to increase (in agreement with e.g. [Ye 03] working on cement pastes with w/c = 0.4-0.55 as well as de-aired cement samples [Kea 89][Zhu 11a] of similar w/c)	Lack of discontinuity in the velocity-gain curves	Advantage of use: allowing setting to be related with actual physical change; independence of variations in mix composition except for change in the paste [Pes 88]; general relation to Biot's theory i.e. existence of percolation transition and transformation from viscous suspension to porous elastic solid with nonvanishing elastic moduli [Lee 04] Disadvantage: difficulty in identification [Pes 88] as well as, in present author's opinion and concerning initial set, too close vicinity of threshold of solid percolation implied by sound-like criterion [Gam 13]; eventually the lack of applicability for air-free mixes [Zhu 11a] Disadvantage: criteria originally proposed for impact-echo method [Pes 88] but working for through-transmission method as well e.g. [Ye 03]
[Bar 01]	Cement pastes with w/c = 0.28-0.4	EN 196-3	After attaining mineral percolation threshold = after minimum value in compressional velocity meaning beginning of the increase of compressional velocity	Not concerned with regard to US measurement	Advantage: Physical meaning of mineral percolation threshold, viz. point at which autogenous shrinkage and chemical shrinkage start to diverge due to local hindrance of volume changes by solid contacts [Bar 01] Disadvantage: Mineral percolation threshold occurs much before knee-point and true suspension-solid transition [Bar 01]

(continued on following page)

Table G.2: Criteria for determination of setting limits applicable to ultrasonic method used other than specifying UPV threshold (*continued*).

Refe-rence	Material investigated and basic recipe attributes	Setting evaluation method (for criterion statement)	Criterion set: Point evaluated: Initial set/ Time of set	Criterion set: Point evaluated: Final set	Theoretical basis or other comment
[Voi 05]	Mortars (w/c = 0.39-0.6) without and with admixtures and concretes (w/c = 0.37 or 0.52); confirmed for cement pastes [Trt 08] and concrete [Rob 08]	ASTM C403	First inflection point (assuming time of increase of penetration resistance = initial set)		Advantage: Hypothesized to be reflecting the microstructural changes better than UPV acc. to [Lee 04] Disadvantage: Disagreement between studies on meaning of inflection point, e.g. final set in opinion of [Lee 04] Dependence on curve shape?
[Dar 11]	CEM III based concretes with w/b (w/c) = 0.45 (confirmed also for CEM I based concretes without and with replacement by pozzolans and w/c = 0.6-1.65 and w/b = 0.41-0.6 [Kho 09])	Both initial and final set: measuring method-ascribed with initial set cross-referenced to Robeyst et al. work; for data given in function of equivalent age [Dar 11] or age [Kho 09]	Identical to [Voi 05]	Slow increase in velocity, indicated by constant value of derivative close to zero (= rate of velocity decreases, alike suggested in [Rob 08]	
[Bel 06]; for mortars also in [Bel 05a]	Concrete with pozzolan, sand and gravel with w/c = 0.3-0.75 (but constant w/cm = 0.3) and admixtures as well as reference mortar with , standard sand, w/c = 0.5 and admixtures	Final set: Time of attaining UPV of 1500 m/s after ref. 8 in [Bel 05a]	If understood as end of workability – the same energy criterion as for final set	Neighbourhood of point of inflection of UPV curve (only in case of concretes) as well as neighbourhood of maximum relative energy (of the first local maximum)	No physical meaning of maximum relative energy, i.e. variable determined as numerical integration of squared amplitude values that is divided by reference energy

(continued on following page)

Table G.2: Criteria for determination of setting limits applicable to ultrasonic method used other than specifying UPV threshold (*continued*).

Refe-rence	Material investigated and basic recipe attributes	Setting evaluation method (for criterion statement)	Criterion set		Theoretical basis or other comment
			Point evaluated		
			Initial set/ Time of set	Final set	
[Lee 04]	Mortars and concretes with w/cm = 0.27-0.5	ASTM C403	Mostly is although needn't be after time of attaining first of intersection points from straight lines tangent to UPV-t curve; instant when UPV begins to develop	For mortars with w/cm ≤ 0.35: Close to but generally before inflection point is attained in UPV-t curve (instant when UPV development rate is maximum)	Advantage of using intersection point: Of practical use as specific UPV threshold to be attained depends only on w/cm and not aggregate graining [Lee 04]
[Zha 12b]	Cementitious pasts, mortars and concretes with w/b = 0.18	ASTM C191 (pastes); ASTM C403 (mortars and concretes)	Close to lasting time for the stage identified as dormant period	Close to arrival at maximum changing rate (inflection point)	
[Rob 08]	Mortars and concretes (beside fine aggregate including coarse aggregates as well) with w/c and w/b = 0.5, respectively; based on two varied cements as well as without or with replacement of cement by blast-furnace slag	ASTM C403, MBE method instead of sieving mortar for testing	Inflection point in UPV-t graph (if understood as time when shear modulus and thus the penetration resistance starts to develop) or 1.45 corresponding to the age when the inflection point occurred (if followed as in ASTM C403)	When rate of UPV decreases = velocity increases more gradually and shows only slow increase (velocity levels off) = when derivative of velocity has decreased to 20 % of its maximum value	Disadvantage: Final setting cannot be determined as unambiguously as initial set
Jacquemmoz et al. Ibid. [Gar 95] and [Smi 02]	Jacquemmoz et al.: Unknown (original reference could not be reached); [Smi 02]: Cement pastes with w/c = 0.33-0.40	Jacquemmoz et al.: Kunhe needle penetration resistance test; [Smi 02]: not clear; mainly relating ultrasonic measurements to hydration models	First of significant modifications of the slope in UPV-t curve = intersection of two slopes /lines tangent to curve	Second of significant modifications of the slope in UPV-t curve = intersection of two slopes/ lines tangent to curve	Advantage: could be found easily using mathematical procedure

(continued on following page)

Table G.2: Criteria for determination of setting limits applicable to ultrasonic method used other than specifying UPV threshold (*continued*).

Refe-rence	Material investigated and basic recipe attributes	Setting evaluation method (for criterion statement)	Criterion set		Theoretical basis or other comment
			Point evaluated		
			Initial set/ Time of set	Final set	
[Her 03]	Mortars and concretes of high w/c			Corresponding to intersection point of two straight lines tangent to velocity evolution in function of degree of reaction, with one showing setting and stiffening and the other hardening and for which degree of reaction is obtained from calorimetric measurements	
[Leh 73]	Builder's gypsum with w/b = 0.33-0.70	DIN 1168 or dip cone	When intensified gain in the amplitude occurs	When travel time obtains a constant value	Advantage: Gypsum is another hydraulic binder
[Jon 96]	Cement pastes and concrete with low w/c	DIN EN 196 (cement pastes); less clear (concretes)	From frequency analysis (20-300 kHz, with the most important being 40-60 kHz): Beginning of increase in curve of relative amplitude, with the relative amplitude obtained as difference of filtered and unfiltered amplitude	End of increase in curve of relative amplitude	Disadvantage: Requires additional software; also it is subjective estimation according to filtering used
[Rei 98]	Among other, cement paste with w/c = 0.26	Vicat needle	From frequency analysis: appearance of amplitude of increasing character in frequency range of ca. 27 kHz	Amplitudes of lowest frequencies start to be weaker while amplitude by the frequency of 27 kHz obtains its maximum	
[Her 03]	Cement pastes with w/c = 0.26 and 0.33	EN 196-3 with confirmation by ESEM	Pronounced increase in the amplitude in the frequency range up to 5 kHz	Beginning with pronounced gain in amplitude at frequency of 27 kHz	

(continued on following page)

Table G.2: Criteria for determination of setting limits applicable to ultrasonic method used other than specifying UPV threshold (*continued*).

Refe-rence	Material investigated and basic recipe attributes	Setting evaluation method (for criterion statement)	Criterion set		Theoretical basis or other comment
			Point evaluated		
			Initial set/ Time of set	Final set	
[Her 03]	Concretes with w/c = 0.45-0.6	ASTM C403 with confirmation by ESEM	Pronounced change in the content of frequency including decay of amplitudes between 1 and 2 kHz	Gain in amplitude by the frequency of 27 kHz	
[Gar 95]	Roller compacted concrete	Mechanical tests of resistance to needle penetration and SEM analysis; also adoption of two distinct slope changes on the UPV-t curve, with initial set defined as beginning of the linkage formation between the grains unreasonably (acc. to [Voi 05]), attributed to ettringite formation while with final set matching formation of large quantity of C-S-H	From maximum amplitude of the limited (15-100 kHz) bandwidth as determined from spectral image in function of time: one of the three singularities on the amplitude-time curve	Another from the three singularities	Advantage: Stopping the growth in amplitude (revealing the singularities) corresponding to modifying or stopping the growth kinetics of one or more constituents
[Bel 05a]	Mortar as in description of [Bel 06] but including variation of cement type as well	As in [Bel 06]	As in [Bel 06]	Frequency shift from 20 to 50 kHz (moment when velocity rate increase is reduced)	Physical meaning relating to setting phenomenon (fully connected solid frame) and signalization of sudden increase of material stiffness

(continued on following page)

Table G.2: Criteria for determination of setting limits applicable to ultrasonic method used other than specifying UPV threshold (*continued*).

Refe-rence	Material investigated and basic recipe attributes	Setting evaluation method (for criterion statement)	Criterion set		Theoretical basis or other comment
			Point evaluated		
			Initial set/ Time of set	Final set	
[Trt 13a]	Cement pastes with w/c = 0.3 or 0.4, without and with admixtures	Initial set: as in [Trt 08], based on comparison of Vicat needle tests and ultrasonic measurement	Based on TG parameter i.e. ratio between maximum amplitudes of two dominant frequency ranges appearing in frequency spectrum of received US signal: Time when amplitudes of both low and high frequencies become equal (TG = 0); coinciding with first inflection point on UPV-t curve and when UPV reaches velocity of water	Not given/respected	Advantage: Physical meaning of TG parameter i.e. following development of rigid bonds between hydrating cement particles and therefore connectivity of solid phases, as in penetration tests [Gam 13]
[Gam 13]	Pure paste with w/c = 0.45, mortars with w/c = 0.40 or 0.45 and fine or very fine aggregate without or with cement content variation and concrete of w/c = 0.35-0.45 with fine and coarse aggregates	EN 196-3 (cement pastes); EN 14488-2 modified by Sika (mortars and concretes)	When TG parameter starts to increase rapidly (from TG value of -1)	When TG parameter stops to increase and reaches its final long-term value close to 1	Advantage: Accurate and unambiguous determination of setting period that is free of effect by different size, type, and amount of aggregates; ability of criterion to detect physical fluid-solid transformation [Gam 13] Disadvantage: In present author's opinion- inability of characteristic points in TG parameter evolution to give the selfsame setting points correspondence after incorporation of aggregates, change of w/c and admixture incorporation

(continued on following page)

Table G.2: Criteria for determination of setting limits applicable to ultrasonic method used other than specifying UPV threshold (*continued*).

Refe-rence	Material investigated and basic recipe attributes	Setting evaluation method (for criterion statement)	Criterion set		Theoretical basis or other comment
			Point evaluated		
			Initial set/ Time of set	Final set	
[Pop 94]	Concretes with coarse and fine aggregates and w/c = 0.5-0.65	Literature based and referring to event on the UPV-t curve	Alternatively to minimum on UPV-t curve, the maximum attenuation (attenuation first going up to a maximum of approx. 80 dB and decreasing onwards in parallel to velocity increase); agreeing with it exteme decrease of sound attenuation in material during setting stated by [Gam 13]	Not given	Advantage: attenuation more sensitive to changes in internal structure than UPV [Pop 94]; in fact, while UPV is primarily influenced by stiffness of paste (modulus of elasticity), measures of attenuation are more closely related to microstructure, morphology, microstructure, microcracks acc. to [Gab 10]. E.g. attenuation is thought decrease with increasing concentration of solid phase resulting from greater extent of hydration [Kim 88]. Disadvantage: threat that UPV and attenuation may be co-variables [Pop 94]; instead of being sensitive, amplitude measurement could be less reliable than measurement of time of flight [Pop 94] Disadvantage (of unknown importance for criterion statement): dip of velocity in UPV-t curve being referenced to as initial set sometimes considered as mineral percolation threshold, on one hand (e.g. [Bar 01]), but never observed for low w/c material, one the other hand (e.g. [Lee 04]) (attribute of high w/c materials, due to increasing tortuosity of pore space [Bou 96])
[Kak 91]	Mortar with w/c = 0.45-0.65	ASTM C403	Not given	Peak time of rate of dynamic bulk modulus	Disadvantage: Limited agreement in w/c range tested

(continued on following page)

Table G.2: Criteria for determination of setting limits applicable to ultrasonic method used other than specifying UPV threshold (*continued*).

Refe-rence	Material investigated and basic recipe attributes	Setting evaluation method (for criterion statement)	Criterion set		Theoretical basis or other comment
			Point evaluated		
			Initial set/ Time of set	Final set	
[Gab 10]	Cement paste with w/c = 0.4-0.6	HRN EN 196-3 (final set at 1300 m/s, irrespectively of w/c)		(1) First inflection point at UPV-t graph; (2) First maximum in duration i.e. one of acoustic emission (AE) parameters, defined as time from the first threshold crossing to the end of the last threshold crossing of the signal in one wave) (3) End of sudden changes including increase and subsequent decrease in risetime i.e. another AE parameter, defined as the time between first threshold crossing and the peak amplitude of the signal in one wave	Advantage: More parameters extracted from the ultrasonic signal confirming attaining important stage of microstructural development Disadvantage: Finding UPV of 1300 m/s at final set for all w/c tested somewhat questionable given typical differences in degree of hydration at final set depending on w/c; higher velocities at final set or even initial set reported in rival studies for similar material [Trt 09]; meanwhile time when the first inflection point appears on the UPV curve for cement pastes sometimes associated with initial set, e.g. [Trt 08]
[Gab 11]	Cement paste with w/c = 0.3	HRN EN 196-3	Leap in the peak frequency of the signal; equivalent to increase of temperature	(1) Steep increase in number of counts i.e. another AE parameter defined as number of oscillations of the signal above a selected voltage threshold (2) Steep increase in signal duration	Advantage/disadvantage: high correlation between AE parameters and setting points is found even though influence of autogenous shrinkage is involved
[Gab 11b]	Concretes with fine and coarse aggregates, and w/c = 0.4-0.65	ASTM C403	Time parameter from regression analysis of a three-parameter exponential model of the UPV-t curve		

(continued on following page)

Table G.2: Criteria for determination of setting limits applicable to ultrasonic method used other than specifying UPV threshold (*continued*).

Refe-rence	Material investigated and basic recipe attributes	Setting evaluation method (for criterion statement)	Criterion set		Theoretical basis or other comment
			Point evaluated		
			Initial set/ Time of set	Final set	
[Rob 09]	As in previous criterion of selfsame author	As in previous criterion of selfsame author	Particular threshold value of relative energy (ultrasonic energy ratio): 0.02 for mortars and 0.01 for concretes	Particular threshold value of relative energy (ultrasonic energy ratio): 0.13 for mortars and 0.07 for concretes; shortly after maximum rate of ultrasonic energy ratio change	Advantage: Dependence of energy on many other factors than UPV; also lower dependence on precision of signal onset time determination; furthermore, in comparison to some criteria, less data demanded for determination of setting phenomena Disadvantage: in present author's opinion, threshold still dependent on mix tested although only showed as dependent on aggregate graining; although less important for time-zero, larger dependence of energy on quality contact with transducer than UPV
[Gar 95]	Roller compacted concrete	Mechanical tests of resistance to needle penetration and SEM analysis; also adoption of two distinct slope changes on the UPV-t curve, with initial set defined as beginning of the linkage formation between the grains unreasonably (acc. to [Voi 05]), attributed to ettringite formation while with final set matching formation of large quantity of C-S-H	From discontinuity in the energy signature	Close to but rather before energy increases to maximum value	Advantage: Stopping decreasing the transmitted energy corresponding to modifying or stopping the growth kinetics of one or more constituents
[Sak 09]	Concrete of non-given composition	Not given but UPV of approx. 3200 m/s at final set		Attaining maximum of energy	

References for Table G.2

For [Bar 01], [Bou 96], [Dar 11], [Gab 11], [Gam 13], [Gar 95], [Kea 89], [Lee 04], [Nei 74], [Pes 88], [Pop 94], [Rob 08], [Rob 09], [Smi 02], [Trt 08], [Trt 13a], [Voi 05], [Ye 03], [Zha 12b], [Zhu 11a] please see Chapter REFERENCES.

[Bel 05a] De Belie, N.; Grosse; C.U.; Kurz, J.; Reinhardt, H.-W.: Ultrasound monitoring of the influence of different accelerating admixtures and cement types for shotcrete on setting and hardening behaviour. *Cement and Concrete Research*, 35(11), 2005, 2087-2094

[Bel 06] De Belie, N.; Grosse, C.U.; Reinhardt, H.-W.: Ultrasonic monitoring of the influence of pozzolanic additions and accelerating admixtures on setting and hardening behaviour of concrete and mortar. In: Reinhardt, H.-W.(Ed.): *Advanced testing of fresh cementitious materials*, Stuttgart, 2006, pp. 55-64

[Doh 69] Dohnalik, M.; Leski, E., Flaga, K.: Ultraschalluntersuchungen der Erstarrungsprozesse von Zement. In: Pohl, E. (Ed.): Zerstörungsfreie Prüf- und Messtechnik für Beton und Stahlbeton, Leipzig, Tagungsbericht, Berlin : Verl. für Bauwesen, 1969, 35-38

[Gab 10] Gabrijel, I.; Mikulić, D.; Bijelić, N.: Ultrasonic characterization of cement composites during hydration. *Technical Gazette*, 17(4), 2010, 493-497

[Gab 11b] Gabrijel, I.; Mikulić, D.: Application of ultrasonic waves for the analysis of setting and hardening in cement composites. fib Symposium Prague 2011, pp. 313-316

[Her 03] Herb, A.T.: *Indirekte Beobachtung des Erstarrens und Erhärtens von Zementleim, Mörtel und Beton mittels Schallwellenausbreitung*. Doctoral Thesis, Universität Stuttgart, 2003

[Jon 96] Jonas, M.: *Einsatzmöglichkeiten der Ultraschall-Frequenzanalyse für die zerstörungsfreie Prüfung von mineralischen Baustoffen und Bauteilen*. Doctoral Thesis, TU Dortmund, 1996

[Kak 91] Kakuta, S.; Kojima, T.: Evaluation of very early age concrete using wave propagation method. In: Taerwe, L.; Lambotte, H. (Eds.): *Quality Control of Concrete Structures*, Ghent, Belgium, June 12-14, 1991 E&FN Spon, Great Britain, 1991, pp. 163-172

[Kho 09] Khokhar, M.I.A.; Staquet, S.; Rozière, E.; Loukili, A.: Ultrasonic monitoring of setting of green concrete containing high cement substitution by mineral additions. NDTCE'09, Non-Destructive Testing in Civil Engineering, Nantes, France, 2009

[Kim 88] Kim, H.C.; Yoon, S.S.: Ultrasonic measurement during early-stage hydration of ordinary Portland cement. *Journal of Materials Science*, 23, 1988, 611-616

[Leh 73] Lehmann, H.; Rieke, K.: Die Verfolgung des Abbindevorganges von Baugirpsen mit dem Ultraschallverfahren. *Tonindustrie Zeitung*, 97(1), 1973, 21-24

[Rei 98] Reinhardt, H.-W.; Grosse, Ch.U.; Herb, A.: Kontinuierliche Ultraschallmessung während des Erstarrens un Erhärtens von Beton als Werkzeug des Qualitätsmanagements. In: Menzel, K.; Schulze, F.; Reinhardt, H.-W. (Eds.): *Beschichtete Bewehrng Ergebnisse sechsjähriger Auslagerungsversuche*, DAfStb, Heft 490, Beuth Verlag, Berlin, 1998, pp. 21-64

[Sak 09] Sakalli, Y.; Trettin, R.: Untersuchung der Einflüsse der Zementzusammensetzung auf die Frühfestigkeitentwicklung und den Hydratationsverlauf von selbstverdichten Beton mittles in situ Ultraschallverfahren. Jahrestagung der Fachgruppe Bauchemie, Freiberg, 2009, GDCh-Monographie Band 41, 2009 pp. 259-262

[Trt 09] Trtnik, G.; Valič, M.I.; Kavčič, F.; Turk, G.: Comparison between two ultrasonic methods in their ability to monitor the setting process of cement pastes. *Cement and Concrete Research*, 39(), 2009, 876-882

[Whi 51] Whitehurst, E.A. Use of the soniscope for measuring setting time of concrete. ASTM Proceedings, vol. 51, pp. 1166-1183

[Woo 57] Woods, K.B.; McLaughlin, J.F.: *Application of pulse velocity tests to several laboratory studies in materials: Technical Report*. Publication FHWA/IN/JHRP-57/36. Joint Highway Research Project, Indiana Department of Transportation and Purdue University. West Lafayette, Indiana, 1957

H Supplementary CT investigation results

The modes of changes in SAP porosity

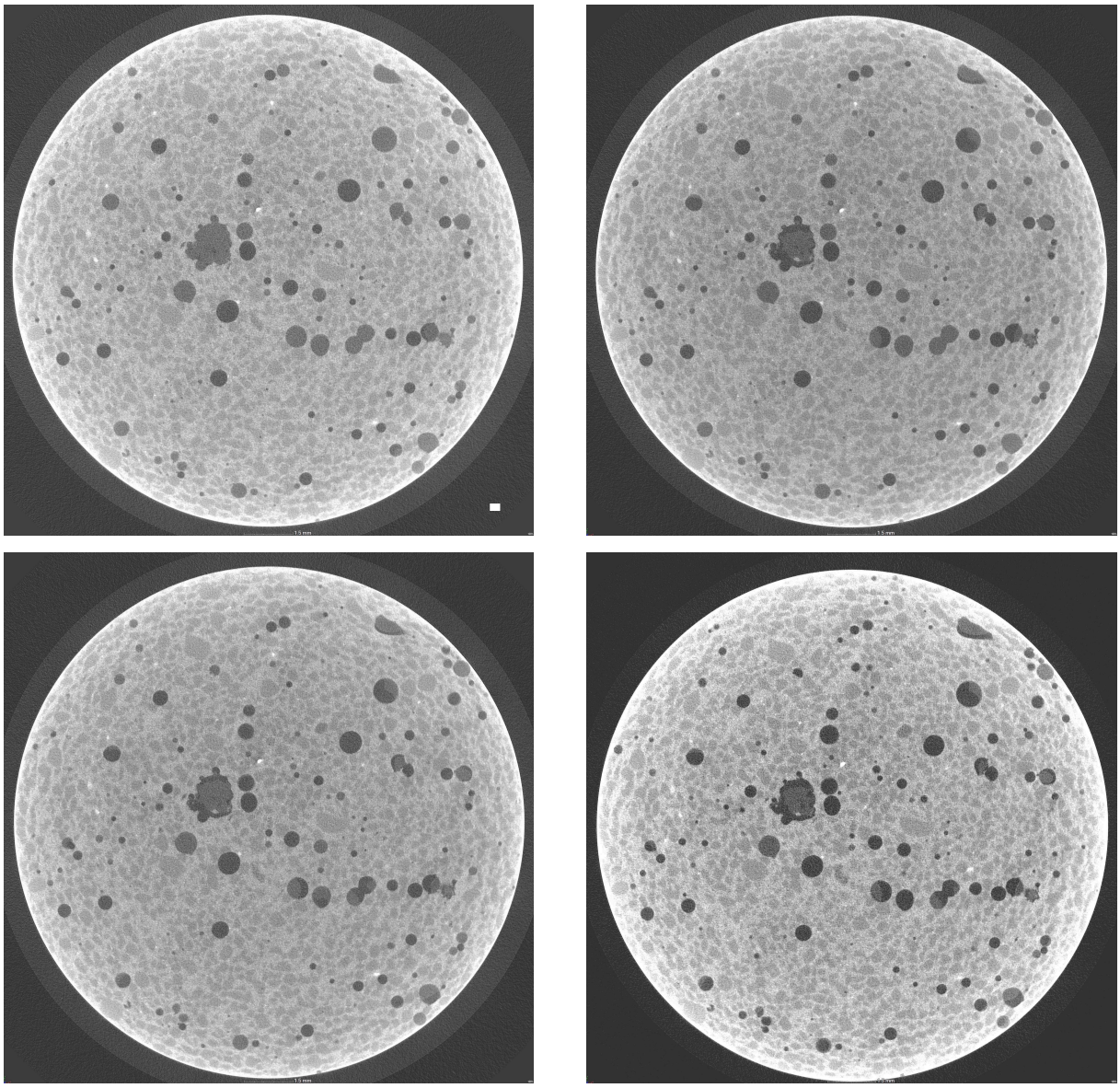

Figure H.1: Modes of changes in full exemplary slice. The order of presentation (from left to right) follows increasing concrete ages at which CT scans were conducted, i.e. 10.5, 13.5 (upper row), 18.5 and 34.5 hours (lower row). The same scale of 300 µm applies to all pictures.

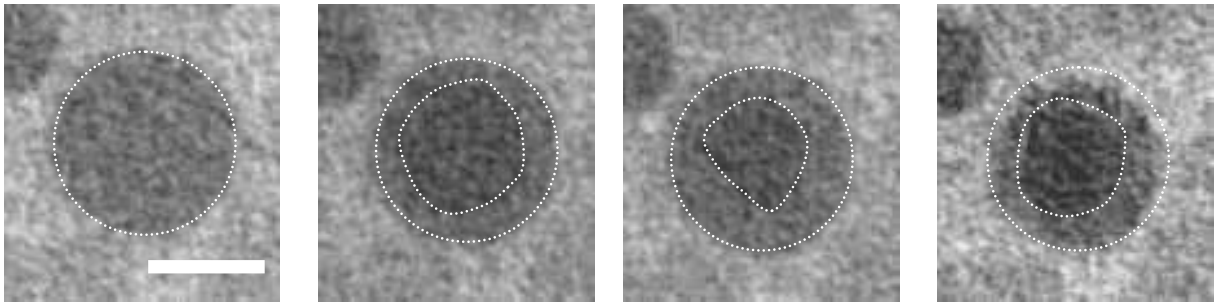

Figure H.2: Mode of changes in exemplary SAP pore 1. The order of presentation (from left to right) follows increasing concrete ages at which CT scans were conducted, i.e. 10.5, 13.5, 18.5 and 34.5 hours. The same scale of 300 µm applies to all pictures.

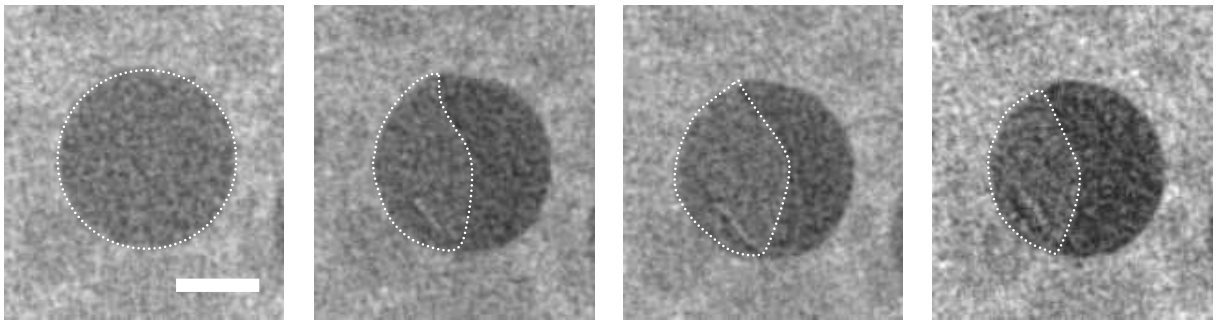

Figure H.3: Mode of changes in exemplary SAP pore 2. The order of presentation (from left to right) follows increasing concrete ages at which CT scans were conducted, i.e. 10.5, 13.5, 18.5 and 34.5 hours. The same scale of 300 µm applies to all pictures.

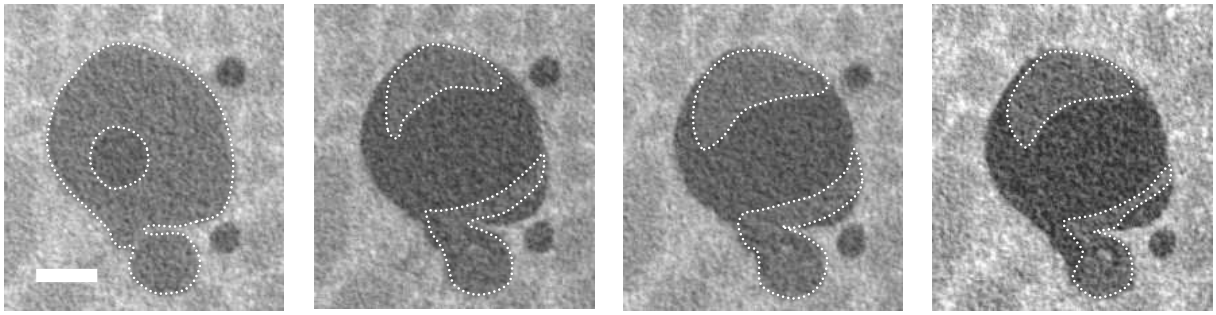

Figure H.4: Mode of changes in exemplary SAP pore 3. The order of presentation (from left to right) follows increasing concrete ages at which CT scans were conducted, i.e. 10.5, 13.5, 18.5 and 34.5 hours. The same scale of 300 µm applies to all pictures.

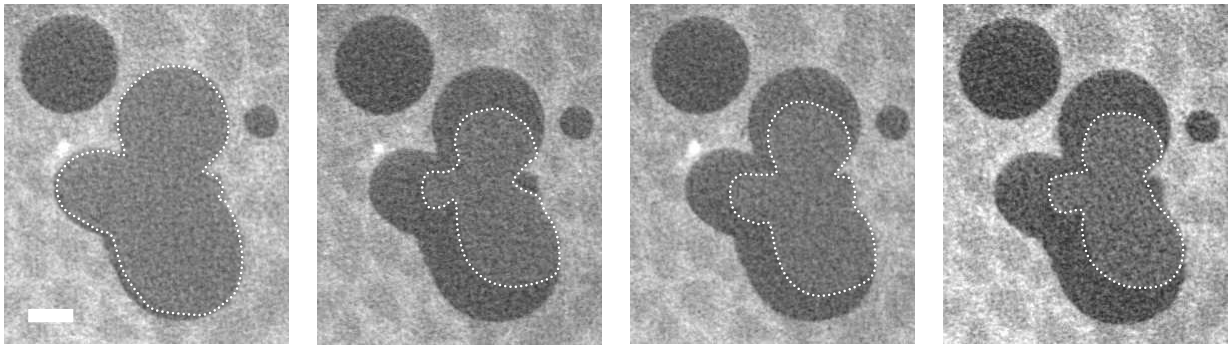

Figure H.5: Mode of changes in exemplary SAP pore 4. The order of presentation (from left to right) follows increasing concrete ages at which CT scans were conducted, i.e. 10.5, 13.5, 18.5 and 34.5 hours. The same scale of 300 µm applies to all pictures.

Frequently observed changes/scenarios in SAP porosity

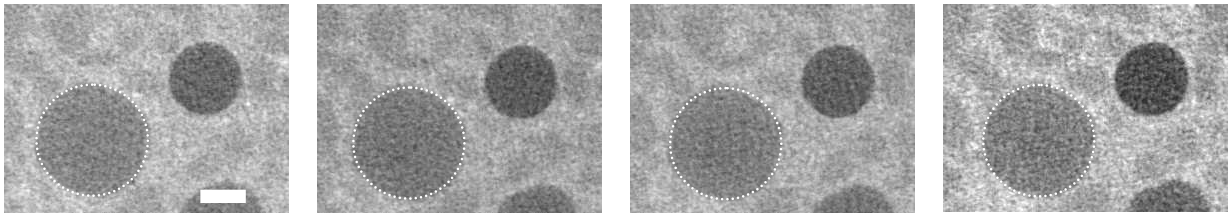

Figure H.6: Mode of changes in exemplary SAP pore 5. The order of presentation (from left to right) follows increasing concrete ages at which CT scans were conducted, i.e. 10.5, 13.5, 18.5 and 34.5 hours. The same scale of 300 µm applies to all pictures.

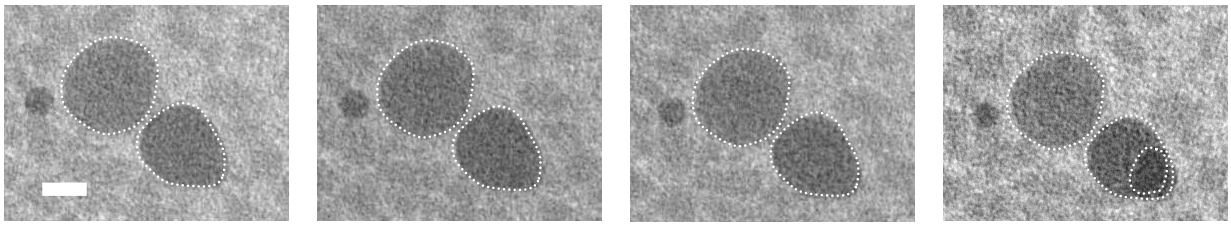

Figure H.7: Mode of changes in exemplary SAP pores 6 and 7. The order of presentation (from left to right) follows increasing concrete ages at which CT scans were conducted, i.e. 10.5, 13.5, 18.5 and 34.5 hours. The same scale of 300 µm applies to all pictures.

Frequently observed changes/scenarios in porosity related to entrapped air of small size

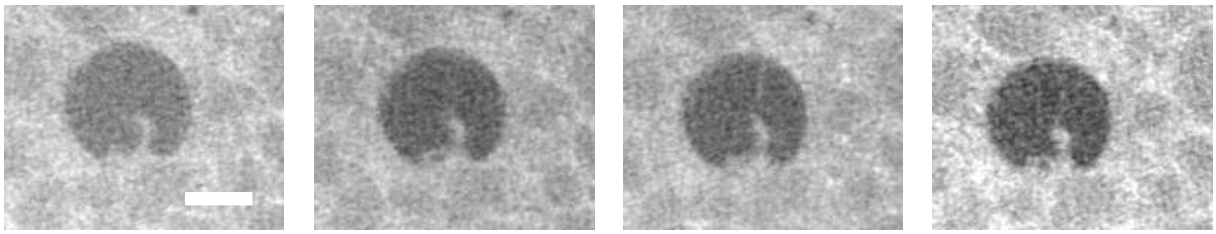

Figure H.8: Mode of changes in unidentified pore. The order of presentation (from left to right) follows increasing concrete ages at which CT scans were conducted, i.e. 10.5, 13.5, 18.5 and 34.5 hours. The same scale of 300 µm applies to all pictures.

Autogenous shrinkage of mixture tested in CT and, for comparison, that of control mix

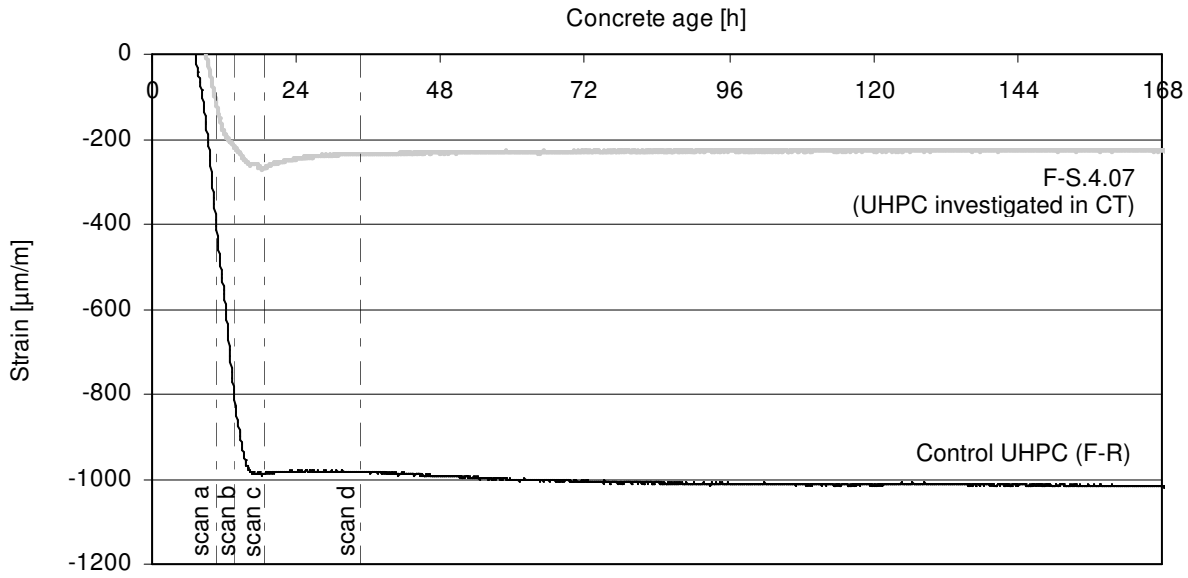

Figure H.9: Autogenous shrinkage data, with indication of concrete ages at which CT scans were performed.

I Supplementary test results – Hardened state

All the results presented herein regard concretes which until the day of testing and, being only the case of instrumented ring tests, also during examination, remained sealed. For other storage/curing conditions, see e.g. [Dud 14] where results of instrumented rings tests under circumferential drying have been published.

Effectiveness of IC in mitigating autogenous shrinkage of finely grained UHPC under additional external restraint as evaluated by means of instrumented ring test and set-up acc. to ASTM C 1581-04

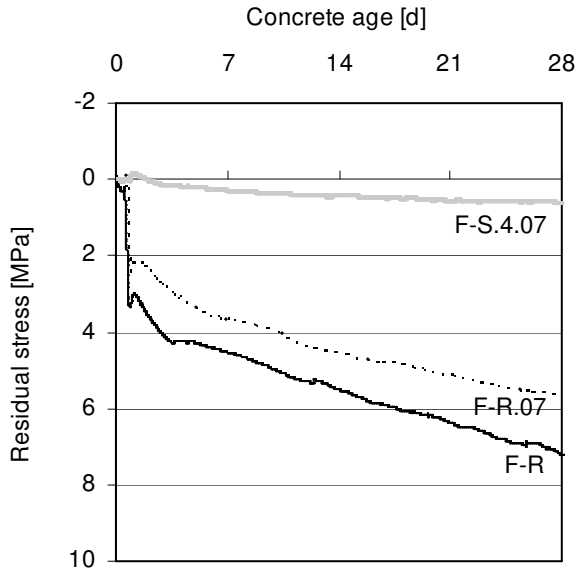

Figure I.1: Evolution of stresses in the instrumented ring tests as measured for mixture incorporating IC (F-S.4.07), mixture of selfsame total w/c but containing no SAP (F-R.07) and control mix (F-R). Mixtures produced from selfsame batch of ingredients.

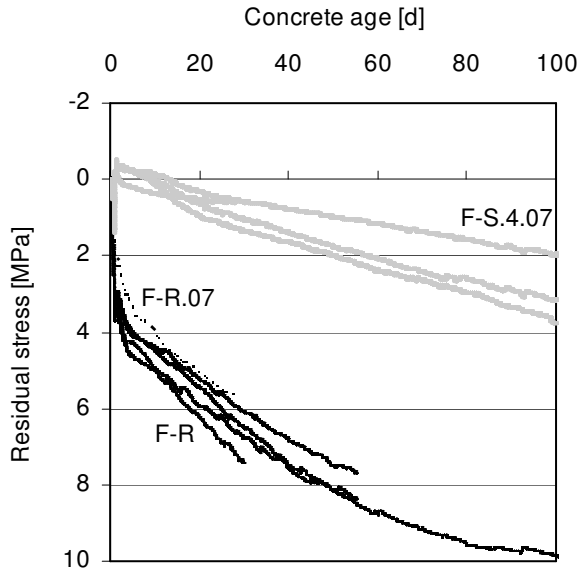

Figure I.2: Long-term evolution of restrained autogenous shrinkage for most important finely grained UHPC compositions tested.

Summary of most important results of instrumented ring tests performed on finely grained UHPCs with set-up acc. to ASTM C 1581-04

Table I.1: Average strains recorded in the restrained ring tests for the sealed finely grained UHPCs (M2Q-based mixtures) using the standardized TUD set-up. Standard deviations are given in parentheses.

Mix	Measured (residual) strain [MPa] (standard deviation)								
	Age evaluated								
	0.5d	**1d**	**3d**	**7d**	**14d**	**21d**	**28d**	**90d**	**At (C)racking/ (E)nd of test**
F-R	-9.2 (9.3)	-43.1 (7.1)	-50.1 (6.3)	-60.6 (4.6)	-69.0 (6.7)	-81.3 (6.7)	-91.5 (7.6)	-136.5 (-)	E: -144.2 at 190.0 d
Ff-R	-7.4 (3.6)	-44.2 (1.5)	-44.4 (-)	-53.7 (-)	-64.8 (-)	-76.7 (-)	-87.3 (-)	-134 (-)	E: -142.2 at 117.0 d
F-R.04	-15.7 (3.0)	-43.3 (1.0)	-49.4 (-)	-55.4 (-)	-64.1 (-)	-	-	-	E: -64.1 at 14.0 d
F-R.07-spvar	-32.0 (-)	-33.0 (-)	-37.3 (-)	-45.2 (-)	-60.2 (-)	-	-	-	E: -74.9 at 20.9 d
F-R.07	1.1 (-)	-33.1 (-)	-38.1 (-)	-51.5 (-)	-64.1 (-)	-72.1 (-)	-79.5 (-)	-	E: -79.4 at 28.0 d
F-S.4.07	-2.8 (2.2)	-1.9 (3.6)	2.5 (2.6)	-1.0 (4.3)	-14.8 (13.8)	-9.4 (3.9)	-12.4 (4.5)	-37.2 (11.4)	**C: -45.5 at 104.7 d**
Ff-S.4.07	-4.4 (0.5)	-4.0 (0.8)	3.5 (-)	0.5 (-)	-9.3 (-)	-16.5 (-)	-21.1 (-)	-55.2 (-)	E: -79.6 at 165.9 d
F-S.6.08	-1.8 (-)	-1.9 (-)	15.3 (-)	9.9 (-)	2.2 (-)	-3.6 (-)	-6.4 (-)	-13.7 (-)	E: -26.7 at 190.0 d

Table I.2: The resultant stresses as derived from restrained ring tests for the sealed finely grained UHPCs (M2Q-based mixtures) using the standardized TUD set-up. Standard deviations are given in parentheses.

Mix	Calculated (residual) stress [MPa] (standard deviation)								
	Age evaluated								
	0.5d	**1d**	**3d**	**7d**	**14d**	**21d**	**28d**	**90d**	**At (C)racking/ (E)nd of test**
F-R	0.7 (0.7)	3.1 (0.5)	3.6 (0.4)	4.3 (0.3)	4.9 (0.5)	5.8 (0.5)	6.5 (0.5)	9.7 (-)	E: 10.3 at 190.0 d
Ff-R	0.5 (0.3)	3.2 (0.1)	3.2 (-)	3.8 (-)	4.6 (-)	5.5 (-)	6.2 (-)	9.6 (-)	E: 10.1 at 55.0 d
F-R.04	1.1 (0.2)	3.1 (0.1)	3.5 (-)	3.9 (-)	4.6 (-)	-	-	-	E: 4.6 at 14.0 d
F-R.07-spvar	2.2 (-)	2.4 (-)	2.7 (-)	3.2 (-)	4.3 (-)	-	-	-	E: 5.3 at 20.9 d
F-R.07	-0.1 (-)	2.4 (-)	2.7 (-)	3.7 (-)	4.6 (-)	5.1 (-)	5.7 (-)	-	E: 5.7 at 28.0 d
F-S.4.07	0.2 (0.2)	0.1 (0.3)	-0.2 (0.2)	0.1 (0.3)	1.1 (1.0)	0.7 (0.3)	0.9 (0.3)	2.7 (0.8)	**C: 3.2 at 104.7 d**
Ff-S.4.07	0.3 (0)	0.3 (0.1)	-0.2 (-)	0 (-)	0.7 (-)	1.2 (-)	1.5 (-)	3.9 (-)	E: 5.7 at 165.9 d
F-S.6.08	0.1 (-)	0.1 (-)	-1.1 (-)	-0.7 (-)	-0.2 (-)	0.3 (-)	0.5 (-)	-	E: 1.9 at 190.0 d

Summary of most important results of instrumented ring tests performed on coarse-grained UHPCs with set-up acc. to ASTM C 1581-04

Table I.3: Average strains recorded in the restrained ring tests for the sealed coarse grained UHPCs (B5Q-based mixtures) using the standardized TUD set-up. Standard deviations are given in parentheses.

Mix	Measured (residual) strain [MPa] (standard deviation)								
	Age evaluated								
	0.5d	1d	3d	7d	14d	21d	28d	90d	At (C)racking/ (E)nd of test
C-R	-37.4 (1.8)	-34.0 (0.2)	-32.6 (-)	-40.2 (-)	-56.7 (-)	-70.6 (-)	-	-	E: -72.6 at 22.0 d
Cf-R	-4.3 (-)	-31.5 (-)	-21.8 (-)	-29.9 (-)	-43.8 (-)	-56.9 (-)	-70.6 (-)	-	E: -73.3 at 29.4 d
Cf-S.3.04	-2.0 (-)	-5.0 (-)	-2.8 (-)	-19.1 (-)	-38.4 (-)	-52.2 (-)	-	-	E: -66.8 at 27.1 d

Table I.4: The resultant stresses as derived from restrained ring tests for the sealed coarse grained UHPCs (B5Q-based mixtures) using the standardized TUD set-up.

Mix	Calculated (residual) stress [MPa] (standard deviation)								
	Age evaluated								
	0.5d	1d	3d	7d	14d	21d	28d	90d	At (C)racking/ (E)nd of test
C-R	2.7 (0.1)	2.4 (-)	2.3 (-)	2.9 (-)	4.0 (-)	5.0 (-)	-	-	E: 5.2 at 22.0 d
Cf-R	0.3 (-)	2.2 (-)	1.6 (-)	2.1 (-)	3.1 (-)	4.1 (-)	5.0 (-)	-	E: 5.2 at 29.4 d
Cf-S.3.04	0.1 (-)	0.4 (-)	0.2 (-)	1.4 (-)	2.7 (-)	3.7 (-)	-	-	E: 4.8 at 27.1 d

Main observations and some important comments (both matrices):

- internal curing introduced to finely grained UHPC matrix led to pronounced decreased in both strains and corresponding tensile stresses measured in the instrumented ring tests; this effect could not be accomplished by adding extra water without the IC agent, as expected
- IC-incorporating mixtures characterized with lower free autogenous shrinkage and furthermore exhibited lower Young's modulus leading to lower stresses under restraint
- the effect was less visible for the B5Q-based mixture, probably due to insufficient amount of IC variables
- one of the IC-incorporating concretes did finally crack (mixture F-S.4.07). Although this could be sign of creep aging and decreasing stress relaxation ability to be expected with increasing concrete age, a more like reason found in own case was sudden

change of temperature shortly before crack was manifested (failure of air-conditioning device during long-term winter measurement)

Cracking potential and normalized cracking potential of most important finely grained UHPCs tested

Table I.5: Cracking potential and normalized cracking potential. Calculation based on average results obtained in the instrumented ring tests and flexural strengths.

Mix	Cracking potential					Normalized cracking potential				
	Age evaluated					Age evaluated				
	1d	3d	7d	28d	90d	1d	3d	7d	28d	90d
F-R	0.30	0.23	0.26	0.36	0.47	100	100	100	100	100
Ff-R	0.16	0.08	0.09	0.15	-	54.5	34.2	35.5	41.3	-
F-R.04	0.32	0.23	0.27	-	-	106.2	98.5	101.8	-	-
F-R.07	0.29	0.20	0.28	0.30	-	94.9	87.5	109.2	85.8	-
F-S.4.07	0.02	-0.02	0.01	0.07	0.17	5.3	-7.6	2.8	20.3	35.2
Ff-S.4.07	0.01	-0.01	0.00	0.04	-	4.7	-3.0	0	11.6	-
F-S.6.08	0.01	-0.09	-0.06	0.04	-	4.1	-40.2	-22.0	10.6	-

Cracking potential and normalized cracking potential of coarse-grained UHPCs tested

Table I.6: Cracking potential and normalized cracking potential. Calculation based on average results obtained in the instrumented ring tests and flexural strengths.

Mix	Cracking potential					Normalized cracking potential				
	Age evaluated					Age evaluated				
	1d	3d	7d	28d	90d	1d	3d	7d	28d	90d
C-R	0.24	0.17	-	-	-	100	100	-	-	-
Cf-R	0.19	0.06	-	0.15	-	78.3	33.3	-	-	-
Cf-S.3.04	0.03	0.01	-	0.14	-	12.4	4.0	-	96.1 rel. to Cf-R	-

Main observations and some important comments (both matrices):

- positive effect of IC also observed in respect to cracking potential
- in view of decreasing stress relaxation ability, all concretes are increasingly more prone to cracking at later ages, irrespectively of IC

Summary of most important results of tests concerning mechanical properties of finely grained UHPCs

Flexural strength and Young's modulus

Table I.7: Average flexural strength and Young's modulus of finely grained UHPCs, with the measurements performed acc. to respective norms on one full prism. Standard deviations are given in parentheses.

Mix	Flexural strength					Young's modulus				
	$f_{cf,\ 1d}$	$f_{cf,\ 3d}$	$f_{cf,\ 7d}$	$f_{cf,\ 28d}$	$f_{cf,\ 90d}$	E_{1d}	E_{3d}	E_{7d}	E_{28d}	E_{90d}
F-R	10.3 (1.3)	15.4 (1.6)	16.5 (1.5)	18.3 (2.9)	20.6 (3.3)	33.2 (1.5)	44.2 (1.2)	47.1 (1.4)	48.8 (1.3)	50.6 (0.5)
F-R-vac	-	17.8 (-)	-	21.5 (-)	-	-	-	-	-	-
Ff-f	19.5 (1.0)	40.0 (6.1)	41.1 (5.5)	42.3 (3.0)	-	-	-	-	-	-
F-S.4	9.8 (1.3)	13.4 (0.9)	14.0 (1.6)	13.0 (2.9)	14.6 (6.5)	-	-	45.9 (1.3)	49.3 (1.0)	-
F-S.4-spvar	2.9 (0.4)	9.2 (0.9)	12.5 (1.0)	15.7 (1.1)	16.1 (1.7)					
F-R.04	9.7 (1.5)	15.2 (1.3)	14.7 (1.8)	17.8 (1.6)	23.1 (0.2)	-	-	-	-	-
F-R.04-vac	-	14.3 (-)	-	15.9 (-)	-	-	-	-	-	-
F-S.3.04	6.5 (1.7)	12.5 (1.4)	14.8 (1.4)	15.5 (2.1)	17.2 (1.4)	26.8 (0.2)	-	-	46.8 (1.3)	49.2 (0.5)
F-S.3.04-vac	-	11.4 (-)	-	13.1 (-)	-	-	-	-	-	-
Ff-S.3.04	17.7 (2.6)	22.7 (0.7)	26.9 (3.4)	30.7 (1.4)	-	-	-	-	-	-
F-S.3.05	8.3 (0.5)	12.8 (0.8)	12.1 (0.2)	13.5 (0.3)	16.8 (1.3)	-	-	-	-	-
F-R.07	8.4 (0.4)	13.2 (1.1)	13.0 (0.6)	18.7 (2.6)	24.2 (2.3)	-	-	-	-	-
F-S.4.065	-	-	-	15.6 (1.5)	-	-	-	-	-	-
F-S.4.07	6.3 (0.9)	11.2 (1.5)	13.9 (0.9)	12.5 (2.9)	16.3 (5.1)	-	35.4 (0.9)	38.7 (2.7)	42.5 (2.0)	47.0 (-)
Ff-S.4.07	21.4 (1.9)	28.9 (2.4)	32.5 (1.1)	36.4 (2.2)	-	-	-	-	-	-
F-R.08	-	16.1 (0.8)	17.3 (0.4)	20.7 (2.3)	-	-	-	-	-	-
F-S.6.08	8.1 (0.5)	11.7 (1.0)	12.2 (0.4)	13.3 (0.2)	8.0 (1.0)	25.6 (0.9)	36.6 (0.9)	40.3 (0.4)	43.4 (0.5)	-
F-S1.0.16	5.4 (0.4)	9.9 (0.5)	11.2 (0.3)	12.5 (1.3)	14.3 (1.0)	-	-	-	-	-

Tensile strength

Table I.8: Average tensile strength of finely grained UHPCs, with the measurements performed on dumbbell-shaped prism. Standard deviations are given in parentheses.

Mix	Tensile strength on dumbbell specimens [MPa]		
	3d	**7d**	**28d**
F-R	4.40 (-)	3.23 (-)	3.83 (-)
Ff-f	6.20 (-)	11.89 (-)	12.99 (-)
F-R.04	-	-	4.28 (1.26) or 5.15 from 2 spec.
F-S.3.04	5.18 (-)	1.95 (-)	2.38 (-)
Ff-S.3.04	7.92 (-)	10.54 (-)	10.03 (-)
F-S.4.07	3.29 (-)	2.33 (-)	2.82 (-)
F-S.6.08	-	-	2.52 (0.75)

Compressive strength (specimens of two different geometries)

Table I.9: Average compressive strength of finely grained UHPCs, with the measurements performed acc. to respective norms on either cubes or prism halves. Standard deviations are given in parentheses.

Mix	Compressive strength on cubes $f_{cm,\ cubes}$ [MPa]				Compressive strength on prism halves $f_{cm,\ prism\ halves}$ [MPa]				
	1d	**3d**	**7d**	**28d**	**1d**	**3d**	**7d**	**28d**	**90d**
F-R	56 (-)	119 (-)	127 (18)	162 (14)	57 (10)	105 (6)	122 (7)	141 (14)	164 (12)
Ff-f	-	-	149 (5)	182 (3)	101 (1)	148 (5)	166 (7)	212 (10)	-
F-S.4	-	-	118 (11)	156 (15)	65 (9)	104 (5)	112 (5)	134 (10)	140 (12)
F-S.4-sp var	-	-	69 (-)	106 (-)	15 (1)	70 (3)	90 (2)	106 (5)	124 (7)
F-R.04	-	-	128 (3)	149 (13)	58 (6)	101 (6)	118 (7)	143 (15)	163 (9)
F-S.3.04	-	-	121 (6)	155 (8)	33 (10)	95 (7)	111 (6)	137 (7)	145 (11)
Ff-S.3.04	-	-	-	168 (4)	75 (3)	125 (6)	142 (3)	181 (5)	-
F-S.3.05	-	-	125 (-)	147 (8)	42 (2)	88 (2)	108 (4)	142 (8)	126 (7)
F-R.07	-	-	110 (-)	149 (25)	40 (1)	100 (2)	108 (3)	136 (7)	147 (4)
F-S.4.065	-	-	-	128 (9)	-	-	-	106 (3)	-
F-S.4.07	43 (-)	97 (-)	95 (15)	130 (13)	35 (6)	86 (3)	94 (4)	123 (10)	135 (7)
Ff-S.4.07	-	-	-	139 (3)	64 (1)	105 (5)	125 (2)	163 (6)	-
F-R.08	-	-	-	-	-	98 (4)	116 (5)	125 (8)	-
F-S.6.08	-	-	-	115 (6)	36 (2)	69 (2)	86 (5)	118 (6)	121 (9)
F-S1.0.16	-	-	53 (-)	97 (-)	27 (1)	66 (1)	75 (2)	85 (3)	97 (1)

Cube compressive strength of finely grained UHPCs for different curing conditions

Table I.10: Evaluation of effect of storage conditions on cube compressive strength of finely grained UHPC. Concrete from the selfsame batch produced tested. Standard deviations are given in parentheses.

Mix	Compressive strength on cubes $f_{cm,\ cubes}$ [MPa]		
	Sealed	**Exposed to ambient**	**7d Water + 21d ambient**
F-R	163 (-)	162 (-)	171 (-)
F-R.07	171 (-)	175 (-)	178 (-)
F-S.4.07	129 (-)	113 (-)	124 (-)

Table I.11: The relationship/ratios between different mechanical properties of M2Q-based mixtures for all ages tested. Results obtained for all individual repetitions within one composition in [MPa] used for deriving the final ratio.

Mix	Flexural strength, $f_{cf}=ax^b$					Compressive strength-prisms halves	
	'a' for the property 'x' related to (R2)						
	$f_{c,\ prism\ halves}$	$f_{c,\ prism\ halves}^{0.5}$	$f_{c,\ prism\ halves}^{2/3}$	$f_{c,\ prism\ halves}^{0.55}$	a,b for R2max	$f_{c,\ full\ prism}$	$f_{c,\ cube}$
F-R	0.134 (0.54)	1.521 (0.71)	0.680 (0.73)	1.196 (0.72)	0.939, 0.6	0.904 (0.94)	0.839 (0.86)
Ff-f	0.223 (0.62)	2.959 (0.61)	1.255 (0.67)	2.289 (0.63)	0.775, 0.76	-	1.165 (0.94)
F-R.04	0.134 (0.78)	1.489 (0.78)	0.672 (0.85)	1.174 (0.81)	0.472, 0.74	-	0.879 (0.97)
F-S.3.04	0.123 (0.74)	1.352 (0.86)	0.613 (0.88)	1.068 (0.88)	0.766, 0.62	0.873 (0.98)	0.876 (-)
Ff-S.3.04	0.183 (0.76)	2.182 (0.93)	0.960 (0.97)	1.707 (0.95)	1.096, 0.64	-	1.080 (-)
F-S.3.05	0.120 (0.15)	1.285 (0.70)	0.586 (0.61)	1.016 (0.69)	1.550, 0.46	-	0.947 (-)
F-R.07	0.145 (0.83)	1.569 (0.68)	0.714 (0.77)	1.240 (0.72)	0.145, 1	-	-
F-S.4.07	0.118 (0.37)	1.237 (0.53)	0.570 (0.52)	0.982 (0.54)	0.937, 0.56	0.868 (0.97)	0.891 (0.99)
Ff-S.4.07	0.251 (0.56)	2.834 (0.98)	1.273 (0.97)	2.231 (0.99)	1.932, 0.58	-	1.170 (-)
F-S.6.08	0.111 (-)	1.141 (-)	0.529 (-)	0.907 (-)	-	-	-
F-S1.0.16	0.149 (0.95)	1.316 (0.90)	0.641 (0.98)	1.061 (0.93)	0.391, 0.78	-	-

Summary of most important results of tests concerning mechanical properties of coarse-grained UHPCs

Flexural strength and Young's modulus

Table I.12: Average flexural strength and Young's modulus of coarse-grained UHPCs, with the measurements performed acc. to respective norms on one full prism. Standard deviations are given in parentheses.

Mix	Flexural strength					Young's modulus			
	$f_{cf,\ 1d}$	$f_{cf,\ 3d}$	$f_{cf,\ 7d}$	$f_{cf,\ 28d}$	$f_{cf,\ 90d}$	E_{1d}	E_{3d}	E_{7d}	E_{28d}
C-R	10.2 (1.3)	13.3 (1.1)	16.2 (1.5)	17.5 (3.0)	-	34.5 (0.5)	44.2 (3.8)	-	51.3 (1.4)
Cf-R	15.5 (3.3)	28.6 (3.3)	-	35.3 (2.8)	39.0 (-)	28.1 (0.9)	44.2 (1.8)	49.1(-)	54.7 (1.1)
C-S.3.04	8.5 (0.6)	11.4 (1.2)	13.8 (0.5)	15.3 (2.5)	-	33.1 (0.9)	41.2 (1.0)	-	49.2 (0.9)
Cf-S.3.04	12.6 (3.0)	26.8 (2.6)	-	34.8 (3.2)	-	27.3 (0.8)	43.0 (0.2)	47.4 (0.5)	53.4 (-)

Tensile strength

Table I.13: Average tensile strength of coarse-grained UHPCs, with the measurements performed on dumbbell-shaped prism. Standard deviations are given in parentheses.

Mix	Tensile strength on dumbbell specimens [MPa]		
	3d	7d	28d
C-R	-	-	4.86 (0.74)
C-S.3.04	-	-	5.32 (0.78) or 4.81 for two samples

Table I.14: Average compressive strength of coarse-grained UHPCs, with the measurements performed acc. to respective norms on either cubes or prism halves. Standard deviations are given in parentheses.

Mix	Compressive strength on cubes $f_{cm,\ cube}$ [MPa]				Compressive strength on prism halves $f_{cm,\ prism\ halves}$ [MPa]				
	1d	3d	7d	28d	1d	3d	7d	28d	90d
C-R	-	-	144 (-)	202 (26)	70 (5)	106 (6)	131 (7)	160 (9)	-
Cf-R	64 (3)	117 (3)	-	188 (6)	71 (16)	142 (7)	-	225 (8)	246 (-)
C-S.3.04	-	-	110 (-)	152 (6)	56 (7)	98 (5)	111 (7)	141 (5)	-
Cf-S.3.04	42 (7)	109 (8)	-	181 (7)	50 (8)	124 (3)	-	207 (7)	-

Table I.15: The relationship/ratios between different mechanical properties of B5Q-based mixtures for all ages tested. Results obtained for all individual repetitions within one composition in [MPa] used for deriving the final ratio.

Mix	Flexural strength, $f_{cf}=ax^b$					Compressive strength- prisms halves	
	'a' for the property 'x' related to (R2)						
	$f_{c,\ prism\ halves}$	$f_{c,\ prism\ halves}^{0.5}$	$f_{c,\ prism\ halves}^{2/3}$	$f_{c,\ prism\ halves}^{0.55}$	a,b for R2max	$f_{c,\ full\ prism}$	$f_{c,\ cube}$
C-R	0.124 (0.76)	1.392 (0.86)	0.625 (0.92)	1.095 (0.88)	0.532, 0.7	0.942 (0.99)	0.812 (-)
Cf-f	0.170 (0.81)	2.322 (0.90)	0.982 (0.95)	1.797 (0.93)	0.982, 0.667	1.333 (0.99)	1.209 (0.99)
C-S.3.04	0.119 (0.70)	1.261 (0.80)	0.578 (0.85)	0.999 (0.83)	0.578, 0.667	0.984 (0.95)	0.950 (0.96)
Cf-S.3.04	0.188 (0.80)	2.305 (0.90)	1.015 (0.95)	1.806 (0.93)	1.015, 0.667	1.283 (0.98)	1.151 (0.99)

Main observations and some important comments (both matrices):

- results of 28d compressive strength: general lack of applicability of size effect in case of concretes based on either of two main UHPC matrices unless fibres are incorporated in the mix. For F-R alike and another but comparable composition of finely grained UHPC, similar observation was made by Orgass and Klug [Org 04] and Boros [Bor 06], respectively
- as far as testing of prisms is concerned, only fibres and tests on full prisms (in arrangement as in measurement of Young's modulus, giving higher values compared to tests on prism halves) are bringing 28day-old concrete based on M2Q matrix to the level expected for UHPC, although not always for mixes with IC
- some damage of microstructure due to swelling and crystallization pressure resulting from some hydration product formation, in addition to large content of unhydrated clinker and high density [Xu 93] and/or repercolation [Ben 06a] likely also affecting strength at later ages
- only addition of fibres and flexural strength tests are making measure of tensile strength reliable in case of UHPC tested
- compressive strength measured on prism halves could be used to predict flexural strength as well as the cube strength although this often requiring special adjustment of the power (0.5 or 2/3 instead of 1) for increasing the ratio accuracy from satisfactory to excellent one. This holds true/applies despite expected difference in rates of development at the beginning of hydration, perhaps due to making first correlation at the age of 1 day (!). Correlation is better for the coarse-grained UHPC mixtures
- statistical average standard deviation never exceeded the standard deviation presented

References (unless not mentioned in Chapter REFERENCES)

[Bor 06] Boros, V.: Ultrasound monitoring of the setting and hardening of Ultra High Performance Concrete. In: *Scientific Student Conference*, Budapest, Hungary, 2006, http://vit.bme.hu/tdk/2006/dolgozatok/boros2006.pdf

[Org 04] Orgass, M.; Klug, Y.: Steel fibre reinforced Ultra-High Strength Concretes. *Leipzig Annual Civil Engineering Report (Lacer)*, 9, 2004, 233 - 244

[Xu 93] Xu, Z.; Tang, M.; Beaudoin, J.J.: Relationships between composition, structure and mechanical properties of very low porosity cementitious systems. *Cement and Concrete Research*, 23(1), 1993, 187-195

Schriftenreihe des Institutes für Baustoffe

Published works of the Institute of Construction Materials

Herausgeber/Editor:
Prof. Dr.-Ing. Viktor Mechtcherine
Institut für Baustoffe
Fakultät Bauingenieurwesen
Technische Universität Dresden
01062 Dresden
Telefon: (0351) 463 36311
Telefax: (0351) 463 37268
E-Mail: i.baustoffe@tu-dresden.de

Heft 2017/1 **Ksenija Vasilic**
A numerical model for self-compacting concrete flow through reinforced sections: A porous medium analogy

Heft 2017/2 **Lukasz Dudziak**
Mitigating autogenous shrinkage of Ultra-High Performance Concrete by means of internal curing using superabsorbent polymers

Weitere Dissertationen am Institut für Baustoffe, die nicht in der Schriftenreihe erschienen sind:

2011 **Sören Eppers**
Assessing the autogenous shrinkage cracking propensity of concrete by means of the restrained ring test

2014 **Oliver Millon**
Analyse und Beschreibung des dynamischen Zugtragverhaltens von ultrahochfestem Beton